UNIVERSITAT DE BARCELONA

Development of an in vitro LTP-model of food anaphylaxis and study of mechanisms driving exacerbated responses

Laia Ollé Boix

UNIVERSITAT DE BARCELONA

Development of an *in vitro* LTP-model of food anaphylaxis and study of mechanisms driving exacerbated mast cell responses

Doctoral program in Biomedicine

Dissertation submitted by:

Laia Ollé Boix

This work was performed at the Department of Biomedicine of the Faculty of Medicine and Health Sciences of the University of Barcelona, under the supervision of Dr. Margarita Martín Andorrà and Dr. Rosa Mª Muñoz Cano.

Laia Ollé Boix Dr. Margarita Martín Andorrà Dr. Rosa Mª Muñoz Cano

Als meus pares, a la meva
germana i a la meva parella

“There is nothing alive simpler than a cell, and nothing can become more complex without first beginning as a cell.”

Mahlon Hoagland

“It is not the strongest of the species that survives, nor the most intelligent that survives. It is the one that is most adaptable to change.”

Leon C. Megginson

“The moment you give up, is the moment you let someone else win.”

Kobe Bryant

ACKNOWLEDGMENTS

TABLE OF CONTENTS

ABSTRACT

Mast cells (MCs), key immune system cells, can be activated via IgE or the MRGPRX2 receptor, releasing proinflammatory mediators that may trigger severe allergic reactions such as anaphylaxis. The study aims to better understand the cellular and molecular mechanisms governing these responses and to identify potential therapeutic targets.

This study develops an *in vitro* model of food allergy mediated by lipid transfer protein (LTP), focusing on the analysis of mast cell (MC) responses in patients with varying degrees of severity. Patients sensitized to Lipid transfer protein (LTP) were classified as anaphylaxis or sensitized depending on the symptoms elicited by LTP-containing food. CD34+-derived MCs from patients and controls were obtained, sensitized with pooled sera, and challenged with Pru p 3 (peach LTP).

MCs from anaphylactic patients exhibited increased degranulation and elevated secretion of PGD2, IL-8, and GM-CSF upon stimulation, which could be related to higher-affinity IgE, produced with the help of $T_{FH}13$ cells, which were more abundant in those patients. In contrast, sensitized MCs showed a protective profile, with higher CCL2 and TGF-β production. At the molecular level, MCs from anaphylactic patients expressed higher levels of genes associated with cell activation, inflammation, and mitochondrial function, including the Microphthalmia-associated transcription factor (MITF). Further dissection shows that inhibition of MITF significantly reduced degranulation, calcium influx, mediator secretion, and mitochondrial activity.

In conclusion, allergic response severity is influenced by both humoral and cellular components. Beyond antibody-driven mechanisms, cellular factors such as MITF expression may amplify mast cell activation and exacerbate allergic reactions. Targeting MITF could represent a therapeutic strategy to reduce mast cell hyperactivation and mitigate severe allergic responses.

Keywords: Mast cells, allergy, anaphylaxis, IgE, MRGPRX2, calcium, degranulation, cytokines, MITF, mitochondrial activity, metabolism.

SUMMARY

DESENVOLUPAMENT D'UN MODEL LTP *IN VITRO* PER A L'ANAFILAXI ALIMENTÀRIA I ESTUDI DELS MECANISMES QUE DIRIGEIXEN RESPOSTES EXACERBADES DELS MASTÒCITS

INTRODUCCIÓ

Els mastòcits (MCs) són cèl·lules del sistema immune, implicades en la defensa de l'hoste, la immunitat innata i adquirida, les respostes homeostàtiques i la immunoregulació (1–4). Diferents mecanismes indueixen l'activació dels mastòcits, com la unió entre la Immunoglobulina E (IgE), unida a l'al·lergen, i FcεRI (Fc Epsilon Receptor) o la unió de fàrmacs amb el receptor MRGPRX2 (Mas related GPR family member X2, receptor acoblat a proteïnes G) (5,6) causant l'alliberament immediat del contingut dels grànuls (7,8). Els mastòcits secreten una àmplia gamma de mediadors preformats i sintetitzats *de novo*, que desencadenen respostes al·lèrgiques com asma, angioedema, urticària, i en els casos més greus, anafilaxi o xoc anafilàctic (9,10).

En les últimes dècades, l'anafilaxi causada per aliments i fàrmacs, ha augmentat de manera crítica i el seu risc és impredictible. La dieta d'evitació d'al·lèrgens o el tractament simptomàtic són els tractaments estàndard per gestionar aquestes patologies; i, la prova de provocació oral amb al·lèrgens segueix sent la principal eina per diagnosticar al·lèrgies a aliments i medicaments, posant en risc la vida del pacient, ja que poden provocar reaccions al·lèrgiques potencialment greus, anafilaxi o fins i tot la mort (11–13). Així doncs, és realment necessari trobar un model *in vitro* que substitueixi la tècnica de provocació oral com a eina de diagnòstic per predir el risc de gravetat. Entendre les bases moleculars i cel·lulars de l'al·lèrgia alimentària ajudaria a desenvolupar un diagnòstic, una prevenció i un tractament més precís.

Estudis recents en pacients al·lèrgics i models murins mostren que l'afinitat de la IgE i el paper de les cèl·lules $T_{FH}13$ (T follicular helper 13 cells) són clau en la desgranulació mastòcitaria i l'anafilaxi (14–16). Per altra banda, la funcionalitat dels mastòcits està regulada per diferents factors de transcripció,

com ara el factor de transcripció associat a la microftàlmia (MITF), el qual està implicat en la biogènesi dels mastòcits i la síntesi de mediadors (17), així com la producció d'ATP (18).

HIPÒTESI

Així doncs, la nostra hipòtesi és que en les reaccions anafilàctiques, tant els components humorals (IgE) com els cel·lulars (mastòcits) contribueixen a la gravetat de la malaltia. A més, MITF, és un regulador clau de la diferenciació i l'activació dels mastòcits i pot representar una potencial diana terapèutica per al tractament de l'anafilaxi en reaccions dependents d'IgE o del receptor MRGPRX2.

RESULTATS

En aquest estudi hem utilitzat un model d'al·lèrgia alimentària relacionada amb la proteïna de transferència de lípids (LTP). La LTP és un "pan-alergen" present en diversos aliments vegetals (hortalisses, fruites, llegums, fruits secs, llavors,...) i és la principal causa d'al·lèrgia alimentària en adults en la regió mediterrània (19–21). L'al·lèrgia a la LTP té una àmplia gamma de símptomes, des de símptomes lleus fins a l'anafilaxi. Els pacients amb al·lèrgia a la LTP poden desenvolupar reaccions amb múltiples aliments vegetals, limitant la seva dieta i afectant la seva qualitat de vida (22).

Població d'estudi

Per tal d'estudiar mecanismes en el model de la LTP, es van reclutar pacients al·lèrgics al Servei d'Al·lèrgies de l'Hospital Clínic de Barcelona. Es van classificar en dos grups en funció de la gravetat de la reacció a la ingestió de préssec: (a) pacients diagnosticats amb al·lèrgia a la LTP i amb antecedents d'anafilaxi a la història clínica, i (b) pacients sensibilitzats a la LTP, però sense símptomes o símptomes locals lleus. També es van reclutar voluntaris sans sense al·lèrgies respiratòries o alimentàries com a controls.

Desenvolupament d'un model cel·lular (mastòcits) per distingir la severitat de la reacció al·lèrgica

Primerament, vam poder establir un model d'al·lèrgia a la LTP *in vitro* que podia diferenciar els pacients amb reaccions greus vers els pacients que només estaven sensibilitzats a la LTP. El test d'activació de mastòcits (MAT) és una eina de diagnòstic *in vitro* que combina l'al·lergen, la IgE específica d'al·lergen i els MCs humans, els tres elements crucials de la fase efectora de les respostes al·lèrgiques mediades per IgE (23). Curiosament, en el nostre model, vam observar que els MCs de pacients anafilàctics induïen una major desgranulació i producció de prostaglandina D2 (PGD_2) que els MCs dels pacients sensibilitzats. A més, vam observar que les LAD2 (línia cel·lular de mastòcits) incubades amb sèrum dels pacients anafilàctics també induïen una major desgranulació i producció de PGD_2 que les LAD2 incubades amb sèrum de pacients sensibilitzats, suggerint que el sèrum (component humoral) dels pacients podia tenir un paper important en la severitat de la reacció. En aquesta línia, vam observar que les cèl·lules $T_{FH}13$, encarregades d'induir la producció d'una IgE de més alta afinitat, eren més abundants en pacients amb anafilaxi que en aquells sensibilitzats, la qual cosa indica que els pacients anafilàctics podrien tenir una IgE específica de més alta afinitat que la dels pacients sensibilitzats.

Diferències en el patró d'activació de mastòcits entre individus sensibilitzats i anafilàctics

A més a més, vam observar que la sensibilització de les cèl·lules amb el sèrum dels pacients anafilàctics, seguida per l'activació de Pru p 3, induïa una major resposta proinflamatòria, augmentant la secreció de IL-8 i GM-CSF. Per contra, la sensibilització de les cèl·lules amb el sèrum dels pacients sensibilitzats, seguida per l'activació de Pru p 3, induïa una resposta més protectora, augmentant la secreció de CCL2 i TGF-β. A partir de la transcriptòmica de MCs sensibilitzats en sèrums de pacients i activats amb Pru p 3, vam observar que vies relacionades amb la secreció de citocines pro-inflamatòries estaven reduïdes en MCs sensibilitzats amb sèrum de pacients sensibilitzats i activades amb Pru p 3, suggerint una senyalització diferencial

en comparació amb els MCs sensibilitzats amb sèrum de pacients anafilàctics i activats amb Pru p 3.

Diferències en l'expressió gènica de mastòcits entre individus sensibilitzats i anafilàctics

L'expressió gènica de diversos factors estava elevada en MCs de pacients anafilàctics en comparació amb els MCs de pacients sensibilitzats o individus sans. Vam observar una elevada expressió de: *FcεRI*, un receptor crucial per l'activació dels MCs; la histidina decarboxilasa, una enzima important en la síntesi d'histamina; la triptasa Alpha/Beta 1, essencial per la producció de triptasa; la proteïna STIM1 (Stromal Interaction Molecule 1), que facilita l'entrada de calci, necessària per l'activació dels MCs; la translocasa de la membrana mitochondrial externa (*TOMM20*), implicada en la biogènesi mitocondrial i COX-IV, proteïna important per l'activitat mitocondrial. A més, també vam observar nivells elevats de mediadors pro-inflamatoris com la interleukina 1 beta (*IL-1B*), la ciclooxigenasa 2 (*COX2*), crucial per la síntesi de prostaglandines; i el receptor de prostaglandines EP3 (*PTGER3*), que indueix l'activació dels MCs. Aquests resultats suggereixen que els pacients anafilàctics podrien tenir una predisposició a patir respostes més severes.

Finalment, els mastòcits de pacients anafilàctics presentaven nivells elevats de *MITF*, un factor de transcripció que, com hem dit anteriorment, està implicat en la diferenciació dels MCs, així com en els mediadors de desgranulació i alliberació dels MCs (24). Vam observar que MITF és un factor clau en la regulació de la desgranulació mastocitària.

Modulacions de l'expressió de MITF condicionen l'alliberació de mediadors pro-inflamatoris i l'activitat mitocondrial

Vam observar que la inhibició de MITF podria disminuir la gravetat de la resposta al·lèrgica mitjançant la regulació de la secreció de mediadors dels mastòcits (preformats i *de novo*) i la funció mitocondrial. Quan MITF estava inhibit o silenciat, hi havia una disminució de la secreció de citoquines pro-inflamatòries (IL-8 i GM-CSF), de l'expressió dels gens *IL-1B, COX2 i*

PTGER3, i de l'expressió de *TOMM20* i *COX-IV*. Així com també, vam observar una disminució de la respiració mitocondrial quan MITF estava inhibit o silenciat.

Resumint, hem observat que els MCs de pacients anafilàctics tenen una desgranulació més forta i una major alliberació de citoquines pro-inflamatòries, probablement causada per una activitat mitocondrial més elevada, una expressió més elevada de gens pro-inflamatoris, així com una secreció de mediadors pro-inflamatoris més elevada, en comparació amb els MCs de pacients sensibilitzats. A més, hem mostrat que aquesta resposta exacerbada es podria regular a la baixa amb el silenciament o la inhibició de MITF.

Conclusions

Els nivells i l'afinitat d'IgE tenen un paper crític en la gravetat de les reaccions al·lèrgiques. A més, l'expressió elevada de certs gens, com MITF, poden estar augmentant la susceptibilitat d'aquests MCs per induir una resposta exacerbada. MITF podria regular les respostes exacerbades dels mastòcits tant per la via depenent de la IgE com per la via depenent de MRGPRX2. Això obre una nova línia d'investigació per explorar: la implicació de MITF en la biologia dels mastòcits, destacant el seu potencial terapèutic en malalties inflamatòries i al·lèrgiques.

Paraules clau: Mastòcits, al·lèrgia, anafilaxi, IgE, MRGPRX2, calci, desgranulació, citoquines, MITF, activitat mitocondrial, metabolisme.

ABBREVIATIONS

2-DG	2-deoxy-D-glucose
5-LO	5-Lipoxygenase
A	Anaphylaxis group
Akt	Protein kinase B
Ap4A	Diadenosine tetraphosphate
APCs	Antigen presenting cells
ATP	Adenosine triphosphate
b-HLH-LZ	Basic helix-loop-helix leucine zipper
B2M	Microglobulina beta 2
BAT	Basophil activation test
BCL2	B-cell lymphoma 2
$_{BC}$MCs	MCs from buffy coat preparations
$_{BC}$MCs-A	$_{BC}$MCs sensitized with sera from anaphylactic patients
$_{BC}$MCs-S	$_{BC}$MCs sensitized with sera from sensitized patients
^{b}IgE	Biotinylated human IgE
BMCPs	Bipotent basophil/mast cell progenitors
BSA	Bovine Serum Albumin
BTK	Bruton tyrosine kinase
C/EBPa	CCAAT/enhancer binding protein alpha
CACNA1H	Calcium voltage-gated channel subunit alpha1 H
CCL	Chemokine C-C motif ligand
CCL11	CC-chemokine ligand 11
CCL18	C-C Motif Chemokine Ligand 18
CCL2	C-C Motif Chemokine Ligand 2
CCL20	C-C Motif Chemokine Ligand 20
CCL5	C-C Motif Chemokine Ligand 5
CCR2	C-C Motif Chemokine receptor type 2
CDK2	Cyclin dependent kinase 2
CIV	Complex IV of the mitochondrial electron chain
CM	Cutaneous mastocytosis
CMA	Chymase 1
CMPs	Common myeloid progenitors
COX1	Cyclooxigenase 1
COX2	Cyclooxigenase 2

COX4I1	Cytochrome C Oxidase Subunit 4I1
CSU	Chronic spontaneous urticaria
CTMCs	Connective tissue-type Mast cells
CXCL	CXC-motif chemokine ligand
CXCL10	C-X-C motif chemokine ligand 10
CXCL8	CXC-motif chemokine ligand 8
CXCR	CXC-motif chemokine receptor
CXCR2	CXC-motif chemokine receptor 2
DAG	Diacylglycerol
DCs	Dendritic cells
DMEM	Dulbecco's Modifies Eagle Medium
DMSO	Dimethyl sulfoxide
DNA	Deoxyribonucleic acid
DNP-HSA	Dinitrophenyl-Human Serum Albumin
DNP-IgE	Dinitrophenyl-IgE
DPT	Drug provocation test
DRP1	Dynamin-related protein 1
ECAR	Extracellular acidification rate
EDTA	Ethylenediaminetetraacetic acid
EFCAB5	EF-hand calcium-binding domain 5
EGTA	Ethylene glycol tetraacetic acid
EMPs	erythro-myeloid progenitors
ER	Endoplasmic reticulum
ERK	Extracellular signal-regulated kinases
ETC	Electron Transfer Chain
FA	Food Allergy
$FADH_2$	Flavin adenine dinucleotide with hydrogen
FBS	Fetal Bovine Serum
FBXL10	F-box and leucine-rich repeat protein 10
FCCP	Carbonyl cyanide-4 (trifluoromethoxy) phenylhydrazone
FcgR	Fc Gamma Receptor
FcRs	Immunoglobulin Fc receptors
FcεR1A	Fc Epsilon Receptor 1 alpha gene
FcεRI	Fc Epsilon Receptor 1

FGF	Fibroblast growth factor
GATA2	GATA binding factor 2
GIST	Gastrointestinal stromal tumor
GlycoPER	Glycolytic Proton Efflux Rate
GM-CSF	Granulocyte-macrophage colony-stimulating factor
GMPs	Granulocyte/monocyte progenitors
GO	Gene Ontology
GSEA	Gene Set Enrichment Analysis
GUSB	Glucuronidase beta
H	Healthy group
H1	Histamine receptor 1
H2	Histamine receptor 2
H3	Histamine receptor 3
H4	Histamine receptor 4
HDC	Histidine decarboxylase
$_{HV}$MCs	MCs from healthy volunteers
HIF1α	Hypoxia-inducible factor 1 alpha
HINT1	Histidine triad nucleotide-binding protein 1
HMC-1	Human mast cell line with KIT mutation in G560V and D860V
HSCs	Hematopoietic stem cells
ICAM-1	Intercellular adhesion molecule 1
IFN-γ	Interferon gamma
IgA	Immunoglobulin A
IgE	Immunoglobulin E
IGF1R	Insulin-like growth factor 1 receptor
IgG	Immunoglobulin G
IgM	Immunoglobulin M
IL	Interleukin
IL-1	Interleukin 1
IL-1β	Interleukin 1 beta
IL-1B	Interleukin 1 beta gene
IL-10	Interleukin 10
IL-13	Interleukin 13

IL-2	Interleukin 2
IL-21	Interleukin 21
IL-25	Interleukin 25
IL-33	Interleukin 33
IL-4	Interleukin 4
IL-5	Interleukin 5
IL-6	Interleukin 6
IL-8	Interleukin 8
IL-9	Interleukin 9
ILC2	Innate lymphoid cells type 2
IMDM	Iscove's Modified Dulbecco's
IP3	Inositol triphosphate
ITAM	Immunoreceptor tyrosine-based activation motif
ITIM	Immunoreceptor tyrosine-based inhibitory motif
KARS	Lysyl-tRNA synthetase 1
LAD2	Laboratory of allergic diseases 2, human leukemia cells
LAD2-A	LAD2 sensitized with sera from anaphylactic patients
LAD2-S	LAD2 sensitized with sera from sensitized patients
LAT	Linker for activation of T cells
LB	Lysogeny broth
lncRNA	Long non-coding RNA
LTB4	Leukotriene B4
LTC4	Leukotriene C4
LTP	Lipid Transfer Protein
LysRS	Lysyl-tRNAsynthetase 1
MAdCAM-1	Mucosal addressin cell adhesion molecule 1
MAPK	Mitogen-activated protein kinase
MAT	Mast cell activation test
MC_C	MC containing chymase
MCPs	Mast cell progenitors
MCs	Mast cells
MCs-A	MCs sensitized with sera from anaphylactic patients
MCs-S	MCs sensitized with sera from sensitized patients
MC_T	MC containing tryptase

MC_{TC}	MC containing tryptase and chymase
MHC	Major histocompatibility complex
MHC-I	Major histocompatibility complex class I
MHC-II	Major histocompatibility complex class II
miRNA	Micro-RNA
MITF	Microphthalmia-associated transcription factor
MMCs	Mucosal mast cells
MPPs	Multipotent progenitors
MRGPRX2	Mas-related G protein-coupled receptor X2
MT-ND6	Mitochondrially encoded NADH:ubiquinone oxidoreductase core subunit 6
mTOR	Mammalian target of rapamycin
NAD^+	Nicotinamide adenine dinucleotide
NADH	Nicotinamide adenine dinucleotide with hydrogen
NC	Negative control
NF-kB	Nuclear Factor kappa-light-chain-enhancer of activated B cells
NFAT	Nuclear Factor of Activated T cells
NFKBIL1	NF-kB inhibitor-like 1 gene
NK	Natural Killer cells
NLRP3	NOD-, LRR- and pyrin domain-containing protein 3
NMBAs	Neuromuscular blocking agents
NSAIDs	Nonsteroidal anti-inflammatory drugs
NUDT2	Nudix hydrolase 2
O/N	Overnight
OCR	Oxygen consumption rate
OFC	Oral food challenge
OIT	Oral food tolerance induction
Opti-MEM	Reduced serum medium
ORAI2	ORAI calcium release-activated calcium modulator 2
OXPHOS	Oxidative phosphorylation
PAMPs	Pathogen associated-molecular pattern molecules
PBMCs	Peripheral blood mononuclear cells
PBS	Phosphate buffered saline

PDH	Pyruvate dehydrogenase
PEG	Polyethylene glycol
PEI	Polyethylenimine
PER	Proton Efflux Rate
PGD_2	Prostaglandin D2
PGE_2	Prostaglandin E2
PI3K	Phosphatidyl inositol 3-OH kinase
PI3KCB	Phosphatidylinositol-4,5-Bisphosphate 3-Kinase Catalytic Subunit Beta
PIP3	Phosphatidylinositol (3,4,5)-trisphosphate
PKC	Protein kinase C
PKCα	Protein kinase C alpha
PLA2	Phospholipase A2
pLAT	Phospho-LAT
PLCγ	Phospholipase C gamma
PRRs	Pattern recognition receptors
PTGER2	Prostaglandin E receptor 2
PTGER3	Prostaglandin E receptor 3
PTGER4	Prostaglandin E receptor 4
pTyr	Phospho-Tyrosine
RANTES	Regulated upon Activation, Normal T Cell Expressed and Secreted
RBL-2H3	Rat basophilic leukemia cells
RNA	Ribonucleic acid
ROS	Oxygen reactive species
rpm	Revolutions per minute
RT	Room Temperature
RT-qPCR	Reverse transcription quantitative polymerase chain reaction
S	Sensitized group
SCF	Stem-cell factor
Ser	Serine
shRNA	Short hairpin-RNA
sIgE	Allergen specific IgE

sIgG4	specific IgG4
SLIT	Sublingual immunotherapy
SM	Systemic mastocytosis
SNP	Single Nucleotide Polymorphism
SOC	Super optimal broth with catabolite repression medium
SOCE	Store-Operated Calcium Entry
SP	Substance P
SPTs	Skin prick tests
STIM1	Stromal Interaction Molecule 1
STV	Streptavidin
SYK	Spleen tyrosine kinase
TAD	Transactivation domain
TCA	Tricarboxylic acid
TEM	Transmission electron microscope
TFH	T follicular helper cells
T_{FH}13	T follicular helper 13 cells
Tfr	T follicular regulatory
TGF-β	Transforming growth factor beta
TGFB1	TGF-β gene
T_H1	T helper 1 cells
T_H17	T helper 17 cells
T_H2	T helper 2 cells
Thr	Threonine
tIgE	Total IgE
TLRs	Toll-like receptors
TNFα	Tumor necrosis factor alpha
TOM	Translocase outer membrane complex
TOMM20	Translocase of outer mitochondrial membrane 20
TPSAB1	Tryptase Alpha/Beta 1
Treg	Regulatory T cells
tRNA	Transfer-RNA
TRPM1	Transient receptor potential cation channel subfamily M member 1
TSLP	Thymic Stromal Lymphopoietin

TTBS	1X Tris-buffered saline with 0.1% Tween 20
VCAM-1	Vascular cell adhesion molecule 1
VEGF	Vascular endothelial growth factor
VIP	Vasoactive intestinal peptide
WB	Western Blot
WHO	World Health Organization
WST-1	Water-Soluble Tetrazolium Dye
WT	Wild-type

INTRODUCTION

1. MAST CELLS

Mast cells (MCs) are immune system cells involved in host defense and pathology. In physiological conditions, MCs are crucial in innate and adaptative immune responses against pathogens. Their strategic location at mucosal surfaces and skin allows them to act at the early stages of the infection and promote the recruitment of effector cells to sites of infection (25). Although MCs have a beneficial role in host defense, they are better known for contributing to several pathologies, such as atopic disorders and anaphylaxis.

1.1. Mast cell biogenesis

Mast cells originate in the bone marrow from hematopoietic stem cells (HSCs). However, recent studies have proposed that MCs may also arise from yolk sac-derived erythro-myeloid progenitors (EMPs) (26,27). HSCs develop into multipotent progenitors (MPPs) that differentiate into common myeloid progenitors (CMPs) (28). These myeloid progenitors develop into granulocyte/monocyte progenitors (GMPs) that mature into different cells: monocytes, neutrophils, eosinophils, basophils, and mast cells (29). GMPs, at some point, can differentiate between basophil or mast cells (bipotent basophil/mast cell progenitors, BMCPs) (30). The expression of transcription factors tightly regulates this process. Upregulation of microphthalmia-associated transcription factor (MITF) and downregulation of CCAAT/enhancer binding protein alpha (C/EBPα) expression is thought to drive mast cell differentiation. At the same time, the inverse induces differentiation to basophils (31). Mast cell differentiation depends on stem cell factor (SCF). For mast cell progenitor cells (MCPs) expressing $CD34^+$ and KIT (or $CD117^+$) receptors, SCF is required for tissue mast cell maturation (32).

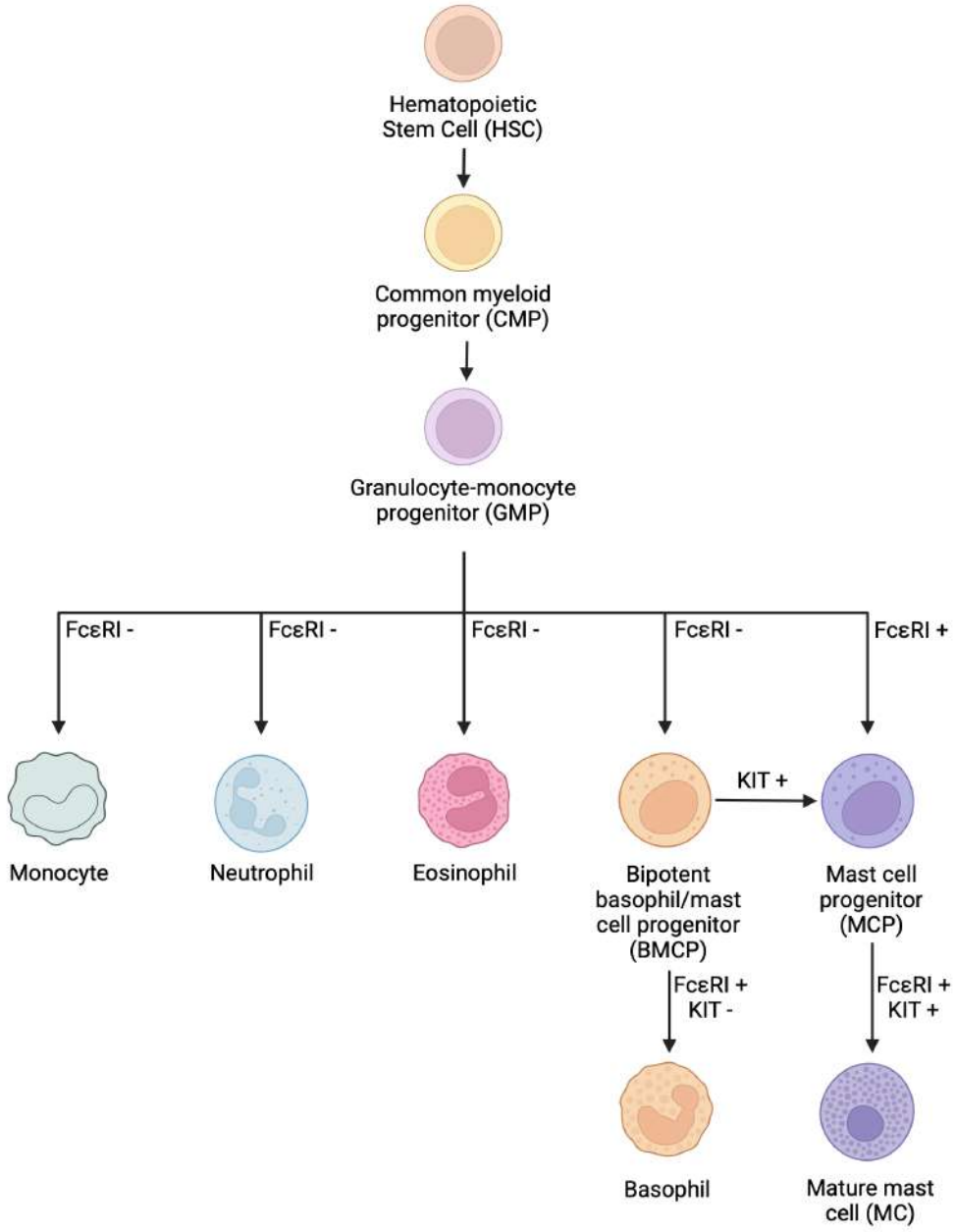

Figure 1. Mast cell differentiation scheme. MCs originate in the bone marrow from HSCs. HSCs derivates in CMPs that differentiate to GMPs. These GMPs could derivate into different cells, including BMCPs and MCPs. Both differentiate into mature MCs in tissues through different stimuli.

MC progenitors migrate to target tissues, mainly by the stimuli of inflammation, where they complete their differentiation and maturation through local growth factors, cytokines, and chemokines. MC localization in the intestinal mucosa is controlled by the adhesive interaction of β7 and α4β7 integrins with its ligands vascular cell adhesion molecule 1 (VCAM-1) and mucosal addressin cell adhesion molecule 1 (MAdCAM-1). This process also needs the expression of CXCR2 (CXC-motif chemokine receptor 2) in mast cell progenitors (28,33). MC homing into the lung is regulated by the interaction of α4β1 and α4β7 with VCAM-1, and this process is controlled by $CD4^+$ and CD11c cells (34). MCP recruitment into the skin is mediated by leukotriene B4 (LTB4), prostaglandin E2 (PGE_2), and the chemokine C-C motif ligand 2 (CCL2) (33).

After maturation, mast cells can be differentiated into various MC subtypes. MC heterogeneity has been described by histochemical analysis. It is mainly divided into two categories in rodents: mucosal mast cells (MMCs), which were primarily present in the mucosa of the gut and lungs, or connective tissue-type MCs (CTMCs), found in the skin and peritoneal cavity (35). In humans, MCs are classified based on their protease composition: MC containing only tryptase (MC_T), MC containing only chymase (MC_C), and MC containing both tryptase and chymase (MC_{TC}). However, the MC distribution in humans is not as well differentiated as in rodents, and most human tissues have a mixed population of MC types (36). Recent transcriptomic analysis revealed that the MC phenotype is dynamic and is distinct in different tissues and physiological conditions (considering degranulation and regranulation afterward) in the same individual (27).

1.2. Mast cell functions

MCs are essential in innate and adaptative immune responses and contribute to tissue remodeling and homeostasis (3). Due to their localization in body barriers, mast cells participate in the early recognition of pathogens (37,38). In physiological conditions, mast cells have a central role in host defense against bacteria and parasites by releasing cytokines and other mediators that recruit other cells to the site of infection (39).

Mast cells recognize harmful antigens by binding directly to a pathogen or associating with pathogen-associated-molecular pattern molecules (PAMPs) through pattern recognition receptors (PRRs) (40). MCs have a broad spectrum of cell surface receptors, such as toll-like receptors (TLRs), immunoglobulin Fc receptors (FcRs), complement receptors, CD48, Mas-related G protein-coupled receptor X2 (MRGPRX2), cytokine and chemokine receptors, which enables them to respond to endogenous and exogenous stimuli (2,41).

Within seconds of stimulation by the antigen, MCs can degranulate, rapidly release pre-formed mediators in the cytoplasmic granules, and activate the synthesis of *de novo* mediators (42). MC activation increases vascular permeability and edema at the site of infection through the release of tumor necrosis factor-alpha (TNFα), some proteases, and vascular endothelial growth factor (VEGF) (43). Cytokine and chemokine production of MCs, including TNFα, interleukins (IL) such as IL-1, IL-4, IL-6, IL-8, IL-13; chemokine C-C motif ligand (CCL) such as CCL11, CCL2 or CXC-motif chemokine ligand (CXCL) such as CXCL8, induce the recruitment of other immune cells to the site of inflammation, such as natural killer (NK) cells (44), eosinophils, and neutrophils (43).

MCs are also involved in adaptative immunity. It is known that MCs can recruit and cooperate with other immune cells, such as dendritic cells (DCs) or T effector cells, through their mediators' release or cell-cell interactions (45–47). The release of TNFα and CCL20 increases the recruitment of dendritic cells (DCs), and CXCL10 and CCL5 enhance the recruitment of T cells (48). Furthermore, MCs can participate as antigen-presenting cells for T cells via major histocompatibility complex (MHC) molecules (49). Additionally, MCs can activate B cells by interacting with CD40-CD40L receptors in B cells and MCs, respectively (50). This receptor interaction is also described in MCs with astrocytes in the central nervous system (51). Finally, MCs can interact with T regulatory cells (Tregs) via the OX40-OX40L axis, inducing the inhibition of MC degranulation (52,53).

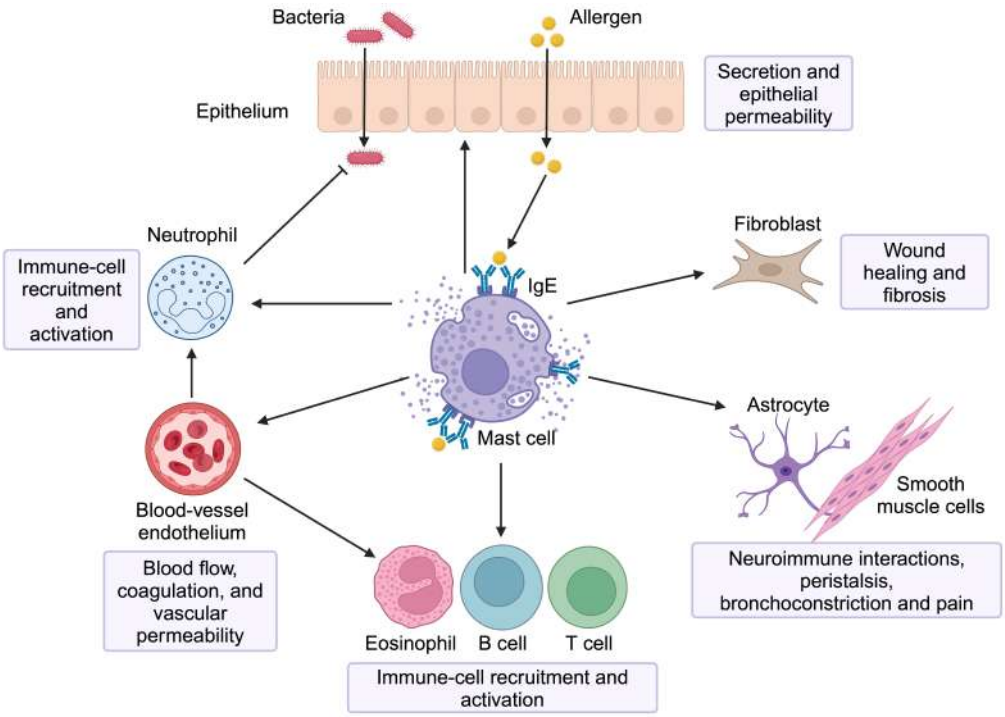

Figure 2. Mast cell functions scheme. Mast cells play a key role in innate and adaptive immunity and contribute to tissue homeostasis and remodeling. Located at body barriers, they detect pathogens early and, under normal conditions, help defend the host against bacteria and parasites by releasing cytokines and other mediators that recruit cells to the site of infection.

1.3. Mast cell mediators

When MCs are activated, a wide range of preformed and *de novo* synthesized mediators such as histamine, proteases, leukotrienes, prostaglandins, chemokines, cytokines, and growth factors are released, resulting in allergic reactions such as anaphylaxis, asthma, angioedema, urticaria, nausea, and fever (54,55).

1.3.1. Preformed mediators

Upon MC activation, degranulation occurs immediately and is completed within 5-10 minutes (56). Although mast cell proteases, such as tryptase,

chymase, and carboxypeptidase, constitute the significant components of mast cell granules, (57–59) histamine is the predominant granule mediator of acute reactions to mast cell activation (60).

Histamine acts through four G protein-coupled histamine receptors (61): H1 receptors reside mainly on bronchial smooth muscle, endothelial cells, and specific neurons and are primarily responsible for bronchoconstriction and increased vascular permeability; H2 receptors are located on vascular smooth muscle and gastric parietal cells and thus mediate vascular dilatation and gastric secretion; H3 receptors are present mainly in the central neuron system whereas H4 receptors are expressed on immune cells including basophils, mast cells, and eosinophils and mediate chemotaxis (62,63). Thus, the main effects of histamine are increased vascular permeability, vasodilatation, and bronchial constriction, which are readily reversed by antihistamines (histamine receptor antagonists) (60).

Lipid mediators, such as leukotriene C4 (LTC4), prostaglandin D2 (PGD_2), and prostaglandin E2 (PGE_2), are generated and released almost simultaneously with the preformed mediators. The generation of these molecules starts with the activation of phospholipase A2 (PLA2), yielding free arachidonic acid (64). This is metabolized through 5-lipoxygenase (5-LO) and cyclooxygenase 2 (COX2) to generate leukotrienes and prostaglandins. Lipid mediators contribute to bronchoconstriction, increased vascular permeability, mucus production, and inflammatory cell recruitment (65).

Proteases are stored in mast cell granules in active form, protected by proteoglycans, allowing their rapid release upon mast cell activation (66). Tryptases are the most abundant proteases and help in protein degradation and defense against pathogens (67). Other important proteases are chymases, which regulate inflammation, and cathepsins, which participate in the degradation of intracellular proteins (68). These proteases play key roles in defense against infection, regulation of inflammation, and tissue remodeling (69). However, its excessive release in diseases such as allergies and asthma can cause inflammation and tissue damage (66).

1.3.2. *De novo* mediators

In contrast to degranulation and eicosanoid release, a delayed process (*de novo* mediators' synthesis) takes several hours after mast cell activation. Mast cells generate various cytokines, such as IL-4, IL-6, IL-8, IL-10, IL-13, IL-33, GM-CSF (Granulocyte-macrophage colony-stimulating factor), and TNFα, and chemokines, including CCL2, CCL5, and CXCL8 (42,70–73). Although it has been proposed that MCs may store specific cytokines, such as TNFα, in their granules, this appears to be minimal compared with the levels generated *de novo* following mast cell activation (74). Under specific circumstances, cytokines and chemokines can be generated and released without degranulation. This suggests that cytokines and chemokines have evolved to play different roles in the body's defense mechanisms against parasites, toxins, and other harmful bioactive agents and organisms. Nevertheless, along with granule components, secreted cytokines manifest pathophysiology associated with allergic inflammation (75–77).

Apart from cytokines and chemokines, MCs produce other *de novo* mediators, such as Thymic Stromal Lymphopoietin (TSLP), which is recognized as an essential mediator in inflammatory responses to allergens, pathogens, and trauma by directing the immune system (through its interaction with dendritic cells and basophils (78)) towards T_H2 (T helper 2 cells) responses (79); or angiogenic mediators (angiopoietin-1, FGF (fibroblast growth factor), and VEGF) (80).

1.3.3. Granule generation and exocytosis

Mast cells use different mechanisms to release their inflammatory mediators in response to specific stimuli. Anaphylactic degranulation is the most rapid process and involves the massive fusion of cytoplasmic granules with the plasma membrane following activation of the high-affinity receptor for Immunoglobulin E (IgE), the FcεRI (Fc Epsilon receptor) (81). In contrast, the regulated secretion of cytokines and chemokines involves a slower and more controlled process. These molecules are synthesized *de novo* in the endoplasmic reticulum, modified in the Golgi apparatus, and targeted to

specific exocytosis (82,83). In addition to these mechanisms, mast cells can release mediators through piecemeal degranulation, a process in which small vesicles selectively transport granule contents to the plasma membrane, allowing partial and prolonged secretion without completely depleting cellular reserves (84).

Moreover, some mediators, such as TNFα, can be stored in endosomal compartments and subsequently released by recycling mechanisms, favoring a more sustained inflammatory response. This set of mechanisms allows mast cells to precisely regulate their inflammatory activity, contributing to defensive immune responses and pathological processes such as allergies and chronic inflammation.

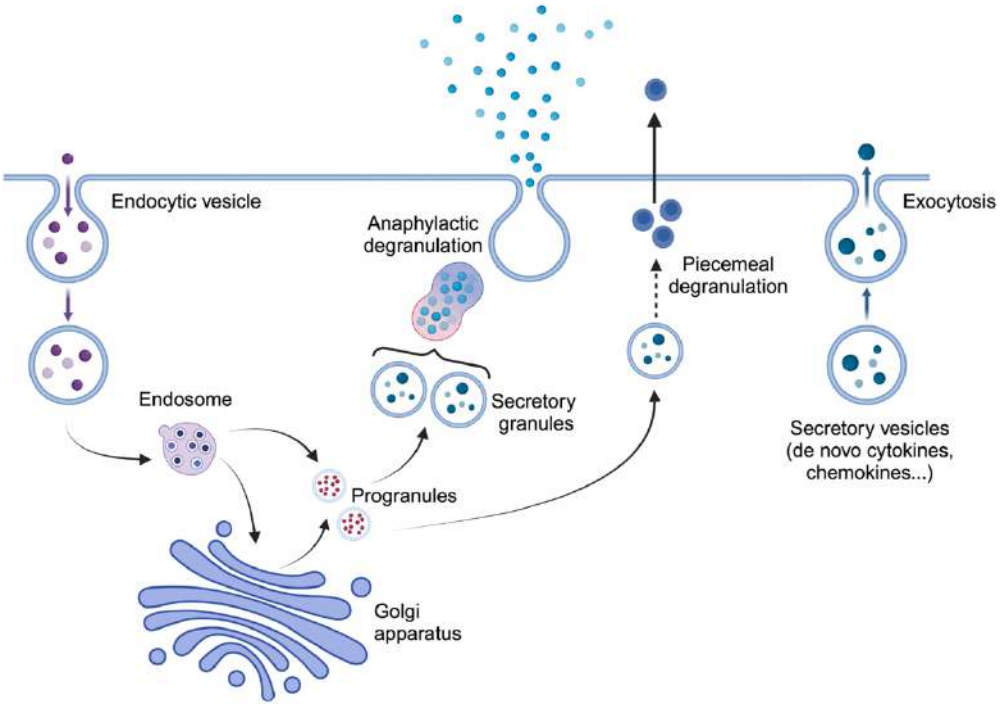

Figure 3. MC granules generation and exocytosis. Upon activation, mast cells immediately release preformed granule contents. Immature progranules from the Golgi apparatus can fuse with endosomes and be secreted by anaphylactic degranulation. *De novo* mediators are packaged in secretory vesicles and released through constitutive exocytosis. Figure adapted from (81,82).

1.4. Mast cell receptors

Mast cells present a wide range of surface and cytoplasmic receptors that make them responsive to a large number of stimuli, the most important ones being KIT (or CD117), the high-affinity receptor for IgE (FcεRI), and MRGPRX2.

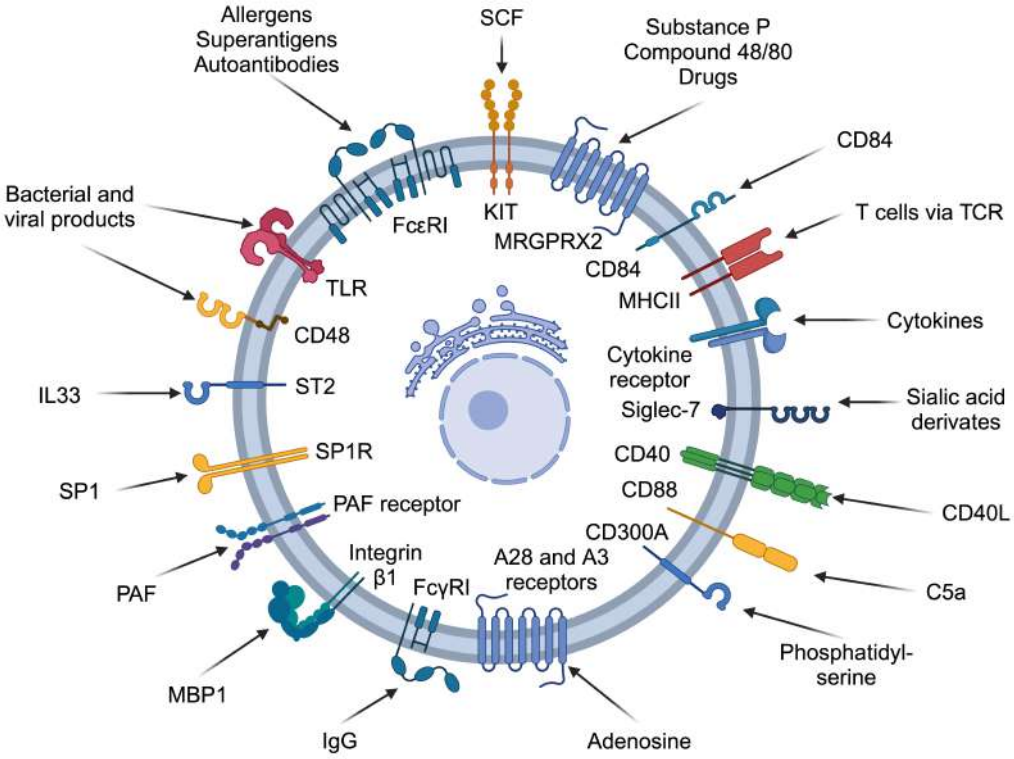

Figure 4. MC receptors. A wide range of receptors can induce mast cell functions, such as degranulation, migration, survival signals, *de novo* mediator production, and secretion.

1.4.1. KIT or CD117

The KIT receptor, CD117, is the primary receptor for mast cell growth, survival, and homing to mast cells into target tissues (85). SCF is the ligand of KIT, and it's produced by different cell types, including fibroblasts and epithelial cells (86).

KIT is a single-chain receptor with protein-tyrosine kinase activity. It comprises an extracellular part comprising five immunoglobulin-like domains (three of them bind to SCF, and the fourth one is important for receptor dimerization) and an intracellular part with a catalytic domain (87).

When SCF binds to KIT, it leads to dimerization and activation of its intrinsic tyrosine residues. SCF activates phospholipase C gamma (PLCγ) and protein kinase C alpha (PKCα) (88). PLCγ has been shown to activate mTOR independent of the conventional PI3K (phosphatidyl inositol 3-OH kinase)/Akt (protein kinase B) pathway using the DAG (diacylglycerol)/PKC (protein kinase C) (26). Moreover, the activation leads to the activation of other signaling molecules, such as LYN, FYN, and PI3K, which activate the MAPK (Mitogen-activated protein kinase) pathways, leading to mast cell growth, differentiation, survival, adhesion, and chemotaxis (86,89). KIT on its own is not enough to cause degranulation but it can enhance degranulation and cytokine production accompanied by FcεRI signals (90,91).

1.4.2. FcεRI

FcεRI is a high-affinity receptor for IgE that plays a central role in allergic reactions. It exists in two forms: a tetrameric form (α, β, and two γ chains) found on mast cells and basophils, and a trimeric form (α and two γ chains) present on antigen-presenting cells (APCs) (92). The α chain binds IgE and ensures proper folding in the endoplasmic reticulum through N-glycosylation. In contrast, the β and γ chains contain ITAM motifs (immunoreceptor tyrosine-based activation motifs) that initiate signaling upon antigen crosslinking of IgE-bound FcεRI (93).

The primary signaling pathway involves LYN phosphorylating ITAMs, which recruit SYK (spleen tyrosine kinase) and amplify the signal. This activation triggers the phosphorylation of LAT (linker for activation of T cells) and subsequent association and phosphorylation of PLCγ-producing inositol triphosphate (IP3) and DAG, leading to calcium mobilization and mast cell degranulation, as well as activating the MAPK/ERK (extracellular signal-

regulated kinases) cascade to promote cytokine production and lipid mediator release (94). A complementary pathway involves FYN phosphorylating GAB2, which activates PI3K to regulate mast cell degranulation and cytokine production. Activated PI3K phosphorylates PIP2 and produces phosphatidylinositol (3,4,5)-trisphosphate (PIP3), enhancing the calcium influx (95).

However, the phosphorylation of two related adaptor proteins, LAT1 and LAT2 (or NTAL), was altered depending on the affinity of IgE (96). These molecules are crucial in organizing signals in mast cells' plasma membrane. As a result, variations in their phosphorylation state correspond to variations in the chemical signals produced. Under high-affinity IgE engagement of FcεRI, the phosphorylation of LAT1 was favored, whereas, under low-affinity IgE binding to FcεRI, stronger phosphorylation of LAT2 (or NTAL) occurred (97). Since LAT1 is essential for mast cell calcium responses and contributes to mast cell degranulation, reducing phosphorylation under low-affinity IgE reduces degranulation (98). LAT2 (or NTAL) appeared to be more critical in driving PI3K activation and downstream signaling in this pathway through Fgr activation, enhancing chemokines production (97).

Once FcεRI signaling is activated, signal transduction cascades are initiated, leading to calcium release from the endoplasmic reticulum (ER), an essential step for mast degranulation. When ER calcium deposits are depleted, the deposit-dependent calcium entry mechanism (SOCE, store-operated calcium entry), which generates a more intense secondary calcium signal, is triggered (94). The sensor that detects the emptying of calcium from the ER has been identified as stromal interacting molecule 1 (STIM1) (99).

FcεRI is critical for IgE-mediated allergic responses and is a key target for understanding and managing allergies and anaphylaxis (100). FcεRI expression is upregulated by IgE levels and IL-4, which promote α-chain production and stabilize the receptor on the cell surface, preventing degradation and leading to accumulation (101,102). Inhibitory mechanisms involve receptors with ITIM (Immunoreceptor tyrosine-based inhibitory motif) motifs that recruit phosphatases like SHP or SHIP to dampen activation (103).

1.4.2.1. STIM1

STIM1 is a dimeric type I transmembrane protein, with the N-terminal located in the limen or ER and the C-terminal soluble in the cytosol (104). Upon MC activation, IP3 binds to its receptor on the ER membrane, causing the release of calcium (105). When calcium concentration in the ER falls, STIM1 oligomerizes and translocates to ER-plasma membrane junction sites to interact with Orai channels, enhancing calcium entry (106–109).

Upon MC activation via FcεRI receptor, NF-κB (Nuclear Factor kappa-light-chain-enhancer of activated B cells) and NFAT (Nuclear Factor of Activated T cells) transcription factors activate, which enhances STIM1 expression. It is reported that STIM1 depletion in mast cells showed less degranulation and cytokine production after IgE-FcεRI cross-linking. Moreover, less blood vessel permeability is reported in STIM1 knockdown mice with FcεRI-mediated passive cutaneous anaphylaxis reactions, suggesting that STIM1 is required for antigen-induced mast-cell mediated passive cutaneous anaphylaxis reactions *in vivo* (110). It is shown that hypoxia-inducible factor 1 alpha (HIF1α) also can directly enhance STIM1 transcription in hypoxia conditions, inducing calcium influx (111). STIM1 and Orai are upregulated in T-cell-mediated immune responses, increasing calcium influx at the region where T cells interact with the APCs. This amplified calcium signaling induces the activation, expansion, and differentiation of T cells (112). It is also shown that in STIM1 deficient mice, the cross-presentation of antigens by DCs is reduced (113). Recently, STIM1 has been studied in cancer diseases, as it seems that it is involved in cancer development, invasion, and metastasis, and it can contribute to resistance against some antitumor therapies (114). However, further investigation of the mechanisms by which STIM1 can regulate tumor cells is needed to consider it as a treatment target in this disease (105). Apart from its role in regulating calcium influx, it has been suggested that STIM1 also regulates cellular metabolism. In cardiomyocytes and T cells, an increase of STIM1 seems to induce a higher uptake of glucose by regulating glucose transporters (115,116). In contrast, a reduction of STIM1 promotes a preference for long-chain fatty acid uptake by regulating its transporters (116).

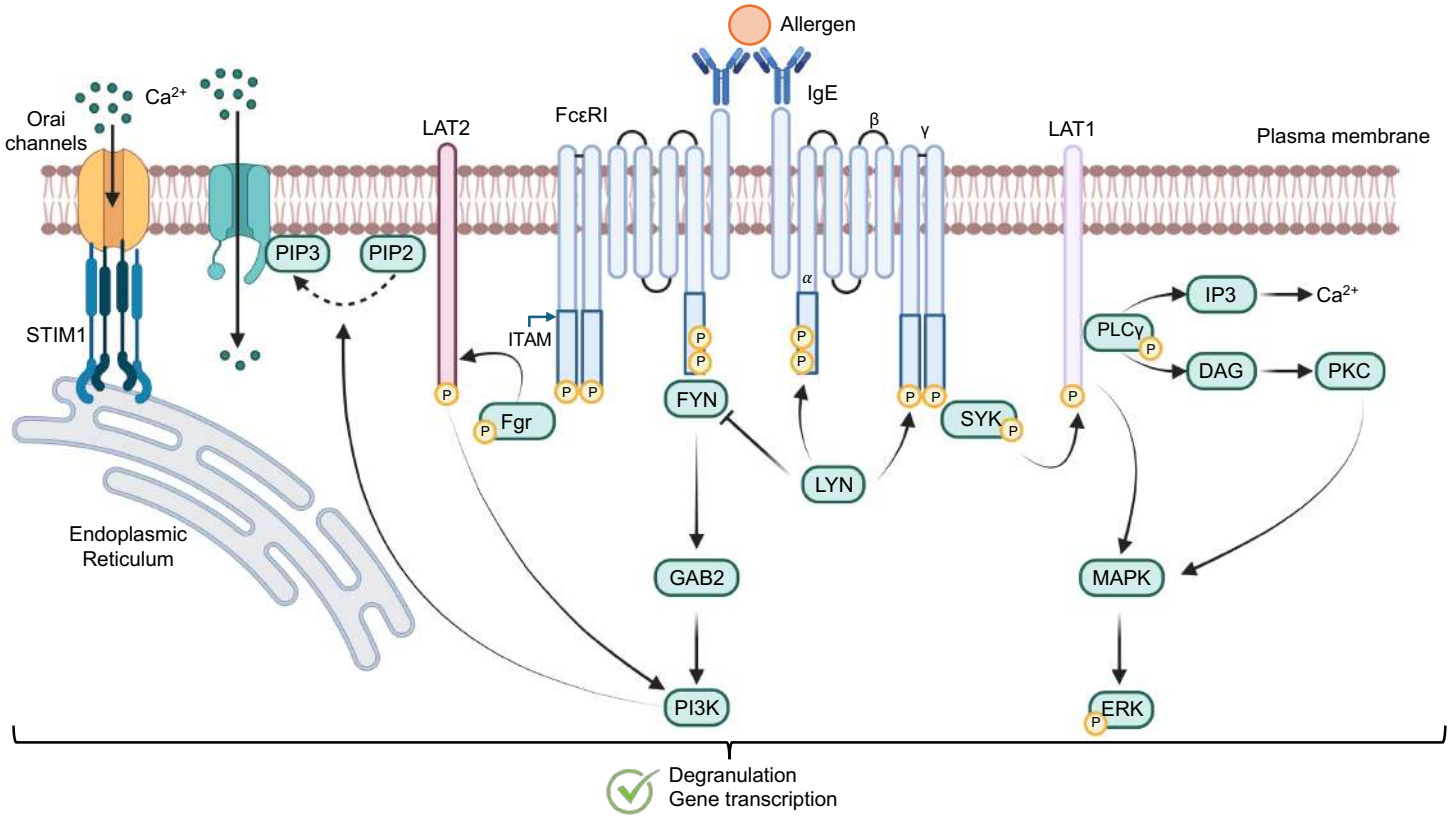

Figure 5. MC activation via FcεRI. FcεRI-IgE crosslinking by antigen leads to an MC signaling cascade. In the case of high-affinity IgE, SYK phosphorylation triggers LAT1 activation, enhancing degranulation and *de novo* cytokine production. In the case of low-affinity IgE, Fgr phosphorylation triggers LAT2 activation, enhancing *de novo* chemokine production.

1.4.3. MRGPRX2

MRGPRX2 is a seven transmembrane G protein-coupled receptor, a Mas-related member expressed almost exclusively by a subset of mast cells that populate connective tissues like the skin (117–119). Its orthologue in mice is the MrgprB2, while the MrgprB3 seems to be the rat orthologue of this receptor (120). Upon activation with some drugs, MRGPRX2 can induce direct MC degranulation and anaphylactic reactions (121). Downstream signaling from MRGPRX2 involves activating the PLCγ and PI3K, which releases preformed and *de novo* synthesized mediators (122,123). As well as in FcεRI signaling, STIM1 is essential in regulating calcium in the MRGPRX2 pathway. Some studies reported that the inhibition of STIM1 can reduce the calcium influx after MC activation through the MRGPRX2 receptor and, consequently, reduce the MC degranulation (102,103).

MRGPRX2-mediated responses seem to be more rapid but transient in comparison to IgE-triggered events (124). The canonical secretagogues activating MRGPRX2 include essential peptides (substance P (SP), Vasoactive intestinal peptide (VIP), cortistatin, neuropeptide Y and compound 48/80), and some drugs (morphine, vancomycin, hydrocodone) capable of producing direct MC degranulation (125–128).

It has been observed that SCF and IL-4 can reduce MRGPRX2 responsiveness both by acutely interfering with the cascade initiated by MRGPRX2 (129) and by restricting expression (130). Moreover, prolonged contact with IL-33 eliminates MRGPRX2 expression, thus suppressing the responsiveness of mast cells to its ligands. In contrast, a brief exposure to IL-33 potentiates the MRGPRX2 allergic pathway (131). This duality in mast cell regulation according to the duration of contact with IL-33 is similar to that observed with the FcεRI receptor: while chronic exposure to IL-33 reduces the responsiveness of human cutaneous mast cells to FcεRI (132), acute exposure potentiates allergic degranulation (133).

Furthermore, we are already aware of several polymorphisms in the MRGPRX2 gene as a result of evolutionary changes (120). Our group

performed an exome analysis with patients who had a drug adverse reaction (126). This analysis shows two MRGPRX2 mutations (Asn16His and Asn62Ser) in two patients and one MRGPRX2 mutation in another patient (Ser313Arg), suggesting that these genetic variants can pose a phenotype predisposing some individuals to immediate drug-induced reactions.

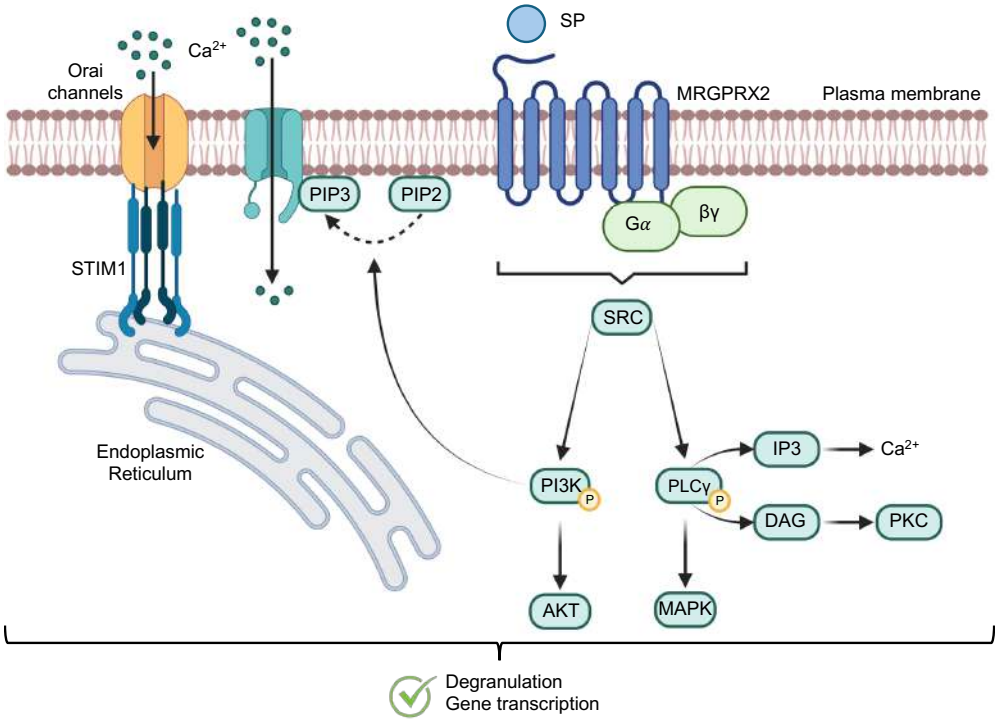

Figure 6. MC activation via MRGPRX2 receptor. Substance P (SP), the natural ligand of the MRGPRX2 receptor, induces the activation of PI3K and PLCγ, promoting degranulation and the activation of gene transcription. Figure adapted from (134,135).

1.5. Microphthalmia-associated transcription factor

MITF is a member of the MiTF/TFE family of basic helix-loop-helix leucine zipper (b-HLH-LZ) transcription factors, which recognizes the E-box (CANNTG) motifs in the promoter region of target genes (136–140). In the N-terminal region, MITF has a transactivation domain (TAD) that facilitates the

activation of gene transcription, and the C-terminal region contains three different areas affluent in threonine, acidic, and serine (141).

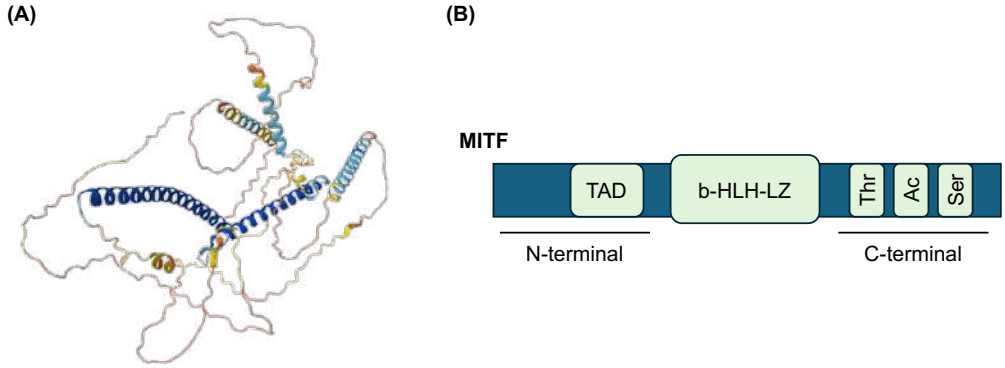

Figure 7. MITF structure. A) MITF 3D predictive structure from Alphafold. B) MITF domain scheme. MITF contains a b-HLH-LZ domain, an N-terminal domain with a transactivation domain (TAD), and a C-terminal region with Threonine (Thr)-, acidic-, and Serine (Ser)-rich domains. Figure adapted from (141).

It is mainly expressed in mast cells, osteoclasts, melanocytes, and retinal pigmented epithelial cells and is involved in their development and function (142–144). MITF was first identified in mice carrying mutations in the *mi* (microphthalmia) locus, which led to the absence of neural crest-derived melanocytes and defects in the retinal pigment epithelium (145). These mutations were also related to hearing loss due to the lack of inner ear melanocytes (146).

The MITF gene has several isoforms: MITF-A, -B, -C, -D, -E, -H, -M, -Mc, and -J, which share common downstream exons from 2 to 9 and differ in their exon 1 (147). MITF-A is the most widely expressed isoform in the mucosal MC (24) and in both $CD34^{+}$-derived mast cells and HMC-1 (human MC line harboring KIT mutations in G560V and D860V) (148).

1.5.1. Regulation of MITF

MITF dysregulation leads to several pathologies. MITF has been extensively studied in melanoma, where it functions as an oncogene (144). It is also highly

expressed in mastocytosis (149). In addition, our group found that MITF is essential for gastrointestinal stromal tumor (GIST) proliferation and survival (150).

Different factors regulate the expression of MITF. It has been described that the activation of MAPK induces the mTOR (mammalian target of rapamycin) inhibition and, consequently, the translocation of MITF to the nucleus in melanocytes (151). Moreover, an elevated PI3K induces MITF activity in melanocytes and B cells (152,153). Also, it is established in melanogenesis that some miRNAs (micro-ribonucleic acid), such as miRNA-137, miRNA-148, and miRNA-182, contribute to the post-transcriptional inhibition of MITF (154–156). Moreover, some MITF interactions with several cofactors that regulate its transcription have been studied. P300/CBP or β-Catenin enhances MITF activity (157). In addition, the SWI/SNF chromatin remodeling or NURF complex controls melanocyte proliferation and differentiation in cooperation with MITF (158). Finally, histidine triad protein 1 (HINT1) is bound to MITF in quiescent conditions, inhibiting its activity (24). Recently, it has been shown that MITF regulates itself. The MITF inhibition or silencing induces the downregulation of MITF (159).

1.5.2. Lysyl-tRNA synthetase – MITF pathway

Aminoacyl transfer-RNA (tRNA) synthetases are critical for translation (160). They catalyze the ligation of amino acids to their matched tRNAs containing the corresponding anticodon to generate aminoacyl tRNAs, which are then transferred to the ribosome for translation (161).

Lysyl-tRNA synthetase (LysRS) is encoded by the KARS gene on chromosome 16 in humans (162). LysRS is a moonlighting protein with both canonical (as an aminoacyl tRNA synthetase) and non-canonical roles (involved in the IgE-dependent MC activation pathway) (163). Upon MC activation, LysRS is phosphorylated on Serine 207 via MAPK (164). This phosphorylation induces a conformational change in LysRS, promoting its translocation to the nucleus and the production of adenosine tetraphosphate

(Ap4A). Then, Ap4A binds to HINT1, leaving MITF free to induce gene transcription (165).

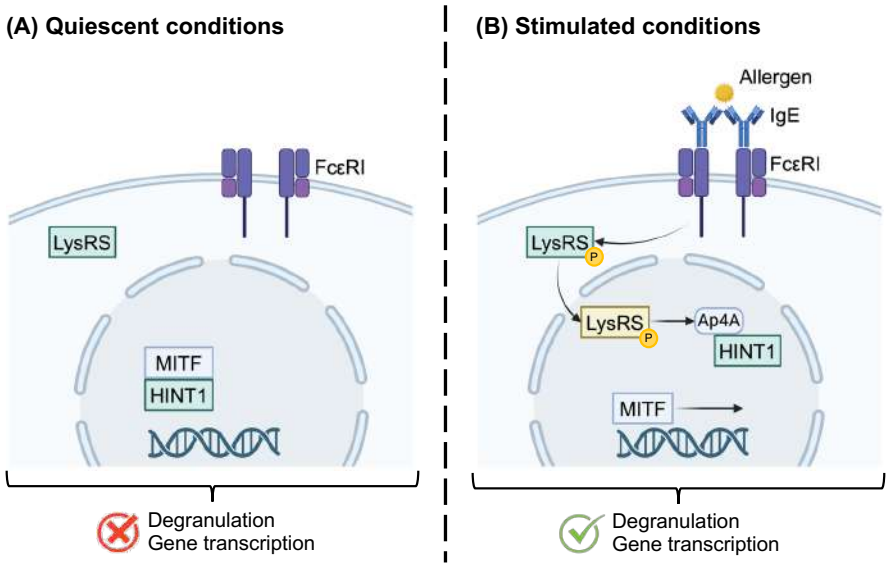

Figure 8. LysRS-MITF pathway. In quiescent conditions, HINT1 represses MITF, but LysRS is phosphorylated and translocated to the nucleus upon activation. This translocation leads to Ap4A production, which binds to HINT1, leaving MITF free for its functions.

1.5.3. MITF is involved in MC biogenesis and function

As mentioned, GMPs can eventually differentiate between basophil and mast cells (BMCPs) (30). At this point, the expression of MITF or C/EBPα is critical. It has been shown that upregulation of MITF induces MC differentiation; instead, upregulation of C/EBPα is critical for basophil differentiation (166). In addition, a relation between MITF and KIT is described. MITF-A would regulate the expression of KIT (166), and conversely, KIT can regulate the expression of MITF at post-transcriptional levels via miRNA-539 and miRNA-381 (167). It is also known that MITF is essential in MCs' differentiation and function due to its downstream of the KIT, MRGPRX2, and FcεRI pathways (168–170).

Furthermore, it has been shown that MITF regulates the expression of some critical genes for the survival of melanocytes and melanoma cells, such as BCL2 (B-cell lymphoma 2), an apoptotic regulator protein, and CDK2 (Cyclin-dependent kinase 2), a cell cycle regulator (24,144,171).

Different transcription factors, such as the MITF and GATA2, regulate MC functionality. It has been shown that the MITF-GATA2 axis is critical for IgE-mast cell-mediated anaphylaxis (172). This study suggests that GATA2 induces a higher expression of MITF and favors the binding of MITF into the *histidine decarboxylase (HDC)* promoter, enhancing the histamine release. It has been described that MITF also regulates some of the key genes, including granzyme B, several proteins (protein kinase C), or proteases such as cathepsin-G (173).

Regarding MC preformed mediators, an interaction between MITF and STIM1 has recently been described. It seems that MITF can regulate STIM1, which, as mentioned before, is a sensor that detects the emptying of calcium from the ER and interacts with the corresponding Orai calcium channel on the cell membrane to allow calcium influx, inducing MC degranulation (99). Regarding *de novo* MC mediators release, it is described that MITF-knockdown in melanoma cells increases the CCL2 secretion (174–177).

Moreover, it has been described that pyruvate dehydrogenase (PDH), essential for the MC metabolism and, consequently, for MC degranulation, interacts with MITF. MC activation via an IgE-dependent pathway induces dephosphorylation of PDH and phosphorylation of MITF, causing the dissociation of PDH-MITF to play their role in mitochondria (178,179). Furthermore, Hua *et al.* (180) show that MITF-overexpression can induce an increase in the expression levels of genes correlated with mitochondrial anti-oxidant functions, mtDNA correlated to mitochondrial biogenesis, and COX-IV correlated with ATP (adenosine triphosphate) production, improving the mitochondrial function. In contrast, it has been shown that MITF can enhance ROS (oxygen reactive species) production in mast cells due to its upregulation of genes involved in ROS generation. Thus, it seems that MITF has a dual

role in ROS production depending on the cellular context and the specific signaling pathways activated (181).

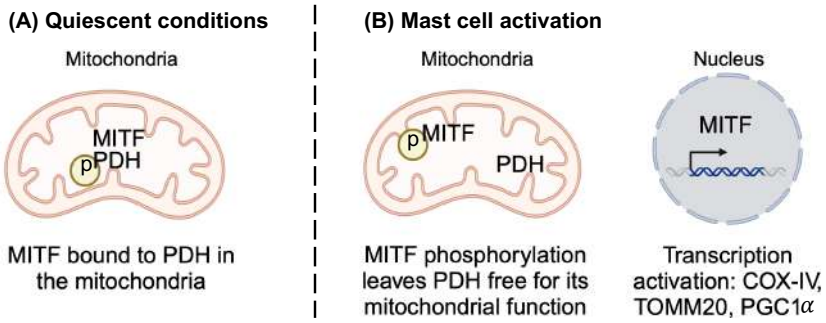

Figure 9. MITF involvement in mitochondrial activity. A) MITF is bound to PDH in the mitochondria in quiescent conditions. B) Upon MC activation, MITF phosphorylation and PDH dephosphorylation leave MITF free for its mitochondrial function. In addition, MITF is activated in the nucleus.

Thus, MITF, as described in the literature, is involved in numerous immunological events.

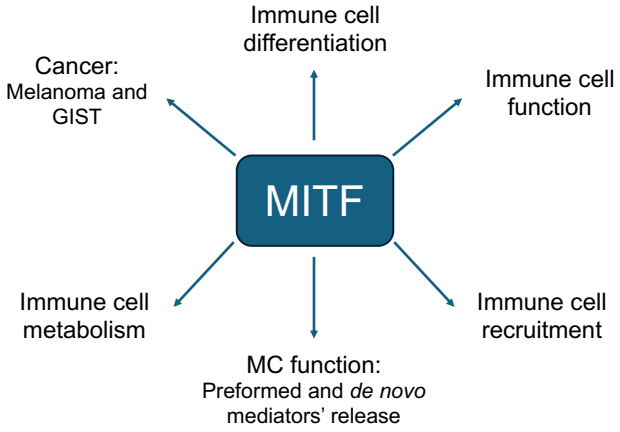

Figure 10. MITF involvement scheme. MITF has been linked to numerous immunological events in immune-related diseases, including cancer and the differentiation, function, metabolism, and recruitment of immune cells (such as T cells, B cells, NK cells, melanocytes, osteoclasts, and mast cells).

1.6. Mast cell metabolism

Cell metabolic processes, including generating energy or creating complex molecules that will eventually be broken down to produce energy, are included in cellular metabolism (182). Catabolism is the process by which molecules are broken down to oxidize and generate energy. This includes traditional metabolic processes like fatty acid oxidation, glycolysis, and mitochondrial respiration. On the other hand, anabolic activities use energy to accumulate complex molecules for later use. The pentose phosphate pathway and gluconeogenesis are two instances of anabolic metabolism. Most studies on mast cell metabolism concentrate on the function of the primary catabolic mechanisms that provide energy, such as mitochondrial respiration and glycolysis (183).

Glycolysis is a metabolic process in which glucose is broken down into two pyruvate molecules, generating energy as ATP and NADH (nicotinamide adenine dinucleotide with hydrogen). It is produced in the cytoplasm and does not require oxygen; it can be aerobic or anaerobic (182). In aerobic conditions, pyruvate is broken down into acetyl-CoA by pyruvate dehydrogenase to enter the Krebs or tricarboxylic acid (TCA) cycle, which occurs in the mitochondria. In the Krebs cycle or TCA, the acetyl-CoA molecule is degraded, forming chemical energy as ATP, NADH, and $FADH_2$ (flavin adenine dinucleotide with hydrogen) (184). The generated NADH and $FADH_2$ transport electrons to the mitochondrial electron transport chain (ETC), enhancing the ATP synthesis through ATP synthetase. The ETC and ATP synthetase processes are termed oxidative phosphorylation (OXPHOS) (185). In anaerobic conditions, pyruvate is converted to lactate, generating NAD^+ (nicotinamide adenine dinucleotide), which is used again in glycolysis to generate energy. This process is called lactic fermentation (182). Usually, this metabolic shift toward lactate production is controlled by HIF1α (186). Lactate cannot be further metabolized; thus, it is secreted out of the cell, acidifying the extracellular environment. It has been shown that even in aerobic conditions, immune cells can shift into lactic fermentation when there is a high energy demand (187).

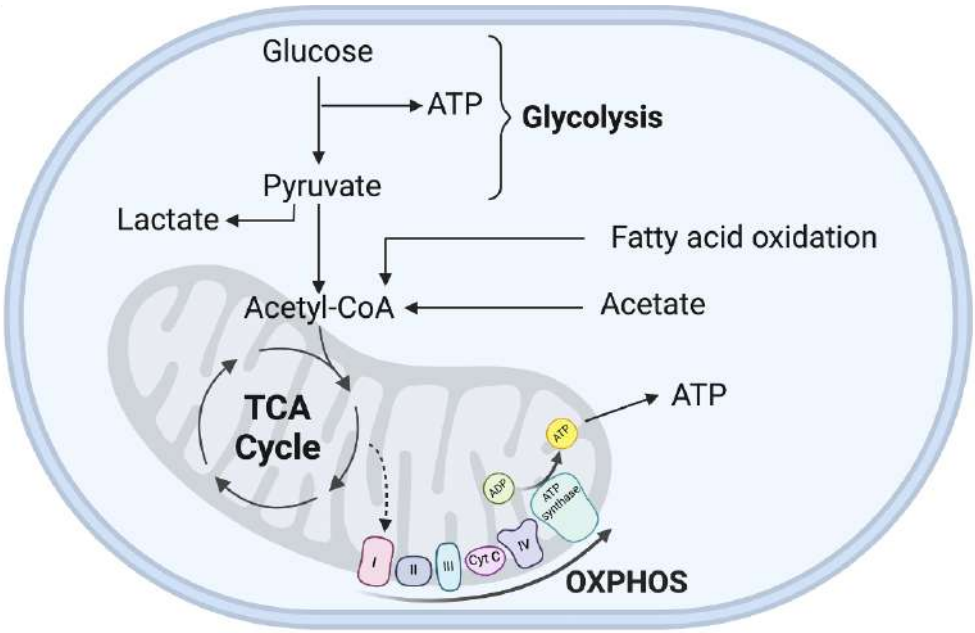

Figure 11. Cell metabolism scheme. Glycolysis and mitochondrial respiration (TCA cycle and OXPHOS) are processed by which molecules are broken down to oxidize and generate energy.

In an allergic reaction, epithelial cells are the first line in contact with the allergens. During allergic inflammation, epithelial cells shift their metabolism towards glycolysis, attended by mitochondrial dysfunction, leading to local inflammation and disrupted barrier integrity (188). This disrupted barrier integrity leads allergens to cross, where dendritic cells or macrophages take it up. It has been reported that those cells display a strongly glycolytic phenotype with a disrupted TCA cycle (189,190). Then, those cells present the antigen to T cells, and glycolysis is essential for T_H2 polarization (191). These type 2 cytokines induce IgE production, enhancing mitochondrial respiration in B cells (192). Upon IgE-FcεRI crosslinking, MC becomes activated, degranulates, and triggers an inflammation cascade.

Mast cell activation increased oxidative phosphorylation (OXPHOS) activity. Inhibition of ATP in mast cells reduces mast cell degranulation and cytokine secretion (193,194). Interestingly, glycolysis is elevated in MC short-term activation (192). Some studies showed that ATP production via glycolysis is significant in IgE-dependent pathways in mast cells. Adding glucose to mast

cell culture increases degranulation, intracellular ROS levels, leukotriene production, and pro-inflammatory cytokines (195,196). Long-term high-glucose culture may make mast cells more sensitive to small amounts of antigen, which could significantly impact the threshold that triggers allergic reactions (195). In human basophils, it has been described that after IgE-mediated activation, there is an extracellular signal controlled by MAPK, inducing an accumulation of HIF1α, which subsequently activates glycolysis (197).

OXPHOS activity depends on dinucleotides (NADH and $FADH_2$) produced by the Krebs cycle, regulated by the pyruvate dehydrogenase. It was observed that PDH inhibition led to reduced anaphylaxis and histamine release in a mouse model (198). It has been shown that mitochondria are involved in cytokine production through cardiolipin, which is found in the inner membrane of the mitochondria and is required for the optimal functioning of the mitochondrial ETC. Cardiolipin can stimulate the generation of pro-inflammatory cytokines by directly binding to the inflammasome NLRP3 (NOD-, LRR-, and pyrin domain-containing protein 3) (199). Indeed, the interaction between mtDNA and TLR9 receptors on neutrophils, monocytes, macrophages, and vascular endothelial cells results in chemotaxis and an increase in the production of pro-inflammatory cytokines (200,201).

Reactive oxygen species generated by mitochondrial electron transport chain activity also play a critical role in mast cell function. Dysregulation of ROS production has been implicated in various allergic conditions, including atopy, dermatitis, and asthma (202,203). ROS can also disturb antigen-dependent mast cell activation by modifying the activities of MAPK and some transcription factors, such as NF-κB and NFAT (204).

Emerging evidence highlights a significant link between mast cell activity and mitochondrial function, suggesting that mitochondria play a crucial role in mast cell-driven pathologies, such as anaphylaxis (203,205,206). Metabolomics has emerged as a promising tool for characterizing metabolic changes during anaphylaxis. In severe reactions, higher levels of glucose, lipids, lipoproteins, and cortisol have been observed, reflecting enhanced immune system

metabolism, increased cell signaling, and mobilization of energy reserves for inflammatory modulation, suggesting a rapid and elevated catabolism response in the first moments of the anaphylactic reaction (207). It has been demonstrated that mast cell sensitization only with IgE without stimulation increases glycolytic capability (183). Furthermore, some studies show increased serum lactate levels and decreased carbohydrates and pyruvate levels in asthmatic and severe allergic patients, suggesting a higher glycolytic activity (208). Although it is known that glycolysis is less efficient than oxidative phosphorylation, it can temporarily achieve energy production rates comparable to those of complete mitochondrial glucose oxidation through the upregulation of glycolytic enzymes induced by HIF1α, which accelerates the rate of glycolysis (208).

Functional mitochondria are necessary for mitochondrial respiration to operate at its best with the least amount of undesirable reactive oxygen species and the highest amount of ATP. Mitochondria can alter their morphology and distribution via fusion, fragmentation, and cytoskeletal movement, adapting to cellular requirements. Mitochondrial translocation to the cell surface near secretory granules is necessary to provide localized energy for exocytosis and maintain optimal calcium levels (209,210). Moreover, upon IgE-dependent stimulation of mast cells, the GTPase DRP1 (dynamin-related protein 1) phosphorylation at Serine 616 via MAPK pathway or dephosphorylation at Serine 637 via Ca^{2+}- activated calcineurin mediates mitochondrial fission, causing degranulation by sustaining local ATP production and calcium balance (211,212). Furthermore, a study with human bronchial epithelial cells and House dust mite allergen reported that mitochondria fragmentation enhances the production of the pro-inflammatory cytokines IL-8 and IL-1β, suggesting a link between pollen allergy and mitochondrial dysfunction (203).

1.7. Mast cell in disease

1.7.1. Hypersensitivity reactions

Coombs and Gell classified hypersensitivity reactions into four types (213,214). Mast cells are critical for the pathogenesis of inflammatory diseases and play a central role in type I hypersensitivity reactions, which are exacerbated immune responses against an allergen (215).

Type I hypersensitivity reactions:

Hypersensitivity reaction type I is an immediate reaction mediated by the immunoglobulin E (216). IgE from mast cells and basophils bind to the allergen, triggering the release of mediators.

There are three main phases during allergic inflammation: sensitization, early-phase, and late-phase reactions (217). First, sensitization to the allergen needs to occur. APCs, mainly dendritic cells, present the allergen to T cells via MHC-II. This presentation induces the polarization of T_H2 cells, causing the production of IgE antibodies by B cells (218). This IgE antibody is bound to the FcεRI on the surface of MCs and basophils, which enhances this sensitization phase (219). When a re-exposure to the sensitized allergen occurs, IgE is bound to the allergen, activating MCs. When mast cells are activated, a wide range of preformed mediators are released immediately, increasing the vascular permeability and inducing vasodilation and bronchoconstriction (81). While a quick and massive release into the bloodstream may result in a severe systemic reaction known as anaphylaxis, symptoms are typically not life-threatening if the mediators are released locally and in a self-limiting manner (220). Apart from these preformed mediators, mast cells produce *de novo* mediators when triggered by an allergen. This process is slower than fast degranulation, and the consequences occur hours after the allergen challenge. In the late-phase reaction, different immune cells are recruited that enhance the severity of the inflammatory response (221).

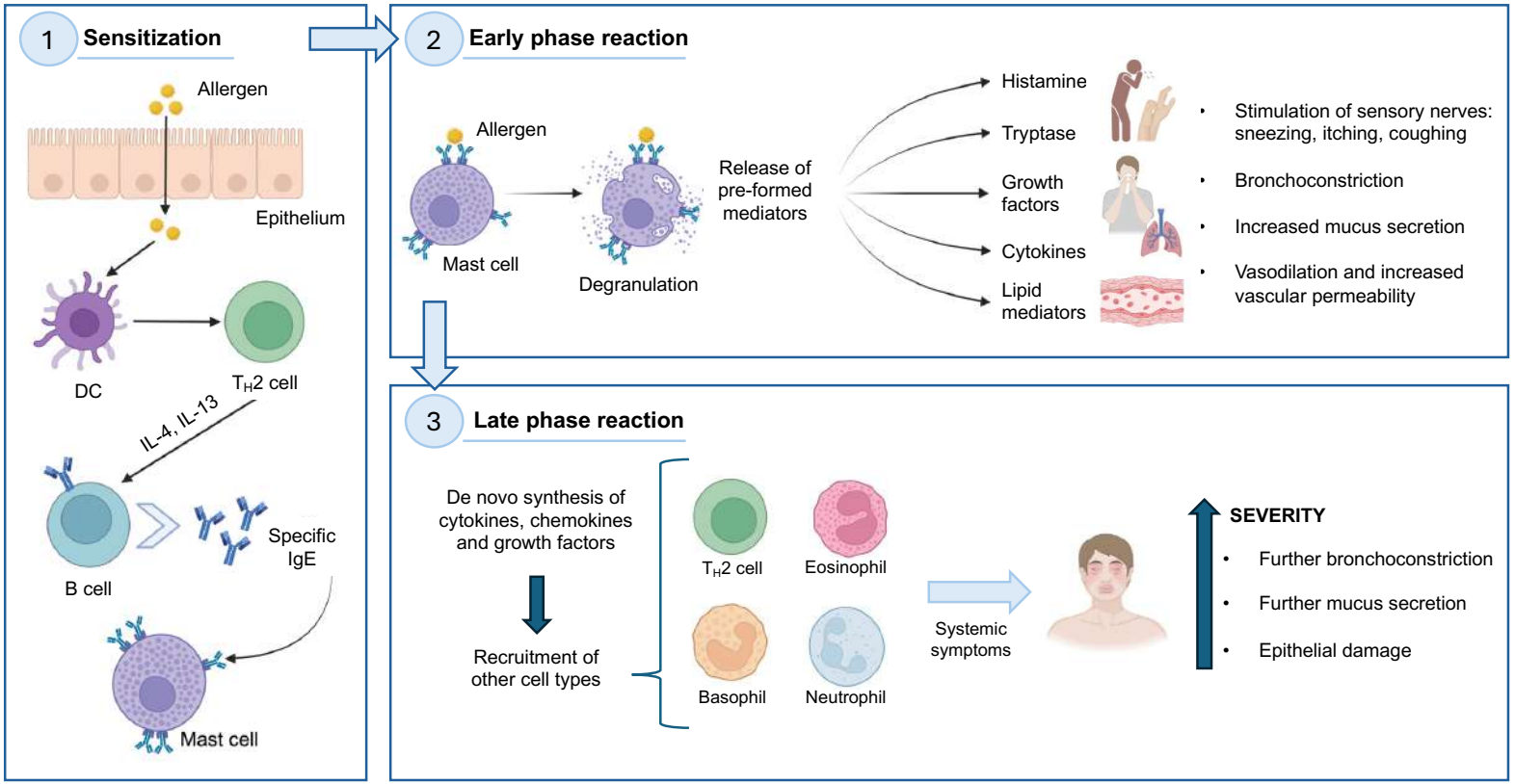

Figure 12. Role of MCs in allergic inflammation. Type 1 hypersensitivity is divided into three phases: 1) Sensitization, where the immune system produces specific IgE against an allergen; 2) early phase, when re-exposure to the allergen causes activation of MCs, leading to the immediate release of mediators such as histamine, causing symptoms such as vasodilatation and increased vascular permeability; and 3) late phase, characterized by the infiltration of immune cells such as eosinophils and neutrophils, which perpetuate inflammation and aggravate symptoms

While classical Type I reactions are IgE-mediated, recent studies have described IgG-mediated anaphylaxis, specifically in response to some drugs (222,223). These reactions entail FcγR interaction on neutrophils, macrophages, and other immune cells such as basophils and mast cells, resulting in the release of mediators such as platelet-activating factor, which is a primary mediator rather than histamine (224). Nevertheless, a higher amount of antigen/drug is required to induce IgG-mediated anaphylaxis, showing the much higher affinity of IgE binding by FcεRI than IgG binding by FcγR (225). However, recent evidence suggests that the simultaneous activation of the IgE and IgG mechanisms may potentially be linked to the most severe food anaphylaxis (226).

Type I hypersensitivity reactions, whether IgE- or IgG-mediated, can be seen in bronchial asthma, allergic rhinitis, allergic dermatitis, food allergy, allergic conjunctivitis, drug-induced allergic reactions and venom allergy (227).

Type II hypersensitivity reactions:

Type II hypersensitivity reactions are mediated by IgG (immunoglobulin G) and IgM (immunoglobulin M), which promote an inflammatory response against cell surface and extracellular matrix proteins (216). The immunoglobulins in this type of reaction induce the activation of the complement system or phagocytosis. Type II hypersensitivity reactions can be seen in immune thrombocytopenia, autoimmune hemolytic anemia, and autoimmune neutropenia (227).

Type III hypersensitivity reactions:

Type III hypersensitivity reactions are mediated by forming antigen-antibody aggregates called "immune complexes.” These immune complexes can precipitate in various tissues and trigger the classical complement pathway. Complement activation leads to the recruitment of inflammatory cells (monocytes and neutrophils) that release lysosomal enzymes and free radicals at the site of immune complexes, causing tissue damage. The most common diseases involving a type III hypersensitivity reaction are serum

sickness, post-streptococcal glomerulonephritis, systemic lupus erythematosus, farmers' lungs (hypersensitivity pneumonitis), and rheumatoid arthritis (227).

Type IV hypersensitivity reactions:

Type IV hypersensitivity reactions are mediated by T cells that induce an inflammatory response against exogenous or endogenous antigens (216). After antigen exposure, there's a local inflammatory response that recruits leukocytes. The antigen is presented to T cells by the macrophages, dendritic cells and monocytes. Activated T cells release cytokines and chemokines, which can cause tissue damage and may result in illnesses. Examples of diseases resulting from type IV hypersensitivity reactions include contact dermatitis and drug hypersensitivity (227).

In recent years, hypersensitivity reactions have been reclassified based on immunological endotypes, reflecting a deeper understanding of the underlying molecular mechanisms. This updated classification introduces a new framework for categorizing hypersensitivity reactions and includes **types V-VI** hypersensitivity reactions which involve epithelial barrier defects and metabolic-induced immune dysregulation, while **type VII** covers direct cellular and inflammatory responses to chemicals (221).

1.7.2. Mastocytosis

Mastocytosis includes a heterogeneous group of disorders characterized by expanding and accumulating neoplastic mast cells in one or more organ systems (228). According to the World Health Organization, mastocytosis is classified into cutaneous mastocytosis (CM), limited to the skin and usually diagnosed in childhood with a good prognosis, and systemic mastocytosis (SM), which affects different organs and is generally diagnosed in adults.

WHO classification divided mastocytosis into several subtypes: cutaneous mastocytosis, systemic mastocytosis and mast cell sarcoma (229).

The diagnosis of systemic mastocytosis is based on the identification of mast cell infiltrates in extracutaneous organs, accompanied by other criteria such as abnormal mast cell morphology, expression of CD2 and CD25 markers, the presence of the KIT D816V (substitution of valine for aspartic acid in codon 816) mutation and elevated blood tryptase levels (230). In the case of cutaneous mastocytosis, the diagnosis is made by skin biopsy, where it has been observed that a count of more than 250 mast cells per square millimeter is highly suggestive of the disease (231).

Advances in treatment have led to the development of therapies targeting the mutations responsible for the proliferation of neoplastic mast cells. These include midostaurin, a tyrosine kinase inhibitor effective against the KIT D816V mutation (232,233), and cladribine, which has shown positive effects in advanced cases (234,235). Other strategies include immunotherapy with monoclonal antibodies directed against specific mast cell markers (236) and bone marrow transplantation in the most aggressive or resistant cases (237).

1.7.3. Asthma

Asthma is a chronic inflammatory disease of the airways, characterized by intermittent chest symptoms, variable airflow obstruction, and bronchial hyperresponsiveness (238). Various cells and inflammatory mediators are involved in its development, and genetic factors partially influence its occurrence (239). Currently, approximately 300 million people worldwide are affected by asthma. It is more common in males during childhood, but its incidence becomes equal in both sexes during puberty. In adulthood, however, it is more prevalent in women. Each year, this disease causes approximately 180.000 deaths (240).

The immune response in allergic asthma begins when an allergen activates dendritic cells in the airway epithelium or when bacterial, viral, or environmental triggers activate epithelial cells (241). This releases cytokines such as TSLP, IL-25, and IL-33, directly activating dendritic cells (242,243) and innate lymphoid cells type 2 (ILC2). ILC2 secrete IL-5, IL-9 and IL-13, which contribute to the recruitment and activation of eosinophils, mast cells

and basophils, as well as the severity of the allergic reaction (244–246). Dendritic cells, in turn, release chemokines like CCL2 and CCL20, which recruit basophils and increase the presence of mast cells in the area (247). The activated dendritic cells then migrate to secondary lymphoid organs, using major histocompatibility complex class II and OX40L to trigger the transcription of GATA3 in naive T cells, promoting their differentiation into T_H2 cells (248). These T_H2 cells secrete IL-4 and IL-13, which induce class switching from IgG to IgE in B cells and stimulate the differentiation of IgE-producing plasma cells specific to the allergen (249). The IgE binds to FcεRI receptors on mast cells and basophils, facilitating their activation and degranulation, which releases preformed mediators like histamine and tryptase, as well as the *de novo* production of prostaglandins, leukotrienes, and other T_H2 cytokines. IL-9 secreted by T_H2 cells further contributes to activating mast cells and basophils (250). Additionally, IL-4 promotes the expression of ICAM-1 (Intercellular adhesion molecule 1) and VCAM-1 on blood vessels, facilitating the adhesion and recruitment of eosinophils, which are attracted by chemokines such as IL-5, eotaxin-1, eotaxin-2, and RANTES (Regulated upon Activation, Normal T Cell Expressed and Secreted) (251).

This inflammatory cascade leads to mucus secretion by goblet cells, bronchoconstriction, and epithelial damage, characteristic of asthma exacerbation. If the inflammation persists, it results in airway remodeling, subepithelial fibrosis, increased epithelial-mesenchymal trophic unit, collagen deposition, eosinophil and mast cell infiltration, and smooth muscle hypertrophy (252). This remodeling causes chronic bronchoconstriction and reduced responsiveness to bronchodilators. Environmental factors such as smoking, hormonal changes, infections, and obesity can alter asthma phenotypes and influence the underlying immunoinflammatory process (253).

Since IgE was recognized as a key trigger in the inflammatory process, the development of therapies targeting IgE has advanced significantly. One of the successful treatments is the anti-IgE biologic omalizumab (248). Omalizumab is a recombinant humanized monoclonal antibody designed to bind to IgE at the Fc portion (constant fragment) at the C epsilon three locus in the same domain where IgE binds to the FcεRI (254,255). Thus, omalizumab can

accelerate the dissociation of the preformed IgE- FcεRI complex on mast cell and basophil surfaces. It can also neutralize free IgE, impairing the IgE-mediated inflammatory signaling cascade (256). Given the complexity of the pathophysiology of asthma, IgE is not the only target in patients with asthma. In recent years, multiple biological treatments have been developed targeting other pathways such as IL-5, IL-5R, TSLP, IL-4/IL-13 (257).

1.7.4. Chronic urticaria

Chronic urticaria can be considered a mast cell–related condition, but it would not traditionally be classified as an IgE-mediated disease. However, since many patients show clinical improvement with anti-IgE therapy, it is often included among IgE-related disorders. Urticaria is a chronic disease characterized by different skin symptoms, such as pruritus and evanescent erythematous, and edematous wheals, lasting from one to 24 hours (258). It can be accompanied by angioedema, which causes painful swelling that lasts up to three days (259). Urticaria is divided into acute urticaria (lasting less than six weeks, often allergic) and chronic spontaneous urticaria (CSU), which persists for over six weeks and affects 86 million people worldwide (260). CSU may involve autoimmune markers in some patients, and its severity is linked to autoimmune serology and resistance to antihistamines (258).

The development of CSU is intimately associated with the interaction of several immune cells, such as mast cells, eosinophils, and basophils, even if the precise mechanism of mast cell degranulation is yet unknown (261). The pathophysiology of CSU involves both immunological and nonimmunological components, with cutaneous mast cells' production of vasoactive mediators being a key component. The most common mediator is histamine, which mainly affects the skin's H1 and H2 receptors (histamine receptors 1 and 2, respectively) to produce edema, vasodilation, and itching. Basopenia, aberrant basophil signaling, and autoimmunity are other processes implicated in CSU (262).

Two main categories of CSU pathophysiology are described (263): Autoallergic (type I), characterized by IgE autoantibodies targeting auto-

antigens, leading to mast cells and basophils activation; and autoimmune (type IIb), involving IgG autoantibodies against IgE or FcεRI, which trigger mast cell and basophil degranulation.

Regarding treatment, H1-antihistamines are the first-line therapy, but many patients do not respond adequately to these medications (264). In such cases, omalizumab, a monoclonal antibody that blocks IgE, is highly effective in controlling symptoms (265). New therapeutic approaches are being investigated because some people are still resistant to this treatment. Among these, BTK (Bruton tyrosine kinase) inhibitors (such as remibrutinib), which disrupt mast cell signaling, exhibit potential (266). It has also explored the role of the MRGPRX2 receptor, involved in mast cell activation, as a potential therapeutic target (267). Additionally, other novel therapies, such as dupilumab (anti-IL-4/IL-13) and ligelizumab (anti-IgE with higher affinity than omalizumab), are also being explored with encouraging early results. Numerous other molecules are currently under investigation; however, further studies are required to establish the efficacy and safety of these emerging treatments (263).

The recommended initial treatment is with antihistamines. If symptom control is inadequate, the dose can be increased up to four times the standard dose. In cases where disease control remains insufficient, the introduction of omalizumab or other immunomodulatory therapies may be considered (268).

2. MAST CELLS IN ALLERGY AND ANAPHYLAXIS

Allergic diseases are type I hypersensitivity reactions of the immune system to typically innocuous substances known as allergens. These reactions occur when the immune system identifies an otherwise non-threatening substance, such as pollen, dust mites, certain foods, or animal dander, as a threat and launches an exaggerated immune response (269,270). Over the past few decades, there has been a significant increase in the prevalence of allergy disorders; estimates indicate that up to 30–40% of the world's population is affected (271).

Research indicates that environmental variables, including pollution, urbanization, and genetic susceptibility (272), contribute to allergy disorders. Developing successful preventative and management strategies for allergy disorders requires understanding the intricate interactions between immune responses and environmental triggers.

While some allergic reactions are localized and relatively mild, such as sneezing, itching, swelling, or gastrointestinal symptoms, specific allergens can trigger a systemic response involving multiple organ systems, leading to anaphylaxis (220,273). According to the 2nd International Symposium on the Definition and Management of anaphylaxis, anaphylaxis is a severe systemic reaction caused by exposure to an antigen. It is typically characterized by respiratory and/or cardiovascular symptoms, often accompanied by skin and/or mucosal involvement (274). Both American and European expert societies define anaphylaxis as a severe and immediate systemic hypersensitivity reaction that can be life-threatening. When severe hypotension (extreme drop in blood pressure) and circulatory failure occur in anaphylaxis, it is called anaphylactic shock, the most severe and potentially life-threatening manifestation of an allergic reaction (275,276).

2.1. Epidemiology of anaphylaxis

Although anaphylaxis is becoming more common, there is still limited epidemiological data available at the general population level. Between 2008 and 2016, the number of Emergency Department visits for the condition increased 3.2 times in the US. Comparably, European rates have risen from 1.5 to 7.9 cases per 100.000 person-years. Age is also a factor, as the risk of anaphylaxis and its severity increases after age 65, with older adults being 2.35 times more likely to experience severe reactions (277–279). Recent global data suggest a prevalence of 0.3% to 5.1% and an incidence of 6.7 to 112 episodes per 100.000 person-years and 3.2 to 10 anaphylactic shocks per 100.000 people, with children primarily triggered by food allergens and adults by medications (280).

The mortality rate of anaphylaxis is estimated to range between 1-2%, increasing to up to 6.5% in cases of anaphylactic shock. It has been estimated that there are 0.05-0.51 per million/year for drug-induced anaphylaxis, 0.03–0.32 per million/year for food-induced anaphylaxis, and 0.09–0.13 per million/year for venom-induced anaphylaxis (281,282).

Lastly, recurrent anaphylactic episodes occur in up to 54% of patients throughout long-term follow-up, highlighting the significance of continued therapy and preventative measures (277).

2.2. Triggers of anaphylaxis

The triggers of anaphylaxis vary with age and differ across geographic regions. For this reason, allergy testing should be tailored to the patient's history and informed by local data on the most common causes of anaphylaxis in the area. The most frequent trigger categories are food, drugs and insect venoms.

The presence of accompanying factors, called cofactors, such as physical exercise, acute infections, drugs, alcohol, menstruation, or emotional stress, may increase the severity of the reaction or decrease the allergen threshold needed to provoke a reaction, increasing its severity. This phenomenon is well described in food allergy and may occur in up to 58% of food anaphylaxis episodes (283,284).

2.2.1. Food

Food allergies have notably increased in the last 20-30 years, especially in industrialized countries (285). This rise may be due to diet changes, lower exposure to specific allergens in childhood, and the increased use of processed foods. About 4% to 8% of the global child population is estimated to have some food allergy (286). The prevalence is lower in adults, ranging from 1% to 2%, but it can vary depending on the region and the foods that most commonly cause reactions (287).

The most common food allergens include milk (especially in young children), egg, nuts (almonds, walnuts, peanuts, etc.), fish and shellfish, wheat, soy, sesame, and fruits (288). In central and north european countries, the most common food allergy in children is peanut allergy, which is the leading cause of food allergy-related death in children (289).

The LTP (lipid transfer protein) is the most frequent food allergy (22) in the Mediterranean region. LTPs are ubiquitous plant proteins engaged in lipid membrane biosynthesis and act as pathogenesis-related proteins (290). Recent studies demonstrated immunological cross-reactivity between LTP from many botanically unrelated fruits and vegetables and concluded that LTP is a pan-allergen (291). A pan-allergen is a type of allergen that is found in a wide variety of different foods or environmental sources (292,293). It refers to allergens structurally similar across multiple species or food types, and therefore, individuals sensitized to one source of a pan-allergen may also develop allergic reactions to other, unrelated sources that contain the same protein or antigen (294). This cross-reactivity occurs because the immune system recognizes similar structures in different allergens (295). It is established that peach (Pru p 3) is considered the primary sensitizer for Mediterranean LTP-driven allergy (296,297). Evaluating studies from Southern Europe, it has been suggested that, in addition to primary sensitization to Pru p 3 and subsequent cross-reactivities with homologous LTPs from pollen and food, pollen LTPs may also induce sensitization, potentially leading to cross-reactivity with food LTPs in certain patients (20).

2.2.2. Drugs

Adverse drug reactions are frequent and can manifest as immediate systemic responses, posing a significant risk to public health (298). While IgE is a well-known mediator in allergic reactions, drug hypersensitivity can involve a variety of mechanisms, including IgG, complement activation, and non-immunological pathways such as the activation of MRGPRX2 receptor and inhibition of cyclooxigenase (225,299).

The signs and symptoms of drug hypersensitivity reactions are almost identical to IgE-mediated symptoms, such as angioedema, urticaria, bronchospasm, gastrointestinal manifestations, skin flushing, headache, edema, hypotension, and anaphylactic shock (300). Such reactions can be triggered by opioid medications, complement activation-related drugs and nonsteroidal anti-inflammatory drugs (NSAIDs). Up to 5-10% of people may experience some form of adverse drug reaction (301).

It has been reported that some exogenous molecules, such as substance P or compound 48/80, can induce MC degranulation via the MRGPRX2 receptor (121). Recently, it has been shown that some drugs, such as fluoroquinolones (ciprofloxacin, levofloxacin, and moxifloxacin), morphine, rocuronium, neuromuscular blocking drugs (atracurium and cisatracurium), and antibiotics (vancomycin), can activate MCs through the MRGPRX2 receptor (6,126).

2.2.3. Venoms

Anaphylactic reactions triggered by insect stings – especially from Hymenoptera species such as bees, wasps, hornets, and fire ants – pose a significant health risk in certain areas. These insects are the primary cause of venom-induced anaphylaxis. For individuals stung by honeybees, wasps, or ants, the allergic response can be severe and even life-threatening. Systemic allergic reactions have been reported in up to 7.5% of adults and 3.4% of children. Among the Hymenoptera, bees and wasps are the most frequently implicated. Individuals with systemic mastocytosis are at a higher risk, not only of developing a venom allergy but also of experiencing more severe and dangerous reactions (302).

2.3. Physiopathology of anaphylaxis

There are different physiopathology mechanisms of anaphylaxis, although the clinical manifestations are the same.

IgE-mediated anaphylaxis (or Type 1 hypersensitivity reaction) is the most frequent mechanism. In this type of anaphylaxis, allergen-specific IgE binds to FcεRI, a high-affinity immunoglobulin IgE receptor displayed at the mature MC or basophil membrane. Upon allergen (usually a protein), cross-linking follows the activation of the IgE-prebound FcεRI and the immediate release of mediators. Despite recent advances, understanding the mechanisms that reactivate memory in allergies, which makes some allergies persistent, remains unknown (303).

Other mechanisms that do not involve IgE are called non-IgE-mediated anaphylaxis. These types of mechanisms (or types II-VII hypersensitivity reactions) can be immunologic when there is an activation of the complement system (C3a, C4a, and C5a) or IgG-mediated anaphylaxis (FcγRs, Fc gamma receptor signaling) or non-immunologic when there's activation through G-protein receptors (such as MRGPRX2) by certain drugs. When no trigger can be identified, it is called idiopathic anaphylaxis.

The triggers of anaphylaxis vary with age and differ across geographic regions. For this reason, allergy testing should be tailored to the patient's history and informed by local data on the most common causes of anaphylaxis in the area. The most frequent trigger categories are food, insect venom, and medications.

The presence of accompanying factors, called cofactors, such as physical exercise, acute infections, drugs, alcohol, menstruation, or emotional stress, may increase the severity of the reaction or decrease the allergen threshold needed to provoke a reaction, increasing its severity, occurring in up to 58% of food anaphylaxis episodes (283,284).

2.3.1. T cells in allergy

Our understanding of the immune basis of food anaphylaxis has increased in recent years. In healthy individuals, different T-cell populations can respond to allergens, producing cytokines, including IFN-γ (interferon gamma) and IL-10, but not inducing T_H2 cytokines, as well as IgG or Immunoglobulin A (IgA)

antibodies but not IgE (304). Most T cells that react against whole extracts are Treg cells expressing Foxp3 (305). It has been shown that mutations in the Foxp3 gene induce a T_H2 polarization, enhancing allergies in humans and mice (306). Furthermore, in healthy individuals, soluble allergens seem to be ignored by the Tregs, allowing T_H2 cell differentiation and allergy development depending on environmental and genetic factors (304). Recently, T_H2 responses were shown to expand Tregs via IL-2, suppressing T_H2 cells in a negative feedback loop (307). Furthermore, different types of T cells that can play a role in the type 2 immune responses have been studied.

ILC2s are tissue-resident cells primarily located in mucosal tissues such as lung, small intestine, skin, and adipose tissue (244). It has been reported that the number of ILC2s increases in the small intestine in mice with IgE-mediated food allergies (78,308). Indeed, ILC2s can impair Treg-mediated tolerance by secreting IL-4, thereby exacerbating food allergy responses (309). As previously mentioned, ILC2s can be activated by epithelial-derived cytokines such as IL-25 and IL-33, and they release several cytokines that recruit mast cells, basophils, eosinophils as well as induce the differentiation of T_H2 and IgE production by B cells (244). Recently, it has been reported that patients with a severe allergy to LTP (specifically Pru p 3), exhibit elevated levels of IL-13 and ILC2s, which correlate with serum Pru p 3 sIgE levels and the number of T_H2 cells (310). This study further reports that stimulation with Pru p 3 leads to an increase of ILC2s, enhancing the differentiation of T_H2. This effect is even more pronounced when Pru p 3 is combined with IL-25 and IL-33. Indeed, in patients with allergy to Pru p 3, sublingual immunotherapy with Pru p 3 reduced both the frequency and activity of these ILC2s (311). These findings suggest that ILC2s may represent a promising therapeutic target in food allergy treatment.

Moreover, studies of food-allergic patients and murine models point to the affinity of IgE as a key factor related to MC degranulation and anaphylaxis (312–315). T follicular helper (T_{FH}) cells direct the affinity and isotype of antibodies synthesized by B cells; the nature of signals that switch to low versus high affinity may differ (316,317). T_H2 cells were described as a way for B cells to control IgE production by activating IL-4 (318). It has been shown

that deleting STAT6 or GATA3 from T_H2 cells reduces IgE production in mice (319). However, T follicular helper cells are a subset of cells, localized into the B cell follicle, that highly express stimulating B cell molecules, such as CD40 ligand, and highly produce IL-4, driving the affinity, longevity, and isotype of antibody produced by B cells (14,320). Those $T_{FH}2$ cells, which slightly express GATA3, induce the switching of IgM to IgE, resulting in low-affinity IgE antibodies (321). Recently, a new subset of T cells, called $T_{FH}13$ cells, has been described, with a different cytokine profile (IL-13^{hi}IL-4^{hi}IL-5^{hi}IL-21^{lo}) and co-expressing the transcription factors BCL6 and GATA3. Those cells promote high- but not low-affinity IgE induction by secreting IL-4 and IL-13 (322,323). These cells are necessary for anaphylactic reactions; therefore, $T_{FH}13$ cells may identify severe patients, as shown (324,325). Furthermore, blocking these $T_{FH}13$ cells might be an alternative therapeutic target to ameliorate anaphylaxis (324).

A novel regulatory T-cell subset, called T follicular regulatory cells (Tfr) has been described as a suppressive counterpart of B-cell-stimulating T follicular helper cells (326). Reduced levels of Tfr cells have been shown in allergic rhinitis individuals compared with healthy individuals (326). Moreover, in Tfr-deficient mice, there is an increase in sIgE, suggesting that Tfr can control $T_{FH}13$ cells (327).

2.4. Diagnosis of anaphylaxis

Anaphylaxis diagnosis is based on a thorough clinical history. Diagnosing anaphylaxis, particularly food-induced anaphylaxis, can be challenging, especially in patients without a prior history of allergy.

Serum tryptase is the most measured of the laboratory markers that have been investigated to support diagnosis. Following an anaphylactic reaction, tryptase levels increase immediately, peak in one to two hours, and then drop to baseline in twenty-four hours. However, normal tryptase levels during the acute phase of an allergic reaction do not rule out anaphylaxis, especially in food-related cases (279). Measuring serum tryptase levels during the acute phase of anaphylaxis is most effective when compared with baseline levels.

The "20+2 rule" is commonly used, where the tryptase level during an acute episode must be at least 20% higher than the baseline level plus 2 ng/mL. This comparison helps confirm the diagnosis of anaphylaxis more accurately, as baseline levels can vary due to conditions like hereditary alpha-tryptasemia or mastocytosis (328). Histamine is another potential marker, as it peaks within 10 minutes of symptom onset and returns to baseline within an hour. Unfortunately, it is rarely helpful in clinical practice since most patients do not arrive at the emergency department early enough to capture the histamine peak (279,329).

The gold standard test for diagnosis of food allergy is an oral food challenge (OFC) in which increasing doses of food are administered under medical supervision (330). However, OFCs are time-consuming and costly and can result in potentially severe allergic reactions, anaphylaxis, or even death (331). In clinical practice, IgE-mediated food allergy is frequently diagnosed by using a surrogate marker and detection of allergen-specific IgE (sIgE) to the implicated food (referred to as sensitization) either in serum or through skin prick tests (SPTs). However, sensitization may fail to correlate with clinical reactivity. A false-positive rate of greater than 50% has been reported in population-based studies (332,333), and consequently, over-diagnosing food allergies is common in non-specialized settings. This results in unnecessary dietary exclusions, social restrictions, and anxiety, which can further impair nutrition and quality of life (332).

For drug allergies, a significant problem in these reactions is that the triggering drug cannot be confirmed in about half of the cases because the allergy test is negative (334,335). The study protocols state that when skin tests with suspected drugs have been negative, a drug provocation test (DPT) should be performed to rule out an allergy (336). However, this type of test is difficult to performed, for example, with neuromuscular blocking agents (NMBAs), such as atracurium or succinylcholine, and other anesthetic drugs. Indeed, similarly to OFC, DPT also carries a high risk, especially in patients who have experienced anaphylaxis (335).

2.4.1. *In vitro* diagnosis

In recent years, more accurate techniques have been developed to diagnose food allergy, especially to distinguish between sensitization and allergy. These techniques are focused on the effector cells of allergic reactions. On one side there is the basophil activation test (BAT), and on the other, the mast cell activation test (MAT). BAT involves incubating fresh blood samples with the allergen and measuring basophil activation markers ($CD63^+$ or CD203c) using flow cytometry. Indeed, BAT is also used for other clinical applications, such as monitoring clinical response following allergen-specific immunotherapy or anti-IgE treatment. A meta-analysis of BAT studies has reported a sensitivity of 73-100% and a specificity of 82-100% to differentiate sensitization from allergy, in a peanut allergy model. However, when Ara h 2 (the primary peanut allergen in some populations) is used in BAT, the sensitivity and the specificity are lower. This test shows a promising diagnostic tool, but there are some limitations: the need for fresh blood samples, which need to be analyzed within 4 to 24 hours after collection, the existence of about 6-17% of the population that have non-realising basophils to IgE-mediated stimulants, and the possibility to have false-negative BAT results after an anaphylactic episode. To avoid these limitations, a passive BAT test has been studied, where the IgE of the donor basophils is stripped following sensitization with the patient's sera before stimulation with the allergen. However, this passive BAT seems less sensitive than the conventional BAT due to the need for high levels of IgE for sensitization (337). The need for such high levels of sIgE in the blood is a significant limitation because, in some patients, sIgE can be low.

The mast cell activation test is a more recent diagnostic tool that involves sensitizing mast cells (either a cell line or $CD34^+$-derived mast cells from the blood) to the patient's sera following allergen stimulation and measuring $CD63^+$-positive mast cells (54,330,338–342). Using peanut extract as an allergen, MAT has shown a sensitivity of 73% and a specificity of 98% (340). The MAT seems a promising diagnostic tool to distinguish between sensitization and allergy, but, as well as BAT, it has some limitations: high cost of generation and mast cell maintenance, long-term cell culture, low amount

of cells from 100 ml of blood, and the need for constant resupply of peripheral blood from healthy donors to generate new batches (337).

These *in vitro* tests offer numerous advantages over OFCs, mainly because they are less invasive and more convenient for patients. Indeed, they are most cost-effective when assessing multiple food allergies simultaneously, but as we mentioned above, they have still some limitations. In summary, BAT can improve diagnostic accuracy in patients, particularly well-studied in children with peanut allergy, but is still technically challenging and limited to a few specialist centers, and lacks the accuracy and reproducibility of a food challenge (331,340). In addition, the basophil's role as effector cells in the pathophysiology of allergic reactions (343) is uncertain. Mast cells have long been regarded as the primary effector cells in individuals who have allergic responses (343); for that reason, MAT can improve the diagnosis of IgE-mediated peanut allergy, and it seems to be more accurate than BAT in distinguishing sensitization versus allergy (54,330). Still, it is time-consuming due to the long differentiation of mast cells *in vitro*. Furthermore, MAT may have some advantages over BAT due its higher specificity, avoiding false positives and over-diagnosing (289). Moreover, unlike basophils, MCs have MRGPRX2 receptors, which can induce degranulation without prior sensitization, allowing the diagnosis of some adverse reactions through this receptor (337).

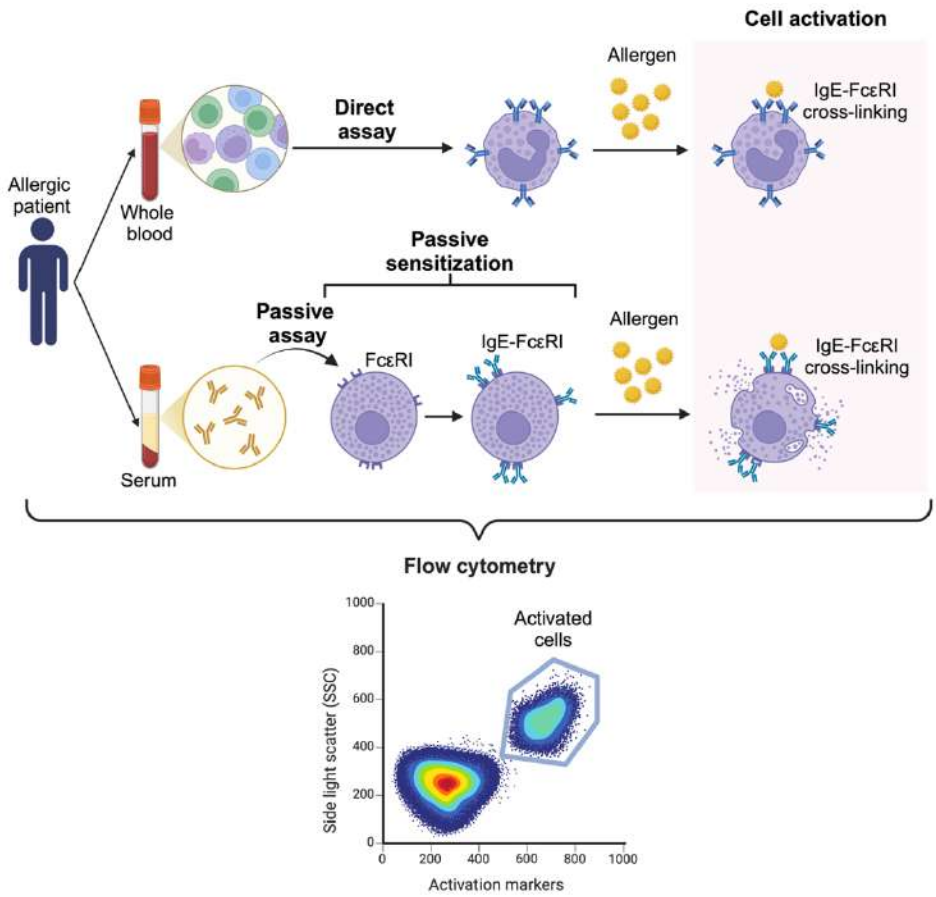

Figure 13. Schematic representation of new diagnostic tools in allergy. Basophil activation test (BAT) is a direct assay that starts with the whole blood of patients and is stimulated with the allergen. On the other hand, the passive assay consists of the previous sensitization of cells with the patient's sera followed by the allergen stimulation. MAT is considered a passive assay, and recently, a passive basophil activation test has also been reported. Figure adapted from (344).

The utilization of primary human MCs for an allergen-induced mast cell activation assay appears to be preferable to cell lines (the humanized rat basophilic leukemia cells, RBL-2H3, the human leukemic mast cells, LAD2, LUVA cells, and wild-type ROSA cells (345–348) because of their tumor origin, maturation storage, *in vitro* cell proliferation, and poor or variable potential to trigger FcεRI -mediated degranulation and to generate mediators (330). To obtain these human MCs for research, several groups have reported methods

for *in vitro* MC culture using bone marrow, peripheral whole blood, or umbilical cord blood as the source of progenitors (54,342,349–352). These approaches are laborious and produce few mast cells for examination, but they make it possible to study dependent and independent IgE pathways in greater depth (342). Another way to have mature MCs is by using human-induced pluripotent cells as progenitors to generate MCs, which is also time-consuming (353). Recently, it has been described a new immortalized MCs: the introduction of an inducible Hoxb8 gene (extracted from the bone marrow of mice) into MC progenitors induces the proliferation of these MC progenitors daily, promoting the differentiation of mature MCs expressing consistent levels of FcεRI within 6 days. These Hoxb8 MCs are highly granulated and can be used for MAT (354).

2.5. Treatment of anaphylaxis

Until recently, the primary approach to managing food allergies involved strict avoidance of allergens and preparation to treat rapidly a severe allergic reaction if accidental ingestion should occur. This strategy resulted in 20% of food-allergic children requiring emergency medical care annually, while 40% experienced at least one severe allergic episode necessitating an emergency room visit at some point in their lives in the United States (355). In drug allergy, management typically involves discontinuing the causative drug and, if possible, using alternatives drugs (356).

The treatment of allergies is usually symptomatic, such as antihistamines, corticosteroids, or bronchodilators, which may reduce symptomatology in case of anaphylaxis, epinephrine should be administered (329).

Epinephrine (or adrenaline) is recognized by the World Health Organization (WHO) as the essential medication for treating anaphylaxis. Its timely administration is critical, as delayed use has been associated with fatal outcomes in many cases (279). Epinephrine is the only drug capable of effectively reversing an anaphylactic reaction by suppressing mediator release by stimulating mast cell β2-adrenergic receptors. The epinephrine interaction with β2-adrenergic receptors induces vasoconstriction (reverse

hypotension) and bronchodilation (relieving airway obstruction), increasing the cardiac output (329).

Literature data show that despite the existence of clinical practice guidelines, more than 50% of anaphylaxis are not diagnosed, and in less than 30% of cases, the treatment of choice, adrenaline, is administered (273,285,357).

2.5.1. Other recent treatments

Sublingual immunotherapy (SLIT) and oral food tolerance induction are emerging treatments for food allergies. SLIT involves placing allergen-containing tablets or drops under the tongue, allowing the allergen to enter the bloodstream through the mucous membranes (358,359). This approach is also used for airborne allergens such as pollen and dust mites. On the other hand, oral food tolerance induction (OTI) consists of gradually introducing small amounts of allergenic foods to help build tolerance (358). Research has mainly focused on foods like milk, eggs, peanuts, and tree nuts. Both therapies aim to reduce allergic reactions and enhance the quality of life for individuals with food allergies. These type of therapies can reduce the T_H2-mediated allergic response, inducing a Treg-mediated immunological tolerance response (269). It is not established whether the induction of clinical tolerance by allergen immunotherapy is mediated, but it is thought that there is a reduction of T_H2 rather than Treg expansion. Also, there is a reduced circulating T_{FH} cells and increased Tfr cells, attended by the induction of IgG4 (360). Indeed, in patients with allergy to Pru p 3, sublingual immunotherapy with Pru p 3 reduced both the frequency and activity of ILC2s, reducing the T_H2-mediated allergic response (311).

Monoclonal antibodies are another known treatment for food allergies. The best-studied monoclonal antibody is omalizumab, an anti-IgE also used in asthma and urticaria (361). A recent publication has shown that omalizumab treatment for 16 weeks increased the reaction threshold for peanut and other common food allergens in patients with multiple food allergies (361).

Microbial therapies are also being developed to treat food allergies because it has been established that the intestinal microbiota of individuals with food allergies is altered (362). In mice, the transfer of allergic microbiota induces susceptibility to food allergy development (363,364). It is thought that microbiota enhance Tregs and suppress T_H2 responses (365,366). Thus, new approaches are being studied by combining immunotherapy treatments with other therapies, such as monoclonal antibodies or microbiota alterations (78).

HYPOTHESIS AND OBJECTIVES

The hypothesis of this thesis is the following:

In hypersensitivity reactions, the humoral (IgE) and cellular (mast cells) components contribute to the severity of the disease. Moreover, MITF, as a key regulator of mast cell differentiation and activation, may represent a potential therapeutic target for the treatment of severe hypersensitivity reactions.

To this aim, the main objectives of this thesis are the following:

1. **To develop an *in vitro* model to assess severity in LTP patients**

   1.1. Differentiate MC from LTP patients and analyze its functionality *in vitro*.
   1.2. Determine the presence of the $T_{FH}13$ cells in our cohort.

2. **To identify new biomarkers to discriminate between sensitization and allergy in an LTP-model**

   2.1. Transcriptomic analysis in mast cells incubated with sera from sensitized or anaphylactic patients and stimulated with peach LTP (Pru p 3).
   2.2. Transcriptomic analysis of MC from healthy, sensitized, and anaphylactic patients incubated with sera from sensitized or anaphylactic patients in baseline and Pru p 3-activated conditions.

3. **To investigate the role of MITF on mast cell release modulation and metabolism**

   3.1. Analyze the role of MITF in the MC mediator's release, both preformed and *de novo*, in the IgE-dependent pathway.
   3.2. Analyze the role of MITF in the MC mediator's release, both preformed and *de novo*, in the IgE-independent pathway (MRGPRX2).

3.3. Study the role of MITF in mitochondrial activity and function.
3.4. Investigate metabolic changes in a MITF-knockdown or MITF-overexpression model.
3.5. Analyze metabolic differences in an LTP patients using a mast cell model.

MATERIALS AND METHODS

1. COMMON METHODS

1.1. Study population

Patients were recruited at the Allergy Department of the Hospital Clínic of Barcelona. Informed consent was obtained from all participating subjects. The study was approved by the local ethics committee of the Hospital Clinic (Barcelona, Spain).

Fourteen patients sensitized to peach LTP-Pru p 3 with sIgE levels ≥ 0.10 KU_A/L (ImmunoCAP®, Thermo Fisher Scientific, Mass, USA), with no other sensitizations identified, including profilins, homologs of Bet v 1, thaumatin-like proteins, gibberellins, tropomyosin or other general storage proteins, were recruited. They were classified into two groups depending on the reaction severity upon peach: (1) *anaphylaxis* patients with a convincing history of anaphylaxis, and (2) *sensitized* patients with no symptoms or only mild local symptoms (contact urticaria, oral allergy syndrome). Oral challenge was not performed in anaphylaxis patients (367), and a recent contact history with peach was required in the sensitized group. Five healthy volunteers with no respiratory or food allergies were also recruited as controls.

Some seras from each group (*anaphylaxis* and *sensitized*) were pooled based on a similar ratio Pru p 3 sIgE / total IgE levels (sIgE:tIgE) to avoid individual variabilities. Total Pru p 3 -sIgE and -specific IgG4 (sIgG4) and tryptase levels were measured by ImmunoCAP® System (Thermo Fisher Scientific). Specific IgE ≥ 0.10 KU_A/L was considered positive.

1.2. $CD34^+$- derived mast cells generation

MCs were obtained from 100 ml of healthy volunteers or LTP patients' peripheral blood or buffy coat preparations (10 ml of concentrated leukocyte suspension from blood) obtained from the blood bank of the Hospital Clínic of Barcelona. Peripheral blood mononuclear cells (PBMCs) were isolated by density gradient centrifugation using Histopaque (Sigma-Aldrich) following the

protocol previously described (9,368). Briefly, blood was diluted with phosphate-buffered saline (PBS, Lonza Bioscience, Morrisville, USA), layered over Histopaque, and centrifuged at room temperature (RT) at 400 xg for 20 minutes. PBMCs were collected, washed, and incubated with MACS Buffer (0.5% bovine serum albumin (BSA, Sigma-Aldrich, St. Louis, MO, USA); 2 mM ethylenediaminetetraacetic acid (EDTA); 50 ml PBS) and CD117 Microbead Kit Human (Myltenyi Biotec, Bergisch Gladbach, Germany). CD117^{+} (or KIT) cells were selected using a magnetic field with LS columns (Myltenyi Biotec) and suspended with mast cell culture medium (Stem-Pro-34 Medium; Thermo Fisher Scientific) supplemented Stem-Pro-34 nutrient (Thermo Fisher Scientific), 1% penicillin/streptomycin (Lonza Bioscience), 1% L-glutamine (Lonza Bioscience), 50 ng/ml rh IL-6 (Immunotools, Friesoythe, Germany), and 100 ng/ml Stem-cell factor (Immunotools). 10 ng/ml rh IL3 (Immunotools) were added at day 0 of the culture. A mast cell culture medium was added to the cell culture every two weeks. At week 7, mast cells were characterized (Figure 14).

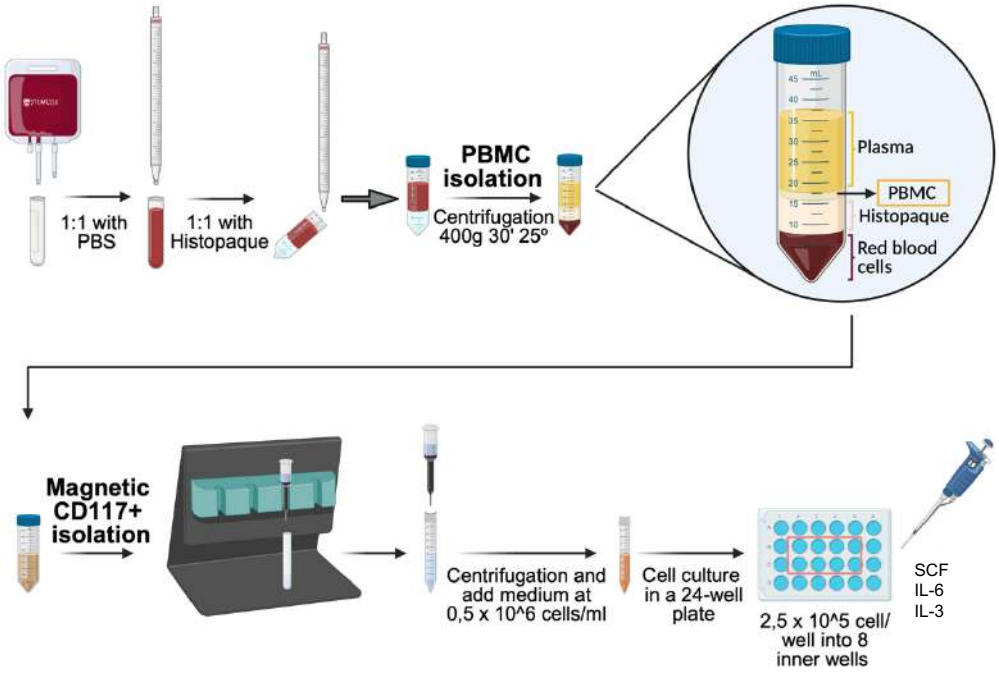

Figure 14. Methodology illustration of MCs generation. 100 ml of blood was used to generate MCs *in vitro* using the CD117-positive PBMC cells.

1.3. Characterization of CD34$^+$- derived mast cells

5x10^4 cells were centrifuged with Cytosipin at 500 revolutions per minute (rpm) for 5 minutes to check the morphology. Then, cells were stained with May-Grünwald Giemsa.

For analysis of mast cell differentiation, 5x10^4 cells were taken from culture, blocked, and stained with APC-conjugated anti-FcεRI (BioLegend, San Diego, CA, USA) and PE-conjugated anti-CD117 (Santa Cruz Biotechnology, Dallas, Texas, USA). Cells were acquired on a FACSCalibur flow cytometer (FACScan; BD Biosciences, Mountain View, CA, USA) and analyzed using FlowJo software version 10.8.

The β-hexosaminidase assay was performed to check the functionality of the CD34$^+$- derived mast cells. 6x10^4 cells were taken from culture and sensitized overnight (O/N) with 0.1 µg/ml biotinylated human IgE (^{b}IgE, Abbiotec, San Diego, CA, USA) in triplicates into 96-well plates. Cells were stimulated with 0.4 µg/ml Streptavidin (STV) (Sigma-Aldrich) for 30 minutes at 37°C. After 30 minutes, plates were centrifuged, and β-hexosaminidase assayed in the supernatants and cell pellets as described (5,369). Degranulation was calculated as the percentage of β-hexosaminidase recovered from the supernatants compared with total cellular content.

1.4. Cell lines

Primary human MCs derived from peripheral blood or buffy coat preparations were obtained as described above (section 1.2) and used to study IgE-dependent pathways.

LAD2 cells kindly provided by Dr. D. Metcalfe (NIH, Bethesda, MD, USA) (370) were grown in Stem-Pro-34 media (Thermo Fisher Scientific), supplemented with Stem-Pro-34 nutrient (Thermo Fisher Scientific), 1% penicillin/streptomycin (Lonza Bioscience), 1% L-glutamine (Lonza Bioscience) and 100 ng/ml SCF (Immunotools).

RBL-2H3 cell model were grown in RPMI media (Corning, NY, USA) supplemented with 1% penicillin/streptomycin (Lonza Bioscience), 1% L-glutamine (Lonza Bioscience), 10% heat-inactivated fetal bovine serum (FBS, Gibco, Dublin, Ireland) and 1% HEPES (Lonza Bioscience). RBL-2H3 model was used to overexpress MITF. As described before for our group (371), Human LysRS (KARS wild-type [WT]) was used to produce the LysRS mutant by site-directed mutagenesis in which proline was replaced by arginine at position 542 (LysRS-P542R). Human LysRS-WT and P542R variants were subcloned into the KpnI and NotI sites of the pcDNA 3.11C-eGFP vector, and the fidelity of all constructs was verified by direct sequencing (GenScript Biotech, Leiden, The Netherlands). RBL-2H3 cells were transfected with GFP-Human LysRS (KARS WT or P542R) plasmids with Lipofectamine (Invitrogen, Mass, USA) and selected with G418 (Gibco). Cells transfected only with GFP were used as control.

Dr. M. Babina (Charité, University of Berlin, Germany) kindly provided human skin MCs used to study the MRGPRX2-dependent pathway. Cells were grown in Iscove's Liquid Medium with Stable Glutamine (with 3.024 g/l NaHCO3, with 15 mg/l Phenol Red; Bio&Sell GmbH, Feucht, Germany) supplemented with 10% heat-inactivated FBS (Bio&Sell GmbH), 1% penicillin/streptomycin (Thermo Fisher Scientific), 1% Amphothericin B (Corning), 227 µM Alpha-Monothioglycerol (Sigma-Aldrich), 1x non-essential amino acids (Sigma – Aldrich), 100 ng/ml SCF (Immunotools) and 20 ng/ml rh IL-4 (Immunotools).

HEK293LTV cell line (Cell Biolabs, San Diego, CA, USA) was used for lentiviral production, described as follows. Cells were grown in Dulbecco’s Modifies Eagle Medium (DMEM) media supplemented with 1% sodium-pyruvate (Lonza Bioscience), 10% heat-inactivated FBS (Gibco), 1% penicillin/streptomycin (Lonza Bioscience), 1% L-glutamine (Lonza Bioscience).

1.5. DNA plasmid amplification and purification

1.5.1. Bacterial transformation

Escherichia coli Stbl3 competent cells (Invitrogen) were used to amplify DNA (deoxyribonucleic acid) plasmids. DNA vector was mixed with bacteria-competent cells and incubated at 42ºC for 30 seconds (heat shock). Immediately, the mixture was cooled on ice for 2 minutes. Then, cells were incubated with SOC medium (super optimal broth with catabolite repression medium, Invitrogen) for 1 hour to allow the cells to express the antibiotic resistance gene, in this case, ampicillin. Subsequently, 100 µl transformed bacteria were seeded on lysogeny broth (LB) agar (Merk, Darmstadt, Germany) plates with 100 µg/ml ampicillin. Plates were incubated overnight at 37ºC (Figure 15).

1.5.2. DNA plasmid amplification and purification

A single colony of ampicillin-resistant bacteria was picked from the LB agar plate and grown in 2 ml of LB medium (Condalab, Madrid, Spain) supplemented with 100 µg/ml ampicillin at 37ºC for 2 hours. Then, these 2 ml were transferred in 200 ml of LB medium (Condalab) and left overnight at 37ºC and 220 rpm. Afterward, plasmids DNA were isolated using the Endotoxin-free plasmid DNA purification kit (Macherey-Nagel, Düren, Germany) following the manufacturer's instructions (Figure 15). The final concentration of DNA was measured using NanoDrop™ One Spectrophotometer (Thermo Fisher Scientific).

1.6. Plasmid transfection and lentivirus production

For the lentiviral particle production, HEK239LTV cells were used. According to the manufacturer's instructions, lentiviral particles to silence MITF gene expression were generated using Mission short hairpin ribonucleic acid (shRNA) technology (Sigma-Aldrich) as previously described (168,169). Briefly, HEK293LTV cells at 80% confluency were transfected with

Polyethylenimine (PEI) and the following plasmids in a ratio 4:1 (4 µg of PEI per 1 µg of DNA): 50 µg shRNA-NT, MITF shRNA-2 or MITF shRNA-3, 17.5 µg pVSV-G and 17.5 µg pdR8.9 in 20 ml of DMEM media (Corning) supplemented with 1% sodium-pyruvate (Lonza Bioscience) for 6 hours. After that, the media was changed, and cells were grown in DMEM media supplemented with 1% sodium-pyruvate (Lonza Bioscience), 10% heat-inactivated FBS (Gibco), 1% penicillin/streptomycin (Lonza Bioscience), 1% L-glutamine (Lonza Bioscience) for 72 hours (Figure 15).

After 72 hours, supernatants were collected and centrifuged at 1500 rpm for 5 minutes to remove cell debris. Then, the supernatant was mixed with 8.5% polyethylene glycol (PEG) and 0.5 M NaCl. The mixture was incubated at 4ºC for a minimum of 2 hours. Afterward, the mixture was centrifuged at 8000 rpm for 15 minutes at 4ºC, and the pellet obtained was resuspended in 1.7 ml Stem-Pro-34 medium (the medium of the cells to be infected) (Figure 15).

LAD2 cells were used for lentivirus transduction. For silencing the shRNA-NT, MITF shRNA-2 and MITF shRNA-3 were used (sequences described in Table 1). These sequences are previously reported as functional in our group (169).

Table 1. Lentivirus shRNA sequences.

	Sequence
shRNA-NT	5’CCGGCAACAAGAGCACCAACTCGAGTTGGTGCTCTTCATCTTGTTGTTTTT3’
MITF shRNA-2	5’CCGGCGGGAAACTTGATTGATCTTTCTCGAGAAAGATCAATCAAGTTTCCCGTTTTTG3’
MITF shRNA-3	5’CCGGGGGAGCTCACAGCGTGTATTTCTCGAGAAATACACGCTGTGAGCTCCCTTTTTG3’

ShRNA-NT was used as a control, and MITF shRNA-2 and MITF shRNA-3 were used to silence MITF.

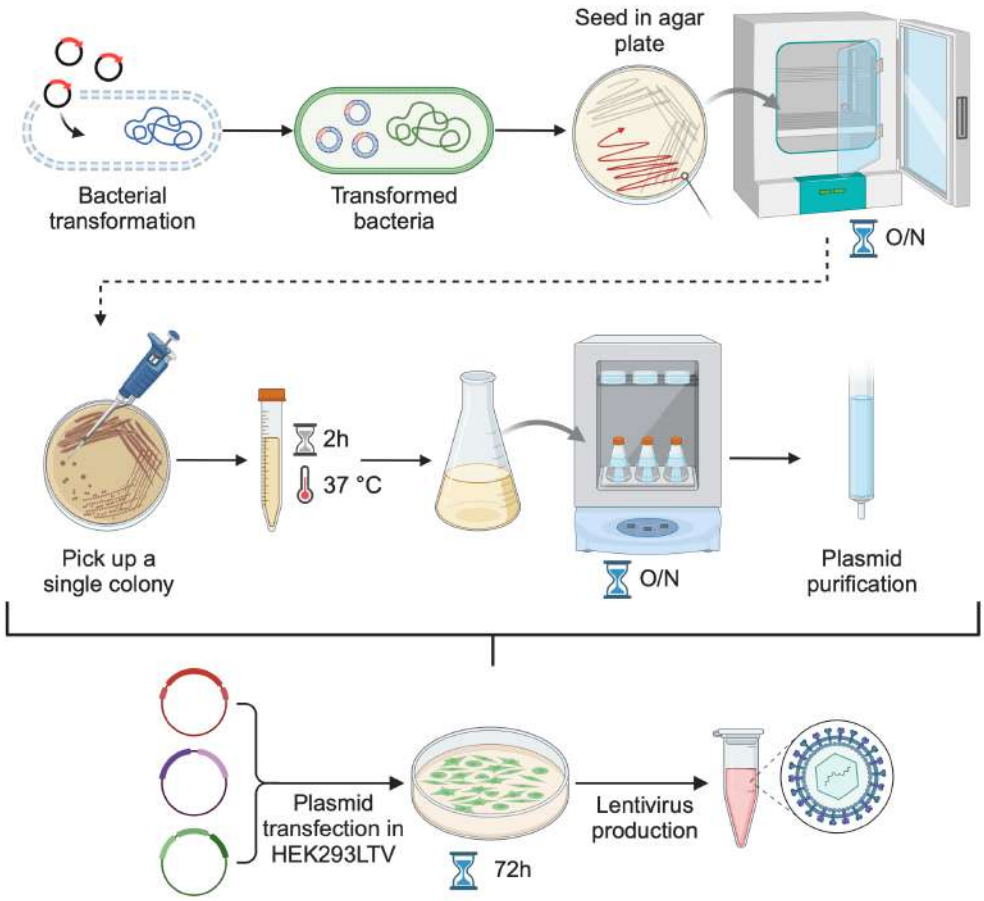

Figure 15. Methodology illustration of DNA amplification, purification, and transfection for lentivirus production. Escherichia coli Stbl3 competent cells were used for DNA amplification and purification. Then, HEK293LTV cells were used for plasmid transfection and lentivirus production.

1.7. Cell treatment

For MITF silencing, LAD2 cells were infected with lentivirus (shRNA-NT, MITF shRNA-2, and MITF shRNA-3) in the presence of 8 µg/ml polybrene (Santa Cruz Biotechnology) for 24 hours. After that, cells were centrifuged and resuspended with new media (complete Stem-Pro-34, as mentioned above, section 1.4) supplemented with 100 ng/ml SCF (Immunotools) and 1 µg/ml puromycin, which is used for selection for 5 days. MITF levels were checked by western blot.

For MITF inhibition, LAD2 cells, MCs derived from blood, skin MCs, and transfected RBL-2H3 cells were treated with MITF inhibitors. As described in the literature, although the exact way ML329 (MedChem Express, Monmouth Junction, NJ, USA) works is unknown, it has been reported to reduce MITF expression and multiple MITF target genes (372). Recently, a new MITF inhibitor, called TT012 (MedChem Express), has been discovered, which binds specifically to dynamic MITF, inhibiting its dimerization, which is necessary for its activity (159). Thus, cells were treated with 2 μM ML329 and 5 or 10 μM TT012 or Dymethil sulfoxide (DMSO, ITW Reagents, Barcelona, Spain), the vehicle as control. For mRNA and protein reduction of MITF, we treated cells for 5 days, but for MITF dimerization inhibition, cells were pre-treated with TT012 for 1 hour, and the reagent was maintained in the medium during the subsequent 24-hour stimulation period, as previously described (159). The levels of MITF were checked by using a western blot.

1.8. Western blotting

Western Blot (WB) analysis was performed to assess the presence of different proteins as described (373,374). First, the total protein concentration of the whole cell lysate samples was determined using the Protein Assay Dye Bio-Rad Kit (Bio-Rad Laboratories, Inc. USA) according to the manufacturer's recommendations. Then, an equal protein amount of each sample (20 μg) was mixed with reducing 5X PierceTM Lane Marker Reducing Sample Buffer and 0.5 μM Dithothreitol. Samples and the molecular marker PageRulerTM Prestained Protein Ladder (Thermo Fisher Scientific) were loaded in a NuPage™ 4-12% Bis-Tris Gel, 1.5 mm x 15 wells (Invitrogen), and electrophoresis was run with NuPage™ MOPS SDS running buffer (Thermo Fisher Scientific). Gels were run in the XCell SureLockTM Novex Mini-Cell system (Invitrogen).

After that, proteins were electrotransferred. There were two ways to perform this step: 1) wet transfer, using polyvinylidene difluoride membranes (Millipore, Bedford, MA, USA) and Transfer Buffer (Thermo Fisher Scientific); or 2) dry transfer, using a nitrocellulose membrane and iBlot2® Transfer Stack support within the iBLOT2® Dry Blotting System (all from Thermo Fisher Scientific).

Ponceau S staining (Sigma-Aldrich) was applied to check a good membrane transfer, and then membranes were washed with 1X Tris-buffered saline with 0.1% Tween 20 (TTBS) and were blocked with 5% non-fat dry milk (Nestlé, Vevey, Switzerland) diluted with TTBS for 1h at room temperature. Blots were then incubated overnight at 4ºC, in agitation, with the primary antibodies listed in Table 2 diluted in TTBS. After primary antibody incubation, membranes were washed three times with TTBS and incubated with the corresponding secondary antibody (Table 2) diluted in TTBS for 1h at RT.

Next, membranes were rewashed with TTBS three times, and proteins were visualized by enhanced chemiluminescence (WesternBright ™ ECL, Advansta, USA) or using SuperSignal™ West Femto Maximum Sensitivity chemiluminescence substrates (Thermo Fisher Scientific). Images were acquired using the Bio-Rad Chemidoc imaging system (Bio-Rad). When required, to allow the incubation of other antibodies within the same membrane, Restore™ PLUS Western Blot Stripping Buffer (Thermo Fisher Scientific) was employed for 12 min. Before other antibody incubation, the membranes were blocked again.

Table 2. List of primary and secondary antibodies used for WB.

	Antigen	MW (kDa)	Host Specie	Dilution	Company	
Primary antibody	phospho Tyrosine HRP conjugated	-	Human	1:1000	BD Transduction Laboratories	Used in first objective
	phospho LAT	38	Human	1:1000	Cell Signaling Technology	
	LAT	38	Human	1:1000	Cell Signaling Technology	
	MITF	60	Human	1:1000	Cell Signaling Technology	Used in the second objective
	STIM1	80	Human/Mouse	1:1000	Cell Signaling Technology	
	phospho DRP	80	Human	1:1000	Cell Signaling Technology	Used in third objective
	DRP	80	Human	1:1000	Cell Signaling Technology	
	phospho ERK	40	Human	1:1000	Cell Signaling Technology	
	ERK	40	Human	1:1000	Cell Signaling Technology	
	COX-IV	18	Human	1:1000	Cell Signaling Technology	
	OXPHOS cocktail	CV (55), CIII (48), CIV (40), CII (30), CI (20)	Human	1:1000	Abcam	
	TOM20	16	Human	1:10000	ProteinTech	
	Actin HRP conjugated	42	Human/Mouse	1:10000	Sigma-Aldrich	Used in all objectives
Secondary antibody	Rabbit	-	Goat		Life Technologies	Used in all objectives
	Mouse	-	Rabbit		DAKO	Used in all objectives

As described in the table, different antibodies were used in each objective section. BD transduction laboratories were from BD Biosciences, Mountain View, CA, USA. Cell Signaling Technology was from Danvers, Massachusetts, USA. Abcam was from Cambridge, UK. ProteinTech from Rosemont, IL, USA. Life Technologies was from Carlsbad, CA, USA. And, DAKO from Carpinteria, CA, USA.

1.9. Cell proliferation and survival assay

Cell proliferation and cell survival were measured using Water-Soluble Tetrazolium Dye (WST-1, MedChem Express).

For cell proliferation, $0.1x10^6$ LAD2 cells sensitized with ^{b}IgE (Abbiotec) or pooled sera from patients and healthy volunteers were incubated overnight in a 96-well plate. Then, cells were washed and incubated with Stem-Pro-34 media for 1, 3, or 5 days. In each time-point, cells were centrifuged at 1500 rpm for 5 minutes at room temperature, and WST-1 was added to diluted 1:10 with cell medium. After 30 minutes, 1 hour, and 2 hours, absorbance was measured at 450 nm in a TECAN Sunrise microplate reader (Tecan Group).

For cell viability, $0.1x10^6$ Treated LAD2 cells with MITF inhibitors or MITF shRNAs were incubated in a 96-well plate for 5 days. Afterward, cells were centrifuged at 1500 rpm, 5 minutes at room temperature, and WST-1 diluted 1:10 with cell medium was added. After 30 minutes, 1 hour, and 2 hours, absorbance was measured at 450 nm in a TECAN Sunrise microplate reader (Tecan Group).

2. SPECIFIC METHODOLOGY FOR OBJECTIVE 1

2.1. Mast cell activation and PGD_2 secretion

$5x10^4$ MCs or LAD2 cells were incubated with 10 ng/ml rh IL-4 (Immunotools) for 5 days (101,375) and sensitized overnight with pooled sera diluted to obtain a total concentration of Pru p 3 sIgE = 1 KU_A/L. Cells were washed and stimulated with 1 µg/ml Pru p 3 (Roxall, Trofa, Portugal) for 30 minutes at 37ºC. The supernatants were kept at -80ºC for later Prostaglandin D2 (PGD_2) analysis using the ELISA kit from Cayman Chemical (Ann Arbor, Mich) as described (371). Cells were blocked and stained with PE-conjugated anti-CD63 (BD Biosciences). Cells were acquired on a FACSCalibur flow cytometer (BD Biosciences) and analyzed using FlowJo software version 10.8

(Figure 16). Experiments were performed in duplicate in patients where possible (limitation: low number of cells obtained).

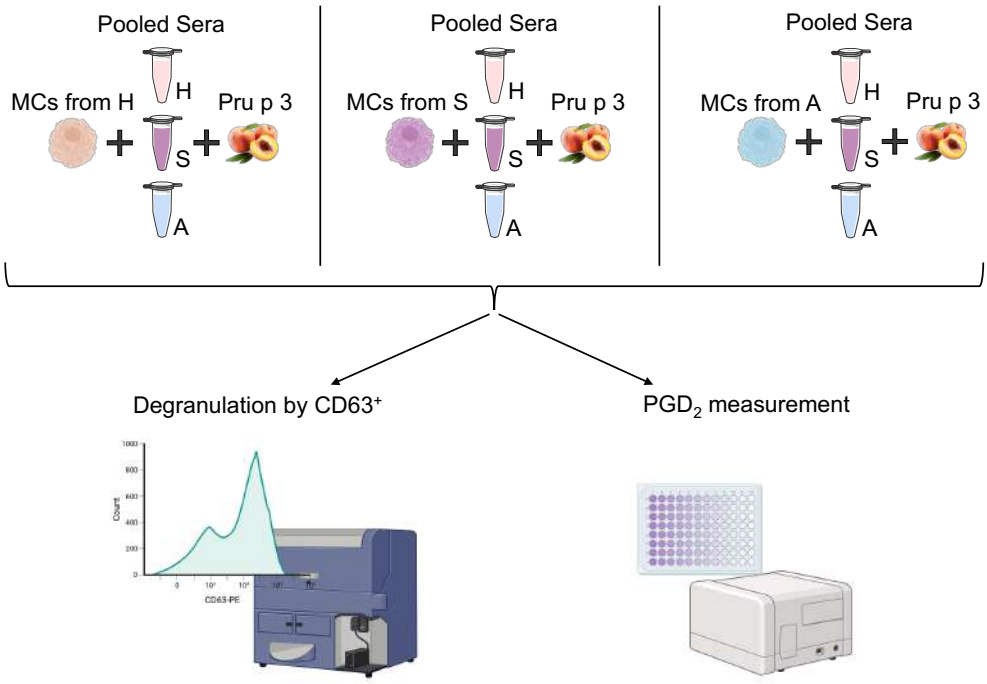

Figure 16. Methodology illustration of MAT and PGD_2 measurement. MCs from healthy donors and patients were sensitized overnight with pooled sera (healthy, sensitized, and anaphylaxis) and then stimulated with Pru p 3. Degranulation was determined with the percentage of CD63-positive cells by flow cytometry, and PGD_2 secretion was assessed by ELISA.

2.2. Detection of $T_{FH}13$ cells

The $T_{FH}13$ cells were detected following the protocol previously described (376). Briefly, PBMCs from patients and healthy volunteers were thawed, and $CD4^+$T cells were isolated using the EasySep Human $CD4^+$T Cell Enrichment Kit (Stemcell Technologies, Vancouver, CAN, USA). $CD4^+$T cells were incubated with Iscove's Modified Dulbecco's medium (IMDM, Gibco) supplemented with 10% heat-inactivated FBS (Gibco), 100 U/mL penicillin-streptomycin (Lonza Biosciences), 2 mmol/L L-glutamine (Lonza Biosciences), 10 mmol/L HEPES (Lonza Biosciences), and 1 mmol/L sodium-

pyruvate (Lonza Biosciences) overnight. Then, $1x10^6$ cells were incubated with IMDM media and 50 ng/ml PMA (Sigma-Aldrich) and 1 µg/ml Ionomycin (Sigma-Aldrich) for 6 hours (after the first hour, Brefaldina A (Invitrogen) is added at 1:1000). After 6 hours, cells were stained with surface antibodies: PerCP-conjugated anti-CD3 (Immunotools), APC-conjugated anti-CD4 (Immunotools), PE-conjugated anti-CD45RA (Immunotools) and APC/Cyanine7-conjugated anti-CXCR5 (BioLegend), fixed with Fixation/Permeabilization Buffer (BD Biosciences) and incubated with Perm/Wash Buffer (BD Biosciences) overnight at 4ºC. Then, cells were stained with intracellular antibodies: FITC-conjugated anti-IL-4 (BioLegend), Brilliant Violet 421-conjugated anti-IL-13 (BioLegend), and PE/Cyanine7-conjugated anti-IFNγ (BioLegend). Cells were acquired on an Attune flow cytometer (Thermo Fisher Scientific) and analyzed using FlowJo software version 10.8.

2.3. Cytokine and chemokine multiplex assay

MCs derived from peripheral blood and LAD2 cells were used to determine the mediator's release. MCs from patients (anaphylaxis and sensitized) were sensitized overnight with pooled sera (anaphylaxis and sensitized, respectively). The next day, $1x10^5$ cells were cultured in a 48-well plate and treated with 1 µg/ml Pru p 3 (Roxall) for 24 hours at 37ºC. In parallel, LAD2 cells were sensitized with both pooled sera from LTP patients (sensitized or anaphylaxis) or with 0.1 µg/ml biotinylated human IgE (Abbiotec) overnight. Then, cells were stimulated with 1 µg/ml Pru p 3 (Roxall) or 0.4 µg/ml STV (Sigma-Aldrich), respectively, for 24 hours at 37ºC.

After 24 hours, the supernatants were kept at -80ºC for later cytokine and chemokine measurement using the ProcartaPlex Multiplex Assay (Invitrogen). In the Multiplex Assay, 50 µl of supernatant was combined with a panel of beads that were covalently bound to an antibody that recognized one of the following cytokines/chemokines: IL-1β, IL-6, IL-8, IL-10, IL-13, GM-CSF, TNFα, TGF-β (transforming growth factor beta), CCL2 (Figure 17).

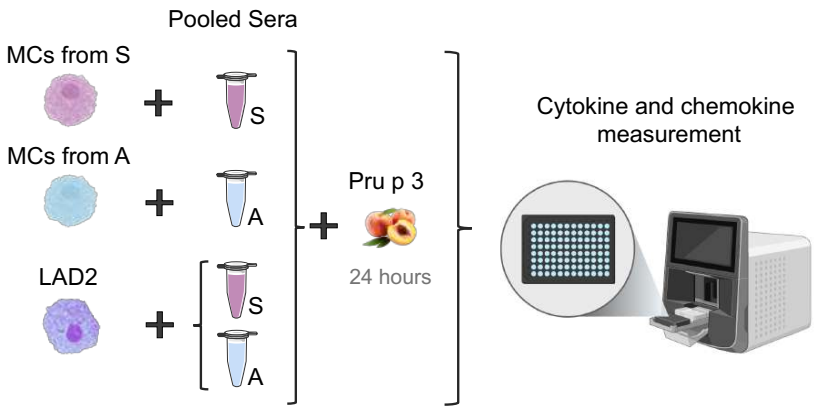

Figure 17. Methodology illustration of cytokine and chemokine multiplex assay. MCs from sensitized and anaphylactic patients were incubated overnight with their corresponding sera (sensitized or anaphylaxis, respectively). LAD2 cells were incubated with both pooled sera from LTP patients overnight. Then, cells were stimulated with Pru p 3 for 24 hours, and cytokine and chemokine were determined using a multiplex assay.

3. SPECIFIC METHODOLOGY FOR OBJECTIVE 2

3.1. RNA extraction and reverse transcription quantitative polymerase chain reaction (RT-qPCR)

$0.5x10^6$ CD34+-derived MCs from anaphylactic and sensitized patients were sensitized with their corresponding pooled sera (anaphylaxis and sensitized, respectively), and MCs from healthy donors were sensitized with sera from both LTP-allergic groups overnight. Then, cells were stimulated with Pru p 3 for 24 hours. After that, cells were pelleted, and RNA extraction was performed using miRNeasy micro kit (Qiagen, Venlo, Netherlands).

RNA from MCs from healthy donors was sent to Macrogen (Incheon, Republic of Korea) for RNA-sequencing. Libraries were sequenced in a 150-base pair paired-end format (140M reads) on Illumina's NovaSeq6000 using the TruSeq Stranded Total RNA Library Prep Gold Kit (Illuminia, San Diego, CA, USA).

RNA from MCs from patients was used to check some genes of interest by RT-qPCR due to the low quantity of DNA obtained. RNA extraction was followed by reverse transcription using the High-capacity cDNA reverse transcription kit (Applied Biosystems, Waltham, Mass, USA). After that, RT-qPCR of STIM1 and GUSB (Glucuronidasa-β, a constitutive gene, used to normalize the results) (all from Invitrogen) were performed in a MicroAmp Fast Optical 96-well Reaction Plate (Applied Biosystems) with a TaqMan Fast Advanced Master Mix (Applied Biosystems). The plate was read in a StepOne™ Real-Time PCR system (Thermo Fisher Scientific) (Figure 18).

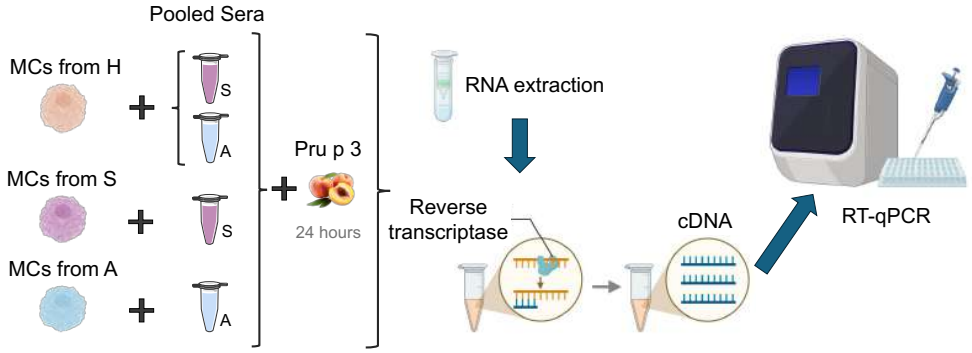

Figure 18. Methodology illustration of RT-qPCR. MCs from healthy donors were sensitized with both pooled sera from LTP patients (sensitized and anaphylaxis) overnight. MCs from sensitized and anaphylaxis patients were sensitized with their corresponding sera (sensitized and anaphylaxis, respectively) overnight. Then, cells were stimulated with Pru p 3 for 24 hours, and RNA extraction was performed, followed by cDNA reverse transcription and RT-qPCR of MITF, STIM1, and GUSB.

3.2. Fluidigm assay

CD34^{+}-derived MCs from peripheral blood from patients, healthy controls, and LAD2 were used to check the expression levels of some genes (listed in Table 3).

On the one hand, MCs from healthy volunteers and patients (sensitized and anaphylaxis) were sensitized with sera from the sensitized or anaphylaxis group. The next day, 1x10^5 cells were cultured in a 48-well plate and treated with 1 µg/ml Pru p 3 (Roxall) for 24 hours at 37ºC. On the other hand, MITF-

silenced LAD2 cells were incubated with 0.1 µg/ml biotinylated human IgE (Abbiotec) and stimulated with 0.4 µg/ml Streptavidin (STV) (Sigma-Aldrich) or 2 µM Substance P (Sigma-Aldrich) (Figure 19). Cell pellet was used to do the validations.

RNA extraction was performed using miRNeasy micro kit (Qiagen) and reverse transcription using the High-capacity cDNA reverse transcription kit (Applied Biosystems). cDNA samples were pre-amplified using PreAmp Master Mix (Izasa Scientific, Barcelona, Spain) and 24 Deltagene assays (Izasa Scientific), and RT-qPCR was performed to check GUSB (Invitrogen), a constitutive gene, to confirm the quality of cDNA. Then, pre-amplified cDNA samples were used to run a qPCR using a 196.24 dynamic array (Fluidigm Corporation, CA, USA) following the manufacturer's protocol (377,378). The 196.24 chip was placed in the BioMark instrument (Fluidigm Corporation) for PCR, and the data was analyzed with Real-Time PCR analysis software in the BioMark instrument (Fluidigm Corporation) (Figure 19).

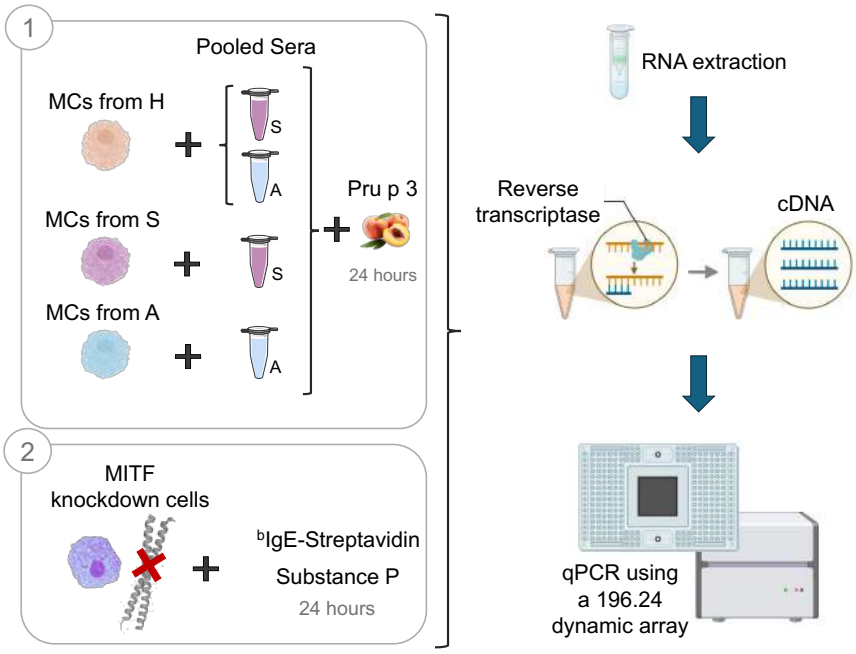

Figure 19. Methodology illustration of fluidigm assay. 1) MCs from healthy donors and patients were sensitized with pooled sera from LTP patients and stimulated with Pru p 3 for 24 hours. 2) LAD2 cells with MITF-inhibited, or MITF-silenced were stimulated with streptavidin or

substance P for 24 hours. After 24 hours, cells were pelleted, and RNA extraction was performed following a cDNA reverse transcription and qPCR by Fluidigm.

Table 3. List of genes used in Fluidigm.

Abbreviation	Description
B2M	Microglobulina beta 2
CCL18	CC Motif Chemokine Ligand 18
CCL2	CC Motif Chemokine Ligand 2
CMA	Chymase 1
COX2	Cyclooxygenase 2
COX4I1	Cytochrome C Oxidase Subunit 4I1
FcεR1A	Fc Epsilon Receptor 1a
GUSB	Glucuronidase beta
HDC	Histidine Decarboxylase
HINT1	Histidine Triad nucleotide binding protein 1
IL1B	Interleukin 1 beta
KARS	Lysyl-tRNA synthetase 1
MITF	Microphpthalmia associated transcription factor
MRGPRX2	Mas related GPR family member X2
NUDT2	Nudix Hydrolase 2
PPARGC1A	Peroxisome Proliferator Activated Receptor Gamma Coactivator 1 alpha
PTGER2	Prostaglandin E receptor 2
PTGER3	Prostaglandin E receptor 3
PTGER4	Prostaglandin E receptor 4
TGFB1	Transforming growth factor beta 1
TOMM20	Translocase of outer mitochondrial membrane 20
TPSAB1	Tryptase alpha/beta 1

All genes were from Deltagene (Izasa Scientific). To normalize all the results, B2M and GUSB were used as housekeeping genes, which are consistently expressed.

4. SPECIFIC METHODOLOGY FOR OBJECTIVE 3

4.1. Calcium release

$0.1x10^6$ transfected RBL-2H3 cells were sensitized overnight with 0.1 µg/ml dinitrophenyl-IgE (DNP-IgE, Sigma-Aldrich), washed and incubated with 2 µM Fluo-4 AM (Invitrogen) for 30 min before cell activation with 1 µg/ml DNP-Human Serum Albumin (DNP-HSA, Sigma-Aldrich), ionomycin, and ethylene glycol tetraacetic acid (EGTA) as described (169,379). Fluorescence was determined every 10 seconds using a TECAN SPARK microplate reader (Tecan Group, Mannedorf, Switzerland).

In parallel, LAD2 cells or primary cells were used to measure calcium influx when MITF was knockdown. LAD2 cells were treated with 5 µM ML329 (MedChem Express) or MITF shRNAs sequences for 5 days. After that, $0.1x10^6$ cells were sensitized with 0.1 µg/ml biotinylated human IgE (Abbiotec) overnight, washed and activated with 0.4 µg/ml STV (Sigma-Aldrich) or 2 µM SP (Sigma-Aldrich). Calcium influx was measured as mentioned above.

Finally, primary human MCs or skin human MCs were treated with MITF inhibitors, 5 µM ML329 or 10 µM TT012 (both from MedChem Express) or DMSO (ITW Reagents) as control, for 5 days. After that, $0.1x10^6$ cells were sensitized with 0.1 µg/ml biotinylated human IgE (Abbiotec) overnight, washed, and activated with 0.4 µg/ml STV (Sigma-Aldrich) or 2 µM SP (Sigma-Aldrich). Calcium influx was measured as mentioned above.

4.2. Cytokine and chemokine multiplex assay

MCs derived from peripheral blood and LAD2 cells were used to determine the mediator's release in a MITF-knockdown situation. LAD2 cells were treated with MITF inhibitors, 5 µM ML329 and 10 µM TT012 (both from MedChem Express) or DMSO (ITW Reagents) as control, or infected with MITF shRNAs (to silence MITF) for 5 days. $3x10^5$ cells were then cultured in a 96-well plate, sensitized with 0.1 µg/ml biotinylated human IgE (Abbiotec),

and stimulated with 0.4 µg/ml STV (Sigma-Aldrich) or 2 µM SP (Sigma-Aldrich) for 24 hours at 37ºC (Figure 20).

In parallel, treated LAD2 cells were also sensitized with both pooled sera from LTP patients (anaphylaxis and sensitized) overnight. Then, $3x10^5$ cells were cultured in a 96-well plate and stimulated with 1 µg/ml Pru p 3 (Roxall) for 24 hours at 37ºC (Figure 20).

Finally, MCs from patients (anaphylaxis and sensitized) were sensitized overnight with their corresponding pooled sera (anaphylaxis and sensitized, respectively). The next day, $1x10^5$ cells were cultured in a 96-well plate and treated with 1 µg/ml Pru p 3 (Roxall) for 24 hours at 37ºC (Figure 20).

After 24 hours, the supernatants were kept at -80ºC for later cytokine and chemokine measurement using the ProcartaPlex Multiplex Assay (Invitrogen). In the Multiplex Assay, 50 µl of supernatant was combined with a panel of beads covalently bound to an antibody that recognized one of the following cytokines/chemokines: IL-8, GM-CSF, CCL2. TGF-β was assessed only in some samples using a ProcartaPlex Simplex Assay (Invitrogen).

In addition, to study IL-8, GM-CSF, and CCL2 secretion in an IgE-independent pathway, we used ELISA kits from R&D Systems (Minneapolis, MN, USA). Thus, LAD2 cells were pre-treated with 5 µM TT012 (MedChem Express) or DMSO (ITW Reagents) for 1 hour, and then activated with 1.5 µM substance P, 250 or 500 µg/ml Vancomycin, 100 or 200 µg/ml Cisatracurium and, 10 or 50 µg/ml Morphine for 24 hours in the continued presence of TT012 or DMSO. Afterward, cells were centrifuged at 1500 rpm for 5 minutes at room temperature, and supernatants were kept at -80ºC for cytokine and chemokine measurements. IL-8, GM-CSF, and CCL2 ELISA kits were used following the manufacturer's recommendations. The same protocol was followed for the transfected RBL-2H3 cells, but only CCL2 secretion was measured.

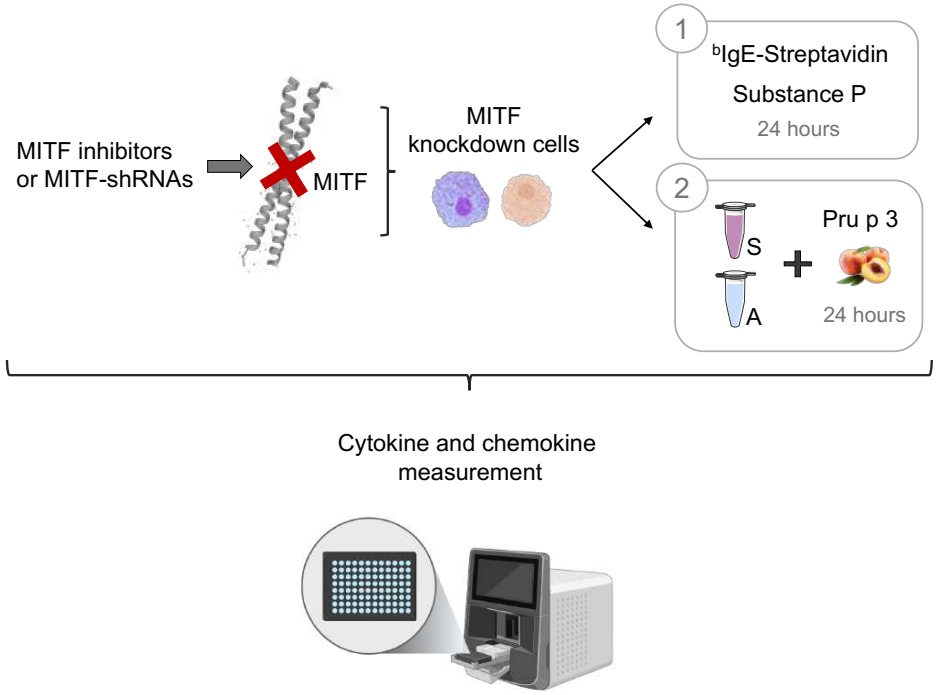

Figure 20. Methodology illustration of cytokine and chemokine multiplex assay in MITF-knockdown cells. LAD2 cells were treated with MITF inhibitors or MITF shRNAs, and CD34^{+}-derived MCs were treated with MITF inhibitors. After 5 days, MITF-knockdown LAD2 cells were first stimulated with streptavidin or substance P. Secondly, MITF-knockdown LAD2 cells or MCs were sensitized with pooled sera from LTP patients and stimulated with Pru p 3. After 24 hours of activation, cytokine and chemokine were determined by Luminex.

4.3. Luciferase assay

Firefly luciferase under the control of transcriptional regulation of TRPM1 and and control vector PGL3-luciferase were a gift from David Fisher (Harvard Medical School), and STIM1 promotor was a gift of Jonathan Soboloff (Institute for Cancer Research and Molecular Biology, Pennsylvania, USA). 1x10^{6} RBL-2H3 cells were transfected with the Firefly TRPM1 and the Renilla reporters at 10:1, respectively, in a reduced serum medium (Opti-MEM, Gibco). Transfections were performed using the AMAXA program T20 (Lonza Biosciences). In parallel, STIM1 was also used at a ratio of 15:1 with Renilla. After transfection, cells were incubated with 0.1 µg/ml DNP-IgE overnight in RPMI complete medium (as mentioned above, section 1.4) and 10 µM TT012 (MedChem Express) or DMSO (ITW Reagents). Then, cells were stimulated

for 6 hours with 1 µg/ml DNP-HSA (Sigma-Aldrich), and luciferase activity was measured using the Dual-Luciferase Reporter Assay system (Promega Corporation, Madison, Wis, USA) following the manufacturer's instructions (Figure 21). Firefly luciferase data were normalized according to Renilla luciferase data.

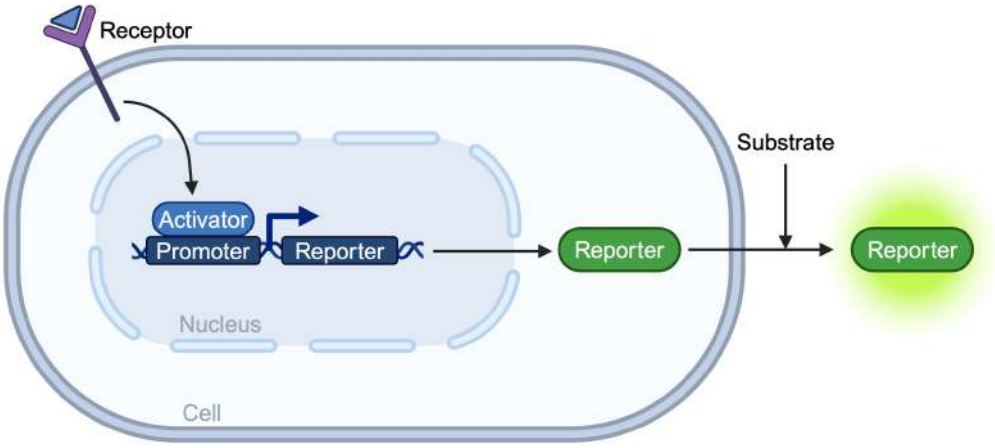

Figure 21. Methodology illustration of luciferase reporter gene assay. Firefly TRPM1 and STIM1 were used as promoters for the luciferase reporter gene. The addition of luciferase substrate produces a stabilized luminescent signal that can be measured. After quantifying the Firefly luminescence, the Renilla luciferase reaction is initiated by adding its substrate. This also makes a stabilized signal from Renilla luciferase that can be measured. Due to the different evolutionary origin, firefly and Renilla luciferases have different enzyme structure and substrate needs. For this reason, it is possible to differentiate its respective bioluminescence signals. Renilla promoter is used as a control due to its constitutive expression.

4.4. RNA-sequencing

LAD2 cells infected with MITF shRNA-2 were used to do transcriptomics. MITF-silenced in LAD2 cells were incubated with 0.1 µg/ml biotinylated human IgE (Abbiotec) and stimulated with 0.4 µg/ml STV (Sigma-Aldrich) or 2 µM SP (Sigma-Aldrich) for 30 minutes. Cells were pelleted, RNA extraction was performed using miRNeasy micro kit (Qiagen), and RNA was sent to the Centre for Genomic Regulation for RNA-sequencing. Libraries were sequenced in a 50 base pair paired-end format (50M reads) on Illumina's

NovaSeq6000 using the TruSeq Stranded Total RNA Library Prep Gold Kit (Illuminia, San Diego, CA, USA).

4.5. Transmission electronic microscopy

As mentioned above (section 1.7), LAD2 cells were infected with lentivirus to silence MITF. After 5 days of infection, cells were sensitized with 0.1 µg/ml biotinylated human IgE (Abbiotec) overnight were activated with 0.4 µg/ml STV (Sigma-Aldrich) or 2 µM SP (Sigma-Aldrich) for 30 min, washed with PBS, and pelleted. The pellet was fixed in 2.5% paraformaldehyde and 2.5% glutaraldehyde in 0.1 M phosphate buffer. Samples were processed for transmission electronic microscopy, and images were taken using a JEOL JEM 1010 100kv transmission electron microscope (TEM).

4.6. Mitochondria and ROS staining

Treated LAD2 cells, CD34-derived MCs, or skin MCs were sensitized with 0.1 µg/ml biotinylated human IgE (Abbiotec) overnight, washed, and activated with 0.4 µg/ml STV (Sigma-Aldrich) or 2 µM SP (Sigma-Aldrich) for 10 minutes at 37ºC. Then, cells were stained with Ghost Dye Violet (BioLegend), 50 nM mitotracker green (Thermo Fisher Scientific), and 25 nM mitotracker red (Thermo Fisher Scientific) for 15 minutes at 37ºC as described (380). Cells were acquired on a FACSFortessa 5L flow cytometer (FACScan; BD Biosciences) and analyzed using FlowJo software version 7. In parallel, treated LAD2 cells were stained with 5 µM CellROX green (Thermo Fisher Scientific) for 30 minutes at 37ºC, washed, and acquired on a CytoFlex flow cytometer (Beckman Coulter, Pasadena, CA, USA). Cells were analyzed using CytoExpert software (Beckman Coulter).

For RBL-2H3, cells were sensitized with 0.1 µg/ml DNP-human IgE (Sigma-Aldrich) overnight, washed, and activated with 1 µg/ml DNP-HSA (Sigma-Aldrich) for 10 minutes at 37ºC. Then, cells were incubated with anti-TOM20 (ProteinTech) primary antibody and stained with Ig-Alexa Fluor 647 (BioLegend) as a secondary antibody and 10 nM mitotracker red (Thermo Fisher Scientific). Finally, cells were stained with DAPI (Thermo Fisher

Scientific), acquired on a FACSFortessa 5L flow cytometer (FACScan; BD Biosciences), and analyzed using FlowJo software version 7.

To measure ROS production in LAD2 cells sensitized with pooled sera from patients and stimulated with the allergen, LAD2 cells were incubated with 10 µg/ml rh IL-4 (Immunotools) for 5 days, sensitized overnight with pooled sera from healthy volunteers, sensitized group and anaphylaxis group, and stimulated with 1 µg/ml Pru p 3 (Roxall) for 3 days. After that, cells were stained with 5 µM CellROX green (Thermo Fisher Scientific) for 30 minutes at 37ºC, washed, and acquired on a CytoFlex flow cytometer (Beckman Coulter, Pasadena, CA, USA). Cells were analyzed using CytoExpert software (Beckman Coulter).

4.7. Mitochondrial Respiration measurement

Oxygen consumption rates (OCR) were measured by Seahorse XFe-24 Flux analyzer (Agilent, Santa Clara, CA, USA). LAD2 cells (treated with ML329 from MedChem Express or MITF shRNA-2), RBL-2H3 (GFP, LysRS-WT or LysRS-P542R transfected cells) or primary mast cells were used to evaluate the mitochondrial respiration as described previously (381–383).

First, the day before the assay, the sensor cartridge was hydrated with Seahorse XF Calibrant (Agilent) at 37ºC in a non-CO^2 incubator overnight. Also, the culture 24-well plate (Agilent) was coated with 100 µl of Poly-D-Lysine (Gibco) and incubated overnight at 37ºC. Then, the culture plate was washed twice using the XF RPMI medium PH 7.4 (Agilent) supplemented with 10 mM glucose (Sigma-Aldrich), 2 mM sodium pyruvate (Sigma-Aldrich), and 2 mM L-glutamine (Gibco). Afterward, $1.5x10^5$ treated LAD2 cells were seeded into the coated plate with XF RPMI complete medium. In parallel, the injection compounds were loaded into the sensor cartridge. Then, cells were incubated at 37ºC without CO_2 for 30 minutes while the Seahorse XFe-24 Flux analyzer calibrated the sensor cartridge. Finally, cells were loaded onto the equipment for mitochondrial respiration analysis using the Mito Stress test. The same protocol was followed with the transfected RBL-2H3 cells, but as

this cell line is adherent, the cells were seeded the day before the assay into the 24-well plate.

For the Mito Stress test, energy consumption was decreased by 1.5 µM oligomycin (Cayman Chemical), an ATP synthase (complex V) inhibitor. After that, 1.5 µM carbonyl cyanide-4 (trifluoromethoxy) phenylhydrazone (FCCP, Cayman Chemical) was added to induce the maximum respiration because it's an uncoupling agent that collapses the proton gradient and disrupts the mitochondrial membrane potential. Finally, 0.5 µM rotenone and antimycin (both from Sigma-Aldrich) were added, inhibitors of complex I and III, respectively, to stop the mitochondrial respiration (Figure 22).

To assess mitochondrial respiration in LAD2 cells sensitized with sera from healthy volunteers and LTP patients, LAD2 cells were incubated for 5 days with 10 µg/ml rh IL-4 (Immunotools). The day before the assay, cells were incubated overnight with pooled sera (with the same amount of sIgE). Then, cells were washed and seeded into the culture 24-well plate, previously coated with Poly-D-Lysine, and loaded into the Seahorse XFe-24 Flux analyzer. In this case, the first injection was 1 µg/ml Pru p 3 (Roxall), and OCR was determined every 5 minutes for 45 minutes, followed by oligomycin, FCCP, rotenone, and antimycin. The same protocol was followed with MCs from a healthy volunteer and LTP patients.

In parallel to the Mito Stress test in MCs from a healthy volunteer and LTP patients, a Glycolytic test was performed. The assay preparation was the same as for the Mito Stress test, but the sensor cartridge was loaded with different compounds to check glycolysis. For the Glycolytic test, as we did before, 1 µg/ml Pru p 3 (Roxall) was injected, and OCR was determined every 5 minutes for 45 minutes. Then, 0.5 µM rotenone and antimycin were injected to inhibit mitochondrial oxygen consumption. Afterward, a 50 mM glucose analog (2-deoxy-D-glucose (2-DG)) was added to inhibit glycolysis through its binding competition for glucose hexokinase (the first enzyme in the glycolytic pathway) to know the total glycolysis rate (Figure 22).

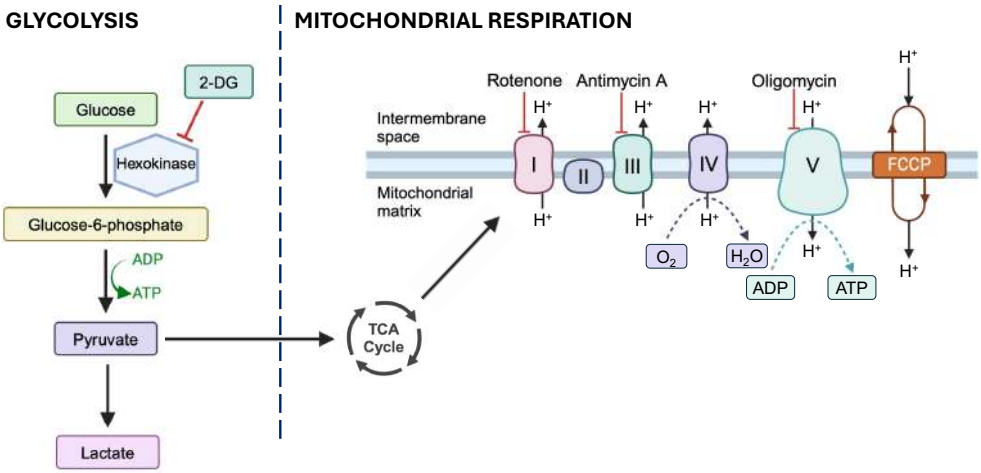

Figure 22. Scheme of cell metabolism pathways. Principles of the Agilent Seahorse XF glycolytic rate test and Mito Stress test. Seahorse is used to determine the respiration of our cells. TCA= Tricarboxylic acid.

5. RESULTS ANALYSIS

5.1. Statistical Analysis

Statistical analysis was performed using PRISM 10 (GraphPad Software, La Jolla, CA, USA). All results are expressed as mean ± standard deviation (SD). After determining the normal distribution of the samples and variance analysis, one-way or Two-way ANOVA (depending on variables) was used to determine significant differences (p-value) between several experimental groups.

5.2. Bioinformatics Analysis

Dreamgenics S.L. (Asturias, Spain) performed the bioinformatics analysis. First, raw FASTQ files were evaluated using FastQC quality checks, and sequence trimming was performed to remove bases, adapters, and other low-quality sequences with fastp software. Next, pseudo-alignment of the sequences against the reference transcriptome for Homo sapiens GRCH38.p14 (Gencode: release 44) and direct quantification of transcripts were carried out using Salmon (v1.10.0). For differential expression analysis

between conditions, the DESeq2 algorithm was used; said analysis was carried out considering both the p-value and the adjusted p-value, using the Benjamini-Hochberg method for adjusting the p-value. Genes with a p-value or adjusted p-value less than 0.05 and a log2FoldChange greater than 1 or less than -1 were considered differentially expressed. Finally, an enrichment study of biological pathways from the Wiki-pathways repository and GO terms (Biological Process, Cellular Component, and Molecular Function) was carried out using the GSEA (Gene Set Enrichment Analysis) algorithm.

RESULTS

1. DEVELOP AN *IN VITRO* MODEL TO ASSESS SEVERITY IN LTP PATIENTS

FA is a pathological immune response triggered by innocuous food protein antigens. LTP is a pan-allergen present in several plant foods (vegetables, fruits, legumes, nuts, seeds…) and is the leading cause of food allergy in adults in the Mediterranean area (384,385). In the last decades, the incidence of food anaphylaxis has increased at a critical rate, and its risk is unpredictable (281,386,387). FA diagnosis is frequently challenging due to the difficulties in differentiating between sensitization and true allergy (388–390).

In recent years, since MCs are considered the primary effector cells of allergy (343), an MC activation test was developed and has already improved the diagnosis of IgE-mediated peanut allergy (54,330).

In this first objective we wanted to identify factors that may differentiate patients at risk of anaphylaxis from those only sensitized. In two opposite phenotypes of LTP-sensitized individuals, i.e., patients with food anaphylaxis and sensitized individuals (with no symptoms), we compared peach-induced (Pru p 3) – the main allergen of LTP – MC activity *in vitro* to understand the FA's molecular and cellular bases.

1.1. Study population and patient characteristics

Patients were recruited at the Allergy Department of the Hospital Clínic of Barcelona. Informed consent was obtained from all participating subjects. The study was approved by the local ethics committee of the Hospital Clinic (Barcelona, Spain).

Patients sensitized to peach LTP-Pru p 3 with sIgE levels (281) 0.10 KU_A/L (ImmunoCAP®, Thermo Fisher Scientific, Uppsala, Sweden), and with no other sensitizations identified, including profilins, homologs of Bet v 1, thaumatin-like proteins, gibberellins, tropomyosin or other general storage proteins, were recruited. They were classified into two groups depending on

the reaction severity upon peach ingestion: (1) anaphylaxis patients – individuals with a convincing history of anaphylaxis and (2) sensitized patients – individuals with no symptoms. The oral challenge was not performed in anaphylaxis patients (391), and a recent history of tolerance to peach was required in the sensitized group. Healthy volunteers with no respiratory or food allergies were also recruited as controls.

To carry out this study, the patients and healthy volunteers recruited were divided into two cohorts to develop the different *in vitro* studies: (1) a cohort to generate pooled sera for MC activation, PGD_2 secretion, and cytokine analysis assays and (2) a second cohort to generate MCs and to detect $T_{FH}13$ (Figure 23).

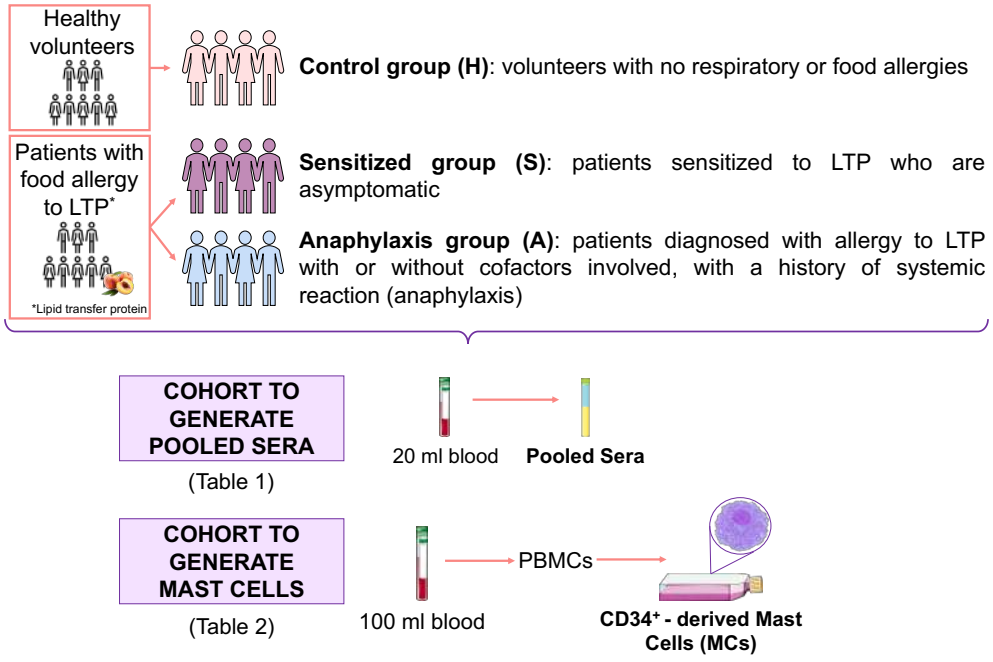

Figure 23. Study populations. The LTP patients and healthy volunteers recruited were divided into two cohorts: one cohort to generate pooled sera for mast cell activation, PGD_2 secretion, and cytokine analysis assays and another cohort to generate MCs and detect $T_{FH}13$.

The characteristics of the patients recruited to obtain (1) serum to create pooled sera (2) $CD34^+$-derived MCs and $T_{FH}13$ are listed in Annex Table 1 and Annex Table 2, respectively.

sIgE values were higher in anaphylaxis than in sensitized patients (19.80 KUA/L and 0.98 KUA/L, respectively); however, the total IgE/specific-IgE ratio (tIgE/sIgE) was higher in sensitized patients (Annex Table 1). The specific IgG4 and IgE ratio (sIgG4/sIgE) was also higher in the anaphylaxis group than in the sensitized group (8.59 and 2.13, respectively) (Annex Table 1). The baseline serum tryptase levels of the patients were measured to rule out tryptasemia (Annex Table 2).

1.2. Sera from anaphylaxis patients induce stronger degranulation and PGD_2 production in $CD34^+$-derived MCs after Pru p 3 stimulation

MCs from patients and healthy volunteers were differentiated ($CD117^+$/$Fc\varepsilon RI^+$) *in vitro* after seven weeks (Supplementary Table 1), and their ability to degranulate to positive stimuli (PMA + Ionomycin and biotinylated IgE plus Streptavidin) was confirmed (Supplementary Figure 1).

MCs from healthy individuals and sensitized and anaphylaxis patients were incubated overnight with pooled sera from healthy controls, anaphylaxis, or sensitized patients. The serum volume was corrected by the sIgE values. Afterward, cells were incubated with Pru p 3 for 30 minutes, and the surface expression of $CD63^+$ was measured using flow cytometry.

MCs from all three groups - healthy controls, anaphylaxis, and sensitized patients - had significantly higher activation when sensitized with pooled anaphylaxis sera, compared with pooled sera from healthy volunteers or sensitized patients (Figure 24A, B, and C, respectively). Sera from sensitized patients induced similar degranulation in healthy individuals. Sera sensitization without Pru p 3 challenge did not activate cells, measured as CD63 expression (Supplementary Table 2).

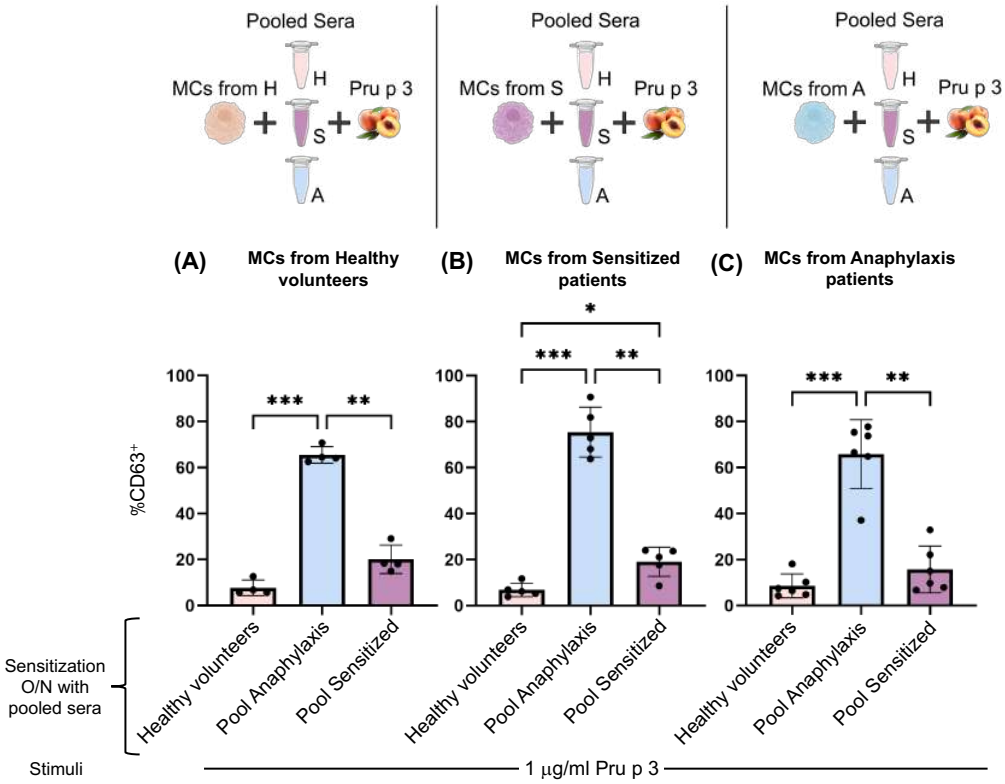

Figure 24. Anaphylaxis sera induce greater MC degranulation. Degranulation measured by CD63 expression was performed in primary mast cells from patients and healthy volunteers. A) MCs from healthy volunteers, B) MCs from sensitized patients, and C) MCs from anaphylaxis patients. MCs were sensitized overnight with pooled sera and stimulated with 1 µg/ml of Pru p 3. Results are expressed as mean ± SD. Significance was determined using one-way ANOVA with Tukey's multiple comparison analysis. P<0.05 was considered statistically significant. *P<0.05; **P<0.01; ***P<0.001. H=Healthy volunteers; A=Anaphylaxis; MC=Mast cell; O/N=Overnight; S=Sensitized.

Next, we aimed to confirm our results by analyzing PGD_2 release under the same conditions. Again, MCs from all three groups, healthy controls, anaphylaxis, and sensitized patients, had a higher PGD_2 production when incubated with pooled anaphylaxis sera compared with pooled healthy volunteers or sensitized sera (Figure 25A, B, and C, respectively). However, it was only significant for MCs from sensitized and anaphylaxis patients, not from healthy individuals. Finally, a significant correlation between degranulation ($CD63^+$) and PGD_2 synthesis was observed in all groups (Supplementary Figure 2).

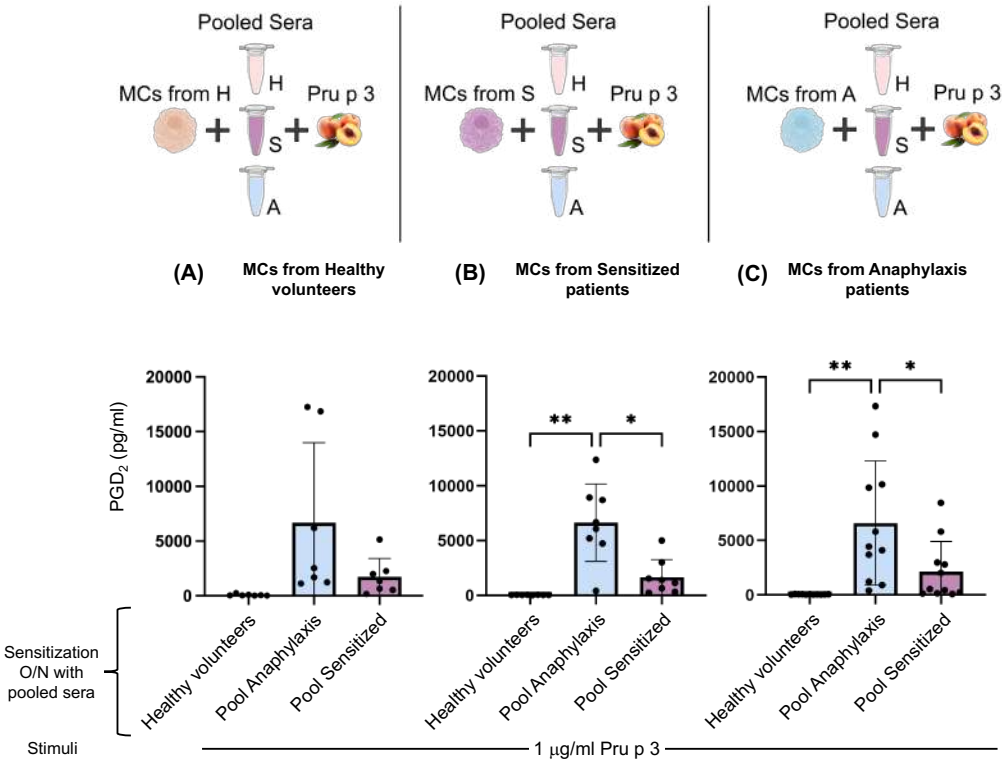

Figure 25. Anaphylaxis sera induce higher PGD_2 secretion. PGD_2 secretion was performed with mast cells from patients and healthy donors. A) MCs from healthy volunteers. B) MCs from sensitized patients. C) MCs from anaphylaxis patients. PGD_2 was measured in post-activation supernatant. Results are expressed as mean ± SD. Significance was determined using one-way ANOVA with Tukey's multiple comparison analysis. P<0.05 was considered statistically significant. *P<0.05; **P<0.01. H=Healthy volunteers; A=Anaphylaxis; MC=Mast cell; O/N=Overnight; S=Sensitized.

1.3. Sera from anaphylaxis patients induce more robust activation in LAD2 cells after Pru p 3 stimulation

We performed the same experiments using LAD2 cells to correct the potential effect of MC phenotype on activation and to reproduce our observations in a different MC model. LAD2 cells sensitized with pooled sera from anaphylaxis patients showed significantly higher degranulation than those incubated with sera from healthy and sensitized individuals (Figure 26A). Furthermore, by WB, we analyzed the intracellular activation pattern after incubation with sera

from the different groups and activation with Pru p 3 in the LAD2 model. The adaptor protein LAT is critical in FcεRI signaling in MCs, linking the IgE high-affinity receptor to calcium influx and degranulation (392). LAD2 cells were sensitized with pooled sera 1:1 overnight and stimulated with 2 µg/ml of Pru p 3. The reaction was stopped at time 0 seconds, 30 seconds, and 2 minutes, and then cells were lysed and WB was performed. As shown in Figure 26B, a pattern of phosphotyrosine proteins was induced, with increased LAT phosphorylation in anaphylaxis patients compared with sensitized patients, in agreement with the higher degranulation (Figure 26A).

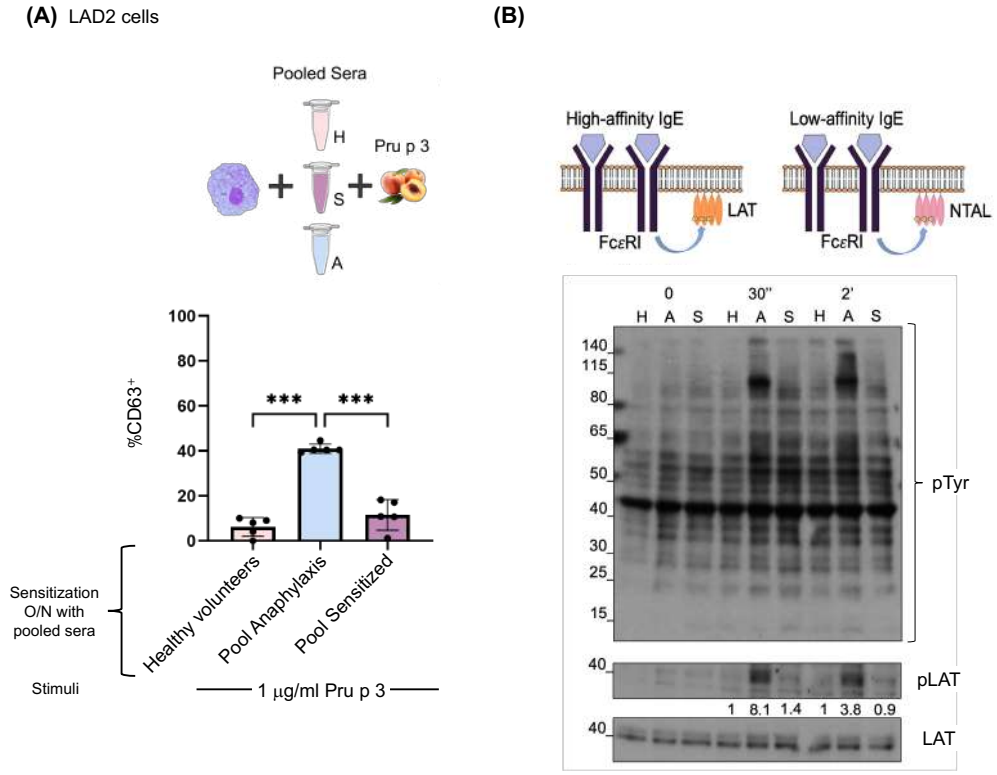

Figure 26. Anaphylaxis sera induce higher LAD2 activation. A) Degranulation measured by CD63 was performed with LAD2 cells sensitized overnight with pooled sera and stimulated with 1 µg/ml Pru p 3 for 30 seconds and 2 minutes. Results are expressed as mean ± SD. Significance was determined using one-way ANOVA with Tukey's multiple comparison analysis. P<0.05 was considered statistically significant. *P<0.05; **P<0.01. B) Western blot of LAD2 cells sensitized overnight with pooled sera and stimulated with 2 µg/ml Pru p 3. pTyr=phospho-Tyrosine; pLAT=phospho-LAT; LAT=Total LAT; H=Healthy volunteers; A=Anaphylaxis; S=Sensitized; O/N=Overnight.

1.4. $T_{FH}13$ cells are more abundant in anaphylaxis patients

Our results showed the marked ability of sIgE in the anaphylaxis pool to yield greater MC degranulation. Recently, $T_{FH}13$ cells have been found to regulate the induction of high-affinity IgE (324). Thus, we investigated the presence of the $T_{FH}13$ population in PBMCs following the gating strategy shown in Supplementary Figure 3 and previously described (323).

We observed that patients from the anaphylaxis group showed a significantly higher number of $T_{FH}13$ cells than the other groups. Sensitized patients presented similar results to healthy individuals. Indeed, we identified a significant correlation between degranulation ($CD63^+$) and the presence of $T_{FH}13$ (Figure 27).

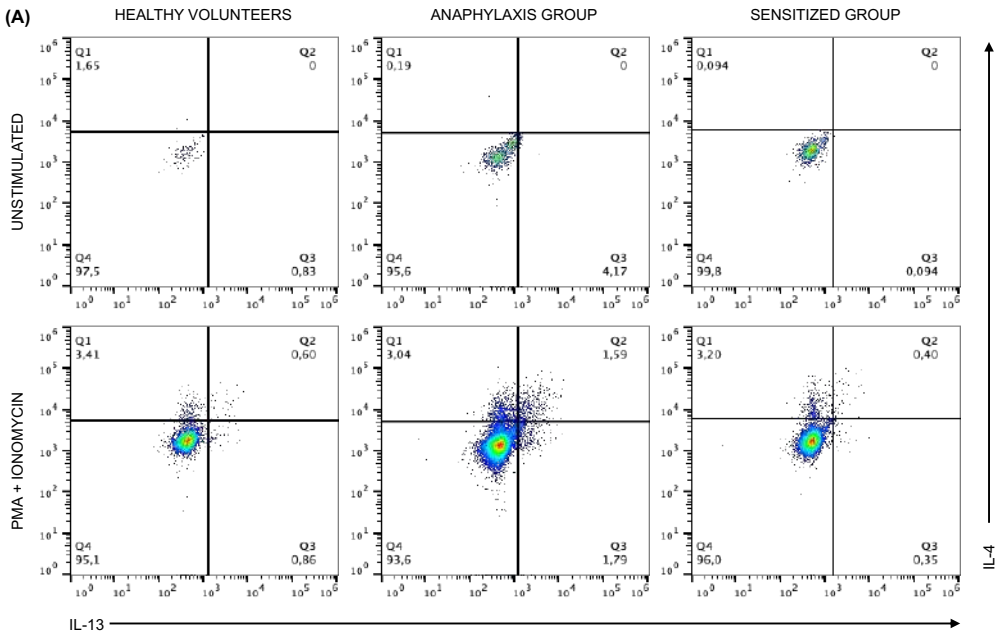

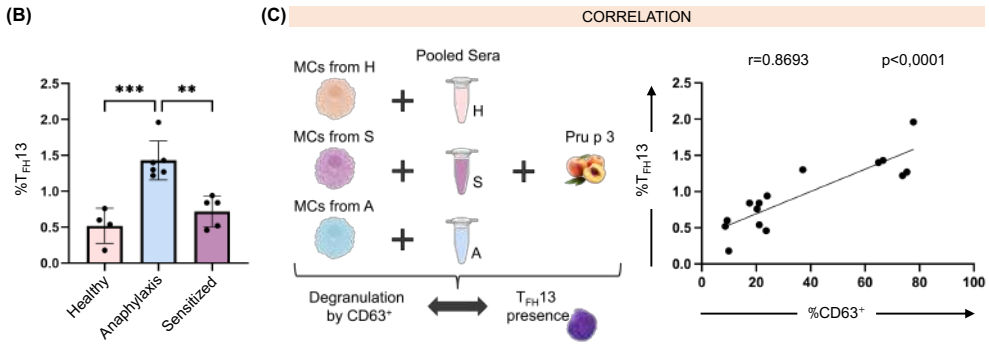

Figure 27. $T_{FH}13$ cells are more abundant in anaphylaxis patients. A) IL-4 and IL-13 intracellular staining in a healthy volunteer, an anaphylaxis patient, and a sensitized patient with or without PMA/ionomycin stimulation (Gated as in Supplementary Figure 3). B) $T_{FH}13$ cells in healthy volunteers, anaphylaxis, and sensitized patients. C) Correlation between degranulation and the percentage of $T_{FH}13$ cells. Results are expressed as mean ± SD. Significance was determined using one-way ANOVA with Tukey's multiple comparison analysis. Correlations were calculated by using Pearson R values. P<0.05 was considered statistically significant. ***P<0.001; ****P<0.0001. H=Healthy volunteers; A=Anaphylaxis; S=Sensitized; MC=Mast cell.

1.5. Analysis of *de novo* mediators release in LTP patients

Thus, in this study, we found that MCs from the anaphylaxis group incubated with pooled anaphylaxis sera produced more significant amounts of IL-8 and GM-CSF (Figure 28A). Thus, they had a higher pro-inflammatory profile than MCs from the sensitized group incubated with pooled sensitized sera. Interestingly, MCs from the sensitized group incubated with pooled sensitized sera produced more TGF-β and CCL2 (Figure 28C), inducing a more protective profile. While we did not find significant differences between groups for the other cytokines (IL-1β, IL-6, IL-10, IL-13, and TNF-α) studied, there was a trend. MCs with pooled anaphylaxis sera produce more cytokines (IL-1β, IL-6, IL-13, and TNF-α) than those incubated with pooled sera from sensitized patients. In contrast, MCs with pooled sensitized sera produce more IL-10 (Supplementary Figure 4).

Similarly, when LAD2 cells were incubated with pooled sera from anaphylaxis patients or with biotinylated human IgE and activated with Pru p 3 or Streptavidin, respectively, they produced more IL-8 and GM-CSF (Figure

28B). Conversely, when LAD2 cells were incubated with pooled sera from sensitized patients and activated with Pru p 3, they produced more TGF-β and CCL2 (Figure 28D).

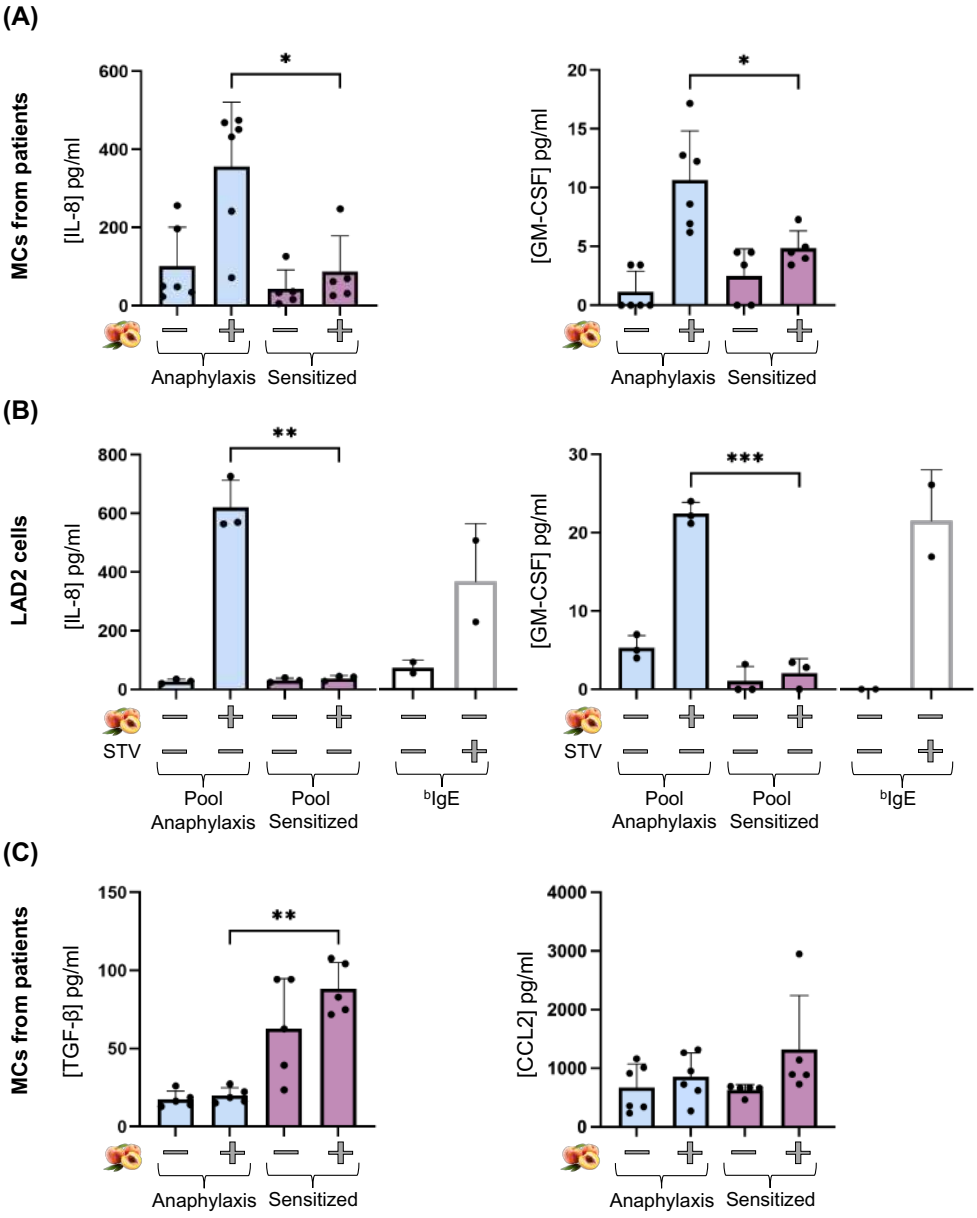

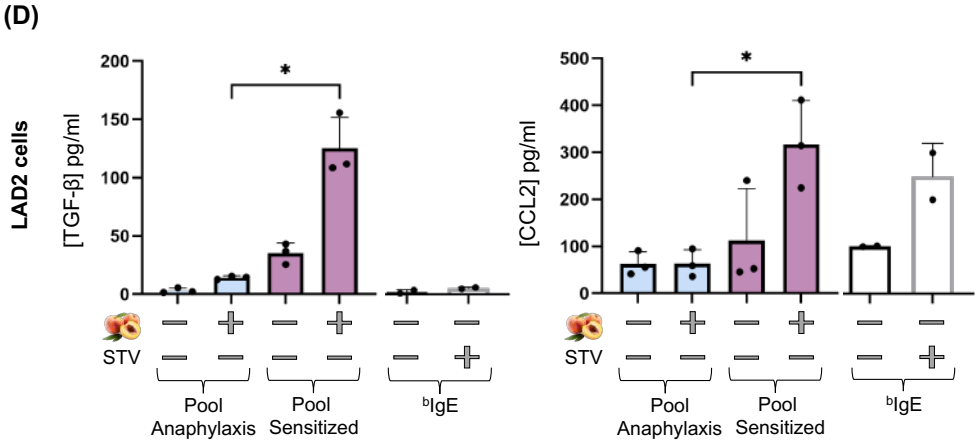

Figure 28. Sera from anaphylaxis patients induce higher pro-inflammatory patterns. A cytokine multiplex assay was performed in MCs from patients and LAD2 cells. A) Pro-inflammatory cytokines in CD34^{+}-derived MCs from anaphylaxis and sensitized patients. B) Pro-inflammatory cytokines in LAD2 cells. C) Anti-inflammatory cytokines in CD34^{+}-derived MCs from anaphylaxis and sensitized patients. B) Anti-inflammatory cytokines in LAD2 cells. Results are expressed as mean ± SD. Significance was determined using a t-test with Welch's correction. P<0.05 was considered statistically significant. *P<0.05; **P<0.01; ****P<0.0001. A=Anaphylaxis; S=Sensitized. ^{b}IgE=biotinylated human IgE; STV=Streptavidin; MC=Mast cell.

1.6. Results Summary

Our results show that serum samples from anaphylaxis patients induce distinguishable MC activation patterns. The $T_{FH}13$ cell population is more abundant in anaphylaxis patients than in sensitized individuals, suggesting their potential use as a risk biomarker of severity.

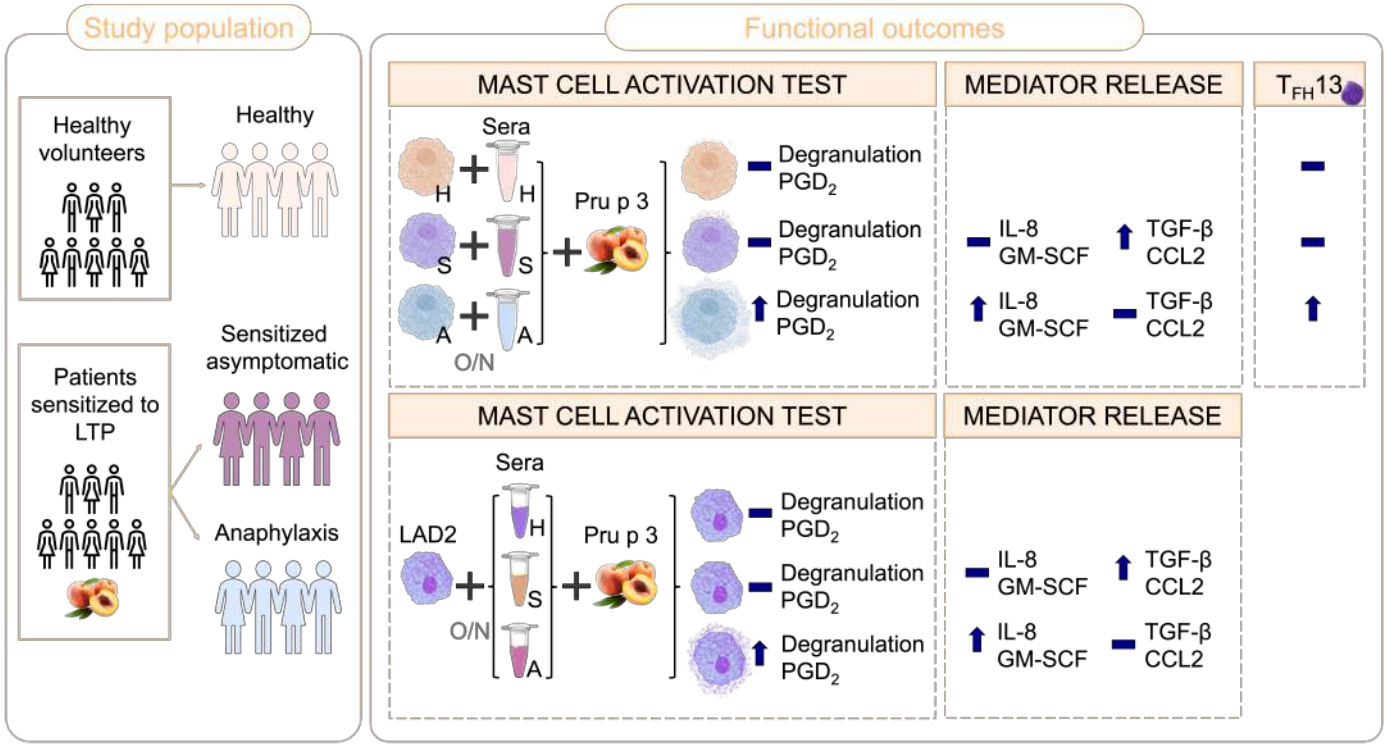

Results Summary 1. Summary of all the data obtained in this first objective. A=Anaphylaxis patients; H=Healthy volunteers; LTP=Lipid Transfer protein; O/N=Overnight; S=Sensitized asymptomatic patient.

1.7. Supplementary Figures and Tables

Supplementary Table 1. CD34^{+}-derived MC characterization.

Group	Subject ID	Number of cells	KIT+ expression	FcεRI+ expression	Viability
Anaphylaxis	1	540000	77.00%	63.50%	70.00%
	2	830000	95.70%	59.80%	72.30%
	3	2000000	64.70%	71.80%	84.50%
	4	500000	95.70%	53.50%	73.30%
	5	300000	64.30%	69.10%	85.00%
	6	1500000	91.50%	86.10%	80.00%
	Mean	945000	81.48%	67.30%	77.52%
Sensitized	7	690000	75.80%	80.80%	74.40%
	8	500000	70.20%	64.20%	80.00%
	9	5000000	75.20%	47.20%	80.00%
	10	2000000	84.80%	86.90%	80.50%
	11	500000	81.30%	57.90%	71.00%
	Mean	1738000	77.46%	67.40%	77.18%
Healthy	12	2000000	95.80%	75.30%	78.00%
	13	2000000	64.60%	52.90%	83.00%
	14	1000000	94.80%	67.50%	70.00%
	15	500000	64.50%	74.90%	85.00%
	Mean	1375000	79.93%	67.65%	79.00%

Characteristics of CD34^{+}-derived MCs from each group of patients (anaphylaxis, sensitized, and healthy volunteers).

Supplementary Table 2. Raw data of the mast cell activation test.

Group	Subject ID	Stimuli	Pooled sera		
			Healthy volunteers	Anaphylaxis	Sensitized
Anaphylaxis	1	Sera	4.0%	5.6%	0.0%
		Sera + Pru p 3	4.3%	73.7%	6.7%
	2	Sera	4.5%	5.2%	0.0%
		Sera + Pru p 3	5.0%	75.3%	22.1%
	3	Sera	2.0%	5.3%	0.0%
		Sera + Pru p 3	4.7%	37.1%	14.9%
	4	Sera	6.2%	7.6%	0.0%
		Sera + Pru p 3	7.6%	66.6%	9.7%
	5	Sera	7.0%	5.9%	0.0%
		Sera + Pru p 3	7.4%	64.9%	7.8%
	6	Sera	7.8%	7.1%	0.0%
		Sera + Pru p 3	10.1%	77.7%	32.9%
Sensitized	7	Sera	0.0%	4.1%	0.1%
		Sera + Pru p 3	3.8%	72.9%	23.6%
	8	Sera	6.6%	4.8%	0.0%
		Sera + Pru p 3	6.9%	90.7%	21.1%
	9	Sera	0.0%	4.8%	0.1%
		Sera + Pru p 3	6.1%	81.9%	17.6%
	10	Sera	7.3%	5.0%	0.0%
		Sera + Pru p 3	11.6%	63.8%	24.0%
	11	Sera	3.1%	4.2%	0.0%
		Sera + Pru p 3	5.3%	68.1%	8.6%
Healthy volunteers	12	Sera	5.0%	5.5%	0.0%
		Sera + Pru p 3	5.6%	62.6%	14.9%
	13	Sera	4.8%	7.4%	0.1%
		Sera + Pru p 3	6.8%	64.5%	29.1%
	14	Sera	3.0%	4.9%	0.0%
		Sera + Pru p 3	5.7%	70.8%	18.0%
	15	Sera	2.0%	5.7%	0.0%
		Sera + Pru p 3	4.1%	64.1%	18.4%

MCs were incubated overnight with different pooled sera (Anaphylaxis, Sensitized, and Healthy volunteers), washed, and activated with Pru p 3.

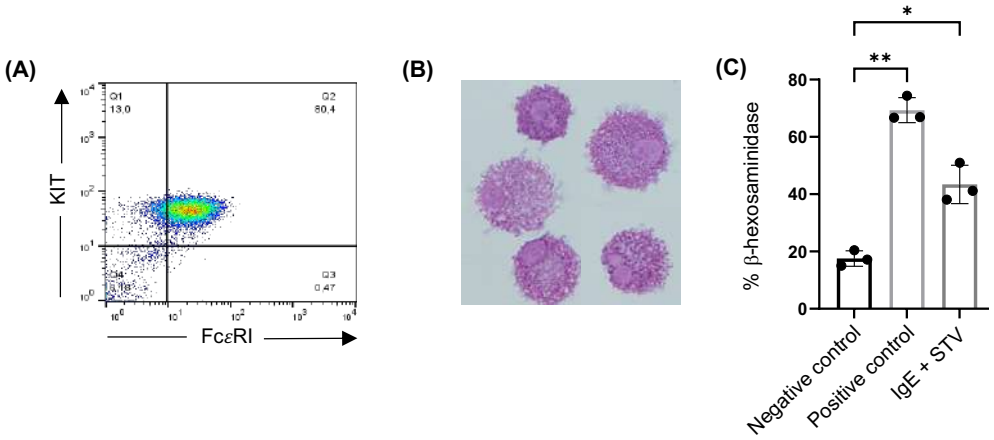

Supplementary Figure 1. CD34⁺-derived mast cells characterization. A) FcεRI and KIT expression of MCs after seven weeks. B) May Grünwald Giemsa staining of MCs. C) Degranulation measured by β-hexosaminidase assay. PMA and Ionomycin were used as a positive control (n=3). Results are expressed as mean ± SD. Significance was determined using one-way ANOVA with Dunkey's multiple comparison analysis. P<0.05 was considered statistically significant. *P<0.05; **P<0.01. The figure shows a representative example. STV=Streptavidin.

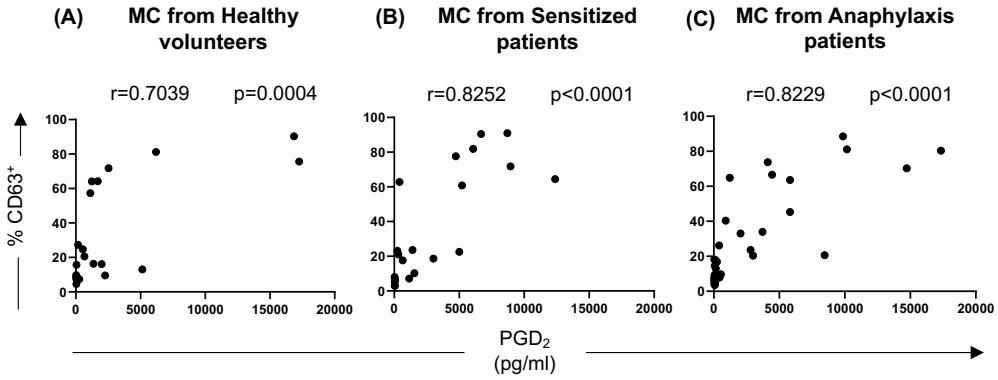

Supplementary Figure 2. Correlation between degranulation by CD63⁺ and PGD_2 secretion. A) MCs from healthy volunteers. B) MCs from sensitized patients. C) MCs from anaphylaxis patients. Correlations were calculated by using Pearson R values. P<0.05 was considered statistically significant.

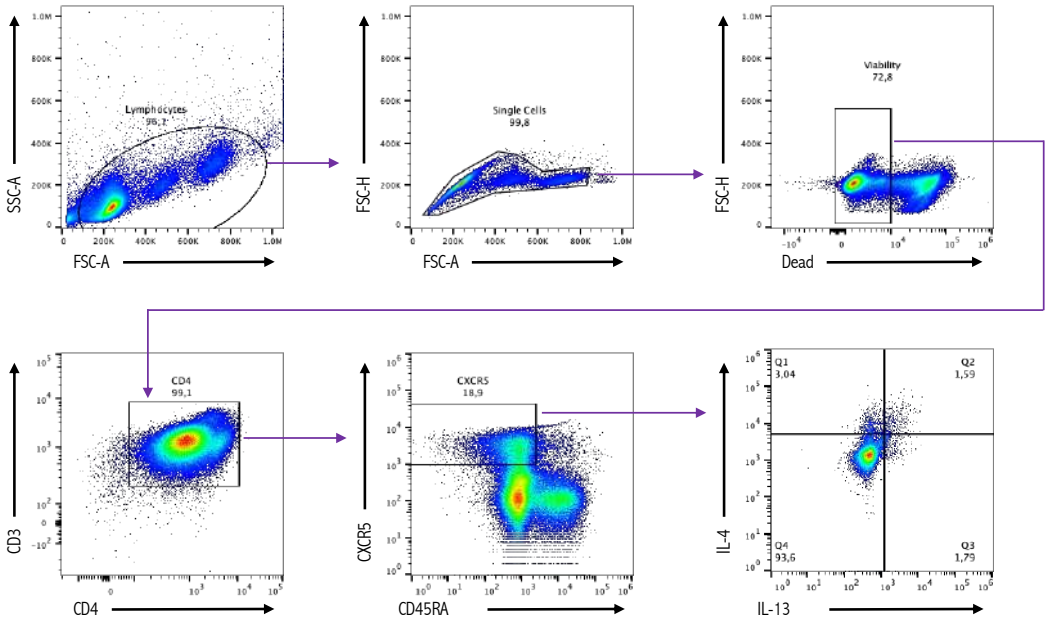

Supplementary Figure 3. Gating strategy for T_{FH}13 cells. Representative flow pot of PBMCs from an LTP-allergic patient stimulated with PMA and Ionomycin.

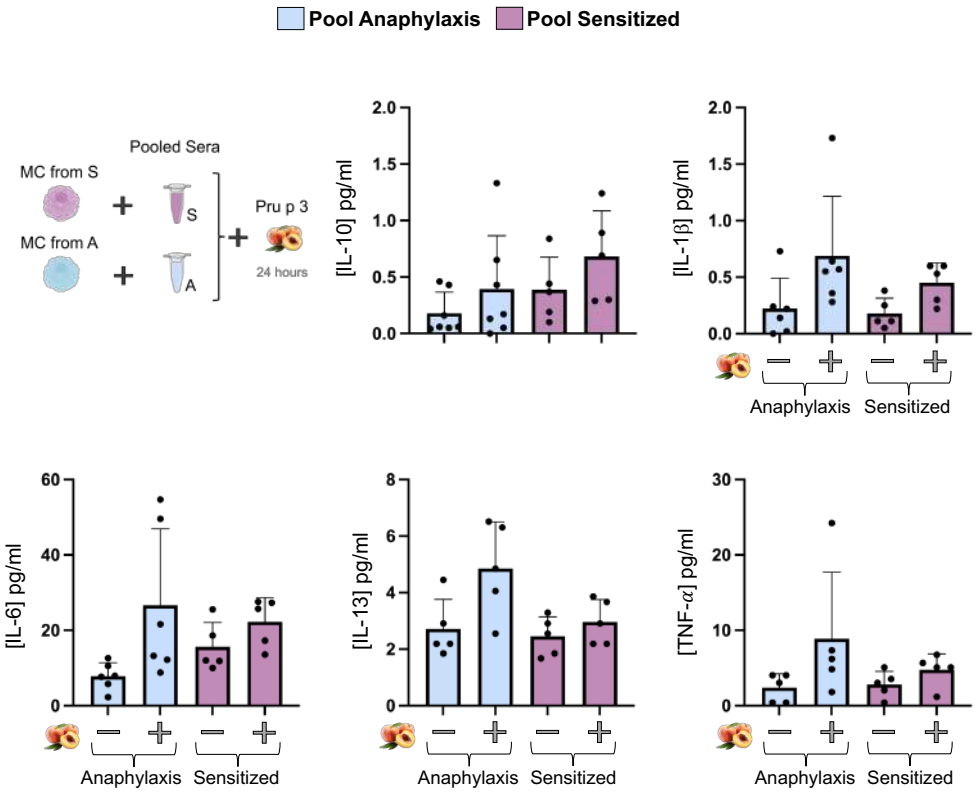

Supplementary Figure 4. Sera from anaphylaxis patients induce a higher pro-inflammatory cytokine secretion. A cytokine multiplex assay was performed in CD34^{+}-derived MCs from anaphylaxis and sensitized patients. Results are expressed as mean ± SD. Significance was determined using a T-test with Welch's correction. P<0.05 was considered statistically significant. A=Anaphylaxis; S=Sensitized; MC=Mast cell.

2. IDENTIFICATION OF NEW BIOMARKERS TO DISCRIMINATE BETWEEN SENSITIZATION AND ALLERGY IN AN LTP-MODEL

Our previous study concluded that MC activation profile analysis may discriminate patients at risk of developing anaphylaxis from those merely sensitized. Interestingly, in our model, we found that the humoral component is far more critical than the cellular one in inducing MC degranulation and PGD_2 production, given that when LAD2 cells were used instead of $CD34^+$-derived MCs from patients, the activation/degranulation patterns were unaltered. Besides, the presence of $T_{FH}13$ cells in anaphylaxis patients points to an essential role of IgE affinity. This is why we wanted to delve into distinguishing the mechanisms induced by the humoral component by performing a transcriptomic analysis of MCs from buffy coat preparations (MC_{BC}) or LAD2 cells sensitized with pooled sera from sensitized and anaphylaxis patients and stimulated with Pru p 3 for 24 hours. A full heatmap and a volcano plot of the genes that are significantly upregulated and downregulated are shown in Supplementary Figure 5. For more detailed results, view ANNEX II, which contains the raw analysis data.

With GSEA, we found in both MCs and LAD2 cells sensitized with sera from sensitized patients, a significant downregulation of senescence (senescence-associated secretory phenotype, SASP) and NF1 (neurofibromin-1) copy variation syndrome. This is related to many cellular processes, such as proliferation and migration, due to its involvement in several signaling pathways, including Ras/MAPK and PI3K/Akt/mTOR (393,394) (Figure 29A and B). These two pathways have been related to cytokine and chemokine secretion. When senescence is induced, cells begin to secrete specific cytokines known as the SASP, which includes a variety of pro-inflammatory cytokines, such as IL-1β, IL-6, IL-8, TNF-α, and GM-CSF (395). In addition, it has been described that MCs in *NF1*-knockout mice increase TGF-β secretion (396,397). This suggests that sera from sensitized patients induce a lower secretion of pro-inflammatory cytokines and a higher secretion of TGF-β than sera from the anaphylaxis group, as we observed previously. Moreover, with the GSEA analysis in LAD2 cells, we observed that TGF-β-signaling was enhanced in LAD2 cells sensitized with sera from sensitized patients and

activated with Pru p 3 (Enrichment Score =0.795 and *p*.adjusted value =0.283). This finding correlates with the higher secretion of TGF-β by MCs from sensitized patients after activation with Pru p 3, as shown in our first study.

As senescence and NF1 are related to cytokine and chemokine secretion, we decided to analyze the MC secretion phenotype. Within the transcriptomic data, we saw that $CD34^+$-derived MCs sensitized with sera from sensitized patients presented upregulated *CCR2* (C-C Motif Chemokine receptor type 2) and *NFKBIL1* (NF-κB inhibitor like 1) compared with MCs sensitized with pooled sera from the anaphylaxis group (Figure 30B). CCR2 is the CCL2 receptor, this chemokine that we found elevated in MCs from sensitized patients after activation with Pru p 3. In addition, the inhibitor of NF-κB, a main cytokine (such as IL-8 or GM-CSF) transcription factor (398–401), was elevated in cells sensitized with sera from sensitized patients, suggesting that this pooled sera may induce the inhibition of some pro-inflammatory cytokine secretion.

Furthermore, calcium is also essential in senescence or NF1 function for cytokine and chemokine secretion due to its involvement as a second messenger (394,395). Thus, we observed that some calcium-related genes were downregulated in MCs sensitized with sera from sensitized patients versus MCs sensitized with pooled anaphylaxis sera. We found that *ORAI2* (ORAI calcium release-activated calcium modulator 2), *EFCAB5* (EF-hand calcium-binding domain 5), and *CACNA1H* (calcium voltage-gated channel subunit alpha1 H) were downregulated (Figure 30B). As expected, this downregulation of calcium-related genes could be associated with the reduced degranulation observed in MCs from sensitized patients.

Furthermore, we observed that MCs sensitized with pooled sera from sensitized patients had upregulated molecules involved in the local acute inflammatory response, such as C3 and C7, two molecules of the complement system (402,403), compared with MCs sensitized with pooled sera from the anaphylaxis group.

Interestingly, we found that the cell cycle pathway was downregulated in the GSEA analysis when LAD2 cells were sensitized with pooled sera from sensitized patients rather than from the anaphylaxis group (Figure 29B). Thus, analyzing the transcriptomic results for genes related to the cell division cycle, many were downregulated, such as *CDCA2, CDCA3, CDCA5, CDCA8, CDC20*, and *CDC25C*, compared with LAD2 cells sensitized with sera from the anaphylaxis group (Figure 30A). This suggests that the sera from sensitized patients may decrease the cell division cycle. To validate this finding, as preliminary data, we performed a WST-1 proliferation assay in LAD2 cells sensitized overnight with sera from healthy donors and the sensitized and anaphylaxis groups. We observed that LAD2 cells sensitized overnight with pooled sera from sensitized patients or healthy volunteers had a significant decrease in proliferation after one, three, and five days compared with LAD2 cells sensitized overnight with pooled sera from the anaphylaxis group or ^{b}IgE (Supplementary Figure 6).

In summary, the transcriptomic data suggest that sera from LTP patients induce different pathways, proposing that sera from sensitized patients induce a more anti-inflammatory pathway regarding cytokine and chemokine secretion, correlating with our previous data.

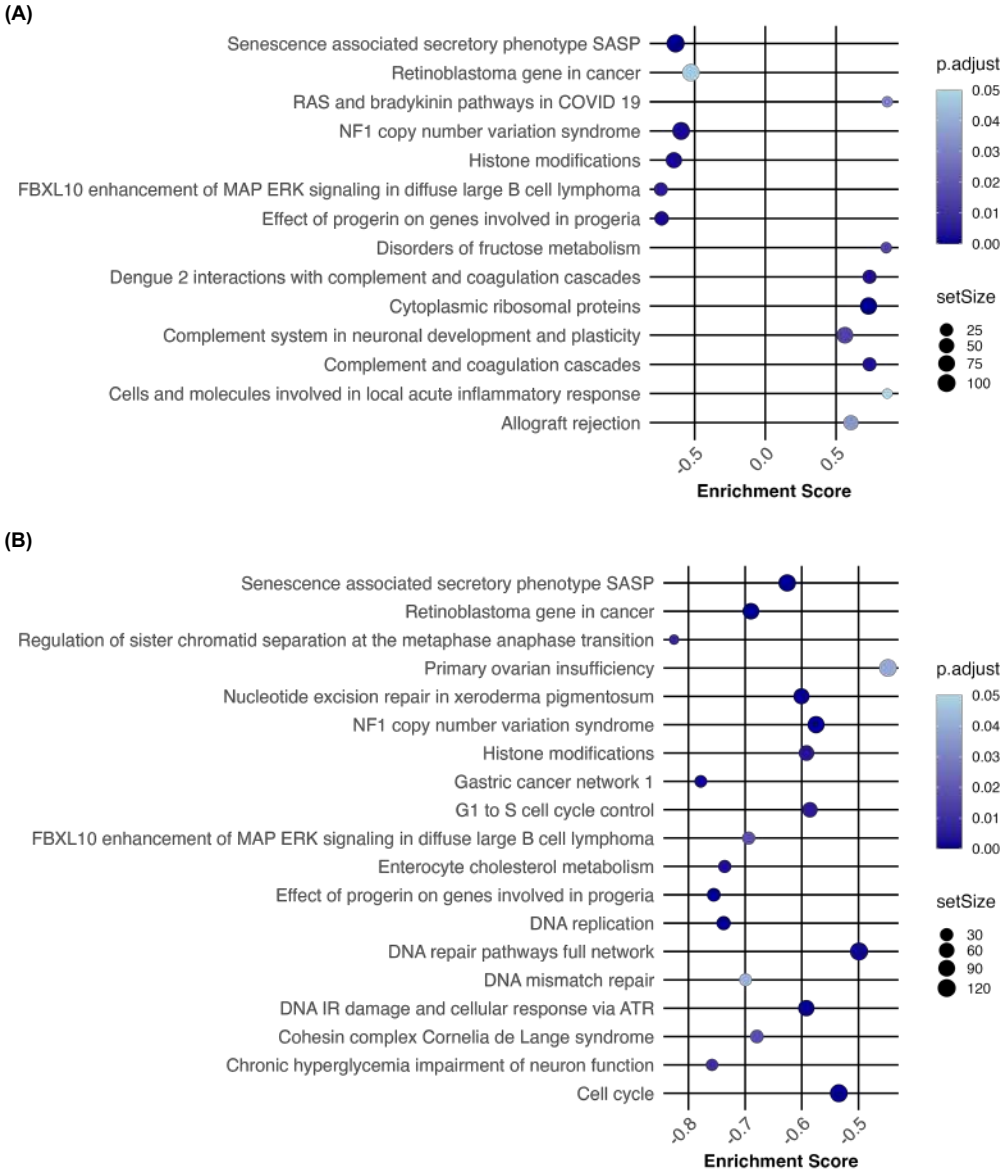

Figure 29. Sera from sensitized patients induce the activation of different signaling pathways in MCs versus sera from anaphylactic patients. CD34^{+}-derived MCs (n=3) and LAD2 cells (n=3) were sensitized with both pooled sera from LTP patients and stimulated with Pru p 3 for 24 hours. Afterward, RNA-sequencing was performed. GSEA was created with RStudio using a log2FoldChange ± 1 and adjusted p-value <0.05. A) GSEA pathways in MCs sensitized with sera from sensitized patients versus MCs sensitized with sera from the anaphylaxis group. B) GSEA pathways in LAD2 cells sensitized with sera from sensitized patients versus LAD2 cells sensitized with sera from the anaphylaxis group.

(A)

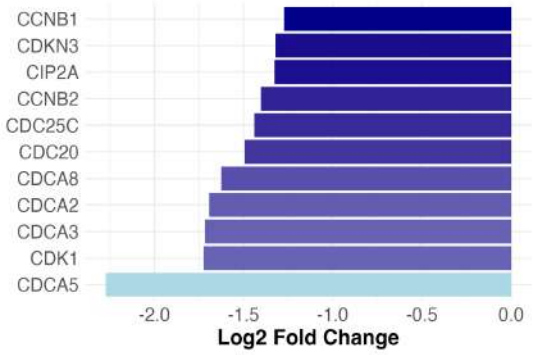

(B)

	Log2FoldChange	p value
CCR2	1.03	0.00
NFKBIL1	0.91	0.00
ORAI2	-1.05	0.00
EFCAB5	-1.64	0.00
CACNA1H	-2.20	0.00

Figure 30. Sera from sensitized patients induce different pathways in MCs versus sera from anaphylactic patients. CD34^{+}-derived MCs (n=3) and LAD2 cells (n=3) were sensitized with both pooled sera from LTP patients and stimulated with Pru p 3 for 24 hours. Afterward, RNA-sequencing was performed. Bar Plots were created with RStudio using a log2FoldChange ± 1 and adjusted p-value <0.05. A) Scheme of upregulated genes in CD34+-derived MCs sensitized with pooled sera from sensitized patients versus cells sensitized with pooled sera from anaphylactic patients. B) Bar Plot of downregulated genes of LAD2 cells sensitized with pooled sera from sensitized patients versus cells sensitized with pooled sera from anaphylactic patients.

In parallel, due to the lower amount of RNA obtained from the MCs from of the patients in our cohort - clinical characteristics of each individual are in Annex Table 3 - we analyzed a set of genes associated with exacerbated MC responses, as described in the literature (see in Table 4 for the gene list and references).

Table 4. Genes evaluated in MCs from LTP patients.

Gene	Description	References	
FcεR1A	Fc Epsilon Receptor 1a	Dispenza *et al.* 2020 (401); Takahashi *et al.* 2005 (402)	Preformed mediator- related genes
HDC	Histidine Decarboxylase	White 1990 (395); Li *et al.* 2023 (396)	
TPSAB1	Tryptase alpha/beta 1	Lang *et al.* 2023 (397); Lyons *et al.* 2021 (398); Caughey 2007 (69)	
CMA	Chymase 1	Caughey 2007 (69); Zhou *et al.* 2011 (399); Scudamore *et al.* 1995 (400)	
STIM1	Stromal Interaction Molecule 1	Baba *et al.* 2008 (110)	
PTGER2	Prostaglandin E receptor 2	Serra-Pages *et al.* 2012 (403); Torres-Atencio *et al.* 2014 (404)	
PTGER3	Prostaglandin E receptor 3	Serra-Pages *et al.* 2012 (403); Torres-Atencio *et al.* 2014 (404)	
PTGER4	Prostaglandin E receptor 4	Serra-Pages *et al.* 2012 (403); Torres-Atencio *et al.* 2014 (404)	
COX2	Cyclooxygenase 2	Kulesza *et al.* 2023 (405); Globig *et al.* 2025 (406); Laouini *et al.* 2005 (407)	
CCL18	CC Motif Chemokine Ligand 18	Cardoso *et al.* 2021 (408); Huoman *et al.* 2021 (409); de Nadaï 2004 (410)	*De novo* mediator- related genes
CCL2	CC Motif Chemokine Ligand 2	Jiang *et al.* 2019 (412); Dijkstra *et al.* 2007 (413); Vantur *et al.* 2020 (414)	
IL1B	Interleukin 1 beta	Yeung *et al.* 2021 (416); Krause *et al.* 2012 (417); H.-R. Wang *et al.* 2023 (418)	
TGFB1	Transforming growth factor beta 1	Schmidt-Weber *et al.* 2006 (420); Tirado-Rodriguez *et al.* 2014 (421)	
HINT1	Histidine Triad nucleotide-binding protein 1	Ribó *et al.* 2021 (358)	MITF-related genes
KARS	Lysyl-tRNA synthetase 1	Ribó *et al.* 2021 (358)	
MITF	Microphpthalmia-associated transcription factor	Li *et al.* 2018 (172); Srivastava *et al.* 2021 (472)	
NUDT2	Nudix Hydrolase 2	Marriott *et al.* 2016 (423)	

2.1. MCs from anaphylactic patients had higher *TPSAB1*, and *FcεR1A* levels

First, we wanted to assess the main MC biomarkers used for diagnosing anaphylaxis: histamine and tryptase (404–406). Thus, we explored the histidine decarboxylase gene (*HDC*, encoding the enzyme that catalyzes histidine to create histamine) (407,408) and tryptase alpha/beta1 (*TPSAB1*, encoding tryptase) (69,409,410). Also, we added the chymase 1 (*CMA*, encoding chymase), a well-known protease released from MCs after cell activation (69,411,412), and *FcεR1A*, which encodes for FcεRI, the high-affinity IgE receptor (413,414).

The analysis of these gene mediators revealed that MCs from LTP patients, both sensitized and anaphylaxis, had an elevated expression of *HDC*, although it was not significant (Figure 31A). Similar results were found for *TPSAB1* gene expression, which was significantly higher in MCs from sensitized and anaphylaxis patients than from healthy volunteers after cell activation with Pru p 3 (Figure 31B).

CMA expression levels were similar in all groups (Figure 31C). Interestingly, the expression of the high-affinity IgE receptor was significantly elevated in MCs from anaphylactic patients upon IgE cell activation (Figure 31D).

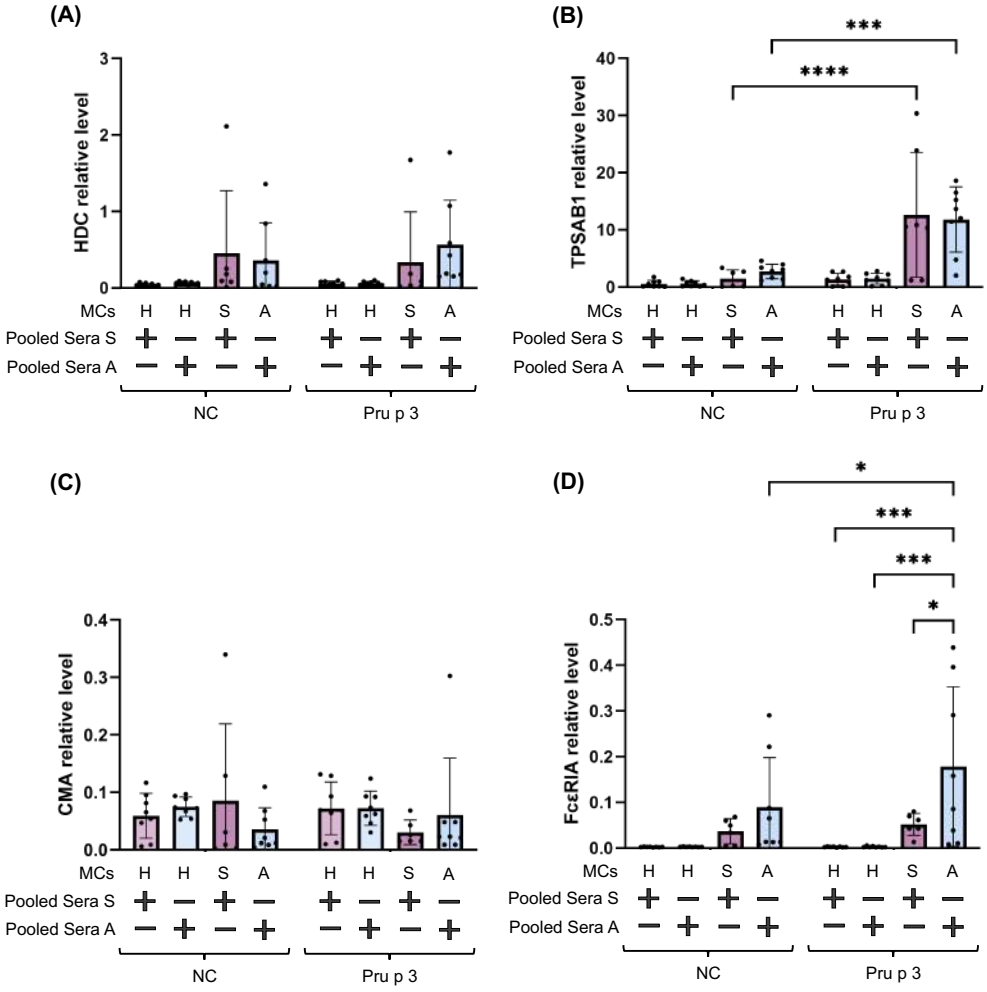

Figure 31. MCs from anaphylactic patients induce more preformed mediators' release. MCs from healthy volunteers (n=8) and LTP patients (sensitized n=6; and anaphylaxis n=8) were used to assess some genes. A) *HDC* gene expression levels. B) *TPSAB1* gene expression levels. C) *CMA* gene expression levels. D) *FcεR1A* gene expression levels. Results are expressed as mean ± SD. Significance was determined using two-way ANOVA with Tukey's multiple comparison analysis. P<0.05 was considered statistically significant. *P<0.05; **P<0.01; ***P<0.001; ****P<0.0001. A=Anaphylaxis; H=Healthy; NC=Negative control; S=Sensitized.

2.2. *STIM1* expression is increased in MCs of anaphylactic patients

MC degranulation depends on intracellular calcium levels regulated by the SOCE pathway. An essential component of SOCE is STIM1, which acts as a calcium sensor within the endoplasmic reticulum. No differences in *STIM1* levels were seen in transcriptomics with MCs sensitized with pooled sera from LTP patients. However, calcium-related genes were found to be downregulated in MCs sensitized with sera from sensitized patients compared with MCs sensitized with anaphylaxis pooled sera, as we showed above. We found *ORAI2* – which encodes Orai calcium channel proteins – to be downregulated; ORAI2 interacts with STIM1 to allow calcium entry. As expected, due to the higher degranulation of MCs from anaphylactic patients, it is possible that these patients had a higher calcium flux than sensitized patients. We found no significant differences in STIM1 expression levels between groups (Figure 32); nevertheless, we did detect an increasing trend in anaphylactic patients, especially after cell activation with Pru p 3.

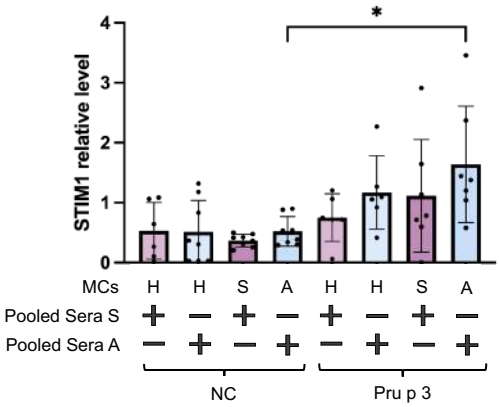

Figure 32. *STIM1* is elevated in MCs from anaphylactic patients. MCs from healthy volunteers (n=8) and from LTP patients (sensitized n=6; and anaphylaxis n=8) were used to assess *STIM1* by RT-qPCR. Results are expressed as mean ± SD. Significance was determined using two-way ANOVA with Tukey's multiple comparison analysis. P<0.05 was considered statistically significant. A=Anaphylaxis; H=Healthy; NC=Negative control; S=Sensitized.

2.3. MCs from anaphylactic patients had higher *PTGER3* and *COX2* levels

Next, we wanted to assess genes related to *de novo* MC mediators. Lipid mediators, such as PGD_2 and PGE_2, are generated and released almost simultaneously with preformed mediators and contribute to bronchoconstriction, increased vascular permeability, mucus production, and inflammatory cell recruitment (65).

Thus, we assessed the expression levels of the *PTGER2, PTGER3*, and *PTGER4*, genes that encode the PGE_2 receptors EP2, EP3, and EP4, respectively. PGE_2 promotes a stimulatory effect through the EP3 receptor and an inhibitory effect through the EP2 and EP4 receptors (415,416).

In this analysis, we found that neither *PTGER2* nor *PTGER4* expression levels showed any significant differences between groups, while *PTGER3* was significantly elevated in MCs from anaphylactic patients under basal or activated conditions. Furthermore, when we measured the PTGER3/PTGER4 ratio, this upregulation of the *PTGER3* gene became even more evident in MCs from anaphylactic patients, suggesting that those patients had many more EP3 receptors than EP4, enhancing the activation in those cells.

We also assessed *PTGS2* or *COX2*, an enzyme that catalyzes the biosynthesis of prostaglandins, mainly PGE_2, during inflammation (417–419). In our cohort, there was no difference in *COX2* levels under basal conditions. However, after activation with Pru p 3, *COX2* expression was significantly higher in MCs from anaphylaxis patients, suggesting a more inflammatory state in those cells.

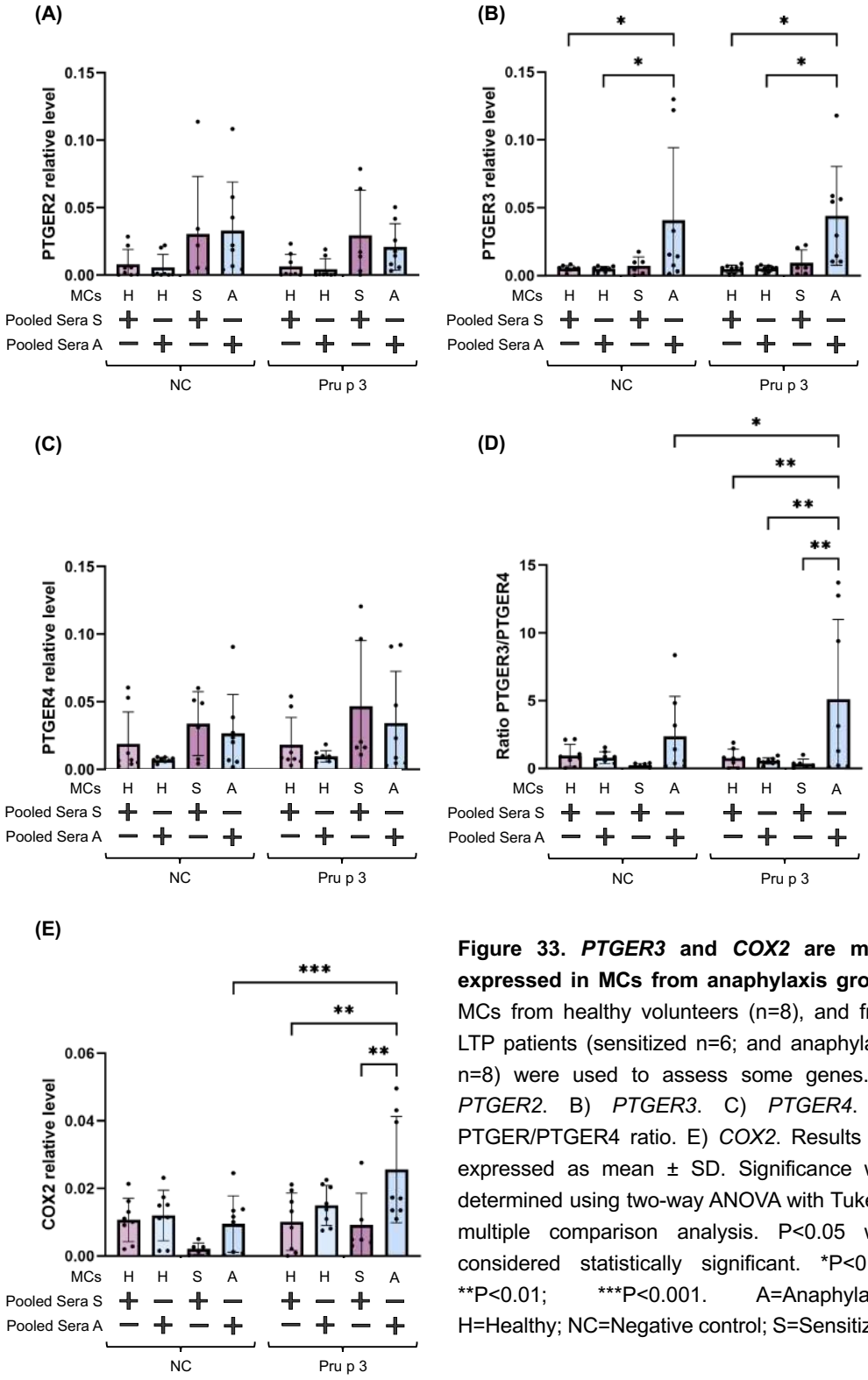

Figure 33. *PTGER3* and *COX2* are more expressed in MCs from anaphylaxis group. MCs from healthy volunteers (n=8), and from LTP patients (sensitized n=6; and anaphylaxis n=8) were used to assess some genes. A) *PTGER2*. B) *PTGER3*. C) *PTGER4*. D) PTGER/PTGER4 ratio. E) *COX2*. Results are expressed as mean ± SD. Significance was determined using two-way ANOVA with Tukey's multiple comparison analysis. P<0.05 was considered statistically significant. *P<0.05; **P<0.01; ***P<0.001. A=Anaphylaxis; H=Healthy; NC=Negative control; S=Sensitized.

2.4. Analysis of *de novo* mediator-related genes in MCs from LTP patients

Regarding *de novo* mediator-related genes, we analyzed a set of pro-inflammatory and protective cytokines synthesized and secreted by MCs, which may influence response severity.

CCL18 is a chemokine mainly associated with a tolerogenic response and is considered a biomarker of sensitization (420–422). We observed that MCs from sensitized patients had elevated levels of *CCL18* under basal conditions and even levels after activation with the allergen (Figure 34A).

CCL2 is a monocyte-chemoattractant (423–426). Interestingly, although we previously saw a higher secretion of CCL2 after Pru p 3 activation in MCs from sensitized patients, in terms of *CCL2* gene expression, there were no significant differences between groups (Figure 34B).

IL-1β is a key mediator of inflammation (427–430). As we expected, we found elevated *IL1B* levels in MCs from anaphylactic patients when cells were activated with Pru p 3.

Finally, TGF-β is an anti-inflammatory mediator (431–433). Correlating with our previous results, we found that MCs from sensitized patients had significantly higher *TGFB1* levels than MCs from anaphylactic patients or healthy volunteers after cell activation with Pru p 3 (Figure 34D).

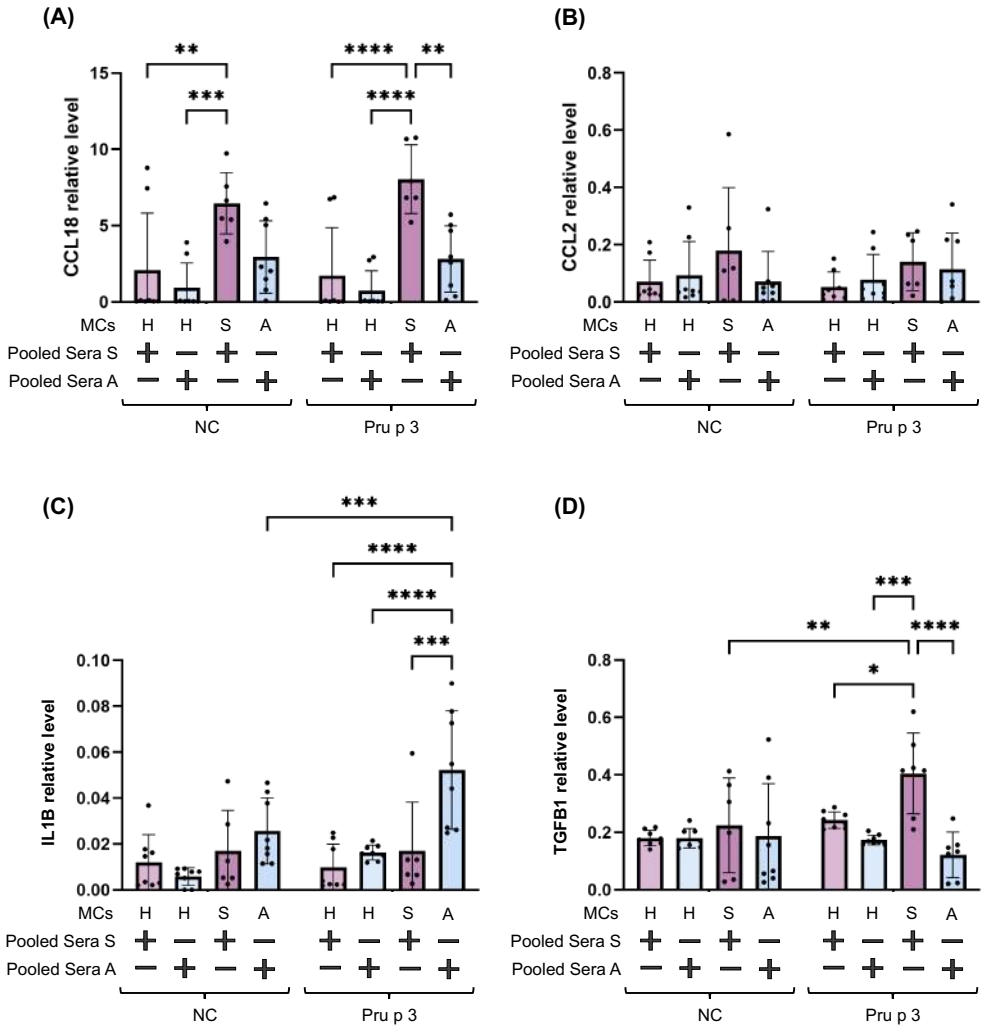

Figure 34. MCs from LTP patients induce a different cytokine/chemokine pattern. MCs from healthy volunteers (n=8) and from LTP patients (sensitized n=6; and anaphylaxis n=8) were used to assess some genes. A) *CCL18* gene expression levels. B) *CCL2* gene expression levels. C) *IL1B* gene expression levels. D) *TGFB1* gene expression levels. Results are expressed as mean ± SD. Significance was determined using two-way ANOVA with Tukey's multiple comparison analysis. P<0.05 was considered statistically significant. *P<0.05; **P<0.01; ***P<0.001; ****P<0.0001. A=Anaphylaxis; H=Healthy; NC=Negative control; S=Sensitized.

2.5. MCs from anaphylactic patients had higher *MITF* levels

It is well established that MITF favors histamine release and the synthesis of other MC mediators, such as granzyme B, PGD_2, and chymases (173,434). Under quiescent conditions, MITF is bound to HINT1, which represses its transcriptional activity. Upon MC stimulation through IgE-crosslinking, LysRS is phosphorylated and translocated to the nucleus, where it synthesizes Ap4A that binds to HINT1, leaving MITF free to induce gene transcription (371). For this reason, we included *MITF* and *HINT1*, as well as *KARS* (encoding LysRS gene) and *NUDT2* (encoding an enzyme that hydrolyses the Ap4A (435)).

First, we observed that MCs from anaphylactic patients had higher *MITF* levels under basal conditions, which were even higher after Pru p 3 activation than other MCs (Figure 35A). Regarding *HINT1* and *KARS*, two genes involved in MITF regulation, no significant differences were found between groups (Figure 35B and C). Finally, *NUDT2*, also involved in MITF regulation, was elevated in MCs from healthy volunteers sensitized with sera from anaphylactic patients, either under basal or activated conditions (Figure 35D).

Given all these results, it seems that MCs from anaphylactic patients appear to be more reactive and activate pro-inflammatory pathways, whereas MCs from sensitized patients enhance more protective pathways. In this genetic analysis, we observed significant differences in MCs from anaphylactic patients for many genes of interest. MCs from anaphylactic patients had higher expression of the *HDC, TPSAB1, FcεR1A, PTGER3, COX2*, and *MITF* genes – suggesting a higher pro-inflammatory response – than MCs from sensitized patients.

As mentioned in the introduction, our group previously identified a LysRS-P542R mutation in a patient with severe anaphylaxis, leading to increased MITF activity. This mutation suggests a potential cellular component involvement in severe reactions, prompting us to focus on this transcription factor to investigate the exacerbated mechanisms in our cohort.

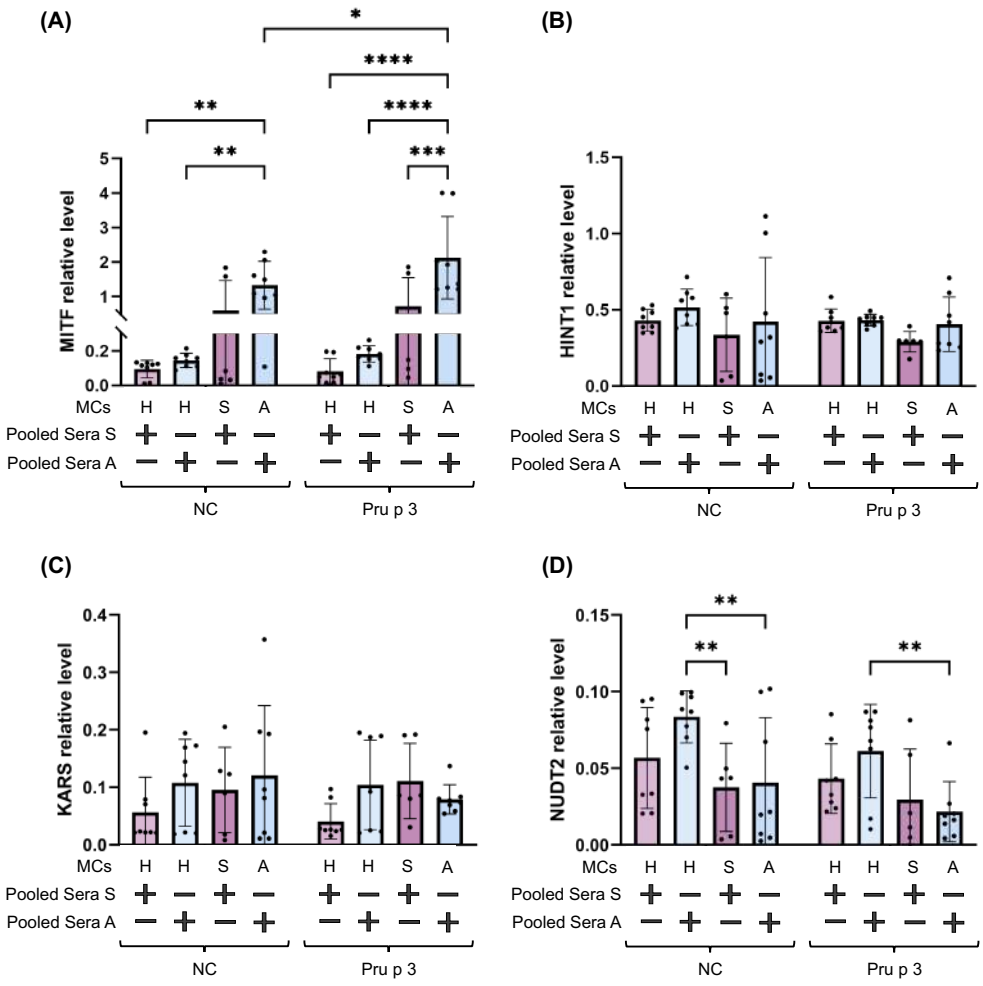

Figure 35. *MITF* is more expressed in MCs from anaphylactic patients. MCs from healthy volunteers (n=8) and from LTP patients (sensitized n=6; and anaphylaxis n=8) were used to assess MITF-related genes. A) *MITF* gene expression levels. B) *HINT1* gene expression levels. C) *KARS* gene expression levels. D) *NUDT2* gene expression levels. Results are expressed as mean ± SD. Significance was determined using two-way ANOVA with Tukey's multiple comparison analysis. P<0.05 was considered statistically significant. *P<0.05; **P<0.01; ****P<0.0001. A=Anaphylaxis; H=Healthy; NC=Negative control; S=Sensitized.

3. INVESTIGATE THE ROLE OF MITF ON MAST CELL RELEASE MODULATION

3.1. MITF involvement in IgE-mediated reactions

To study MITF involvement in MC activation through different pathways, we used different cell models: 1) RBL-2H3 cells transfected with the LysRS-P542R mutation as an MITF-overexpression model and 2) MCs treated with MITF inhibitors or infected with shRNA sequences as a MITF-knockdown model. As mentioned in the methodology section, to inhibit MITF, we used ML329, which inhibits the MITF pathway (372), and TT012, which inhibits MITF dimerization (159). To silence *MITF*, we used two different shRNA sequences (detailed in the methodology section) that were previously reported (150,168,169). In all experiments, we assessed the expression of receptors and cell viability.

3.1.1. Quantification of gene expression associated with exacerbated MC responses in MITF-knockdown cells upon FcεRI stimulation

We used a qPCR dynamic array to assess whether MITF is involved in the transcription of different genes related to exacerbated MC responses (those explored above in MCs from patients). LAD2 cells were treated with MITF shRNAs for five days, sensitized overnight with ^{b}IgE, and stimulated with STV for 24 hours.

First, we assessed the expression of *MITF*, which we confirmed was significantly downregulated in cells treated with MITF shRNAs (Figure 36A). Then, we observed that in MITF-knockdown cells, *KARS, NUTD2*, and *HINT1* expression was significantly decreased, both under basal and stimulated conditions (Figure 36B, C and D).

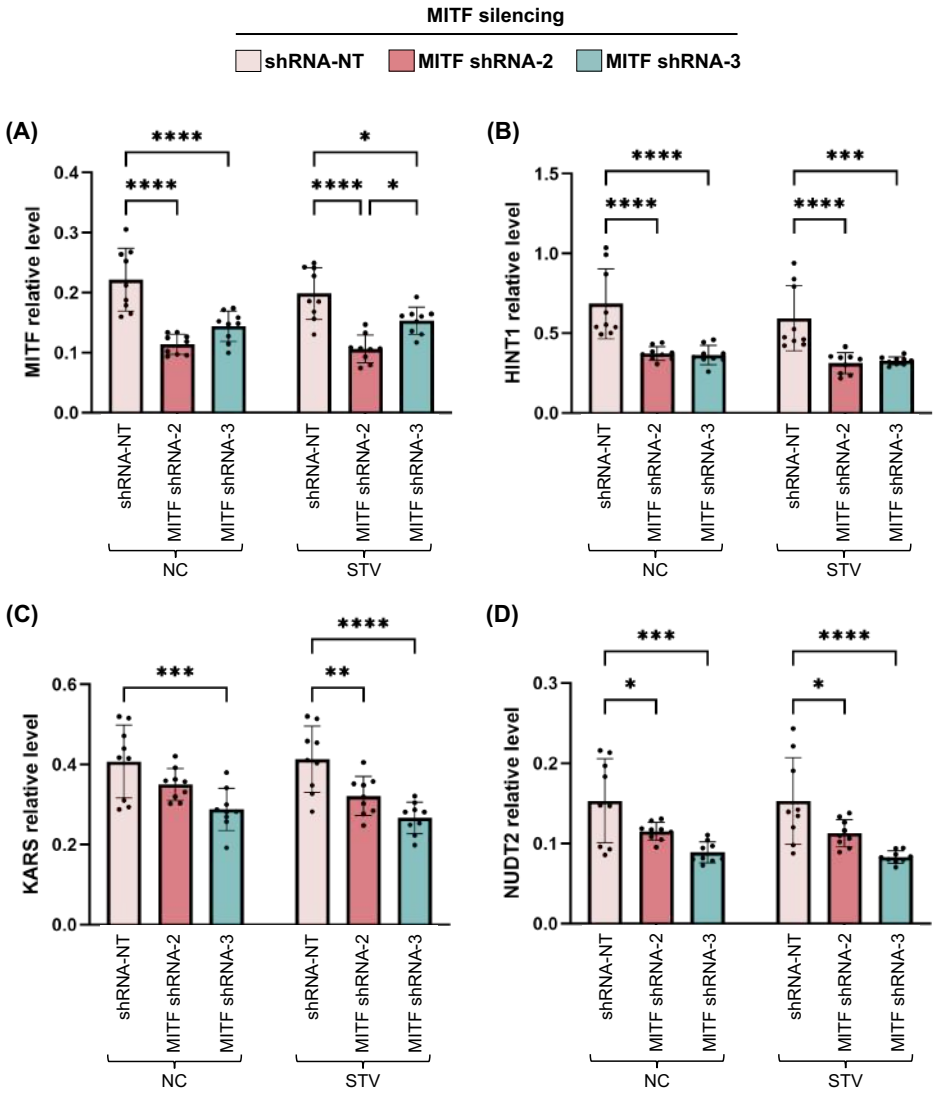

Figure 36. Genes involved in MITF regulation are decreased in MITF-silenced cells via the FcεRI receptor. MITF-silenced LAD2 cells were used to assess some genes (n=9). A) *MITF* gene expression levels. B) *HINT1* gene expression levels. C) *KARS* gene expression levels. D) *NUDT2* gene expression levels. Results are expressed as mean ± SD. Significance was determined using two-way ANOVA with Tukey's multiple comparison analysis. P<0.05 was considered statistically significant. *P<0.05; **P<0.01; ***P<0.001; ****P<0.0001. NC=Negative control; STV=Streptavidin.

Then, we assessed *STIM1* expression, finding that it was downregulated in MITF-silenced cells after stimulation with ^{b}IgE + STV (Figure 37).

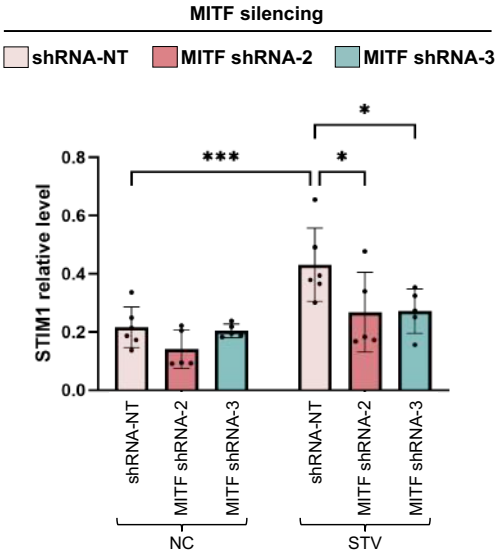

Figure 37. *MITF* silencing reduces *STIM1* levels in the IgE-dependent pathway. MITF-silenced LAD2 cells were used to assess *STIM1* (n=9). Results are expressed as mean ± SD. Significance was determined using two-way ANOVA with Tukey's multiple comparison analysis. P<0.05 was considered statistically significant. *P<0.05; ***P<0.001. NC=Negative control; STV=Streptavidin.

Furthermore, we observed that control cells presented elevated levels of *CCL18* and *IL1B* compared with MITF-knockdown both under basal conditions and after activation with ^{b}IgE + STV. No differences were found for *CCL2* and *TGFB1* (Figure 38).

Moreover, we did not observe differences in *PTGER2* gene expression, but MITF-knockdown cells presented lower *PTGER3* expression levels and higher *PTGER4* expression levels than control cells, both under basal and activated conditions (Figure 39B and C). In addition, *COX2* is elevated in control cells after cell activation with ^{b}IgE + STV (Figure 39D).

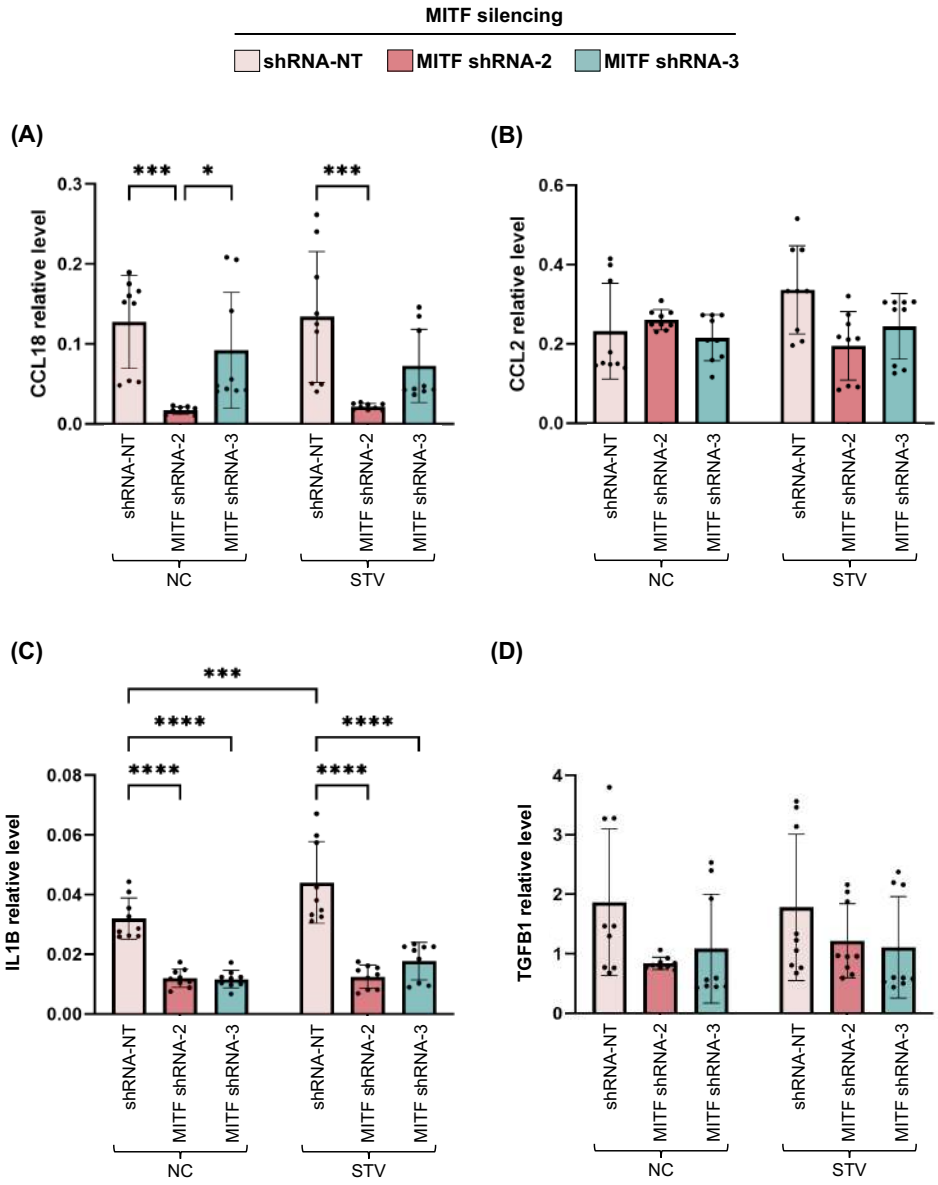

Figure 38. Cytokine and chemokine gene level changes in MITF-knockdown cells. MITF-silenced LAD2 cells were used to assess some genes (n=9). A) *CCL18* gene expression levels. B) *CCL2* gene expression levels. C) *IL1B* gene expression levels. D) *TGFB1* gene expression levels. Results are expressed as mean ± SD. Significance was determined using two-way ANOVA with Tukey's multiple comparison analysis. P<0.05 was considered statistically significant. *P<0.05; **P<0.01; ***P<0.001; ****P<0.0001. NC=Negative control; STV=Streptavidin.

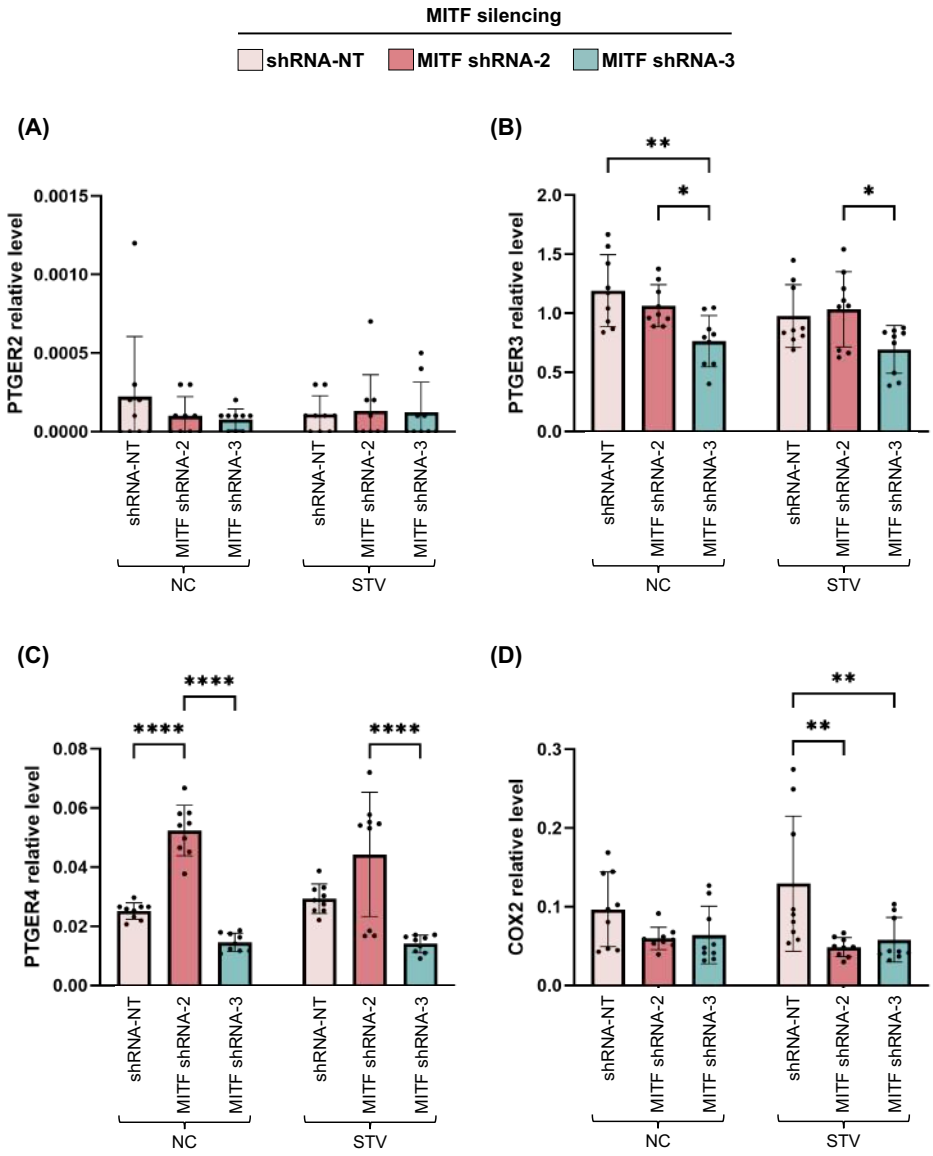

Figure 39. *PTGER4* is increased in MITF-knockdown cells. MITF-silenced LAD2 cells were used to assess some genes (n=9). A) *PTGER2* gene expression levels. B) *PTGER3* gene expression levels. C) *PTGER4* gene expression levels. D) *COX2* gene expression levels. Results are expressed as mean ± SD. Significance was determined using two-way ANOVA with Tukey's multiple comparison analysis. P<0.05 was considered statistically significant. *P<0.05; **P<0.01; ***P<0.001; ****P<0.0001. NC=Negative control; STV=Streptavidin.

All these results suggest that MITF may play an important role in regulating the pro-inflammatory pattern. *MITF* silencing showed elevated levels of *PTGER4* but a reduction in *IL1B, COX2, PTGER3, NUDT2, KARS*, and *HINT1*, suggesting a lower pro-inflammatory pattern in those cells.

3.1.2. MITF regulation of calcium influx in MCs through the FcεRI receptor

We previously reported a decrease in MC degranulation after MITF inhibition with ML329 (168). Moreover, an increase in MC degranulation has been demonstrated in an MITF-overexpression model (371). We recently reported a decrease in calcium influx after MITF inhibition with ML329 or silencing via the MRGPRX2 pathway (169), suggesting that MITF influences MC differentiation and modulates functional responses by controlling calcium dynamics. Recently, it has been shown that STIM1 is a key player in calcium signaling and a target of transcriptional regulation by MITF in melanocytes. Chromatin Immunoprecipitation (ChIP) and functional analysis confirmed the MITF-STIM1 interaction (436). Thus, in this section, we wanted to study MITF involvement in calcium release through its interaction with STIM1.

3.1.2.1. MITF-knockdown reduces calcium influx through STIM1

As we saw that *MITF* silencing reduces *STIM1* gene expression, we wanted to validate this MITF-STIM axis. Thus, we treated LAD2 cells with ML329, TT012 or MITF shRNAs for five days and after then, STIM1 was evaluated by western blot. MITF-knockdown cells, either with MITF inhibitors or with MITF shRNAs, had significantly lower STIM1 protein expression than control cells (Figure 40).

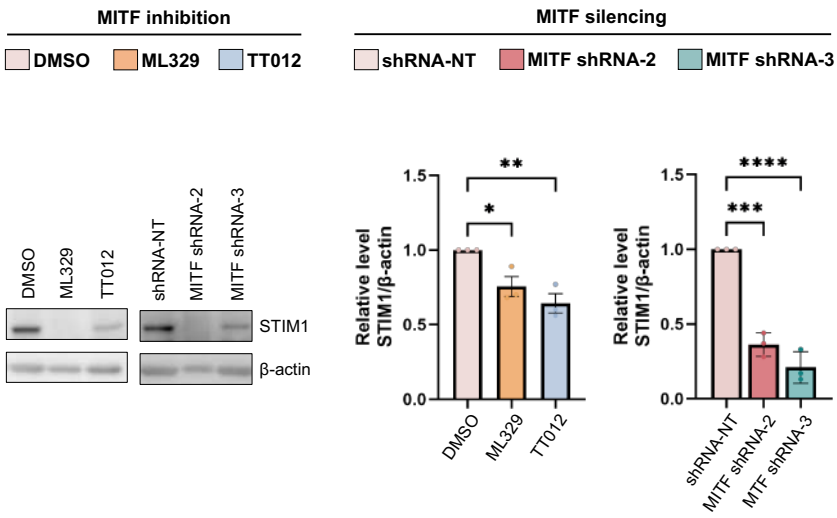

Figure 40. MITF-knockdown reduces STIM1 levels in a mast cell model. LAD2 cells were treated with MITF inhibitors, ML329 and TT012, and MITF shRNAs for five days, and then STIM1 protein expression was measured by western blot (n=3). Results are expressed as mean ± SD. Significance was determined using one-way ANOVA with Tukey's multiple comparison analysis. P<0.05 was considered statistically significant. *P<0.05; **P<0.01; ***P<0.001.

Next, we wanted to analyze the calcium influx in MITF-knockdown cells. LAD2 cells were treated with MITF inhibitors or infected with MITF shRNAs for five days, sensitized overnight with ^{b}IgE, and calcium influx was measured after cell activation with STV (Figure 41A). LAD2 cells treated with ML329 or MITF shRNAs, showed significantly lower levels of calcium influx after cell activation with STV than control cells (Figure 41B and C). Moreover, we used primary cells to further confirm this MITF-calcium axis. MC_{BC} were treated with MITF inhibitors for five days and sensitized overnight with ^{b}IgE, and then calcium influx was measured after cell activation with STV. MITF-silenced MCs showed significantly lower levels of calcium influx after cell activation (Figure 41D), as we observed in LAD2 cells.

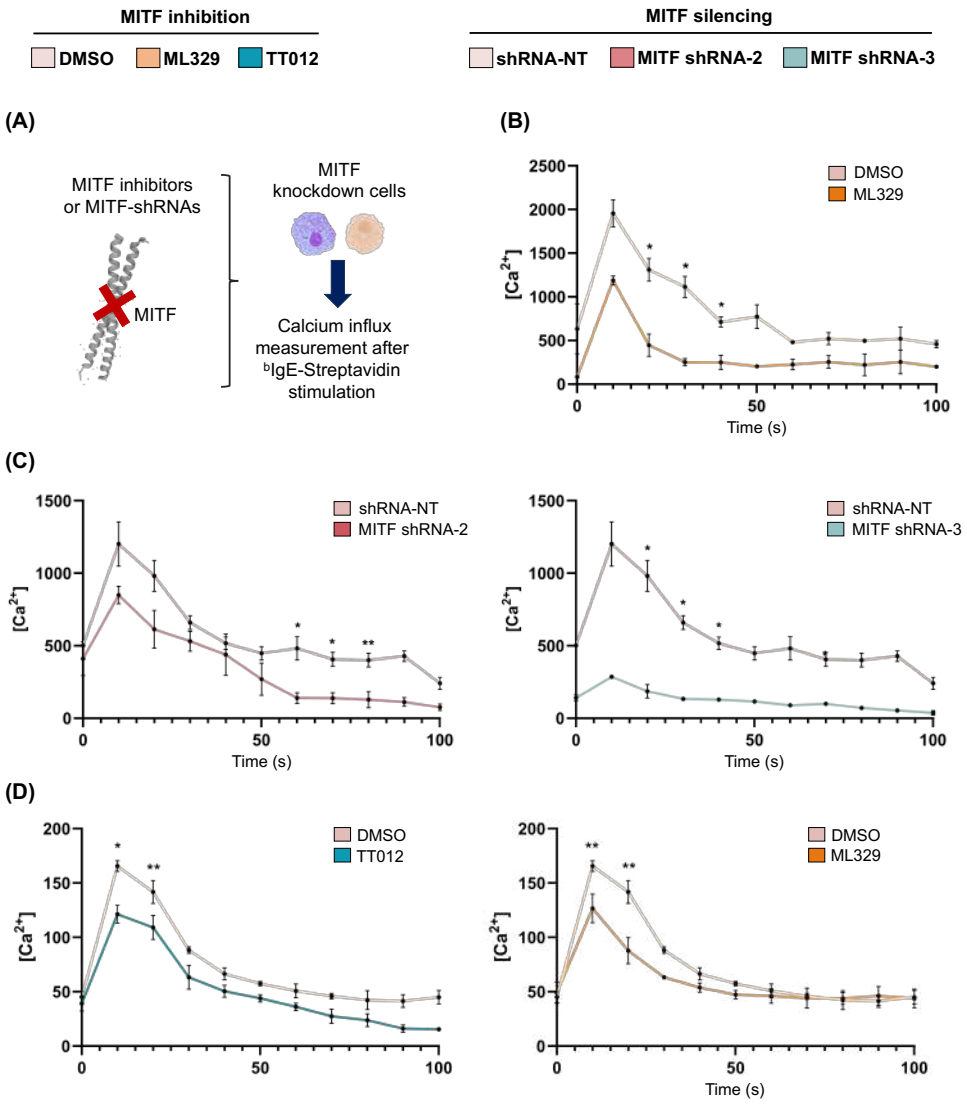

Figure 41. Calcium influx is impaired in MITF-knockdown cells via the FcεRI receptor. LAD2 cells or primary MCs were treated with MITF inhibitors or shRNAs, and calcium influx was measured after cell activation with streptavidin (STV). A) Methodology illustration. B) LAD2 cells treated with ML329 for five days and stimulated with STV (n=3). C) LAD2 cells infected with MITF shRNA-2 and MITF shRNA-3 for five days and activated with STV (n=3). D) Primary MCs treated with TT012 or ML329 for five days and stimulated with STV (n=3). Results are expressed as mean ± SD. Significance was determined using two-way ANOVA with Tukey's multiple comparison analysis. P<0.05 was considered statistically significant. *P<0.05; **P<0.01; ***P<0.001.

MITF is involved in cell viability, as shown in other studies (24,144,171). Thus, we believed that this calcium influx decreases might be due to reduced cell viability. However, to conduct this experiment, we used the same amount of live cells for each condition, avoiding this possible effect. Another thing to consider was that *MITF* silencing induces a reduction in the gene and protein expression of *FcεRI*, which could induce a lower signaling through this pathway in those cells. Beyond the possible effects on viability and FcεRI expression, there was an association with the MITF-calcium influx axis, as we also observed a reduction in STIM1 in MITF-knockdown cells. Moreover, to confirm this interaction, we used an MITF-overexpression model, where neither the viability nor FcεRI expression was affected.

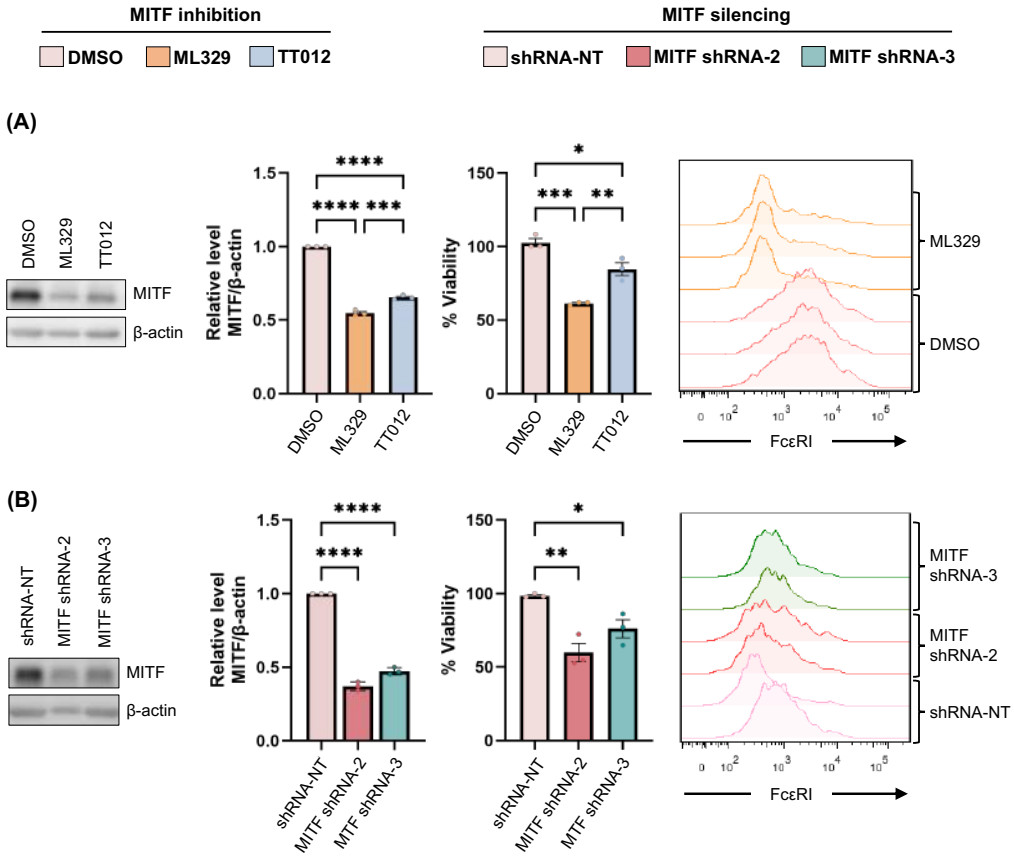

Figure 42. MITF is involved in cell viability and FcεRI expression. LAD2 cells were treated with MITF inhibitors or shRNAs, cell viability was measured by WST-1 and FcεRI expression was measured by flow cytometry. A) Cells treated with MITF inhibitors (n=3). B) LAD2 cells infected with shRNAs (n=3). Results are expressed as mean ± SD. Significance was

determined using two-way ANOVA with Tukey's multiple comparison analysis. P<0.05 was considered statistically significant. *P<0.05; **P<0.01; ***P<0.001; ****P<0.0001.

3.1.2.2. MITF-overexpression increases calcium influx through STIM1

Once we observed that MITF inhibition decreases the calcium influx, we wanted to see whether MITF-overexpression would produce the opposite effect. As previously mentioned, the LysRS-P542R mutation was found in a patient with severe anaphylaxis. Thus, RBL-2H3 cells transfected with the LysRS-P542R mutation is an approximated *in vitro* anaphylaxis model, which we used here to investigate this MITF-calcium axis. As mentioned, LysRS-P542R cells had constitutive GFP-LysRS expression in the nucleus, enhancing MITF expression (Figure 43A and B). Consequently, after cell activation with DNP-HSA, we observed that LysRS-P542R mutation cells had significantly higher calcium influx than LysRS-WT or control cells (Figure 43B).

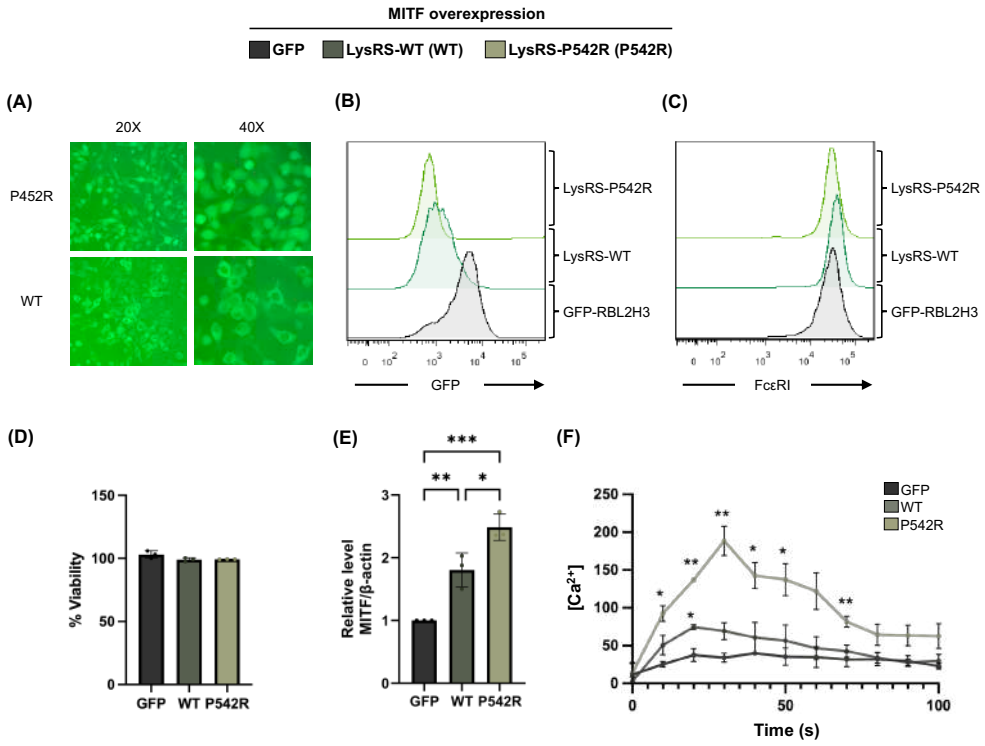

Figure 43. MITF-overexpression enhances calcium influx in a transfected RBL-2H3 model. The LysRS-P542R mutation in RBL-2H3 cells, as an MITF-overexpression model, was

used to assess calcium influx. A) Microscope photos of LysRS-P542R and WT cells. B) GFP levels in transfected RBL-2H3 cells by flow cytometry. C) FcεRI levels in transfected RBL-2H3 cells by flow cytometry. D) Cell viability in transfected RBL-2H3 cells by WST-1. E) MITF levels in transfected RBL-2H3 cells by flow cytometry (n=3). F) Calcium influx in the transfected RBL-2H3 model. Results are expressed as mean ± SD. Significance was determined using one-way ANOVA with Tukey's multiple comparison analysis. P<0.05 was considered statistically significant. *P<0.05; **P<0.01; ***P<0.001. P54R as LysRS-P542R and WT as LysRS-WT.

Assessing STIM1 in the MITF-overexpression model, we found that LysRS-P542R cells had higher STIM1 protein levels than LysRS-WT and even more so than RBL-2H3-GFP (control), correlating with MITF levels (Figure 44B and C). This suggests that when MITF is overexpressed, STIM1 is upregulated. Knowing that, these cells were treated with MITF inhibitors (ML329 and TT012) to study STIM1 expression. Cells treated with MITF inhibitors reduced their levels but also reduced their STIM1 levels, suggesting that when MITF was inhibited, STIM1 levels were downregulated, either with ML329 or TT012 inhibitors (Figure 44B and C).

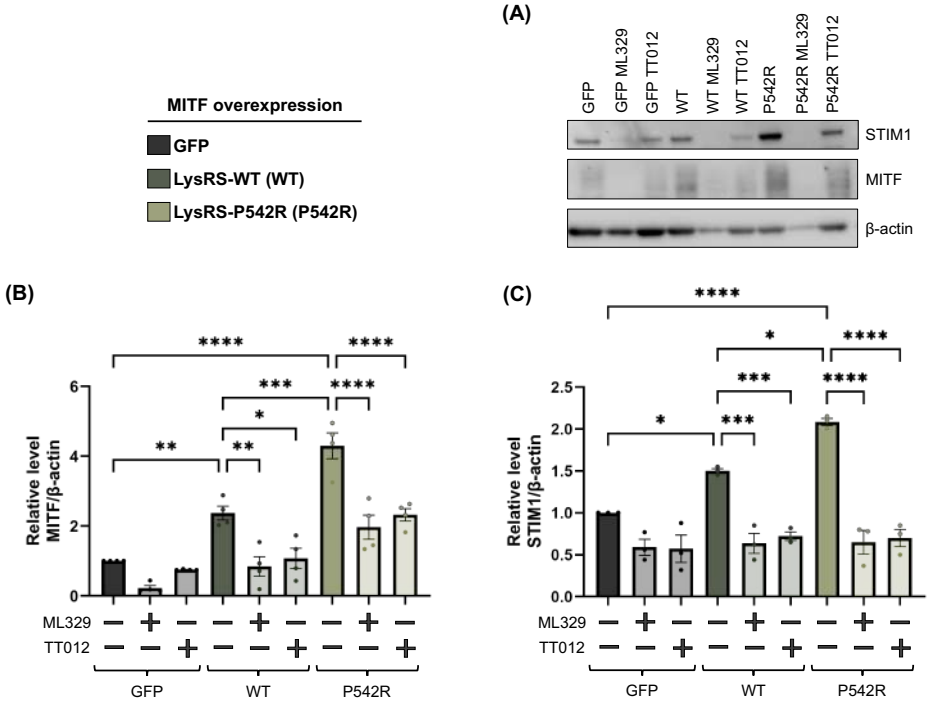

Figure 44. Increased MITF expression enhances STIM1 expression and calcium influx in a transfected RBL-2H3 model. The LysRS-P542R mutation in RBL-2H3 cells, as an MITF-

overexpression model, was used to assess STIM1 levels. A) Representative WB of transfected RBL-2H3 treated with MITF inhibitors. B) MITF levels when cells were treated with MITF inhibitors (n=4). C) STIM1 levels when cells were treated with MITF inhibitors (n=3). Results are expressed as mean ± SD. Significance was determined using two-way ANOVA with Tukey's multiple comparison analysis. P<0.05 was considered statistically significant. *P<0.05; **P<0.01; ***P<0.001; ****P<0.0001. P54R as LysRS-P542R and WT as LysRS-WT.

All these results suggest a correlation between MITF and STIM1, thus regulating calcium flux.

3.1.2.3. MITF inhibition reduces STIM1 activity in RBL-2H3 cells

Next, we measured whether MITF was directly involved in STIM1 transcriptional activity. We used STIM1 promotor-controlled firefly luciferase, which was transfected to RBL-2H3 cells together with a Renilla luciferase reporter gene, and cells were incubated with TT012 and DNP-IgE overnight. Then, cells were activated with DNP-HSA, and Luciferase expression, which correlates with MITF activity, was measured. In parallel, we used TRPM1 (Transient receptor potential melastatin-related 1), a well-known MITF target (437), as a control.

We observed that LysRS-P542R had higher MITF activity than LysRS-WT and even more so than RBL-2H3-GFP. In addition, when cells were treated with TT012 overnight, MITF activity was reduced significantly in all transfected cells (Figure 45A and B).

These results suggest that MITF might participate in regulating STIM1 as inhibiting MITF reduces its activity, which is evaluated through the STIM1-promotor gene.

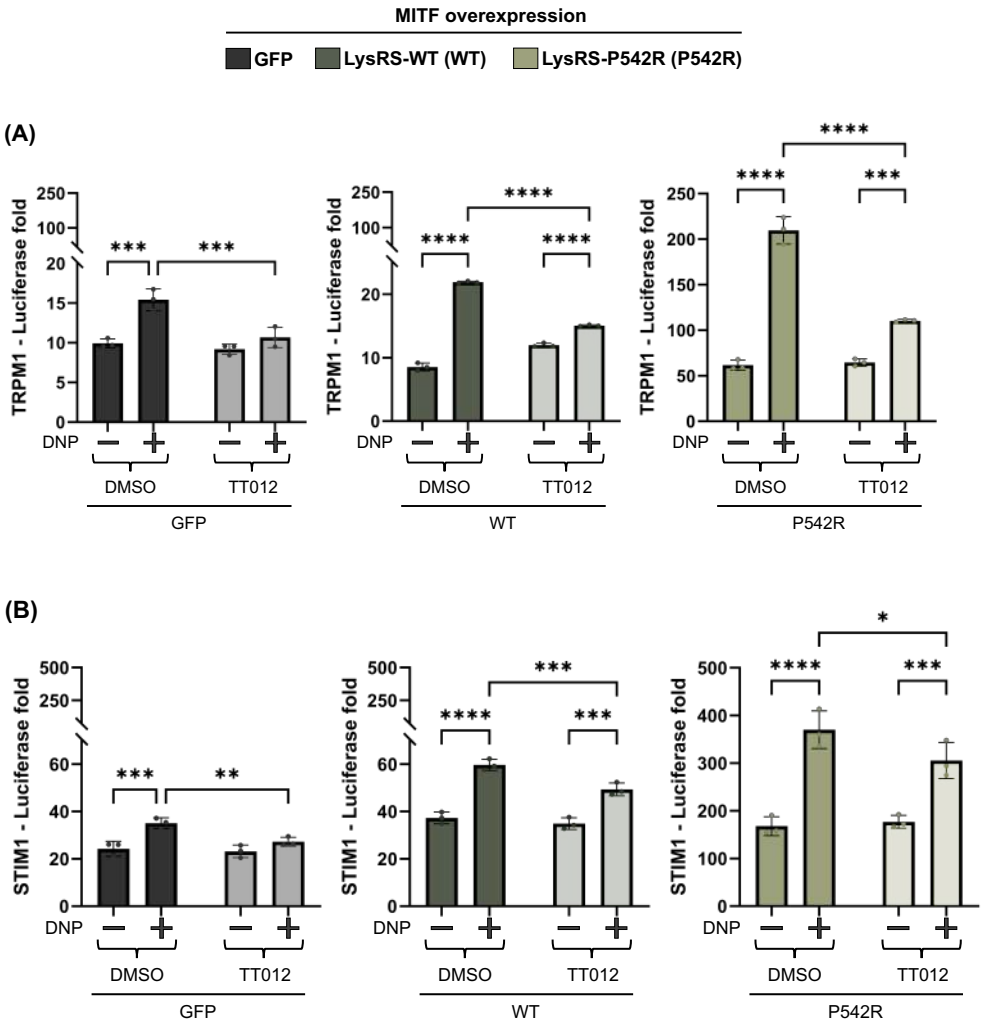

Figure 45. STIM1 activity is regulated by MITF. The Luciferase technique was used to assess STIM1 activity in transfected RBL-2H3 cells using TRPM1 in parallel as a control. These cells were treated with TT012 overnight after cell transfection with luciferase. A) MITF activity through the TRPM1 promotor (n=3). B) MITF activity through the STIM1 promotor (n=3). Results are expressed as mean ± SD. Significance was determined using two-way ANOVA with Tukey's multiple comparison analysis. P<0.05 was considered statistically significant. *P<0.05; **P<0.01; ***P<0.001; ****P<0.0001. DNP as DNP-HSA=dinitrophenyl- Human serum albumin; P54R as LysRS-P542R and WT as LysRS-WT.

3.1.3. MITF regulation of *de novo* mediators release in mast cells through the FcεRI receptor

MCs produce a wide range of cytokines, chemokines, and growth factors upon activation with stimuli such as allergens, pathogens, or physical injury. This secretion includes pro-inflammatory cytokines, such as IL-8 and GM-CSF, as well as anti-inflammatory cytokines like TGF-β, or chemokines such as CCL2 (which disrupts immune cell infiltration and T-cell function) (175,438).

MC functionality is regulated by transcription factors such as MITF and GATA2, whose activation induces the transcription of mediator genes (173,434). Thus, in this section, we wanted to study the involvement of MITF in *de novo* mediator secretion in MCs.

3.1.3.1. Analysis of *de novo* mediators release in MITF-knockdown cells

First, as in the first study, we observed that MCs from anaphylactic patients produce more pro-inflammatory cytokines than those from sensitized patients. MCs from the anaphylaxis group had higher *MITF* levels. Thus, LAD2 cells were treated with ML329 or MITF shRNAs, and IL-8, GM-CSF, CCL2, and TGF-β were measured after cell activation with ^{b}IgE+STV for 24 hours. Our results showed that MITF inhibition with ML329 or silenced with shRNAs significantly reduces IL-8 and GM-CSF secretion compared with control cells after cell activation with ^{b}IgE+STV (Figure 46A and B).

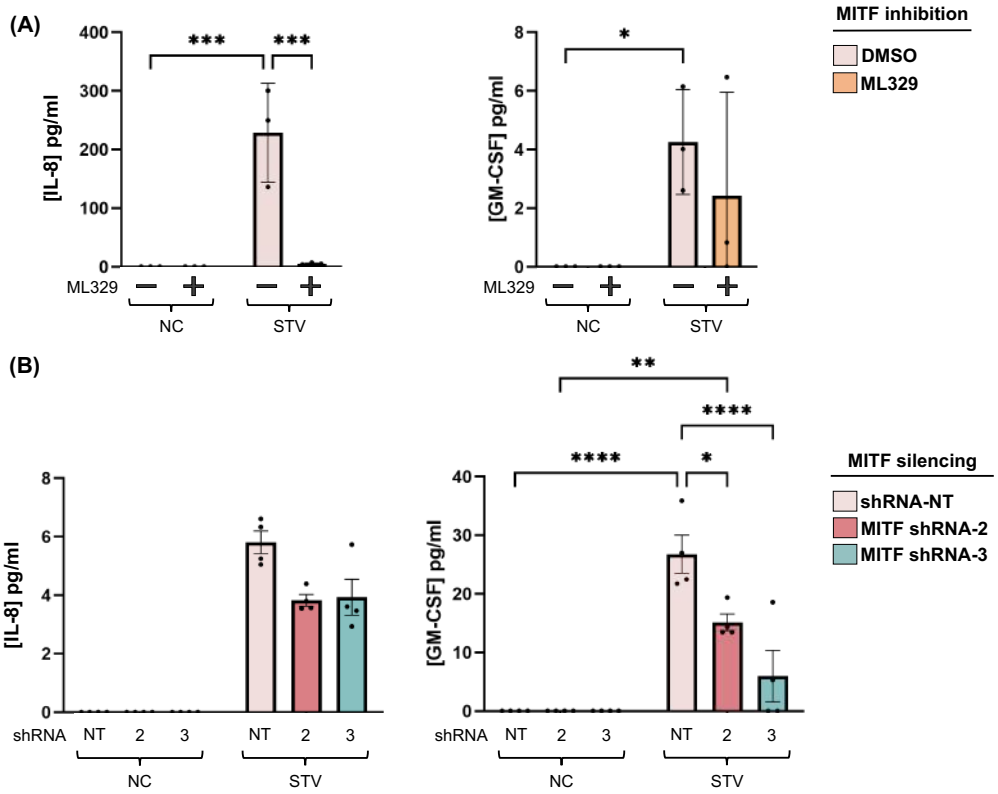

Figure 46. Pro-inflammatory cytokines are reduced in MITF-knockdown cells. LAD2 cells were treated with ML329 or shRNAs to inhibit or silence MITF, and IL-8 and GM-CSF were measured after activation with streptavidin. A) IL-8 and GM-CSF secretion in LAD2 cells with MITF inhibition (n=3). B) IL-8 and GM-CSF secretion in LAD2 cells with MITF-silenced (n=4). Results are expressed as mean ± SD. Significance was determined using two-way ANOVA with Tukey's multiple comparison analysis. P<0.05 was considered statistically significant. *P<0.05; **P<0.01; ***P<0.001; ****P<0.0001. NC=Negative control; STV=Streptavidin.

Interestingly, we found that LAD2 cells with MITF-knockdown, either with ML329 and MITF shRNAs, produced more TGF-β and CCL2 than control cells after activation with STV (Figure 47A and B).

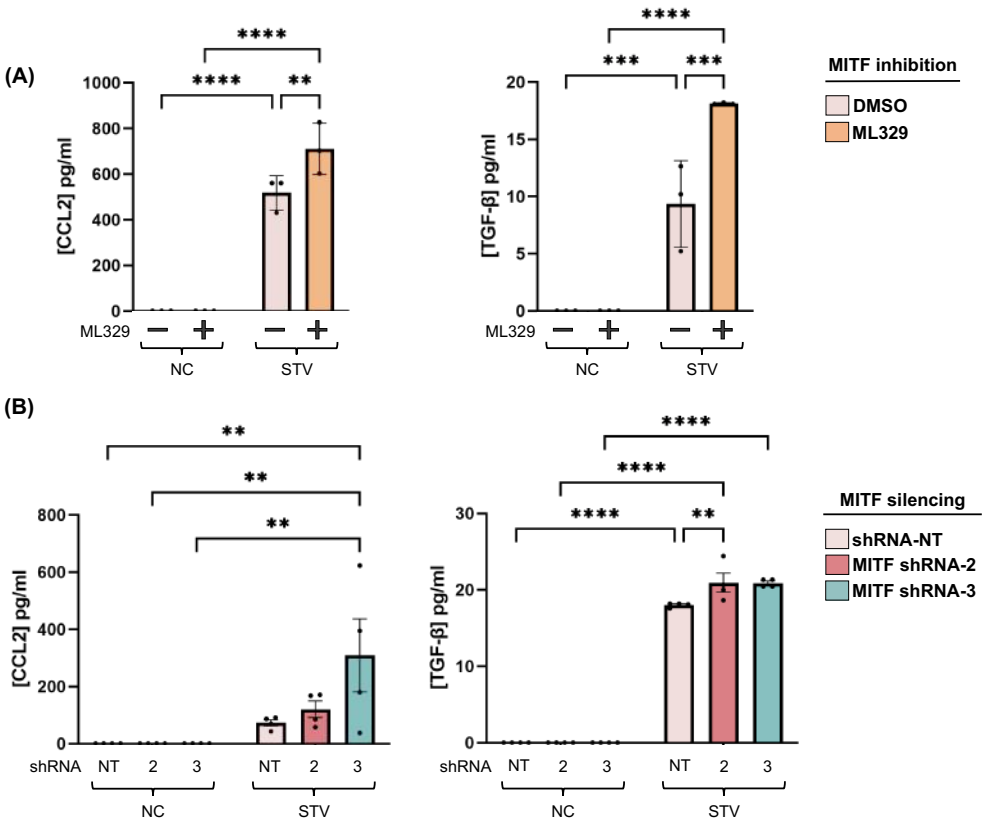

Figure 47. TGF-β and CCL2 secretion is increased in MITF-knockdown cells. LAD2 cells were treated with ML329 or shRNAs to inhibit or silence MITF, and TGF-β and CCL2 were measured after activation with streptavidin. A) CCL2 and TGF-β secretion in LAD2 cells with MITF inhibition (n=3). B) CCL2 and TGF-β secretion in LAD2 cells with MITF-silenced (n=4). Results are expressed as mean ± SD. Significance was determined using two-way ANOVA with Tukey's multiple comparison analysis. P<0.05 was considered statistically significant. **P<0.01; ***P<0.001; ****P<0.0001. NC=Negative control; STV=Streptavidin.

3.1.3.2. MITF-knockdown changes the cytokine pattern in cells sensitized with pooled sera from LTP patients and challenged with Pru p 3

In our first study, we showed that LAD2 and primary cells sensitized with sera from the anaphylaxis group produced more IL-8 and GM-CSF than cells sensitized with pooled sera from sensitized patients. In addition, we found that anaphylactic patients had higher *MITF* levels than sensitized patients.

Furthermore, we verified that MITF-knockdown may induce changes in the cytokine pattern after cell activation in LAD2 cells. Thus, we wanted to analyze whether *MITF* levels are the basis of this differential secretion.

LAD2 cells were treated with ML329, TT012, or shRNAs for five days. Afterward, cells were sensitized with sera from both groups of patients and stimulated with Pru p 3. In parallel, $CD34^+$-derived MCs were treated with both MITF inhibitors for five days, sensitized with sera from anaphylaxis and sensitized patients and stimulated with Pru p 3. IL-8, GM-CSF, and CCL2 were measured.

We observed that cells with MITF-knockdown, either when cells were sensitized with pooled sera from the anaphylaxis or sensitized group, reduced the amount of IL-8 secretion in LAD2 cells and $CD34^+$-derived MCs (Figure 48). Similar results were found when GM-CSF was measured. Cells with MITF-knockdown sensitized with pooled sera from LTP patients, both sensitized and anaphylaxis, produced lower amounts of GM-CSF than control cells (Figure 49).

Conversely, in MITF-knockdown cells – when sensitized with pooled sera from the anaphylaxis or sensitized group – in some cases, we observed no differences (Figure 50A) and in others, there was a slightly significant increase in CCL2 secretion (Figure 50B and C).

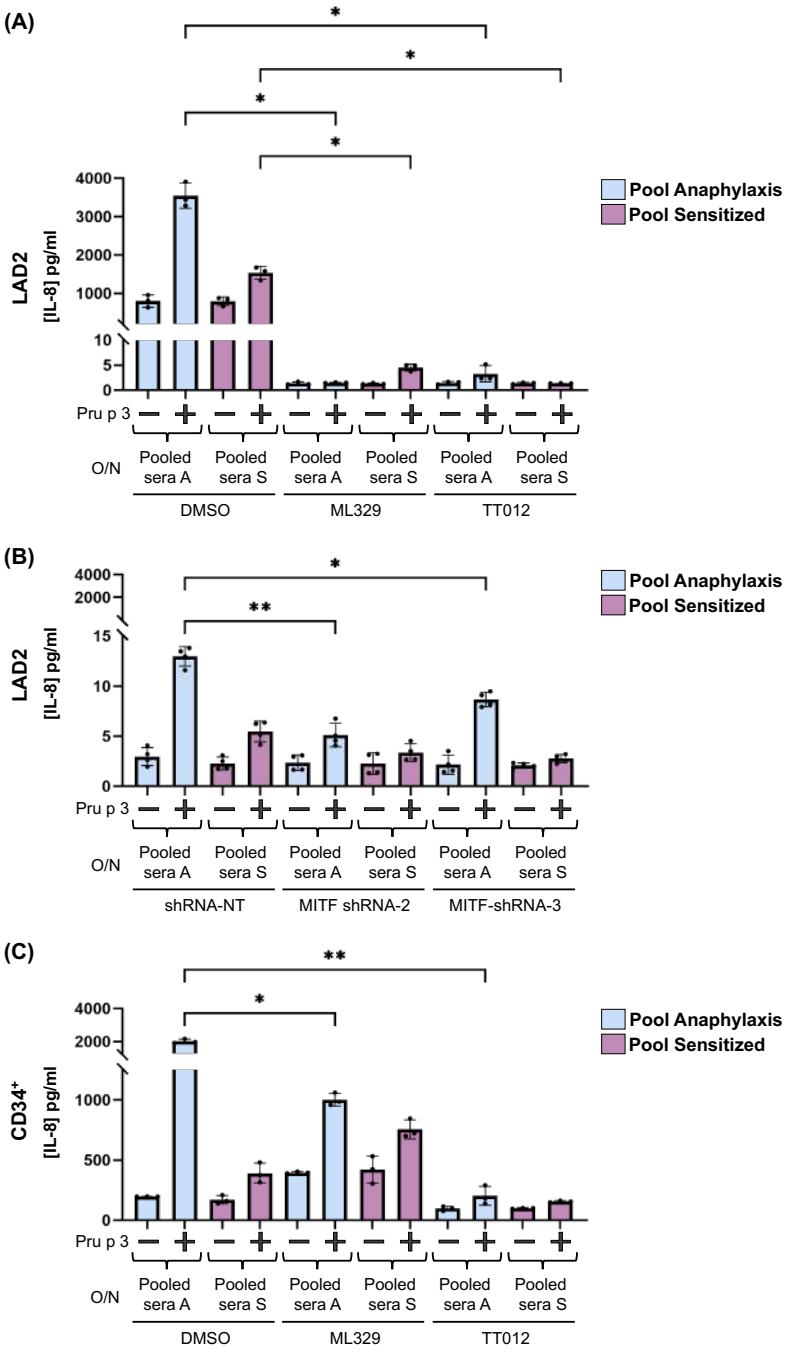

Figure 48. MITF-knockdown reduces IL-8 cytokine secretion in sensitized cells. LAD2 and primary cells were treated with ML329, TT012, or MITF shRNAs, sensitized with sera from LTP patients and stimulated with allergen. A) LAD2 cells with MITF inhibition (n=3). B) LAD2 cells with MITF-silenced (n=4). C) Primary cells with MITF inhibition (n=3). Results are expressed as mean ± SD. Significance was determined using two-way ANOVA with Tukey's multiple

comparison analysis. P<0.05 was considered statistically significant. *P<0.05; **P<0.01. A=Anaphylaxis; O/N=Overnight; S=Sensitized.

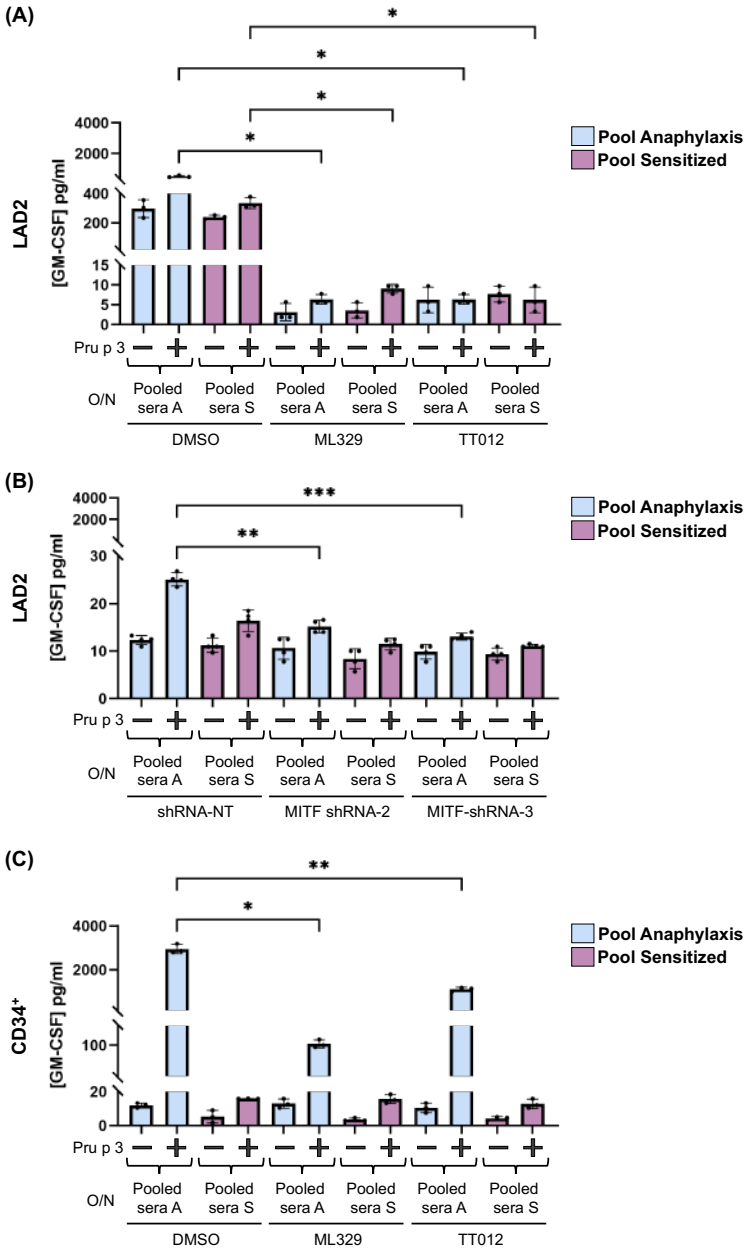

Figure 49. MITF-knockdown reduces GM-CSF cytokine secretion in sensitized cells. LAD2 and primary cells were treated with ML329, TT012 or MITF shRNAs, sensitized with sera from LTP patients and stimulated with allergen. A) LAD2 cells with MITF inhibition (n=3). B) LAD2 cells with MITF-silenced (n=4). C) Primary cells with MITF inhibition (n=3). Results are

expressed as mean ± SD. Significance was determined using two-way ANOVA with Tukey's multiple comparison analysis. P<0.05 was considered statistically significant. *P<0.05; **P<0.01; ***P<0.001. A=Anaphylaxis; O/N=Overnight; S=Sensitized.

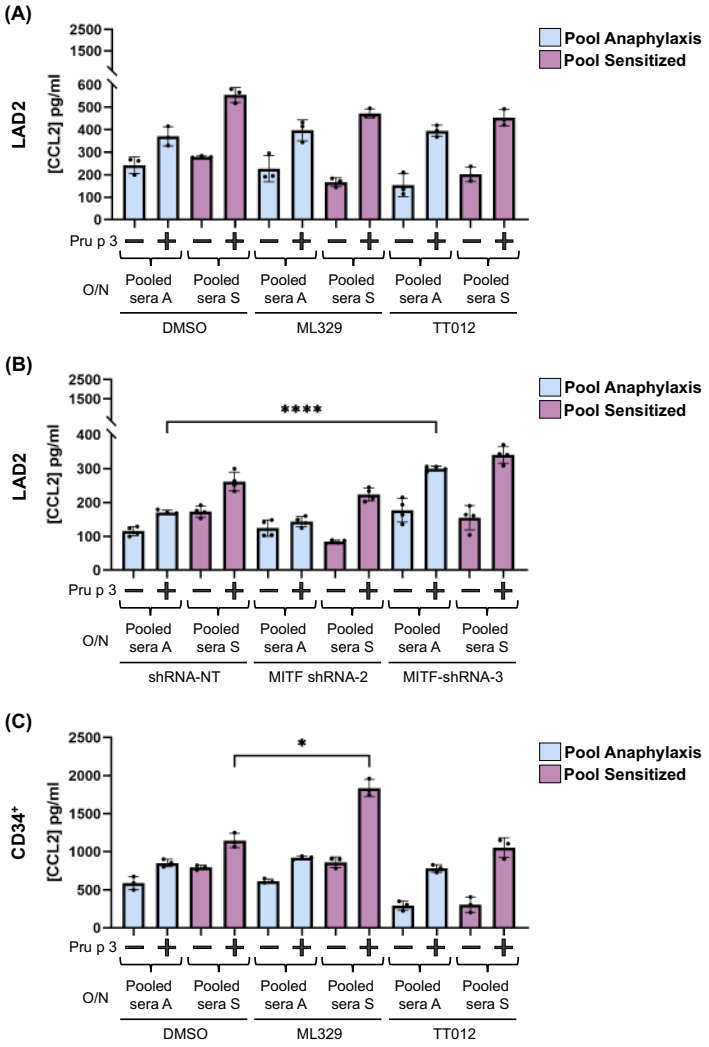

Figure 50. MITF-knockdown increases CCL2 secretion in sensitized cells. LAD2 and primary cells were treated with ML329, TT012 or MITF shRNAs, sensitized with sera from LTP patients and stimulated with allergen. A) LAD2 cells with MITF inhibition (n=3). B) LAD2 cells with MITF-silenced (n=4). C) Primary cells with MITF inhibition (n=3). Results are expressed as mean ± SD. Significance was determined using two-way ANOVA with Tukey's multiple comparison analysis. P<0.05 was considered statistically significant. *P<0.05; ****P<0.0001. A=Anaphylaxis; O/N=Overnight; S=Sensitized.

3.2. MITF involvement in drug hypersensitivity reactions

We previously reported that MRGPRX2 activation with substance P or drugs increases MITF activity (169) and MITF is involved in adverse reactions; therefore, we decided to further investigate MITF involvement in MC mediator's release abilities to deepen our understanding of drug hypersensitivity reactions.

3.2.1. Quantification of gene expression associated with exacerbated MC responses in MITF-knockdown cells upon MRGPRX2 stimulation

We used a qPCR dynamic array to assess whether MITF is involved in the transcription of different genes (those explored above) related to exacerbated MC responses via the MRGPRX2 receptor.

LAD2 cells were treated with MITF shRNAs for five days and stimulated with SP for 24 hours. Afterward, some genes were assessed by qPCR dynamic array. First, we evaluated the expression of *MITF* and saw a significant downregulation in cells treated with MITF shRNAs, both under basal and activated conditions, confirming MITF silencing. Then, we assessed genes involved in the MITF pathway, as before. In MITF-silenced cells, *KARS*, *NUTD2*, and *HINT1* were significantly decreased, both under basal and stimulated conditions (Figure 51), as observed in the IgE-dependent pathway.

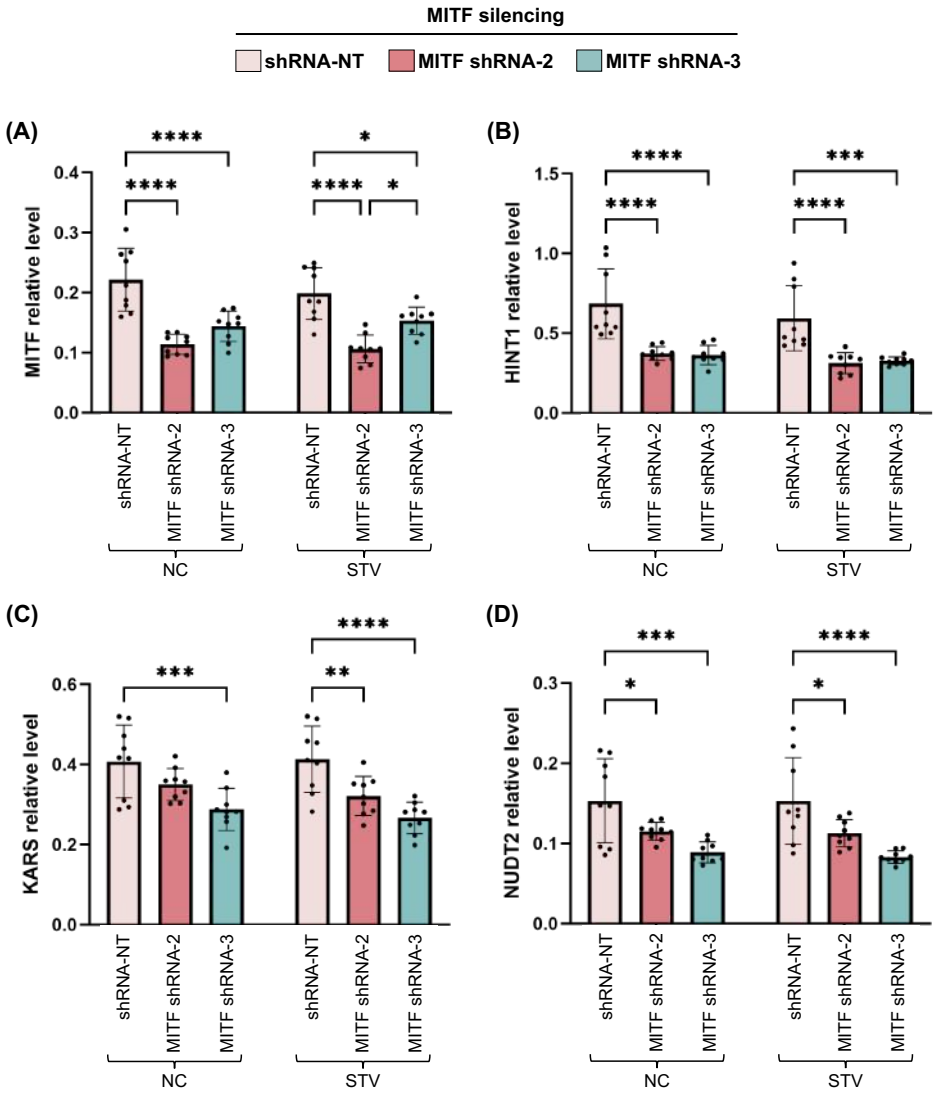

Figure 51. Genes involved in MITF regulation are reduced in MITF-silenced cells via the MRGPRX2 receptor. MITF-silenced LAD2 cells were used to assess some genes (n=9). A) *MITF* gene expression levels. B) *HINT1* gene expression levels. C) *KARS* gene expression levels. D) *NUDT2* gene expression levels. Results are expressed as mean ± SD. Significance was determined using two-way ANOVA with Tukey's multiple comparison analysis. P<0.05 was considered statistically significant. *P<0.05; **P<0.01; ***P<0.001; ****P<0.0001. NC=Negative control; SP=Substance P.

Afterward, we assessed *STIM1* and observed that after cell activation with SP, the levels of *STIM1* in MITF-knockdown cells were lower than in control cells (Figure 52).

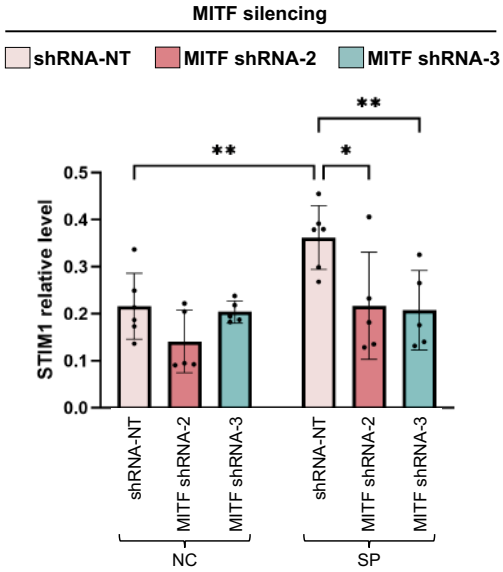

Figure 52. MITF silencing reduces STIM1 levels in the MRGPRX2 pathway. MITF-silenced LAD2 cells were used to assess *STIM1* (n=9). Results are expressed as mean ± SD. Significance was determined using two-way ANOVA with Tukey's multiple comparison analysis. P<0.05 was considered statistically significant. *P<0.05; **P<0.01. NC=Negative control; SP=Substance P.

Furthermore, assessing the cytokine and chemokine genes, we observed that control cells presented elevated levels of *CCL18* and *IL1B* after cell activation with SP (Figure 53A and C). No significant differences were found in *CCL2* and *TGFB1* levels (Figure 53B and D).

Then, we evaluated the prostaglandin receptors genes. No significant differences were found in the expression of *PTGER2*; however, MITF-knockdown cells presented lower *PTGER3* expression levels and higher *PTGER4* expression levels than control cells, both under basal and activated conditions (Figure 54B and C). In addition, *COX2* is elevated in control cells after cell activation with SP (Figure 54D).

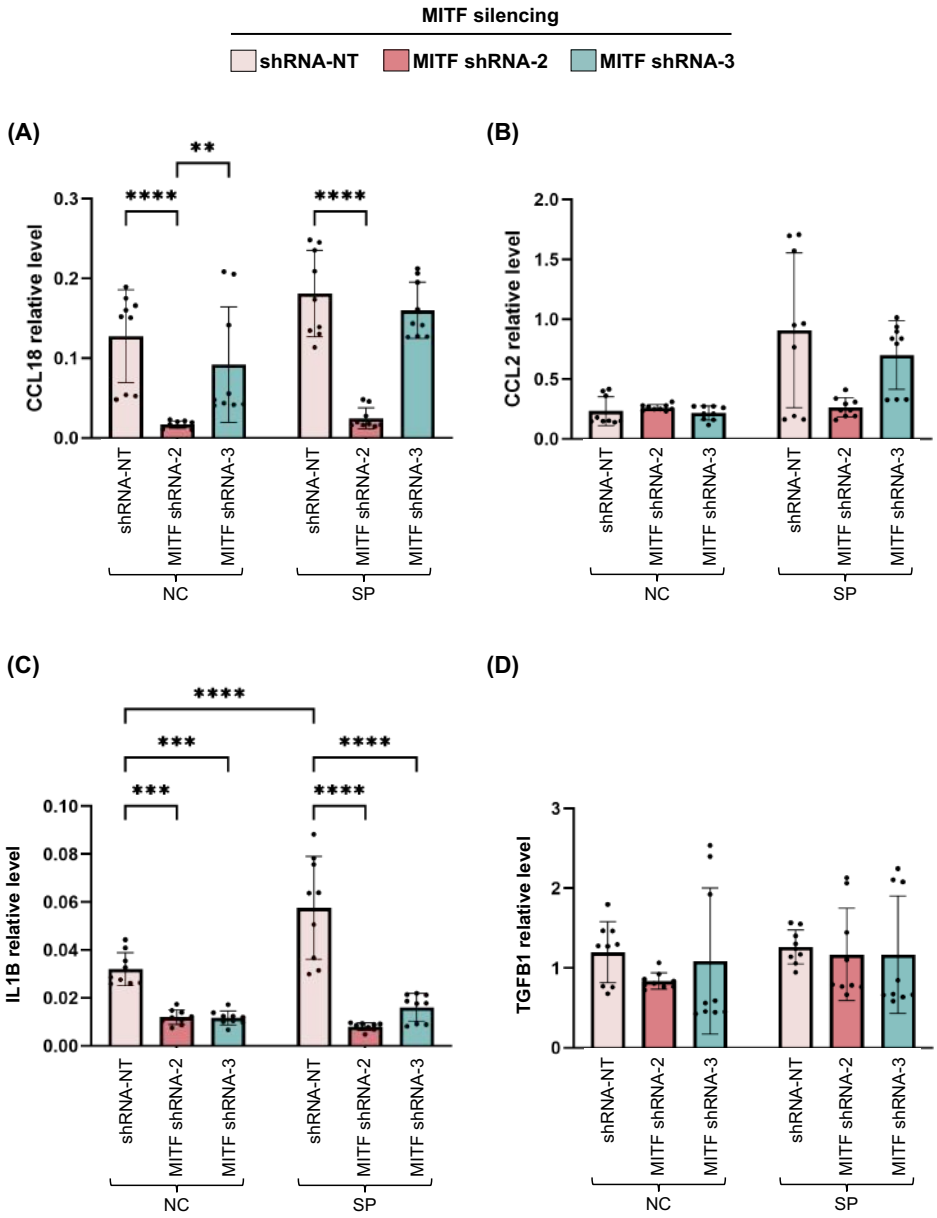

Figure 53. MITF-knockdown cytokine and chemokine gene levels in the MRGPRX2 pathway. MITF-silenced LAD2 cells were used to assess some genes (n=9). A) *CCL18* gene expression levels. B) *CCL2* gene expression levels. C) *IL1B* gene expression levels. D) *TGFB1* gene expression levels. Results are expressed as mean ± SD. Significance was determined using two-way ANOVA with Tukey's multiple comparison analysis. P<0.05 was considered statistically significant. **P<0.01; ***P<0.001; ****P<0.0001. NC=Negative control; SP=Substance P.

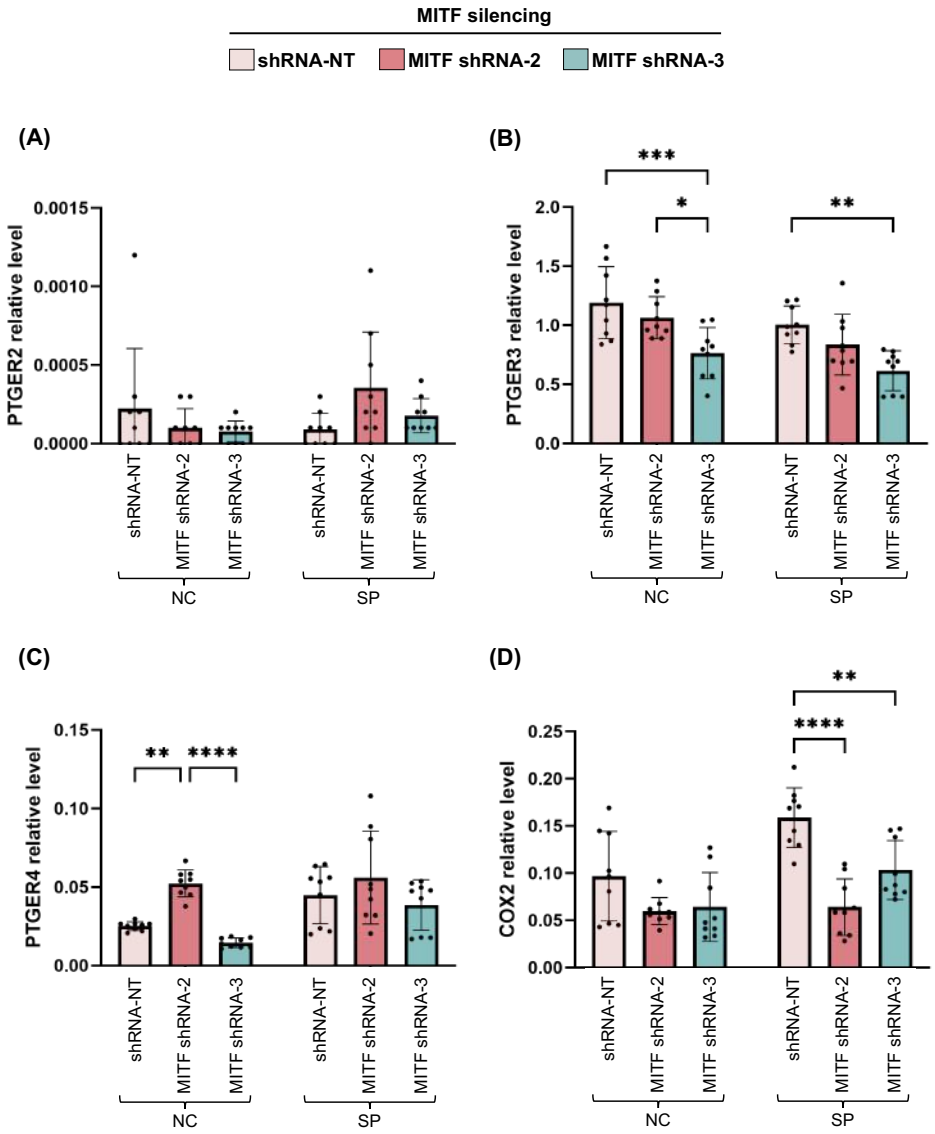

Figure 54. *PTGER4* is elevated in MITF-knockdown cells in the MRGPRX2 pathway. MITF-silenced LAD2 cells were used to assess some genes (n=9). A) *PTGER2* gene expression levels. B) *PTGER3* gene expression levels. C) *PTGER4* gene expression levels. D) *COX2* gene expression levels. Results are expressed as mean ± SD. Significance was determined using two-way ANOVA with Tukey's multiple comparison analysis. P<0.05 was considered statistically significant. *P<0.05; **P<0.01; ***P<0.001; ****P<0.0001. NC=Negative control; SP=Substance P.

Finally, we assessed *MRGPRX2* receptor gene levels to assess whether MITF can regulate this receptor. We observed that in MITF-silenced cells, *MRGPRX2* is significantly downregulated (Figure 55A). Indeed, when we assessed protein expression by flow cytometry, we found a decreased MRGPRX2 expression levels, especially when MITF is silenced (Figure 55A and B).

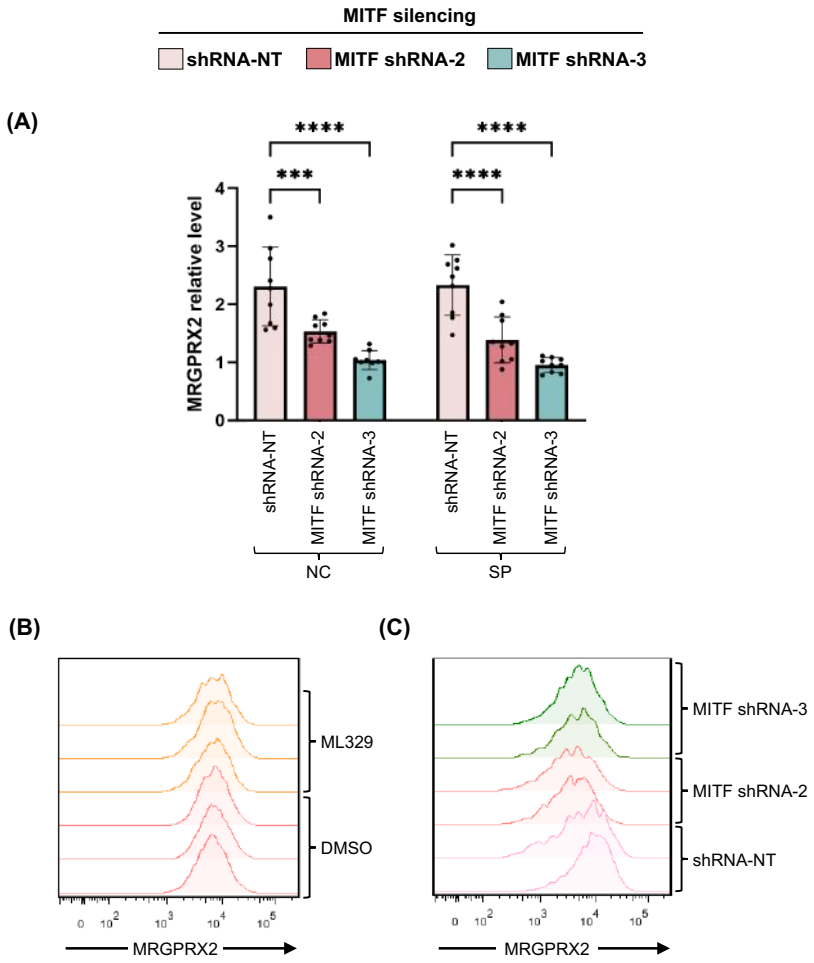

Figure 55. MRGPRX2 receptor expression is reduced in MITF-knockdown cells. MITF-knockdown LAD2 cells were used to assess *MRGPRX2* gene expression levels (n=9) by qPCR, and MRGPRX2 protein expression levels by flow cytometry. A) *MRGPRX2* gene expression levels. B) MRGPRX2 expression in MITF-inhibited cells. C) MRGPRX2 expression in MITF-silenced cells. Results are expressed as mean ± SD. Significance was determined using two-way ANOVA with Tukey's multiple comparison analysis. P<0.05 was considered statistically significant. ***P<0.001; ****P<0.0001. NC=Negative control; SP=Substance P.

Again, all these results suggest that MITF may play an important role in regulating exacerbated responses. The inhibition of this transcription factor reduced the expression of *IL1B, COX2, PTGER3, NUDT2, KARS*, and *HINT1*, promoting a less pro-inflammatory response.

3.2.2. MITF regulation of calcium influx in MCs via the MRGPRX2 receptor

After assessing MITF involvement in STIM1 expression and, consequently, in calcium influx in an IgE-dependent pathway, we measured the calcium influx under MITF-knockdown conditions after cell activation with SP (Figure 56A).

As we previously reported (169), LAD2 cells treated with ML329 or MITF shRNAs presented significantly lower levels of calcium influx after cell activation with SP than control cells (Figure 56B and C). Moreover, we used primary cells to further confirm this MITF-calcium axis. Skin MCs were treated with MITF inhibitors (ML329 and TT012) for five days, and then calcium influx was measured after cell activation with SP. MITF-silenced MCs presented significantly lower levels of calcium influx after cell activation (Figure 56), as observed in LAD2 cells.

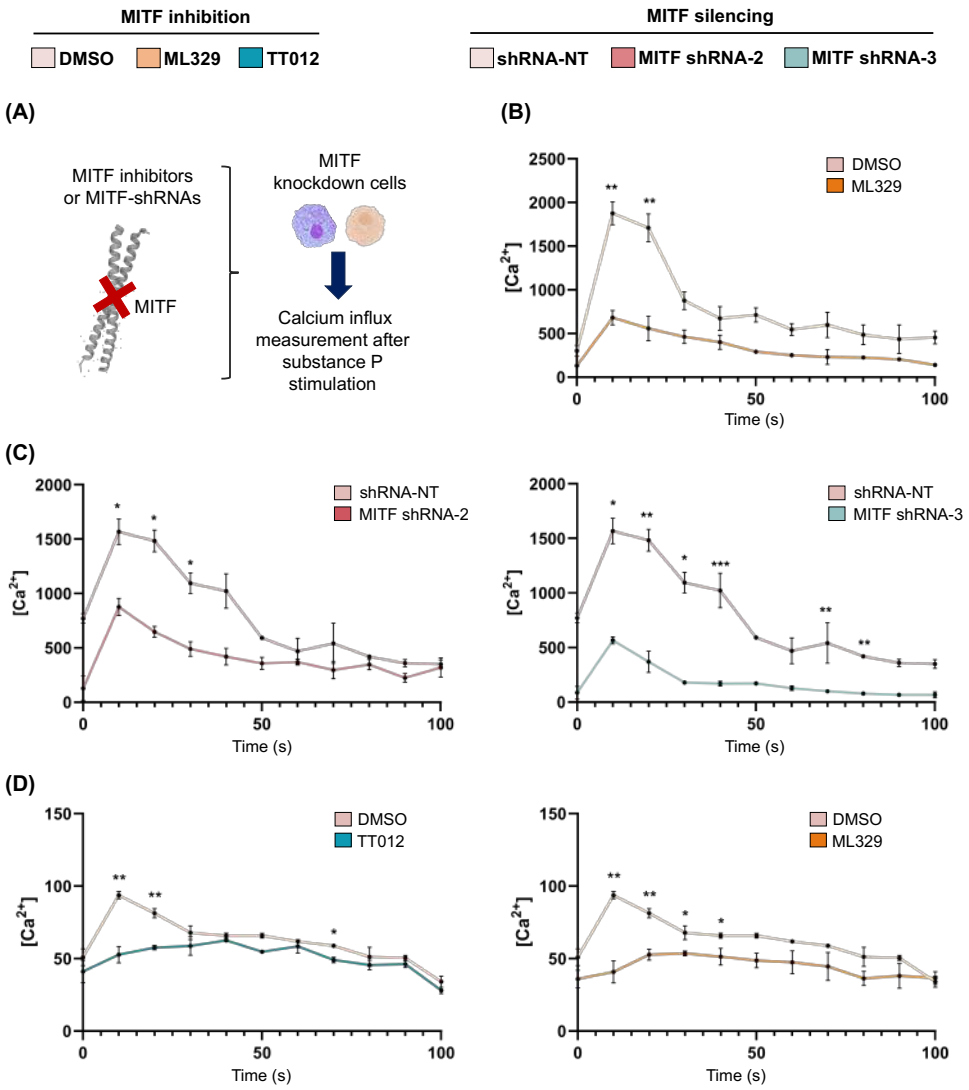

Figure 56. Calcium influx is impaired in MITF-knockdown cells via the MRGPRX2 receptor. LAD2 cells treated with MITF inhibitors or infected with MITF shRNAs for five days and stimulated with substance P (SP) were used to measure calcium influx. A) Methodology illustration. B) LAD2 cells treated with ML329 for five days and stimulated with SP (n=3). C) LAD2 cells infected with MITF shRNA-2 and MITF shRNA-3 for five days and activated with SP (n=3). D) Skin MCs treated with TT012 or ML329 for five days and stimulated with SP (n=3). Results are expressed as mean ± SD. Significance was determined using two-way ANOVA with Tukey's multiple comparison analysis. P<0.05 was considered statistically significant. *P<0.05; **P<0.01; ***P<0.001.

3.2.3. MITF regulation of *de novo* mediators release in mast cells via the MRGPRX2 receptor through substance P

Similarly, we first analyzed the cytokine and chemokine release with MITF inhibition and MITF silencing. As we observed with the IgE-dependent pathway, MITF inhibition and MITF silencing reduce the IL-8 and GM-CSF secretion after cell activation with SP, the natural ligand of the MRGPRX2 receptor (Figure 57); in contrast, it increases the CCL2 and TGF-β secretion (Figure 58).

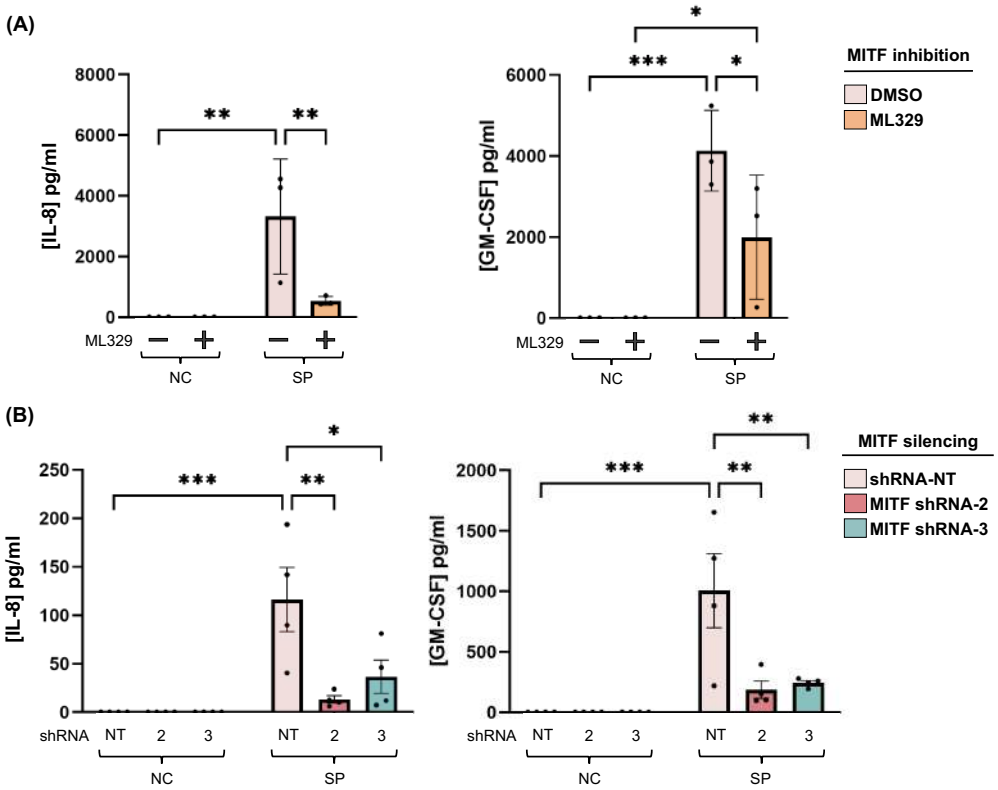

Figure 57. MITF-knockdown reduces IL-8 and GM-CSF secretion in MCs after activation with SP. LAD2 cells were treated with ML329 or shRNAs to inhibit or silence MITF, and IL-8 and GM-CSF were measured after activation with streptavidin. A) IL-8 and GM-CSF secretion in LAD2 cells with MITF inhibition (n=3). B) IL-8 and GM-CSF secretion in LAD2 cells with MITF-silenced (n=4). Results are expressed as mean ± SD. Significance was determined using two-way ANOVA with Tukey's multiple comparison analysis. P<0.05 was considered statistically significant. *P<0.05; **P<0.01; ***P<0.001. NC=Negative control; SP=Substance P.

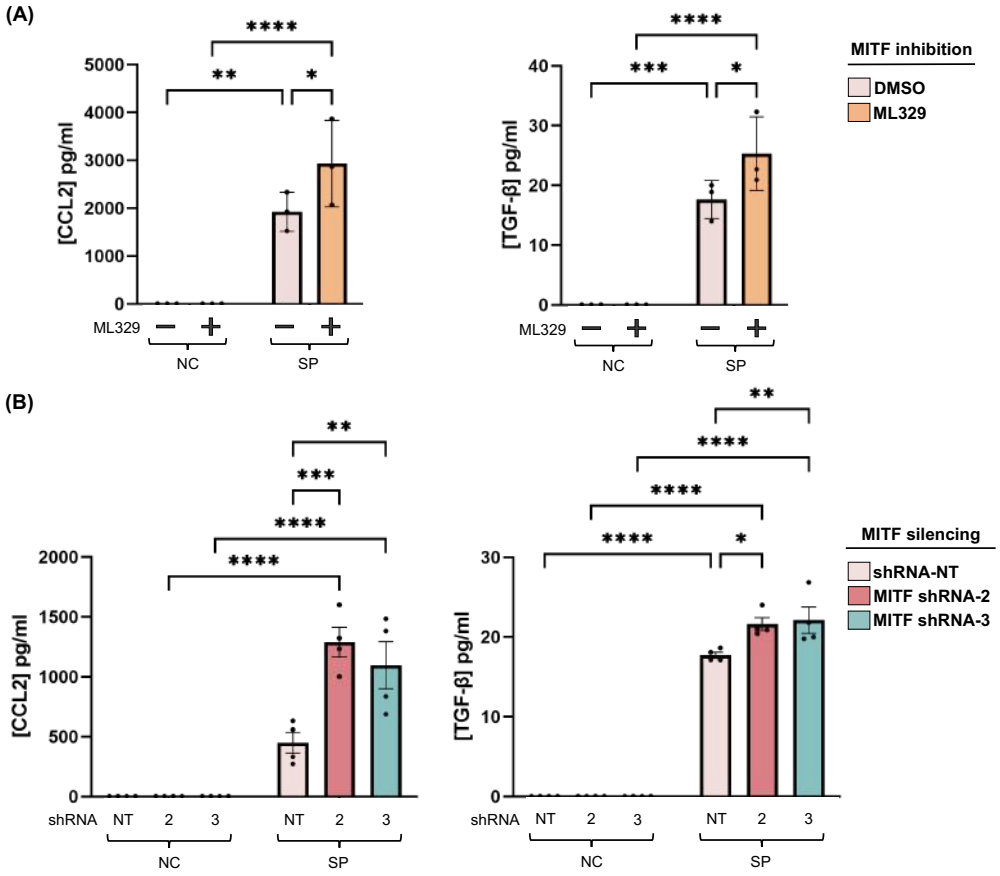

Figure 58. MITF-knockdown increases CCL2 and TGF-β secretion in MCs after activation with SP. LAD2 cells were treated with ML329 or shRNAs to inhibit or silence MITF, and IL-8 and GM-CSF were measured after activation with streptavidin. A) CCL2 and TGF-β secretion in LAD2 cells with MITF inhibition (n=3). B) CCL2 and TGF-β secretion in LAD2 cells with MITF-silenced (n=4). Results are expressed as mean ± SD. Significance was determined using two-way ANOVA with Tukey's multiple comparison analysis. P<0.05 was considered statistically significant. *P<0.05; **P<0.01; ***P<0.001; ****P<0.0001. NC=Negative control; SP=Substance P.

Next, we decided to use a novel MITF inhibitor, TT012, that acts by inhibiting the dimerization of MITF. We wanted to evaluate whether this inhibition was sufficient to impair the cytokine and chemokine secretion. Thus, LAD2 cells were pre-treated with TT012 for one hour and then stimulated to assess IL-8, GM-CSF and CCL2 secretion in the continued presence of TT012.

First, a dose-response curve was constructed to find the optimal TT012 concentration for the best inhibition effect. Thus, after cell treatment with different concentrations of TT012 (1.25, 2.5, 5, and 10 μM), SP was used to activate. Upon measuring IL-8, GM-CSF, and CCL2, we observed that all TT012 concentrations could reduce cytokine and chemokine secretion, although 5 and 10 μM seem the best for clear inhibition. Thus, we selected 5 μM to perform all the following experiments (Figure 59).

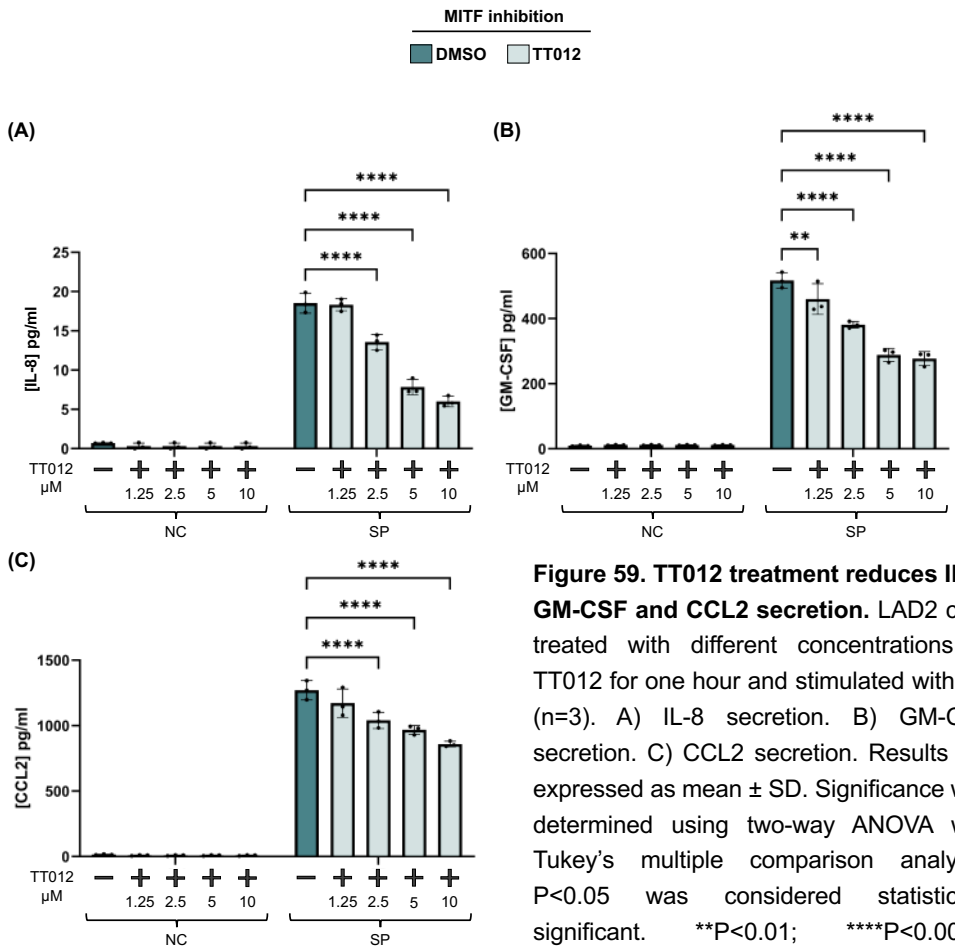

Figure 59. TT012 treatment reduces IL-8, GM-CSF and CCL2 secretion. LAD2 cells treated with different concentrations of TT012 for one hour and stimulated with SP (n=3). A) IL-8 secretion. B) GM-CSF secretion. C) CCL2 secretion. Results are expressed as mean ± SD. Significance was determined using two-way ANOVA with Tukey's multiple comparison analysis. P<0.05 was considered statistically significant. **P<0.01; ****P<0.0001. NC=Negative control; SP=Substance P.

Controversially with these results, we previously observed that cells treated with ML329 for 5 days increased CCL2 secretion. It's important to consider that TT012 acts by inhibiting the dimerization of MITF but not affecting MITF levels even after 25 hours of continuous exposure (1 hour of preincubation plus 24 hours of activation) (159). Thus, we treated LAD2 cells with TT012 for five days to assess whether MITF-knockdown could change CCL2 secretion. After five days of treatment with TT012, we saw a reduced expression of MITF and a higher secretion of CCL2 compared with control cells (Figure 60). This results suggest a controversial role of MITF in regulating CCL2 secretion.

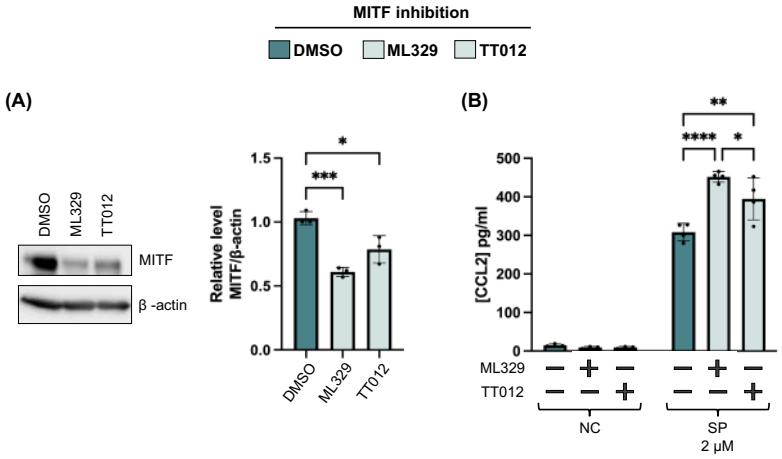

Figure 60. TT012 treatment for five days increases CCL2 secretion. LAD2 cells were treated with 10 μM TT012 or 2 μM ML329 for 5 days, stimulated with substance P, and CCL2 was measured after 24 hours of stimulation (n=4). A) MITF expression after five days of MITF inhibition. C) CCL2 secretion. Results are expressed as mean ± SD. Significance was determined using two-way ANOVA with Tukey's multiple comparison analysis. P<0.05 was considered statistically significant. *P<0.05; **P<0.01; ****P<0.0001. NC=Negative control; SP=Substance P.

3.2.4. MITF regulation of *de novo* mediators release in mast cells via the MRGPRX2 receptor through drugs

After selecting the TT012 concentration, LAD2 cells were treated with this MITF inhibitor for one hout or with ML329 for five days and activated with different drugs at different concentrations. IL-8, GM-CSF, and CCL2 were measured.

LAD2 cells activated with vancomycin, morphine and cisatracurium produced high levels of IL-8, especially with vancomycin and morphine. Conversely, when LAD2 cells were treated with MITF inhibitors, this IL-8 secretion was significantly reduced in all cases (Figure 61A). Similar results were observed with GM-CSF secretion. LAD2 cells activated with vancomycin and morphine produced more GM-CSF, especially at the highest concentrations, than LAD2 cells stimulated with cisatracurium. Moreover, when these cells were treated with ML329 or TT012, there was a reduction in GM-CSF secretion after drugs stimulation (Figure 61B).

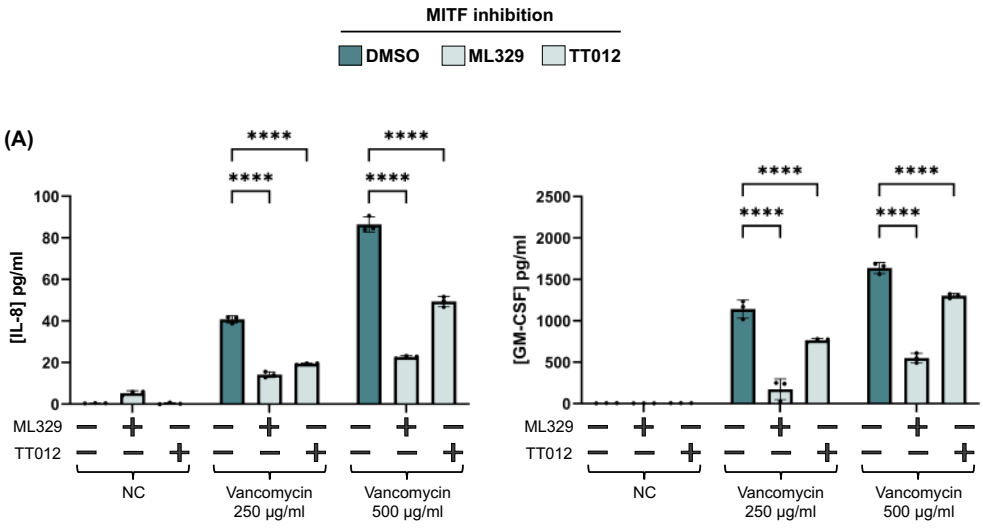

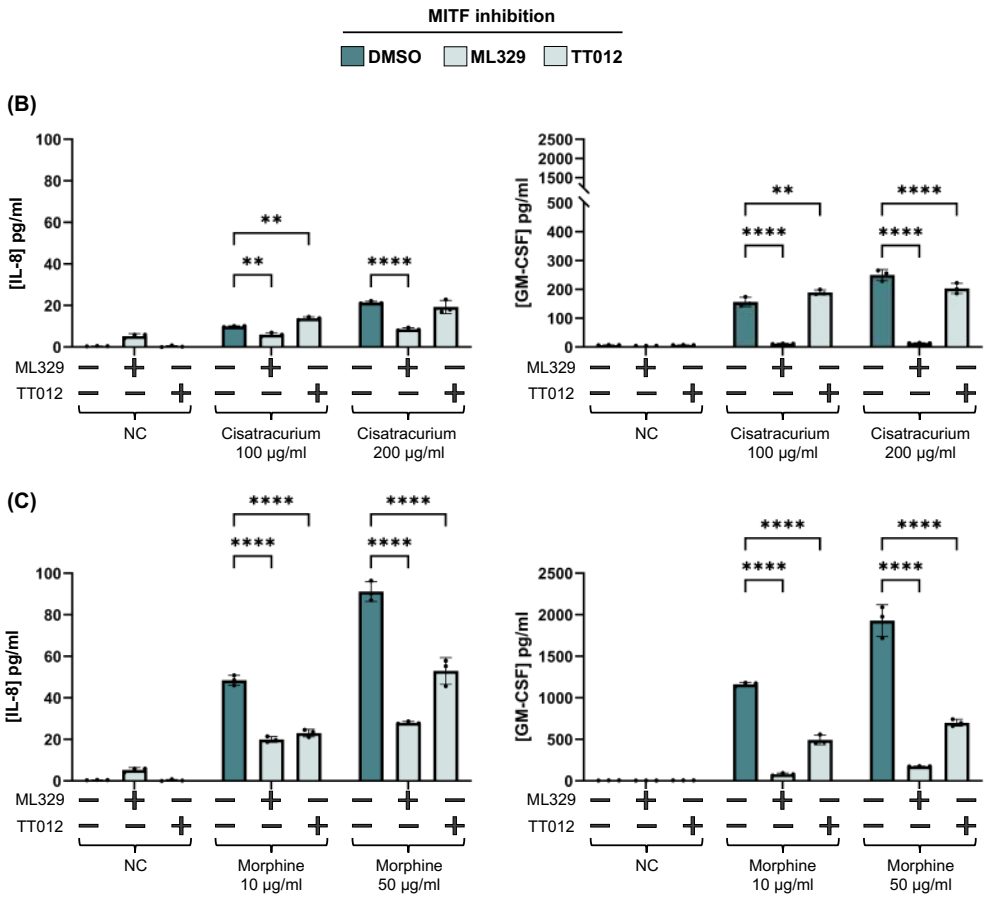

Figure 61. IL-8 and GM-CSF secretion is reduced in MITF-inhibited cells stimulated with drugs. LAD2 cells treated with ML329 for five days or TT012 (1 hour of preincubation plus 24 hours of activation) and stimulated with different concentrations of vancomycin, morphine and cisatracurium (n=3). A) IL-8 and GM-CSF secretion in LAD2 cells treated with TT012 and stimulated with different vancomycin concentrations. B) IL-8 and GM-CSF secretion in LAD2 cells treated with TT012 and stimulated with different cisatracurium concentrations. C) IL-8 and GM-CSF secretion in LAD2 cells treated with TT012 and stimulated with different morphine concentrations. Results are expressed as mean ± SD. Significance was determined using two-way ANOVA with Tukey's multiple comparison analysis. P<0.05 was considered statistically significant. **P<0.01; ****P<0.0001. NC=Negative control.

Finally, we analyzed CCL2 secretion. We also used TT012 at 5 μM to treat cells for 25 hours (1 hour of preincubation plus 24 hours of activation) and ML329 to treat cells for five days before cell activation with drugs. LAD2 cells treated with ML329 for five days produced more CCL2 than control cells after cell activation with vancomycin, morphine and cisatracurium. Conversely, when LAD2 cells were treated with TT012 for 25 hours, CCL2 secretion was significantly reduced (Figure 62).

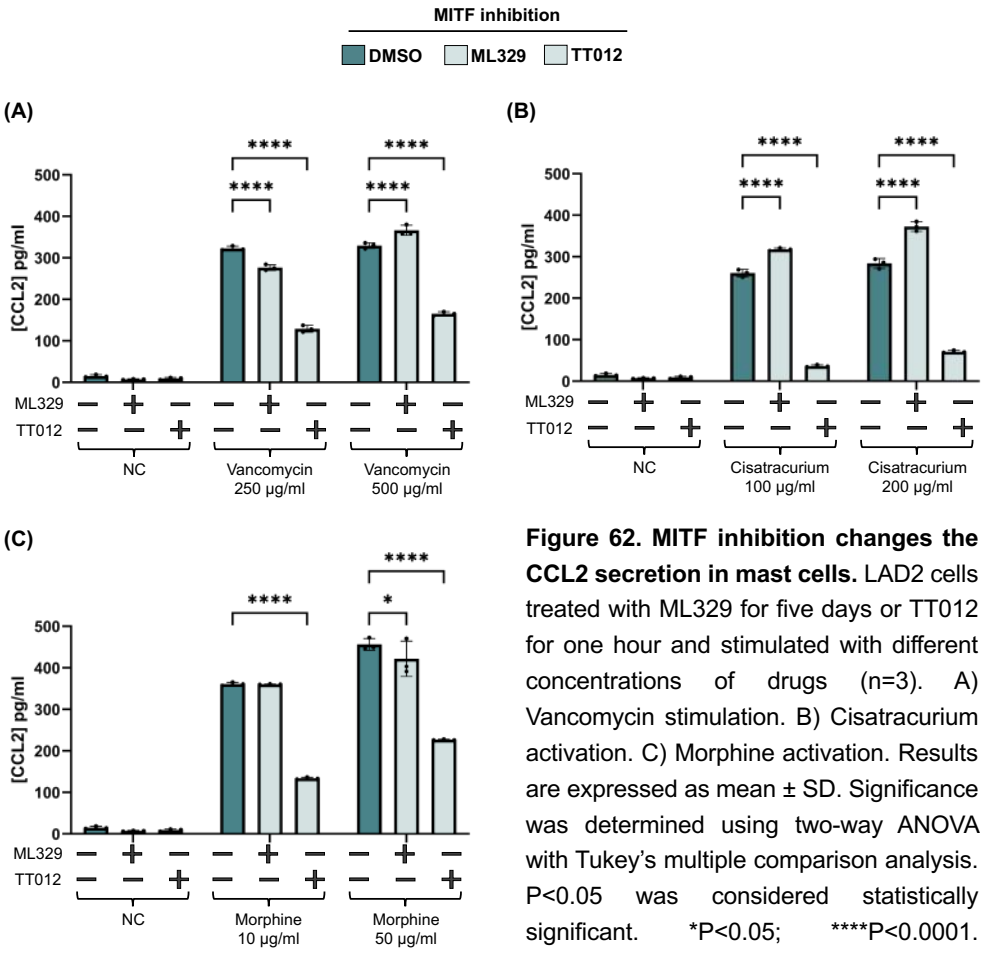

Figure 62. MITF inhibition changes the CCL2 secretion in mast cells. LAD2 cells treated with ML329 for five days or TT012 for one hour and stimulated with different concentrations of drugs (n=3). A) Vancomycin stimulation. B) Cisatracurium activation. C) Morphine activation. Results are expressed as mean ± SD. Significance was determined using two-way ANOVA with Tukey's multiple comparison analysis. P<0.05 was considered statistically significant. *P<0.05; ****P<0.0001. NC=Negative control; SP=Substance P.

To confirm the findings described above, we used another MC model. Skin MCs were treated with TT012 for 25 hours or ML329 for five days. Then, cells were activated with different drugs at different concentrations, and IL-8, GM-CSF, and CCL2 secretion were measured. When cells were treated with MITF inhibitors, there was a significant reduction in the IL-8 and GM-CSF production after cell activation with all drugs (Figure 63A and B).

Assessing the CCL2 secretion, we saw that cells treated with ML329 for five days produced more CCL2 than control cells. Conversely, cells treated with TT012 for one hour before activation induced a lower secretion of CCL2 than control cells (Figure 63C).

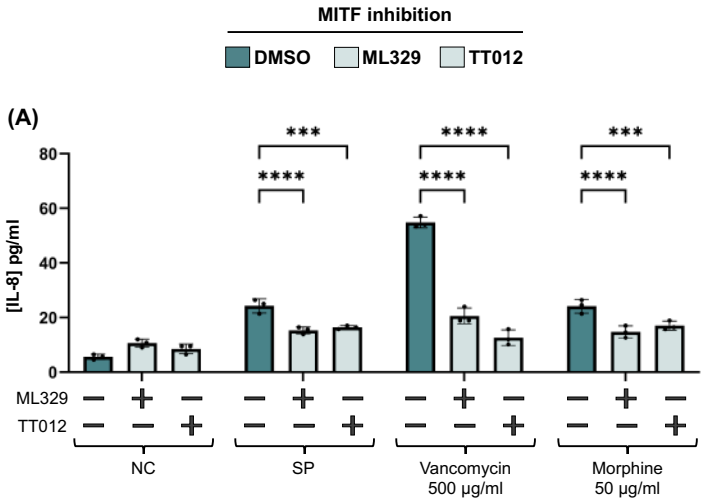

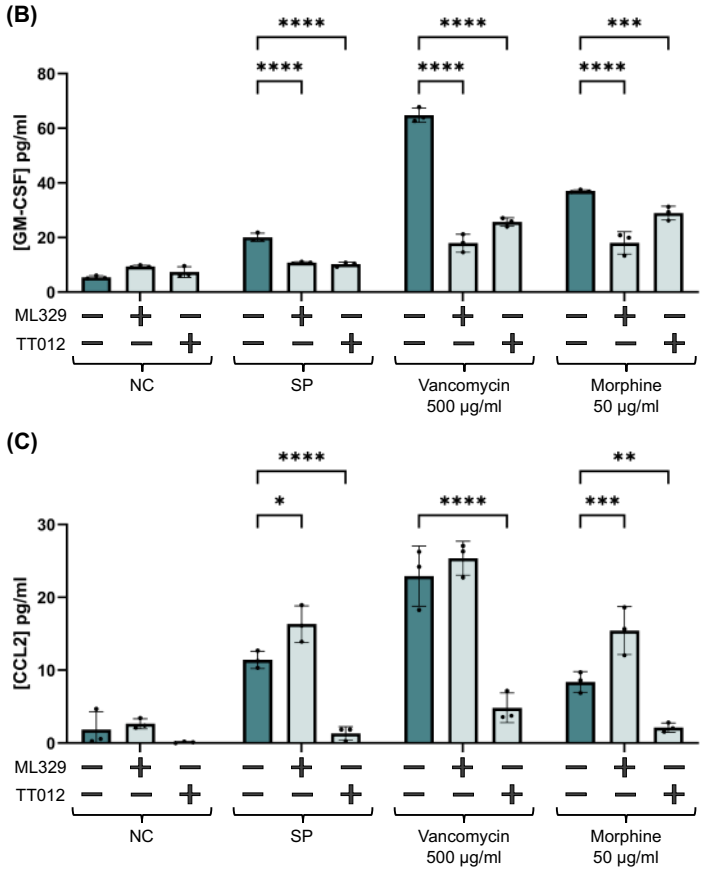

Figure 63. MITF inhibition changes the cytokine/chemokine pattern in skin mast cells. Primary cells were treated with ML329 for five days or TT012 (1 hour of preincubation plus 24 hours of activation) and then stimulated with SP, vancomycin and morphine (n=3). A) IL-8 secretion. B) GM-CSF secretion. C) CCL2 secretion. Results are expressed as mean ± SD. Significance was determined using two-way ANOVA with Tukey's multiple comparison analysis. P<0.05 was considered statistically significant. *P<0.05; **P<0.01; ***P<0.001; ****P<0.0001. NC=Negative control; SP=Substance P.

3.3. Results summary

In summary, MITF-knockdown may reduce the severity of the allergic response, both in the IgE-dependent or MRGPRX2-dependent pathway, reducing pro-inflammatory conditions (IL-8, GM-CSF, *IL1B, COX2, PTGER3*, and *FcεR1A*) and increasing anti-inflammatory conditions (CCL2 and *PTGER4*) (Results Summary 2).

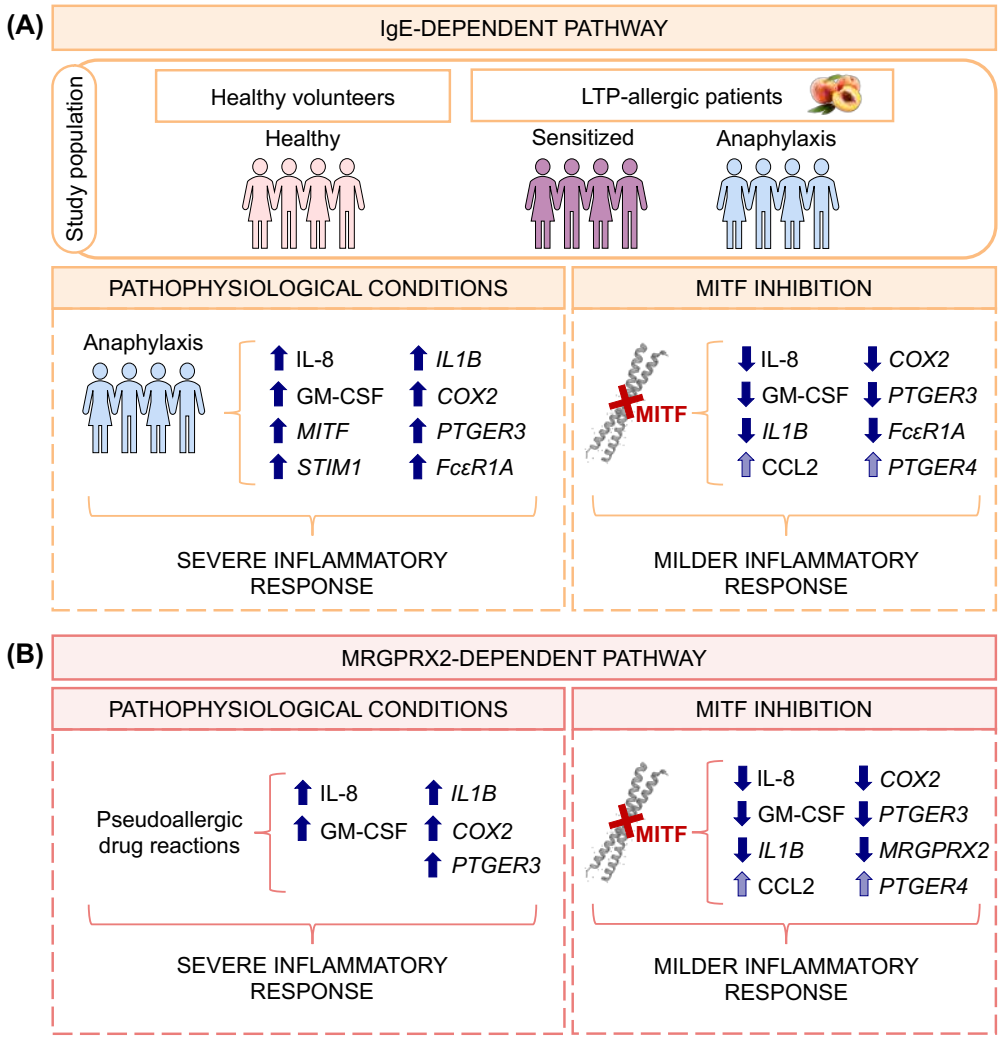

Results Summary 2. Summary of all data obtained in these second and third sections. A) IgE-dependent pathway. B) MRGPRX2-dependent pathway. LTP=Lipid Transfer protein.

3.4. Supplementary Figures and Tables

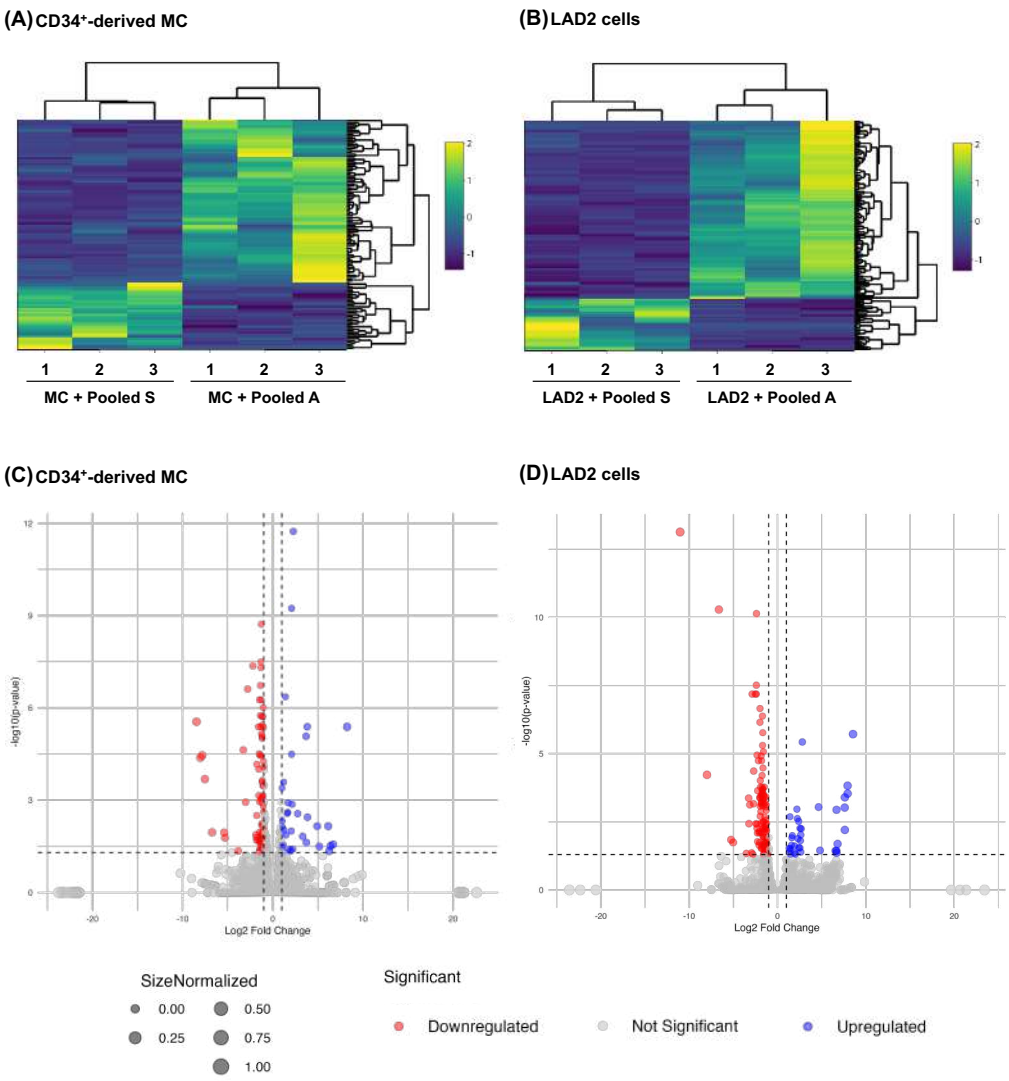

Supplementary Figure 5. RNA-sequencing analysis. CD34+-derived MCs and LAD2 cells were sensitized with both pooled sera from LTP patients and stimulated with Pru p 3 for 24h. Next, RNA-sequencing was performed. Volcano Plots were created with RStudio using a log2FoldChange ± 1 and adjusted p-value <0.05. A) Heatmap of CD34^{+}-derived MCs sensitized with pooled sera from sensitized patients versus cells sensitized with pooled sera from anaphylactic patients. B) Heatmap of LAD2 cells sensitized with pooled sera from sensitized patients versus cells sensitized with pooled sera from anaphylactic patients. C) Volcano Plot of CD34^{+}-derived MCs sensitized with pooled sera from sensitized patients versus cells sensitized with pooled sera from anaphylactic patients. B) Volcano Plot of LAD2 cells sensitized with

pooled sera from sensitized patients versus cells sensitized with pooled sera from anaphylactic patients. A=Anaphylaxis; S=Sensitized.

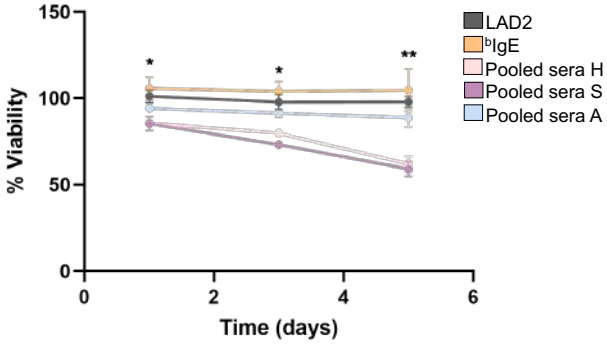

Supplementary Figure 6. Cell viability test in LAD2 cells sensitized with pooled sera. LAD2 cells were incubated overnight with pooled sera from healthy donors and LTP-allergic groups, and WST-1 was measured after one, three and five days. A=Anaphylaxis; [b]IgE=Biotinylated human IgE; H=Healthy; S=Sensitized.

4. TRANSCRIPTOMIC ANALYSIS OF MITF-DEPENDENT TARGETS IN MAST CELLS REVEALED A METABOLIC SIGNATURE

In our previous results, we saw that MCs from anaphylaxis patients presented higher MITF expression levels, and we demonstrated the involvement of MITF in those exacerbated MC responses, suggesting that MITF-knockdown might diminish the pro-inflammatory conditions.

Emerging evidence highlights a significant link between MC activity and mitochondrial function, suggesting that mitochondria play a crucial role in MC-driven pathologies, such as anaphylaxis (203,205,206). Metabolomics has revealed significant metabolic changes during severe anaphylactic reactions, indicating elevated immune metabolism and a rapid catabolic response (207).

Recently, it was found that MITF is involved in regulating MC mitochondrial activity (193). MC activation resulted in an increase in OXPHOS activity, that depends on dinucleotides produced by the Krebs cycle, regulated by PDH, which is bound to MITF in quiescent conditions. Furthermore, that MC activation, through the IgE-dependent pathway, induces dephosphorylation of PDH and phosphorylation of MITF, causing the dissociation of PDH-MITF to exert their roles in mitochondria (178,179). MITF-overexpression in retinal pigment epithelial cells has been shown to enhance mitochondrial function by increasing the expression of genes related to mitochondrial biogenesis, antioxidant responses, and ATP production, further underscoring its importance in MCs (180).

Altogether, this demonstrates the complex relationship between MITF, mitochondria, MC activation, and systemic allergic responses. Thus, in this fourth objective, we aim to delve into the metabolism of MCs to further investigate the differences between these two groups of patients, exploring MITF's role in MC activation, with a specific focus on mitochondrial function.

4.1. Transcriptomic analysis in MITF-knockdown cells

Due to transcriptomic limitations in MCs from patients, we conducted transcriptomic analysis on a cell line to identify differences in molecules regulated by MITF in the context of two receptors, FcεRI and MRGPRX2 (as previous observations had also indicated potential implications). Thus, we performed RNA-sequencing in MITF-knockdown LAD2 cells. PCA and a full heatmap of transcriptomic results are included in Supplementary Figure 7. Indeed, the raw data from the entire analysis can be found in the ANNEX II. GSEA revealed that when MITF is silenced, different metabolic pathways are affected. When MITF-knockdown cells were activated with ^{b}IgE + STV, there was a reduction in oxidative phosphorylation, glycolysis, and gluconeogenesis, and electron transport chain OXPHOS mitochondrial system (Figure 64A). Similar results were observed when MITF-knockdown cells were activated with SP: there was a reduction in oxidative phosphorylation, mitochondrial complex I assembly, and electron transport chain OXPHOS mitochondrial system (Figure 64B). Furthermore, in both cases, there were other signaling pathways affected, such as downregulation of cell cycle and G1 and S cell cycle control, and downregulation of inflammatory pathways in infections: Type I interferon induction and signaling during SARS CoV 2 infection, SARS CoV 2 innate immunity evasion and cell-specific immune response, Escherichia Coli infection, immune response to tuberculosis.

Moreover, GO cellular component analysis revealed the downregulation of different mitochondrial compartments in MITF-knockdown cells compared with control cells. After cell activation with ^{b}IgE + STV or SP, we observed a downregulation of the following cellular components: NADH dehydrogenase complex, mitochondrial respiratory chain complex I, mitochondrial respiratory chain, mitochondrial protein complex, mitochondrial membrane part, mitochondrial matrix, mitochondrial inner membrane (Figure 65).

(A)

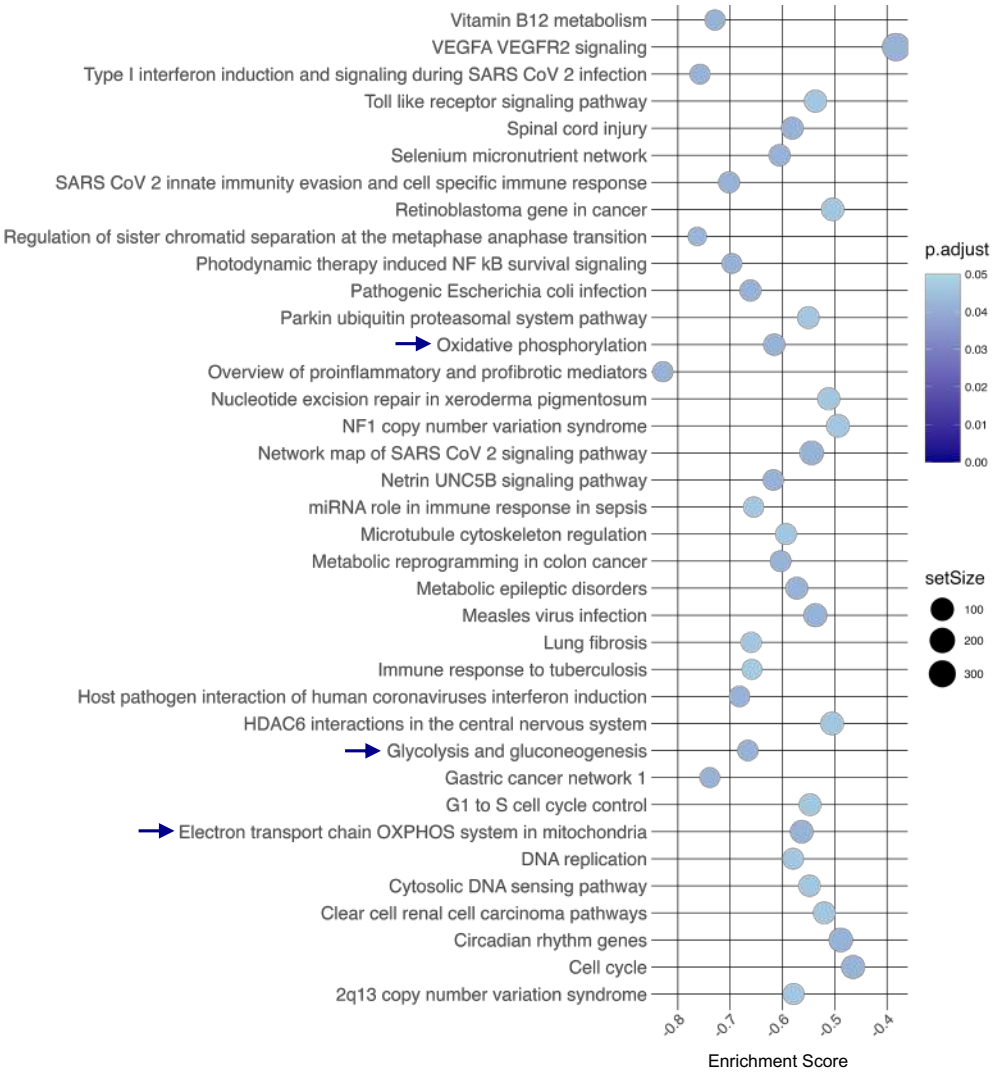
Vitamin B12 metabolism
VEGFA VEGFR2 signaling
Type I interferon induction and signaling during SARS CoV 2 infection
Toll like receptor signaling pathway
Spinal cord injury
Selenium micronutrient network
SARS CoV 2 innate immunity evasion and cell specific immune response
Retinoblastoma gene in cancer
Regulation of sister chromatid separation at the metaphase anaphase transition
Photodynamic therapy induced NF kB survival signaling
Pathogenic Escherichia coli infection
Parkin ubiquitin proteasomal system pathway
Oxidative phosphorylation
Overview of proinflammatory and profibrotic mediators
Nucleotide excision repair in xeroderma pigmentosum
NF1 copy number variation syndrome
Network map of SARS CoV 2 signaling pathway
Netrin UNC5B signaling pathway
miRNA role in immune response in sepsis
Microtubule cytoskeleton regulation
Metabolic reprogramming in colon cancer
Metabolic epileptic disorders
Measles virus infection
Lung fibrosis
Immune response to tuberculosis
Host pathogen interaction of human coronaviruses interferon induction
HDAC6 interactions in the central nervous system
Glycolysis and gluconeogenesis
Gastric cancer network 1
G1 to S cell cycle control
Electron transport chain OXPHOS system in mitochondria
DNA replication
Cytosolic DNA sensing pathway
Clear cell renal cell carcinoma pathways
Circadian rhythm genes
Cell cycle
2q13 copy number variation syndrome
-0.8
-0.7
-0.6
-0.5
-0.4
Enrichment Score
p.adjust
0.05
0.04
0.03
0.02
0.01
0.00
setSize
100
200
300

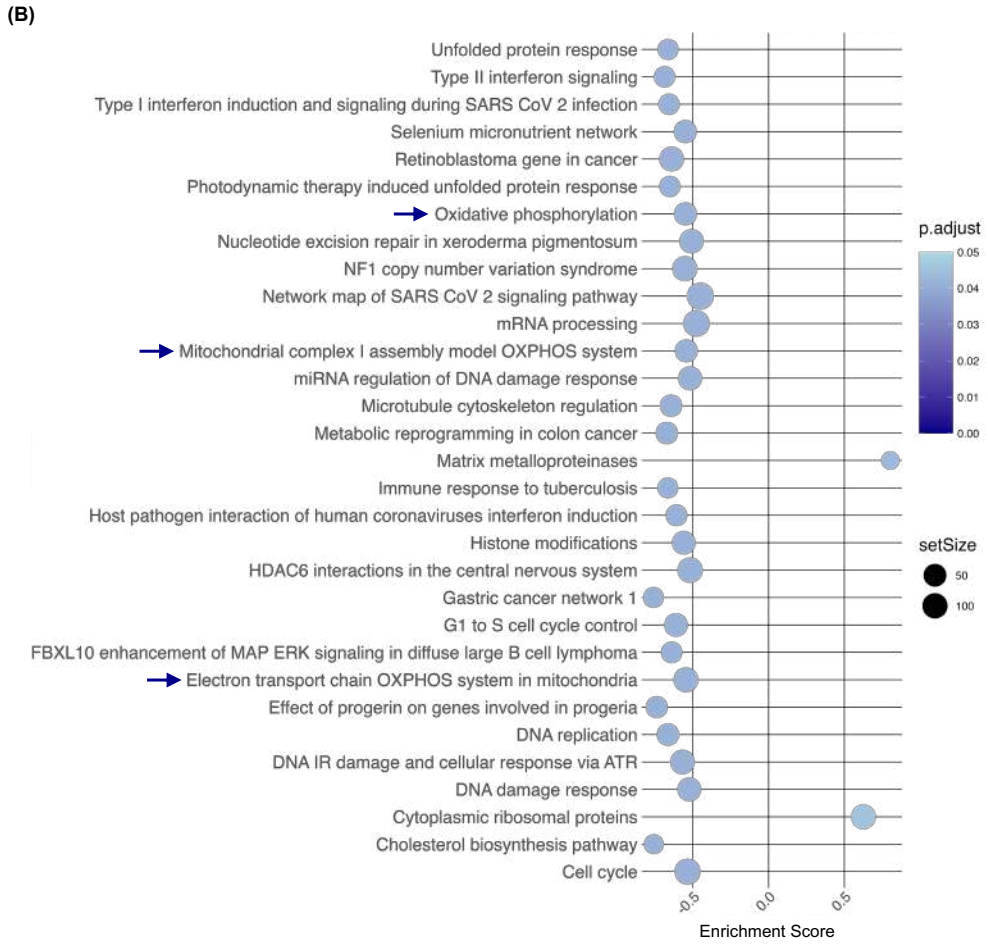

Figure 64. MITF-knockdown reduces metabolic pathways in mast cells. LAD2 cells infected with shRNA-NT (as control) and MITF shRNA-2 were sensitized with 0.1 µg/ml biotinylated human IgE overnight and were activated with ^{b}IgE + STV or SP for 30 min (n=9). Then, cells were pelleted, and RNA-sequencing was performed. Gene ontology enrichment pathways were created with RStudio using a log2FoldChange ± 1 and adjusted p-value <0.05. A) LAD2 cells with MITF shRNA-D versus shRNA-NT, when cells were activated with STV. B) LAD2 cells with MITF shRNA-D versus shRNA-NT, when cells were activated with SP. STV=Streptavidin; SP=Substance P.

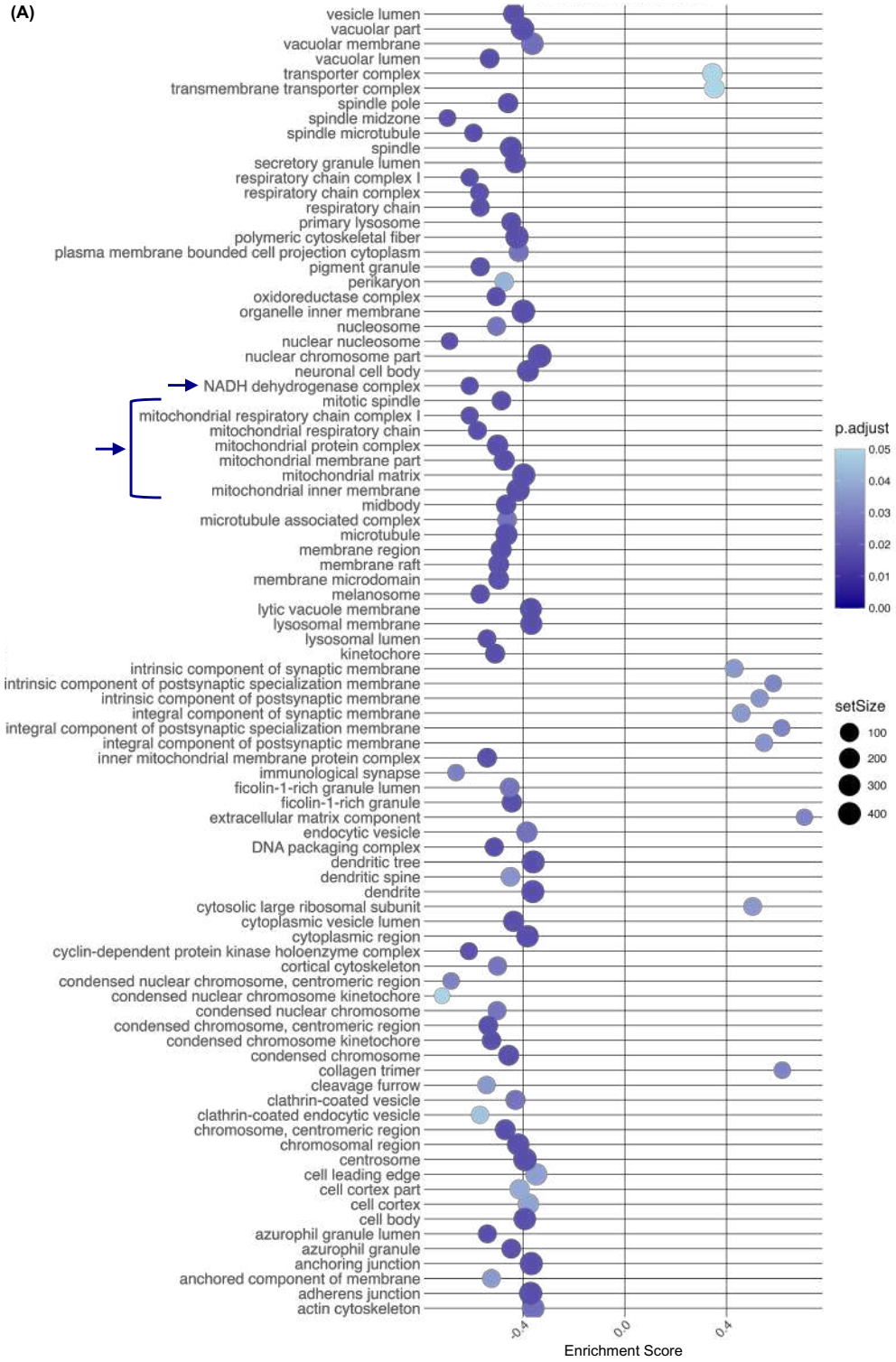
(A)
vesicle lumen
vacuolar part
vacuolar membrane
vacuolar lumen
transporter complex
transmembrane transporter complex
spindle pole
spindle midzone
spindle microtubule
spindle
secretory granule lumen
respiratory chain complex I
respiratory chain complex
respiratory chain
primary lysosome
polymeric cytoskeletal fiber
plasma membrane bounded cell projection cytoplasm
pigment granule
perikaryon
oxidoreductase complex
organelle inner membrane
nucleosome
nuclear nucleosome
nuclear chromosome part
neuronal cell body
NADH dehydrogenase complex
mitotic spindle
mitochondrial respiratory chain complex I
mitochondrial respiratory chain
mitochondrial protein complex
mitochondrial membrane part
mitochondrial matrix
mitochondrial inner membrane
midbody
microtubule associated complex
microtubule
membrane region
membrane raft
membrane microdomain
melanosome
lytic vacuole membrane
lysosomal membrane
lysosomal lumen
kinetochore
intrinsic component of synaptic membrane
intrinsic component of postsynaptic specialization membrane
intrinsic component of postsynaptic membrane
integral component of synaptic membrane
integral component of postsynaptic specialization membrane
integral component of postsynaptic membrane
inner mitochondrial membrane protein complex
immunological synapse
ficolin-1-rich granule lumen
ficolin-1-rich granule
extracellular matrix component
endocytic vesicle
DNA packaging complex
dendritic tree
dendritic spine
dendrite
cytosolic large ribosomal subunit
cytoplasmic vesicle lumen
cytoplasmic region
cyclin-dependent protein kinase holoenzyme complex
cortical cytoskeleton
condensed nuclear chromosome, centromeric region
condensed nuclear chromosome kinetochore
condensed nuclear chromosome
condensed chromosome, centromeric region
condensed chromosome kinetochore
condensed chromosome
collagen trimer
cleavage furrow
clathrin-coated vesicle
clathrin-coated endocytic vesicle
chromosome, centromeric region
chromosomal region
centrosome
cell leading edge
cell cortex part
cell cortex
cell body
azurophil granule lumen
azurophil granule
anchoring junction
anchored component of membrane
adherens junction
actin cytoskeleton
-0.4
0.0
0.4
Enrichment Score
p.adjust
0.05
0.04
0.03
0.02
0.01
0.00
setSize
100
200
300
400

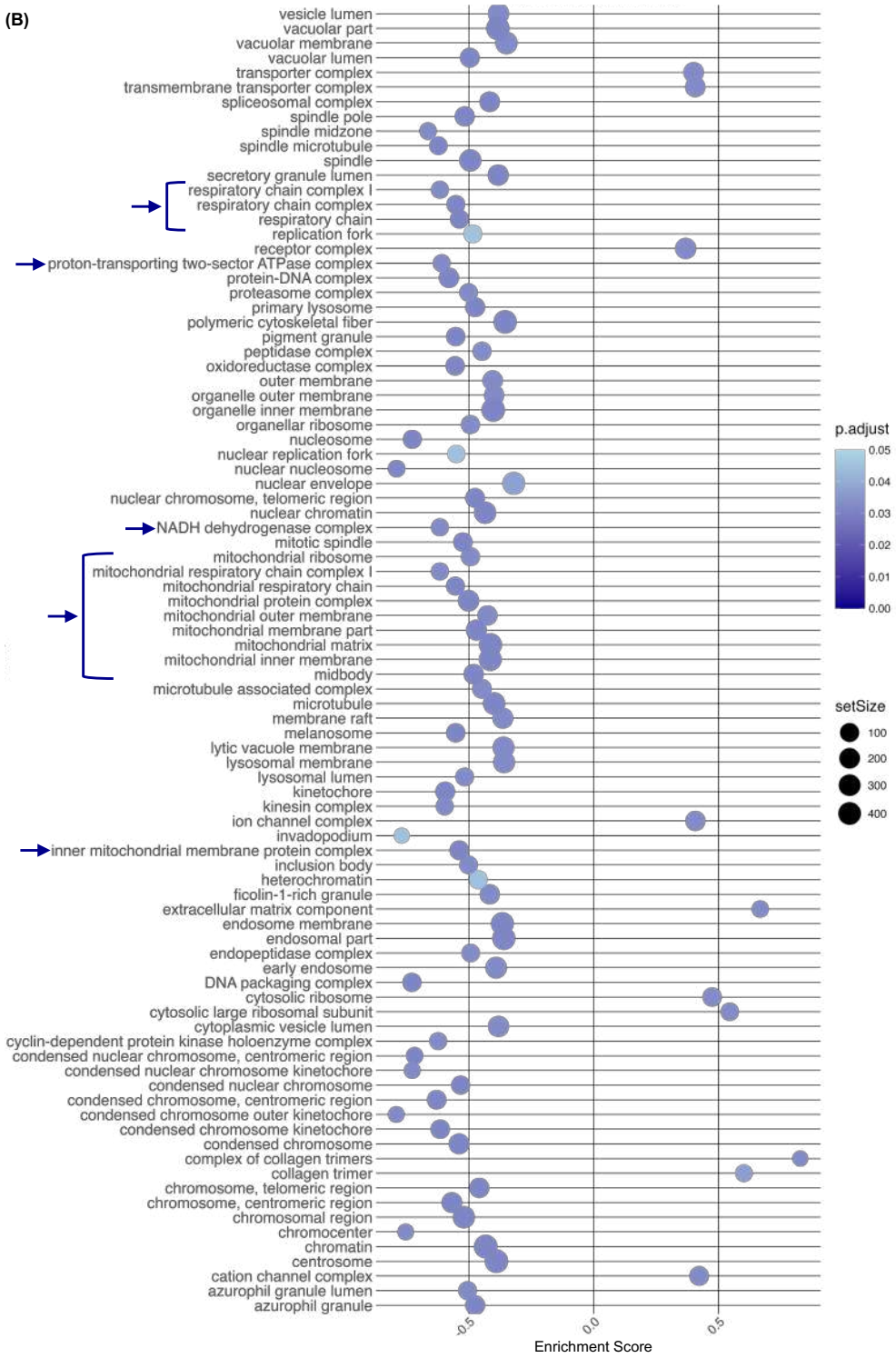

Figure 65. MITF-knockdown reduces mitochondrial cellular components in mast cells. LAD2 cells infected with shRNA-NT (as control) and MITF shRNA-2 were sensitized with 0.1

µg/ml biotinylated human IgE overnight and were activated with ^{b}IgE + STV or SP for 30 min (n=9). Then cells were pelleted, and RNA-sequencing was performed. Gene ontology enrichment pathways were created with RStudio using a log2FoldChange ± 1 and adjusted p-value <0.05. A) LAD2 cells with MITF shRNA-D versus shRNA-NT, when cells were activated with STV. B) LAD2 cells with MITF shRNA-D versus shRNA-NT, when cells were activated with SP. STV=Streptavidin; SP=Substance P.

In summary, with the transcriptomic analysis of MITF-knockdown cells compared with control cells, we gathered a good deal of interesting information that can be used to study different cellular mechanisms affected by MITF. However, based on the results of the GSEA and GO cellular components analysis, we decided to focus on the mitochondrial as MITF seems to play an important role.

4.2. Assessing mitochondrial function in MITF-knockdown mast cells

Knowing that many mitochondrial pathways are affected in MITF-knockdown cells, we wanted to delve deeper into the mitochondrial function; in this case, we evaluated mitochondrial membrane potential. First, to know the best time to assess mitochondrial membrane potential, we used LAD2 cells to conduct a dose-response curve with SP and ^{b}IgE + STV, finding that the greatest variation in membrane potential was observed at 10 minutes (Supplementary Figure 8).

Afterward, LAD2 cells were treated with ML329 and TT012 or infected with lentivirus and, after five days, stimulated with ^{b}IgE + STV or SP for 10 minutes. The viability of treated cells after five days was significantly reduced, with MITF inhibitors and shRNAs; however, when we analyzed mitochondrial parameters, we excluded dead cells by flow cytometry, thus leaving the same percentage of live cells per condition (Figure 67B).

When cells were treated with MITF inhibitors (ML329 and TT012), they exhibited more dysfunctional mitochondria, which was more significant with ML329 treatment, and less mitochondrial membrane potential after cell activation, either with ^{b}IgE + STV or SP, than control cells (Figure 66C and D).

In addition, we observed that MITF inhibition induces more ROS, especially when cells were treated with ML329 (Figure 66E).

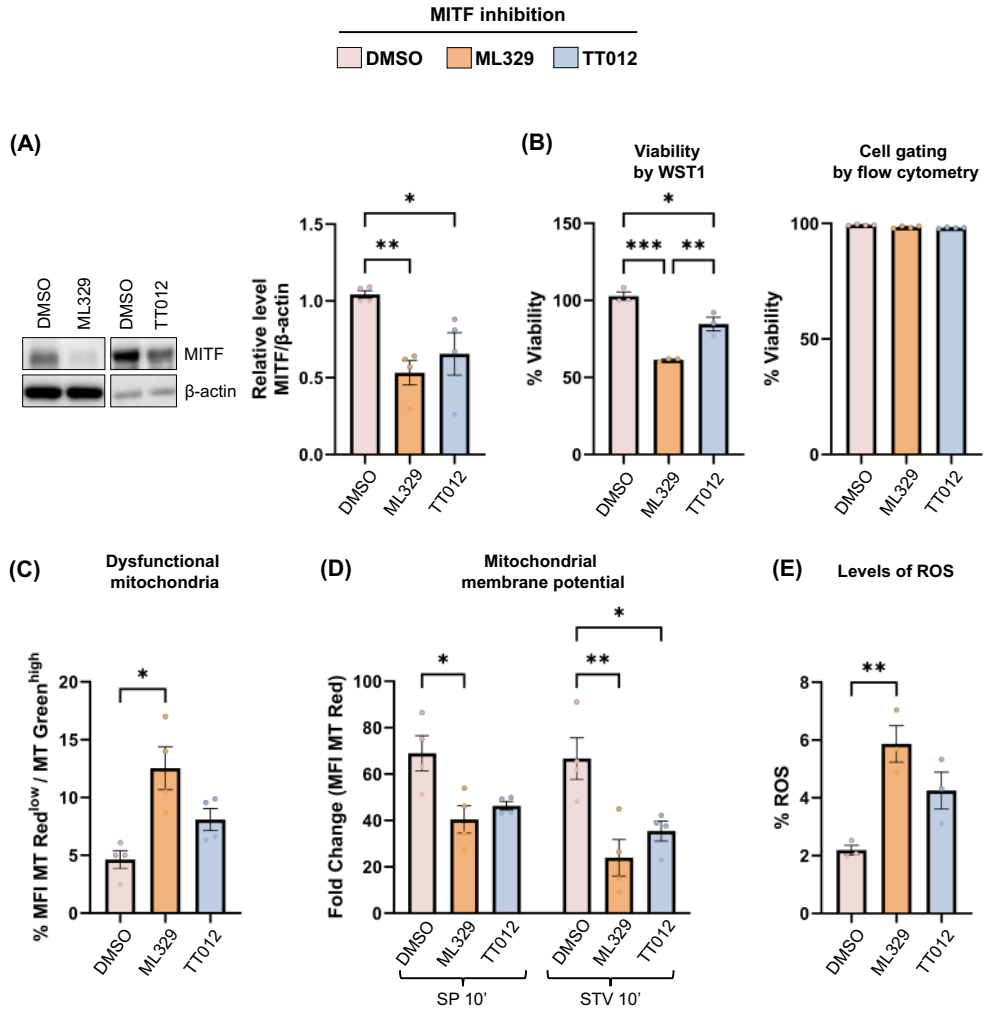

Figure 66. MITF inhibition induces mitochondrial dysfunction. LAD2 cells were treated with MITF inhibitors (ML329 and TT012), and cells were analyzed by flow cytometry using Mitotrackers and CellROX (n=4). Treated LAD2 cells were activated with ^{b}IgE + streptavidin or substance P for 10 min. A) Levels of MITF. B) Cell viability. C) Dysfunctional mitochondria. D) Mitochondrial membrane potential. E) ROS levels. Results are expressed as mean ± SD. Significance was determined using one or two-way ANOVA with Tukey's multiple comparison analysis. P<0.05 was considered statistically significant. *P<0.05; **P<0.01; ***P<0.001. STV=Streptavidin; SP=Substance P.

Similar results were obtained when *MITF* was silenced. MITF shRNA-2 and MITF shRNA-3 had more dysfunctional mitochondria and produced more ROS. Although not statistically significant, MITF-knockdown cells tend to have a lower mitochondrial membrane potential than control cells (shRNA-NT) after cell activation either with [b]IgE + STV and SP (Figure 67).

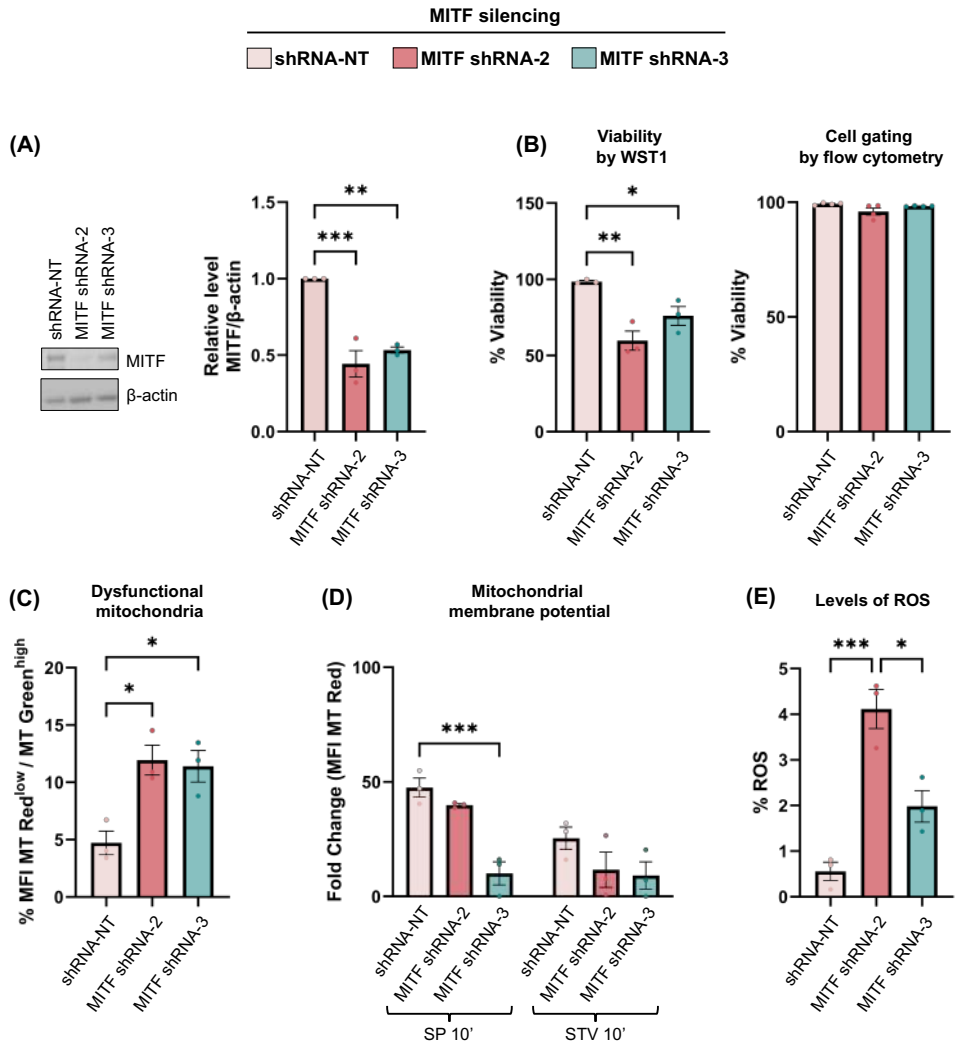

Figure 67. MITF silencing induces mitochondrial dysfunction. shRNAs were used to silence MITF in LAD2 cells. Then cells were analyzed by flow cytometry using Mitotrackers and CellROX. Treated LAD2 cells were activated with streptavidin or substance P for 10 min (n=4). A) MITF levels. B) Cell viability. C) Dysfunctional mitochondria. D) Mitochondrial membrane potential. E) ROS levels. Results are expressed as mean ± SD. Significance was determined

using one or two-way ANOVA with Tukey's multiple comparison analysis. P<0.05 was considered statistically significant. *P<0.05; **P<0.01; ***P<0.001. STV=Streptavidin; SP=Substance P.

4.3. MITF-knockdown reduces mitochondrial function in primary mast cells

To validate previous results, we used primary MCs. CD34^{+}-derived or skin MCs were treated with ML329 or TT012 and, after five days, stimulated with ^{b}IgE + STV or SP. MITF inhibition, in both cell models, causes more dysfunctional mitochondria and less mitochondrial membrane potential after cell activation than control cells (Figure 68).

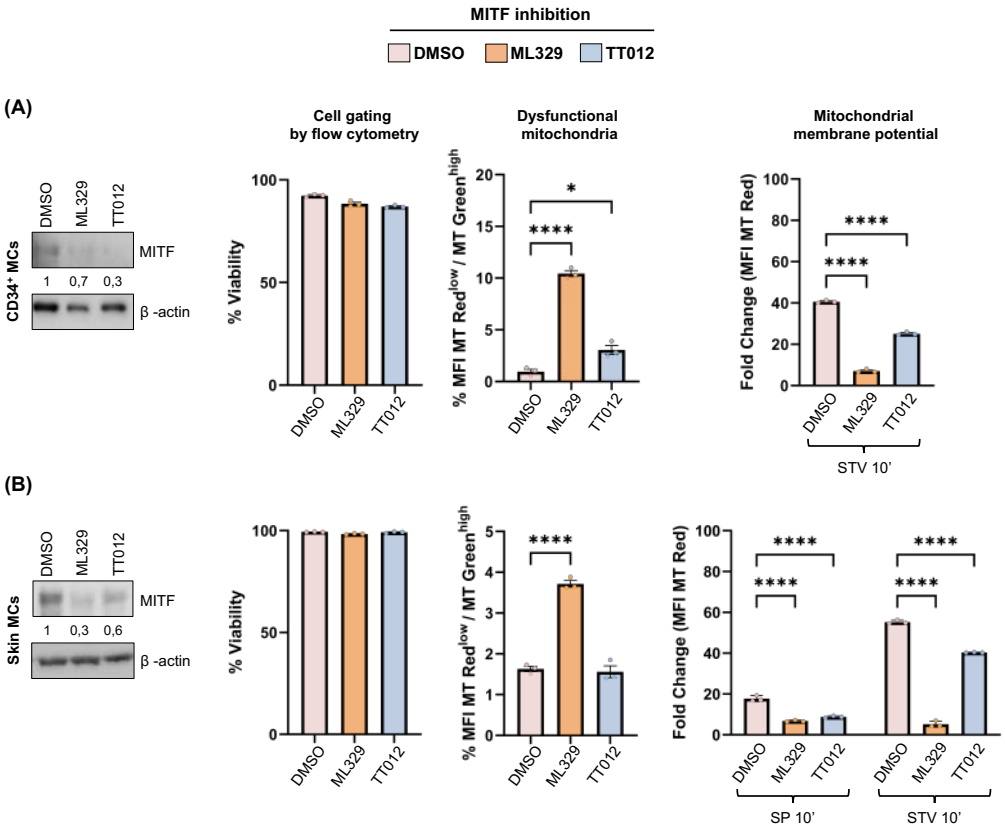

Figure 68. MITF inhibition reduces mitochondrial activity in primary mast cells. MITF-knockdown cells were analyzed by flow cytometry using Mitotrackers. Cells were sensitized with 0.1 µg/ml biotinylated human IgE overnight and were activated with ^{b}IgE + STV or SP for

10 min (n=4). A) CD34+-derived MCs were treated with ML329, TT012 or DMSO (control). B) Skin MCs were treated with ML329, TT012 or DMSO (control). Results are expressed as mean ± SD. Significance was determined using one or two-way ANOVA with Tukey's multiple comparison analysis. P<0.05 was considered statistically significant. *P<0.05; ****P<0.0001. STV=Streptavidin; SP=Substance P.

4.4. Evaluating mitochondrial activity in an *in vitro* anaphylaxis cell model

We observed that MITF-knockdown decreases the mitochondrial membrane potential; however, we also wanted to know what happened when MITF is overexpressed. To do so, RBL-2H3 cells were used to overexpress MITF by transfection with LysRS-WT and LysRS-P542R plasmids. This LysRS-P542R mutation, as we mentioned above, promotes a constitutive nuclear location of LysRS-P542R enhancing MITF gene transcription in the absence of stimulation (371). Cells transfected only with GFP were used as control. Transfected RBL-2H3 treated with either ML329 and TT012, causes more dysfunctional mitochondria (Figure 69A and B). Analyzing the mitochondrial membrane potential, first we observed that LysRS-P542R had more mitochondrial membrane potential than LysRS-WT and control cells after activation with IgE-DNP + DNP-HSA, suggesting that the MITF-overexpression can induce more mitochondrial membrane potential. Moreover, when cells were treated with MITF inhibitors, there was a reduction in mitochondrial membrane potential after activation with IgE-DNP + DNP-HSA (Figure 69C).

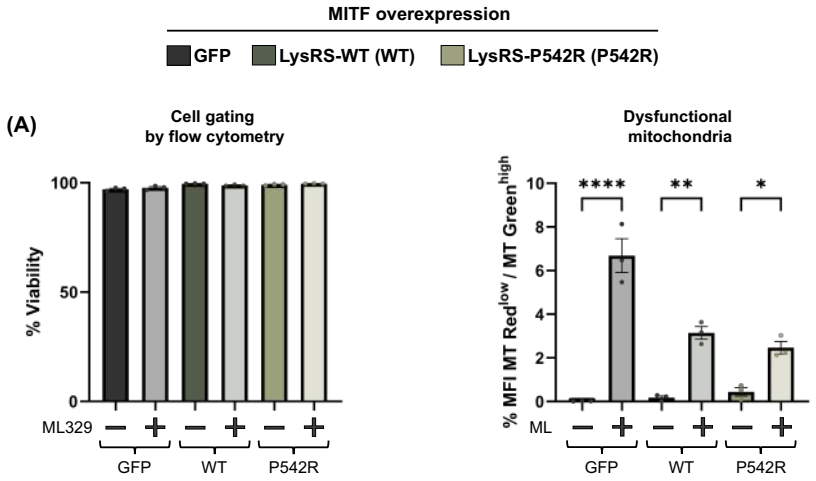

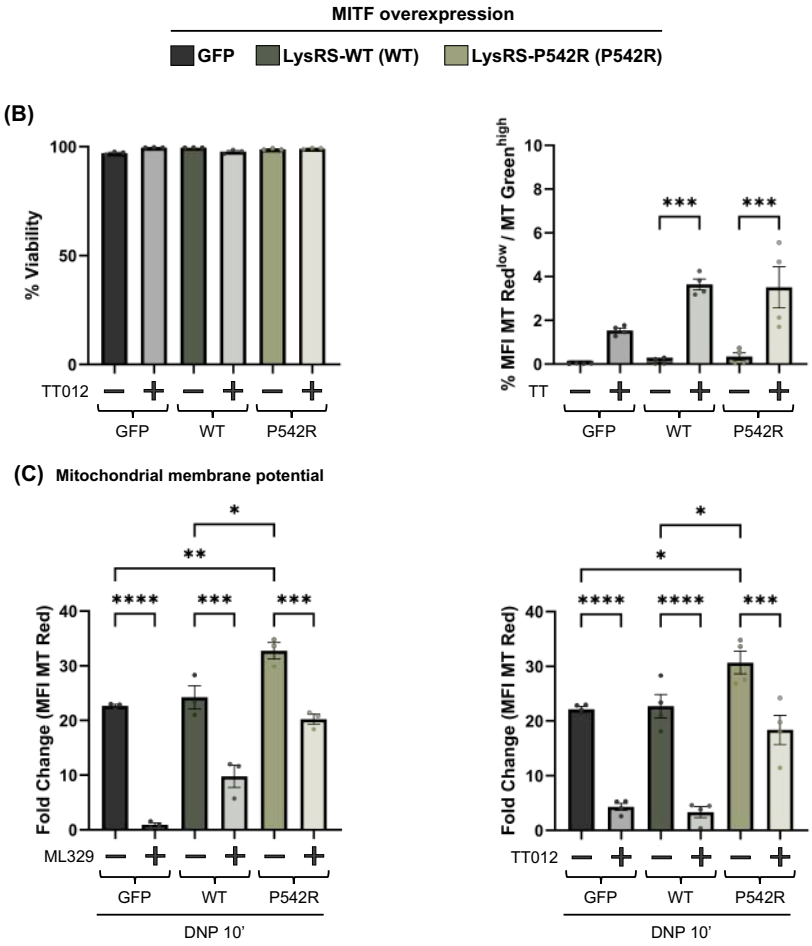

Figure 69. Mitochondrial inhibition reduces mitochondrial activity in the MITF-overexpression model. RBL-2H3 cells were analyzed by flow cytometry using Mitotrackers. Cells were sensitized with 0.1 µg/ml DNP-human IgE overnight, washed and activated with DNP-BSA for 10 minutes (n=4). A) Viability and dysfunctional mitochondria analysis of RBL-2H3 cells treated with ML329 or DMSO (control). B) Viability and dysfunctional mitochondria analysis of RBL-2H3 cells treated with TT012 or DMSO (control). C) Mitochondrial membrane potential of treated RBL-2H3 cells. Results are expressed as mean ± SD. Significance was determined using two-way ANOVA with Tukey's multiple comparison analysis. P<0.05 was considered statistically significant. *P<0.05; **P<0.01; ***P<0.001; ****P<0.0001. DNP as DNP-HSA=Dinitrophenyl-Human serum albumin; P54R as LysRS-P542R and WT as LysRS-WT.

4.5. MITF inhibition reduces mitochondrial membrane potential in MCs from an anaphylactic patient

Based on the above showed, we hypothesized that MCs from LTP patients may have different mitochondrial functionality, due to their different MITF expression levels. Thus, as preliminary data, we used MCs from one healthy volunteer and one anaphylactic patient (clinical characteristics are shown in Annex Table 4), and we performed a mitochondrial analysis.

First, as we had already demonstrated that *MITF* was elevated in MCs from anaphylaxis, we performed an RT-qPCR of these MCs to assess *MITF* levels. We observed that *MITF* was more expressed in MCs from the anaphylactic patient than from the healthy volunteer (Annex Table 4). Indeed, if MITF is elevated in the anaphylaxis group, and MITF is related to the mitochondrial function, treating MCs from the anaphylactic patient with an MITF inhibitor may reduce the higher allergic response in those cells. To test this hypothesis, MCs were treated with TT012 for five days. Afterward, cells were sensitized with their sera and stimulated with Pru p 3 for 10 minutes. MCs from the healthy donor treated with TT012, had more dysfunctional mitochondria than control cells (DMSO), but no significant difference was found in MCs from the anaphylactic patient (Figure 70A).

As we observed in the MITF-overexpression model (LysRS-P542R), the mitochondrial membrane potential was higher in MCs from the anaphylactic patient than from the healthy donor. Furthermore, this decreased significantly when the MCs of both were treated with TT012 (Figure 70B).

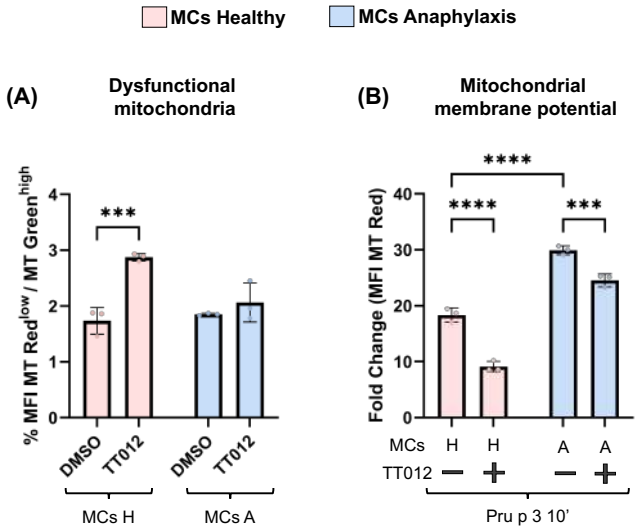

Figure 70. MITF inhibition reduces mitochondrial activity in MCs from an anaphylactic patient. MCs from a healthy volunteer (n=1) and an anaphylaxis patient (n=1) were sensitized with their sera overnight and activated with 1 µg/ml Pru p 3. Technical triplicates were performed in each case. A) Dysfunctional mitochondria analyzed by flow cytometry in MCs from the anaphylaxis patient and healthy donor treated with TT012 or DMSO (control) (technical triplicates). C) Mitochondrial membrane potential analyzed by flow cytometry in MCs from the anaphylaxis patient and healthy donor treated with TT012 or DMSO (control) (technical triplicates). Results are expressed as mean ± SD. Significance was determined using one-way ANOVA with Tukey's multiple comparison analysis. P<0.05 was considered statistically significant. ***P<0.001; ****P<0.0001. H=Healthy volunteer; A=Anaphylaxis.

4.6. Mitochondrial protein import is reduced in MITF-knockdown cells

Interestingly, in the transcriptomics results, some mitochondrial genes were affected in MITF-knockdown cells, most being significantly downregulated (Figure 71). Many genes of the TOM family (translocases of the outer mitochondrial membrane) were downregulated – including *TOMM20* – when MITF was silenced after cell activation with ^{b}IgE + STV, and even more so with SP. The TOM family proteins are the main entry point for proteins into the mitochondria, suggesting that lower expression of these genes can disrupt mitochondrial protein import (439).

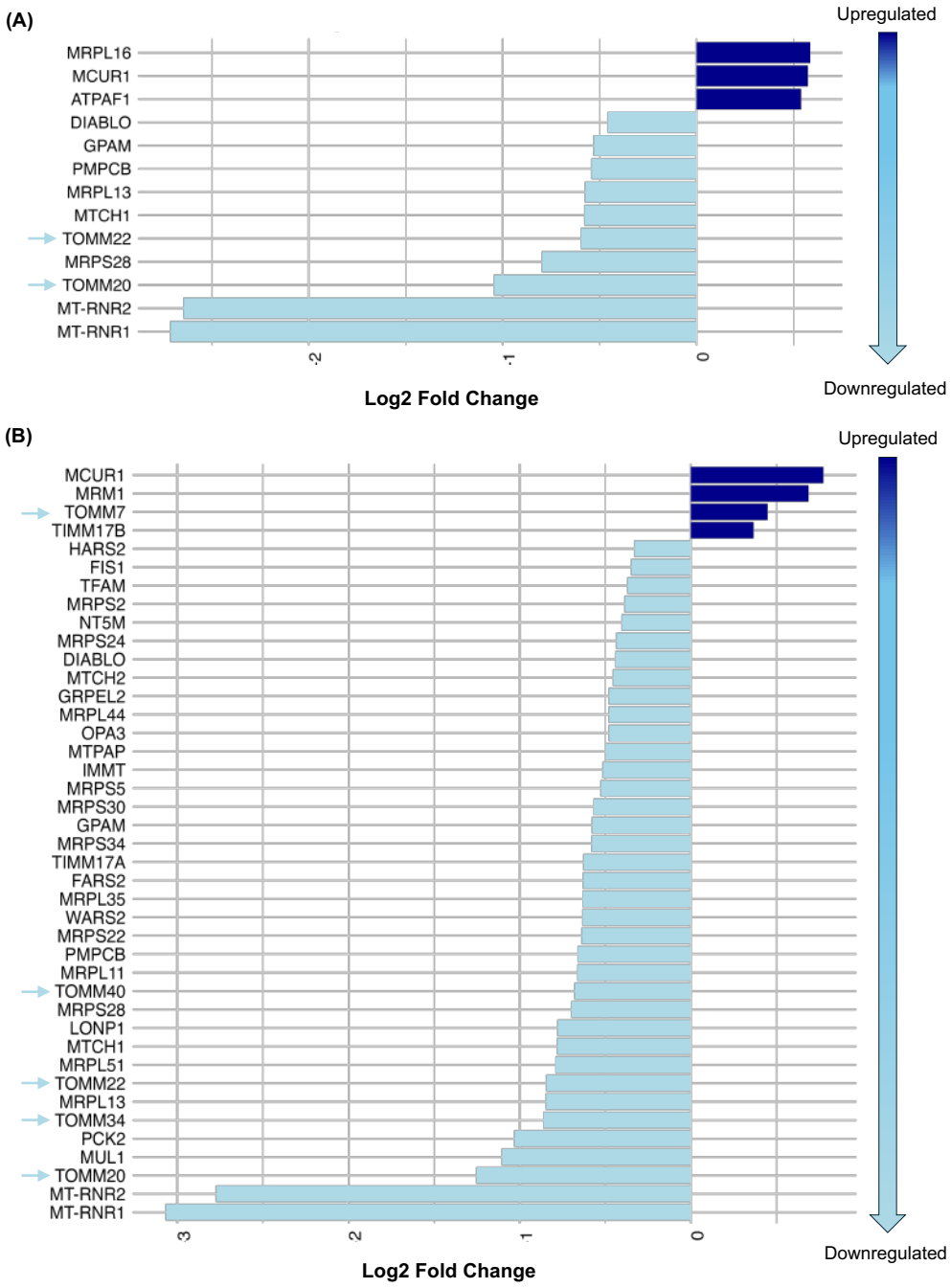

Figure 71. Mitochondrial gene expression from RNA-sequencing. LAD2 cells infected with shRNA-NT (control) and MITF shRNA-2 were sensitized with 0.1 µg/ml biotinylated human IgE overnight and were activated with ^{b}IgE + STV or SP for 30 min. Then cells were pelleted, and RNA-sequencing was performed. Gene mitochondrial bar plot was created with RStudio using a log2FoldChange ± 1 and adjusted p-value <0.05. A) LAD2 cells with MITF shRNA-D versus

shRNA-NT, when cells were activated with ^{b}IgE + STV. B) LAD2 cells with MITF shRNA-D versus shRNA-NT, when cells were activated with SP.

These results were validated by RT-qPCR on more samples, confirming a significantly lower expression of *TOMM20* in MITF-knockdown cells (Figure 72), suggesting a low mitochondrial protein import in MITF-silenced cells.

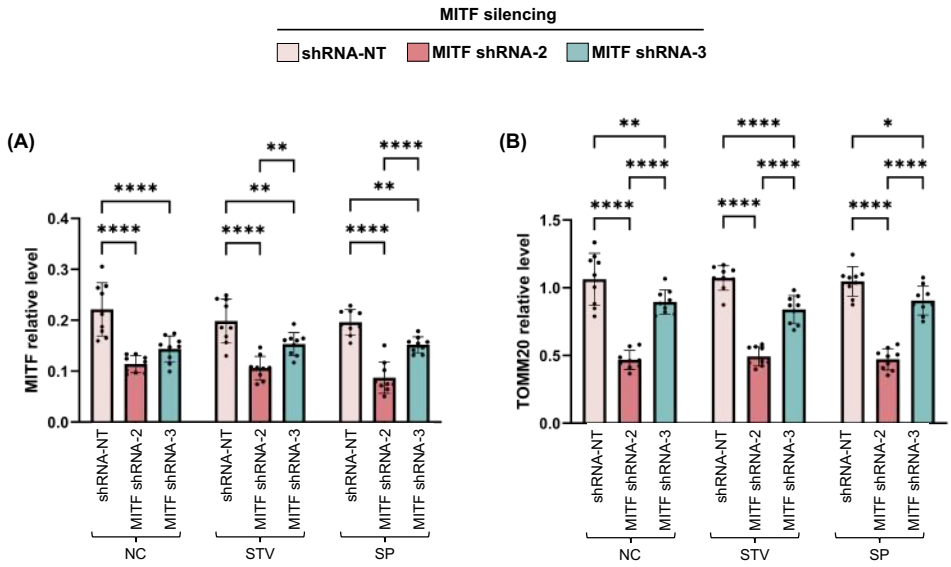

Figure 72. *TOMM20* is reduced in MITF silencing. LAD2 cells were infected with MITF shRNAs (NT, 2 and 3) and stimulated with streptavidin or substance P for 24h (n=9). After 24h, gene expression levels were assessed with Fluidigm. A) *MITF* gene expression levels. B) *TOMM20* gene expression levels. Results are expressed as mean ± SD. Significance was determined using two-way ANOVA with Tukey's multiple comparison analysis. P<0.05 was considered statistically significant. *P<0.05; **P<0.01; ****P<0.0001. STV=Streptavidin; SP=Substance P.

4.7. MITF-knockdown reduces pSer616-DRP1 levels in mast cells

As we observed that MITF regulates the mitochondrial protein import through TOM20 and with the GO cellular components analysis, that MITF silencing could disrupt many mitochondrial components, we wanted to investigate mitochondrial dynamics, which are essential for MCs activation.

The GTPase DRP1 controls mitochondrial fission through phosphorylation. DRP1 contains two phosphorylation sites: while DRP1 activity is blocked by phosphorylation of Ser637, it is induced by phosphorylation of Ser616. MITF-silenced LAD2 cells exhibited a reduction in phospho-DRP1^{Ser616} after activation either with ^{b}IgE + STV or SP compared with control cells, suggesting less fission in these cells (Figure 73A and B).

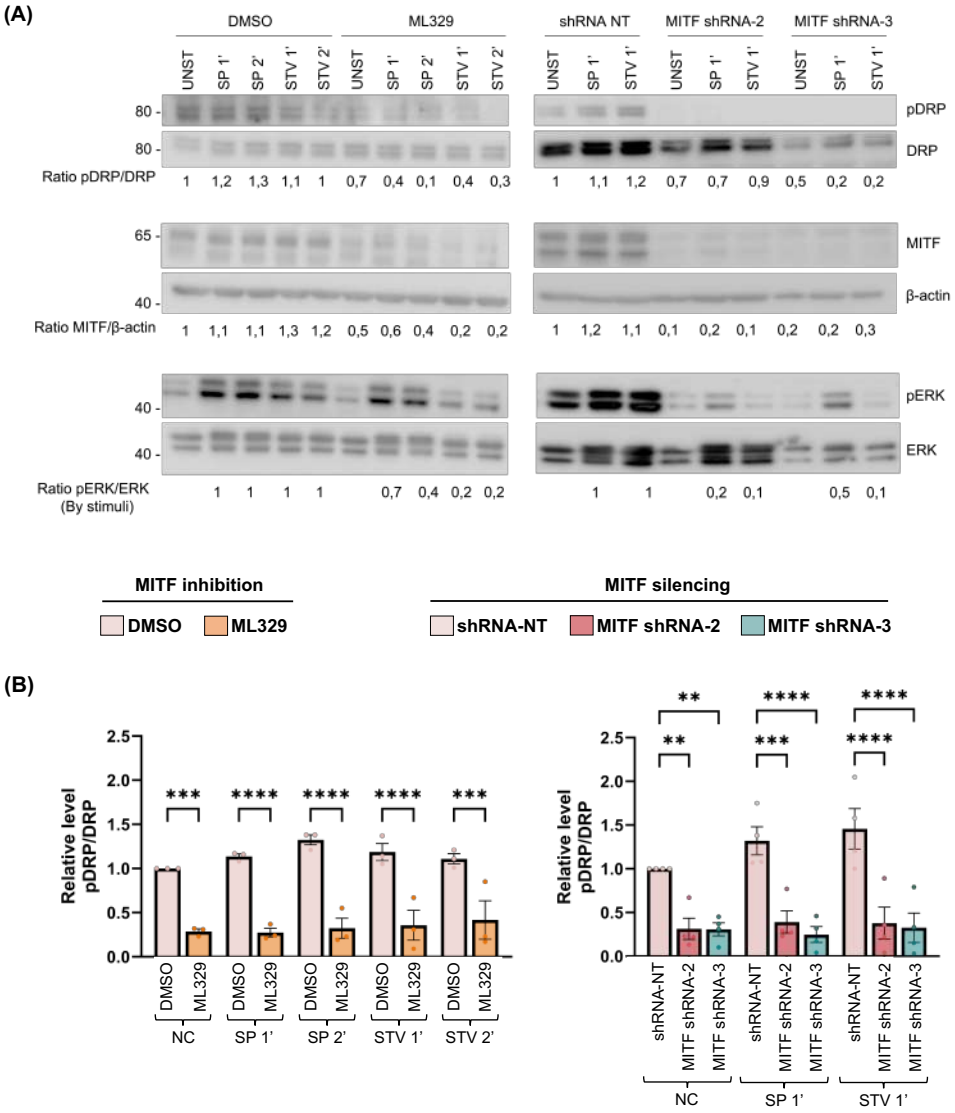

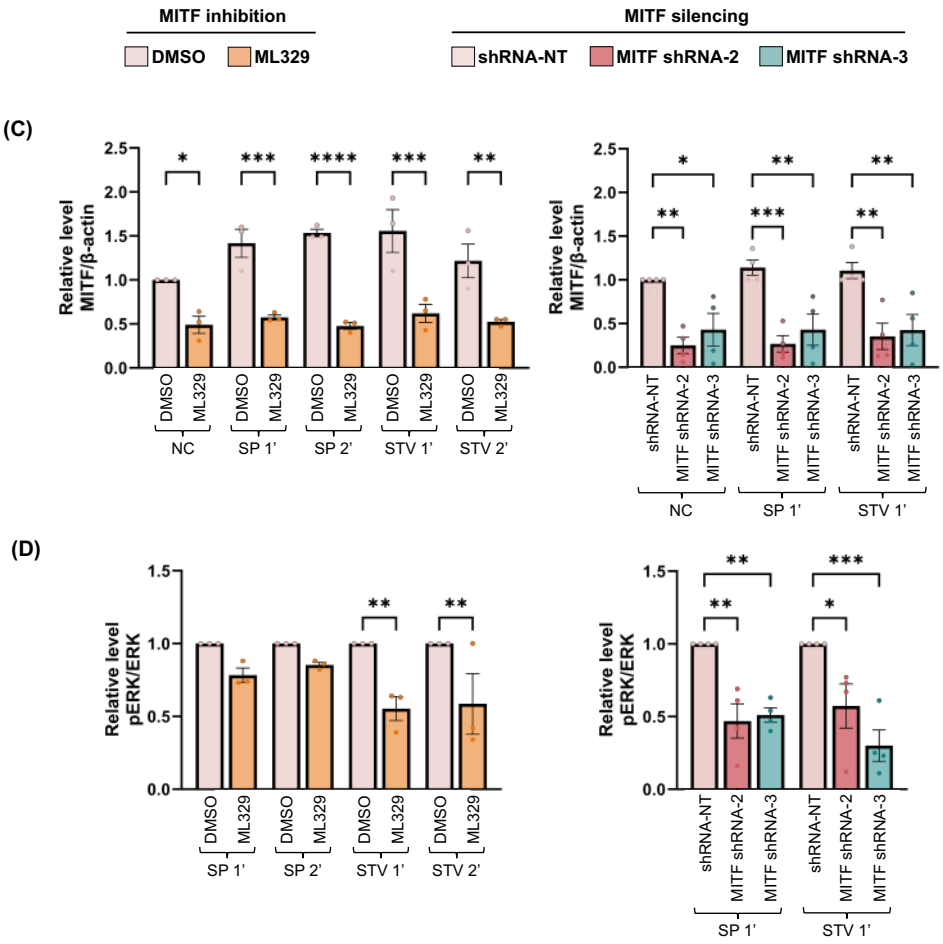

Figure 73. MITF-knockdown reduces phosphorylation of pDRP1^{Ser616}. MITF-knockdown cells were analyzed by western blot. Treated LAD2 cells were sensitized with 0.1 µg/ml biotinylated human IgE overnight and were activated with ^{b}IgE + STV or SP for 1 or 2 min. A) Representative western blot of LAD2 cells treated with ML329 (n=3) or MITF- shRNA (n=4). B) MITF statistical analysis of western blot fission results. B) pDRP1 levels analysis. C) pERK levels analysis. Results are expressed as mean ± SD. Significance was determined using two-way ANOVA with Tukey's multiple comparison analysis. P<0.05 was considered statistically significant. *P<0.05; **P<0.01; ***P<0.001; ****P<0.0001. STV=Streptavidin; SP=Substance P.

Interestingly, MITF-knockdown LAD2 cells also had low levels of phospho-ERK (Figure 73D), a member of the mitogen-activated protein kinase family, which is involved in the MC activation pathway.

4.8. MITF-knockdown reduces mitochondrial fission after cell activation via the FcεRI or MRGPRX2 pathways

Next, we assessed the mitochondrial fission by TEM. LAD2 cells were infected with lentivirus to silence MITF. After five days, cells were activated using ^{b}IgE + STV and SP. Figure 74A shows an example of fused or fragmented mitochondria in our samples. In unstimulated conditions, there was no difference in the number of fused mitochondria. After cell activation with SP, MITF-knockdown cells, although when comparing unstimulated and stimulated samples, there were significant differences in the number of fused mitochondria, there was also a significant increase in these when compared with the control group (Figure 74).

After cell activation with ^{b}IgE + STV, MITF-knockdown cells had a higher number of fused mitochondria than control cells, and there were non-significant differences when comparing unstimulated and stimulated conditions in these cells (Figure 74). Correlating with our results above, LAD2 cells treated with shRNAs to silence MITF, had lower phospho-DRP1^{Ser616} levels, and consequently, less mitochondrial fission.

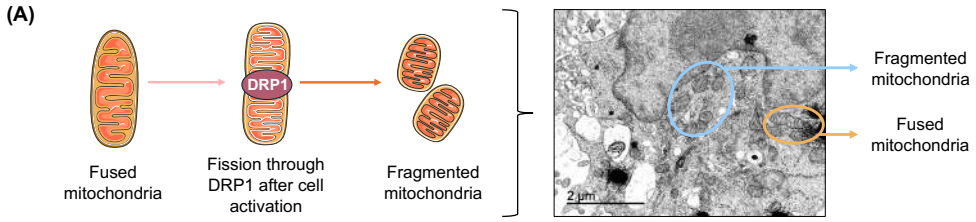

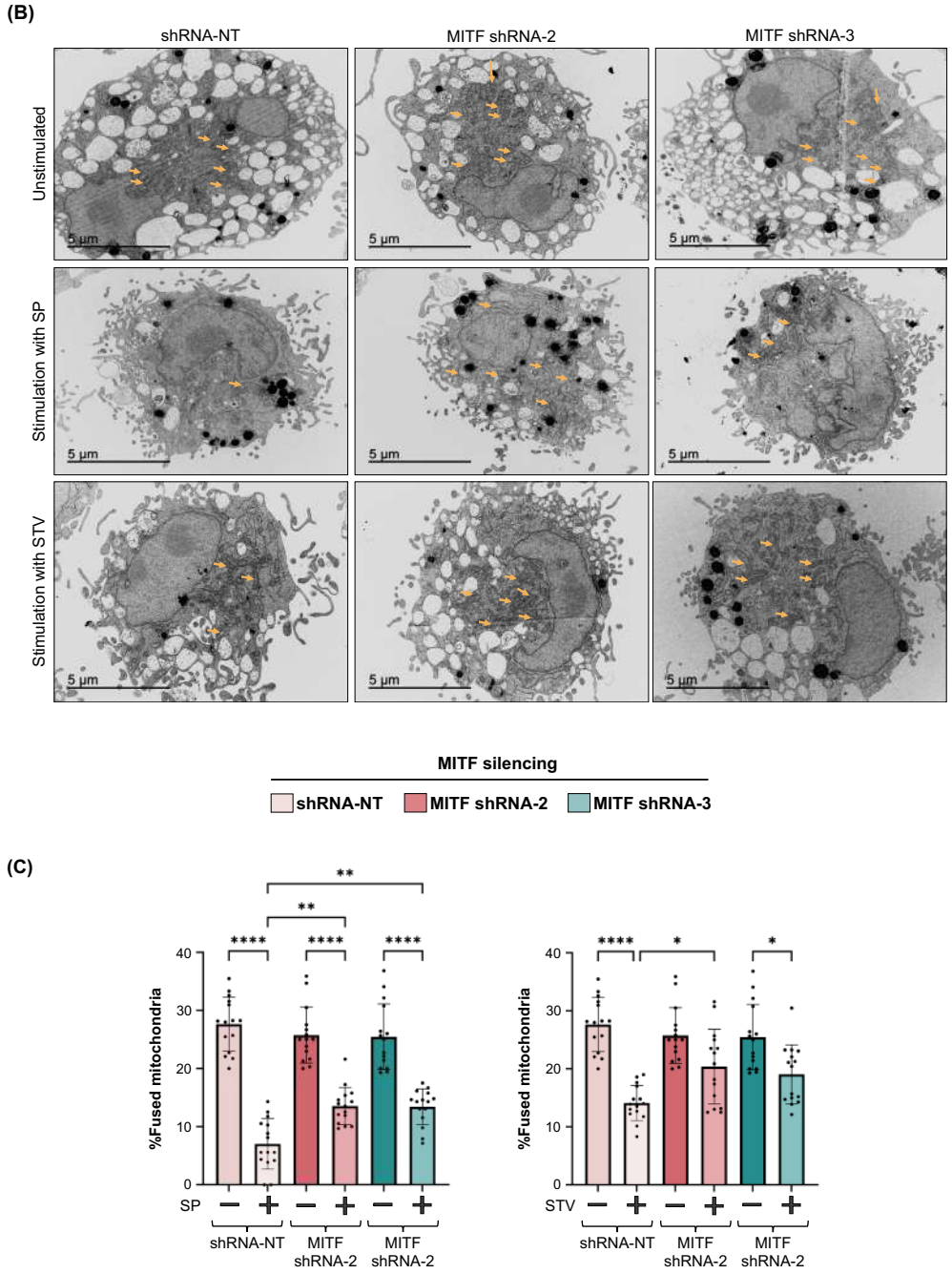

Figure 74. Mitochondrial fission is impaired with MITF silencing. MITF-knockdown cells were analyzed by TEM. Treated LAD2 cells were sensitized with 0.1 µg/ml biotinylated human IgE overnight and were activated with streptavidin or substance P for 1 or 2 minutes. Cells were pelleted and assessed under TEM. A) Scheme of fused and fragmented mitochondria. B)

Representative TEM photos of MITF-knockdown cells activated with SP or [b]IgE + STV. Fused mitochondria are identified by orange arrows. C) Statistical analysis of fused mitochondria when cells were activated with SP (n=15). D) Statistical analysis of fused mitochondria when cells were activated with [b]IgE + STV (n=15). Results are expressed as mean ± SD. Significance was determined using two-way ANOVA with Tukey's multiple comparison analysis. P<0.05 was considered statistically significant. *P<0.05; **P<0.01; ****P<0.0001. STV=Streptavidin; SP=Substance P.

4.9. MITF-knockdown reduces the expression of other mitochondrial enzymes involved in metabolism

In addition, as Hua *et al.* reported that MITF regulates *COX-IV* (a nuclear gene that encodes for the COX-IV subunit of complex IV (CIV) in retinal pigment epithelial cells (440), we decided to assess it in our model of MITF-knockdown cells. We observed a significantly lower expression of *COX-IV* in MITF-knockdown cells than in control cells (Figure 75).

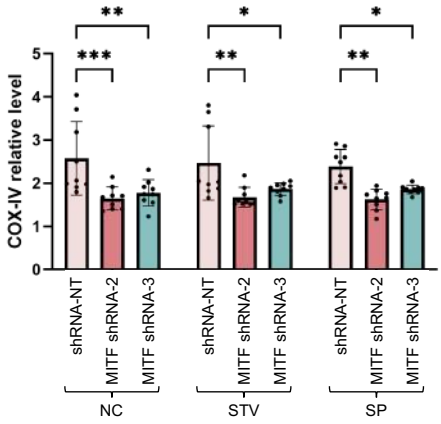

Figure 75. MITF-knockdown cells reduce *COX-IV* expression. LAD2 cells were infected with MITF shRNAs (NT, 2 and 3) and stimulated with streptavidin or substance P for 24h (n=9). After 24h, *COX-IV* gene expression levels were assessed by Fluidigm. Results are expressed as mean ± SD. Significance was determined using two-way ANOVA with Tukey's multiple comparison analysis. P<0.05 was considered statistically significant. *P<0.05; **P<0.01; ***P<0.001. STV=Streptavidin; SP=Substance P.

As we demonstrated that MITF is involved in mitochondrial protein import (*TOMM20*) and *COX-IV* regulation, and previously we observed that MITF-knockdown cells had different mitochondrial components downregulated (GO cellular components analysis), we performed a deeper analysis of some mitochondrial OXPHOS proteins in a MITF-knockdown model.

In terms of protein levels, first, we evaluated for COX-IV, finding significantly reduced levels in cells with MITF inhibition or silencing, correlating with a reduction in its gene expression levels in MITF-knockdown cells (Figure 76A), suggesting lower activity in these cells versus control cells.

Furthermore, we saw that silencing or inhibiting MITF in LAD2 cells induces a reduction in TOM20 protein levels, as we expected due to the lower expression of this gene in MITF-knockdown cells, suggesting less mitochondrial mass in these cells versus control cells.

In addition, when cells were treated with ML329, other OXPHOS complexes regulated by mtDNA (CI, CII and CIII) were reduced, suggesting a lower metabolic activity in these cells than in control cells. In MITF-silenced LAD2 cells, no significant differences between OXPHOS complexes regulated by mtDNA were found; just significantly reduced CII was found in MITF-shRNA-3 cells (Figure 76B).

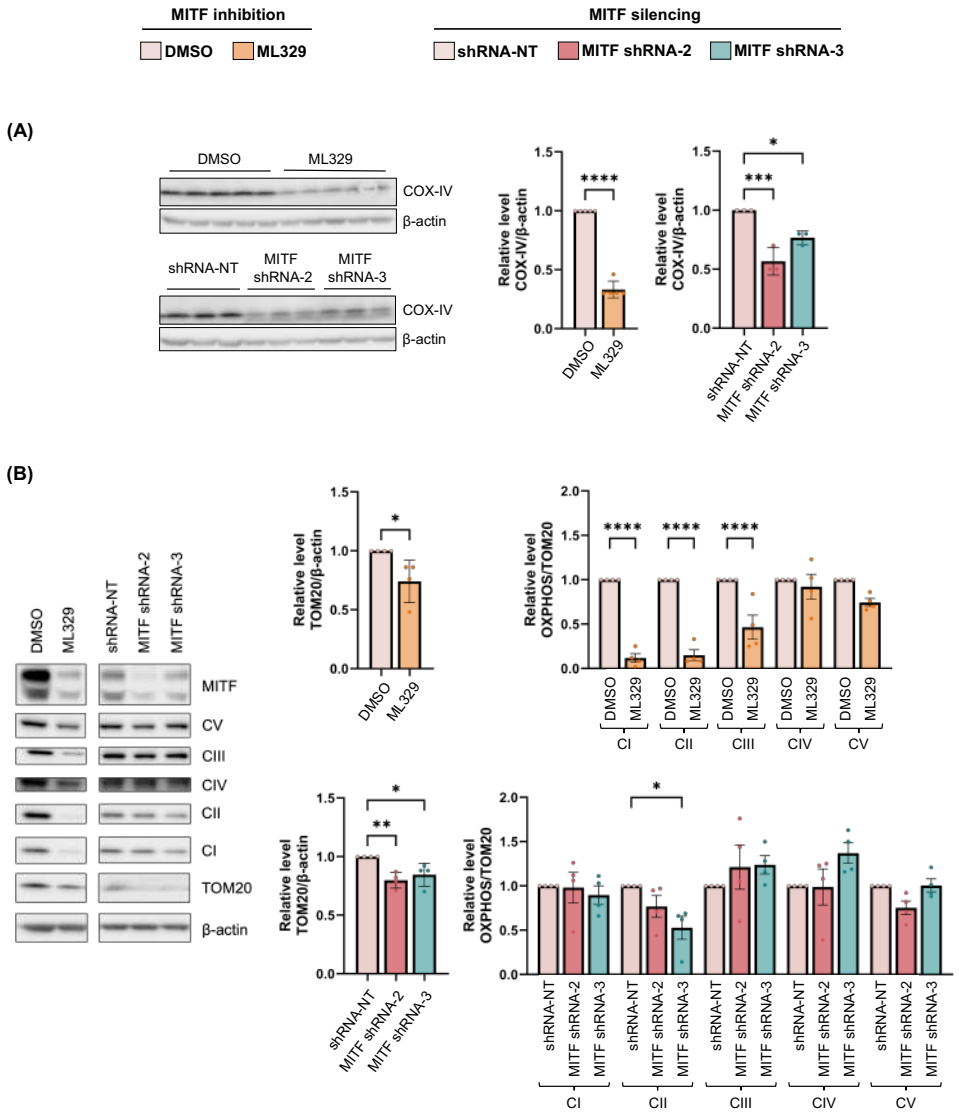

Figure 76. TOM20 and COX-IV proteins are reduced in MITF-knockdown cells. MITF-knockdown cells were used to assess mitochondrial proteins by western blot. A) The COX-IV subunit of CIV of the mitochondrial electron chain in LAD2 cells treated with ML329 (n=5) or MITF- shRNA (n=3). B) OXPHOS mitochondrial complexes (encoded in mitochondrial DNA) in LAD2 cells treated with ML329 or MITF- shRNA (n=4). Results are expressed as mean ± SD. Significance was determined using two-way ANOVA with Tukey's multiple comparison analysis. P<0.05 was considered statistically significant. *P<0.05; **P<0.01; ***P<0.001; ****P<0.0001. STV=Streptavidin; SP=Substance P.

4.10. Anaphylaxis patients have higher levels of *TOMM20* and *COX-IV*

As we saw that MITF regulates *TOMM20* and *COX-IV*, we used our cohort of LTP patients (Annex Table 3) to assess the expression of these genes. CD34^{+}-derived MCs from patients and healthy donors were sensitized with pooled sera (anaphylaxis and sensitized) overnight and stimulated with Pru p 3 for 24 hours. Afterward, cells were pelleted, and Fluidigm was performed.

TOMM20 was significantly more expressed in MCs from anaphylactic patients when cells were activated with Pru p 3. In addition, *COX-IV* was highly expressed in both MCs from anaphylactic patients and healthy volunteers sensitized with pooled sera from the anaphylaxis group under stimulation conditions (Figure 77). These findings suggest that the cellular component is important for these severe allergic reactions; nonetheless, the humoral component also plays an important role.

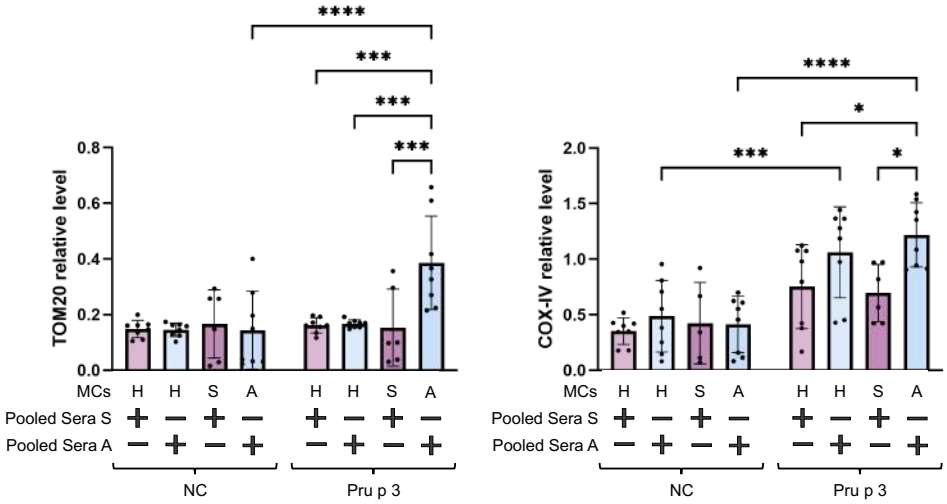

Figure 77. *TOMM20* and *COX-IV* are increased in MCs from the anaphylaxis group. MCs from LTP patients (sensitized n=6; and anaphylaxis n=8) and healthy volunteers (n=8) were sensitized with pooled sera overnight. Then, cells were washed and stimulated with 1 µg/ml Pru p 3 for 24 hours. Afterward, cells were pelleted and RNA extracted, followed by reverse transcription and Fluidigm were performed to assess *TOMM20* and *COX-IV* levels. Results are expressed as mean ± SD. Significance was determined using two-way ANOVA with Tukey's multiple comparison analysis. P<0.05 was considered statistically significant. *P<0.05;

***P<0.001; ****P<0.0001. H=Healthy volunteer; S=Sensitized patients; A=Anaphylaxis patients.

4.11. MITF regulates mitochondrial respiration

Knowing that MITF is involved in mitochondrial protein import and function, we wanted to delve into cell respiration to validate the results observed in the GSEA analysis, where we found different downregulated OXPHOS-related pathways. To do so, we measured the OCR in LAD2 cells with MITF-inhibited or silenced (treated with ML329 or infected with MITF shRNA-2), and in transfected RBL-2H3 cells, where MITF is overexpressed.

In this study, we showed that MITF inhibition or silencing reduces the levels of OCR, basal respiration, ATP production, and maximum respiration of the cells (Figure 78A and C), suggesting lower mitochondrial activity in these cells. This lower mitochondrial activity might be due to the reduced expression of TOM20, which is important for mitochondrial protein import, and COX-IV, which is important for oxidative phosphorylation. Indeed, we observed a reduction in the ECAR levels in cells with MITF-knockdown (Figure 78B), suggesting a lower glycolysis in these cells.

Furthermore, when we assessed mitochondrial respiration in the MITF-overexpression model, there were no significant differences; however, there was a trend. LysRS-P542R cells, with high MITF protein levels, had elevated OCR levels, as well as more basal respiration, ATP production, proton leak, and maximum respiration, followed by LysRS-WT (Figure 79). Indeed, we observed that LysRS-P542R cells exhibited higher ECAR levels after oxidative phosphorylation was blocked by oligomycin, suggesting that these cells rely more on glycolysis to compensate for the loss of mitochondrial ATP production compared with LysRS-WT or control cells (Figure 79).

Altogether, it suggests that MITF may play a role in oxidative phosphorylation: MITF-knockdown induces low mitochondrial respiration while MITF-overexpression induces high mitochondrial respiration.

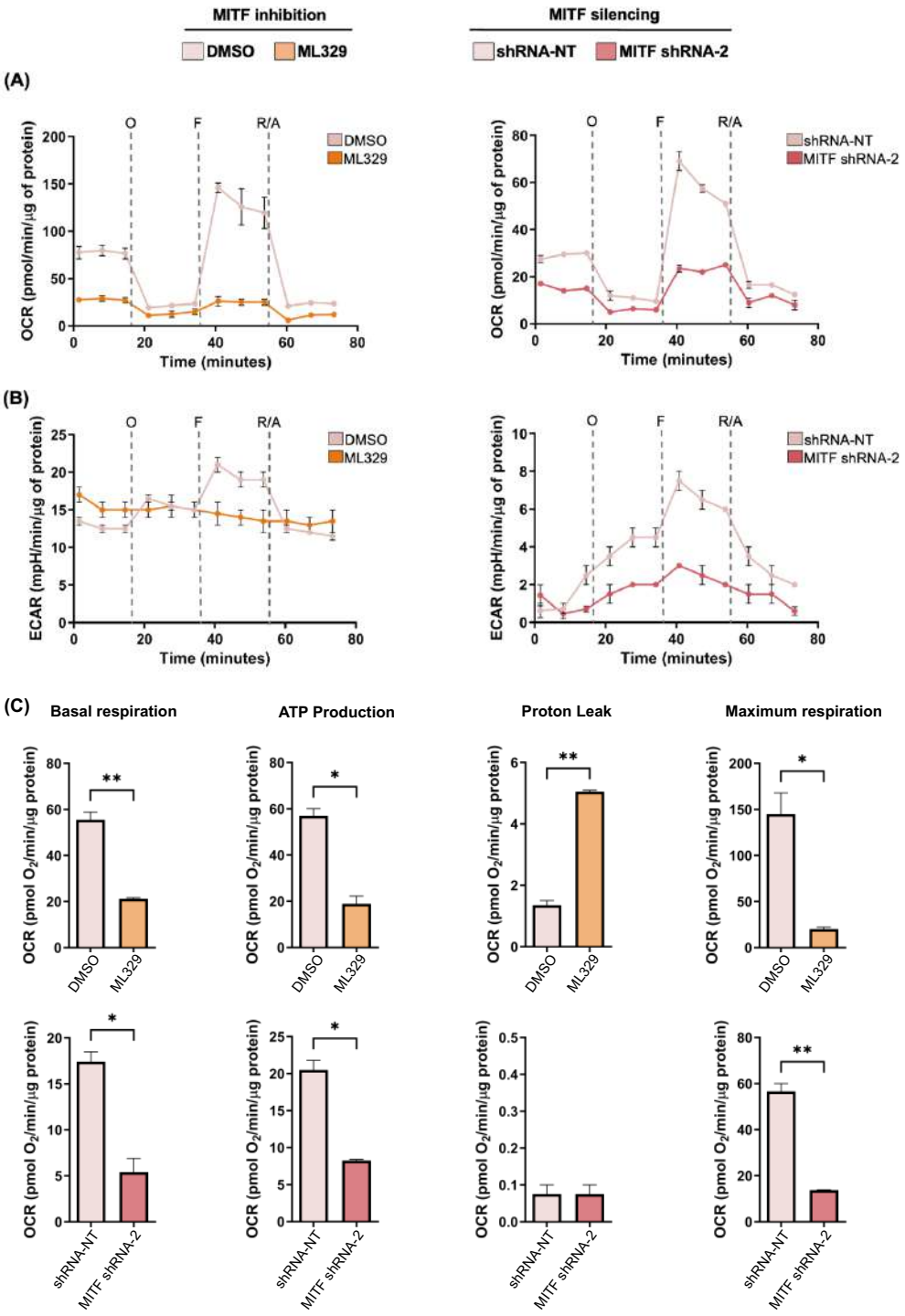

Figure 78. Mitochondrial respiration is decreased in MITF-knockdown cells. LAD2 cells were used to analyze mitochondrial respiration using Seahorse (n=3). A) Oxygen consumption

rate of LAD2 cells treated with ML329 or shRNA. B) Extracellular acidification rate of LAD2 cells treated with ML329 or shRNA. C) Analysis of different parameters of the MitoStress Test in treated LAD2 cells. Results are expressed as mean ± SD. Significance was determined using one-way ANOVA with Tukey's multiple comparison analysis. P<0.05 was considered statistically significant. *P<0.05; **P<0.01. O=Oligomycin; F=FCCP; R/T=Rotenone/Antimycin.

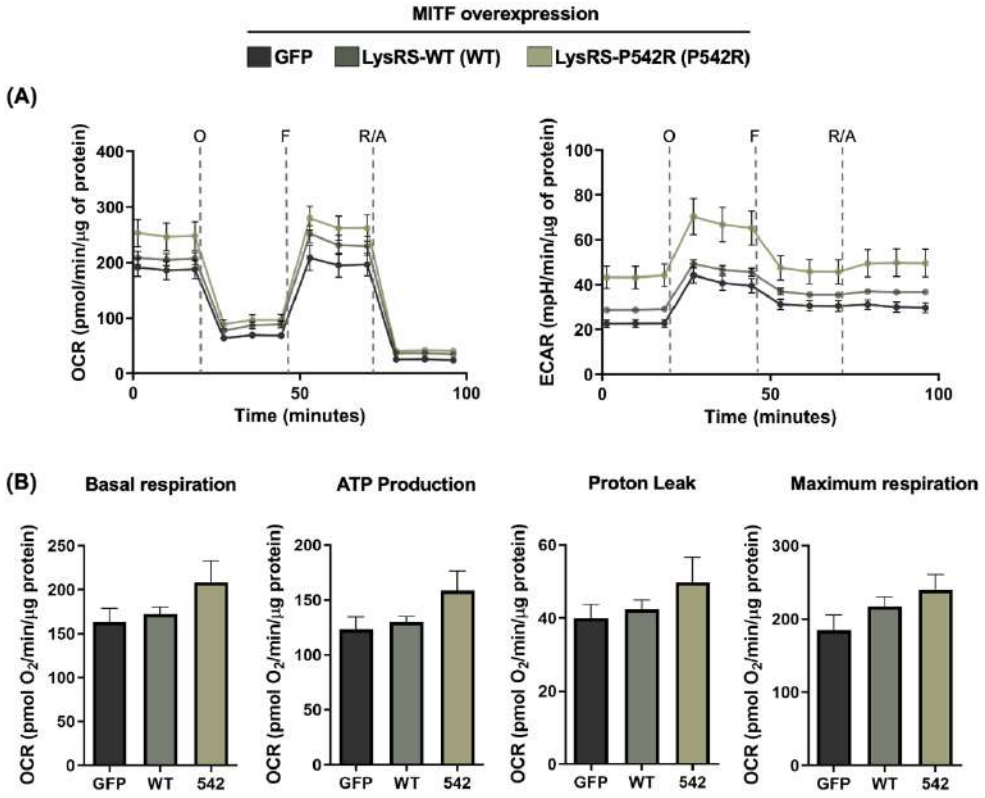

Figure 79. LysRS-P542R mutation induces a higher mitochondrial respiration. Transfected RBL-2H3 cells (LysRS-WT, LysRS-P542R and, GFP as a control) were used to analyze mitochondrial respiration by Seahorse (n=3). The MitoStress test was performed with oligomycin, FCCP and Rotenone/Antimycin. A) Oxygen consumption rate and extracellular acidification rate of transfected RBL-2H3. C) Analysis of different parameters of MitoStress Test in transfected RBL-2H3. Results are expressed as mean ± SD. Significance was determined using two-way ANOVA with Tukey's multiple comparison analysis. P<0.05 was considered statistically significant. P54R as LysRS-P542R and WT as LysRS-WT. O=Oligomycin; F=FCCP; R/T=Rotenone/Antimycin.

4.12. Sera from LTP patients induce a higher mitochondrial respiration

With this preliminary evidence that MITF plays a role in metabolism and TOM20 and COX-IV seem to be higher in MCs from anaphylactic patients, we wanted to assess whether both the humoral and cellular components of our cohort might induce changes in MC metabolism. First, LAD2 cells were sensitized with pooled sera from patients (sensitized and anaphylaxis) and healthy volunteers overnight. Then, cells were washed, and mitochondrial respiration was measured using Seahorse.

LAD2 cells sensitized with pooled sera from LTP patients had a higher oxygen consumption rate than those sensitized with sera from healthy donors. Analyzing different parameters, we observed that basal mitochondrial respiration and ATP production were higher when LAD2 cells were sensitized with pooled sera from sensitized patients, but even more so when sensitized with pooled sera from the anaphylaxis group than from healthy volunteers.

In addition, LAD2 cells sensitized with pooled sera from LTP patients had greater proton leak and maximum mitochondrial respiration than cells sensitized with pooled sera from healthy donors (Figure 80). Thus, it seems that sera from LTP patients may induce higher mitochondrial activity than sera from healthy individuals, again suggesting that the humoral component from LTP patients has an essential role in the severity of the allergic reactions.

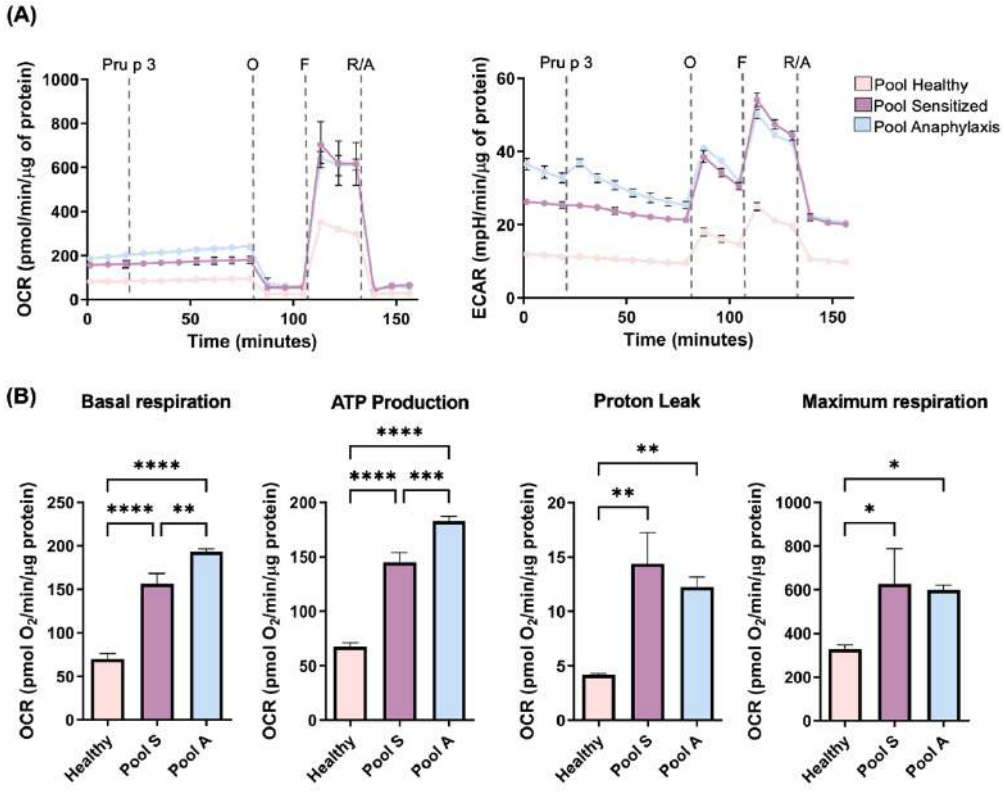

Figure 80. Sera from LTP patients induce more mitochondrial respiration. LAD2 cells were sensitized with pooled sera from patients (sensitized and anaphylaxis) and healthy volunteers overnight. Then, cells were washed, and mitochondrial respiration was assessed by Seahorse (n=3). After basal measurements, 1 µg/ml Pru p 3 was added, and respiration was measured for 45 minutes. Then, oligomycin, FCCP and Rotenone/Antimycin were used to measure other mitochondrial respiration parameters. A) The MitoStress test was performed with oligomycin, FCCP and Rotenone/Antimycin after Pru p 3 injection. B) Statistics of MitoStress measurement. Results are expressed as mean ± SD. Significance was determined using one-way ANOVA with Tukey's multiple comparison analysis. P<0.05 was considered statistically significant. *P<0.05; **P<0.01; ***P<0.001; ****P<0.0001. H=Healthy volunteer; S=Sensitized patients; A=Anaphylaxis patients; O=Oligomycin; F=FCCP; R/T=Rotenone/Antimycin.

4.13. Sera from LTP patients induce higher ROS production after Pru p 3 stimulation

Next, we assessed ROS production in LAD2 cells sensitized with pooled sera from healthy volunteers and LTP patients and stimulated with Pru p 3 for three days. We observed that, after three days of Pru p 3 stimulation, ROS

production increased in LAD2 cells sensitized with pooled sera from sensitized patients, and was even higher in cells sensitized with pooled sera from the anaphylaxis group (Figure 81).

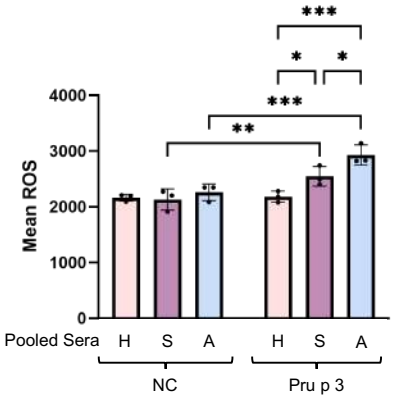

Figure 81. ROS production is elevated in LAD2 cells sensitized with pooled sera from the anaphylaxis group and stimulated with Pru p 3. LAD2 cells were incubated with IL-4 for five days, sensitized overnight with pooled sera from healthy volunteers and the sensitized and anaphylaxis groups, and then stimulated with Pru p 3. ROS production was measured after three days of activation. Results are expressed as mean ± SD. Significance was determined using one-way ANOVA with Tukey's multiple comparison analysis. P<0.05 was considered statistically significant. *P<0.05; **P<0.01. H=Healthy volunteer; S=Sensitized patients; A=Anaphylaxis patients.

4.14. MCs from LTP patients have a higher mitochondrial activity

Afterward, we assessed whether the cellular component might change mitochondrial metabolism. To do so, we differentiated *in vitro* MCs from the blood of one healthy volunteer, one sensitized patient, and one anaphylactic patient (clinical characteristics are in Annex Table 4), and performed a mitochondrial analysis. As expected, we found higher *MITF* levels in the anaphylactic patient, followed by the sensitized patient, than in the healthy volunteer (Annex Table 4), suggesting that MITF might play a role in the metabolic regulation of these cells.

First, we used Seahorse to assess mitochondrial respiration, finding that cells from sensitized and anaphylactic patients had a higher OCR than those of the

healthy volunteer. Regarding ECAR, MCs from the anaphylactic patient seemed to have higher acidification media than other MCs, especially after Pru p 3 injection (Figure 82A). When oxidative phosphorylation parameters were analyzed, MCs from the two LTP patients showed greater basal respiration and ATP production than cells from the healthy donor. Also, cells from the patients, although not significant, tended toward increased proton leak and maximum respiration (Figure 82B).

Secondly, although the ECAR results afford an idea of cellular glycolysis, we used MCs from the healthy donor to perform a Seahorse glycolytic test to better distinguish differences in this metabolic pathway. MCs from the healthy individual were sensitized overnight with its serum and serum from the anaphylactic patient. Then, cells were used to perform the glycolytic test, first adding Pru p 3. After allergen addition, we observed that MCs from the healthy volunteer sensitized with serum from the anaphylactic patient induced a higher glycolytic proton efflux rate (glycoPER), signifying a faster glycolytic response than MCs from the healthy individual sensitized with its own serum (Figure 82C). In addition, after the injection of mitochondrial inhibitors, the compensatory glycolysis was higher in MCs from the healthy volunteer sensitized with serum from the anaphylactic patient, suggesting that this anaphylactic patient's serum had the ability to modify the metabolic cell demand to a more glycolytic pattern.

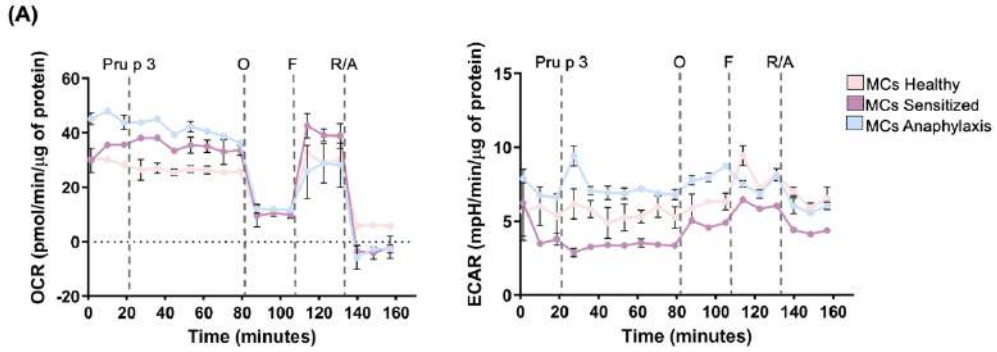

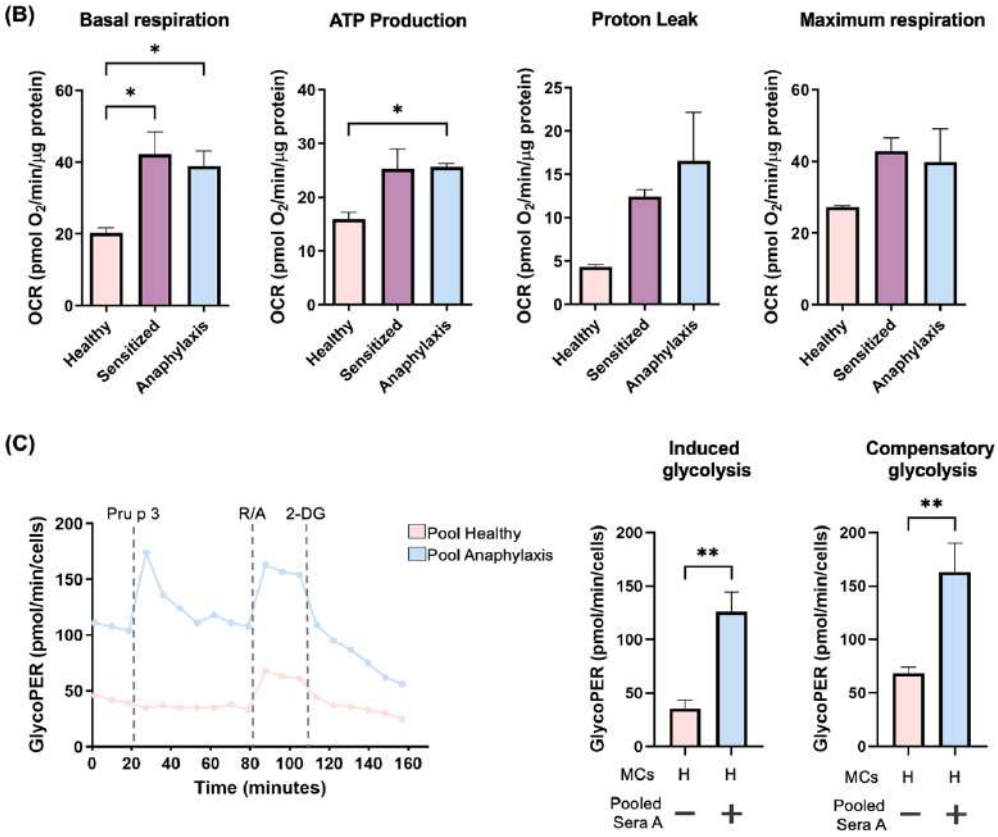

Figure 82. Mitochondrial respiration is elevated in MCs from LTP patients. MCs from one healthy donor (n=1), one sensitized patient (n=1) and one anaphylaxis (n=1) patient were sensitized with their serum overnight (in triplicate). Then, cells were used to assess mitochondrial respiration. A) The MitoStress test was performed with oligomycin, FCCP and Rotenone/Antimycin after 1 µg/ml Pru p 3 injection. B) Statistics of MitoStress measurement. C) Glycolytic test was performed with R/A and 2-deoxy-D-glucose (2-DG) after Pru p 3 injection. Results are expressed as mean ± SD. Significance was determined using one-way ANOVA with Tukey's multiple comparison analysis. P<0.05 was considered statistically significant. *P<0.05; **P<0.01. H=Healthy volunteer; S=Sensitized patients; A=Anaphylaxis patients; O=Oligomycin; F=FCCP; R/T=Rotenone/Antimycin.

4.15. Results Summary

Our findings suggest that MITF may fine-tune MC responses by regulating mitochondrial function (Results Summary 3). This uncovers a novel aspect of MITF's involvement in MC biology, shedding light on its potential as a therapeutic target in inflammatory and allergic diseases. Also, the interest in

metabolic activity during anaphylactic reactions is increasing, and it must be further studied to discover new therapies for these severe reactions.

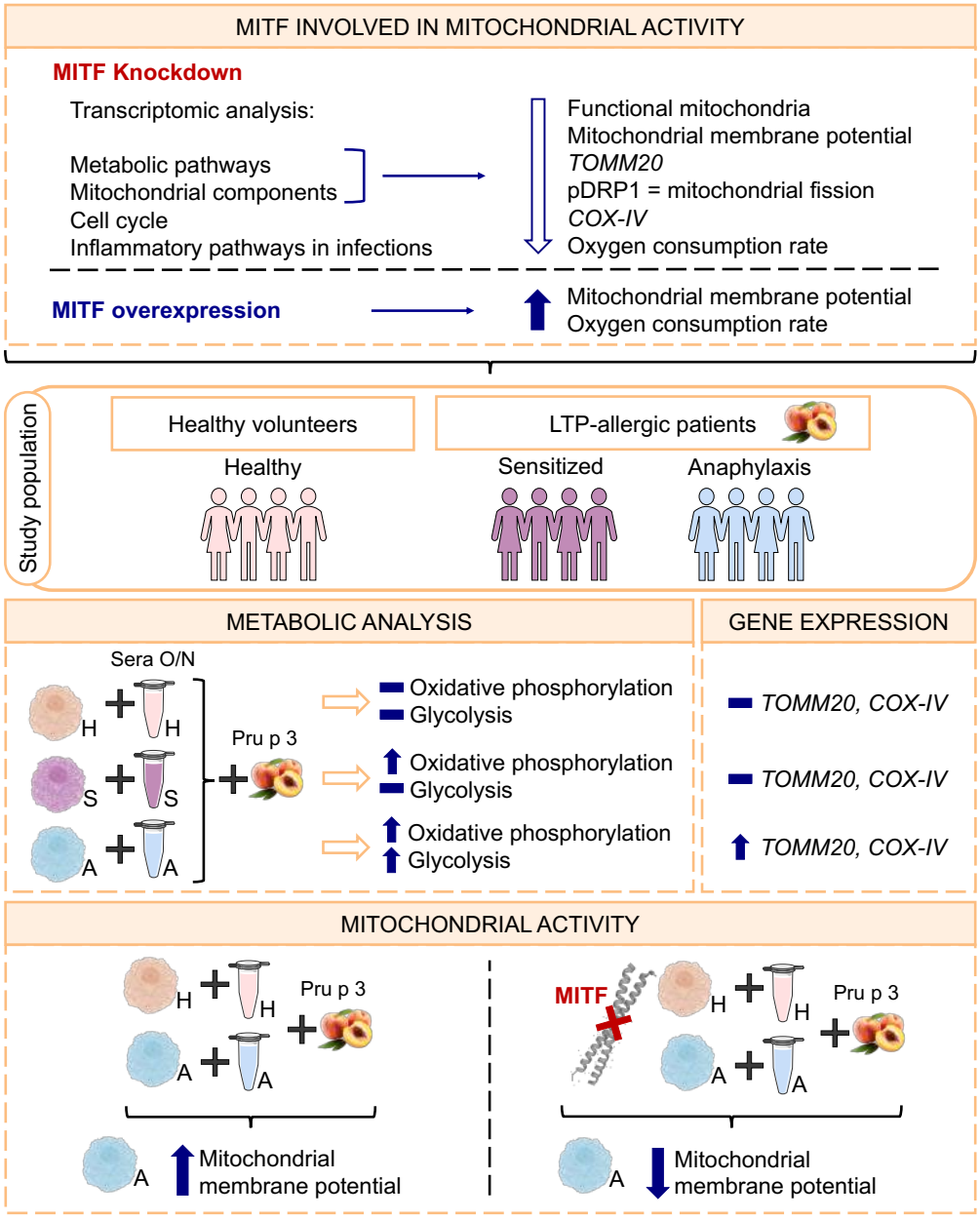

Results Summary 3. Summary of all the data obtained in this last section. A=Anaphylaxis patients; H=Healthy volunteers; LTP=Lipid Transfer protein; O/N=Overnight; PDH=Pyruvate dehydrogenase; pDRP=phospho-DRP^{Ser616}; S=Sensitized patients.

4.16. Supplementary Figures and Tables

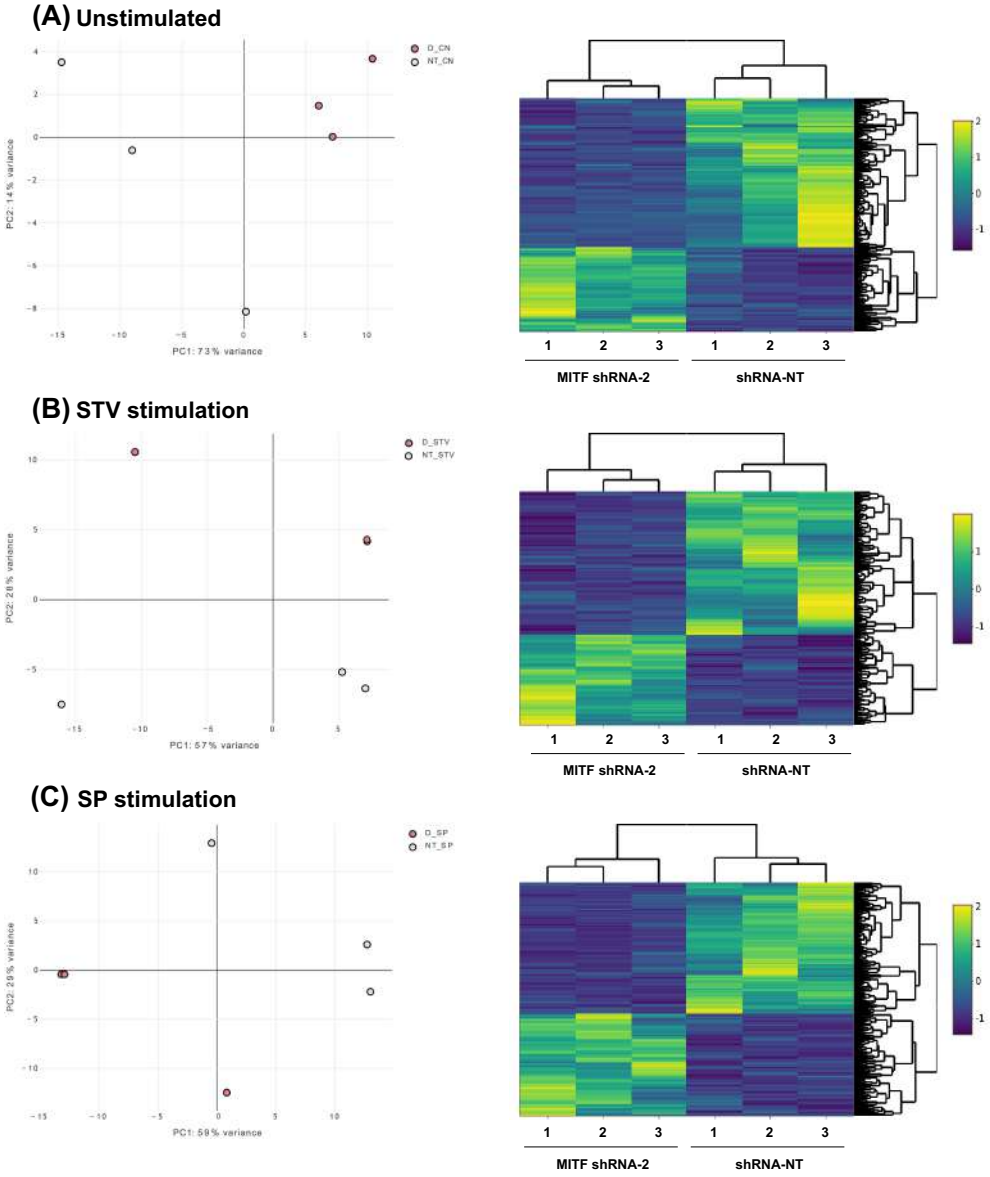

Supplementary Figure 7. Differential analysis from RNA-sequencing. LAD2 cells infected with shRNA-NT (as control) and MITF shRNA-2 were activated with streptavidin or substance P, and RNA-sequencing was performed. PCA plot and heatmap were created with RStudio using a log2FoldChange ± 1 and adjusted p-value <0.05. A) Unstimulated cells. B) Cells activated with ^{b}IgE + STV. C) Cells activated with SP. STV=Streptavidin; SP=Substance P.

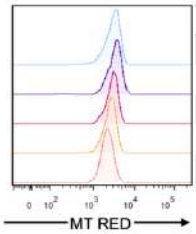

	Mean MT Red
SP 15'	2850
SP 10'	3194
SP 5'	2799
SP 2'	2453
CN	2150

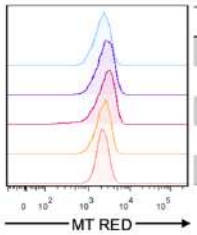

	Mean MT Red
STV 15'	2134
STV 10'	2564
STV 5'	2521
STV 2'	2225
CN	2150

Supplementary Figure 8. Mitochondrial membrane potential curve. LAD2 cells were activated with either ^{b}IgE + streptavidin and substance P for 2, 5, 10 and 15 minutes, and the mitochondrial membrane potential was assessed by flow cytometry. STV=Streptavidin; SP=Substance P.

DISCUSSION

MCs are immune system cells that play a role in host defense, innate and acquired immunity, homeostatic responses, and immunoregulation (1–4). Various mechanisms can trigger MC activation, such as the binding of IgE and antigen to FcεRI, or the attachment of drugs to the MRGPRX2 receptor, which leads to the immediate release of contents from the granules (7,8). MCs release a wide array of preformed and newly synthesized mediators that elicit allergic responses, including asthma, angioedema, urticaria, and anaphylaxis or anaphylactic shock in the most severe cases (9,10).

FA is a pathological immune response triggered by harmless food protein antigens. LTPs are common plant food allergens that contribute to some of the most prevalent FAs in the Mediterranean region (384,385). In recent decades, the incidence of food anaphylaxis – the most severe form of allergic reaction – has significantly increased, and its risk remains unpredictable (281,386,387). The allergen avoidance diet and symptomatic treatment are standard approaches to managing these conditions. In contrast, the oral challenge test with allergens continues to be the gold standard for diagnosing food and drug allergies. This is time-consuming, requires an specialized setting and poses a risk to patients' lives, as it can lead to potentially severe allergic reactions, including anaphylaxis or even death (12-14).

Thus, having a reliable predictive model to anticipate potential allergic responses, especially the severe ones. Identifying severity markers will enable us to stratify patient risk, personalize treatments, and improve clinical management. Understanding the molecular and cellular bases of FAs will lead to accurate diagnosis, prevention, and treatment while allowing us to apply our findings to other conditions characterized by increased MC activation, such as drug allergic reactions.

1. IDENTIFYING BIOMARKERS TO DISTINGUISH BETWEEN ALLERGY AND SENSITIZATION

1.1. Development of a mast cell activation test to diagnose LTP-allergy

Allergy sensitization in food allergy often fails to correlate with clinical reactivity, which can lead to the overdiagnosis of FAs. This results in unnecessary dietary exclusions, social restrictions, and anxiety, further impairing nutrition and quality of life (332).

New techniques for diagnosing FAs have emerged recently, such as BAT and MAT. These tests can differentiate, with high sensitivity, between sensitization and allergy in some food allergy models. However, MAT appears to be superior to BAT, exhibiting greater specificity (337,337) – although BAT seems to be easier to perform, as it is a direct assay where only blood and allergen are needed.

It has been shown that BAT can be used for other clinical applications, such as monitoring clinical response following allergen-specific immunotherapy or anti-IgE treatment. Furthermore, its usefulness for studying cofactors has been proven. Adding nonsteroidal anti-inflammatory drugs (NSAIDs) before the allergen enhances IgE-mediated activation in human basophils in patients with food anaphylaxis (441). Indeed, in mugwort pollen-related peach allergy that BAT could predict the severity of the reaction (442). Conversely, a recent study has showed that BAT can distinguish between Pru p 3 allergy and tolerance but cannot predict the reaction severity (443). The authors suggest that the contradictory results between these two studies could be explained by the diagnostic work-up relying on subjective symptoms and a clinical process with limited accuracy.

However, the basophil's role as an effector cell in the pathophysiology of allergic reactions (343) is uncertain. MCs have long been regarded as the primary effector cells in individuals with allergic responses (343). Unlike basophils, MCs have MRGPRX2 receptors, which can induce degranulation without prior sensitization, leading to diagnostic drug hypersensitivity

reactions through this receptor (337). Additionally, basophils have consistently low MITF expression (31), which is crucial for basophils and MC differentiation. Therefore, using mast cells allows us to better study the mechanisms underlying food allergy. MAT is an *in vitro* diagnostic tool that combines the allergen, allergen-specific IgE, and human MCs - three crucial elements of the effector phase of IgE-mediated allergic responses (444).

In our study, we found that the MC activation profile could differentiate patients with severe reactions from those who are only sensitized to LTP. We tested 11 LTP patients, six of whom suffered anaphylaxis, and confirmed that MAT is an excellent assay to assess peach allergen (Pru p 3) reactivity. MAT may help identify patients with the highest risk of severe anaphylaxis, confirming its status as a highly sensitive assay. Our results align with previous studies that used peanuts as the allergen in MATs (54,330,445,446).

MCs were obtained from peripheral blood, resulting in around one million cells from an extraction of 70–100 mL. The efficiency of our results aligns with the existing literature (342,352). Apart from the few cells obtained, the differentiation of $CD34^+$ cells to MCs takes around two months. To solve this problem, in the context of diagnostics, some groups used LAD2 cells as a cell model. LAD2 cells closely resemble primary human MC cultures, which are slow-growing, dependent on SCF for proliferation, carry functional FcεRI receptors on their surfaces, and can degranulate in response to immunological stimuli (346). Recently, new immortalized MCs – Hoxb8 MCs – have been described, which are highly granulated and can be used for MAT (354). The differentiation of mature Hoxb8 MCs (extracted from the bone marrow of mice) expressing consistent levels of FcεRI takes only six days (354). Further studies are needed to assess its efficacy in MAT; however, this new cell line could significantly improve using MAT's use as a diagnostic tool.

In this study, we also conducted a MAT with LAD2 cells sensitized with sera from healthy, sensitized, or anaphylaxis individuals and stimulated with the allergen. We observed that LAD2 cells had a lower degranulation rate than primary MCs under the same conditions as reported in other studies (331). This lower activation, measured by the expression of CD63, could suggest

that MAT with LAD2 would not be as specific as MAT with primary MCs. However, the differences observed between groups were the same regardless the MC type used – higher CD63 expression when cells were sensitized with sera from the anaphylaxis group than from the sera from sensitized group after Pru p 3 challenge, suggesting that the humoral component is essential in the severity of the reaction.

1.2. IgE affinity might play a role in the severity of allergic responses

Determination of the tIgE/sIgE (total IgE / specific IgE) ratio is commonly used for diagnostic purposes, as the clinical relevance of the sIgE levels depends on their proportion relative to tIgE when analyzing the receptor occupancy rate of effector cells. Furthermore, measuring allergen-specific IgG_4 ($sIgG_4$) could provide additional insights into tolerance development in FA patients (447–449). Although there is only one study involving milk food allergy, some studies on aeroallergens have shown that the serum IgG_4 levels are higher among asymptomatic atopic patients (450); thus, the IgG_4/IgE ratio is greater in nonatopic and asymptomatic atopic individuals than in allergic patients (451,452). The anaphylactic patients in our cohort had significantly lower tIgE/sIgE and $sIgG_4$/sIgE ratios, indicating higher relative sIgE values in those patients compared with sensitized patients and healthy volunteers. However, evidence regarding the utility of these ratios remains limited (453).

The higher sIgE levels in the anaphylaxis group than in the sensitized group, could account for the higher activation of the first group, as reported in other studies (446). Tam *et al*., (444) reported that MCs from healthy donors responded to high sIgE levels but not to low ones. To eliminate this confounding factor, we standardized the sIgE levels for each group and used the same quantity of sIgE for MC sensitization. Therefore, our results suggest that MC responses may depend on other factors, not only sIgE levels.

Our study showed that $T_{FH}13$ cells were more abundant in patients with anaphylaxis than those merely sensitized. T follicular helper (T_{FH}) cells are a subset of cells, localized in B-cell follicles. They express high levels of B-cell-stimulating molecules, such as CD40 ligand, and produce large amounts of

IL-4, thereby promoting the affinity maturation, longevity, and isotype switching of antibodies produced by B cells (14,320). Recently, $T_{FH}13$ cells have been discovered, which induce anaphylactic IgE by secreting IL-4 and IL-13 (324). Thus, our results suggest that patients from the anaphylaxis group might have higher affinity sIgE than individuals who are just sensitized, signifying that this anaphylactic IgE could be related with a more intense response in MCs from anaphylactic patients, as proposed in other studies (330).

1.3. IgE affinity induces different signaling pathways

Furthermore, the affinity of IgE could induce different signaling patterns. As some studies have reported (313,392), a high-affinity IgE can yield a more robust activation of phospho-LAT1, increasing degranulation and cytokine production with greater recruitment of neutrophils at the site of inflammation. On the contrary, a low-affinity IgE can induce the activation of other molecules, such as phospho-LAT2 or phospho-Fgr, increasing the production of the chemokines such as CCL2, CCL3, and CCL4, which are monocyte or macrophage-attracting factors. So, the affinity of IgE could switch the cellular response via molecular signals (313).

In our study, we show that sera from anaphylaxis patients induce a more robust activation of phospho-LAT1 in LAD2 cells, producing a higher amount of IL-8 and GM-CSF in both $CD34^+$-derived MCs from patients and LAD2 cells, suggesting a stronger pro-inflammatory profile. Otherwise, sera from sensitized patients induce a higher amount of TGF-β and CCL2 in both $CD34^+$-derived MCs and LAD2 cells, indicating a more protective profile. TGF-β was reported to suppress MC activity and to inhibit MC FcεRI expression in mice (454,455). These results reinforce the idea that differences in IgE affinity lead to different cell activation pathways, possibly leading to anaphylaxis in a high-affinity context.

Another interesting factor to consider is epitope diversity related to the affinity of sIgE. Some studies reported a higher epitope diversity with a high-affinity sIgE in allergic patients compared with those with tolerance, correlating with

the severity of allergic reactions (456–458). However, our study did not assess epitope diversity or its relationship with sIgE affinity. Nevertheless, it would be interesting to characterize the range of epitopes recognized and their potential impact on allergic responses.

In summary, the MC activation profile analysis and the identification of the $T_{FH}13$ population in peripheral blood may discriminate patients at risk of developing anaphylaxis from those merely sensitized, helping to stratify risk before an OFC.

1.4. Pru p 3 induces a different signaling pathway in sensitized and allergic patients

Following the findings of our first study, we performed RNA-sequencing of both $_{BC}$MCs and LAD2 cells sensitized with sera from both groups of patients and stimulated with Pru p 3 for 24 hours. The transcriptomic data showed that $_{BC}$MCs sensitized with sera from the sensitized group ($_{BC}$MCs-S) induced different pathways than those from the anaphylaxis group ($_{BC}$MCs-A). We detected clearly differentiated patterns; however, it must be taken into consideration that we were looking at selective activation (MC sensitized with patient sera and activated with allergen) under specific conditions (24 hours); therefore, it is possible that we missed some of the differentially expressed genes. In addition, we focused on coding genes, although we also observed lncRNA (long non-coding RNA) and miRNA (microRNA) that were differentially expressed and which would be interesting to study.

The GSEA analysis revealed that senescence, cell cycle, and NF1 pathways were downregulated in $_{BC}$MCs-S than from $_{BC}$MCs-A after stimulation with Pru p 3. Cellular senescence is a state of proliferation arrest in which senescent cells develop a hypersecretory phenotype (SASP). This indicates that they secrete certain factors into their microenvironment that can modulate biological activities, both locally and systemically, contributing to chronic inflammation. Some of these SASP components are cytokines (e.g., IL-1, IL-6, and IL-8), chemokines (e.g., CCL2 and CCL5), and growth factors (e.g., GM-CSF) (395). We observed an increase in IL-8 and GM-CSF production in

MCs from anaphylactic patients, which may correlate with the higher state of senescence in these cells. However, we noted that MCs from sensitized patients produce more CCL2, a chemokine also related to senescence. Senescence is described to comprise two different stages: an early stage, with an intention of tissue repair, and a later stage, with the development of chronic inflammation (459). This early stage has been suggested to have CCL2 higher secretion, which induces the recruitment of monocytes and macrophages attempting to repair the damage. However, an advanced state of senescence is associated with increased secretion of pro-inflammatory cytokines, contributing to chronic inflammation (460). Thus, based on our results, it might be that MCs from sensitized patients secrete more CCL2 in an early stage of senescence to restore the local inflammatory situation. In contrast, MCs from anaphylactic patients may develop a chronic inflammatory state, with a higher production of pro-inflammatory cytokines and an elevated state of senescence.

In addition, the secretion of these pro-inflammatory factors depends on calcium homeostasis (395). Our analysis found that several calcium-related genes – such as *ORAI2, EFCAB5*, and *CACNA1H* – were downregulated in LAD2 cells sensitized with sera from sensitized patients (LAD2-S) compared with those sensitized with sera from the anaphylaxis group (LAD2-A), suggesting a lower secretion of pro-inflammatory cytokines. Furthermore, calcium is also needed for MC degranulation, therefore, these results also correlated with our previous findings, where we found a decrease in degranulation and secretion of pro-inflammatory cytokines in MCs-S or LAD2-S compared with MCs-A or LAD2-A.

Moreover, we found a higher expression of the *CCR2* and *NFKBIL1* genes in $_{BC}$MCs-S than in $_{BC}$MCs-A. *NFKBIL1* encodes an NF-κB inhibitor, reducing the pro-inflammatory response by modulating the antigenic presentation of dendritic cells (461). CCR2 is the primary chemokine receptor that induces macrophage and monocyte recruitment, and regulates the T-cell responses (462). An increase in CCR2 is reported to induce the switching of T cells into T_H1 or T_H17 (T helper 1 or T helper 17 cells), promoting local inflammation (463,464). This correlates with the GSEA results obtained in $_{BC}$MCs-S, where

local acute inflammatory response pathways were upregulated compared with $_{BC}$MCs-A. These findings are related to the clinical symptoms of sensitized patients with no symptoms or only mild local symptoms (contact urticaria, oral allergy syndrome).

In addition, NF1 is related to many cellular processes, such as proliferation and migration, through its involvement in many signaling pathways, including Ras/MAPK and PI3K/Akt/mTOR (393,394). MCs from *NF1*-knockout mice were reported to have increased TGF-β secretion (396,397). This correlated with our findings; MCs-S induced a lower production of TGF-β than MCs-A. Furthermore, TGF-β signaling pathways are upregulated in LAD2-S, suggesting an attenuated response in these cells. TGF-β was proven to modulate allergic inflammation by inhibiting MC degranulation and T_H2 responses and promoting Treg (regulatory T cells) differentiation (455,465,466).

These results correlate with our previous findings, proposing that the humoral component plays a vital role in the severity of allergic reactions. Nevertheless, MCs were described as being able to contribute to the severity of allergic responses. An increased risk of severe anaphylaxis has been linked to hereditary copy number variations of the *TPSAB1* gene, which encodes tryptase (467). In our first study, serum tryptase values below 8 µg/L in all MC donors made the presence of hereditary alpha tryptasemia unlikely. A mutation in *KIT* (D816V) can contribute to MC hyperreactivity (270), all patients in our study were thoroughly evaluated and none of them had a clinical suspicion of systemic mastocytosis. In contrast, Hyper-IgE syndrome patients (AD-HIES) with dominant negative *STAT3* mutations are protective against anaphylaxis (468). Thus, in parallel to the transcriptomic data of MC_{BC} or LAD2 cells sensitized with sera from LTP patients, we were interested in looking at the expression of some genes related to exacerbated responses in patient MCs.

1.5. Pru p 3 induces a stronger pro-inflammatory response in MCs from anaphylactic patients in comparison with sensitized individuals

We observed increased *CCL18* and *TGFB1* gene expression in MCs from sensitized patients, suggesting induction of Treg and, consequently, less pro-inflammatory conditions. CCL18 is a chemokine with a dual role in regulating T_H2 and Treg cells. Under non-pathologic conditions, it promotes a tolerogenic differentiation of dendritic cells and a polarization of Treg; however, in a severe inflammatory context, it can promote polarization to T_H2 (469). CCL18 is increased in allergic diseases, such as asthma and atopic dermatitis, and may be a biomarker of atopy due to its correlation with allergic sensitization measured by skin prick test in children from 1 to 16 years-old (421). In addition, CCL18 in healthy individuals induces an adaptative Treg response and induces natural killer cytotoxicity, but not in individuals allergic to aeroallergens (470,471).

Pru p 3 increased *TPSAB1* gene expression in both MCs from sensitized and anaphylactic patients, as well as of the *HDC* gene, suggesting higher levels of tryptase and histamine – two of the primary mediators released by MCs in allergic reactions. However, these findings are insufficient to distinguish between sensitization and anaphylaxis since histamine is a biomarker with a short half-life, making it difficult to detect, and tryptase is not always elevated in cases of anaphylaxis (472–475).

Evaluating the *CMA* gene – which encodes chymase, another MC mediator – we did not observe any differences between groups. Interestingly, we found that *FcεRI*, the high-affinity IgE receptor, was much more expressed in MCs from the anaphylaxis group than from the sensitized group or healthy volunteers after cell activation with Pru p 3. These results suggest that this receptor is upregulated in these patients after allergen contact. As shown in other studies, IgE upregulates FcεRI primarily through stabilization of the receptor at the cell surface in human mast cells and mouse basophils, thereby enhancing immediate type I hypersensitivity responses in allergic individuals

(102,476–478). Indeed, increased *FCER1A* mRNA expression has been reported in eosinophils from asthmatic patients after allergen challenge (479).

Along with MC mediators, we found that MCs from the anaphylaxis group induced higher levels of *PTGER3* – the EP3 receptor of prostaglandin E2 – compared with those from sensitized patients or healthy individuals under basal and stimulated conditions. PGE_2 is a bioactive molecule secreted by MCs that can promote stimulatory or inhibitory effects depending on its interaction with receptors. Some studies found that PGE_2 might diminish MC activation through the EP2 and EP4 receptors, protecting against anaphylactic reactions (480,481). Regarding EP receptors, when MCs have an EP2- or EP4-dominant expression, PGE_2 induces the inhibition of MC responses. Yet, when MCs have an EP3-dominant expression, PGE_2 enhances the FcεRI-induced degranulation (415,482). Thus, we suggest that PGE_2 in MCs from anaphylactic patients could enhance the anaphylactic reaction due to the higher expression of *PTGER3*. A higher expression of EP3 and a lower expression of EP4 have been described in isolated basophils from food-anaphylaxis patients compared with healthy controls (480). In addition, PGE_2 is produced from arachidonic acid by cyclooxygenase enzymes, specifically *COX1* and *COX2*. In our cohort, *COX2* is elevated in MCs from anaphylactic patients after cell activation with Pru p 3, suggesting higher PGE_2 secretion and, consequently, higher MC activation through *PTGER3*.

Moreover, we demonstrated an increase in *IL1B* in MCs from the anaphylaxis group after Pru p 3 stimulation. IL-1β is a key cytokine in inflammatory conditions, and it has also been related to allergic diseases, such as allergic rhinitis, asthma, and atopic dermatitis (430). Signaling via the IL-1 receptor has been proven necessary to sensitize and activate the inflammatory response in atopic dermatitis (429). In addition, some studies in mice revealed that IL-1β enhances T_H2 responses by infiltrating these cells into tissues and increasing the expression of pro-inflammatory cytokines (428,430). Moreover, as we mentioned above, a higher secretion of IL-1β is related to cellular senescence, inducing chronic inflammation in those patients that may increase the possibility of having a severe reaction (395,459). Indeed, it has been described that IL-1β increases COX2 expression via the NF-κB and

MAPK pathways in various cell types, including astrocytes, fibroblasts, epithelial cells, endothelial cells, macrophages, as well as in certain tumor cell lines (483–486). Thus, a higher expression of *IL1B* in MCs from the anaphylaxis group after Pru p 3 stimulation could enhance the *COX2* expression in those cells.

Furthermore, we found that MCs from the anaphylaxis group had higher *MITF* levels compared with sensitized group. MITF has been reported to be critical for IgE-MC-mediated anaphylaxis in a mice model due to its interaction with the *HDC* promoter, enhancing histamine synthesis in an IgE-dependent pathway (172). Thus, as we mentioned before, MCs from anaphylactic patients showed an elevated expression of *HDC*, which could be increased mainly by the higher levels of *MITF*.

There are several mechanisms of MITF regulation. A recent study by our group reported a mutation in *KARS* (encoding LysRS), which increases MITF activity, MC degranulation, and pro-inflammatory responses associated with severe anaphylaxis to hymenopters venoms (371). This mutation results in a constitutive LysRS translocation to the nuclei and higher Ap4A production, which binds to HINT1, releasing MITF and enhancing its transcriptional activity without stimulation. After MC stimulation, degranulation is further enhanced, as well as PGD_2 synthesis and secretion (371). We did not find any significant differences in *KARS* or *HINT1* expression in our cohort. Nonetheless, we found differences in *NUDT2*, which encodes an enzyme that hydrolyses Ap4A. We found higher *NUDT2* expression levels in $_{HV}$MCs-S and even higher levels in $_{HV}$MCs-A. These results suggest that MCs from anaphylactic patients have a lower hydrolysis rate of Ap4A, favoring the activity of MITF, and therefore MC activation.

Moreover, although not significant, we found that in $_{HV}$MCs-A and challenged with Pru p 3 tended to have higher *MITF* expression. This suggests that the signaling pathways induced by allergen exposure in anaphylactic patients differ from those in sensitized individuals, indicating enhances MITF activity in anaphylaxis. In addition, MAPK/ERK signaling enhancement induced by F-box and leucine-rich repeat protein 10 (FBXL10) was significantly

downregulated in $_{BC}$MCs-S compared with $_{BC}$MCs-A. It was described that ERK phosphorylates MITF at Ser73, enhancing its activity in melanoma cells (487). Moreover, elevated PI3K induces MITF activity in melanocytes and B cells (152,153). Interestingly, in our transcriptomic data, we found Phosphatidylinositol-4,5-Bisphosphate 3-Kinase Catalytic Subunit Beta (*PI3KCB*, a PI3K subunit) and Insulin-like growth factor 1 receptor (*IGF1R*, receptor of insulin-like growth factor 1 that can activate PI3K) significantly downregulated in $_{BC}$MCs-S, suggesting lower PI3K activity, and consequently, a lower MITF activity in these cells compared with $_{BC}$MCs-A. However, further studies are needed to identify the mechanism of MITF upregulation in MCs from anaphylactic patients.

In summary, allergen induces a differential signaling in MCs from patients with anaphylaxis than those just sensitized, contributing to the differential severity of the allergic responses, as previously described (17). Thus, since *MITF* expression was increased in MCs from anaphylactic patients, suggesting a pivotal role in exacerbated MC responses, we decided to assess its role in IgE-dependent and -independent reactions.

2. STUDY OF MITF AS A CANDIDATE FOR EXACERBATED MAST CELL RESPONSES

MITF is essential for MC development as it regulates several critical genes in MC differentiation and activation (488). The *MITF* knockout affects the maturation, differentiation, and granularity of MCs, however, the implications of MITF in mature MCs are not yet fully characterized (24,489).

2.1. MITF regulates calcium influx through STIM1

As mentioned above, MCs from anaphylactic patients had higher *MITF* levels, and although not significant, there was an upward trend in *STIM1* expression in these cells. Our previous study found that MCs from the anaphylaxis group had a stronger degranulation response, possibly due to the higher levels of *MITF* and *STIM1* and, consequently, higher calcium influx. In previous studies

by our group, we found a decrease in calcium influx in MITF-knockdown cells (169). However, in this thesis, we found that MITF might regulate the calcium dynamics necessary for MC degranulation by regulating STIM1 expression. We showed that MITF-knockdown reduces the calcium influx after cell activation with either ^{b}IgE + STV or SP and STIM1 expression. At the same time, MITF-overexpression enhances calcium influx after cell activation with DNP-HSA and STIM1 expression. Interestingly *STIM1* transcription is inhibited after MITF inhibition using a reporter gene assay. Similar results were found in melanocytes (490).

STIM1 depletion in MCs exhibited less degranulation and cytokine production after IgE-FcεRI cross-linking. Moreover, it was shown that STIM1 is required for antigen-induced mast-cell-mediated passive cutaneous anaphylaxis reactions *in vivo* in *STIM1*-knockdown mice (110). Correlating with these results, as mentioned above, our transcriptomic data revealed that calcium-related genes – such as *ORAI2* – were downregulated in MCs sensitized with sera from anaphylaxis patients. The *ORAI2* gene encodes the Orai2 protein, which belongs to the Orai family of proteins involved in calcium entry. The intact communication between STIM1 and Orai is critical for calcium dynamics and, consequently, proper cell function (491,492). STIM1 deficiency in knockout mice was shown to impair MC degranulation and anaphylactic responses (110,493).

Thus, the STIM1-MITF axis may play a role in the pathogenesis of anaphylaxis.

2.2. MITF regulates *de novo* mediator's release in the IgE-dependent pathway

It is well established that calcium is required for IgE-mediated release of *de novo* mediators (99). As MITF is involved in calcium dynamics, our study is the first in the literature to show cytokine and chemokine secretion in MCs, within the context of MITF. We reported that MITF inhibition or silencing reduces pro-inflammatory cytokines, such as IL-8 and GM-CSF, but induces a higher CCL2 secretion. This increase correlates with previous reports that

described the CCL2-MITF axis as an essential component in cell senescence, with induction of CCL2 when *MITF* is knocked down in melanoma cells (174–176).

2.3. MITF-knockdown induces less pro-inflammatory conditions

We observed that MITF inhibition or silencing may decrease IL-8 and GM-CSF secretion in MCs-A, reducing exacerbated MC responses. In addition, MITF-knockdown cells may induce a higher secretion of CCL2 in cells sensitized with sera from both LTP patients after stimulation with Pru p 3. Interestingly MCs from sensitized patients with lower *MITF* expression than anaphylactics produce higher levels of CCL2, suggesting an inverse relation between levels of *MITF* and CCL2 synthesis and release, as shown in melanoma cells (174).

MITF expression aligns with a more pro-inflammatory profile. In this study, we reported that MITF inhibition or silencing induces a reduction of pro-inflammatory genes, such as *IL1B, COX2,* and *PTGER3*, via an IgE-dependent pathway, suggesting a less inflammatory response in these cells. On the contrary, MITF inhibition or silencing increases the expression of the *PTGER4* gene, which encodes the EP4 receptor, known to decrease MC activation upon PGE_2 binding (480,481).

All these results suggest that MITF inhibition or silencing might modulate the allergic response by inducing a less pro-inflammatory condition.

2.4. MITF reduces cell viability and MRGPRX2 expression

It is also well-established that MITF is involved in cell survival. Some studies showed that MITF inhibition reduces cell viability through CDK2 and BCL2 in melanoma cells (171,494). Furthermore, our group reported that MITF silencing reduces viability and cell proliferation through the reduction of KIT, CDK2, and BCL2 in GIST (gastrointestinal stromal tumor) cell lines and HMC-

1 cells (168). In line with these findings, we observed that MITF inhibition or silencing reduces cell viability in LAD2 cells.

Moreover, MITF is involved in the FcεRI and MRGPRX2 signaling pathways (169,495), but there is not data regarding its role in their expression. We observed that FcεRI, in terms of protein expression, was similar in MITF knockdown cells and control cells. However, the gene and protein expression of the MRGPRX2 receptor was significantly decreased in MITF-knockdown cells.

Given MITF's involvement in cell survival and MRGPRX2 expression, all experiments were carefully monitored for these variables. Whenever possible, live cells were sorted, and receptor expression was assessed. While MITF silencing or inhibition reduces pro-inflammatory cytokines, we also observed an increase in the secretion of protective cytokines. These data suggest that MITF silencing shifts MCs toward a more protective and anti-inflammatory role.

2.5. MITF regulates *de novo* mediator's release in the MRGPRX2-dependent pathway

These findings concerning in the IgE-dependent pathway were also found when cells were activated with natural ligands such as SP and, more interestingly, with drugs that were proposed to trigger the MRGPRX2 receptor. In recent years, MRGPRX2 has been associated with non-IgE drug-induced allergic reactions (121,298,496). *In vitro* studies have demonstrated that MCs stimulated with different drugs can degranulate through this receptor (5,497,498). Our study showed that MCs could secrete IL-8, GM-CSF, and CCL2 when cells were activated with its natural ligand (SP) or with different drugs, such as vancomycin, cisatracurium, and morphine. However, we observed that activation of mast cells through the MRGPRX2 receptor by SP leads to reduced secretion of IL-8 and GM-CSF but increased secretion of CCL2, compared with MC activation via MRGPRX2 with other drugs. SP is an endogenous neuropeptide secreted by neurons and is involved in many biological processes, such as nociception and inflammation (499,500). Thus,

our results suggest that MC activation with SP is less pro-inflammatory and more related to repairing tissue damage than the MC activation with drugs, which is more pro-inflammatory and might potentially induce drug hypersensitivity reactions. However, under in pathological conditions, such as atopic dermatitis or chronic spontaneous urticaria, SP in the skin and MRGPRX2 in are overexpressed. This keeps MCs hyperactivated, releasing histamine and other mediators that trigger itching and skin inflammation (501). Thus, using a higher concentration of SP could alter the balance of the inflammatory response, leading to MC hyperactivation resulting in the excessive release of pro-inflammatory mediators. This disruption could contribute to increased inflammation and trigger reactions, such as those observed in conditions like urticaria. Interestingly, we saw that MC activation with vancomycin and morphine was more pronounced than with cisatracurium.

Next, we observed that MITF inhibition with ML329 and TT012 reduced the secretion of IL-8 and GM-CSF after cell activation with SP or drugs. However, after five days of inhibition we observed an increase of the CCL2 production after cell activation. In contrast, MITF inhibition with TT012 for 25 hours reduced the CCL2 secretion, showing the complexity of CCL2 regulation by MITF. As mentioned above, MITF-knockdown induces CCL2 secretion in melanoma cells (174); however, TT012 acts by inhibiting MITF dimerization, it does not affect MITF levels within 25 hours of incubation. This could be why 25 hours with TT012 is insufficient to induce higher CCL2 secretion.

Afterward, we validated our results in primary skin MCs. We obtained the same results as with LAD2 cells; however, we observed that skin MCs secreted lower amounts of cytokines and chemokines than LAD2 cells, possibly due to their hyperresponsiveness towards MRGPRX2 ligands. Recent studies have shown that LAD2 cells inefficiently regulate MRGPRX2, contributing to hyperresponsiveness through this receptor. It was proposed that the efficient intrinsic regulatory mechanisms are those that protect human skin cells from excessive activation of MRGPRX2 (502). In addition, studies in human skin MCs have proposed that arrestin may regulate the MRGPRX2

response because the depletion of β-arrestin-1 can increase MRGPRX2 expression on the cell surface (503).

Finally, we tested MITF's involvement in gene regulation via the MRGPRX2-dependent pathway. Thus, after cell activation with SP, we demonstrated that MITF inhibition or silencing induces a reduction of pro-inflammatory genes, such as *IL1B, COX2,* and *PTGER3*, and increases the expression of *PTGER4* gene, skewing the response towards a less inflammatory environment, as we observed in the IgE-dependent pathway.

In summary, MITF may influence the activation profile of MCs also through the MRGPRX2 pathway by regulating the release of both preformed and newly synthesized mediators. To further explore MITF's role in MC signaling pathways, we conducted a transcriptomic analysis using MITF-silenced cells following activation via the FcεRI and MRGPRX2 receptors.

2.6. MITF is involved in MC metabolism

The GSEA of MITF-silenced cells in our study showed downregulation of pathways related to inflammation in infections, cell cycle, and metabolism after cell activation with ^{b}IgE + STV or SP. Moreover, GO cellular component analysis also revealed the downregulation of different mitochondrial compartments in MITF-knockdown cells. Recently, MC activation, through an IgE-dependent pathway, was shown to induce the dephosphorylation of PDH and phosphorylation of MITF, causing the disassociation of PDH-MITF to play their individual roles in mitochondria (178,179). Thus, we decided to delve into MITF's involvement in MC metabolism.

2.6.1. MITF regulates the mitochondrial membrane potential

First, we evaluated mitochondrial function by analyzing the mitochondrial membrane potential under conditions where MITF was silenced or inhibited. Our results found that MITF inhibition or silencing decreases the mitochondrial membrane potential after cell activation with ^{b}IgE + STV or SP. Moreover,

MITF-overexpression in the LysRS transfected-RBL-2H3 model increases the mitochondrial membrane potential after cell activation with DNP-IgE + DNP-HSA, which can be inhibited by the treatment with MITF inhibitors (TT012 or ML329). Additionally, we found that MCs from anaphylactic patients – who had elevated *MITF* levels – also had a higher mitochondrial membrane potential after activation with Pru p 3 than MCs from healthy individuals, correlating with the higher degranulation seen in MCs from anaphylactic patients. The mitochondrial membrane potential generated by the electron transport chain modulates MC degranulation, as demonstrated in one study where uncoupling OXPHOS reduces degranulation, as mitochondrial ATP is the primary energy source for this process (504). Treating these cells with MITF inhibitor could significantly diminish this mitochondrial membrane potential in these patients, suggesting that MITF is involved in mitochondrial function.

2.6.2. MITF regulates mitochondrial protein import and function

Furthermore, analyzing the transcriptomic data, we observed that some genes related to mitochondrial protein import (TOM family proteins) and function (*COX-IV*) were downregulated in MITF-silenced cells. We observed that when *MITF* expression is down, *TOMM20* and *COX-IV* expression decreases at the mRNA and protein level. MITF-overexpression was reported to enhance mitochondrial function by increasing the expression of genes related to mitochondrial biogenesis, antioxidant responses, and ATP production in retinal pigment epithelial cells, further underscoring its importance in MCs (180). TOM20 is a translocase of the outer mitochondrial membrane, regulating the main entry point of proteins into the mitochondria (439,505). *COX-IV* is a nuclear gene that encodes for the COX-IV subunit of the OXPHOS complex IV (CIV), the last enzyme in the mitochondrial electron transfer chain, representing the regulatory center of oxidative phosphorylation (506). Thus, the decrease in TOM20 and COX-IV in the MITF-knockdown cells suggests lower mitochondrial protein import and function. Moreover, COX-IV needs to be translocated into the mitochondria, and this protein import is reported to be regulated by TOM proteins (507). Thus, apart from the decrease in COX-IV expression, there could also be a decrease in the amount

of this protein in the mitochondria since MITF downregulates genes of the TOM family.

As we found elevated MITF levels in MCs from anaphylactic patients, we evaluated *TOMM20* and *COX-IV* in our study cohort. Interestingly, we observed that *TOMM20* and *COX-IV* were elevated in MCs from anaphylactic patients compared with MCs from sensitized patients and healthy volunteers, suggesting a higher mitochondrial activity in these cells.

Furthermore, MITF has been described to regulate the expression of *PPARGC1A*, which encodes PGC1α, the primary regulator of mitochondrial biogenesis. PGC1α drives the expression of nuclear-encoded mitochondrial proteins. Many of these proteins must be imported via TOM20, linking *TOMM20* to mitochondrial biogenesis, although this connection requires further investigation. It has been shown that PGC1α promotes oxidative phosphorylation metabolism (508). MITF enhances PGC1α expression, increasing mitochondrial metabolism and survival under oxidative stress conditions. On the contrary, MITF-knockdown in melanoma cells reduces negative PGC1α expression, driving cells to a more glycolytic metabolism and higher sensitivity to oxidative stress conditions (509,510). In this study, we analyzed *PPARGC1A* expression, but it was too low to draw any conclusions.

2.6.3. MITF regulates mitochondrial fission in MCs

Knowing that MITF is involved in mitochondrial protein import and function, we analyzed its role in mitochondrial dynamics. Upon MC activation via IgE or non-IgE stimuli, mitochondria undergo fission and translocate from the perinuclear region to the cell surface (504,511,512). Interestingly, while some mitochondria remain in the perinuclear area to sustain general cellular functions, others translocate on demand (513). This appears to be reversible; mitochondria return to the perinuclear region 24 hours after non-IgE stimulation (504). This mitochondrial translocation is tightly regulated by post-translational modifications of Drp1. Dephosphorylation at Ser-637 by calcium-activated calcineurin facilitates Drp1 recruitment from the cytoplasm to the mitochondrial outer membrane, while phosphorylation at Ser-616 regulates

Drp1 activity, driving mitochondrial fission (513). Our results showed decreased levels of phosphor-DRP1$^{Ser-616}$ in MITF-silenced cells compared with control cells after activation with SP or ^{b}IgE+STV. DRP1 phosphorylation at Ser-616 is reported to be mediated by the MAPK-ERK1/2 signaling pathway, underscoring its role in mitochondrial dynamics and energy metabolism (210). Our study found decreased phospho-ERK1/2 levels in MITF-knockdown cells compared with control cells after activation with either SP or ^{b}IgE+STV. Thus, this decrease in phospho-ERK1/2 might induce lower phosphorylation of Ser-616 DRP1 in these cells. On the other hand, as previously mentioned, there was reduced calcium influx in MITF-knockdown cells compared with control cells, which may promote mitochondrial fusion. The decreased calcium influx in MITF-knockdown cells may reduce the dephosphorylation of Ser-637 DRP1, leading to mitochondrial fusion (210). Moreover, we validated these results with TEM, finding that MITF-silenced LAD2 cells with lower phospho-DRP1$^{Ser-616}$, had more fused mitochondria than control cells when activated by either SP or ^{b}IgE+STV.

2.6.4. MITF regulates mitochondrial metabolism

Some metabolic studies reported that mitochondrial morphology also affects the metabolic pathways. Notably, inhibition of DRP1 and mitochondrial fission disrupts ATP production from OXPHOS, potentially contributing to increased cellular senescence (504). Interestingly, in our study, MITF-silenced or inhibited cells, with less phopho-DRP1 and less mitochondrial fission, had a lower OCR than control cells. This could increase cellular senescence through the secretion of CCL2, which is elevated in these cells, as mentioned above. However, previously, we showed that MCs from anaphylactic patients – who presented elevated *MITF* levels – also induce cell senescence. It has been reported in melanoma cells that MITF plays a critical role in maintaining the balance between proliferation and cellular senescence. When MITF levels are too low, cells may enter a senescent state due to a lack of signals necessary for proliferation. On the other hand, when MITF levels are excessively high, senescence may also be triggered, possibly due to the disruption of normal cellular regulatory pathways in response to cellular damage, stress, or an

unfavorable environment (514–516). Nevertheless, further studies are needed to understand the connection between MITF, anaphylaxis, and senescence.

Furthermore, the lower OCR in MITF-silenced cells could also be due to the downregulation of TOM20 and COX-IV in those cells, as described in astrocytes and fibroblasts (517–519).

Recently, Nishikiori *et al.* demonstrated that MITF is associated with a higher glycolytic activity through the enhanced expression of HIF-1α in a melanoma cell line (494). This study used ECAR measurement to evaluate glycolytic activity through the Seahorse's MitoStress Test. We also saw greater glycolytic activity when evaluating ECAR rate in the LysRS-P542R cells – which overexpress MITF – after adding oligomycin, an oxidative phosphorylation inhibitor. These results suggest that LysRS-P54R cells rely more on glycolysis to compensate for the loss of mitochondrial ATP production than LysRS-WT or control cells. ECAR is an indirect measure of glycolysis, as it reflects lactic acid production. However, it is not exact because ECAR can also be influenced by other metabolic processes that produce acid, such as proton pump activity, which may not be directly related to glycolysis. Thus, it would be interesting to evaluate the glycolytic activity with Seahorse's glycolytic test, which is a more accurate technique than ECAR measurement. Indeed, we showed that when MITF is overexpressed through the LysRS-P542R model, there is higher mitochondrial respiration than in LysRS-WT or control cells.

Furthermore, we showed that MITF-knockdown cells produced more ROS than control cells. MITF is known to play a dual role in ROS production depending on the cellular context and the specific signaling pathways activated (181). In melanoma cells, MITF can act as an antioxidant (180). However, ROS production can be enhanced in activated MCs due to MITF's upregulation of genes involved in ROS generation. The generation of ROS can influence MC activation and immune responses (520). Some studies showed that MC exposure to ROS induces histamine and serotonin release, and allergen-mediated ROS production promotes T_H2 cytokine secretion,

driving T_H2 immune responses. Conversely, reduced ROS levels or antioxidant treatments induce T_H17 differentiation (521).

Stimulation of FcεRI triggers rapid intracellular ROS generation, which influences calcium regulation (504). Mitochondrial dysfunction, characterized by excessive ROS production, has been linked to premature cell senescence and impaired mitophagy. These dysfunctions may contribute to allergic diseases and asthma. Chronic stress on mucosal epithelial cells can lead to epigenetic changes that impair mitochondrial function, elevate ROS production, and reduce ATP levels, perpetuating allergic responses (513).

2.7. LTP patients present differences in MC metabolism

The metabolic flexibility of MCs is essential for their activation. Recently, it was described that some mitochondrial DNA (mtDNA) or nuclear variants in sensitized patients (to egg white, milk, peanut, soybean, wheat, or aeroallergens) can impair mitochondrial function (206), suggesting an essential link between mitochondria and allergies. During anaphylaxis, mitochondria enhance ATP production to release MC mediators, contributing to the clinical signs. However, mitochondrial function may become impaired due to increased oxidative stress. In a peanut allergy mouse model, elevated oxidative stress during anaphylaxis was shown to reduce OXPHOS efficiency declined through complexes I and III (504).

2.7.1. Sera from patients induce more mitochondrial activity

In this study, we showed that LAD2 cells sensitized with sera from patients (sensitized or anaphylactic) and stimulated with Pru p 3 had an increased OCR, and those sensitized with sera from anaphylactic patients also had an elevated ECAR. These results suggest that both patient groups had more mitochondrial activity than healthy volunteers. A previous work performing a metabolomic analysis comparing IgE- and non-IgE-mediated degranulation in MCs, revealed higher concentrations of glycolytic and TCA cycle metabolites (excluding citrate and succinate) in IgE-mediated degranulation (183). These

findings align with other studies reporting a heightened catabolic activity in allergen-induced degranulation. Also, our results suggest that an anaphylactic response induces a higher glycolysis rate. It was previously reported that allergen-induced degranulation would lead to increased oxygen consumption (in rat peritoneal MCs) and a significant acute increase in ECAR as measured using Seahorse (in mice bone marrow-derived MCs) (183).

Furthermore, we found greater ROS production in LAD2-A after Pru p 3 stimulation than in LAD2-S.

In summary, LAD2-S or LAD2-A showed increased mitochondrial activity. Indeed, LAD2-A presented a higher glycolysis rate and elevated ROS production upon Pru p 3 stimulation.

2.7.2. MCs from patients induce distinct metabolic pathways

Noting that sera from LTP patients influenced MC metabolic activity, we next assessed mitochondrial respiration in MCs derived from patients.

In this study, we presented preliminary data, where MCs from anaphylactic and sensitized patients seem to have greater oxygen consumption than those from healthy donors. However, with the addition of FCCP – to induce maximal mitochondrial respiration – MCs from the anaphylactic patient did not have a higher response than those from the healthy volunteer. In contrast, MCs from the sensitized patient had a much higher response than MCs from either the anaphylactic patient or healthy donor. These results suggest that MCs from the anaphylactic patient may collapse with the addition of FCCP and a higher oxidative stress environment, causing impairment in OXPHOS. Interestingly, MCs from the anaphylactic patient had a higher ECAR than others when Pru p 3 was added, suggesting elevated glycolytic metabolism in these cells, however, further investigation is required to draw definitive conclusions.

Moreover, we used $_{HV}$MCs-A to study glycolysis more accurately. Here, we blocked glycolysis using a glucose analog (2-DG) and induced glycolysis, inhibiting oxidative phosphorylation with rotenone and antimycin. This test

showed that $_{HV}$MCs-A induced rapid glycolysis after Pru p 3 injection (decreasing over time). Indeed, both by blocking or inducing glycolysis, $_{HV}$MCs-A showed increased glycolysis usage. Short-term MC activation via FcεRI has been reported to primarily increase glycolysis, whereas prolonged activation shifts the metabolic profile toward OXPHOS (521). One study on macrophages (522), found that pro-inflammatory macrophages had higher ATP production from glycolysis associated with increased pro-inflammatory cytokine secretion. In contrast, a higher level of OXPHOS was associated with increased anti-inflammatory cytokines.

In summary, MCs from anaphylactic patients show a high glycolytic capacity, producing more pro-inflammatory cytokines than those from sensitized patients. On the contrary, OXPHOS metabolism is enhanced in MCs from the sensitized group, related with the production of anti-inflammatory cytokines.

2.7.3. MITF involvement in anaphylactic MC metabolism

Our study found increased levels of *MITF* in MCs from anaphylactic patients compared with those from sensitized patients, particularly enhancing the glycolytic pathway. Indeed, in LAD2 cells sensitized with sera from the anaphylaxis group, we observed an increase in ROS production compared with LAD2 cells sensitized with sera from sensitized patients, generating a higher oxidative stress environment. Moreover, we observed an increase in the senescence pathway, enhancing pro-inflammatory cytokine secretion and an increase in *ORAI2* gene expression in $_{BC}$MCs-A, enhancing calcium influx in these cells and, consequently, degranulation.

It has been shown that MITF can act as an anti-oxidant in melanoma cells and MITF inhibition induces ROS production (180), however, as we demonstrated, increased MITF expression in MCs can enhance ROS production (181). In addition, it has been reported that MITF may induce HIF-1α (523), a hypoxia-induced factor that can accelerate glycolysis (192) and senescence (524) in macrophages and fibroblasts. Moreover, Orai2 increases in hypoxic environments through HIF-1α (491), increasing the calcium influx. To date, no scientific articles have explored the correlation between hypoxia and

anaphylaxis; nevertheless, hypoxia is well-established in asthma, as airway constriction and inflammation during asthma attacks reduce oxygen levels in the blood (525).

2.7.4. MITF as a therapeutical target in LTP patients

Our findings suggest that MITF could regulate exacerbated MC responses through both the IgE-dependent and MRGPRX2-dependent pathways by regulating MC degranulation, mediator secretion, and mitochondrial function. This reveals a novel aspect of the involvement of MITF in MC biology, highlighting it as a potential therapeutic target in inflammatory and allergic diseases (Figure 83).

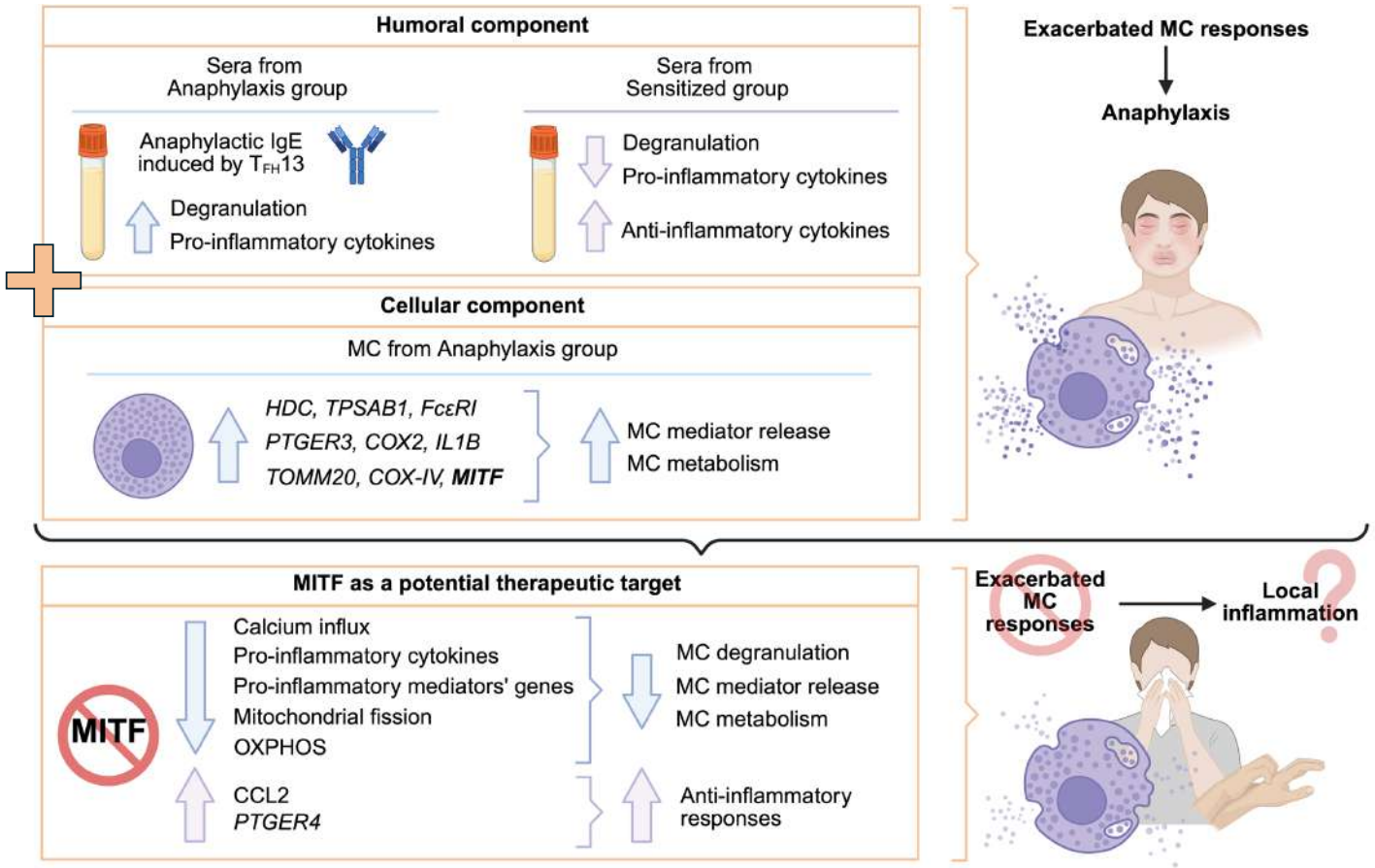

Figure 83. MITF as a potential therapeutic target to reduce exacerbated MC responses. MITF-knockdown changes MC activation patterns at different levels, inducing a less pro-inflammatory response. Thus, we propose that MITF can lessen the severity of anaphylactic reactions; further studies are needed to delimit its actions.

3. STUDY LIMITATIONS

One significant limitation of this study is the number of patients allergic to LTPs. The Hospital Clínic of Barcelona treats many allergic patients. Yet, it is difficult to find individuals with LTP allergy willing to participate in the study by donating 100 ml of blood. Even so, the results are consistent and statistically significant, allowing us to get interesting conclusions, although larger studies may be needed to confirm our observations.

Another limitation is that the MC's phenotype in the tissue may differ from that observed in the $CD34^+$-derived MCs (27). Yet, we observed a different pattern in $CD34^+$-derived sensitized and anaphylactic cells, which is remarkable.

In vitro MC differentiation approaches are laborious and produce few MCs for examination, nonetheless, they allow for a more in-depth of study of IgE-mediated pathways. However, the few MCs obtained from blood make it difficult to conduct large-scale studies. It would be interesting to perform a transcriptomic study comparing MCs from sensitized and anaphylactic patients to analyze the differences between these patients and thus establish new therapeutic targets.

Finally, it would also be desirable to obtain skin MCs from patients with drug hypersensitivity reactions to delve into the MRGPRX2-mediated pathways.

CONCLUSIONS

1. The mast cell activation test (MAT) may discriminate patients at risk of developing anaphylaxis from those that are merely sensitized, helping in the risk stratification before an oral food challenge.
2. Allergen induces a stronger degranulation and PGD_2, IL-8, and GM-CSF secretion in anaphylactic MCs, and a protective response in sensitized MCs, with a higher production of CCL2 and TGF-β.
3. $T_{FH}13$ cells may be a risk biomarker of anaphylaxis.
4. *MITF* is elevated in mast cells from anaphylactic patients at baseline and increases after allergen activation, and considering that is a key regulator of mast cell differentiation and activation, these results suggest a predisposition to suffer severe allergic reactions.
5. MITF regulates calcium influx in MC through STIM1, in both FcεRI and MRGPRX2 activation models.
6. MITF regulates the expression of pro-inflammatory genes such as IL1B, COX2, and PTGER3, and the secretion of pro-inflammatory cytokines, such as IL-8 and GM-CSF in both FcεRI and MRGPRX2 activation models.
7. MITF regulates mitochondria function through TOM20 and COX-IV, mitochondria fission through DRP-1 phosphorylation, mitochondrial membrane potential and respiration.
8. Mast cells from anaphylactic patients exhibit a higher mitochondrial membrane potential and *TOMM20* and *COX-IV* expression, probably due an increased *MITF* expression.
9. Allergen stimulation induces a higher mitochondrial respiration and enhances the glycolytic pathway in anaphylaxis MCs compared with sensitized MCs.
10. MITF may regulate the severity of allergic response in the IgE-dependent and MRGPRX2-dependent pathways by regulating MC mediators' release (preformed and *de novo*) and mitochondrial function.

General conclusion:

Allergic response severity is influenced by both humoral and cellular components. Beyond antibody-driven mechanisms, cellular factors such as MITF expression may amplify mast cell activation and exacerbate allergic reactions. Targeting MITF could represent a therapeutic strategy to reduce mast cell hyperactivation and mitigate severe allergic responses.

ANNEX I: Clinical data of patients

Annex Table 1. Subjects selected for preparing "pooled sera".

Pool	Subject ID	Total IgE (KUA/L)	Pru p 3 IgE (KUA/L)	Ratio tIgE:sIgE	Pru p 3 IgG4 (KUA/L)	Ratio sIgG4/sIgE	Symptomatology
Anaphylaxis	1	48.2	11.3	4.26	ND	ND	Anaphylaxis (urticaria, bronchoespasm) with pomegranate.
	2	117	10.7	10.93	ND	ND	Anaphylaxis (urticaria, bronchoespasm, hipotension, loss of conciousness) with tomato and cofactor (NSAID).
	3	136	61	2.22	ND	ND	Anaphylaxis (urticaria, vomiting, bronchospasm) with apple and cofactor (physical exercise). OAS with peanut. Contact urticaria with peach.
	4	177	9.46	18.71	ND	ND	Anaphylaxis (urticaria, hipotension, bronchospasm) with peach, hazelnut and peanut. Contact urticaria with peach.
	5	139	7.96	17.46	ND	ND	Anaphylaxis (urticaria, diarrhea, bronchospasm) with peanut. Urticaria with corn, peanut and hazelnut. OAS with peach, tomato and lettuce.
	6	96.6	5.8	16.65	ND	ND	Anaphylaxis (urticaria, bronchospasm) with walnut and cofactor (alcohol). Contact urticaria with peach. OAS with walnut and hazelnut.
	7	132	16.5	8.00	ND	ND	OAS with apple, hazelnut. Urticaria and angioedema with tomato. Anaphylaxis (angioedema, diarrhea, bronchospasm, hipotensión) with walnut and cofactor (physical exercise).
	8	159	17.7	8.98	ND	ND	Gastrointestinal symptoms with lettuce, tomato, green beans. OAS with hazelnut, peanut and walnut. Anaphylaxis (urticaria, angiedema, hipotension) with walnut with cofactor (NSAID).
	Pool	ND	19.80	ND	2.31	8.59	

Pool	Subject ID	Total IgE (KUA/L)	Pru p 3 IgE (KUA/L)	Ratio tIgE:sIgE	Pru p 3 IgG4 (KUA/L)	Ratio sIgG4/sIgE	Symptomatology
Sensitized	9	229	0.88	260.22	ND	ND	Asymptomatic sensitization
	10	160	1.25	128.00	ND	ND	Asymptomatic sensitization
	11	228	1.64	139.02	ND	ND	Asymptomatic sensitization
	12	316	1.22	259.01	ND	ND	Asymptomatic sensitization
	Pool	ND	0.98	ND	0.46	2.13	
Healthy	13	ND	<0.10	ND	ND	ND	Healthy individuals
	14	ND	<0.10	ND	ND	ND	Healthy individuals
	15	ND	<0.10	ND	ND	ND	Healthy individuals
	16	ND	<0.10	ND	ND	ND	Healthy individuals
	17	ND	<0.10	ND	ND	ND	Healthy individuals
	Pool	ND	<0.10	ND	0.09	0.56	

Characteristics of subjects selected for pooled sera. All healthy volunteers had Pru p 3 sIgE <0.10 KUA/L. ND= Not determined. OAS= Oral Allergy Syndrome. NSAID= non-steroidal anti-inflammatory drugs.

Annex Table 2. Subjects selected for CD34+-derived MCs and $T_{FH}13$ detection.

Subject ID	Group	Gender	Age	Pru p 3 IgE (KUA/L)	Tryptase (µg/L)	Symptomatology
1	Anaphylaxis	Male	30	24.7	2.2	OAS with sunflower seed, pistachio, almond, peanut, walnut, hazelnut, lettuce, lentil, apple, grapefruit, avocado, banana, orange. Anaphylaxis (urticaria, hipotension, bronchoespasm) without cofactor with nuts, sunflower seeds, peach juice, vegetable mix.
2	Anaphylaxis	Male	50	1.05	2.3	Urticaria and angioedema with seeds. Anaphylaxis (urticaria, angioedema and bronchoespasm) with apple. Contact urticaria with peach. OAS with several nuts (hazelnut, walnut, peanut).
3	Anaphylaxis	Male	55	7.96	4.5	Anaphylaxis (urticaria, abdominal pain, vomitin, bronchospasm) without cofactor with peach, hazelnut, and walnut.
4	Anaphylaxis	Female	42	8.76	ND	Urticaria with ingestion of mixed vegetables, apple. Gastrointestinal symptoms with green beans. Anaphylaxis (urticaria, angioedema, bronchospasm) with almonds and cofactor (NSAID).
5	Anaphylaxis	Female	32	13.00	2.4	Anaphylaxis (urticaria, bronchospasm, hipotension) without cofactor with peach and walnut.
6	Anaphylaxis	Male	56	16.50	5.4	OAS with ingestion of peanut, corn, walnut. Gastrointestinal symptoms with mixed vegetables and peach. Urticaria and angioedema with peach and nuts. Anaphylactic shock (urticaria, lingual angioedema, hipotension, loss of conciousness) with nectarine with cofactor (physical exercise).

Subject ID	Group	Gender	Age	Pru p 3 IgE (KUA/L)	Tryptase (µg/L)	Symptomatology
7	Sensitized	Male	63	0.43	5.7	Asymptomatic sensitization
8	Sensitized	Female	46	41.20	3.9	Asymptomatic sensitization
9	Sensitized	Female	37	28.70	6.3	Asymptomatic sensitization
10	Sensitized	Male	48	0.66	5.2	Asymptomatic sensitization
11	Sensitized	Female	74	1.25	4.4	Asymptomatic sensitization
12	Healthy	Male	30	0.03	ND	Healthy indiviuals
13	Healthy	Female	22	0.03	ND	Healthy indiviuals
14	Healthy	Male	28	0.02	ND	Healthy indiviuals
15	Healthy	Male	35	0.03	ND	Healthy indiviuals

Characteristics of subjects selected for $CD34^{+}$-derived MCs and $T_{FH}13$ detection. ND= Not determined. OAS= Oral Allergy Syndrome. NSAID= non-steroidal anti-inflammatory drugs.

Annex Table 3. Subjects selected for CD34^{+}-derived MCs to perform qPCR array.

Subject ID	Group	Gender	Age	Pru p 3 IgE (KUA/L)	Tryptase (µg/L)	Symptomatology
1	Anaphylaxis	Male	30	24.7	2.2	OAS with ingestion of sunflower seed, pistachio, almond, peanut, walnut, hazelnut, lettuce, lentil, apple, grapefruit, avocado, banana, orange. Anaphylaxis without cofactor with ingestion of nuts, sunflower seeds, peach juice, vegetable mix.
2	Anaphylaxis	Male	50	1.05	2.3	Urticaria and angioedema with seeds.
3	Anaphylaxis	Male	55	7.96	4.5	Anaphylaxis without cofactor with peach.
4	Anaphylaxis	Female	42	8.76	ND	Urticaria with ingestion of mixed vegetables, apple. Gastrointestinal symptoms with green beans. Anaphylaxis with almonds with cofactor (NSAID).
5	Anaphylaxis	Female	32	13.00	2.4	Anaphylaxis without cofactor with peach.
6	Anaphylaxis	Male	56	16.50	5.4	OAS with ingestion of peanut, corn, walnut. Gastrointestinal symptoms with mixed vegetables and peach. Urticaria and angioedema with peach and nuts. Anaphylactic shock with nectarine with cofactor (physical exercise).
7	Anaphylaxis	Male	56	7.96	ND	Anaphylaxis with peanut. Urticaria with corn, peanut and hazelnut. OAS with peach, tomato and lettuce.
8	Anaphylaxis	Male	46	1.79	ND	Urticaria with orange, melon and apple. OAS with corn ingestion. Anaphylaxis with apple and cofactor.

Subject ID	Group	Gender	Age	Pru p 3 IgE (KUA/L)	Tryptase (µg/L)	Symptomatology
9	Sensitized	Male	63	0.43	5.7	Asymptomatic sensitized.
10	Sensitized	Female	46	41.20	3.9	Asymptomatic sensitized.
11	Sensitized	Female	37	28.70	6.3	Asymptomatic sensitized.
12	Sensitized	Male	48	0.66	5.2	Asymptomatic sensitized.
13	Sensitized	Female	74	1.25	4.4	Asymptomatic sensitized.
14	Sensitized	Female	22	0.11	ND	Asymptomatic sensitized.
15	Healthy	Male	30	<0.10	ND	Asymptomatic.
16	Healthy	Female	22	<0.10	ND	Asymptomatic.
17	Healthy	Male	28	<0.10	ND	Asymptomatic.
18	Healthy	Female	22	<0.10	ND	Asymptomatic.
19	Healthy	Male	26	<0.10	ND	Asymptomatic.
20	Healthy	Male	26	<0.10	ND	Asymptomatic.
21	Healthy	Female	23	<0.10	ND	Asymptomatic.
22	Healthy	Male	35	<0.10	ND	Asymptomatic.

Characteristics of subjects selected for $CD34^{+}$-derived MCs to check some genes. ND= Not determined. OAS= Oral Allergy Syndrome. NSAID= non-steroidal anti-inflammatory drugs.

Annex Table 4. Subjects selected for CD34^{+}-derived MCs to do mitochondrial analysis.

Subject ID	Group	Gender	Age	Pru p 3 IgE (KU$_{A}$/L)	Symptomatology	MITF levels
1	Anaphylaxis	Female	25	3.12	OAS, urticaria and angioedema with peanut and almond.	3.14
2	Sensitized	Female	26	0.11	Asymptomatic sensitized.	2.40
3	Healthy	Male	26	ND	Asymptomatic.	1.10

Characteristics of subjects selected for CD34^{+}-derived MCs to do Seahorse. ND= Not determined. OAS= Oral Allergy Syndrome.

ANNEX II: RNA-sequencing results

In this Thesis we performed two RNA-sequencing:

- To investigate whether the humoral component of LTP patients was able to activate different signaling pathways that would allow us to distinguish between anaphylactic and sensitized patients. Thus, we used mast cells derived from buffy coat preparations or LAD2 cells, sensitized with pooled sera from LTP patients (both sensitized and anaphylaxis) and stimulated with the allergen (Pru p 3) for 24 hours. Those cells that were sensitized with pooled sera from sensitized group were compared with cells sensitized with pooled sera from anaphylaxis group.
- To study signaling pathways activated in the presence or absence of MITF. Thus, we used LAD2 cells with MITF-silenced by the MITF shRNA-2 sequence. Those cells were stimulated with streptavidin or substance P for 24 hours and compared with control samples (LAD2 cells treated with shRNA-NT).

As we mentioned in the methodology section the bioinformatics analysis was performed by Dreamgenics S.L. (Asturias, Spain). In this annex, we attach the data obtained on differential gene expression (p-value less than 0.05 and a log2FoldChange greater than 1 or less than -1), and on pathways enriched using GSEA algorithm.

Annex Table 5. GSEA pathways in MCs sensitized with pooled sera from sensitized patients versus MCs sensitized with pooled sera from anaphylactic patients. MCs from buffy coat preparations were sensitized with pooled sera from LTP patients and stimulated with Pru p 3 for 24 hours.

Description	setSize	enrichmentScore	padj	qvalue	core_enrichment
Senescence associated secretory phenotype SASP	103	-0,626	0,000	0,000	H2AC6/UBC/H2BC7/CDK4/H3-3B/H2AZ2/H2BC8/H4C11/H2AC20/UBB/CDKN2A/H4C5/H2AC7/JUN/H2BC26/UBE2S/H4C2/H4C16/H2BC5/H3C4/CDKN2C/H2AZ1/FZR1/H4C9/H2AC8/H2BC4/H4C12/H3C13/H2BC12/H4C6/H2BC21/H4C8/H2BC6/CDK2/H2AC18/CDKN2D/H2BC14/H4C13/H2BC10/H4C3/H3C10/H3C1/H2BC15/H2AX/H3C12/H4C4/H2BC13/H2BC9/H2BC11/H2BC3/CCNA2/H4C1/H2AC14/H4C14/H2AC4/H2BC17/H3C3/H3C8/UBE2C/H3C7/H3C2/H3C15
Retinoblastoma gene in cancer	86	-0,690	0,000	0,000	SAP30/RFC4/CDK4/HMGB1/CCND3/RRM1/PRMT2/POLA1/PRIM1/CCNE2/MCM3/BARD1/SUV39H1/H2AZ1/DCK/RPA3/WEE1/CDC7/CDK2/HMGB2/POLE2/SMC2/PCNA/RFC5/CDC25B/RFC3/MCM7/CCNB1/TTK/CDT1/CDC25A/STMN1/CCNB2/CCNA2/TYMS/ORC1/ANLN/DHFR/PLK4/CHEK1/TOP2A/CDK1/KIF4A/RRM2/E2F1/CDC45/E2F2
DNA replication	42	-0,738	0,000	9,72E+09	MCM4/POLD3/GMNN/UBC/RFC4/POLA1/RFC2/PRIM1/ORC6/MCM3/RPA4/DBF4/RPA3/CDC7/CDK2/POLE2/PCNA/RFC5/MCM2/RFC3/MCM7/POLD1/CDT1/MCM10/ORC1/CDC6/MCM5/CDC45
Effect of progerin on genes involved in progeria	35	-0,755	0,000	0,000	SUV39H1/H3C4/H3C13/MBD3/H3C10/H3C1/H3C12/H3C3/H3C8/H3C7/E2F1/H3C2/H3C15
NF1 copy number variation syndrome	98	-0,575	0,000	0,000	TEFM/H4C11/RFC2/LIMK1/CCNE2/H4C5/H4C2/H4C16/SYN1/H3C4/RAD9A/H4C9/H4C12/H3C13/H4C6/H4C8/TUBB/RAD51/H4C13/PCNA/RFC5/ATAD5/H4C3/RFC3/H3C10/H3C1/H3C12/H4C4/CCNA2/H4C1/H4C14/H3C3/H3C8/H3C7/H3C2/H3C15
Cell cycle	117	-0,535	0,000	0,000	BUB3/CCND2/CDKN2A/CCNE2/YWHAQ/ORC6/MAD1L1/MCM3/RBL1/CDKN2C/FZR1/GADD45G/DBF4/MAD2L2/WEE1/CDC7/CDK2/CDKN2D/PCNA/CDC25B/MCM2/BUB1/PLK1/MCM7/PTTG1/ESPL1/CCNB1/TTK/CDC25A/PKMYT1/CCNB2/CDC25C/CCNA2/CDC20/ORC1/CDC6/MCM5/CHEK1/CDK1/E2F1/CDC45/E2F2

Description	setSize	enrichmentScore	padj	qvalue	core_enrichment
DNA IR damage and cellular response via ATR	81	-0,592	0,000	0,000	BARD1/BRCA1/RAD9A/BRCA2/RECQL4/RAD51/CDK2/PCNA/MCM2/PLK1/BRIP1/FANCA/H2AX/CDC25C/FANCI/CLSPN/CHEK1/CDK1/FEN1/FOXM1/E2F1/CDC45/EXO1
Nucleotide excision repair in xeroderma pigmentosum	75	-0,601	0,000	0,000	POLD2/DDB2/ERCC3/POLE4/ERCC1/RPA1/XRCC1/GTF2H3/POLD3/CHD1L/HMGN1/H2AC6/POLE3/GTF2H4/RFC4/H3-3B/XPC/H4C11/RFC2/H4C5/H4C2/H4C16/BRCA1/H4C9/LIG1/RPA3/H4C12/H4C6/H4C8/POLE2/RAD18/H4C13/PCNA/RFC5/H4C3/RFC3/POLD1/H4C4/H4C1/H4C14
Gastric cancer network 1	25	-0,778	0,001	0,001	H4C16/ECT2/KIF20B/LIN9/CENPF/AURKA/TPX2/TOP2A/KIF15/UBE2C/MYBL2/E2F7
DNA repair pathways full network	120	-0,499	0,001	0,001	NBN/MSH6/OGG1/UNG/GTF2H5/MRE11/TERF2/RPA2/FANCF/POLD2/DDB2/ERCC3/PARP2/POLE4/ERCC1/RPA1/XRCC1/USP1/GTF2H3/POLD3/POLE3/NEIL2/GTF2H4/RFC4/HMGB1/XPC/FANCD2/RFC2/RAD51C/MPG/FANCM/FANCE/BRCA1/NEIL3/FAAP100/BRCA2/LIG1/RPA3/RAD51/POLE2/PCNA/RFC5/BRIP1/RFC3/FANCA/FANCB/POLD1/H2AX/FANCI/CHEK1/FEN1/EXO1
Enterocyte cholesterol metabolism	29	-0,736	0,003	0,003	DHCR24/HSD17B7/FDFT1/IDI1/TM7SF2/NSDHL/LSS/HMGCR/DGAT1/LDLR/EBP/HMGCS1/CD36/CYP51A1/DHCR7/SQLE/MVD/FDPS/ACAT2/ABCA1/MTTP
Histone modifications	63	-0,592	0,004	0,004	H4C2/H4C16/SUV39H1/H3C4/KMT5C/H4C9/KMT5A/H4C12/H3C13/H4C6/H4C8/H4C13/H4C3/H3C10/H3C1/H3C12/H4C4/H4C1/H3C8/H3C7/H3C15
G1 to S cell cycle control	63	-0,586	0,005	0,005	CCND2/PRIM1/CDKN2A/CCNE2/ORC6/MCM3/CDKN2C/RPA3/WEE1/CDK2/POLE2/CDKN2D/PCNA/MCM2/MCM7/CCNB1/CDC25A/ORC1/MCM5/CDK1/E2F1/CDC45/E2F2
Regulation of sister chromatid separation at the metaphase anaphase transition	14	-0,825	0,007	0,007	BUB3/MAD1L1/BUB1/CENPE/PTTG1/ESPL1/MAD2L1/CDC20/BUB1B
Chronic hyperglycemia impairment of neuron function	22	-0,758	0,009	0,009	AGER/MMP23B/MMP2/NOS2/SCN8A/MMP24/MMP14

Description	setSize	enrichmentScore	padj	qvalue	core_enrichment
Cohesin complex Cornelia de Lange syndrome	33	-0,679	0,017	0,017	REC8/SGO2/PLK1/PTTG1/ESPL1/CDK1/SGO1/AURKB/ESCO2/CDCA5
FBXL10 enhancement of MAP ERK signaling in diffuse large B cell lymphoma	28	-0,694	0,017	0,017	EZH2/PCGF1/H3-3B/H2AZ2/H3C4/H2AZ1/H3C13/H3C10/H3C1/H2AX/H3C12/H3C8/H3C7/H3C15
Primary ovarian insufficiency	103	-0,448	0,040	0,038	RFWD3/MGME1/AMHR2/FANCM/CLPP/AMH/BLM/SOX8/BRCA2/RECQL4/SGO2/RAD51/HROB/MCM8/DMC1/XRCC2/KASH5/FANCA/CENPE/BMPR1B/FOXL2/FANCI/WDR62/HMMR/MND1/PSMC3IP/POF1B/CAV1/EXO1
DNA mismatch repair	23	-0,699	0,041	0,039	RPA2/POLD2/POLE4/RPA1/POLD3/POLE3/RFC4/RFC2/LIG1/RPA3/POLE2/PCNA/RFC5/RFC3/POLD1/EXO1

Annex Table 6. Differential gene expression in MCs sensitized with pooled sera from sensitized patients versus MCs sensitized with pooled sera from anaphylactic patients. MCs from buffy coat preparations were sensitized with pooled sera from LTP patients and stimulated with Pru p 3 for 24 hours.

Gene	Log2FoldChange	padj	Biotype	Description
ENSG00000228782	-8,46	0,00		
ENSG00000290612	-8,03	0,00		
ENSG00000275400	-7,83	0,00		
ENSG00000275993	-7,53	0,00		
ENSG00000285953	-6,73	0,01		
PELO-AS1	-5,39	0,01	lncRNA	PELO antisense RNA 1 [Source:HGNC Symbol;Acc:HGNC:56263]
DKK3	-5,30	0,02	protein_coding	dickkopf WNT signaling pathway inhibitor 3 [Source:HGNC Symbol;Acc:HGNC:2893]
SYN3	-3,83	0,04	protein_coding	synapsin III [Source:HGNC Symbol;Acc:HGNC:11496]

Gene	Log2FoldChange	padj	Biotype	Description
ENSG00000229618	-3,27	0,00		
LINC00310	-3,02	0,00	lncRNA	long intergenic non-protein coding RNA 310 [Source:HGNC Symbol;Acc:HGNC:16414]
E2F7	-2,78	0,00	protein_coding	E2F transcription factor 7 [Source:HGNC Symbol;Acc:HGNC:23820]
NR4A3	-2,21	0,00	protein_coding	nuclear receptor subfamily 4 group A member 3 [Source:HGNC Symbol;Acc:HGNC:7982]
SNORA53	-1,87	0,01	snoRNA	small nucleolar RNA, H/ACA box 53 [Source:HGNC Symbol;Acc:HGNC:32646]
OR14A2	-1,83	0,02	protein_coding	olfactory receptor family 14 subfamily A member 2 [Source:HGNC Symbol;Acc:HGNC:15024]
PTPRF	-1,79	0,02	protein_coding	protein tyrosine phosphatase receptor type F [Source:HGNC Symbol;Acc:HGNC:9670]
IGF1R	-1,78	0,00	protein_coding	insulin like growth factor 1 receptor [Source:HGNC Symbol;Acc:HGNC:5465]
KANK2	-1,76	0,00	protein_coding	KN motif and ankyrin repeat domains 2 [Source:HGNC Symbol;Acc:HGNC:29300]
ERMN	-1,62	0,02	protein_coding	ermin [Source:HGNC Symbol;Acc:HGNC:29208]
CIT	-1,59	0,00	protein_coding	citron rho-interacting serine/threonine kinase [Source:HGNC Symbol;Acc:HGNC:1985]
ARHGAP17	-1,55	0,00	protein_coding	Rho GTPase activating protein 17 [Source:HGNC Symbol;Acc:HGNC:18239]
XYLT1	-1,55	0,00	protein_coding	xylosyltransferase 1 [Source:HGNC Symbol;Acc:HGNC:15516]
FANCA	-1,51	0,00	protein_coding	FA complementation group A [Source:HGNC Symbol;Acc:HGNC:3582]
RTL8A	-1,49	0,05	protein_coding	retrotransposon Gag like 8A [Source:HGNC Symbol;Acc:HGNC:24514]
EXO1	-1,49	0,01	protein_coding	exonuclease 1 [Source:HGNC Symbol;Acc:HGNC:3511]
RGPD5	-1,49	0,04	protein_coding	RANBP2 like and GRIP domain containing 5 [Source:HGNC Symbol;Acc:HGNC:32418]
BCL9	-1,47	0,00	protein_coding	BCL9 transcription coactivator [Source:HGNC Symbol;Acc:HGNC:1008]
ABCA1	-1,47	0,00	protein_coding	ATP binding cassette subfamily A member 1 [Source:HGNC Symbol;Acc:HGNC:29]
SPAG1	-1,45	0,02	protein_coding	sperm associated antigen 1 [Source:HGNC Symbol;Acc:HGNC:11212]
CCDC150	-1,42	0,05	protein_coding	coiled-coil domain containing 150 [Source:HGNC Symbol;Acc:HGNC:26834]
PLK4	-1,41	0,00	protein_coding	polo like kinase 4 [Source:HGNC Symbol;Acc:HGNC:11397]
IQGAP3	-1,39	0,01	protein_coding	IQ motif containing GTPase activating protein 3 [Source:HGNC Symbol;Acc:HGNC:20669]
H3C8	-1,38	0,00	protein_coding	H3 clustered histone 8 [Source:HGNC Symbol;Acc:HGNC:4772]
NSRP1	-1,37	0,03	protein_coding	nuclear speckle splicing regulatory protein 1 [Source:HGNC Symbol;Acc:HGNC:25305]
CTPS2	-1,36	0,02	protein_coding	CTP synthase 2 [Source:HGNC Symbol;Acc:HGNC:2520]
NCAPG	-1,36	0,00	protein_coding	non-SMC condensin I complex subunit G [Source:HGNC Symbol;Acc:HGNC:24304]
H3C3	-1,33	0,00	protein_coding	H3 clustered histone 3 [Source:HGNC Symbol;Acc:HGNC:4768]
MND1	-1,32	0,03	protein_coding	meiotic nuclear divisions 1 [Source:HGNC Symbol;Acc:HGNC:24839]

Gene	Log2FoldChange	padj	Biotype	Description
TYMS	-1,31	0,00	protein_coding	thymidylate synthetase [Source:HGNC Symbol;Acc:HGNC:12441]
H3C2	-1,31	0,00	protein_coding	H3 clustered histone 2 [Source:HGNC Symbol;Acc:HGNC:4776]
SHCBP1	-1,30	0,00	protein_coding	SHC binding and spindle associated 1 [Source:HGNC Symbol;Acc:HGNC:29547]
RORA	-1,27	0,00	protein_coding	RAR related orphan receptor A [Source:HGNC Symbol;Acc:HGNC:10258]
KDM6B	-1,27	0,04	protein_coding	lysine demethylase 6B [Source:HGNC Symbol;Acc:HGNC:29012]
GOLGA1	-1,27	0,00	protein_coding	golgin A1 [Source:HGNC Symbol;Acc:HGNC:4424]
OR9H1P	-1,26	0,04	protein_coding	olfactory receptor family 9 subfamily H member 1 pseudogene [Source:HGNC Symbol;Acc:HGNC:15038]
TUBB3	-1,25	0,00	protein_coding	tubulin beta 3 class III [Source:HGNC Symbol;Acc:HGNC:20772]
PLK1	-1,25	0,00	protein_coding	polo like kinase 1 [Source:HGNC Symbol;Acc:HGNC:9077]
FANCB	-1,24	0,01	protein_coding	FA complementation group B [Source:HGNC Symbol;Acc:HGNC:3583]
CHAF1A	-1,22	0,01	protein_coding	chromatin assembly factor 1 subunit A [Source:HGNC Symbol;Acc:HGNC:1910]
CDT1	-1,20	0,02	protein_coding	chromatin licensing and DNA replication factor 1 [Source:HGNC Symbol;Acc:HGNC:24576]
H2AC16	-1,19	0,00	protein_coding	H2A clustered histone 16 [Source:HGNC Symbol;Acc:HGNC:4730]
H2BC17	-1,19	0,00	protein_coding	H2B clustered histone 17 [Source:HGNC Symbol;Acc:HGNC:4758]
H2AC14	-1,19	0,00	protein_coding	H2A clustered histone 14 [Source:HGNC Symbol;Acc:HGNC:4727]
GTF2H4	-1,18	0,00	protein_coding	general transcription factor IIH subunit 4 [Source:HGNC Symbol;Acc:HGNC:4658]
DTX4	-1,18	0,00	protein_coding	deltex E3 ubiquitin ligase 4 [Source:HGNC Symbol;Acc:HGNC:29151]
H2AC4	-1,17	0,00	protein_coding	H2A clustered histone 4 [Source:HGNC Symbol;Acc:HGNC:4734]
JAG2	-1,17	0,01	protein_coding	jagged canonical Notch ligand 2 [Source:HGNC Symbol;Acc:HGNC:6189]
ENSG00000290385	-1,16	0,01		
TRRAP	-1,16	0,02	protein_coding	transformation/transcription domain associated protein [Source:HGNC Symbol;Acc:HGNC:12347]
GEN1	-1,16	0,00	protein_coding	GEN1 Holliday junction 5' flap endonuclease [Source:HGNC Symbol;Acc:HGNC:26881]
H2BC11	-1,15	0,00	protein_coding	H2B clustered histone 11 [Source:HGNC Symbol;Acc:HGNC:4761]
GPSM2	-1,14	0,00	protein_coding	G protein signaling modulator 2 [Source:HGNC Symbol;Acc:HGNC:29501]
ASF1B	-1,13	0,01	protein_coding	anti-silencing function 1B histone chaperone [Source:HGNC Symbol;Acc:HGNC:20996]
KDM7A	-1,11	0,00	protein_coding	lysine demethylase 7A [Source:HGNC Symbol;Acc:HGNC:22224]
ALPK3	-1,10	0,00	protein_coding	alpha kinase 3 [Source:HGNC Symbol;Acc:HGNC:17574]
TRIM66	-1,09	0,04	protein_coding	tripartite motif containing 66 [Source:HGNC Symbol;Acc:HGNC:29005]
KIF18A	-1,08	0,00	protein_coding	kinesin family member 18A [Source:HGNC Symbol;Acc:HGNC:29441]
H3C15	-1,08	0,00	protein_coding	H3 clustered histone 15 [Source:HGNC Symbol;Acc:HGNC:20505]

Gene	Log2FoldChange	padj	Biotype	Description
ANLN	-1,08	0,00	protein_coding	anillin, actin binding protein [Source:HGNC Symbol;Acc:HGNC:14082]
HJURP	-1,06	0,00	protein_coding	Holliday junction recognition protein [Source:HGNC Symbol;Acc:HGNC:25444]
PIK3CB	-1,06	0,01	protein_coding	phosphatidylinositol-4,5-bisphosphate 3-kinase catalytic subunit beta [Source:HGNC Symbol;Acc:HGNC:8976]
LMO7	-1,05	0,03	protein_coding	LIM domain 7 [Source:HGNC Symbol;Acc:HGNC:6646]
ARHGAP31	-1,04	0,01	protein_coding	Rho GTPase activating protein 31 [Source:HGNC Symbol;Acc:HGNC:29216]
CELSR1	-1,04	0,01	protein_coding	cadherin EGF LAG seven-pass G-type receptor 1 [Source:HGNC Symbol;Acc:HGNC:1850]
CKAP2L	-1,03	0,03	protein_coding	cytoskeleton associated protein 2 like [Source:HGNC Symbol;Acc:HGNC:26877]
ANKRD9	-1,03	0,00	protein_coding	ankyrin repeat domain 9 [Source:HGNC Symbol;Acc:HGNC:20096]
CCDC18	-1,03	0,01	protein_coding	coiled-coil domain containing 18 [Source:HGNC Symbol;Acc:HGNC:30370]
FCHO2	-1,03	0,00	protein_coding	FCH and mu domain containing endocytic adaptor 2 [Source:HGNC Symbol;Acc:HGNC:25180]
PRC1	-1,02	0,00	protein_coding	protein regulator of cytokinesis 1 [Source:HGNC Symbol;Acc:HGNC:9341]
H2BC3	-1,02	0,00	protein_coding	H2B clustered histone 3 [Source:HGNC Symbol;Acc:HGNC:4751]
TEAD1	-1,02	0,03	protein_coding	TEA domain transcription factor 1 [Source:HGNC Symbol;Acc:HGNC:11714]
SLC4A7	-1,01	0,01	protein_coding	solute carrier family 4 member 7 [Source:HGNC Symbol;Acc:HGNC:11033]
SMC4	-1,01	0,01	protein_coding	structural maintenance of chromosomes 4 [Source:HGNC Symbol;Acc:HGNC:14013]
SLC43A2	1,01	0,03	protein_coding	solute carrier family 43 member 2 [Source:HGNC Symbol;Acc:HGNC:23087]
CCR2	1,03	0,00	protein_coding	C-C motif chemokine receptor 2 [Source:HGNC Symbol;Acc:HGNC:1603]
TMEM74B	1,05	0,00	protein_coding	transmembrane protein 74B [Source:HGNC Symbol;Acc:HGNC:15893]
HLA-DMA	1,07	0,01	protein_coding	major histocompatibility complex, class II, DM alpha [Source:HGNC Symbol;Acc:HGNC:4934]
MYCBP	1,17	0,03	protein_coding	MYC binding protein [Source:HGNC Symbol;Acc:HGNC:7554]
HBD	1,20	0,00	protein_coding	hemoglobin subunit delta [Source:HGNC Symbol;Acc:HGNC:4829]
ENSG00000289720	1,22	0,05		
TMEM9B-AS1	1,25	0,01	lncRNA	TMEM9B antisense RNA 1 [Source:HGNC Symbol;Acc:HGNC:19230]
LYZ	1,40	0,00	protein_coding	lysozyme [Source:HGNC Symbol;Acc:HGNC:6740]
CDCA7L	1,46	0,01	protein_coding	cell division cycle associated 7 like [Source:HGNC Symbol;Acc:HGNC:30777]
ZEB1	1,62	0,00	protein_coding	zinc finger E-box binding homeobox 1 [Source:HGNC Symbol;Acc:HGNC:11642]
LINC01571	1,67	0,00	lncRNA	long intergenic non-protein coding RNA 1571 [Source:HGNC Symbol;Acc:HGNC:51384]
PNMA2	1,69	0,00	protein_coding	PNMA family member 2 [Source:HGNC Symbol;Acc:HGNC:9159]
SEPTIN1	1,85	0,04	protein_coding	septin 1 [Source:HGNC Symbol;Acc:HGNC:2879]
VCX	1,99	0,04	protein_coding	variable charge X-linked [Source:HGNC Symbol;Acc:HGNC:12667]

Gene	Log2FoldChange	padj	Biotype	Description
TMOD2	2,05	0,01	protein_coding	tropomodulin 2 [Source:HGNC Symbol;Acc:HGNC:11872]
TCN1	2,08	0,00	protein_coding	transcobalamin 1 [Source:HGNC Symbol;Acc:HGNC:11652]
ATP10A	2,09	0,00	protein_coding	ATPase phospholipid transporting 10A (putative) [Source:HGNC Symbol;Acc:HGNC:13542]
DAB2	2,14	0,00	protein_coding	DAB adaptor protein 2 [Source:HGNC Symbol;Acc:HGNC:2662]
ZNF208	2,22	0,04	protein_coding	zinc finger protein 208 [Source:HGNC Symbol;Acc:HGNC:12999]
ENSG00000271793	2,28	0,00		
FKBP10	2,76	0,00	protein_coding	FKBP prolyl isomerase 10 [Source:HGNC Symbol;Acc:HGNC:18169]
PLN	3,31	0,01	protein_coding	phospholamban [Source:HGNC Symbol;Acc:HGNC:9080]
FCRLA	3,69	0,00	protein_coding	Fc receptor like A [Source:HGNC Symbol;Acc:HGNC:18504]
ENSG00000274276	3,72	0,02		
KCNK9	3,82	0,00	protein_coding	potassium two pore domain channel subfamily K member 9 [Source:HGNC Symbol;Acc:HGNC:6283]
BMP7	3,85	0,00	protein_coding	bone morphogenetic protein 7 [Source:HGNC Symbol;Acc:HGNC:1074]
DGKG	4,92	0,01	protein_coding	diacylglycerol kinase gamma [Source:HGNC Symbol;Acc:HGNC:2853]
ASB5	5,16	0,03	protein_coding	ankyrin repeat and SOCS box containing 5 [Source:HGNC Symbol;Acc:HGNC:17180]
LRTOMT	6,15	0,01	protein_coding	leucine rich transmembrane and O-methyltransferase domain containing [Source:HGNC Symbol;Acc:HGNC:25033]
ENSG00000167807	6,26	0,05		
ENSG00000270008	6,40	0,03		
PCBP3	6,68	0,03	protein_coding	poly(rC) binding protein 3 [Source:HGNC Symbol;Acc:HGNC:8651]
TCAF2C	8,24	0,00	protein_coding	TRPM8 channel associated factor 2C [Source:HGNC Symbol;Acc:HGNC:53641]

Annex Table 7. GSEA pathways in LAD2 cells sensitized with pooled sera from sensitized patients versus LAD2 cells sensitized with pooled sera from anaphylactic patients. LAD2 cells were sensitized with pooled sera from LTP patients and stimulated with Pru p 3 for 24 hours.

Description	setSize	enrichmentScore	padj	qvalue	core_enrichment
Retinoblastoma gene in cancer	86	-0,690	0,000	0,000	SAP30/RFC4/CDK4/HMGB1/CCND3/RRM1/PRMT2/POLA1/PRIM1/CCNE2/MCM3/BARD1/SUV39H1/H2AZ1/DCK/RPA3/WEE1/CDC7/CDK2/HMGB2/POLE2/SMC2/PCNA/RFC5/CDC25B/RFC3/MCM7/CCNB1/TTK/CDT1/CDC25A/STMN1/CCNB2/CCNA2/TYMS/ORC1/ANLN/DHFR/PLK4/CHEK1/TOP2A/CDK1/KIF4A/RRM2/E2F1/CDC45/E2F2
Senescence associated secretory phenotype SASP	103	-0,626	0,000	0,000	H2AC6/UBC/H2BC7/CDK4/H3-3B/H2AZ2/H2BC8/H4C11/H2AC20/UBB/CDKN2A/H4C5/H2AC7/JUN/H2BC26/UBE2S/H4C2/H4C16/H2BC5/H3C4/CDKN2C/H2AZ1/FZR1/H4C9/H2AC8/H2BC4/H4C12/H3C13/H2BC12/H4C6/H2BC21/H4C8/H2BC6/CDK2/H2AC18/CDKN2D/H2BC14/H4C13/H2BC10/H4C3/H3C10/H3C1/H2BC15/H2AX/H3C12/H4C4/H2BC13/H2BC9/H2BC11/H2BC3/CCNA2/H4C1/H2AC14/H4C14/H2AC4/H2BC17/H3C3/H3C8/UBE2C/H3C7/H3C2/H3C15
DNA replication	42	-0,738	0,000	0,000	MCM4/POLD3/GMNN/UBC/RFC4/POLA1/RFC2/PRIM1/ORC6/MCM3/RPA4/DBF4/RPA3/CDC7/CDK2/POLE2/PCNA/RFC5/MCM2/RFC3/MCM7/POLD1/CDT1/MCM10/ORC1/CDC6/MCM5/CDC45
Effect of progerin on genes involved in progeria	35	-0,755	0,000	0,000	SUV39H1/H3C4/H3C13/MBD3/H3C10/H3C1/H3C12/H3C3/H3C8/H3C7/E2F1/H3C2/H3C15
NF1 copy number variation syndrome	98	-0,575	0,000	0,000	TEFM/H4C11/RFC2/LIMK1/CCNE2/H4C5/H4C2/H4C16/SYN1/H3C4/RAD9A/H4C9/H4C12/H3C13/H4C6/H4C8/TUBB/RAD51/H4C13/PCNA/RFC5/ATAD5/H4C3/RFC3/H3C10/H3C1/H3C12/H4C4/CCNA2/H4C1/H4C14/H3C3/H3C8/H3C7/H3C2/H3C15
Cell cycle	117	-0,535	0,000	0,000	BUB3/CCND2/CDKN2A/CCNE2/YWHAQ/ORC6/MAD1L1/MCM3/RBL1/CDKN2C/FZR1/GADD45G/DBF4/MAD2L2/WEE1/CDC7/CDK2/CDKN2D/PCNA/CDC25B/MCM2/BUB1/PLK1/MCM7/PTTG1/ESPL1/CCNB1/TTK/CDC25A/PKMYT1/CCNB2/CDC25C/CCNA2/CDC20/ORC1/CDC6/MCM5/CHEK1/CDK1/E2F1/CDC45/E2F2

Description	setSize	enrichmentScore	padj	qvalue	core_enrichment
DNA IR damage and cellular response via ATR	81	-0,592	0,000	0,000	BARD1/BRCA1/RAD9A/BRCA2/RECQL4/RAD51/CDK2/PCNA/MCM2/PLK1/BRIP1/FANCA/H2AX/CDC25C/FANCI/CLSPN/CHEK1/CDK1/FEN1/FOXM1/E2F1/CDC45/EXO1
Nucleotide excision repair in xeroderma pigmentosum	75	-0,601	0,000	0,000	POLD2/DDB2/ERCC3/POLE4/ERCC1/RPA1/XRCC1/GTF2H3/POLD3/CHD1L/HMGN1/H2AC6/POLE3/GTF2H4/RFC4/H3-3B/XPC/H4C11/RFC2/H4C5/H4C2/H4C16/BRCA1/H4C9/LIG1/RPA3/H4C12/H4C6/H4C8/POLE2/RAD18/H4C13/PCNA/RFC5/H4C3/RFC3/POLD1/H4C4/H4C1/H4C14
Gastric cancer network 1	25	-0,778	0,001	0,00	H4C16/ECT2/KIF20B/LIN9/CENPF/AURKA/TPX2/TOP2A/KIF15/UBE2C/MYBL2/E2F7
DNA repair pathways full network	120	-0,499	0,001	0,001	NBN/MSH6/OGG1/UNG/GTF2H5/MRE11/TERF2/RPA2/FANCF/POLD2/DDB2/ERCC3/PARP2/POLE4/ERCC1/RPA1/XRCC1/USP1/GTF2H3/POLD3/POLE3/NEIL2/GTF2H4/RFC4/HMGB1/XPC/FANCD2/RFC2/RAD51C/MPG/FANCM/FANCE/BRCA1/NEIL3/FAAP100/BRCA2/LIG1/RPA3/RAD51/POLE2/PCNA/RFC5/BRIP1/RFC3/FANCA/FANCB/POLD1/H2AX/FANCI/CHEK1/FEN1/EXO1
Enterocyte cholesterol metabolism	29	-0,736	0,003	0,00	DHCR24/HSD17B7/FDFT1/IDI1/TM7SF2/NSDHL/LSS/HMGCR/DGAT1/LDLR/EBP/HMGCS1/CD36/CYP51A1/DHCR7/SQLE/MVD/FDPS/ACAT2/ABCA1/MTTP
Histone modifications	63	-0,592	0,004	0,004	H4C2/H4C16/SUV39H1/H3C4/KMT5C/H4C9/KMT5A/H4C12/H3C13/H4C6/H4C8/H4C13/H4C3/H3C10/H3C1/H3C12/H4C4/H4C1/H3C8/H3C7/H3C15
G1 to S cell cycle control	63	-0,586	0,005	0,00	CCND2/PRIM1/CDKN2A/CCNE2/ORC6/MCM3/CDKN2C/RPA3/WEE1/CDK2/POLE2/CDKN2D/PCNA/MCM2/MCM7/CCNB1/CDC25A/ORC1/MCM5/CDK1/E2F1/CDC45/E2F2
Regulation of sister chromatid separation at the metaphase anaphase transition	14	-0,825	0,007	0,007	BUB3/MAD1L1/BUB1/CENPE/PTTG1/ESPL1/MAD2L1/CDC20/BUB1B

Description	setSize	enrichmentScore	padj	qvalue	core_enrichment
Chronic hyperglycemia impairment of neuron function	22	-0,758	0,009	0,01	AGER/MMP23B/MMP2/NOS2/SCN8A/MMP24/MMP14
Cohesin complex Cornelia de Lange syndrome	33	-0,679	0,017	0,017	REC8/SGO2/PLK1/PTTG1/ESPL1/CDK1/SGO1/AURKB/ESCO2/CDCA5
FBXL10 enhancement of MAP ERK signaling in diffuse large B cell lymphoma	28	-0,694	0,017	0,02	EZH2/PCGF1/H3-3B/H2AZ2/H3C4/H2AZ1/H3C13/H3C10/H3C1/H2AX/H3C12/H3C8/H3C7/H3C15
Primary ovarian insufficiency	103	-0,448	0,040	0,038	RFWD3/MGME1/AMHR2/FANCM/CLPP/AMH/BLM/SOX8/BRCA2/RECQL4/SGO2/RAD51/HROB/MCM8/DMC1/XRCC2/KASH5/FANCA/CENPE/BMPR1B/FOXL2/FANCI/WDR62/HMMR/MND1/PSMC3IP/POF1B/CAV1/EXO1
DNA mismatch repair	23	-0,699	0,041	0,04	RPA2/POLD2/POLE4/RPA1/POLD3/POLE3/RFC4/RFC2/LIG1/RPA3/POLE2/PCNA/RFC5/RFC3/POLD1/EXO1

Annex Table 8. Differential gene expression in LAD2 cells sensitized with pooled sera from sensitized patients versus LAD2 cells sensitized with pooled sera from anaphylactic patients. LAD2 cells were sensitized with pooled sera from LTP patients and stimulated with Pru p 3 for 24 hours.

Gene	Log2FoldChange	padj	Biotype	Description
ENSG00000273590	-11,03	0,00		
ENSG00000282143	-7,99	0,00		
ENSG00000268400	-6,64	0,00		
TMEM38A	-5,26	0,01	protein_coding	transmembrane protein 38A [Source:HGNC Symbol;Acc:HGNC:28462]
CDC42BPG	-5,03	0,02	protein_coding	CDC42 binding protein kinase gamma [Source:HGNC Symbol;Acc:HGNC:29829]
FAM111B	-3,53	0,05	protein_coding	FAM111 trypsin like peptidase B [Source:HGNC Symbol;Acc:HGNC:24200]
E2F7	-3,27	0,00	protein_coding	E2F transcription factor 7 [Source:HGNC Symbol;Acc:HGNC:23820]
CENPM	-3,23	0,00	protein_coding	centromere protein M [Source:HGNC Symbol;Acc:HGNC:18352]
EXO1	-3,14	0,00	protein_coding	exonuclease 1 [Source:HGNC Symbol;Acc:HGNC:3511]
SULT1A4	-2,93	0,04	protein_coding	sulfotransferase family 1A member 4 [Source:HGNC Symbol;Acc:HGNC:30004]
PCLAF	-2,87	0,00	protein_coding	PCNA clamp associated factor [Source:HGNC Symbol;Acc:HGNC:28961]
E2F2	-2,81	0,05	protein_coding	E2F transcription factor 2 [Source:HGNC Symbol;Acc:HGNC:3114]
DDIAS	-2,72	0,00	protein_coding	DNA damage induced apoptosis suppressor [Source:HGNC Symbol;Acc:HGNC:26351]
HASPIN	-2,70	0,00	protein_coding	histone H3 associated protein kinase [Source:HGNC Symbol;Acc:HGNC:19682]
NCAPG	-2,52	0,00	protein_coding	non-SMC condensin I complex subunit G [Source:HGNC Symbol;Acc:HGNC:24304]
IQGAP3	-2,45	0,00	protein_coding	IQ motif containing GTPase activating protein 3 [Source:HGNC Symbol;Acc:HGNC:20669]
H1-5	-2,40	0,00	protein_coding	H1.5 linker histone, cluster member [Source:HGNC Symbol;Acc:HGNC:4719]
H3C15	-2,40	0,00	protein_coding	H3 clustered histone 15 [Source:HGNC Symbol;Acc:HGNC:20505]
H3C2	-2,38	0,00	protein_coding	H3 clustered histone 2 [Source:HGNC Symbol;Acc:HGNC:4776]
RAD51AP1	-2,32	0,01	protein_coding	RAD51 associated protein 1 [Source:HGNC Symbol;Acc:HGNC:16956]
SPC24	-2,32	0,00	protein_coding	SPC24 component of NDC80 kinetochore complex [Source:HGNC Symbol;Acc:HGNC:26913]
CENPA	-2,32	0,00	protein_coding	centromere protein A [Source:HGNC Symbol;Acc:HGNC:1851]
CDCA5	-2,27	0,01	protein_coding	cell division cycle associated 5 [Source:HGNC Symbol;Acc:HGNC:14626]
RRM2	-2,26	0,02	protein_coding	ribonucleotide reductase regulatory subunit M2 [Source:HGNC Symbol;Acc:HGNC:10452]
NEURL1B	-2,24	0,00	protein_coding	neuralized E3 ubiquitin protein ligase 1B [Source:HGNC Symbol;Acc:HGNC:35422]
PBK	-2,16	0,00	protein_coding	PDZ binding kinase [Source:HGNC Symbol;Acc:HGNC:18282]
ESCO2	-2,10	0,01	protein_coding	establishment of sister chromatid cohesion N-acetyltransferase 2 [Source:HGNC Symbol;Acc:HGNC:27230]
ZWINT	-2,09	0,02	protein_coding	ZW10 interacting kinetochore protein [Source:HGNC Symbol;Acc:HGNC:13195]
TICRR	-2,06	0,01	protein_coding	TOPBP1 interacting checkpoint and replication regulator [Source:HGNC Symbol;Acc:HGNC:28704]

Gene	Log2FoldChange	padj	Biotype	Description
RAD54L	-2,03	0,02	protein_coding	RAD54 like [Source:HGNC Symbol;Acc:HGNC:9826]
POLQ	-2,02	0,00	protein_coding	DNA polymerase theta [Source:HGNC Symbol;Acc:HGNC:9186]
H3C7	-1,99	0,00	protein_coding	H3 clustered histone 7 [Source:HGNC Symbol;Acc:HGNC:4773]
TRIP13	-1,99	0,00	protein_coding	thyroid hormone receptor interactor 13 [Source:HGNC Symbol;Acc:HGNC:12307]
PRC1	-1,99	0,00	protein_coding	protein regulator of cytokinesis 1 [Source:HGNC Symbol;Acc:HGNC:9341]
PSRC1	-1,96	0,00	protein_coding	proline and serine rich coiled-coil 1 [Source:HGNC Symbol;Acc:HGNC:24472]
BIRC5	-1,96	0,00	protein_coding	baculoviral IAP repeat containing 5 [Source:HGNC Symbol;Acc:HGNC:593]
UBE2C	-1,95	0,00	protein_coding	ubiquitin conjugating enzyme E2 C [Source:HGNC Symbol;Acc:HGNC:15937]
DEPDC1	-1,93	0,00	protein_coding	DEP domain containing 1 [Source:HGNC Symbol;Acc:HGNC:22949]
SKA1	-1,92	0,01	protein_coding	spindle and kinetochore associated complex subunit 1 [Source:HGNC Symbol;Acc:HGNC:28109]
FOXM1	-1,91	0,00	protein_coding	forkhead box M1 [Source:HGNC Symbol;Acc:HGNC:3818]
H2AC16	-1,90	0,00	protein_coding	H2A clustered histone 16 [Source:HGNC Symbol;Acc:HGNC:4730]
AURKB	-1,89	0,00	protein_coding	aurora kinase B [Source:HGNC Symbol;Acc:HGNC:11390]
ERCC6L	-1,86	0,03	protein_coding	ERCC excision repair 6 like, spindle assembly checkpoint helicase [Source:HGNC Symbol;Acc:HGNC:20794]
H3C8	-1,86	0,00	protein_coding	H3 clustered histone 8 [Source:HGNC Symbol;Acc:HGNC:4772]
TROAP	-1,86	0,00	protein_coding	trophinin associated protein [Source:HGNC Symbol;Acc:HGNC:12327]
KIF15	-1,84	0,00	protein_coding	kinesin family member 15 [Source:HGNC Symbol;Acc:HGNC:17273]
PRR11	-1,80	0,00	protein_coding	proline rich 11 [Source:HGNC Symbol;Acc:HGNC:25619]
FEN1	-1,79	0,03	protein_coding	flap structure-specific endonuclease 1 [Source:HGNC Symbol;Acc:HGNC:3650]
NDC80	-1,77	0,00	protein_coding	NDC80 kinetochore complex component [Source:HGNC Symbol;Acc:HGNC:16909]
PIMREG	-1,77	0,01	protein_coding	PICALM interacting mitotic regulator [Source:HGNC Symbol;Acc:HGNC:25483]
H3C3	-1,77	0,00	protein_coding	H3 clustered histone 3 [Source:HGNC Symbol;Acc:HGNC:4768]
KIF4A	-1,75	0,00	protein_coding	kinesin family member 4A [Source:HGNC Symbol;Acc:HGNC:13339]
SGO1	-1,74	0,00	protein_coding	shugoshin 1 [Source:HGNC Symbol;Acc:HGNC:25088]
KIF20A	-1,73	0,00	protein_coding	kinesin family member 20A [Source:HGNC Symbol;Acc:HGNC:9787]
CDK1	-1,73	0,00	protein_coding	cyclin dependent kinase 1 [Source:HGNC Symbol;Acc:HGNC:1722]
GAS7	-1,72	0,00	protein_coding	growth arrest specific 7 [Source:HGNC Symbol;Acc:HGNC:4169]
CDCA3	-1,72	0,02	protein_coding	cell division cycle associated 3 [Source:HGNC Symbol;Acc:HGNC:14624]
H1-3	-1,71	0,00	protein_coding	H1.3 linker histone, cluster member [Source:HGNC Symbol;Acc:HGNC:4717]
TOP2A	-1,70	0,00	protein_coding	DNA topoisomerase II alpha [Source:HGNC Symbol;Acc:HGNC:11989]

Gene	Log2FoldChange	padj	Biotype	Description
H2BC17	-1,70	0,00	protein_coding	H2B clustered histone 17 [Source:HGNC Symbol;Acc:HGNC:4758]
H2AC4	-1,70	0,01	protein_coding	H2A clustered histone 4 [Source:HGNC Symbol;Acc:HGNC:4734]
CDCA2	-1,69	0,00	protein_coding	cell division cycle associated 2 [Source:HGNC Symbol;Acc:HGNC:14623]
DLGAP5	-1,69	0,00	protein_coding	DLG associated protein 5 [Source:HGNC Symbol;Acc:HGNC:16864]
KIF2C	-1,67	0,00	protein_coding	kinesin family member 2C [Source:HGNC Symbol;Acc:HGNC:6393]
KIF11	-1,66	0,00	protein_coding	kinesin family member 11 [Source:HGNC Symbol;Acc:HGNC:6388]
FBXO5	-1,65	0,01	protein_coding	F-box protein 5 [Source:HGNC Symbol;Acc:HGNC:13584]
HMMR	-1,65	0,00	protein_coding	hyaluronan mediated motility receptor [Source:HGNC Symbol;Acc:HGNC:5012]
BUB1B	-1,65	0,00	protein_coding	BUB1 mitotic checkpoint serine/threonine kinase B [Source:HGNC Symbol;Acc:HGNC:1149]
NUSAP1	-1,63	0,00	protein_coding	nucleolar and spindle associated protein 1 [Source:HGNC Symbol;Acc:HGNC:18538]
NCAPH	-1,63	0,00	protein_coding	non-SMC condensin I complex subunit H [Source:HGNC Symbol;Acc:HGNC:1112]
CDCA8	-1,62	0,00	protein_coding	cell division cycle associated 8 [Source:HGNC Symbol;Acc:HGNC:14629]
H4C14	-1,62	0,01	protein_coding	H4 clustered histone 14 [Source:HGNC Symbol;Acc:HGNC:4794]
GTSE1	-1,62	0,00	protein_coding	G2 and S-phase expressed 1 [Source:HGNC Symbol;Acc:HGNC:13698]
FAM83D	-1,61	0,05	protein_coding	family with sequence similarity 83 member D [Source:HGNC Symbol;Acc:HGNC:16122]
NEK2	-1,60	0,00	protein_coding	NIMA related kinase 2 [Source:HGNC Symbol;Acc:HGNC:7745]
NCAPG2	-1,60	0,00	protein_coding	non-SMC condensin II complex subunit G2 [Source:HGNC Symbol;Acc:HGNC:21904]
KIFC1	-1,60	0,03	protein_coding	kinesin family member C1 [Source:HGNC Symbol;Acc:HGNC:6389]
ENSG00000284946	-1,60	0,00		
CLSPN	-1,58	0,01	protein_coding	claspin [Source:HGNC Symbol;Acc:HGNC:19715]
ANLN	-1,58	0,03	protein_coding	anillin, actin binding protein [Source:HGNC Symbol;Acc:HGNC:14082]
H2AC14	-1,57	0,00	protein_coding	H2A clustered histone 14 [Source:HGNC Symbol;Acc:HGNC:4727]
ASPM	-1,57	0,00	protein_coding	assembly factor for spindle microtubules [Source:HGNC Symbol;Acc:HGNC:19048]
TYMS	-1,56	0,02	protein_coding	thymidylate synthetase [Source:HGNC Symbol;Acc:HGNC:12441]
WDR62	-1,54	0,02	protein_coding	WD repeat domain 62 [Source:HGNC Symbol;Acc:HGNC:24502]
HJURP	-1,53	0,04	protein_coding	Holliday junction recognition protein [Source:HGNC Symbol;Acc:HGNC:25444]
H4C1	-1,50	0,02	protein_coding	H4 clustered histone 1 [Source:HGNC Symbol;Acc:HGNC:4781]
CDC20	-1,49	0,01	protein_coding	cell division cycle 20 [Source:HGNC Symbol;Acc:HGNC:1723]
KIF14	-1,49	0,00	protein_coding	kinesin family member 14 [Source:HGNC Symbol;Acc:HGNC:19181]
FANCI	-1,47	0,01	protein_coding	FA complementation group I [Source:HGNC Symbol;Acc:HGNC:25568]

Gene	Log2FoldChange	padj	Biotype	Description
H2BC3	-1,47	0,01	protein_coding	H2B clustered histone 3 [Source:HGNC Symbol;Acc:HGNC:4751]
KIF23	-1,45	0,00	protein_coding	kinesin family member 23 [Source:HGNC Symbol;Acc:HGNC:6392]
APOBEC3B	-1,45	0,04	protein_coding	apolipoprotein B mRNA editing enzyme catalytic subunit 3B [Source:HGNC Symbol;Acc:HGNC:17352]
CDC25C	-1,44	0,02	protein_coding	cell division cycle 25C [Source:HGNC Symbol;Acc:HGNC:1727]
H2BC11	-1,43	0,04	protein_coding	H2B clustered histone 11 [Source:HGNC Symbol;Acc:HGNC:4761]
TPX2	-1,43	0,00	protein_coding	TPX2 microtubule nucleation factor [Source:HGNC Symbol;Acc:HGNC:1249]
AURKA	-1,42	0,00	protein_coding	aurora kinase A [Source:HGNC Symbol;Acc:HGNC:11393]
CCNB2	-1,40	0,01	protein_coding	cyclin B2 [Source:HGNC Symbol;Acc:HGNC:1580]
H2BC9	-1,40	0,00	protein_coding	H2B clustered histone 9 [Source:HGNC Symbol;Acc:HGNC:4755]
CENPF	-1,39	0,01	protein_coding	centromere protein F [Source:HGNC Symbol;Acc:HGNC:1857]
H2BC13	-1,38	0,03	protein_coding	H2B clustered histone 13 [Source:HGNC Symbol;Acc:HGNC:4748]
H4C4	-1,37	0,04	protein_coding	H4 clustered histone 4 [Source:HGNC Symbol;Acc:HGNC:4782]
H2AC12	-1,33	0,00	protein_coding	H2A clustered histone 12 [Source:HGNC Symbol;Acc:HGNC:13671]
CENPN	-1,33	0,00	protein_coding	centromere protein N [Source:HGNC Symbol;Acc:HGNC:30873]
CIP2A	-1,33	0,02	protein_coding	cellular inhibitor of PP2A [Source:HGNC Symbol;Acc:HGNC:29302]
CDKN3	-1,32	0,00	protein_coding	cyclin dependent kinase inhibitor 3 [Source:HGNC Symbol;Acc:HGNC:1791]
MAD2L1	-1,30	0,00	protein_coding	mitotic arrest deficient 2 like 1 [Source:HGNC Symbol;Acc:HGNC:6763]
LIN9	-1,29	0,03	protein_coding	lin-9 DREAM MuvB core complex component [Source:HGNC Symbol;Acc:HGNC:30830]
TUBB3	-1,28	0,02	protein_coding	tubulin beta 3 class III [Source:HGNC Symbol;Acc:HGNC:20772]
CCNB1	-1,27	0,00	protein_coding	cyclin B1 [Source:HGNC Symbol;Acc:HGNC:1579]
NUF2	-1,27	0,00	protein_coding	NUF2 component of NDC80 kinetochore complex [Source:HGNC Symbol;Acc:HGNC:14621]
CENPH	-1,26	0,03	protein_coding	centromere protein H [Source:HGNC Symbol;Acc:HGNC:17268]
PPP2R3B	-1,25	0,04	protein_coding	protein phosphatase 2 regulatory subunit B"beta [Source:HGNC Symbol;Acc:HGNC:13417]
H2BC15	-1,25	0,01	protein_coding	H2B clustered histone 15 [Source:HGNC Symbol;Acc:HGNC:4749]
H2AC13	-1,24	0,02	protein_coding	H2A clustered histone 13 [Source:HGNC Symbol;Acc:HGNC:4725]
SPAG5	-1,24	0,01	protein_coding	sperm associated antigen 5 [Source:HGNC Symbol;Acc:HGNC:13452]
H3C1	-1,23	0,05	protein_coding	H3 clustered histone 1 [Source:HGNC Symbol;Acc:HGNC:4766]
PARPBP	-1,23	0,01	protein_coding	PARP1 binding protein [Source:HGNC Symbol;Acc:HGNC:26074]
H3C10	-1,23	0,03	protein_coding	H3 clustered histone 10 [Source:HGNC Symbol;Acc:HGNC:4775]
PTTG1	-1,22	0,00	protein_coding	PTTG1 regulator of sister chromatid separation, securin [Source:HGNC Symbol;Acc:HGNC:9690]

Gene	Log2FoldChange	padj	Biotype	Description
ARHGAP11A	-1,22	0,01	protein_coding	Rho GTPase activating protein 11A [Source:HGNC Symbol;Acc:HGNC:15783]
KNL1	-1,17	0,02	protein_coding	kinetochore scaffold 1 [Source:HGNC Symbol;Acc:HGNC:24054]
IBA57	-1,10	0,05	protein_coding	iron-sulfur cluster assembly factor IBA57 [Source:HGNC Symbol;Acc:HGNC:27302]
H1-2	-1,07	0,05	protein_coding	H1.2 linker histone, cluster member [Source:HGNC Symbol;Acc:HGNC:4716]
NAIP	1,29	0,03	protein_coding	NLR family apoptosis inhibitory protein [Source:HGNC Symbol;Acc:HGNC:7634]
SMIM11	1,41	0,00	protein_coding	small integral membrane protein 11 [Source:HGNC Symbol;Acc:HGNC:1293]
RHOBTB2	1,43	0,03	protein_coding	Rho related BTB domain containing 2 [Source:HGNC Symbol;Acc:HGNC:18756]
ZEB1	1,44	0,04	protein_coding	zinc finger E-box binding homeobox 1 [Source:HGNC Symbol;Acc:HGNC:11642]
HLA-DPB1	1,46	0,05	protein_coding	major histocompatibility complex, class II, DP beta 1 [Source:HGNC Symbol;Acc:HGNC:4940]
NAALADL2	1,58	0,02	protein_coding	N-acetylated alpha-linked acidic dipeptidase like 2 [Source:HGNC Symbol;Acc:HGNC:23219]
LRP1B	1,62	0,01	protein_coding	LDL receptor related protein 1B [Source:HGNC Symbol;Acc:HGNC:6693]
RUNDC3A-AS1	1,67	0,01	lncRNA	RUNDC3A antisense RNA 1 [Source:HGNC Symbol;Acc:HGNC:51344]
LINC02732	1,89	0,04	lncRNA	long intergenic non-protein coding RNA 2732 [Source:HGNC Symbol;Acc:HGNC:54249]
FABP5	1,92	0,02	protein_coding	fatty acid binding protein 5 [Source:HGNC Symbol;Acc:HGNC:3560]
ENSG00000227733	2,02	0,05		
CPM	2,19	0,00	protein_coding	carboxypeptidase M [Source:HGNC Symbol;Acc:HGNC:2311]
GSAP	2,24	0,00	protein_coding	gamma-secretase activating protein [Source:HGNC Symbol;Acc:HGNC:28042]
PDK4	2,31	0,01	protein_coding	pyruvate dehydrogenase kinase 4 [Source:HGNC Symbol;Acc:HGNC:8812]
TIE1	2,39	0,00	protein_coding	tyrosine kinase with immunoglobulin like and EGF like domains 1 [Source:HGNC Symbol;Acc:HGNC:11809]
EEPD1	2,40	0,03	protein_coding	endonuclease/exonuclease/phosphatase family domain containing 1 [Source:HGNC Symbol;Acc:HGNC:22223]
NINL	2,53	0,03	protein_coding	ninein like [Source:HGNC Symbol;Acc:HGNC:29163]
ADGRL3	2,55	0,01	protein_coding	adhesion G protein-coupled receptor L3 [Source:HGNC Symbol;Acc:HGNC:20974]
FAM227A	2,59	0,02	protein_coding	family with sequence similarity 227 member A [Source:HGNC Symbol;Acc:HGNC:44197]
GCNT2	2,62	0,04	protein_coding	glucosaminyl (N-acetyl) transferase 2 (I blood group) [Source:HGNC Symbol;Acc:HGNC:4204]
C2orf16	2,63	0,01		

Gene	Log2FoldChange	padj	Biotype	Description
P2RY10	2,67	0,01	protein_coding	P2Y receptor family member 10 [Source:HGNC Symbol;Acc:HGNC:19906]
EXTL3-AS1	2,80	0,00	lncRNA	EXTL3 antisense RNA 1 [Source:HGNC Symbol;Acc:HGNC:27985]
CXorf65	4,65	0,00	protein_coding	chromosome X open reading frame 65 [Source:HGNC Symbol;Acc:HGNC:33713]
ENSG00000269026	4,81	0,04		
ENSG00000286885	6,57	0,04		
PSG11-AS1	6,67	0,04	lncRNA	PSG11, PSG2 and PSG5 antisense RNA 1 [Source:HGNC Symbol;Acc:HGNC:56358]
PTPRN	6,67	0,00	protein_coding	protein tyrosine phosphatase receptor type N [Source:HGNC Symbol;Acc:HGNC:9676]
XIST	6,68	0,04	lncRNA	X inactive specific transcript [Source:HGNC Symbol;Acc:HGNC:12810]
ENSG00000285772	6,80	0,02		
INMT-MINDY4	7,60	0,00	protein_coding	INMT-MINDY4 readthrough (NMD candidate) [Source:HGNC Symbol;Acc:HGNC:41995]
OR1H1P	7,62	0,00	unprocessed_pseudogene	olfactory receptor family 1 subfamily H member 1 pseudogene [Source:HGNC Symbol;Acc:HGNC:8206]
TGIF2-RAB5IF	7,62	0,01	protein_coding	TGIF2-RAB5IF readthrough [Source:HGNC Symbol;Acc:HGNC:44664]
PDE10A	7,93	0,00	protein_coding	phosphodiesterase 10A [Source:HGNC Symbol;Acc:HGNC:8772]
STAG3L3	7,94	0,00	transcribed_unprocessed_pseudogene	STAG3 cohesin complex component like 3 (pseudogene) [Source:HGNC Symbol;Acc:HGNC:33845]
ENSG00000282740	8,54	0,00		

Annex Table 9. Differential gene expression in LAD2 cells with MITF-silenced versus LAD2 cells with shRNA-NT, in an IgE-independent pathway (MRGPRX2). LAD2 cells were infected with lentivirus (shRNA-NT and MITF shRNA-2) for 5 days. Unstimulated cells were compared.

Gene	Log2FoldChange	padj	Biotype	Description
AK4	-3,871	0,045	protein_coding	adenylate kinase 4 [Source:HGNC Symbol;Acc:HGNC:363]
RGS20	-3,423	0,000	protein_coding	regulator of G protein signaling 20 [Source:HGNC Symbol;Acc:HGNC:14600]
ADM	-3,184	0,024	protein_coding	adrenomedullin [Source:HGNC Symbol;Acc:HGNC:259]
ENSG00000267166	-3,092	0,000		
HILPDA-AS1	-3,059	0,030	lncRNA	HILPDA antisense RNA 1 [Source:HGNC Symbol;Acc:HGNC:55641]
EPHA5-AS1	-3,028	0,000	lncRNA	EPHA5 antisense RNA 1 [Source:HGNC Symbol;Acc:HGNC:50602]
MIR210HG	-3,022	0,019	lncRNA	MIR210 host gene [Source:HGNC Symbol;Acc:HGNC:39524]
DEFB119	-2,978	0,000	protein_coding	defensin beta 119 [Source:HGNC Symbol;Acc:HGNC:18099]
TSBP1	-2,904	0,000	protein_coding	testis expressed basic protein 1 [Source:HGNC Symbol;Acc:HGNC:13922]
GPA33	-2,900	0,001	protein_coding	glycoprotein A33 [Source:HGNC Symbol;Acc:HGNC:4445]
HILPDA	-2,845	0,034	protein_coding	hypoxia inducible lipid droplet associated [Source:HGNC Symbol;Acc:HGNC:28859]
HIF1A-AS3	-2,831	0,045	lncRNA	HIF1A antisense RNA 3 [Source:HGNC Symbol;Acc:HGNC:54284]
CTAGE6	-2,727	0,044	protein_coding	CTAGE family member 6 [Source:HGNC Symbol;Acc:HGNC:28644]
TRPM2	-2,665	0,000	protein_coding	transient receptor potential cation channel subfamily M member 2 [Source:HGNC Symbol;Acc:HGNC:12339]
PDE1A	-2,649	0,001	protein_coding	phosphodiesterase 1A [Source:HGNC Symbol;Acc:HGNC:8774]
CA2	-2,602	0,000	protein_coding	carbonic anhydrase 2 [Source:HGNC Symbol;Acc:HGNC:1373]
IFI44L	-2,592	0,000	protein_coding	interferon induced protein 44 like [Source:HGNC Symbol;Acc:HGNC:17817]
LINC02925	-2,589	0,007	lncRNA	long intergenic non-protein coding RNA 2925 [Source:HGNC Symbol;Acc:HGNC:55756]
ENSG00000286223	-2,583	0,000		
PRTN3	-2,542	0,000	protein_coding	proteinase 3 [Source:HGNC Symbol;Acc:HGNC:9495]
DCDC2	-2,530	0,000	protein_coding	doublecortin domain containing 2 [Source:HGNC Symbol;Acc:HGNC:18141]
RASSF4	-2,528	0,007	protein_coding	Ras association domain family member 4 [Source:HGNC Symbol;Acc:HGNC:20793]
USP2	-2,451	0,000	protein_coding	ubiquitin specific peptidase 2 [Source:HGNC Symbol;Acc:HGNC:12618]
TPBGL-AS1	-2,442	0,005	lncRNA	TPBGL antisense RNA 1 [Source:HGNC Symbol;Acc:HGNC:55506]

Gene	Log2FoldChange	padj	Biotype	Description
EEPD1	-2,426	0,000	protein_coding	endonuclease/exonuclease/phosphatase family domain containing 1 [Source:HGNC Symbol;Acc:HGNC:22223]
ENSG00000181514	-2,422	0,000		
CCL18	-2,410	0,000	protein_coding	C-C motif chemokine ligand 18 [Source:HGNC Symbol;Acc:HGNC:10616]
CCL3L3	-2,400	0,000	protein_coding	C-C motif chemokine ligand 3 like 3 [Source:HGNC Symbol;Acc:HGNC:30554]
ENSG00000213068	-2,300	0,002		
ZC3H11B	-2,290	0,000	protein_coding	zinc finger CCCH-type containing 11B [Source:HGNC Symbol;Acc:HGNC:25659]
TM4SF19-DYNLT2B	-2,271	0,000	protein_coding	TM4SF19-DYNLT2B readthrough (NMD candidate) [Source:HGNC Symbol;Acc:HGNC:49190]
C15orf48	-2,256	0,000	protein_coding	chromosome 15 open reading frame 48 [Source:HGNC Symbol;Acc:HGNC:29898]
GRIP1	-2,240	0,000	protein_coding	glutamate receptor interacting protein 1 [Source:HGNC Symbol;Acc:HGNC:18708]
PGM1	-2,220	0,011	protein_coding	phosphoglucomutase 1 [Source:HGNC Symbol;Acc:HGNC:8905]
CHCHD6	-2,216	0,000	protein_coding	coiled-coil-helix-coiled-coil-helix domain containing 6 [Source:HGNC Symbol;Acc:HGNC:28184]
CD109	-2,202	0,000	protein_coding	CD109 molecule [Source:HGNC Symbol;Acc:HGNC:21685]
PDK1-AS1	-2,193	0,002		
NDRG4	-2,190	0,003	protein_coding	NDRG family member 4 [Source:HGNC Symbol;Acc:HGNC:14466]
RORA	-2,166	0,001	protein_coding	RAR related orphan receptor A [Source:HGNC Symbol;Acc:HGNC:10258]
HMGB3P7	-2,134	0,000	processed_pseudogene	high mobility group box 3 pseudogene 7 [Source:HGNC Symbol;Acc:HGNC:39299]
OR2T8	-2,118	0,004	protein_coding	olfactory receptor family 2 subfamily T member 8 [Source:HGNC Symbol;Acc:HGNC:15020]
HAND2	-2,118	0,004	protein_coding	heart and neural crest derivatives expressed 2 [Source:HGNC Symbol;Acc:HGNC:4808]
VAT1L	-2,115	0,000	protein_coding	vesicle amine transport 1 like [Source:HGNC Symbol;Acc:HGNC:29315]
MYO1E	-2,102	0,027	protein_coding	myosin IE [Source:HGNC Symbol;Acc:HGNC:7599]
SORBS3	-2,094	0,000	protein_coding	sorbin and SH3 domain containing 3 [Source:HGNC Symbol;Acc:HGNC:30907]
ENSG00000236841	-2,090	0,000		
ENSG00000287897	-2,078	0,013		
CCR8	-2,074	0,032	protein_coding	C-C motif chemokine receptor 8 [Source:HGNC Symbol;Acc:HGNC:1609]
ENSG00000288754	-2,045	0,005		
MEOX2	-2,007	0,016	protein_coding	mesenchyme homeobox 2 [Source:HGNC Symbol;Acc:HGNC:7014]
KCNQ5-DT	-1,998	0,000	lncRNA	KCNQ5 divergent transcript [Source:HGNC Symbol;Acc:HGNC:55469]
ACVR1C	-1,994	0,046	protein_coding	activin A receptor type 1C [Source:HGNC Symbol;Acc:HGNC:18123]

Gene	Log2FoldChange	padj	Biotype	Description
ENSG00000289316	-1,984	0,000		
FAM227A	-1,982	0,003	protein_coding	family with sequence similarity 227 member A [Source:HGNC Symbol;Acc:HGNC:44197]
ADAMTS18	-1,951	0,047	protein_coding	ADAM metallopeptidase with thrombospondin type 1 motif 18 [Source:HGNC Symbol;Acc:HGNC:17110]
GPRC5C	-1,934	0,000	protein_coding	G protein-coupled receptor class C group 5 member C [Source:HGNC Symbol;Acc:HGNC:13309]
TRAC	-1,909	0,002	TR_C_gene	T cell receptor alpha constant [Source:HGNC Symbol;Acc:HGNC:12029]
PATL1-DT	-1,905	0,000	lncRNA	PATL1 divergent transcript [Source:HGNC Symbol;Acc:HGNC:55501]
PLSCR5	-1,887	0,000	protein_coding	phospholipid scramblase family member 5 [Source:HGNC Symbol;Acc:HGNC:19952]
CTSH	-1,873	0,000	protein_coding	cathepsin H [Source:HGNC Symbol;Acc:HGNC:2535]
SLC2A3	-1,860	0,026	protein_coding	solute carrier family 2 member 3 [Source:HGNC Symbol;Acc:HGNC:11007]
LINC01050	-1,850	0,022	lncRNA	long intergenic non-protein coding RNA 1050 [Source:HGNC Symbol;Acc:HGNC:49044]
IL1B	-1,839	0,000	protein_coding	interleukin 1 beta [Source:HGNC Symbol;Acc:HGNC:5992]
ABCA1	-1,834	0,000	protein_coding	ATP binding cassette subfamily A member 1 [Source:HGNC Symbol;Acc:HGNC:29]
RTN4R	-1,810	0,000	protein_coding	reticulon 4 receptor [Source:HGNC Symbol;Acc:HGNC:18601]
ENSG00000288849	-1,806	0,004		
OR3D1P	-1,799	0,000	unprocessed_pseudogene	olfactory receptor family 3 subfamily D member 1 pseudogene [Source:HGNC Symbol;Acc:HGNC:25339]
TSPAN10	-1,781	0,000	protein_coding	tetraspanin 10 [Source:HGNC Symbol;Acc:HGNC:29942]
CXCL16	-1,781	0,000	protein_coding	C-X-C motif chemokine ligand 16 [Source:HGNC Symbol;Acc:HGNC:16642]
ENSG00000203279	-1,770	0,023		
ENSG00000264695	-1,764	0,004		
CADM1	-1,760	0,000	protein_coding	cell adhesion molecule 1 [Source:HGNC Symbol;Acc:HGNC:5951]
ENSG00000287891	-1,758	0,000		
FSTL1	-1,758	0,003	protein_coding	follistatin like 1 [Source:HGNC Symbol;Acc:HGNC:3972]
LINC01226	-1,748	0,000	lncRNA	long intergenic non-protein coding RNA 1226 [Source:HGNC Symbol;Acc:HGNC:49678]
LDB3	-1,741	0,000	protein_coding	LIM domain binding 3 [Source:HGNC Symbol;Acc:HGNC:15710]
C7orf57	-1,739	0,023	protein_coding	chromosome 7 open reading frame 57 [Source:HGNC Symbol;Acc:HGNC:22247]
OR14K1	-1,728	0,000	protein_coding	olfactory receptor family 14 subfamily K member 1 [Source:HGNC Symbol;Acc:HGNC:15025]
ENSG00000235749	-1,708	0,000		
ENSG00000289613	-1,695	0,018		

Gene	Log2FoldChange	padj	Biotype	Description
FAM167A	-1,683	0,038	protein_coding	family with sequence similarity 167 member A [Source:HGNC Symbol;Acc:HGNC:15549]
XIRP1	-1,677	0,000	protein_coding	xin actin binding repeat containing 1 [Source:HGNC Symbol;Acc:HGNC:14301]
DARS1-AS1	-1,675	0,001	lncRNA	DARS1 antisense RNA 1 [Source:HGNC Symbol;Acc:HGNC:40170]
TMEM268	-1,670	0,000	protein_coding	transmembrane protein 268 [Source:HGNC Symbol;Acc:HGNC:24513]
GGH	-1,669	0,001	protein_coding	gamma-glutamyl hydrolase [Source:HGNC Symbol;Acc:HGNC:4248]
OR9H1P	-1,666	0,000	protein_coding	olfactory receptor family 9 subfamily H member 1 pseudogene [Source:HGNC Symbol;Acc:HGNC:15038]
ENSG00000289351	-1,649	0,025		
MX1	-1,642	0,000	protein_coding	MX dynamin like GTPase 1 [Source:HGNC Symbol;Acc:HGNC:7532]
JPH4	-1,635	0,000	protein_coding	junctophilin 4 [Source:HGNC Symbol;Acc:HGNC:20156]
RGS4	-1,629	0,013	protein_coding	regulator of G protein signaling 4 [Source:HGNC Symbol;Acc:HGNC:10000]
CCL3	-1,616	0,000	protein_coding	C-C motif chemokine ligand 3 [Source:HGNC Symbol;Acc:HGNC:10627]
ENTPD8	-1,615	0,014	protein_coding	ectonucleoside triphosphate diphosphohydrolase 8 [Source:HGNC Symbol;Acc:HGNC:24860]
PDK1	-1,609	0,016	protein_coding	pyruvate dehydrogenase kinase 1 [Source:HGNC Symbol;Acc:HGNC:8809]
OR2G3	-1,608	0,000	protein_coding	olfactory receptor family 2 subfamily G member 3 [Source:HGNC Symbol;Acc:HGNC:15008]
ENSG00000276012	-1,608	0,000		
ITGBL1	-1,605	0,000	protein_coding	integrin subunit beta like 1 [Source:HGNC Symbol;Acc:HGNC:6164]
LINC02890	-1,604	0,033	lncRNA	long intergenic non-protein coding RNA 2890 [Source:HGNC Symbol;Acc:HGNC:55220]
HAVCR1	-1,600	0,009	protein_coding	hepatitis A virus cellular receptor 1 [Source:HGNC Symbol;Acc:HGNC:17866]
MXI1	-1,595	0,042	protein_coding	MAX interactor 1, dimerization protein [Source:HGNC Symbol;Acc:HGNC:7534]
CCL4L2	-1,586	0,000	protein_coding	C-C motif chemokine ligand 4 like 2 [Source:HGNC Symbol;Acc:HGNC:24066]
ENSG00000272397	-1,585	0,000		
HRH4	-1,582	0,000	protein_coding	histamine receptor H4 [Source:HGNC Symbol;Acc:HGNC:17383]
ANGPT4	-1,581	0,000	protein_coding	angiopoietin 4 [Source:HGNC Symbol;Acc:HGNC:487]
DYNLT4	-1,577	0,031	protein_coding	dynein light chain Tctex-type 4 [Source:HGNC Symbol;Acc:HGNC:32315]
OAS3	-1,576	0,000	protein_coding	2'-5'-oligoadenylate synthetase 3 [Source:HGNC Symbol;Acc:HGNC:8088]
CAMK4	-1,566	0,006	protein_coding	calcium/calmodulin dependent protein kinase IV [Source:HGNC Symbol;Acc:HGNC:1464]
HNRNPH2	-1,563	0,000	protein_coding	heterogeneous nuclear ribonucleoprotein H2 [Source:HGNC Symbol;Acc:HGNC:5042]
P4HA1	-1,560	0,017	protein_coding	prolyl 4-hydroxylase subunit alpha 1 [Source:HGNC Symbol;Acc:HGNC:8546]
SERPINF1	-1,554	0,005	protein_coding	serpin family F member 1 [Source:HGNC Symbol;Acc:HGNC:8824]

Gene	Log2FoldChange	padj	Biotype	Description
PEPD	-1,541	0,000	protein_coding	peptidase D [Source:HGNC Symbol;Acc:HGNC:8840]
DPEP2	-1,536	0,001	protein_coding	dipeptidase 2 [Source:HGNC Symbol;Acc:HGNC:23028]
CTSA	-1,534	0,000	protein_coding	cathepsin A [Source:HGNC Symbol;Acc:HGNC:9251]
SYNE2	-1,534	0,000	protein_coding	spectrin repeat containing nuclear envelope protein 2 [Source:HGNC Symbol;Acc:HGNC:17084]
APOC1	-1,529	0,003	protein_coding	apolipoprotein C1 [Source:HGNC Symbol;Acc:HGNC:607]
ZMYND15	-1,524	0,000	protein_coding	zinc finger MYND-type containing 15 [Source:HGNC Symbol;Acc:HGNC:20997]
BIRC7	-1,516	0,003	protein_coding	baculoviral IAP repeat containing 7 [Source:HGNC Symbol;Acc:HGNC:13702]
DENND6A-DT	-1,509	0,004	lncRNA	DENND6A divergent transcript [Source:HGNC Symbol;Acc:HGNC:51592]
KCNQ5	-1,503	0,000	protein_coding	potassium voltage-gated channel subfamily Q member 5 [Source:HGNC Symbol;Acc:HGNC:6299]
CTTN	-1,501	0,000	protein_coding	cortactin [Source:HGNC Symbol;Acc:HGNC:3338]
SERPINB1	-1,499	0,000	protein_coding	serpin family B member 1 [Source:HGNC Symbol;Acc:HGNC:3311]
OR14L1P	-1,493	0,003		
IFI6	-1,482	0,000	protein_coding	interferon alpha inducible protein 6 [Source:HGNC Symbol;Acc:HGNC:4054]
LRRC38	-1,480	0,023	protein_coding	leucine rich repeat containing 38 [Source:HGNC Symbol;Acc:HGNC:27005]
ENSG00000237422	-1,478	0,000		
LINC00589	-1,468	0,005	lncRNA	long intergenic non-protein coding RNA 589 [Source:HGNC Symbol;Acc:HGNC:32299]
OR2G2	-1,461	0,000	protein_coding	olfactory receptor family 2 subfamily G member 2 [Source:HGNC Symbol;Acc:HGNC:15007]
DNAH7	-1,455	0,000	protein_coding	dynein axonemal heavy chain 7 [Source:HGNC Symbol;Acc:HGNC:18661]
ENO2	-1,449	0,017	protein_coding	enolase 2 [Source:HGNC Symbol;Acc:HGNC:3353]
PRAG1	-1,449	0,014	protein_coding	PEAK1 related, kinase-activating pseudokinase 1 [Source:HGNC Symbol;Acc:HGNC:25438]
MEGF6	-1,447	0,000	protein_coding	multiple EGF like domains 6 [Source:HGNC Symbol;Acc:HGNC:3232]
ADGRA2	-1,440	0,000	protein_coding	adhesion G protein-coupled receptor A2 [Source:HGNC Symbol;Acc:HGNC:17849]
ERMN	-1,434	0,000	protein_coding	ermin [Source:HGNC Symbol;Acc:HGNC:29208]
ENSG00000276627	-1,421	0,005		
TSHZ2	-1,420	0,000	protein_coding	teashirt zinc finger homeobox 2 [Source:HGNC Symbol;Acc:HGNC:13010]
LINC00930	-1,416	0,025	lncRNA	long intergenic non-protein coding RNA 930 [Source:HGNC Symbol;Acc:HGNC:48620]
RPL17P50	-1,409	0,039	processed_pseudogene	ribosomal protein L17 pseudogene 50 [Source:HGNC Symbol;Acc:HGNC:45098]
SBF2-AS1	-1,407	0,000	lncRNA	SBF2 antisense RNA 1 [Source:HGNC Symbol;Acc:HGNC:27438]

Gene	Log2FoldChange	padj	Biotype	Description
SNX21	-1,407	0,025	protein_coding	sorting nexin family member 21 [Source:HGNC Symbol;Acc:HGNC:16154]
C1orf54	-1,403	0,000	protein_coding	chromosome 1 open reading frame 54 [Source:HGNC Symbol;Acc:HGNC:26258]
VLDLR	-1,399	0,003	protein_coding	very low density lipoprotein receptor [Source:HGNC Symbol;Acc:HGNC:12698]
BTBD17	-1,390	0,046	protein_coding	BTB domain containing 17 [Source:HGNC Symbol;Acc:HGNC:33758]
ENSG00000176349	-1,388	0,047		
OAS2	-1,385	0,000	protein_coding	2'-5'-oligoadenylate synthetase 2 [Source:HGNC Symbol;Acc:HGNC:8087]
ENSG00000287611	-1,381	0,000		
MAS1	-1,380	0,000	protein_coding	MAS1 proto-oncogene, G protein-coupled receptor [Source:HGNC Symbol;Acc:HGNC:6899]
HS3ST2	-1,369	0,000	protein_coding	heparan sulfate-glucosamine 3-sulfotransferase 2 [Source:HGNC Symbol;Acc:HGNC:5195]
IFIT1	-1,369	0,000	protein_coding	interferon induced protein with tetratricopeptide repeats 1 [Source:HGNC Symbol;Acc:HGNC:5407]
FXYD1	-1,369	0,005	protein_coding	FXYD domain containing ion transport regulator 1 [Source:HGNC Symbol;Acc:HGNC:4025]
TM4SF19	-1,367	0,000	protein_coding	transmembrane 4 L six family member 19 [Source:HGNC Symbol;Acc:HGNC:25167]
STARD10	-1,363	0,000	protein_coding	StAR related lipid transfer domain containing 10 [Source:HGNC Symbol;Acc:HGNC:10666]
GPR153	-1,362	0,000	protein_coding	G protein-coupled receptor 153 [Source:HGNC Symbol;Acc:HGNC:23618]
TNNI2	-1,352	0,005	protein_coding	troponin I2, fast skeletal type [Source:HGNC Symbol;Acc:HGNC:11946]
GPNMB	-1,352	0,000	protein_coding	glycoprotein nmb [Source:HGNC Symbol;Acc:HGNC:4462]
ENSG00000259952	-1,346	0,031		
TMEM178A	-1,344	0,018	protein_coding	transmembrane protein 178A [Source:HGNC Symbol;Acc:HGNC:28517]
AMACR	-1,338	0,000	protein_coding	alpha-methylacyl-CoA racemase [Source:HGNC Symbol;Acc:HGNC:451]
EPHA5	-1,336	0,006	protein_coding	EPH receptor A5 [Source:HGNC Symbol;Acc:HGNC:3389]
STXBP5-AS1	-1,334	0,000	lncRNA	STXBP5 antisense RNA 1 [Source:HGNC Symbol;Acc:HGNC:44183]
MAP3K6	-1,327	0,000	protein_coding	mitogen-activated protein kinase kinase kinase 6 [Source:HGNC Symbol;Acc:HGNC:6858]
ENSG00000288965	-1,323	0,016		
ENSG00000279464	-1,319	0,038		
ENSG00000229771	-1,318	0,000		
ENSG00000286376	-1,317	0,004		
NDRG1	-1,312	0,000	protein_coding	N-myc downstream regulated 1 [Source:HGNC Symbol;Acc:HGNC:7679]
FGR	-1,310	0,000	protein_coding	FGR proto-oncogene, Src family tyrosine kinase [Source:HGNC Symbol;Acc:HGNC:3697]

Gene	Log2FoldChange	padj	Biotype	Description
AKAP5	-1,309	0,000	protein_coding	A-kinase anchoring protein 5 [Source:HGNC Symbol;Acc:HGNC:375]
UBA6	-1,307	0,033	protein_coding	ubiquitin like modifier activating enzyme 6 [Source:HGNC Symbol;Acc:HGNC:25581]
PADI2	-1,303	0,000	protein_coding	peptidyl arginine deiminase 2 [Source:HGNC Symbol;Acc:HGNC:18341]
BPNT2	-1,289	0,000	protein_coding	3'(2'), 5'-bisphosphate nucleotidase 2 [Source:HGNC Symbol;Acc:HGNC:26019]
CMTM7	-1,286	0,001	protein_coding	CKLF like MARVEL transmembrane domain containing 7 [Source:HGNC Symbol;Acc:HGNC:19178]
ABCA6	-1,284	0,040	protein_coding	ATP binding cassette subfamily A member 6 [Source:HGNC Symbol;Acc:HGNC:36]
CXXC4	-1,281	0,000	protein_coding	CXXC finger protein 4 [Source:HGNC Symbol;Acc:HGNC:24593]
LINC01010	-1,276	0,000	lncRNA	long intergenic non-protein coding RNA 1010 [Source:HGNC Symbol;Acc:HGNC:48978]
RPL17P43	-1,273	0,040	processed_pseudogene	ribosomal protein L17 pseudogene 43 [Source:HGNC Symbol;Acc:HGNC:35996]
ISCA2	-1,270	0,000	protein_coding	iron-sulfur cluster assembly 2 [Source:HGNC Symbol;Acc:HGNC:19857]
GUCA1C	-1,264	0,000	protein_coding	guanylate cyclase activator 1C [Source:HGNC Symbol;Acc:HGNC:4680]
RTN4RL1	-1,258	0,000	protein_coding	reticulon 4 receptor like 1 [Source:HGNC Symbol;Acc:HGNC:21329]
ENSG00000230882	-1,256	0,000		
ZEB1	-1,255	0,002	protein_coding	zinc finger E-box binding homeobox 1 [Source:HGNC Symbol;Acc:HGNC:11642]
LINC00511	-1,249	0,000	lncRNA	long intergenic non-protein coding RNA 511 [Source:HGNC Symbol;Acc:HGNC:43564]
ENSG00000287737	-1,247	0,005		
ZFYVE26	-1,243	0,031	protein_coding	zinc finger FYVE-type containing 26 [Source:HGNC Symbol;Acc:HGNC:20761]
ROCK1P1	-1,243	0,000	transcribed_unprocessed_pseudogene	Rho associated coiled-coil containing protein kinase 1 pseudogene 1 [Source:HGNC Symbol;Acc:HGNC:37832]
NOX5	-1,240	0,022	protein_coding	NADPH oxidase 5 [Source:HGNC Symbol;Acc:HGNC:14874]
CCNG2	-1,239	0,000	protein_coding	cyclin G2 [Source:HGNC Symbol;Acc:HGNC:1593]
LINC01117	-1,238	0,005	lncRNA	long intergenic non-protein coding RNA 1117 [Source:HGNC Symbol;Acc:HGNC:49260]
ENSG00000271858	-1,236	0,008		
NUP62CL	-1,234	0,043	protein_coding	nucleoporin 62 C-terminal like [Source:HGNC Symbol;Acc:HGNC:25960]
RABGEF1P3	-1,232	0,000	transcribed_unprocessed_pseudogene	RABGEF1 pseudogene 3 [Source:HGNC Symbol;Acc:HGNC:55753]
TDRD3	-1,232	0,000	protein_coding	tudor domain containing 3 [Source:HGNC Symbol;Acc:HGNC:20612]
LINC02365	-1,229	0,018	lncRNA	long intergenic non-protein coding RNA 2365 [Source:HGNC Symbol;Acc:HGNC:53285]
STAMBPL1	-1,228	0,000	protein_coding	STAM binding protein like 1 [Source:HGNC Symbol;Acc:HGNC:24105]
THBS4-AS1	-1,222	0,000	lncRNA	THBS4 antisense RNA 1 [Source:HGNC Symbol;Acc:HGNC:40583]

Gene	Log2FoldChange	padj	Biotype	Description
VWA1	-1,220	0,000	protein_coding	von Willebrand factor A domain containing 1 [Source:HGNC Symbol;Acc:HGNC:30910]
PRKAR1A	-1,207	0,000	protein_coding	protein kinase cAMP-dependent type I regulatory subunit alpha [Source:HGNC Symbol;Acc:HGNC:9388]
CLIC4	-1,203	0,014	protein_coding	chloride intracellular channel 4 [Source:HGNC Symbol;Acc:HGNC:13518]
YPEL4	-1,203	0,005	protein_coding	yippee like 4 [Source:HGNC Symbol;Acc:HGNC:18328]
PDZD7	-1,198	0,003	protein_coding	PDZ domain containing 7 [Source:HGNC Symbol;Acc:HGNC:26257]
HPS4	-1,197	0,000	protein_coding	HPS4 biogenesis of lysosomal organelles complex 3 subunit 2 [Source:HGNC Symbol;Acc:HGNC:15844]
CRYGC	-1,191	0,000	protein_coding	crystallin gamma C [Source:HGNC Symbol;Acc:HGNC:2410]
IFIT2	-1,191	0,000	protein_coding	interferon induced protein with tetratricopeptide repeats 2 [Source:HGNC Symbol;Acc:HGNC:5409]
AMZ2	-1,190	0,000	protein_coding	archaelysin family metallopeptidase 2 [Source:HGNC Symbol;Acc:HGNC:28041]
RGS5-AS1	-1,187	0,018	lncRNA	RGS5 antisense RNA 1 [Source:HGNC Symbol;Acc:HGNC:40504]
ANLN	-1,186	0,004	protein_coding	anillin, actin binding protein [Source:HGNC Symbol;Acc:HGNC:14082]
ENSG00000255750	-1,185	0,008		
ULK4P1	-1,184	0,025	lncRNA	ULK4 pseudogene 1 [Source:NCBI gene (formerly Entrezgene);Acc:89838]
MDGA2	-1,180	0,014	protein_coding	MAM domain containing glycosylphosphatidylinositol anchor 2 [Source:HGNC Symbol;Acc:HGNC:19835]
ARMC2	-1,179	0,014	protein_coding	armadillo repeat containing 2 [Source:HGNC Symbol;Acc:HGNC:23045]
ENSG00000273771	-1,176	0,029		
MAP9-AS1	-1,176	0,036	lncRNA	MAP9 antisense RNA 1 [Source:HGNC Symbol;Acc:HGNC:56110]
CDSN	-1,175	0,011	protein_coding	corneodesmosin [Source:HGNC Symbol;Acc:HGNC:1802]
C5orf47	-1,174	0,025	protein_coding	chromosome 5 open reading frame 47 [Source:HGNC Symbol;Acc:HGNC:27026]
DTX1	-1,170	0,003	protein_coding	deltex E3 ubiquitin ligase 1 [Source:HGNC Symbol;Acc:HGNC:3060]
ENSG00000234389	-1,169	0,001		
CCND2	-1,168	0,013	protein_coding	cyclin D2 [Source:HGNC Symbol;Acc:HGNC:1583]
ELFN1	-1,167	0,000	protein_coding	extracellular leucine rich repeat and fibronectin type III domain containing 1 [Source:HGNC Symbol;Acc:HGNC:33154]
ENTPD1	-1,166	0,001	protein_coding	ectonucleoside triphosphate diphosphohydrolase 1 [Source:HGNC Symbol;Acc:HGNC:3363]
DERL3	-1,166	0,029	protein_coding	derlin 3 [Source:HGNC Symbol;Acc:HGNC:14236]
AK5	-1,162	0,000	protein_coding	adenylate kinase 5 [Source:HGNC Symbol;Acc:HGNC:365]
CPNE5	-1,157	0,046	protein_coding	copine 5 [Source:HGNC Symbol;Acc:HGNC:2318]
OAS1	-1,154	0,000	protein_coding	2'-5'-oligoadenylate synthetase 1 [Source:HGNC Symbol;Acc:HGNC:8086]

Gene	Log2FoldChange	padj	Biotype	Description
ZC3H12C	-1,154	0,014	protein_coding	zinc finger CCCH-type containing 12C [Source:HGNC Symbol;Acc:HGNC:29362]
OR10D1P	-1,152	0,005	unprocessed_pseudogene	olfactory receptor family 10 subfamily D member 1 pseudogene [Source:HGNC Symbol;Acc:HGNC:8166]
PLXNA1	-1,152	0,000	protein_coding	plexin A1 [Source:HGNC Symbol;Acc:HGNC:9099]
CTSF	-1,148	0,000	protein_coding	cathepsin F [Source:HGNC Symbol;Acc:HGNC:2531]
ENSG00000290729	-1,148	0,002		
ACTA2-AS1	-1,147	0,015	lncRNA	ACTA2 antisense RNA 1 [Source:HGNC Symbol;Acc:HGNC:45169]
DST	-1,145	0,040	protein_coding	dystonin [Source:HGNC Symbol;Acc:HGNC:1090]
LDHAP7	-1,139	0,013	processed_pseudogene	lactate dehydrogenase A pseudogene 7 [Source:HGNC Symbol;Acc:HGNC:23144]
CTSD	-1,138	0,000	protein_coding	cathepsin D [Source:HGNC Symbol;Acc:HGNC:2529]
NSG2	-1,137	0,018	protein_coding	neuronal vesicle trafficking associated 2 [Source:HGNC Symbol;Acc:HGNC:24955]
MCF2L2	-1,131	0,000	protein_coding	MCF.2 cell line derived transforming sequence-like 2 [Source:HGNC Symbol;Acc:HGNC:30319]
CLSPN	-1,131	0,002	protein_coding	claspin [Source:HGNC Symbol;Acc:HGNC:19715]
ESR2	-1,131	0,000	protein_coding	estrogen receptor 2 [Source:HGNC Symbol;Acc:HGNC:3468]
KREMEN1	-1,130	0,000	protein_coding	kringle containing transmembrane protein 1 [Source:HGNC Symbol;Acc:HGNC:17550]
SNAPC1	-1,130	0,000	protein_coding	small nuclear RNA activating complex polypeptide 1 [Source:HGNC Symbol;Acc:HGNC:11134]
ENSG00000287481	-1,126	0,008		
SULT1C2	-1,124	0,000	protein_coding	sulfotransferase family 1C member 2 [Source:HGNC Symbol;Acc:HGNC:11456]
ARPIN-AP3S2	-1,123	0,039	protein_coding	ARPIN-AP3S2 readthrough [Source:HGNC Symbol;Acc:HGNC:38824]
HTN1	-1,117	0,048	protein_coding	histatin 1 [Source:HGNC Symbol;Acc:HGNC:5283]
ENSG00000254362	-1,116	0,001		
CCNE1	-1,116	0,040	protein_coding	cyclin E1 [Source:HGNC Symbol;Acc:HGNC:1589]
SLC43A3	-1,115	0,000	protein_coding	solute carrier family 43 member 3 [Source:HGNC Symbol;Acc:HGNC:17466]
DHX58	-1,105	0,000	protein_coding	DExH-box helicase 58 [Source:HGNC Symbol;Acc:HGNC:29517]
ENSG00000260337	-1,099	0,019		
AQP10	-1,098	0,000	protein_coding	aquaporin 10 [Source:HGNC Symbol;Acc:HGNC:16029]
HERC6	-1,096	0,000	protein_coding	HECT and RLD domain containing E3 ubiquitin protein ligase family member 6 [Source:HGNC Symbol;Acc:HGNC:26072]
WNT9A	-1,092	0,004	protein_coding	Wnt family member 9A [Source:HGNC Symbol;Acc:HGNC:12778]
PDZD4	-1,090	0,000	protein_coding	PDZ domain containing 4 [Source:HGNC Symbol;Acc:HGNC:21167]

Gene	Log2FoldChange	padj	Biotype	Description
SCD	-1,088	0,019	protein_coding	stearoyl-CoA desaturase [Source:HGNC Symbol;Acc:HGNC:10571]
SNX3	-1,088	0,000	protein_coding	sorting nexin 3 [Source:HGNC Symbol;Acc:HGNC:11174]
NT5DC3	-1,088	0,000	protein_coding	5'-nucleotidase domain containing 3 [Source:HGNC Symbol;Acc:HGNC:30826]
LINC01011	-1,085	0,002	lncRNA	long intergenic non-protein coding RNA 1011 [Source:HGNC Symbol;Acc:HGNC:33812]
RHPN1	-1,074	0,014	protein_coding	rhophilin Rho GTPase binding protein 1 [Source:HGNC Symbol;Acc:HGNC:19973]
IFI30	-1,073	0,022	protein_coding	IFI30 lysosomal thiol reductase [Source:HGNC Symbol;Acc:HGNC:5398]
MAPT	-1,066	0,036	protein_coding	microtubule associated protein tau [Source:HGNC Symbol;Acc:HGNC:6893]
CEP55	-1,066	0,027	protein_coding	centrosomal protein 55 [Source:HGNC Symbol;Acc:HGNC:1161]
DTL	-1,064	0,020	protein_coding	denticleless E3 ubiquitin protein ligase homolog [Source:HGNC Symbol;Acc:HGNC:30288]
KANK2	-1,063	0,003	protein_coding	KN motif and ankyrin repeat domains 2 [Source:HGNC Symbol;Acc:HGNC:29300]
MIR3150BHG	-1,060	0,003	lncRNA	MIR3150B host gene [Source:HGNC Symbol;Acc:HGNC:52000]
ENSG00000274767	-1,057	0,001		
LINC02298	-1,055	0,002	lncRNA	long intergenic non-protein coding RNA 2298 [Source:HGNC Symbol;Acc:HGNC:53216]
REPS2	-1,054	0,007	protein_coding	RALBP1 associated Eps domain containing 2 [Source:HGNC Symbol;Acc:HGNC:9963]
TOMM20	-1,053	0,000	protein_coding	translocase of outer mitochondrial membrane 20 [Source:HGNC Symbol;Acc:HGNC:20947]
HAVCR2	-1,051	0,000	protein_coding	hepatitis A virus cellular receptor 2 [Source:HGNC Symbol;Acc:HGNC:18437]
USE1	-1,049	0,007	protein_coding	unconventional SNARE in the ER 1 [Source:HGNC Symbol;Acc:HGNC:30882]
LINC01119	-1,046	0,040	lncRNA	long intergenic non-protein coding RNA 1119 [Source:HGNC Symbol;Acc:HGNC:49262]
LMF1-AS1	-1,044	0,000	lncRNA	LMF1 antisense RNA 1 [Source:HGNC Symbol;Acc:HGNC:50469]
TMEM18	-1,042	0,000	protein_coding	transmembrane protein 18 [Source:HGNC Symbol;Acc:HGNC:25257]
OTOAP1	-1,041	0,021	transcribed_unprocessed_pseudogene	OTOA pseudogene 1 [Source:HGNC Symbol;Acc:HGNC:53869]
IFITM1	-1,040	0,000	protein_coding	interferon induced transmembrane protein 1 [Source:HGNC Symbol;Acc:HGNC:5412]
ADAMTSL4	-1,034	0,002	protein_coding	ADAMTS like 4 [Source:HGNC Symbol;Acc:HGNC:19706]
FRMD6	-1,031	0,034	protein_coding	FERM domain containing 6 [Source:HGNC Symbol;Acc:HGNC:19839]
FAM117B	-1,029	0,001	protein_coding	family with sequence similarity 117 member B [Source:HGNC Symbol;Acc:HGNC:14440]
ODF3B	-1,028	0,009		
PCED1B	-1,027	0,000	protein_coding	PC-esterase domain containing 1B [Source:HGNC Symbol;Acc:HGNC:28255]
ATP5F1B	-1,027	0,000	protein_coding	ATP synthase F1 subunit beta [Source:HGNC Symbol;Acc:HGNC:830]

Gene	Log2FoldChange	padj	Biotype	Description
PLIN2	-1,026	0,000	protein_coding	perilipin 2 [Source:HGNC Symbol;Acc:HGNC:248]
SLAMF7	-1,026	0,000	protein_coding	SLAM family member 7 [Source:HGNC Symbol;Acc:HGNC:21394]
AP1S2	-1,023	0,000	protein_coding	adaptor related protein complex 1 subunit sigma 2 [Source:HGNC Symbol;Acc:HGNC:560]
DUSP14	-1,020	0,000	protein_coding	dual specificity phosphatase 14 [Source:HGNC Symbol;Acc:HGNC:17007]
CUL4A	-1,018	0,000	protein_coding	cullin 4A [Source:HGNC Symbol;Acc:HGNC:2554]
IFIT3	-1,012	0,000	protein_coding	interferon induced protein with tetratricopeptide repeats 3 [Source:HGNC Symbol;Acc:HGNC:5411]
HCN2	-1,011	0,000	protein_coding	hyperpolarization activated cyclic nucleotide gated potassium and sodium channel 2 [Source:HGNC Symbol;Acc:HGNC:4846]
TRAV8-5	-1,009	0,002	TR_V_pseudogene	T cell receptor alpha variable 8-5 (pseudogene) [Source:HGNC Symbol;Acc:HGNC:12150]
ADAMTSL3	-1,007	0,000	protein_coding	ADAMTS like 3 [Source:HGNC Symbol;Acc:HGNC:14633]
ENSG00000289851	-1,007	0,027		
OTOA	-1,006	0,001	protein_coding	otoancorin [Source:HGNC Symbol;Acc:HGNC:16378]
MYO10	-1,005	0,000	protein_coding	myosin X [Source:HGNC Symbol;Acc:HGNC:7593]
CCL4	-1,001	0,008	protein_coding	C-C motif chemokine ligand 4 [Source:HGNC Symbol;Acc:HGNC:10630]
ARTN	1,000	0,000	protein_coding	artemin [Source:HGNC Symbol;Acc:HGNC:727]
TNXB	1,000	0,000	protein_coding	tenascin XB [Source:HGNC Symbol;Acc:HGNC:11976]
RFLNB	1,002	0,018	protein_coding	refilin B [Source:HGNC Symbol;Acc:HGNC:28705]
ENSG00000267436	1,015	0,038		
PERPP2	1,017	0,031	transcribed_processed_pseudogene	PERP pseudogene 2 [Source:HGNC Symbol;Acc:HGNC:56620]
DUSP6	1,018	0,000	protein_coding	dual specificity phosphatase 6 [Source:HGNC Symbol;Acc:HGNC:3072]
ENSG00000279129	1,020	0,005		
MT1E	1,020	0,000	protein_coding	metallothionein 1E [Source:HGNC Symbol;Acc:HGNC:7397]
FSIP2	1,022	0,000	protein_coding	fibrous sheath interacting protein 2 [Source:HGNC Symbol;Acc:HGNC:21675]
LINC02475	1,026	0,040	lncRNA	long intergenic non-protein coding RNA 2475 [Source:HGNC Symbol;Acc:HGNC:53418]

Gene	Log2FoldChange	padj	Biotype	Description
SPOCK1	1,026	0,022	protein_coding	SPARC (osteonectin), cwcv and kazal like domains proteoglycan 1 [Source:HGNC Symbol;Acc:HGNC:11251]
SLC22A20P	1,030	0,000	transcribed_unitary_pseudogene	solute carrier family 22 member 20, pseudogene [Source:HGNC Symbol;Acc:HGNC:29867]
SLC23A3	1,035	0,024	protein_coding	solute carrier family 23 member 3 [Source:HGNC Symbol;Acc:HGNC:20601]
ENSG00000280537	1,037	0,031		
AMH	1,039	0,000	protein_coding	anti-Mullerian hormone [Source:HGNC Symbol;Acc:HGNC:464]
TSPAN6	1,042	0,020	protein_coding	tetraspanin 6 [Source:HGNC Symbol;Acc:HGNC:11858]
C1GALT1P2	1,045	0,000	processed_pseudogene	C1GALT1 pseudogene 2 [Source:HGNC Symbol;Acc:HGNC:51615]
ITPRID2-DT	1,046	0,000	lncRNA	ITPRID2 divergent transcript [Source:HGNC Symbol;Acc:HGNC:55386]
IGSF3	1,059	0,000	protein_coding	immunoglobulin superfamily member 3 [Source:HGNC Symbol;Acc:HGNC:5950]
KCNIP1-OT1	1,059	0,001	lncRNA	KCNIP1 overlapping transcript 1 [Source:HGNC Symbol;Acc:HGNC:40320]
KCNIP1	1,064	0,002	protein_coding	potassium voltage-gated channel interacting protein 1 [Source:HGNC Symbol;Acc:HGNC:15521]
POU2F2	1,068	0,050	protein_coding	POU class 2 homeobox 2 [Source:HGNC Symbol;Acc:HGNC:9213]
EFCAB12	1,074	0,023	protein_coding	EF-hand calcium binding domain 12 [Source:HGNC Symbol;Acc:HGNC:28061]
PILRA	1,076	0,001	protein_coding	paired immunoglobin like type 2 receptor alpha [Source:HGNC Symbol;Acc:HGNC:20396]
ENSG00000250397	1,076	0,031		
ANKRD55	1,077	0,016	protein_coding	ankyrin repeat domain 55 [Source:HGNC Symbol;Acc:HGNC:25681]
ENSG00000260182	1,079	0,000		
ENSG00000247679	1,080	0,000		
CNRIP1	1,085	0,000	protein_coding	cannabinoid receptor interacting protein 1 [Source:HGNC Symbol;Acc:HGNC:24546]
RN7SL587P	1,087	0,027	misc_RNA	RNA, 7SL, cytoplasmic 587, pseudogene [Source:HGNC Symbol;Acc:HGNC:46603]
WFIKKN1	1,096	0,000	protein_coding	WAP, follistatin/kazal, immunoglobulin, kunitz and netrin domain containing 1 [Source:HGNC Symbol;Acc:HGNC:30912]
FGF11	1,113	0,000	protein_coding	fibroblast growth factor 11 [Source:HGNC Symbol;Acc:HGNC:3667]
ENSG00000233968	1,113	0,000		
ENSG00000232828	1,115	0,011		

Gene	Log2FoldChange	padj	Biotype	Description
RIPOR2	1,115	0,000	protein_coding	RHO family interacting cell polarization regulator 2 [Source:HGNC Symbol;Acc:HGNC:13872]
SAP25	1,116	0,000	protein_coding	Sin3A associated protein 25 [Source:HGNC Symbol;Acc:HGNC:41908]
SPTBN2	1,119	0,000	protein_coding	spectrin beta, non-erythrocytic 2 [Source:HGNC Symbol;Acc:HGNC:11276]
ENSG00000242861	1,120	0,001		
ENSG00000264659	1,123	0,000		
GFRA2	1,130	0,042	protein_coding	GDNF family receptor alpha 2 [Source:HGNC Symbol;Acc:HGNC:4244]
ZNF521	1,136	0,000	protein_coding	zinc finger protein 521 [Source:HGNC Symbol;Acc:HGNC:24605]
NID2	1,139	0,000	protein_coding	nidogen 2 [Source:HGNC Symbol;Acc:HGNC:13389]
ABCA15P	1,145	0,001	transcribed_unitary_pseudogene	ATP binding cassette subfamily A member 15, pseudogene [Source:HGNC Symbol;Acc:HGNC:34405]
ENSG00000248015	1,157	0,000		
FAT3	1,158	0,015	protein_coding	FAT atypical cadherin 3 [Source:HGNC Symbol;Acc:HGNC:23112]
AIFM3	1,166	0,004	protein_coding	apoptosis inducing factor mitochondria associated 3 [Source:HGNC Symbol;Acc:HGNC:26398]
MCOLN2	1,166	0,021	protein_coding	mucolipin TRP cation channel 2 [Source:HGNC Symbol;Acc:HGNC:13357]
CYP27B1	1,177	0,016	protein_coding	cytochrome P450 family 27 subfamily B member 1 [Source:HGNC Symbol;Acc:HGNC:2606]
ENSG00000236833	1,180	0,049		
AFF2	1,182	0,000	protein_coding	ALF transcription elongation factor 2 [Source:HGNC Symbol;Acc:HGNC:3776]
KIF9	1,185	0,002	protein_coding	kinesin family member 9 [Source:HGNC Symbol;Acc:HGNC:16666]
AP1G2-AS1	1,188	0,000	lncRNA	AP1G2 antisense RNA 1 [Source:HGNC Symbol;Acc:HGNC:55442]
RPL5P21	1,200	0,000	processed_pseudogene	ribosomal protein L5 pseudogene 21 [Source:HGNC Symbol;Acc:HGNC:37029]
RRM2P3	1,200	0,003	processed_pseudogene	ribonucleotide reductase M2 polypeptide pseudogene 3 [Source:HGNC Symbol;Acc:HGNC:10455]
FGFR4	1,202	0,003	protein_coding	fibroblast growth factor receptor 4 [Source:HGNC Symbol;Acc:HGNC:3691]
CFP	1,209	0,011	protein_coding	complement factor properdin [Source:HGNC Symbol;Acc:HGNC:8864]
SYTL4	1,209	0,000	protein_coding	synaptotagmin like 4 [Source:HGNC Symbol;Acc:HGNC:15588]
SPRED3	1,220	0,003	protein_coding	sprouty related EVH1 domain containing 3 [Source:HGNC Symbol;Acc:HGNC:31041]
CEBPA	1,223	0,037	protein_coding	CCAAT enhancer binding protein alpha [Source:HGNC Symbol;Acc:HGNC:1833]
NKD2	1,224	0,000	protein_coding	NKD inhibitor of WNT signaling pathway 2 [Source:HGNC Symbol;Acc:HGNC:17046]
GRIN2C	1,230	0,000	protein_coding	glutamate ionotropic receptor NMDA type subunit 2C [Source:HGNC Symbol;Acc:HGNC:4587]
ENSG00000248791	1,232	0,009		

Gene	Log2FoldChange	padj	Biotype	Description
PDE3A	1,234	0,000	protein_coding	phosphodiesterase 3A [Source:HGNC Symbol;Acc:HGNC:8778]
ACAA2P1	1,238	0,003	transcribed_processed_pseudogene	ACAA2 pseudogene 1 [Source:HGNC Symbol;Acc:HGNC:55880]
F2RL3	1,251	0,000	protein_coding	F2R like thrombin or trypsin receptor 3 [Source:HGNC Symbol;Acc:HGNC:3540]
SNX29P1	1,252	0,016	unprocessed_pseudogene	sorting nexin 29 pseudogene 1 [Source:HGNC Symbol;Acc:HGNC:31913]
TG	1,273	0,000	protein_coding	thyroglobulin [Source:HGNC Symbol;Acc:HGNC:11764]
KCND1	1,277	0,000	protein_coding	potassium voltage-gated channel subfamily D member 1 [Source:HGNC Symbol;Acc:HGNC:6237]
MYCN	1,277	0,044	protein_coding	MYCN proto-oncogene, bHLH transcription factor [Source:HGNC Symbol;Acc:HGNC:7559]
LY6G5C	1,283	0,000	protein_coding	lymphocyte antigen 6 family member G5C [Source:HGNC Symbol;Acc:HGNC:13932]
TAS1R3	1,291	0,008	protein_coding	taste 1 receptor member 3 [Source:HGNC Symbol;Acc:HGNC:15661]
HLF	1,294	0,049	protein_coding	HLF transcription factor, PAR bZIP family member [Source:HGNC Symbol;Acc:HGNC:4977]
ITGA2B	1,306	0,000	protein_coding	integrin subunit alpha 2b [Source:HGNC Symbol;Acc:HGNC:6138]
ENSG00000290665	1,310	0,047		
ENSG00000286607	1,310	0,008		
NKPD1	1,321	0,005	protein_coding	NTPase KAP family P-loop domain containing 1 [Source:HGNC Symbol;Acc:HGNC:24739]
ENSG00000270149	1,326	0,016		
LAIR1	1,329	0,018	protein_coding	leukocyte associated immunoglobulin like receptor 1 [Source:HGNC Symbol;Acc:HGNC:6477]
MAP3K5-AS2	1,331	0,023	lncRNA	MAP3K5 antisense RNA 2 [Source:HGNC Symbol;Acc:HGNC:56125]
ASGR1	1,332	0,000	protein_coding	asialoglycoprotein receptor 1 [Source:HGNC Symbol;Acc:HGNC:742]
TREX2	1,334	0,041	protein_coding	three prime repair exonuclease 2 [Source:HGNC Symbol;Acc:HGNC:12270]
CHRNA5	1,339	0,038	protein_coding	cholinergic receptor nicotinic alpha 5 subunit [Source:HGNC Symbol;Acc:HGNC:1959]
DISP2	1,354	0,000	protein_coding	dispatched RND transporter family member 2 [Source:HGNC Symbol;Acc:HGNC:19712]
TEX15	1,355	0,001	protein_coding	testis expressed 15, meiosis and synapsis associated [Source:HGNC Symbol;Acc:HGNC:11738]
ENSG00000278997	1,360	0,000		
PDGFC	1,364	0,000	protein_coding	platelet derived growth factor C [Source:HGNC Symbol;Acc:HGNC:8801]
BCAN-AS1	1,368	0,000	lncRNA	BCAN antisense RNA 1 [Source:HGNC Symbol;Acc:HGNC:55233]
MIR181A1HG	1,378	0,003	lncRNA	MIR181A1 host gene [Source:HGNC Symbol;Acc:HGNC:48659]
LAMB2P1	1,382	0,000	unprocessed_pseudogene	laminin subunit beta 2 pseudogene 1 [Source:HGNC Symbol;Acc:HGNC:6488]

Gene	Log2FoldChange	padj	Biotype	Description
GARIN1B	1,392	0,027	protein_coding	golgi associated RAB2 interactor 1B [Source:HGNC Symbol;Acc:HGNC:30704]
CHRNE	1,411	0,007	protein_coding	cholinergic receptor nicotinic epsilon subunit [Source:HGNC Symbol;Acc:HGNC:1966]
KCNJ14	1,412	0,000	protein_coding	potassium inwardly rectifying channel subfamily J member 14 [Source:HGNC Symbol;Acc:HGNC:6260]
VGF	1,414	0,002	protein_coding	VGF nerve growth factor inducible [Source:HGNC Symbol;Acc:HGNC:12684]
FLRT3	1,422	0,019	protein_coding	fibronectin leucine rich transmembrane protein 3 [Source:HGNC Symbol;Acc:HGNC:3762]
KAZN	1,426	0,000	protein_coding	kazrin, periplakin interacting protein [Source:HGNC Symbol;Acc:HGNC:29173]
NANOG	1,431	0,010	protein_coding	Nanog homeobox [Source:HGNC Symbol;Acc:HGNC:20857]
RAB3C	1,433	0,000	protein_coding	RAB3C, member RAS oncogene family [Source:HGNC Symbol;Acc:HGNC:30269]
KCNN3	1,439	0,043	protein_coding	potassium calcium-activated channel subfamily N member 3 [Source:HGNC Symbol;Acc:HGNC:6292]
RUNDC3A	1,443	0,001	protein_coding	RUN domain containing 3A [Source:HGNC Symbol;Acc:HGNC:16984]
C17orf99	1,443	0,002	protein_coding	chromosome 17 open reading frame 99 [Source:HGNC Symbol;Acc:HGNC:34490]
PID1	1,449	0,000	protein_coding	phosphotyrosine interaction domain containing 1 [Source:HGNC Symbol;Acc:HGNC:26084]
GABRB2	1,467	0,000	protein_coding	gamma-aminobutyric acid type A receptor subunit beta2 [Source:HGNC Symbol;Acc:HGNC:4082]
RASGRP2	1,476	0,000	protein_coding	RAS guanyl releasing protein 2 [Source:HGNC Symbol;Acc:HGNC:9879]
RSPH4A	1,494	0,023	protein_coding	radial spoke head component 4A [Source:HGNC Symbol;Acc:HGNC:21558]
CCR5	1,504	0,000	protein_coding	C-C motif chemokine receptor 5 [Source:HGNC Symbol;Acc:HGNC:1606]
DPYS	1,505	0,028	protein_coding	dihydropyrimidinase [Source:HGNC Symbol;Acc:HGNC:3013]
SNORD3B-2	1,511	0,038	snoRNA	small nucleolar RNA, C/D box 3B-2 [Source:HGNC Symbol;Acc:HGNC:33190]
PDE4D	1,517	0,006	protein_coding	phosphodiesterase 4D [Source:HGNC Symbol;Acc:HGNC:8783]
CA1	1,518	0,003	protein_coding	carbonic anhydrase 1 [Source:HGNC Symbol;Acc:HGNC:1368]
ENSG00000280211	1,521	0,046		
STRC	1,524	0,000	protein_coding	stereocilin [Source:HGNC Symbol;Acc:HGNC:16035]
OR5AU1	1,529	0,048	protein_coding	olfactory receptor family 5 subfamily AU member 1 [Source:HGNC Symbol;Acc:HGNC:15362]
FGFR2	1,532	0,000	protein_coding	fibroblast growth factor receptor 2 [Source:HGNC Symbol;Acc:HGNC:3689]
CSMD3	1,537	0,043	protein_coding	CUB and Sushi multiple domains 3 [Source:HGNC Symbol;Acc:HGNC:19291]
ENSG00000286797	1,567	0,000		
RNVU1-7	1,571	0,016	snRNA	RNA, variant U1 small nuclear 7 [Source:HGNC Symbol;Acc:HGNC:37500]
PTPN21	1,576	0,023	protein_coding	protein tyrosine phosphatase non-receptor type 21 [Source:HGNC Symbol;Acc:HGNC:9651]

Gene	Log2FoldChange	padj	Biotype	Description
SOX4	1,578	0,000	protein_coding	SRY-box transcription factor 4 [Source:HGNC Symbol;Acc:HGNC:11200]
SNORD3B-1	1,591	0,000	snoRNA	small nucleolar RNA, C/D box 3B-1 [Source:HGNC Symbol;Acc:HGNC:10168]
SPECC1L-ADORA2A	1,593	0,002	protein_coding	SPECC1L-ADORA2A readthrough (NMD candidate) [Source:HGNC Symbol;Acc:HGNC:49185]
ENSG00000289865	1,604	0,010		
ENSG00000285888	1,613	0,013		
ENSG00000269892	1,618	0,036		
SLC43A1	1,619	0,000	protein_coding	solute carrier family 43 member 1 [Source:HGNC Symbol;Acc:HGNC:9225]
CHADL	1,633	0,024	protein_coding	chondroadherin like [Source:HGNC Symbol;Acc:HGNC:25165]
EGR3	1,650	0,001	protein_coding	early growth response 3 [Source:HGNC Symbol;Acc:HGNC:3240]
MYC	1,665	0,033	protein_coding	MYC proto-oncogene, bHLH transcription factor [Source:HGNC Symbol;Acc:HGNC:7553]
SLC18A2-AS1	1,674	0,000	lncRNA	SLC18A2 antisense RNA 1 [Source:HGNC Symbol;Acc:HGNC:55843]
ENSG00000267149	1,678	0,031		
WNK4	1,720	0,010	protein_coding	WNK lysine deficient protein kinase 4 [Source:HGNC Symbol;Acc:HGNC:14544]
RD3	1,728	0,000	protein_coding	RD3 regulator of GUCY2D [Source:HGNC Symbol;Acc:HGNC:19689]
ITGA4	1,742	0,000	protein_coding	integrin subunit alpha 4 [Source:HGNC Symbol;Acc:HGNC:6140]
ENSG00000258811	1,762	0,005		
IQCN	1,765	0,000	protein_coding	IQ motif containing N [Source:HGNC Symbol;Acc:HGNC:29350]
SMANTIS	1,780	0,000	lncRNA	SMARCA4 interacting SWI/SNF chromatin remodeling complex scaffold lncRNA [Source:HGNC Symbol;Acc:HGNC:54417]
GAL3ST4	1,808	0,002	protein_coding	galactose-3-O-sulfotransferase 4 [Source:HGNC Symbol;Acc:HGNC:24145]
ENOX1	1,852	0,000	protein_coding	ecto-NOX disulfide-thiol exchanger 1 [Source:HGNC Symbol;Acc:HGNC:25474]
ZGLP1	1,859	0,011	protein_coding	zinc finger GATA like protein 1 [Source:HGNC Symbol;Acc:HGNC:37245]
EPS8L2	1,901	0,001	protein_coding	EPS8 like 2 [Source:HGNC Symbol;Acc:HGNC:21296]
ST8SIA5	1,902	0,050	protein_coding	ST8 alpha-N-acetyl-neuraminide alpha-2,8-sialyltransferase 5 [Source:HGNC Symbol;Acc:HGNC:17827]
ASIC4	1,908	0,000	protein_coding	acid sensing ion channel subunit family member 4 [Source:HGNC Symbol;Acc:HGNC:21263]
ENSG00000266980	1,911	0,020		
PRSS57	1,930	0,002	protein_coding	serine protease 57 [Source:HGNC Symbol;Acc:HGNC:31397]
CLEC12A	1,942	0,002	protein_coding	C-type lectin domain family 12 member A [Source:HGNC Symbol;Acc:HGNC:31713]
NFE2	1,948	0,000	protein_coding	nuclear factor, erythroid 2 [Source:HGNC Symbol;Acc:HGNC:7780]

Gene	Log2FoldChange	padj	Biotype	Description
USP13	1,986	0,000	protein_coding	ubiquitin specific peptidase 13 [Source:HGNC Symbol;Acc:HGNC:12611]
SLC22A17	2,077	0,004	protein_coding	solute carrier family 22 member 17 [Source:HGNC Symbol;Acc:HGNC:23095]
ENSG00000259283	2,161	0,000		
KCNAB3	2,208	0,000	protein_coding	potassium voltage-gated channel subfamily A regulatory beta subunit 3 [Source:HGNC Symbol;Acc:HGNC:6230]
NHLH1	2,238	0,002	protein_coding	nescient helix-loop-helix 1 [Source:HGNC Symbol;Acc:HGNC:7817]
GPR132	2,250	0,004	protein_coding	G protein-coupled receptor 132 [Source:HGNC Symbol;Acc:HGNC:17482]
C2orf66	2,263	0,000	protein_coding	chromosome 2 open reading frame 66 [Source:HGNC Symbol;Acc:HGNC:33809]
ALCAM	2,265	0,001	protein_coding	activated leukocyte cell adhesion molecule [Source:HGNC Symbol;Acc:HGNC:400]
MGAM2	2,268	0,000	protein_coding	maltase-glucoamylase 2 (putative) [Source:HGNC Symbol;Acc:HGNC:28101]
CHMP1B2P	2,394	0,005	transcribed_unitary_pseudogene	charged multivesicular body protein 1B2, pseudogene [Source:HGNC Symbol;Acc:HGNC:49380]
SCN3A	2,428	0,000	protein_coding	sodium voltage-gated channel alpha subunit 3 [Source:HGNC Symbol;Acc:HGNC:10590]
NTRK3	2,453	0,000	protein_coding	neurotrophic receptor tyrosine kinase 3 [Source:HGNC Symbol;Acc:HGNC:8033]
PEAR1	2,476	0,000	protein_coding	platelet endothelial aggregation receptor 1 [Source:HGNC Symbol;Acc:HGNC:33631]
FLNC	2,559	0,008	protein_coding	filamin C [Source:HGNC Symbol;Acc:HGNC:3756]
PTCHD1	2,793	0,000	protein_coding	patched domain containing 1 [Source:HGNC Symbol;Acc:HGNC:26392]
ADCYAP1	2,874	0,000	protein_coding	adenylate cyclase activating polypeptide 1 [Source:HGNC Symbol;Acc:HGNC:241]
AKAP12	3,333	0,000	protein_coding	A-kinase anchoring protein 12 [Source:HGNC Symbol;Acc:HGNC:370]
CNTNAP5	3,877	0,000	protein_coding	contactin associated protein family member 5 [Source:HGNC Symbol;Acc:HGNC:18748]
GNL3LP1	7,911	0,000	processed_pseudogene	G protein nucleolar 3 like pseudogene 1 [Source:HGNC Symbol;Acc:HGNC:25733]

Annex Table 10. GSEA pathways in LAD2 cells with MITF-silenced versus LAD2 cells with shRNA-NT, in an IgE-independent pathway (MRGPRX2). LAD2 cells were infected with lentivirus (shRNA-NT and MITF shRNA-2) for 5 days and stimulated with substance P for 24 hours.

Description	setSize	enrichmentScore	padj	qvalues	core_enrichment
Network map of SARS CoV 2 signaling pathway	141	-0,4510	0,0410	0,0340	RAC1/TGFBR2/IRAK1/VPS36/DEPTOR/DUSP1/IRF9/AKT1S1/MYD88/PTGS2/TRAF2/CCL3/EIF4A2/CCL4/HRG/STAT1/TRAF3/IFITM3/CD247/C1R/ACTB/IL1A/IFITM1/IFIH1/CCL5/IL18RAP/CCL2/HSPA8/GSN/APOC1/CEBPB/IFI27/CTSD/CTSL/IFI6/IFIT1/CCNB2/OAS2/CCNB1/MX1/CDK1/BIRC5/CXCL16/GTSE1/IL1B/RRM2/TRPM2/IFI44L
Cell cycle	114	-0,5353	0,0410	0,0340	PKMYT1/CCNA1/SMAD3/CUL1/CDK4/YWHAQ/TTK/CDKN2C/PLK1/CCND3/CDC16/MCM2/TGFB2/ESPL1/ANAPC13/MCM5/CDK2/CDKN2B/CCNA2/MCM6/CDC20/WEE1/MCM4/CCNB2/CHEK1/CDC25C/CCNB1/CDC45/CDK1/CDC6/CCND2/E2F1/E2F2
mRNA processing	125	-0,4764	0,0410	0,0340	PTBP2/SRSF10/SRP54/SRSF7/TRA2B/EFTUD2/CPSF3/XRN2/RBM39/HNRNPR/SREK1/CSTF2/DHX9/SNRPD2/SNRPB2/LSM7/PRMT2/HNRNPA2B1/SF3B4/SF3A3/CSTF1/HNRNPU/RNGTT/HNRNPK/SRSF5/HNRNPH1/DHX15/NUDT21/SNRPF/PRPF3/PRMT1/SNRNP70/SRSF9/HNRNPA1/SRSF1/SUPT5H/DICER1/PCBP2/CELF1/SRSF3/HNRNPC/POLR2A/SF3B3/NXF1/SFPQ/CDC40/SF3B5/HNRNPM/SNRPB/DDX20/RBMX/TMED10/SMC1A/PRPF4/SRSF2/RBM17/HNRNPL/U2AF1/PAPOLA/HNRNPD/RNPS1/YBX1/PRPF6/CPSF2/TXNL4A/SF3B2/DNAJC8/HNRNPH2
NF1 copy number variation syndrome	94	-0,5529	0,0410	0,0340	PRMT5/H3C12/RFC2/RFC3/EXOC5/EVI2A/CRY1/H3C11/TUBB/H4C3/H4C6/H4C4/COPRS/H4C13/H3C10/H3C6/H4C14/CCNA2/H4C1/H4C9/H3C3/H3C15/H3C2/H3C7/H3C8/H3C4/BCL2/RTN4R
HDAC6 interactions in the central nervous system	96	-0,5187	0,0410	0,0340	HDAC11/KAT5/SGK1/NDUFV1/MAP1LC3A/DYNC1I2/CSNK2B/CTNNB1/SMAD2/XRCC6/MAPK1/HSPB1/MDH1/SIRT2/SOD1/STUB1/OPTN/RAC1/ATXN3/MAP1B/PRDX2/MAPK3/HSP90AA1/MYD88/TPPP/PRDX1/SQSTM1/TUBB3/VHL/TUBB/TUBA1C/CNOT6/HSPA4/RAD23B/GRK2/AURKA/HSPA8/ISG15/PPP1CA/VIM/GARS1/CDC20/MAP3K5/BIRC5/BCL2

Description	setSize	enrichmentScore	p.adjust	qvalues	core_enrichment
Electron transport chain OXPHOS system in mitochondria	90	-0,5459	0,0410	0,0340	SDHC/NDUFS6/NDUFA4/ATP5PD/ATP5MC1/COX8A/COX11/UQCR10/NDUFA3/COX4I1/SDHA/ATP5PB/NDUFB7/NDUFA13/NDUFB8/NDUFB2/NDUFV1/COX6A1/SLC25A6/NDUFB4/SLC25A5/NDUFB10/NDUFA11/UCP2/NDUFS4/COX5B/NDUFV2/COX15/NDUFB6/ATP5F1D/NDUFA9/ATP5IF1/COX7B/COX6C/ATP5F1A/NDUFS2/COX5A/NDUFS1/UQCRC2/COX7A2/COX7A1/ATP5PO/SDHD/SLC25A4/ATP5MC3/UQCRC1/NDUFS7/NDUFS8/NDUFC2/NDUFA6/NDUFAB1/NDUFA8/ATP5F1E/NDUFB5/SDHB/NDUFB1/UQCRFS1/NDUFA1/NDUFS3/ATP5F1C/ATP5F1B
Retinoblastoma gene in cancer	85	-0,6407	0,0410	0,0340	SUV39H1/RRM1/RFC3/TYMS/HMGB1/CCND3/PLK4/POLE2/RPA3/STMN1/DHFR/CDK2/CCNA2/ANLN/MCM6/WEE1/MCM4/H2AZ1/TOP2A/CCNB2/CHEK1/CCNB1/KIF4A/CDC45/CDK1/CDT1/E2F1/RRM2/E2F2
miRNA regulation of DNA damage response	66	-0,5191	0,0410	0,0340	CYCS/CCND3/H2AX/CDK2/CCNB2/CHEK1/CDC25C/CCNB1/CDK1/CCND2/E2F1
DNA damage response	66	-0,5235	0,0410	0,0340	CYCS/CCND3/H2AX/CDK2/CCNB2/CHEK1/CDC25C/CCNB1/CDK1/CCND2/E2F1
DNA IR damage and cellular response via ATR	81	-0,5686	0,0410	0,0340	MDM2/RECQL/TP53/CEP164/NBN/XPA/ABRAXAS1/IKBKG/RECQL4/PML/POLB/RAD1/RMI1/RAD51/RPA1/SEM1/RAD17/PCNA/SMC1A/BARD1/MLH1/DCLRE1A/BRCA2/FEN1/PLK1/EXO1/MCM2/H2AX/FANCA/CDK2/BRIP1/CHEK1/CDC25C/FOXM1/CDC45/CDK1/E2F1/CLSPN
Nucleotide excision repair in xeroderma pigmentosum	74	-0,5090	0,0410	0,0340	H4C11/POLD1/H4C2/RPA1/CUL4B/POLE4/RBX1/PCNA/H4C8/RFC4/ERCC2/CETN2/RFC2/RFC3/POLD2/POLE2/H4C3/H4C6/RPA3/RAD23B/H4C4/CUL4A/H4C13/H4C14/H4C1/H4C9
Histone modifications	62	-0,5601	0,0410	0,0340	EZH2/SUV39H1/H3C12/H3C11/SMYD3/H4C3/H4C6/SETDB2/H4C4/H4C13/H3C10/H3C6/SETD7/H4C1/H4C9/H3C15/H3C7/H3C8/H3C4
G1 to S cell cycle control	62	-0,6117	0,0410	0,0340	CCND3/MCM2/POLE2/RPA3/MCM5/CDK2/CDKN2B/MCM6/WEE1/CCNG2/MCM4/CCNB1/CDC45/CDK1/CCND2/E2F1/E2F2

Description	setSize	enrichmentScore	p.adjust	qvalues	core_enrichment
FBXL10 enhancement of MAP ERK signaling in diffuse large B cell lymphoma	29	-0,6400	0,0410	0,0340	MAPK3/EZH2/H3C12/H3C11/H2AX/H3C10/H3C6/H3C15/H2AZ1/H3C7/H3C8/H3C4
Selenium micronutrient network	52	-0,5498	0,0410	0,0340	SELENOH/SOD1/SELENOW/PRDX2/TXNRD1/SCARB1/TXN/SELENOI/SELENOM/PTGS2/CAT/LDLR/PRDX1/GSR/SELENOT/TXNRD3/CTH/ICAM1/PNPO/CCL2/SOD2/PRDX3/GPX1/IL1B/CBS
Oxidative phosphorylation	52	-0,5487	0,0410	0,0340	NDUFS6/NDUFA4/ATP5PD/ATP5MC1/NDUFA3/ATP5PB/NDUFB7/NDUFB8/NDUFB2/NDUFV1/GZMB/NDUFB4/NDUFB10/NDUFA11/NDUFS4/NDUFV2/NDUFB6/ATP5F1D/NDUFA9/ATP5F1A/ATP6AP1/ATP6AP2/NDUFS2/NDUFS1/ATP5PO/ATP5MC3/NDUFS7/NDUFS8/NDUFC2/NDUFA6/NDUFAB1/NDUFA8/ATP5F1E/NDUFB5/NDUFB1/NDUFS3/ATP5F1B
Type II interferon signaling	27	-0,6874	0,0410	0,0340	IRF9/PTPN11/GBP1/STAT2/STAT1/ICAM1/CIITA/EIF2AK2/H4C14/ISG15/IFIT2/IFI6/OAS1/IL1B
Mitochondrial complex I assembly model OXPHOS system	50	-0,5429	0,0410	0,0340	NDUFAF2/NDUFA3/NDUFB7/NDUFA13/NDUFB8/NDUFB2/NDUFV1/NDUFB4/NDUFB10/DMAC2/NDUFAF1/NDUFS4/TMEM126B/NDUFV2/NDUFB6/NDUFAF4/DMAC1/NDUFS2/TMEM70/NDUFS1/NDUFC2/NDUFA6/NDUFAB1/NDUFA8/NDUFB5/NDUFB1/NDUFA1/NDUFS3
Photodynamic therapy induced unfolded protein response	26	-0,6526	0,0410	0,0340	HSP90B1/DNAJC3/EIF2A/XBP1/NARS1/ATF4/HSPA5/EDEM1/DDIT3/TRIB3/ERP27/WARS1
Type I interferon induction and signaling during SARS CoV 2 infection	26	-0,6574	0,0410	0,0340	IRF9/MYD88/STAT2/STAT1/TRAF3/TLR6/IFIH1/EIF2AK2/TLR3/OAS1/OAS2/OAS3
DNA replication	42	-0,6645	0,0410	0,0340	RFC2/RFC3/POLD2/MCM2/POLE2/RPA3/MCM5/CDK2/MCM6/MCM4/MCM10/CDC45/CDT1/CDC6
Host pathogen interaction of human coronaviruses interferon induction	31	-0,6079	0,0410	0,0340	IRF9/MYD88/STAT2/STAT1/TRAF3/IFIH1/EIF2AK2/OAS1/OAS2/OAS3
Gastric cancer network 1	22	-0,7601	0,0410	0,0340	TPX2/CCNA1/E2F7/KIF20B/ECT2/AURKA/KIF15/MCM4/CENPF/UBE2C/TOP2A/MYBL2

Description	setSize	enrichmentScore	p.adjust	qvalues	core_enrichment
Immune response to tuberculosis	22	-0,6653	0,0410	0,0340	IRF9/STAT2/STAT1/IFI35/PSMB8/IFITM1/IFIT3/OAS1/IFIT1/MX1
Cholesterol biosynthesis pathway	15	-0,7575	0,0410	0,0340	SQLE/SC5D/FDFT1/CYP51A1/MVK/HMGCR/DHCR7/NSDHL/HMGCS1/MVD/IDI1/FDPS/MSMO1/LSS
Effect of progerin on genes involved in progeria	35	-0,7387	0,0410	0,0340	SUV39H1/H3C12/H3C11/CBX5/H3C10/H3C6/H3C3/H3C15/H3C2/H3C7/H3C8/H3C4/E2F1
Microtubule cytoskeleton regulation	41	-0,6442	0,0410	0,0340	PAK1/RAC1/MAP1B/CLIP1/DPYSL2/TRIO/PARD6A/TPPP/GNAQ/PRKCA/DIAPH1/MAPKAPK2/STMN1/SRC/TESK2/CDC42/AURKB/KIF2C/CDK1
Metabolic reprogramming in colon cancer	41	-0,6723	0,0410	0,0340	PKM/PGAM1/GART/PGK1/IDH3A/FH/TIGAR/GLUD1/PAICS/PDHA1/PGD/G6PD/SUCLG2/DLST/ENO1/SLC2A1/FASN/IDH2/ACO2/SDHB/HK3/PSPH/PYCR1/PSAT1
Unfolded protein response	24	-0,6636	0,0410	0,0340	TP53/PPP1R15A/TXNIP/RTCB/EIF2S1/XBP1/ATF4/HSPA5/DDIT3/MBTPS2/CASP1/BCL2/IL1B
Matrix metalloproteinases	11	0,8034	0,0430	0,0357	MMP2/TNF/MMP14/TIMP1/TIMP3
Cytoplasmic ribosomal proteins	86	0,6257	0,0452	0,0375	RPS18/RPL26/RPL37/RPS24/RPL27A/RPS11/RPS10/RPS6KA3/RPL13A/RPS19/RPL10A/RPL17/RPS25/RPL7/RPL11/RPLP0/RPS28/RPL13/RPLP2/RPL31/RPS23/RPL36/UBA52/RPS6/RPL34/RPS27/RPL36A/RPS3/RPL30/RPL12/RPS12/RPL6/RPS14/RPL27/RPS15A/RPL23A/RPL32/RPS2/RPL35/RPS5/RPL29/RPS29/RPS27A/RPS21/RPL7A/RPL39/RPL37A/RPL15/RPL9/RPLP1/FAU/RPL35A/RPL18/RPL23/RPL5/RPS6KA1/RPS15/RPL24/RPS16/RPS9/RPL38/RPL4/RPS26/RPL21

Annex Table 11. Differential gene expression in LAD2 cells with MITF-silenced versus LAD2 cells with shRNA-NT, in an IgE-dependent pathway. LAD2 cells were infected with lentivirus (shRNA-NT and MITF shRNA-2) for 5 days and stimulated with substance P for 24 hours.

Gene	Log2FoldChange	padj	Biotype	Description
GPR45	-5,373	0,001	protein_coding	G protein-coupled receptor 45 [Source:HGNC Symbol;Acc:HGNC:4503]
IFI44L	-3,779	0,000	protein_coding	interferon induced protein 44 like [Source:HGNC Symbol;Acc:HGNC:17817]
BMP7	-3,681	0,000	protein_coding	bone morphogenetic protein 7 [Source:HGNC Symbol;Acc:HGNC:1074]
ENSG00000267166	-3,652	0,000		
KLHDC7B	-3,638	0,001	protein_coding	kelch domain containing 7B [Source:HGNC Symbol;Acc:HGNC:25145]
DEFB119	-3,480	0,000	protein_coding	defensin beta 119 [Source:HGNC Symbol;Acc:HGNC:18099]
ENSG00000286752	-3,320	0,000		
LINC02890	-3,266	0,000	lncRNA	long intergenic non-protein coding RNA 2890 [Source:HGNC Symbol;Acc:HGNC:55220]
HMGB3P7	-3,220	0,000	processed_pseudogene	high mobility group box 3 pseudogene 7 [Source:HGNC Symbol;Acc:HGNC:39299]
ENSG00000181514	-3,180	0,000		
PSAT1	-3,177	0,005	protein_coding	phosphoserine aminotransferase 1 [Source:HGNC Symbol;Acc:HGNC:19129]
MT-RNR1	-3,069	0,044	Mt_rRNA	mitochondrially encoded 12S rRNA [Source:HGNC Symbol;Acc:HGNC:7470]
NEURL1B	-3,063	0,000	protein_coding	neuralized E3 ubiquitin protein ligase 1B [Source:HGNC Symbol;Acc:HGNC:35422]
EEPD1	-3,014	0,000	protein_coding	endonuclease/exonuclease/phosphatase family domain containing 1 [Source:HGNC Symbol;Acc:HGNC:22223]
E2F2	-2,931	0,000	protein_coding	E2F transcription factor 2 [Source:HGNC Symbol;Acc:HGNC:3114]
CPNE3	-2,921	0,012	protein_coding	copine 3 [Source:HGNC Symbol;Acc:HGNC:2316]
LINC01050	-2,878	0,000	lncRNA	long intergenic non-protein coding RNA 1050 [Source:HGNC Symbol;Acc:HGNC:49044]
RTL9	-2,852	0,000	protein_coding	retrotransposon Gag like 9 [Source:HGNC Symbol;Acc:HGNC:29245]
CLSPN	-2,803	0,000	protein_coding	claspin [Source:HGNC Symbol;Acc:HGNC:19715]
ANGPT4	-2,782	0,000	protein_coding	angiopoietin 4 [Source:HGNC Symbol;Acc:HGNC:487]
MT-RNR2	-2,775	0,044	Mt_rRNA	mitochondrially encoded 16S rRNA [Source:HGNC Symbol;Acc:HGNC:7471]
NCAPG	-2,757	0,000	protein_coding	non-SMC condensin I complex subunit G [Source:HGNC Symbol;Acc:HGNC:24304]
CHCHD6	-2,716	0,000	protein_coding	coiled-coil-helix-coiled-coil-helix domain containing 6 [Source:HGNC Symbol;Acc:HGNC:28184]

Gene	Log2FoldChange	padj	Biotype	Description
TRPM2	-2,648	0,002	protein_coding	transient receptor potential cation channel subfamily M member 2 [Source:HGNC Symbol;Acc:HGNC:12339]
ATP6V0D2	-2,644	0,042	protein_coding	ATPase H+ transporting V0 subunit d2 [Source:HGNC Symbol;Acc:HGNC:18266]
RRM2	-2,624	0,000	protein_coding	ribonucleotide reductase regulatory subunit M2 [Source:HGNC Symbol;Acc:HGNC:10452]
CDSN	-2,623	0,000	protein_coding	corneodesmosin [Source:HGNC Symbol;Acc:HGNC:1802]
RTN4R	-2,599	0,000	protein_coding	reticulon 4 receptor [Source:HGNC Symbol;Acc:HGNC:18601]
DCDC2	-2,594	0,000	protein_coding	doublecortin domain containing 2 [Source:HGNC Symbol;Acc:HGNC:18141]
ADAMTS18	-2,572	0,000	protein_coding	ADAM metallopeptidase with thrombospondin type 1 motif 18 [Source:HGNC Symbol;Acc:HGNC:17110]
HS3ST2	-2,565	0,000	protein_coding	heparan sulfate-glucosamine 3-sulfotransferase 2 [Source:HGNC Symbol;Acc:HGNC:5195]
BHLHE41	-2,555	0,000	protein_coding	basic helix-loop-helix family member e41 [Source:HGNC Symbol;Acc:HGNC:16617]
KCNQ5-DT	-2,553	0,000	lncRNA	KCNQ5 divergent transcript [Source:HGNC Symbol;Acc:HGNC:55469]
IL1B	-2,509	0,000	protein_coding	interleukin 1 beta [Source:HGNC Symbol;Acc:HGNC:5992]
DENND6A-DT	-2,419	0,000	lncRNA	DENND6A divergent transcript [Source:HGNC Symbol;Acc:HGNC:51592]
E2F1	-2,412	0,000	protein_coding	E2F transcription factor 1 [Source:HGNC Symbol;Acc:HGNC:3113]
TSBP1	-2,368	0,000	protein_coding	testis expressed basic protein 1 [Source:HGNC Symbol;Acc:HGNC:13922]
ANKH	-2,333	0,000	protein_coding	ANKH inorganic pyrophosphate transport regulator [Source:HGNC Symbol;Acc:HGNC:15492]
ADM2	-2,312	0,001	protein_coding	adrenomedullin 2 [Source:HGNC Symbol;Acc:HGNC:28898]
CCL18	-2,284	0,000	protein_coding	C-C motif chemokine ligand 18 [Source:HGNC Symbol;Acc:HGNC:10616]
ENSG00000276012	-2,262	0,000		
MYBL2	-2,224	0,001	protein_coding	MYB proto-oncogene like 2 [Source:HGNC Symbol;Acc:HGNC:7548]
CHRNA6	-2,208	0,000	protein_coding	cholinergic receptor nicotinic alpha 6 subunit [Source:HGNC Symbol;Acc:HGNC:15963]
GGH	-2,207	0,000	protein_coding	gamma-glutamyl hydrolase [Source:HGNC Symbol;Acc:HGNC:4248]
CPNE5	-2,206	0,000	protein_coding	copine 5 [Source:HGNC Symbol;Acc:HGNC:2318]
LURAP1L-AS1	-2,204	0,019	lncRNA	LURAP1L antisense RNA 1 [Source:HGNC Symbol;Acc:HGNC:49761]
OIP5	-2,201	0,018	protein_coding	Opa interacting protein 5 [Source:HGNC Symbol;Acc:HGNC:20300]
RTKN2	-2,186	0,005	protein_coding	rhotekin 2 [Source:HGNC Symbol;Acc:HGNC:19364]
ITGBL1	-2,170	0,000	protein_coding	integrin subunit beta like 1 [Source:HGNC Symbol;Acc:HGNC:6164]
EPHA5	-2,158	0,000	protein_coding	EPH receptor A5 [Source:HGNC Symbol;Acc:HGNC:3389]
ENSG00000287891	-2,155	0,000		

Gene	Log2FoldChange	padj	Biotype	Description
KIAA0319	-2,149	0,040	protein_coding	KIAA0319 [Source:HGNC Symbol;Acc:HGNC:21580]
CEP55	-2,137	0,000	protein_coding	centrosomal protein 55 [Source:HGNC Symbol;Acc:HGNC:1161]
CTSH	-2,123	0,000	protein_coding	cathepsin H [Source:HGNC Symbol;Acc:HGNC:2535]
NDRG4	-2,119	0,000	protein_coding	NDRG family member 4 [Source:HGNC Symbol;Acc:HGNC:14466]
MEGF6	-2,112	0,000	protein_coding	multiple EGF like domains 6 [Source:HGNC Symbol;Acc:HGNC:3232]
ENSG00000261888	-2,107	0,000		
GTSE1	-2,100	0,000	protein_coding	G2 and S-phase expressed 1 [Source:HGNC Symbol;Acc:HGNC:13698]
ENSG00000229771	-2,087	0,000		
TSPAN10	-2,085	0,000	protein_coding	tetraspanin 10 [Source:HGNC Symbol;Acc:HGNC:29942]
RGS20	-2,078	0,043	protein_coding	regulator of G protein signaling 20 [Source:HGNC Symbol;Acc:HGNC:14600]
ENSG00000286223	-2,052	0,000		
SNX21	-2,037	0,022	protein_coding	sorting nexin family member 21 [Source:HGNC Symbol;Acc:HGNC:16154]
SLAMF7	-2,028	0,000	protein_coding	SLAM family member 7 [Source:HGNC Symbol;Acc:HGNC:21394]
TMEM268	-2,024	0,000	protein_coding	transmembrane protein 268 [Source:HGNC Symbol;Acc:HGNC:24513]
SYNE2	-2,015	0,000	protein_coding	spectrin repeat containing nuclear envelope protein 2 [Source:HGNC Symbol;Acc:HGNC:17084]
OAS3	-2,007	0,000	protein_coding	2'-5'-oligoadenylate synthetase 3 [Source:HGNC Symbol;Acc:HGNC:8088]
CTSA	-2,007	0,000	protein_coding	cathepsin A [Source:HGNC Symbol;Acc:HGNC:9251]
RNA5SP484	-2,001	0,011	rRNA_pseudogene	RNA, 5S ribosomal pseudogene 484 [Source:HGNC Symbol;Acc:HGNC:43384]
DTX1	-1,998	0,000	protein_coding	deltex E3 ubiquitin ligase 1 [Source:HGNC Symbol;Acc:HGNC:3060]
BCL2	-1,977	0,017	protein_coding	BCL2 apoptosis regulator [Source:HGNC Symbol;Acc:HGNC:990]
CXCL16	-1,976	0,000	protein_coding	C-X-C motif chemokine ligand 16 [Source:HGNC Symbol;Acc:HGNC:16642]
HNRNPH2	-1,972	0,000	protein_coding	heterogeneous nuclear ribonucleoprotein H2 [Source:HGNC Symbol;Acc:HGNC:5042]
DYNLT2B	-1,970	0,000	protein_coding	dynein light chain Tctex-type 2B [Source:HGNC Symbol;Acc:HGNC:28482]
CCND2	-1,965	0,000	protein_coding	cyclin D2 [Source:HGNC Symbol;Acc:HGNC:1583]
GUCA1C	-1,964	0,000	protein_coding	guanylate cyclase activator 1C [Source:HGNC Symbol;Acc:HGNC:4680]
ERCC6L	-1,963	0,001	protein_coding	ERCC excision repair 6 like, spindle assembly checkpoint helicase [Source:HGNC Symbol;Acc:HGNC:20794]
CDC6	-1,955	0,001	protein_coding	cell division cycle 6 [Source:HGNC Symbol;Acc:HGNC:1744]
SORBS3	-1,954	0,000	protein_coding	sorbin and SH3 domain containing 3 [Source:HGNC Symbol;Acc:HGNC:30907]

Gene	Log2FoldChange	padj	Biotype	Description
OTOAP1	-1,952	0,000	transcribed_unprocessed_pseudogene	OTOA pseudogene 1 [Source:HGNC Symbol;Acc:HGNC:53869]
PLXNA1	-1,952	0,000	protein_coding	plexin A1 [Source:HGNC Symbol;Acc:HGNC:9099]
MKI67	-1,946	0,000	protein_coding	marker of proliferation Ki-67 [Source:HGNC Symbol;Acc:HGNC:7107]
CDT1	-1,941	0,000	protein_coding	chromatin licensing and DNA replication factor 1 [Source:HGNC Symbol;Acc:HGNC:24576]
TMEM178A	-1,940	0,000	protein_coding	transmembrane protein 178A [Source:HGNC Symbol;Acc:HGNC:28517]
TM4SF19	-1,913	0,000	protein_coding	transmembrane 4 L six family member 19 [Source:HGNC Symbol;Acc:HGNC:25167]
ATP5F1B	-1,910	0,000	protein_coding	ATP synthase F1 subunit beta [Source:HGNC Symbol;Acc:HGNC:830]
BIRC5	-1,905	0,000	protein_coding	baculoviral IAP repeat containing 5 [Source:HGNC Symbol;Acc:HGNC:593]
RNU6ATAC12P	-1,893	0,019	snRNA	RNA, U6atac small nuclear 12, pseudogene [Source:HGNC Symbol;Acc:HGNC:46911]
ANXA2	-1,884	0,009	protein_coding	annexin A2 [Source:HGNC Symbol;Acc:HGNC:537]
C1orf54	-1,877	0,000	protein_coding	chromosome 1 open reading frame 54 [Source:HGNC Symbol;Acc:HGNC:26258]
NCF2	-1,873	0,007	protein_coding	neutrophil cytosolic factor 2 [Source:HGNC Symbol;Acc:HGNC:7661]
PTPRM	-1,858	0,042	protein_coding	protein tyrosine phosphatase receptor type M [Source:HGNC Symbol;Acc:HGNC:9675]
ENSG00000289351	-1,856	0,010		
CDK1	-1,854	0,000	protein_coding	cyclin dependent kinase 1 [Source:HGNC Symbol;Acc:HGNC:1722]
PEPD	-1,841	0,000	protein_coding	peptidase D [Source:HGNC Symbol;Acc:HGNC:8840]
MX1	-1,840	0,000	protein_coding	MX dynamin like GTPase 1 [Source:HGNC Symbol;Acc:HGNC:7532]
ITPR2-AS1	-1,833	0,001	lncRNA	ITPR2 and SSPN antisense RNA 1 [Source:HGNC Symbol;Acc:HGNC:56072]
CDC45	-1,833	0,024	protein_coding	cell division cycle 45 [Source:HGNC Symbol;Acc:HGNC:1739]
HTR2B	-1,820	0,025	protein_coding	5-hydroxytryptamine receptor 2B [Source:HGNC Symbol;Acc:HGNC:5294]
FOXM1	-1,796	0,000	protein_coding	forkhead box M1 [Source:HGNC Symbol;Acc:HGNC:3818]
MCM10	-1,787	0,002	protein_coding	minichromosome maintenance 10 replication initiation factor [Source:HGNC Symbol;Acc:HGNC:18043]
MAP3K5	-1,783	0,000	protein_coding	mitogen-activated protein kinase kinase kinase 5 [Source:HGNC Symbol;Acc:HGNC:6857]
MAFB	-1,777	0,000	protein_coding	MAF bZIP transcription factor B [Source:HGNC Symbol;Acc:HGNC:6408]
GLRA4	-1,775	0,042	transcribed_unitary_pseudogene	glycine receptor alpha 4 (pseudogene) [Source:HGNC Symbol;Acc:HGNC:31715]

Gene	Log2FoldChange	padj	Biotype	Description
CHILL1	-1,773	0,003	lncRNA	cancer hallmarks in lung lncRNA 1 [Source:HGNC Symbol;Acc:HGNC:55933]
ARPIN-AP3S2	-1,772	0,001	protein_coding	ARPIN-AP3S2 readthrough [Source:HGNC Symbol;Acc:HGNC:38824]
NUF2	-1,771	0,000	protein_coding	NUF2 component of NDC80 kinetochore complex [Source:HGNC Symbol;Acc:HGNC:14621]
CDCA2	-1,767	0,000	protein_coding	cell division cycle associated 2 [Source:HGNC Symbol;Acc:HGNC:14623]
FMNL2	-1,766	0,000	protein_coding	formin like 2 [Source:HGNC Symbol;Acc:HGNC:18267]
DLGAP5	-1,759	0,000	protein_coding	DLG associated protein 5 [Source:HGNC Symbol;Acc:HGNC:16864]
STARD10	-1,746	0,000	protein_coding	StAR related lipid transfer domain containing 10 [Source:HGNC Symbol;Acc:HGNC:10666]
NTM	-1,725	0,025	protein_coding	neurotrimin [Source:HGNC Symbol;Acc:HGNC:17941]
TRAC	-1,719	0,001	TR_C_gene	T cell receptor alpha constant [Source:HGNC Symbol;Acc:HGNC:12029]
KIF4A	-1,717	0,000	protein_coding	kinesin family member 4A [Source:HGNC Symbol;Acc:HGNC:13339]
H3C8	-1,711	0,000	protein_coding	H3 clustered histone 8 [Source:HGNC Symbol;Acc:HGNC:4772]
PADI2	-1,701	0,000	protein_coding	peptidyl arginine deiminase 2 [Source:HGNC Symbol;Acc:HGNC:18341]
PBK	-1,698	0,000	protein_coding	PDZ binding kinase [Source:HGNC Symbol;Acc:HGNC:18282]
TROAP	-1,692	0,000	protein_coding	trophinin associated protein [Source:HGNC Symbol;Acc:HGNC:12327]
C5orf47	-1,690	0,000	protein_coding	chromosome 5 open reading frame 47 [Source:HGNC Symbol;Acc:HGNC:27026]
PPARGC1A	-1,687	0,004	protein_coding	PPARG coactivator 1 alpha [Source:HGNC Symbol;Acc:HGNC:9237]
CENPA	-1,681	0,000	protein_coding	centromere protein A [Source:HGNC Symbol;Acc:HGNC:1851]
NEK2	-1,672	0,000	protein_coding	NIMA related kinase 2 [Source:HGNC Symbol;Acc:HGNC:7745]
KRT19P1	-1,667	0,008	processed_pseudogene	keratin 19 pseudogene 1 [Source:HGNC Symbol;Acc:HGNC:33422]
APOBEC3B	-1,619	0,000	protein_coding	apolipoprotein B mRNA editing enzyme catalytic subunit 3B [Source:HGNC Symbol;Acc:HGNC:17352]
COMMD3-BMI1	-1,619	0,009	protein_coding	COMMD3-BMI1 readthrough [Source:HGNC Symbol;Acc:HGNC:48326]
ENSG00000288849	-1,612	0,036		
KIF20A	-1,611	0,000	protein_coding	kinesin family member 20A [Source:HGNC Symbol;Acc:HGNC:9787]
RTN4RL1	-1,600	0,000	protein_coding	reticulon 4 receptor like 1 [Source:HGNC Symbol;Acc:HGNC:21329]
HTN3	-1,597	0,000	protein_coding	histatin 3 [Source:HGNC Symbol;Acc:HGNC:5284]
SPP1	-1,589	0,006	protein_coding	secreted phosphoprotein 1 [Source:HGNC Symbol;Acc:HGNC:11255]
CCNB1	-1,588	0,000	protein_coding	cyclin B1 [Source:HGNC Symbol;Acc:HGNC:1579]
THBS4-AS1	-1,581	0,000	lncRNA	THBS4 antisense RNA 1 [Source:HGNC Symbol;Acc:HGNC:40583]

Gene	Log2FoldChange	padj	Biotype	Description
H2BC3	-1,581	0,007	protein_coding	H2B clustered histone 3 [Source:HGNC Symbol;Acc:HGNC:4751]
MYO10	-1,576	0,019	protein_coding	myosin X [Source:HGNC Symbol;Acc:HGNC:7593]
KIF2C	-1,571	0,000	protein_coding	kinesin family member 2C [Source:HGNC Symbol;Acc:HGNC:6393]
JPH4	-1,568	0,000	protein_coding	junctophilin 4 [Source:HGNC Symbol;Acc:HGNC:20156]
IFI30	-1,562	0,000	protein_coding	IFI30 lysosomal thiol reductase [Source:HGNC Symbol;Acc:HGNC:5398]
ENSG00000278095	-1,562	0,036		
ENSG00000281974	-1,560	0,000		
ZC3H11B	-1,560	0,005	protein_coding	zinc finger CCCH-type containing 11B [Source:HGNC Symbol;Acc:HGNC:25659]
KCP	-1,558	0,000	protein_coding	kielin cysteine rich BMP regulator [Source:HGNC Symbol;Acc:HGNC:17585]
CKAP2L	-1,538	0,000	protein_coding	cytoskeleton associated protein 2 like [Source:HGNC Symbol;Acc:HGNC:26877]
ENSG00000255750	-1,536	0,019		
STRIP2	-1,533	0,042	protein_coding	striatin interacting protein 2 [Source:HGNC Symbol;Acc:HGNC:22209]
PATL1-DT	-1,532	0,003	lncRNA	PATL1 divergent transcript [Source:HGNC Symbol;Acc:HGNC:55501]
ENSG00000234139	-1,529	0,000		
ROCK1P1	-1,527	0,000	transcribed_unprocessed_pseudogene	Rho associated coiled-coil containing protein kinase 1 pseudogene 1 [Source:HGNC Symbol;Acc:HGNC:37832]
SPACA3	-1,527	0,009	protein_coding	sperm acrosome associated 3 [Source:HGNC Symbol;Acc:HGNC:16260]
BUB1B	-1,525	0,000	protein_coding	BUB1 mitotic checkpoint serine/threonine kinase B [Source:HGNC Symbol;Acc:HGNC:1149]
PIMREG	-1,522	0,001	protein_coding	PICALM interacting mitotic regulator [Source:HGNC Symbol;Acc:HGNC:25483]
ST3GAL6	-1,518	0,001	protein_coding	ST3 beta-galactoside alpha-2,3-sialyltransferase 6 [Source:HGNC Symbol;Acc:HGNC:18080]
SPTBN1	-1,511	0,005	protein_coding	spectrin beta, non-erythrocytic 1 [Source:HGNC Symbol;Acc:HGNC:11275]
ZSWIM8-AS1	-1,506	0,000	lncRNA	ZSWIM8 antisense RNA 1 [Source:HGNC Symbol;Acc:HGNC:45103]
SOX13	-1,503	0,000	protein_coding	SRY-box transcription factor 13 [Source:HGNC Symbol;Acc:HGNC:11192]
SPC24	-1,499	0,002	protein_coding	SPC24 component of NDC80 kinetochore complex [Source:HGNC Symbol;Acc:HGNC:26913]
MAST1	-1,492	0,025	protein_coding	microtubule associated serine/threonine kinase 1 [Source:HGNC Symbol;Acc:HGNC:19034]
ERP27	-1,487	0,000	protein_coding	endoplasmic reticulum protein 27 [Source:HGNC Symbol;Acc:HGNC:26495]
ABI3BP	-1,486	0,000	protein_coding	ABI family member 3 binding protein [Source:HGNC Symbol;Acc:HGNC:17265]
NCAPH	-1,480	0,000	protein_coding	non-SMC condensin I complex subunit H [Source:HGNC Symbol;Acc:HGNC:1112]
CDC25C	-1,478	0,005	protein_coding	cell division cycle 25C [Source:HGNC Symbol;Acc:HGNC:1727]

Gene	Log2FoldChange	padj	Biotype	Description
CXCR3	-1,476	0,043	protein_coding	C-X-C motif chemokine receptor 3 [Source:HGNC Symbol;Acc:HGNC:4540]
C15orf48	-1,470	0,023	protein_coding	chromosome 15 open reading frame 48 [Source:HGNC Symbol;Acc:HGNC:29898]
OAS2	-1,470	0,004	protein_coding	2'-5'-oligoadenylate synthetase 2 [Source:HGNC Symbol;Acc:HGNC:8087]
H3C7	-1,468	0,000	protein_coding	H3 clustered histone 7 [Source:HGNC Symbol;Acc:HGNC:4773]
ENSG00000260306	-1,464	0,000		
CHEK1	-1,463	0,010	protein_coding	checkpoint kinase 1 [Source:HGNC Symbol;Acc:HGNC:1925]
CDCA5	-1,463	0,000	protein_coding	cell division cycle associated 5 [Source:HGNC Symbol;Acc:HGNC:14626]
MORC1	-1,459	0,000	protein_coding	MORC family CW-type zinc finger 1 [Source:HGNC Symbol;Acc:HGNC:7198]
IQGAP3	-1,459	0,001	protein_coding	IQ motif containing GTPase activating protein 3 [Source:HGNC Symbol;Acc:HGNC:20669]
KIF11	-1,459	0,000	protein_coding	kinesin family member 11 [Source:HGNC Symbol;Acc:HGNC:6388]
NME1-NME2	-1,455	0,001	protein_coding	NME1-NME2 readthrough [Source:HGNC Symbol;Acc:HGNC:33531]
CCNB2	-1,455	0,000	protein_coding	cyclin B2 [Source:HGNC Symbol;Acc:HGNC:1580]
AMIGO2	-1,447	0,000	protein_coding	adhesion molecule with Ig like domain 2 [Source:HGNC Symbol;Acc:HGNC:24073]
MELTF	-1,442	0,000	protein_coding	melanotransferrin [Source:HGNC Symbol;Acc:HGNC:7037]
KIF18A	-1,442	0,000	protein_coding	kinesin family member 18A [Source:HGNC Symbol;Acc:HGNC:29441]
HASPIN	-1,439	0,000	protein_coding	histone H3 associated protein kinase [Source:HGNC Symbol;Acc:HGNC:19682]
TOP2A	-1,436	0,000	protein_coding	DNA topoisomerase II alpha [Source:HGNC Symbol;Acc:HGNC:11989]
AURKB	-1,433	0,000	protein_coding	aurora kinase B [Source:HGNC Symbol;Acc:HGNC:11390]
CACNA1H	-1,433	0,000	protein_coding	calcium voltage-gated channel subunit alpha1 H [Source:HGNC Symbol;Acc:HGNC:1395]
ASPM	-1,429	0,000	protein_coding	assembly factor for spindle microtubules [Source:HGNC Symbol;Acc:HGNC:19048]
GINS1	-1,425	0,010	protein_coding	GINS complex subunit 1 [Source:HGNC Symbol;Acc:HGNC:28980]
FCRL3	-1,423	0,013	protein_coding	Fc receptor like 3 [Source:HGNC Symbol;Acc:HGNC:18506]
H2AZ1	-1,422	0,000	protein_coding	H2A.Z variant histone 1 [Source:HGNC Symbol;Acc:HGNC:4741]
MAS1	-1,421	0,000	protein_coding	MAS1 proto-oncogene, G protein-coupled receptor [Source:HGNC Symbol;Acc:HGNC:6899]
PRC1	-1,420	0,000	protein_coding	protein regulator of cytokinesis 1 [Source:HGNC Symbol;Acc:HGNC:9341]
MELK	-1,419	0,000	protein_coding	maternal embryonic leucine zipper kinase [Source:HGNC Symbol;Acc:HGNC:16870]
ENSG00000231612	-1,416	0,003		
UBE2C	-1,416	0,000	protein_coding	ubiquitin conjugating enzyme E2 C [Source:HGNC Symbol;Acc:HGNC:15937]

Gene	Log2FoldChange	padj	Biotype	Description
LINC00494	-1,415	0,000	lncRNA	long intergenic non-protein coding RNA 494 [Source:HGNC Symbol;Acc:HGNC:27657]
AMACR	-1,413	0,000	protein_coding	alpha-methylacyl-CoA racemase [Source:HGNC Symbol;Acc:HGNC:451]
RYR1	-1,412	0,000	protein_coding	ryanodine receptor 1 [Source:HGNC Symbol;Acc:HGNC:10483]
H2AC4	-1,403	0,001	protein_coding	H2A clustered histone 4 [Source:HGNC Symbol;Acc:HGNC:4734]
ENSG00000280088	-1,399	0,000		
IFIT1	-1,396	0,000	protein_coding	interferon induced protein with tetratricopeptide repeats 1 [Source:HGNC Symbol;Acc:HGNC:5407]
OAS1	-1,393	0,000	protein_coding	2'-5'-oligoadenylate synthetase 1 [Source:HGNC Symbol;Acc:HGNC:8086]
ENSG00000253214	-1,389	0,039		
IFI6	-1,388	0,000	protein_coding	interferon alpha inducible protein 6 [Source:HGNC Symbol;Acc:HGNC:4054]
OR14K1	-1,387	0,023	protein_coding	olfactory receptor family 14 subfamily K member 1 [Source:HGNC Symbol;Acc:HGNC:15025]
KCNE5	-1,384	0,000	protein_coding	potassium voltage-gated channel subfamily E regulatory subunit 5 [Source:HGNC Symbol;Acc:HGNC:6241]
NRIP3	-1,384	0,000	protein_coding	nuclear receptor interacting protein 3 [Source:HGNC Symbol;Acc:HGNC:1167]
GPNMB	-1,383	0,000	protein_coding	glycoprotein nmb [Source:HGNC Symbol;Acc:HGNC:4462]
PRKAR1A	-1,383	0,000	protein_coding	protein kinase cAMP-dependent type I regulatory subunit alpha [Source:HGNC Symbol;Acc:HGNC:9388]
SPIRE1	-1,379	0,000	protein_coding	spire type actin nucleation factor 1 [Source:HGNC Symbol;Acc:HGNC:30622]
AMZ2	-1,377	0,000	protein_coding	archaelysin family metallopeptidase 2 [Source:HGNC Symbol;Acc:HGNC:28041]
SNX3	-1,375	0,000	protein_coding	sorting nexin 3 [Source:HGNC Symbol;Acc:HGNC:11174]
LY6S	-1,373	0,000	protein_coding	lymphocyte antigen 6 family member S [Source:HGNC Symbol;Acc:HGNC:54397]
ZNF367	-1,371	0,003	protein_coding	zinc finger protein 367 [Source:HGNC Symbol;Acc:HGNC:18320]
TRGC1	-1,370	0,016	TR_C_gene	T cell receptor gamma constant 1 [Source:HGNC Symbol;Acc:HGNC:12275]
ENSG00000288895	-1,370	0,040		
DPEP2	-1,368	0,007	protein_coding	dipeptidase 2 [Source:HGNC Symbol;Acc:HGNC:23028]
H3C2	-1,367	0,001	protein_coding	H3 clustered histone 2 [Source:HGNC Symbol;Acc:HGNC:4776]
LINC02683	-1,366	0,008	lncRNA	long intergenic non-protein coding RNA 2683 [Source:HGNC Symbol;Acc:HGNC:54179]
PTP4A2	-1,363	0,000	protein_coding	protein tyrosine phosphatase 4A2 [Source:HGNC Symbol;Acc:HGNC:9635]
ENSG00000286852	-1,357	0,022		
ENSG00000273196	-1,356	0,031		
ZWINT	-1,350	0,008	protein_coding	ZW10 interacting kinetochore protein [Source:HGNC Symbol;Acc:HGNC:13195]

Gene	Log2FoldChange	padj	Biotype	Description
PDLIM1P4	-1,346	0,011	processed_pseudogene	PDZ and LIM domain 1 pseudogene 4 [Source:HGNC Symbol;Acc:HGNC:48947]
GPX1	-1,346	0,000	protein_coding	glutathione peroxidase 1 [Source:HGNC Symbol;Acc:HGNC:4553]
CXXC4	-1,343	0,001	protein_coding	CXXC finger protein 4 [Source:HGNC Symbol;Acc:HGNC:24593]
ISCA2	-1,342	0,000	protein_coding	iron-sulfur cluster assembly 2 [Source:HGNC Symbol;Acc:HGNC:19857]
ATP5F1C	-1,338	0,000	protein_coding	ATP synthase F1 subunit gamma [Source:HGNC Symbol;Acc:HGNC:833]
ADAMTSL3	-1,337	0,000	protein_coding	ADAMTS like 3 [Source:HGNC Symbol;Acc:HGNC:14633]
LNCTSI	-1,337	0,000	lncRNA	lncRNA TGF-beta/SMAD3 pathway interacting [Source:HGNC Symbol;Acc:HGNC:56660]
IZUMO1	-1,335	0,001	protein_coding	izumo sperm-oocyte fusion 1 [Source:HGNC Symbol;Acc:HGNC:28539]
PRDX3	-1,334	0,000	protein_coding	peroxiredoxin 3 [Source:HGNC Symbol;Acc:HGNC:9354]
YAP1	-1,329	0,042	protein_coding	Yes1 associated transcriptional regulator [Source:HGNC Symbol;Acc:HGNC:16262]
ENSG00000236841	-1,326	0,002		
H2AC14	-1,321	0,000	protein_coding	H2A clustered histone 14 [Source:HGNC Symbol;Acc:HGNC:4727]
ARHGAP11A	-1,317	0,000	protein_coding	Rho GTPase activating protein 11A [Source:HGNC Symbol;Acc:HGNC:15783]
GCNA	-1,317	0,001	protein_coding	germ cell nuclear acidic peptidase [Source:HGNC Symbol;Acc:HGNC:15805]
H3C15	-1,312	0,003	protein_coding	H3 clustered histone 15 [Source:HGNC Symbol;Acc:HGNC:20505]
CENPF	-1,312	0,000	protein_coding	centromere protein F [Source:HGNC Symbol;Acc:HGNC:1857]
HES4	-1,311	0,001	protein_coding	hes family bHLH transcription factor 4 [Source:HGNC Symbol;Acc:HGNC:24149]
RASIP1	-1,307	0,000	protein_coding	Ras interacting protein 1 [Source:HGNC Symbol;Acc:HGNC:24716]
SULT1C2	-1,304	0,000	protein_coding	sulfotransferase family 1C member 2 [Source:HGNC Symbol;Acc:HGNC:11456]
GEM	-1,302	0,011	protein_coding	GTP binding protein overexpressed in skeletal muscle [Source:HGNC Symbol;Acc:HGNC:4234]
DNAH7	-1,300	0,005	protein_coding	dynein axonemal heavy chain 7 [Source:HGNC Symbol;Acc:HGNC:18661]
GAS2L1	-1,297	0,000	protein_coding	growth arrest specific 2 like 1 [Source:HGNC Symbol;Acc:HGNC:16955]
KIF18B	-1,297	0,000	protein_coding	kinesin family member 18B [Source:HGNC Symbol;Acc:HGNC:27102]
LDB3	-1,294	0,013	protein_coding	LIM domain binding 3 [Source:HGNC Symbol;Acc:HGNC:15710]
ZMYND15	-1,292	0,000	protein_coding	zinc finger MYND-type containing 15 [Source:HGNC Symbol;Acc:HGNC:20997]
ENSG00000287481	-1,288	0,024		
S100A5	-1,286	0,000	protein_coding	S100 calcium binding protein A5 [Source:HGNC Symbol;Acc:HGNC:10495]
SCIN	-1,286	0,047	protein_coding	scinderin [Source:HGNC Symbol;Acc:HGNC:21695]

Gene	Log2FoldChange	padj	Biotype	Description
DUSP14	-1,285	0,000	protein_coding	dual specificity phosphatase 14 [Source:HGNC Symbol;Acc:HGNC:17007]
COMT	-1,282	0,000	protein_coding	catechol-O-methyltransferase [Source:HGNC Symbol;Acc:HGNC:2228]
PARP14	-1,281	0,000	protein_coding	poly(ADP-ribose) polymerase family member 14 [Source:HGNC Symbol;Acc:HGNC:29232]
TBC1D2	-1,280	0,000	protein_coding	TBC1 domain family member 2 [Source:HGNC Symbol;Acc:HGNC:18026]
ENSG00000269553	-1,279	0,000		
MNDA	-1,279	0,000	protein_coding	myeloid cell nuclear differentiation antigen [Source:HGNC Symbol;Acc:HGNC:7183]
ENSG00000274370	-1,274	0,000		
FGF18	-1,273	0,026	protein_coding	fibroblast growth factor 18 [Source:HGNC Symbol;Acc:HGNC:3674]
HMMR	-1,271	0,000	protein_coding	hyaluronan mediated motility receptor [Source:HGNC Symbol;Acc:HGNC:5012]
SLC7A7	-1,268	0,000	protein_coding	solute carrier family 7 member 7 [Source:HGNC Symbol;Acc:HGNC:11065]
PCLAF	-1,256	0,004	protein_coding	PCNA clamp associated factor [Source:HGNC Symbol;Acc:HGNC:28961]
TDRD3	-1,256	0,000	protein_coding	tudor domain containing 3 [Source:HGNC Symbol;Acc:HGNC:20612]
TOMM20	-1,253	0,000	protein_coding	translocase of outer mitochondrial membrane 20 [Source:HGNC Symbol;Acc:HGNC:20947]
IFIT2	-1,253	0,000	protein_coding	interferon induced protein with tetratricopeptide repeats 2 [Source:HGNC Symbol;Acc:HGNC:5409]
GPC1	-1,252	0,000	protein_coding	glypican 1 [Source:HGNC Symbol;Acc:HGNC:4449]
DIAPH3	-1,250	0,000	protein_coding	diaphanous related formin 3 [Source:HGNC Symbol;Acc:HGNC:15480]
MCM4	-1,246	0,003	protein_coding	minichromosome maintenance complex component 4 [Source:HGNC Symbol;Acc:HGNC:6947]
SPATA12	-1,243	0,000	protein_coding	spermatogenesis associated 12 [Source:HGNC Symbol;Acc:HGNC:23221]
SMIM14	-1,243	0,000	protein_coding	small integral membrane protein 14 [Source:HGNC Symbol;Acc:HGNC:27321]
H3C3	-1,240	0,004	protein_coding	H3 clustered histone 3 [Source:HGNC Symbol;Acc:HGNC:4768]
UNK	-1,237	0,000	protein_coding	unk zinc finger [Source:HGNC Symbol;Acc:HGNC:29369]
CLDN14-AS1	-1,233	0,000	lncRNA	CLDN14 antisense RNA 1 [Source:HGNC Symbol;Acc:HGNC:55953]
CCNG2	-1,233	0,000	protein_coding	cyclin G2 [Source:HGNC Symbol;Acc:HGNC:1593]
FBXO7	-1,233	0,000	protein_coding	F-box protein 7 [Source:HGNC Symbol;Acc:HGNC:13586]
GXYLT1P6	-1,227	0,000	processed_pseudogene	GXYLT1 pseudogene 6 [Source:HGNC Symbol;Acc:HGNC:50425]
TMEM187	-1,226	0,001	protein_coding	transmembrane protein 187 [Source:HGNC Symbol;Acc:HGNC:13705]
SLC7A8	-1,223	0,000	protein_coding	solute carrier family 7 member 8 [Source:HGNC Symbol;Acc:HGNC:11066]
WEE1	-1,223	0,000	protein_coding	WEE1 G2 checkpoint kinase [Source:HGNC Symbol;Acc:HGNC:12761]

Gene	Log2FoldChange	padj	Biotype	Description
VAT1	-1,222	0,000	protein_coding	vesicle amine transport 1 [Source:HGNC Symbol;Acc:HGNC:16919]
MBNL2	-1,222	0,000	protein_coding	muscleblind like splicing regulator 2 [Source:HGNC Symbol;Acc:HGNC:16746]
LRRC58	-1,222	0,000	protein_coding	leucine rich repeat containing 58 [Source:HGNC Symbol;Acc:HGNC:26968]
ENSG00000254092	-1,221	0,000		
KIF14	-1,220	0,000	protein_coding	kinesin family member 14 [Source:HGNC Symbol;Acc:HGNC:19181]
KREMEN1	-1,220	0,000	protein_coding	kringle containing transmembrane protein 1 [Source:HGNC Symbol;Acc:HGNC:17550]
GBP2	-1,218	0,000	protein_coding	guanylate binding protein 2 [Source:HGNC Symbol;Acc:HGNC:4183]
VAT1L	-1,218	0,034	protein_coding	vesicle amine transport 1 like [Source:HGNC Symbol;Acc:HGNC:29315]
DLGAP1-AS1	-1,218	0,000	lncRNA	DLGAP1 antisense RNA 1 [Source:HGNC Symbol;Acc:HGNC:31676]
ENSG00000267193	-1,214	0,045		
TRIM69	-1,213	0,000	protein_coding	tripartite motif containing 69 [Source:HGNC Symbol;Acc:HGNC:17857]
SYCP3	-1,213	0,000	protein_coding	synaptonemal complex protein 3 [Source:HGNC Symbol;Acc:HGNC:18130]
PYGL	-1,213	0,000	protein_coding	glycogen phosphorylase L [Source:HGNC Symbol;Acc:HGNC:9725]
ENSG00000259623	-1,212	0,004		
ENSG00000273956	-1,208	0,000		
GPR34	-1,206	0,000	protein_coding	G protein-coupled receptor 34 [Source:HGNC Symbol;Acc:HGNC:4490]
KCNN4	-1,205	0,000	protein_coding	potassium calcium-activated channel subfamily N member 4 [Source:HGNC Symbol;Acc:HGNC:6293]
SGPP1	-1,204	0,000	protein_coding	sphingosine-1-phosphate phosphatase 1 [Source:HGNC Symbol;Acc:HGNC:17720]
AK5	-1,201	0,001	protein_coding	adenylate kinase 5 [Source:HGNC Symbol;Acc:HGNC:365]
GAS6	-1,201	0,008	protein_coding	growth arrest specific 6 [Source:HGNC Symbol;Acc:HGNC:4168]
WDR76	-1,199	0,001	protein_coding	WD repeat domain 76 [Source:HGNC Symbol;Acc:HGNC:25773]
UBA2	-1,199	0,000	protein_coding	ubiquitin like modifier activating enzyme 2 [Source:HGNC Symbol;Acc:HGNC:30661]
NANS	-1,198	0,000	protein_coding	N-acetylneuraminate synthase [Source:HGNC Symbol;Acc:HGNC:19237]
NDC80	-1,197	0,000	protein_coding	NDC80 kinetochore complex component [Source:HGNC Symbol;Acc:HGNC:16909]
CTSL	-1,196	0,000	protein_coding	cathepsin L [Source:HGNC Symbol;Acc:HGNC:2537]
RASGRP3	-1,189	0,002	protein_coding	RAS guanyl releasing protein 3 [Source:HGNC Symbol;Acc:HGNC:14545]
ENSG00000236525	-1,186	0,000		
OTOA	-1,186	0,018	protein_coding	otoancorin [Source:HGNC Symbol;Acc:HGNC:16378]

Gene	Log2FoldChange	padj	Biotype	Description
LAT2	-1,186	0,000	protein_coding	linker for activation of T cells family member 2 [Source:HGNC Symbol;Acc:HGNC:12749]
ENSG00000279365	-1,183	0,000		
IARS1	-1,176	0,002	protein_coding	isoleucyl-tRNA synthetase 1 [Source:HGNC Symbol;Acc:HGNC:5330]
ADGRE2	-1,176	0,000	protein_coding	adhesion G protein-coupled receptor E2 [Source:HGNC Symbol;Acc:HGNC:3337]
PRNP	-1,175	0,001	protein_coding	prion protein [Source:HGNC Symbol;Acc:HGNC:9449]
LINC02732	-1,174	0,000	lncRNA	long intergenic non-protein coding RNA 2732 [Source:HGNC Symbol;Acc:HGNC:54249]
PC	-1,171	0,001	protein_coding	pyruvate carboxylase [Source:HGNC Symbol;Acc:HGNC:8636]
DLGAP1-AS2	-1,169	0,000	lncRNA	DLGAP1 antisense RNA 2 [Source:HGNC Symbol;Acc:HGNC:28146]
HYLS1	-1,167	0,006	protein_coding	HYLS1 centriolar and ciliogenesis associated [Source:HGNC Symbol;Acc:HGNC:26558]
HOOK1	-1,164	0,017	protein_coding	hook microtubule tethering protein 1 [Source:HGNC Symbol;Acc:HGNC:19884]
FKBP9	-1,164	0,000	protein_coding	FKBP prolyl isomerase 9 [Source:HGNC Symbol;Acc:HGNC:3725]
LINC02908	-1,163	0,025	lncRNA	long intergenic non-protein coding RNA 2908 [Source:HGNC Symbol;Acc:HGNC:31426]
KPNA2	-1,159	0,000	protein_coding	karyopherin subunit alpha 2 [Source:HGNC Symbol;Acc:HGNC:6395]
CAPN2	-1,158	0,000	protein_coding	calpain 2 [Source:HGNC Symbol;Acc:HGNC:1479]
HINT3	-1,157	0,000	protein_coding	histidine triad nucleotide binding protein 3 [Source:HGNC Symbol;Acc:HGNC:18468]
CDC20	-1,156	0,000	protein_coding	cell division cycle 20 [Source:HGNC Symbol;Acc:HGNC:1723]
ENSG00000255299	-1,152	0,000		
ENSG00000257639	-1,151	0,000		
NDUFS3	-1,150	0,000	protein_coding	NADH:ubiquinone oxidoreductase core subunit S3 [Source:HGNC Symbol;Acc:HGNC:7710]
ENSG00000287188	-1,149	0,000		
AHNAK2	-1,149	0,000	protein_coding	AHNAK nucleoprotein 2 [Source:HGNC Symbol;Acc:HGNC:20125]
NDST2	-1,149	0,000	protein_coding	N-deacetylase and N-sulfotransferase 2 [Source:HGNC Symbol;Acc:HGNC:7681]
TMX1	-1,146	0,000	protein_coding	thioredoxin related transmembrane protein 1 [Source:HGNC Symbol;Acc:HGNC:15487]
H4C9	-1,146	0,000	protein_coding	H4 clustered histone 9 [Source:HGNC Symbol;Acc:HGNC:4793]
LMF1-AS1	-1,146	0,000	lncRNA	LMF1 antisense RNA 1 [Source:HGNC Symbol;Acc:HGNC:50469]
LINC02427	-1,144	0,017	lncRNA	long intergenic non-protein coding RNA 2427 [Source:HGNC Symbol;Acc:HGNC:53358]
PCED1B	-1,144	0,000	protein_coding	PC-esterase domain containing 1B [Source:HGNC Symbol;Acc:HGNC:28255]
TRIB3	-1,144	0,004	protein_coding	tribbles pseudokinase 3 [Source:HGNC Symbol;Acc:HGNC:16228]

Gene	Log2FoldChange	padj	Biotype	Description
ENSG00000234389	-1,141	0,001		
PRR11	-1,139	0,000	protein_coding	proline rich 11 [Source:HGNC Symbol;Acc:HGNC:25619]
RAB27A	-1,138	0,000	protein_coding	RAB27A, member RAS oncogene family [Source:HGNC Symbol;Acc:HGNC:9766]
KRT19	-1,134	0,000	protein_coding	keratin 19 [Source:HGNC Symbol;Acc:HGNC:6436]
PAFAH2	-1,133	0,000	protein_coding	platelet activating factor acetylhydrolase 2 [Source:HGNC Symbol;Acc:HGNC:8579]
CCT8	-1,129	0,000	protein_coding	chaperonin containing TCP1 subunit 8 [Source:HGNC Symbol;Acc:HGNC:1623]
PHLDA2	-1,129	0,013	protein_coding	pleckstrin homology like domain family A member 2 [Source:HGNC Symbol;Acc:HGNC:12385]
LONRF3	-1,126	0,000	protein_coding	LON peptidase N-terminal domain and ring finger 3 [Source:HGNC Symbol;Acc:HGNC:21152]
CTSD	-1,124	0,000	protein_coding	cathepsin D [Source:HGNC Symbol;Acc:HGNC:2529]
LINC02577	-1,124	0,000	lncRNA	long intergenic non-protein coding RNA 2577 [Source:HGNC Symbol;Acc:HGNC:53749]
ENSG00000286346	-1,123	0,000		
PDP2	-1,122	0,000	protein_coding	pyruvate dehydrogenase phosphatase catalytic subunit 2 [Source:HGNC Symbol;Acc:HGNC:30263]
ENSG00000289261	-1,122	0,000		
GARS1	-1,117	0,002	protein_coding	glycyl-tRNA synthetase 1 [Source:HGNC Symbol;Acc:HGNC:4162]
RAB3IL1	-1,114	0,001	protein_coding	RAB3A interacting protein like 1 [Source:HGNC Symbol;Acc:HGNC:9780]
GOLGA7B	-1,110	0,003	protein_coding	golgin A7 family member B [Source:HGNC Symbol;Acc:HGNC:31668]
EZR	-1,108	0,000	protein_coding	ezrin [Source:HGNC Symbol;Acc:HGNC:12691]
LINC00589	-1,108	0,021	lncRNA	long intergenic non-protein coding RNA 589 [Source:HGNC Symbol;Acc:HGNC:32299]
MUL1	-1,107	0,000	protein_coding	mitochondrial E3 ubiquitin protein ligase 1 [Source:HGNC Symbol;Acc:HGNC:25762]
TARP	-1,102	0,019	protein_coding	TCR gamma alternate reading frame protein [Source:NCBI gene (formerly Entrezgene);Acc:445347]
CIT	-1,102	0,000	protein_coding	citron rho-interacting serine/threonine kinase [Source:HGNC Symbol;Acc:HGNC:1985]
IFI27	-1,101	0,000	protein_coding	interferon alpha inducible protein 27 [Source:HGNC Symbol;Acc:HGNC:5397]
CD68	-1,101	0,000	protein_coding	CD68 molecule [Source:HGNC Symbol;Acc:HGNC:1693]
COA6	-1,100	0,000	protein_coding	cytochrome c oxidase assembly factor 6 [Source:HGNC Symbol;Acc:HGNC:18025]
PIGAP1	-1,099	0,050	processed_pseudogene	phosphatidylinositol glycan anchor biosynthesis class A pseudogene 1 [Source:HGNC Symbol;Acc:HGNC:8958]
CIART	-1,099	0,033	protein_coding	circadian associated repressor of transcription [Source:HGNC Symbol;Acc:HGNC:25200]
NCS1	-1,098	0,000	protein_coding	neuronal calcium sensor 1 [Source:HGNC Symbol;Acc:HGNC:3953]
NUSAP1	-1,097	0,000	protein_coding	nucleolar and spindle associated protein 1 [Source:HGNC Symbol;Acc:HGNC:18538]

Gene	Log2FoldChange	padj	Biotype	Description
PROCR	-1,096	0,000	protein_coding	protein C receptor [Source:HGNC Symbol;Acc:HGNC:9452]
FGR	-1,095	0,000	protein_coding	FGR proto-oncogene, Src family tyrosine kinase [Source:HGNC Symbol;Acc:HGNC:3697]
ENSG00000273997	-1,094	0,016		
VIM	-1,090	0,000	protein_coding	vimentin [Source:HGNC Symbol;Acc:HGNC:12692]
GAS2L3	-1,090	0,000	protein_coding	growth arrest specific 2 like 3 [Source:HGNC Symbol;Acc:HGNC:27475]
LRRC39	-1,089	0,000	protein_coding	leucine rich repeat containing 39 [Source:HGNC Symbol;Acc:HGNC:28228]
TMEM266	-1,089	0,000	protein_coding	transmembrane protein 266 [Source:HGNC Symbol;Acc:HGNC:26763]
ENSG00000259336	-1,088	0,000		
OR10D1P	-1,086	0,013	unprocessed_pseudogene	olfactory receptor family 10 subfamily D member 1 pseudogene [Source:HGNC Symbol;Acc:HGNC:8166]
ERMAP	-1,082	0,000	protein_coding	erythroblast membrane associated protein (Scianna blood group) [Source:HGNC Symbol;Acc:HGNC:15743]
OR9H1P	-1,078	0,037	protein_coding	olfactory receptor family 9 subfamily H member 1 pseudogene [Source:HGNC Symbol;Acc:HGNC:15038]
CNBP	-1,077	0,000	protein_coding	CCHC-type zinc finger nucleic acid binding protein [Source:HGNC Symbol;Acc:HGNC:13164]
HROB	-1,076	0,010	protein_coding	homologous recombination factor with OB-fold [Source:HGNC Symbol;Acc:HGNC:28460]
MCM6	-1,074	0,000	protein_coding	minichromosome maintenance complex component 6 [Source:HGNC Symbol;Acc:HGNC:6949]
APPL1	-1,074	0,000	protein_coding	adaptor protein, phosphotyrosine interacting with PH domain and leucine zipper 1 [Source:HGNC Symbol;Acc:HGNC:24035]
SBF2-AS1	-1,071	0,000	lncRNA	SBF2 antisense RNA 1 [Source:HGNC Symbol;Acc:HGNC:27438]
OSBP	-1,071	0,000	protein_coding	oxysterol binding protein [Source:HGNC Symbol;Acc:HGNC:8503]
HCCS	-1,070	0,000	protein_coding	holocytochrome c synthase [Source:HGNC Symbol;Acc:HGNC:4837]
HINT1	-1,068	0,000	protein_coding	histidine triad nucleotide binding protein 1 [Source:HGNC Symbol;Acc:HGNC:4912]
ENSG00000272916	-1,065	0,001		
PLEKHN1	-1,061	0,000	protein_coding	pleckstrin homology domain containing N1 [Source:HGNC Symbol;Acc:HGNC:25284]
ENSG00000285895	-1,061	0,000		
WTIP	-1,058	0,001	protein_coding	WT1 interacting protein [Source:HGNC Symbol;Acc:HGNC:20964]
RPS2P36	-1,057	0,004	processed_pseudogene	ribosomal protein S2 pseudogene 36 [Source:HGNC Symbol;Acc:HGNC:36784]

Gene	Log2FoldChange	padj	Biotype	Description
HEXB	-1,054	0,000	protein_coding	hexosaminidase subunit beta [Source:HGNC Symbol;Acc:HGNC:4879]
MACIR	-1,048	0,000	protein_coding	macrophage immunometabolism regulator [Source:HGNC Symbol;Acc:HGNC:25052]
SOD2	-1,047	0,000	protein_coding	superoxide dismutase 2 [Source:HGNC Symbol;Acc:HGNC:11180]
TUBA1B	-1,044	0,004	protein_coding	tubulin alpha 1b [Source:HGNC Symbol;Acc:HGNC:18809]
ESR2	-1,044	0,000	protein_coding	estrogen receptor 2 [Source:HGNC Symbol;Acc:HGNC:3468]
CDCA3	-1,040	0,002	protein_coding	cell division cycle associated 3 [Source:HGNC Symbol;Acc:HGNC:14624]
POTEI	-1,039	0,032	protein_coding	POTE ankyrin domain family member I [Source:HGNC Symbol;Acc:HGNC:37093]
LRP11	-1,038	0,020	protein_coding	LDL receptor related protein 11 [Source:HGNC Symbol;Acc:HGNC:16936]
TCIRG1	-1,038	0,000	protein_coding	T cell immune regulator 1, ATPase H+ transporting V0 subunit a3 [Source:HGNC Symbol;Acc:HGNC:11647]
FAHD1	-1,037	0,000	protein_coding	fumarylacetoacetate hydrolase domain containing 1 [Source:HGNC Symbol;Acc:HGNC:14169]
HTATSF1	-1,036	0,000	protein_coding	HIV-1 Tat specific factor 1 [Source:HGNC Symbol;Acc:HGNC:5276]
MLPH	-1,036	0,000	protein_coding	melanophilin [Source:HGNC Symbol;Acc:HGNC:29643]
H4C1	-1,035	0,000	protein_coding	H4 clustered histone 1 [Source:HGNC Symbol;Acc:HGNC:4781]
RAB7B	-1,034	0,043	protein_coding	RAB7B, member RAS oncogene family [Source:HGNC Symbol;Acc:HGNC:30513]
CCDC78	-1,034	0,003	protein_coding	coiled-coil domain containing 78 [Source:HGNC Symbol;Acc:HGNC:14153]
HRH4	-1,033	0,000	protein_coding	histamine receptor H4 [Source:HGNC Symbol;Acc:HGNC:17383]
FLVCR2	-1,033	0,000	protein_coding	FLVCR choline and putative heme transporter 2 [Source:HGNC Symbol;Acc:HGNC:20105]
PCK2	-1,032	0,000	protein_coding	phosphoenolpyruvate carboxykinase 2, mitochondrial [Source:HGNC Symbol;Acc:HGNC:8725]
ANK2	-1,031	0,000	protein_coding	ankyrin 2 [Source:HGNC Symbol;Acc:HGNC:493]
SLC25A1	-1,029	0,000	protein_coding	solute carrier family 25 member 1 [Source:HGNC Symbol;Acc:HGNC:10979]
OR5B21	-1,028	0,000	protein_coding	olfactory receptor family 5 subfamily B member 21 [Source:HGNC Symbol;Acc:HGNC:19616]
YAP1P1	-1,026	0,000	processed_pseudogene	YAP1 pseudogene 1 [Source:HGNC Symbol;Acc:HGNC:38016]
INTS6L	-1,025	0,000	protein_coding	integrator complex subunit 6 like [Source:HGNC Symbol;Acc:HGNC:27334]
RGS11	-1,024	0,005	protein_coding	regulator of G protein signaling 11 [Source:HGNC Symbol;Acc:HGNC:9993]
OSTM1	-1,021	0,000	protein_coding	osteoclastogenesis associated transmembrane protein 1 [Source:HGNC Symbol;Acc:HGNC:21652]
SEC11C	-1,020	0,000	protein_coding	SEC11 homolog C, signal peptidase complex subunit [Source:HGNC Symbol;Acc:HGNC:23400]
CACNA2D1	-1,019	0,000	protein_coding	calcium voltage-gated channel auxiliary subunit alpha2delta 1 [Source:HGNC Symbol;Acc:HGNC:1399]
FASTK	-1,016	0,000	protein_coding	Fas activated serine/threonine kinase [Source:HGNC Symbol;Acc:HGNC:24676]

Gene	Log2FoldChange	padj	Biotype	Description
TYMP	-1,016	0,000	protein_coding	thymidine phosphorylase [Source:HGNC Symbol;Acc:HGNC:3148]
USP18	-1,016	0,000	protein_coding	ubiquitin specific peptidase 18 [Source:HGNC Symbol;Acc:HGNC:12616]
ENSG00000273226	-1,015	0,023		
UROD	-1,012	0,000	protein_coding	uroporphyrinogen decarboxylase [Source:HGNC Symbol;Acc:HGNC:12591]
ENSG00000284946	-1,004	0,001		
PDE12	-1,003	0,000	protein_coding	phosphodiesterase 12 [Source:HGNC Symbol;Acc:HGNC:25386]
CEBPB	-1,003	0,000	protein_coding	CCAAT enhancer binding protein beta [Source:HGNC Symbol;Acc:HGNC:1834]
NR1D2	-1,002	0,000	protein_coding	nuclear receptor subfamily 1 group D member 2 [Source:HGNC Symbol;Acc:HGNC:7963]
XKR3	-1,002	0,025	protein_coding	XK related 3 [Source:HGNC Symbol;Acc:HGNC:28778]
APOC1	-1,000	0,012	protein_coding	apolipoprotein C1 [Source:HGNC Symbol;Acc:HGNC:607]
ZFPM1	1,002	0,000	protein_coding	zinc finger protein, FOG family member 1 [Source:HGNC Symbol;Acc:HGNC:19762]
LINC02193	1,002	0,027		
SLC40A1	1,003	0,032	protein_coding	solute carrier family 40 member 1 [Source:HGNC Symbol;Acc:HGNC:10909]
OSBPL6	1,003	0,013	protein_coding	oxysterol binding protein like 6 [Source:HGNC Symbol;Acc:HGNC:16388]
SPOCK2	1,004	0,004	protein_coding	SPARC (osteonectin), cwcv and kazal like domains proteoglycan 2 [Source:HGNC Symbol;Acc:HGNC:13564]
ANKRD30BP2	1,006	0,006	transcribed_unprocessed_pseudogene	ankyrin repeat domain 30B pseudogene 2 [Source:HGNC Symbol;Acc:HGNC:16620]
ENSG00000267436	1,006	0,040		
CLDN9	1,007	0,002	protein_coding	claudin 9 [Source:HGNC Symbol;Acc:HGNC:2051]
PRMT6	1,010	0,000	protein_coding	protein arginine methyltransferase 6 [Source:HGNC Symbol;Acc:HGNC:18241]
ENSG00000230773	1,011	0,001		
ENSG00000227733	1,011	0,015		
ENSG00000264808	1,012	0,041		
ENSG00000284606	1,013	0,033		
C6orf132	1,015	0,019	protein_coding	chromosome 6 open reading frame 132 [Source:HGNC Symbol;Acc:HGNC:21288]
CXCL14	1,015	0,021	protein_coding	C-X-C motif chemokine ligand 14 [Source:HGNC Symbol;Acc:HGNC:10640]
ACVR1B	1,016	0,000	protein_coding	activin A receptor type 1B [Source:HGNC Symbol;Acc:HGNC:172]
GPR141	1,018	0,000	protein_coding	G protein-coupled receptor 141 [Source:HGNC Symbol;Acc:HGNC:19997]
BMS1P14	1,026	0,049	lncRNA	BMS1 pseudogene 14 [Source:HGNC Symbol;Acc:HGNC:49159]

Gene	Log2FoldChange	padj	Biotype	Description
TRIB2	1,027	0,009	protein_coding	tribbles pseudokinase 2 [Source:HGNC Symbol;Acc:HGNC:30809]
PALD1	1,029	0,045	protein_coding	phosphatase domain containing paladin 1 [Source:HGNC Symbol;Acc:HGNC:23530]
TWF1	1,031	0,000	protein_coding	twinfilin actin binding protein 1 [Source:HGNC Symbol;Acc:HGNC:9620]
TIMP1	1,040	0,000	protein_coding	TIMP metallopeptidase inhibitor 1 [Source:HGNC Symbol;Acc:HGNC:11820]
CCDC102B	1,040	0,007	protein_coding	coiled-coil domain containing 102B [Source:HGNC Symbol;Acc:HGNC:26295]
ENSG00000285650	1,041	0,038		
RIC3	1,043	0,000	protein_coding	RIC3 acetylcholine receptor chaperone [Source:HGNC Symbol;Acc:HGNC:30338]
ZFHX3-AS1	1,044	0,007	lncRNA	ZFHX3 antisense RNA 1 [Source:HGNC Symbol;Acc:HGNC:56033]
BMAL1	1,046	0,001	protein_coding	basic helix-loop-helix ARNT like 1 [Source:HGNC Symbol;Acc:HGNC:701]
EFCAB15P	1,052	0,037	transcribed_unitary_pseudogene	EF-hand calcium binding domain 15, pseudogene [Source:HGNC Symbol;Acc:HGNC:55140]
ENSG00000197550	1,052	0,001		
SYNPO2	1,056	0,000	protein_coding	synaptopodin 2 [Source:HGNC Symbol;Acc:HGNC:17732]
SPTBN2	1,058	0,000	protein_coding	spectrin beta, non-erythrocytic 2 [Source:HGNC Symbol;Acc:HGNC:11276]
AQP7B	1,059	0,014	protein_coding	aquaporin 7B [Source:HGNC Symbol;Acc:HGNC:53895]
CSF2	1,061	0,010	protein_coding	colony stimulating factor 2 [Source:HGNC Symbol;Acc:HGNC:2434]
ZEB2-AS1	1,061	0,023	lncRNA	ZEB2 antisense RNA 1 [Source:HGNC Symbol;Acc:HGNC:37149]
ENSG00000270557	1,061	0,021		
MUC20P1	1,062	0,000	unprocessed_pseudogene	mucin 20, cell surface associated pseudogene 1 [Source:HGNC Symbol;Acc:HGNC:51921]
MIR181A1HG	1,063	0,013	lncRNA	MIR181A1 host gene [Source:HGNC Symbol;Acc:HGNC:48659]
CRACD	1,064	0,000	protein_coding	capping protein inhibiting regulator of actin dynamics [Source:HGNC Symbol;Acc:HGNC:29219]
ENSG00000272103	1,064	0,028		
FAM174A-DT	1,065	0,020	lncRNA	FAM174A divergent transcript [Source:HGNC Symbol;Acc:HGNC:55584]
ENSG00000260912	1,066	0,000		
CDH23	1,068	0,002	protein_coding	cadherin related 23 [Source:HGNC Symbol;Acc:HGNC:13733]
CFAP70	1,069	0,000	protein_coding	cilia and flagella associated protein 70 [Source:HGNC Symbol;Acc:HGNC:30726]
MTSS1	1,074	0,004	protein_coding	MTSS I-BAR domain containing 1 [Source:HGNC Symbol;Acc:HGNC:20443]
ENSG00000290549	1,077	0,010		
TEX15	1,077	0,038	protein_coding	testis expressed 15, meiosis and synapsis associated [Source:HGNC Symbol;Acc:HGNC:11738]

Gene	Log2FoldChange	padj	Biotype	Description
CNRIP1	1,079	0,000	protein_coding	cannabinoid receptor interacting protein 1 [Source:HGNC Symbol;Acc:HGNC:24546]
ENSG00000233968	1,080	0,000		
ENSG00000278997	1,084	0,000		
ACER2	1,085	0,000	protein_coding	alkaline ceramidase 2 [Source:HGNC Symbol;Acc:HGNC:23675]
TSPAN7	1,087	0,000	protein_coding	tetraspanin 7 [Source:HGNC Symbol;Acc:HGNC:11854]
NEIL1	1,087	0,005	protein_coding	nei like DNA glycosylase 1 [Source:HGNC Symbol;Acc:HGNC:18448]
KIAA1958	1,087	0,019	protein_coding	KIAA1958 [Source:HGNC Symbol;Acc:HGNC:23427]
FAM234B	1,088	0,000	protein_coding	family with sequence similarity 234 member B [Source:HGNC Symbol;Acc:HGNC:29288]
RPL5P21	1,088	0,002	processed_pseudogene	ribosomal protein L5 pseudogene 21 [Source:HGNC Symbol;Acc:HGNC:37029]
ENSG00000260470	1,101	0,000		
MAP3K5-AS2	1,102	0,010	lncRNA	MAP3K5 antisense RNA 2 [Source:HGNC Symbol;Acc:HGNC:56125]
PAIP2B	1,105	0,006	protein_coding	poly(A) binding protein interacting protein 2B [Source:HGNC Symbol;Acc:HGNC:29200]
ADCY4	1,107	0,000	protein_coding	adenylate cyclase 4 [Source:HGNC Symbol;Acc:HGNC:235]
LINC02302	1,109	0,000	lncRNA	long intergenic non-protein coding RNA 2302 [Source:HGNC Symbol;Acc:HGNC:53221]
FBXO39	1,113	0,000	protein_coding	F-box protein 39 [Source:HGNC Symbol;Acc:HGNC:28565]
LRP1B	1,113	0,002	protein_coding	LDL receptor related protein 1B [Source:HGNC Symbol;Acc:HGNC:6693]
ADPRHL1	1,115	0,007	protein_coding	ADP-ribosylhydrolase like 1 [Source:HGNC Symbol;Acc:HGNC:21303]
PPAN-P2RY11	1,115	0,001	protein_coding	PPAN-P2RY11 readthrough [Source:HGNC Symbol;Acc:HGNC:33526]
CCR2	1,116	0,000	protein_coding	C-C motif chemokine receptor 2 [Source:HGNC Symbol;Acc:HGNC:1603]
ENSG00000228463	1,116	0,016		
PLAC8	1,117	0,010	protein_coding	placenta associated 8 [Source:HGNC Symbol;Acc:HGNC:19254]
ENSG00000288049	1,121	0,000		
ENSG00000286943	1,121	0,037		
AMMECR1	1,124	0,000	protein_coding	AMMECR nuclear protein 1 [Source:HGNC Symbol;Acc:HGNC:467]
HSPE1P13	1,126	0,013	processed_pseudogene	heat shock protein family E (Hsp10) member 1 pseudogene 13 [Source:HGNC Symbol;Acc:HGNC:49332]
ENSG00000284292	1,134	0,005		
ZNF252P-AS1	1,135	0,001	lncRNA	ZNF252P antisense RNA 1 [Source:HGNC Symbol;Acc:HGNC:27821]
AGBL2	1,136	0,003	protein_coding	AGBL carboxypeptidase 2 [Source:HGNC Symbol;Acc:HGNC:26296]

Gene	Log2FoldChange	padj	Biotype	Description
HIC1	1,138	0,016	protein_coding	HIC ZBTB transcriptional repressor 1 [Source:HGNC Symbol;Acc:HGNC:4909]
PRICKLE1	1,140	0,009	protein_coding	prickle planar cell polarity protein 1 [Source:HGNC Symbol;Acc:HGNC:17019]
LRATD1	1,146	0,000	protein_coding	LRAT domain containing 1 [Source:HGNC Symbol;Acc:HGNC:20743]
SPRED3	1,147	0,000	protein_coding	sprouty related EVH1 domain containing 3 [Source:HGNC Symbol;Acc:HGNC:31041]
FRAS1	1,148	0,012	protein_coding	Fraser extracellular matrix complex subunit 1 [Source:HGNC Symbol;Acc:HGNC:19185]
ENSG00000261582	1,148	0,033		
CNIH2	1,150	0,014	protein_coding	cornichon family AMPA receptor auxiliary protein 2 [Source:HGNC Symbol;Acc:HGNC:28744]
CFAP47	1,150	0,000	protein_coding	cilia and flagella associated protein 47 [Source:HGNC Symbol;Acc:HGNC:26708]
NR4A3	1,152	0,006	protein_coding	nuclear receptor subfamily 4 group A member 3 [Source:HGNC Symbol;Acc:HGNC:7982]
GSTM4	1,152	0,009	protein_coding	glutathione S-transferase mu 4 [Source:HGNC Symbol;Acc:HGNC:4636]
SLC15A2	1,152	0,047	protein_coding	solute carrier family 15 member 2 [Source:HGNC Symbol;Acc:HGNC:10921]
PIM1	1,152	0,009	protein_coding	Pim-1 proto-oncogene, serine/threonine kinase [Source:HGNC Symbol;Acc:HGNC:8986]
SP2-AS1	1,153	0,010	lncRNA	SP2 antisense RNA 1 [Source:HGNC Symbol;Acc:HGNC:51341]
GSTM3	1,155	0,004	protein_coding	glutathione S-transferase mu 3 [Source:HGNC Symbol;Acc:HGNC:4635]
LINC01094	1,156	0,023	lncRNA	long intergenic non-protein coding RNA 1094 [Source:HGNC Symbol;Acc:HGNC:49219]
FSCB	1,158	0,037	protein_coding	fibrous sheath CABYR binding protein [Source:HGNC Symbol;Acc:HGNC:20494]
ENSG00000240219	1,162	0,000		
RYR3	1,169	0,000	protein_coding	ryanodine receptor 3 [Source:HGNC Symbol;Acc:HGNC:10485]
ENSG00000224400	1,173	0,032		
FAM183BP	1,174	0,000	processed_pseudogene	family with sequence similarity 183 member B, pseudogene [Source:HGNC Symbol;Acc:HGNC:34511]
ZNF469	1,179	0,000	protein_coding	zinc finger protein 469 [Source:HGNC Symbol;Acc:HGNC:23216]
SASH3	1,181	0,004	protein_coding	SAM and SH3 domain containing 3 [Source:HGNC Symbol;Acc:HGNC:15975]
IKZF3	1,181	0,002	protein_coding	IKAROS family zinc finger 3 [Source:HGNC Symbol;Acc:HGNC:13178]
PCAT6	1,183	0,006	lncRNA	prostate cancer associated transcript 6 [Source:HGNC Symbol;Acc:HGNC:43714]
TMEM198	1,185	0,000	protein_coding	transmembrane protein 198 [Source:HGNC Symbol;Acc:HGNC:33704]
PCYT1B	1,190	0,020	protein_coding	phosphate cytidylyltransferase 1B, choline [Source:HGNC Symbol;Acc:HGNC:8755]
LRRC8B	1,190	0,000	protein_coding	leucine rich repeat containing 8 VRAC subunit B [Source:HGNC Symbol;Acc:HGNC:30692]
KCND1	1,193	0,000	protein_coding	potassium voltage-gated channel subfamily D member 1 [Source:HGNC Symbol;Acc:HGNC:6237]

Gene	Log2FoldChange	padj	Biotype	Description
MYCN	1,209	0,004	protein_coding	MYCN proto-oncogene, bHLH transcription factor [Source:HGNC Symbol;Acc:HGNC:7559]
ABCA15P	1,213	0,008	transcribed_unitary_pseudogene	ATP binding cassette subfamily A member 15, pseudogene [Source:HGNC Symbol;Acc:HGNC:34405]
EEF1A1P24	1,213	0,001	processed_pseudogene	eukaryotic translation elongation factor 1 alpha 1 pseudogene 24 [Source:HGNC Symbol;Acc:HGNC:37897]
MEF2C	1,213	0,013	protein_coding	myocyte enhancer factor 2C [Source:HGNC Symbol;Acc:HGNC:6996]
ENSG00000248015	1,213	0,000		
RD3	1,214	0,015	protein_coding	RD3 regulator of GUCY2D [Source:HGNC Symbol;Acc:HGNC:19689]
ITGA10	1,223	0,014	protein_coding	integrin subunit alpha 10 [Source:HGNC Symbol;Acc:HGNC:6135]
ENOX1	1,224	0,042	protein_coding	ecto-NOX disulfide-thiol exchanger 1 [Source:HGNC Symbol;Acc:HGNC:25474]
ENSG00000261159	1,225	0,025		
TJP3	1,230	0,011	protein_coding	tight junction protein 3 [Source:HGNC Symbol;Acc:HGNC:11829]
ENSG00000263033	1,236	0,028		
EXOC6B	1,242	0,000	protein_coding	exocyst complex component 6B [Source:HGNC Symbol;Acc:HGNC:17085]
ENSG00000247679	1,250	0,000		
MAST4	1,254	0,000	protein_coding	microtubule associated serine/threonine kinase family member 4 [Source:HGNC Symbol;Acc:HGNC:19037]
SEPTIN14P6	1,269	0,001	transcribed_processed_pseudogene	septin 14 pseudogene 6 [Source:HGNC Symbol;Acc:HGNC:51690]
ARHGAP8	1,271	0,000	protein_coding	Rho GTPase activating protein 8 [Source:HGNC Symbol;Acc:HGNC:677]
SLC16A6	1,274	0,000	protein_coding	solute carrier family 16 member 6 [Source:HGNC Symbol;Acc:HGNC:10927]
ITGA4	1,277	0,000	protein_coding	integrin subunit alpha 4 [Source:HGNC Symbol;Acc:HGNC:6140]
ENSG00000286797	1,282	0,001		
FMNL1-AS1	1,282	0,000	lncRNA	FMNL1 antisense RNA 1 [Source:HGNC Symbol;Acc:HGNC:55717]
MT1X	1,283	0,000	protein_coding	metallothionein 1X [Source:HGNC Symbol;Acc:HGNC:7405]
RRM2P3	1,285	0,002	processed_pseudogene	ribonucleotide reductase M2 polypeptide pseudogene 3 [Source:HGNC Symbol;Acc:HGNC:10455]
ENSG00000240401	1,286	0,001		
AP1G2-AS1	1,287	0,000	lncRNA	AP1G2 antisense RNA 1 [Source:HGNC Symbol;Acc:HGNC:55442]
LY6G5C	1,288	0,000	protein_coding	lymphocyte antigen 6 family member G5C [Source:HGNC Symbol;Acc:HGNC:13932]

Gene	Log2FoldChange	padj	Biotype	Description
MYCN	1,209	0,004	protein_coding	MYCN proto-oncogene, bHLH transcription factor [Source:HGNC Symbol;Acc:HGNC:7559]
ABCA15P	1,213	0,008	transcribed_unitary_pseudogene	ATP binding cassette subfamily A member 15, pseudogene [Source:HGNC Symbol;Acc:HGNC:34405]
EEF1A1P24	1,213	0,001	processed_pseudogene	eukaryotic translation elongation factor 1 alpha 1 pseudogene 24 [Source:HGNC Symbol;Acc:HGNC:37897]
MEF2C	1,213	0,013	protein_coding	myocyte enhancer factor 2C [Source:HGNC Symbol;Acc:HGNC:6996]
ENSG00000248015	1,213	0,000		
RD3	1,214	0,015	protein_coding	RD3 regulator of GUCY2D [Source:HGNC Symbol;Acc:HGNC:19689]
ITGA10	1,223	0,014	protein_coding	integrin subunit alpha 10 [Source:HGNC Symbol;Acc:HGNC:6135]
ENOX1	1,224	0,042	protein_coding	ecto-NOX disulfide-thiol exchanger 1 [Source:HGNC Symbol;Acc:HGNC:25474]
ENSG00000261159	1,225	0,025		
TJP3	1,230	0,011	protein_coding	tight junction protein 3 [Source:HGNC Symbol;Acc:HGNC:11829]
ENSG00000263033	1,236	0,028		
EXOC6B	1,242	0,000	protein_coding	exocyst complex component 6B [Source:HGNC Symbol;Acc:HGNC:17085]
ENSG00000247679	1,250	0,000		
MAST4	1,254	0,000	protein_coding	microtubule associated serine/threonine kinase family member 4 [Source:HGNC Symbol;Acc:HGNC:19037]
SEPTIN14P6	1,269	0,001	transcribed_processed_pseudogene	septin 14 pseudogene 6 [Source:HGNC Symbol;Acc:HGNC:51690]
ARHGAP8	1,271	0,000	protein_coding	Rho GTPase activating protein 8 [Source:HGNC Symbol;Acc:HGNC:677]
SLC16A6	1,274	0,000	protein_coding	solute carrier family 16 member 6 [Source:HGNC Symbol;Acc:HGNC:10927]
ITGA4	1,277	0,000	protein_coding	integrin subunit alpha 4 [Source:HGNC Symbol;Acc:HGNC:6140]
ENSG00000286797	1,282	0,001		
FMNL1-AS1	1,282	0,000	lncRNA	FMNL1 antisense RNA 1 [Source:HGNC Symbol;Acc:HGNC:55717]
MT1X	1,283	0,000	protein_coding	metallothionein 1X [Source:HGNC Symbol;Acc:HGNC:7405]
RRM2P3	1,285	0,002	processed_pseudogene	ribonucleotide reductase M2 polypeptide pseudogene 3 [Source:HGNC Symbol;Acc:HGNC:10455]

Gene	Log2FoldChange	padj	Biotype	Description
ENSG00000240401	1,286	0,001		
AP1G2-AS1	1,287	0,000	lncRNA	AP1G2 antisense RNA 1 [Source:HGNC Symbol;Acc:HGNC:55442]
LY6G5C	1,288	0,000	protein_coding	lymphocyte antigen 6 family member G5C [Source:HGNC Symbol;Acc:HGNC:13932]
ENSG00000271344	1,292	0,004		
KCNJ14	1,292	0,000	protein_coding	potassium inwardly rectifying channel subfamily J member 14 [Source:HGNC Symbol;Acc:HGNC:6260]
ENSG00000273901	1,292	0,004		
FSIP2	1,293	0,000	protein_coding	fibrous sheath interacting protein 2 [Source:HGNC Symbol;Acc:HGNC:21675]
MMP14	1,293	0,039	protein_coding	matrix metallopeptidase 14 [Source:HGNC Symbol;Acc:HGNC:7160]
SLC23A3	1,293	0,003	protein_coding	solute carrier family 23 member 3 [Source:HGNC Symbol;Acc:HGNC:20601]
FBN1	1,294	0,000	protein_coding	fibrillin 1 [Source:HGNC Symbol;Acc:HGNC:3603]
RDH10	1,294	0,000	protein_coding	retinol dehydrogenase 10 [Source:HGNC Symbol;Acc:HGNC:19975]
CHIT1	1,296	0,025	protein_coding	chitinase 1 [Source:HGNC Symbol;Acc:HGNC:1936]
SLC22A20P	1,296	0,005	transcribed_unitary_pseudogene	solute carrier family 22 member 20, pseudogene [Source:HGNC Symbol;Acc:HGNC:29867]
B3GALT2	1,298	0,036	protein_coding	beta-1,3-galactosyltransferase 2 [Source:HGNC Symbol;Acc:HGNC:917]
SYTL4	1,299	0,004	protein_coding	synaptotagmin like 4 [Source:HGNC Symbol;Acc:HGNC:15588]
NECTIN3	1,301	0,001	protein_coding	nectin cell adhesion molecule 3 [Source:HGNC Symbol;Acc:HGNC:17664]
SOX4	1,319	0,003	protein_coding	SRY-box transcription factor 4 [Source:HGNC Symbol;Acc:HGNC:11200]
ENSG00000290522	1,320	0,019		
TSPAN6	1,322	0,000	protein_coding	tetraspanin 6 [Source:HGNC Symbol;Acc:HGNC:11858]
DISP2	1,327	0,000	protein_coding	dispatched RND transporter family member 2 [Source:HGNC Symbol;Acc:HGNC:19712]
ENSG00000280537	1,328	0,001		
EGR3	1,328	0,007	protein_coding	early growth response 3 [Source:HGNC Symbol;Acc:HGNC:3240]
GRIN2C	1,332	0,000	protein_coding	glutamate ionotropic receptor NMDA type subunit 2C [Source:HGNC Symbol;Acc:HGNC:4587]
ENSG00000260370	1,332	0,017		
ENSG00000248791	1,336	0,002		
ENSG00000285820	1,341	0,002		
GATM	1,344	0,006	protein_coding	glycine amidinotransferase [Source:HGNC Symbol;Acc:HGNC:4175]
SSPOP	1,348	0,021	transcribed_unitary_pseudogene	SCO-spondin, pseudogene [Source:HGNC Symbol;Acc:HGNC:21998]

Gene	Log2FoldChange	padj	Biotype	Description
ENSG00000263508	1,353	0,010		
ENSG00000236833	1,354	0,006		
MEX3A	1,357	0,000	protein_coding	mex-3 RNA binding family member A [Source:HGNC Symbol;Acc:HGNC:33482]
ENSG00000286015	1,361	0,014		
MYH3	1,365	0,003	protein_coding	myosin heavy chain 3 [Source:HGNC Symbol;Acc:HGNC:7573]
PLEKHA8P1	1,367	0,000	transcribed_processed_pseudogene	pleckstrin homology domain containing A8 pseudogene 1 [Source:HGNC Symbol;Acc:HGNC:30222]
RPS3AP19	1,369	0,043	processed_pseudogene	RPS3A pseudogene 19 [Source:HGNC Symbol;Acc:HGNC:36467]
RIMKLA	1,373	0,024	protein_coding	ribosomal modification protein rimK like family member A [Source:HGNC Symbol;Acc:HGNC:28725]
HYDIN	1,376	0,017	protein_coding	HYDIN axonemal central pair apparatus protein [Source:HGNC Symbol;Acc:HGNC:19368]
CCRL2	1,377	0,006	protein_coding	C-C motif chemokine receptor like 2 [Source:HGNC Symbol;Acc:HGNC:1612]
BMP1	1,377	0,000	protein_coding	bone morphogenetic protein 1 [Source:HGNC Symbol;Acc:HGNC:1067]
SMANTIS	1,382	0,000	lncRNA	SMARCA4 interacting SWI/SNF chromatin remodeling complex scaffold lncRNA [Source:HGNC Symbol;Acc:HGNC:54417]
LGALS12	1,388	0,011	protein_coding	galectin 12 [Source:HGNC Symbol;Acc:HGNC:15788]
ENSG00000290717	1,390	0,031		
MAK	1,390	0,002	protein_coding	male germ cell associated kinase [Source:HGNC Symbol;Acc:HGNC:6816]
ENSG00000279186	1,394	0,001		
ENSG00000260927	1,394	0,000		
PRSS57	1,404	0,013	protein_coding	serine protease 57 [Source:HGNC Symbol;Acc:HGNC:31397]
STRC	1,411	0,001	protein_coding	stereocilin [Source:HGNC Symbol;Acc:HGNC:16035]
SLC4A3	1,415	0,028	protein_coding	solute carrier family 4 member 3 [Source:HGNC Symbol;Acc:HGNC:11029]
RPL17P22	1,419	0,000	processed_pseudogene	ribosomal protein L17 pseudogene 22 [Source:HGNC Symbol;Acc:HGNC:35761]
C17orf99	1,421	0,002	protein_coding	chromosome 17 open reading frame 99 [Source:HGNC Symbol;Acc:HGNC:34490]
CCP110	1,424	0,000	protein_coding	centriolar coiled-coil protein 110 [Source:HGNC Symbol;Acc:HGNC:24342]
LINC00954	1,428	0,008	lncRNA	long intergenic non-protein coding RNA 954 [Source:HGNC Symbol;Acc:HGNC:48668]
ZNF662	1,437	0,007	protein_coding	zinc finger protein 662 [Source:HGNC Symbol;Acc:HGNC:31930]

Gene	Log2FoldChange	padj	Biotype	Description
AREG	1,437	0,028	protein_coding	amphiregulin [Source:HGNC Symbol;Acc:HGNC:651]
BCAN-AS1	1,438	0,000	lncRNA	BCAN antisense RNA 1 [Source:HGNC Symbol;Acc:HGNC:55233]
C1GALT1P2	1,442	0,000	processed_pseudogene	C1GALT1 pseudogene 2 [Source:HGNC Symbol;Acc:HGNC:51615]
ENSG00000288758	1,449	0,001		
ZNF415	1,455	0,013	protein_coding	zinc finger protein 415 [Source:HGNC Symbol;Acc:HGNC:20636]
SLC27A3	1,466	0,000	protein_coding	solute carrier family 27 member 3 [Source:HGNC Symbol;Acc:HGNC:10997]
MED12L	1,486	0,000	protein_coding	mediator complex subunit 12L [Source:HGNC Symbol;Acc:HGNC:16050]
ALOX15	1,497	0,046	protein_coding	arachidonate 15-lipoxygenase [Source:HGNC Symbol;Acc:HGNC:433]
SLC22A17	1,500	0,008	protein_coding	solute carrier family 22 member 17 [Source:HGNC Symbol;Acc:HGNC:23095]
COL11A2	1,503	0,000	protein_coding	collagen type XI alpha 2 chain [Source:HGNC Symbol;Acc:HGNC:2187]
PMS2P13	1,504	0,001	transcribed_unprocessed_pseudogene	PMS1 homolog 2, mismatch repair system component pseudogene 13 [Source:HGNC Symbol;Acc:HGNC:55748]
ENSG00000264451	1,506	0,005		
ENSG00000240497	1,510	0,000		
LYPD8	1,513	0,001	protein_coding	LY6/PLAUR domain containing 8 [Source:HGNC Symbol;Acc:HGNC:44208]
CACNB3	1,524	0,001	protein_coding	calcium voltage-gated channel auxiliary subunit beta 3 [Source:HGNC Symbol;Acc:HGNC:1403]
ENSG00000260182	1,526	0,000		
ENSG00000290461	1,528	0,000		
RAB3C	1,530	0,000	protein_coding	RAB3C, member RAS oncogene family [Source:HGNC Symbol;Acc:HGNC:30269]
SNX29P1	1,533	0,006	unprocessed_pseudogene	sorting nexin 29 pseudogene 1 [Source:HGNC Symbol;Acc:HGNC:31913]
ENSG00000272692	1,537	0,007		
ENSG00000253736	1,542	0,026		
SNORD3B-2	1,545	0,046	snoRNA	small nucleolar RNA, C/D box 3B-2 [Source:HGNC Symbol;Acc:HGNC:33190]
OR10D4P	1,546	0,019	unprocessed_pseudogene	olfactory receptor family 10 subfamily D member 4 pseudogene [Source:HGNC Symbol;Acc:HGNC:14770]
DPYS	1,552	0,010	protein_coding	dihydropyrimidinase [Source:HGNC Symbol;Acc:HGNC:3013]
LINC02751	1,557	0,023	lncRNA	long intergenic non-protein coding RNA 2751 [Source:HGNC Symbol;Acc:HGNC:54271]

Gene	Log2FoldChange	padj	Biotype	Description
TMTC1	1,558	0,010	protein_coding	transmembrane O-mannosyltransferase targeting cadherins 1 [Source:HGNC Symbol;Acc:HGNC:24099]
ITPRID2-DT	1,559	0,000	lncRNA	ITPRID2 divergent transcript [Source:HGNC Symbol;Acc:HGNC:55386]
ENSG00000249881	1,562	0,000		
TUBB8	1,563	0,003	protein_coding	tubulin beta 8 class VIII [Source:HGNC Symbol;Acc:HGNC:20773]
ITGA2B	1,576	0,000	protein_coding	integrin subunit alpha 2b [Source:HGNC Symbol;Acc:HGNC:6138]
NCAM2	1,579	0,004	protein_coding	neural cell adhesion molecule 2 [Source:HGNC Symbol;Acc:HGNC:7657]
KRT72	1,580	0,000	protein_coding	keratin 72 [Source:HGNC Symbol;Acc:HGNC:28932]
LRRTM2	1,581	0,000	protein_coding	leucine rich repeat transmembrane neuronal 2 [Source:HGNC Symbol;Acc:HGNC:19409]
ATP1B1	1,584	0,000	protein_coding	ATPase Na+/K+ transporting subunit beta 1 [Source:HGNC Symbol;Acc:HGNC:804]
MIR194-2HG	1,604	0,016	lncRNA	MIR194-2 host gene [Source:HGNC Symbol;Acc:HGNC:51946]
GIHCG	1,607	0,000	lncRNA	GIHCG inhibitor of miR-200b/200a/429 expression [Source:HGNC Symbol;Acc:HGNC:52649]
SLC18A2-AS1	1,610	0,000	lncRNA	SLC18A2 antisense RNA 1 [Source:HGNC Symbol;Acc:HGNC:55843]
ENSG00000246203	1,610	0,040		
SYCE1L	1,610	0,031	protein_coding	synaptonemal complex central element protein 1 like [Source:HGNC Symbol;Acc:HGNC:37236]
SLC26A8	1,634	0,044	protein_coding	solute carrier family 26 member 8 [Source:HGNC Symbol;Acc:HGNC:14468]
NHLH1	1,636	0,012	protein_coding	nescient helix-loop-helix 1 [Source:HGNC Symbol;Acc:HGNC:7817]
WFIKKN1	1,660	0,000	protein_coding	WAP, follistatin/kazal, immunoglobulin, kunitz and netrin domain containing 1 [Source:HGNC Symbol;Acc:HGNC:30912]
MT2A	1,663	0,000	protein_coding	metallothionein 2A [Source:HGNC Symbol;Acc:HGNC:7406]
AIFM3	1,664	0,000	protein_coding	apoptosis inducing factor mitochondria associated 3 [Source:HGNC Symbol;Acc:HGNC:26398]
FLNC	1,679	0,032	protein_coding	filamin C [Source:HGNC Symbol;Acc:HGNC:3756]
ENSG00000205890	1,682	0,038		
ENSG00000272884	1,685	0,000		
DDIT4L	1,686	0,025	protein_coding	DNA damage inducible transcript 4 like [Source:HGNC Symbol;Acc:HGNC:30555]
GSTM2	1,691	0,000	protein_coding	glutathione S-transferase mu 2 [Source:HGNC Symbol;Acc:HGNC:4634]
CROT	1,698	0,000	protein_coding	carnitine O-octanoyltransferase [Source:HGNC Symbol;Acc:HGNC:2366]
TRIP6	1,706	0,042	protein_coding	thyroid hormone receptor interactor 6 [Source:HGNC Symbol;Acc:HGNC:12311]
KRT73	1,707	0,000	protein_coding	keratin 73 [Source:HGNC Symbol;Acc:HGNC:28928]
TMEM119	1,721	0,016	protein_coding	transmembrane protein 119 [Source:HGNC Symbol;Acc:HGNC:27884]

Gene	Log2FoldChange	padj	Biotype	Description
LAMB2P1	1,726	0,000	unprocessed_pseudogene	laminin subunit beta 2 pseudogene 1 [Source:HGNC Symbol;Acc:HGNC:6488]
ENSG00000273328	1,729	0,000		
SPOCK1	1,736	0,000	protein_coding	SPARC (osteonectin), cwcv and kazal like domains proteoglycan 1 [Source:HGNC Symbol;Acc:HGNC:11251]
LINC01252	1,745	0,020	lncRNA	long intergenic non-protein coding RNA 1252 [Source:HGNC Symbol;Acc:HGNC:27888]
CSMD3	1,754	0,001	protein_coding	CUB and Sushi multiple domains 3 [Source:HGNC Symbol;Acc:HGNC:19291]
ALCAM	1,761	0,000	protein_coding	activated leukocyte cell adhesion molecule [Source:HGNC Symbol;Acc:HGNC:400]
KAZN	1,762	0,000	protein_coding	kazrin, periplakin interacting protein [Source:HGNC Symbol;Acc:HGNC:29173]
MT1E	1,769	0,000	protein_coding	metallothionein 1E [Source:HGNC Symbol;Acc:HGNC:7397]
PDE3A	1,771	0,000	protein_coding	phosphodiesterase 3A [Source:HGNC Symbol;Acc:HGNC:8778]
LINGO2	1,774	0,030	protein_coding	leucine rich repeat and Ig domain containing 2 [Source:HGNC Symbol;Acc:HGNC:21207]
ENSG00000258811	1,788	0,003		
TNFRSF9	1,788	0,000	protein_coding	TNF receptor superfamily member 9 [Source:HGNC Symbol;Acc:HGNC:11924]
LINC01410	1,795	0,037	lncRNA	long intergenic non-protein coding RNA 1410 [Source:HGNC Symbol;Acc:HGNC:50702]
P2RY2	1,820	0,003	protein_coding	purinergic receptor P2Y2 [Source:HGNC Symbol;Acc:HGNC:8541]
GARIN1B	1,821	0,000	protein_coding	golgi associated RAB2 interactor 1B [Source:HGNC Symbol;Acc:HGNC:30704]
FBXW10B	1,821	0,001	protein_coding	F-box and WD repeat domain containing 10B [Source:HGNC Symbol;Acc:HGNC:14379]
DACH1	1,830	0,000	protein_coding	dachshund family transcription factor 1 [Source:HGNC Symbol;Acc:HGNC:2663]
NMUR1	1,845	0,002	protein_coding	neuromedin U receptor 1 [Source:HGNC Symbol;Acc:HGNC:4518]
FGFR2	1,851	0,000	protein_coding	fibroblast growth factor receptor 2 [Source:HGNC Symbol;Acc:HGNC:3689]
NFAM1	1,867	0,000	protein_coding	NFAT activating protein with ITAM motif 1 [Source:HGNC Symbol;Acc:HGNC:29872]
ENSG00000285888	1,868	0,000		
ALDH2	1,871	0,000	protein_coding	aldehyde dehydrogenase 2 family member [Source:HGNC Symbol;Acc:HGNC:404]
GAL3ST4	1,871	0,000	protein_coding	galactose-3-O-sulfotransferase 4 [Source:HGNC Symbol;Acc:HGNC:24145]
KCNMB4	1,872	0,023	protein_coding	potassium calcium-activated channel subfamily M regulatory beta subunit 4 [Source:HGNC Symbol;Acc:HGNC:6289]
AFF2	1,873	0,000	protein_coding	ALF transcription elongation factor 2 [Source:HGNC Symbol;Acc:HGNC:3776]
KCNJ2	1,882	0,008	protein_coding	potassium inwardly rectifying channel subfamily J member 2 [Source:HGNC Symbol;Acc:HGNC:6263]
GCNT1	1,884	0,005	protein_coding	glucosaminyl (N-acetyl) transferase 1 [Source:HGNC Symbol;Acc:HGNC:4203]
AGBL1	1,898	0,011	protein_coding	AGBL carboxypeptidase 1 [Source:HGNC Symbol;Acc:HGNC:26504]

Gene	Log2FoldChange	padj	Biotype	Description
LINC00552	1,907	0,040	TEC	long intergenic non-protein coding RNA 552 [Source:HGNC Symbol;Acc:HGNC:43692]
RGS16	1,911	0,001	protein_coding	regulator of G protein signaling 16 [Source:HGNC Symbol;Acc:HGNC:9997]
ENSG00000273428	1,917	0,003		
CA1	1,921	0,000	protein_coding	carbonic anhydrase 1 [Source:HGNC Symbol;Acc:HGNC:1368]
WNK4	1,933	0,000	protein_coding	WNK lysine deficient protein kinase 4 [Source:HGNC Symbol;Acc:HGNC:14544]
EBI3	1,943	0,041	protein_coding	Epstein-Barr virus induced 3 [Source:HGNC Symbol;Acc:HGNC:3129]
CLEC12A	1,952	0,009	protein_coding	C-type lectin domain family 12 member A [Source:HGNC Symbol;Acc:HGNC:31713]
COL3A1	1,961	0,034	protein_coding	collagen type III alpha 1 chain [Source:HGNC Symbol;Acc:HGNC:2201]
GABRB2	1,972	0,000	protein_coding	gamma-aminobutyric acid type A receptor subunit beta2 [Source:HGNC Symbol;Acc:HGNC:4082]
CLK3P2	1,979	0,002	processed_pseudogene	CDC like kinase 3 pseudogene 2 [Source:HGNC Symbol;Acc:HGNC:49786]
FAT3	1,979	0,000	protein_coding	FAT atypical cadherin 3 [Source:HGNC Symbol;Acc:HGNC:23112]
INSRR	1,981	0,000	protein_coding	insulin receptor related receptor [Source:HGNC Symbol;Acc:HGNC:6093]
GFRA2	1,982	0,000	protein_coding	GDNF family receptor alpha 2 [Source:HGNC Symbol;Acc:HGNC:4244]
PARD6G	1,983	0,000	protein_coding	par-6 family cell polarity regulator gamma [Source:HGNC Symbol;Acc:HGNC:16076]
GPR132	2,001	0,013	protein_coding	G protein-coupled receptor 132 [Source:HGNC Symbol;Acc:HGNC:17482]
ANXA3	2,006	0,000	protein_coding	annexin A3 [Source:HGNC Symbol;Acc:HGNC:541]
ZNF286A-TBC1D26	2,030	0,037	protein_coding	ZNF286A-TBC1D26 readthrough (NMD candidate) [Source:HGNC Symbol;Acc:HGNC:55384]
PDE4D	2,034	0,000	protein_coding	phosphodiesterase 4D [Source:HGNC Symbol;Acc:HGNC:8783]
CTTN-DT	2,042	0,022	lncRNA	CTTN divergent transcript [Source:HGNC Symbol;Acc:HGNC:55592]
IQCN	2,090	0,000	protein_coding	IQ motif containing N [Source:HGNC Symbol;Acc:HGNC:29350]
EXT1	2,092	0,000	protein_coding	exostosin glycosyltransferase 1 [Source:HGNC Symbol;Acc:HGNC:3512]
PRF1	2,109	0,035	protein_coding	perforin 1 [Source:HGNC Symbol;Acc:HGNC:9360]
NFE2	2,114	0,000	protein_coding	nuclear factor, erythroid 2 [Source:HGNC Symbol;Acc:HGNC:7780]
ZFP91-CNTF	2,125	0,049	protein_coding	ZFP91-CNTF readthrough (NMD candidate) [Source:HGNC Symbol;Acc:HGNC:33441]
COL7A1	2,166	0,000	protein_coding	collagen type VII alpha 1 chain [Source:HGNC Symbol;Acc:HGNC:2214]
ENSG00000250696	2,172	0,002		
KCNAB3	2,197	0,000	protein_coding	potassium voltage-gated channel subfamily A regulatory beta subunit 3 [Source:HGNC Symbol;Acc:HGNC:6230]
ENSG00000260011	2,198	0,005		

Gene	Log2FoldChange	padj	Biotype	Description
ENSG00000234147	2,202	0,046		
PEAR1	2,255	0,000	protein_coding	platelet endothelial aggregation receptor 1 [Source:HGNC Symbol;Acc:HGNC:33631]
NTRK3	2,298	0,000	protein_coding	neurotrophic receptor tyrosine kinase 3 [Source:HGNC Symbol;Acc:HGNC:8033]
ADCYAP1	2,309	0,011	protein_coding	adenylate cyclase activating polypeptide 1 [Source:HGNC Symbol;Acc:HGNC:241]
ENSG00000230570	2,326	0,000		
DNM1P46	2,333	0,030	transcribed_unprocessed_pseudogene	dynamin 1 pseudogene 46 [Source:HGNC Symbol;Acc:HGNC:35199]
SLC35F1	2,337	0,001	protein_coding	solute carrier family 35 member F1 [Source:HGNC Symbol;Acc:HGNC:21483]
HES7	2,351	0,001	protein_coding	hes family bHLH transcription factor 7 [Source:HGNC Symbol;Acc:HGNC:15977]
FAM225B	2,368	0,010	lncRNA	family with sequence similarity 225 member B [Source:HGNC Symbol;Acc:HGNC:21865]
MMP2	2,378	0,010	protein_coding	matrix metallopeptidase 2 [Source:HGNC Symbol;Acc:HGNC:7166]
ASIC4	2,400	0,000	protein_coding	acid sensing ion channel subunit family member 4 [Source:HGNC Symbol;Acc:HGNC:21263]
ENSG00000290058	2,414	0,004		
ASAH2	2,429	0,001	protein_coding	N-acylsphingosine amidohydrolase 2 [Source:HGNC Symbol;Acc:HGNC:18860]
ENSG00000289640	2,453	0,003		
MGAM2	2,465	0,000	protein_coding	maltase-glucoamylase 2 (putative) [Source:HGNC Symbol;Acc:HGNC:28101]
TRPC3	2,494	0,008	protein_coding	transient receptor potential cation channel subfamily C member 3 [Source:HGNC Symbol;Acc:HGNC:12335]
ENSG00000255367	2,613	0,049		
CD36	2,627	0,000	protein_coding	CD36 molecule [Source:HGNC Symbol;Acc:HGNC:1663]
C2orf66	2,649	0,000	protein_coding	chromosome 2 open reading frame 66 [Source:HGNC Symbol;Acc:HGNC:33809]
DAAM2-AS1	2,670	0,001	lncRNA	DAAM2 antisense RNA 1 [Source:HGNC Symbol;Acc:HGNC:40830]
MMP2-AS1	2,683	0,000	lncRNA	MMP2 antisense RNA 1 [Source:HGNC Symbol;Acc:HGNC:53142]
PREX1	2,688	0,000	protein_coding	phosphatidylinositol-3,4,5-trisphosphate dependent Rac exchange factor 1 [Source:HGNC Symbol;Acc:HGNC:32594]
ENSG00000286504	2,768	0,004		
PLAC4	2,849	0,017	lncRNA	placenta enriched 4 [Source:HGNC Symbol;Acc:HGNC:14616]
ELFN2	2,863	0,000	lncRNA	extracellular leucine rich repeat and fibronectin type III domain containing 2 [Source:NCBI gene (formerly Entrezgene);Acc:114794]

Gene	Log2FoldChange	padj	Biotype	Description
TMBIM7P	3,024	0,000	transcribed_unitary_pseudogene	transmembrane BAX inhibitor motif containing 7, pseudogene [Source:HGNC Symbol;Acc:HGNC:49212]
SCG2	3,082	0,000	protein_coding	secretogranin II [Source:HGNC Symbol;Acc:HGNC:10575]
ENSG00000283423	3,234	0,005		
MDGA1	3,286	0,000	protein_coding	MAM domain containing glycosylphosphatidylinositol anchor 1 [Source:HGNC Symbol;Acc:HGNC:19267]
ARX	3,335	0,010	protein_coding	aristaless related homeobox [Source:HGNC Symbol;Acc:HGNC:18060]
DYSF	3,381	0,000	protein_coding	dysferlin [Source:HGNC Symbol;Acc:HGNC:3097]
IL3	3,419	0,001	protein_coding	interleukin 3 [Source:HGNC Symbol;Acc:HGNC:6011]
ARNT2	3,426	0,000	protein_coding	aryl hydrocarbon receptor nuclear translocator 2 [Source:HGNC Symbol;Acc:HGNC:16876]
APLN	3,427	0,002	protein_coding	apelin [Source:HGNC Symbol;Acc:HGNC:16665]
CRTAM	3,562	0,000	protein_coding	cytotoxic and regulatory T cell molecule [Source:HGNC Symbol;Acc:HGNC:24313]
ENSG00000259283	3,632	0,000		
CPHL1P	3,642	0,000	transcribed_unitary_pseudogene	ceruloplasmin and hephaestin like 1, pseudogene [Source:HGNC Symbol;Acc:HGNC:31714]
LINC02539	3,713	0,001	lncRNA	long intergenic non-protein coding RNA 2539 [Source:HGNC Symbol;Acc:HGNC:53572]
CNTNAP5	4,421	0,000	protein_coding	contactin associated protein family member 5 [Source:HGNC Symbol;Acc:HGNC:18748]

Annex Table 12. GSEA pathways in LAD2 cells with MITF-silenced versus LAD2 cells with shRNA-NT, without cell activation. LAD2 cells were infected with lentivirus (shRNA-NT and MITF shRNA-2) for 5 days and stimulated with streptavidin for 24 hours.

Description	setSize	enrichmentScore	padj	qvalues	core_enrichment
VEGFA VEGFR2 signaling	352	-0,3827	0,0416	0,0342	FADD/ARF4/TPM3/TMOD1/MAP2K3/EWSR1/HSP90AA1/MYO1C/COPG1/SHC2/EIF4G1/ACTG1/TMOD3/PTMA/NOTCH4/IQGAP1/SDCBP/TXNDC5/MAPK3/AKT1S1/NRP2/MAP2K4/ATF4/SH3BGRL3/SARS1/TPP1/SLC7A1/MAPKAPK2/RAC1/PLAU/HSPB1/INPP4B/EPRS1/QKI/NOS3/PIK3R2/TFAM/CCT7/TRAF3IP2/GRSF1/PGD/HMGB1/GIPC1/MAPK1/EGR3/PRDX2/SLC25A11/PRKCA/PTPN11/TBCA/LDHA/EIF2A/PTPN14/PGK1/ALDOA/TXNIP/ARF6/JAG1/ICAM1/LRRC59/PRKRA/TUBA1C/PLA2G4A/GAPDH/SSR3/CDC42/ITGB1/CYCS/PGF/TMSB4X/S1PR1/PBK/IDH2/PPP1CA/CAPN2/NDRG1/CACNA2D1/FYN/NR4A1/SH2D2A/EZR/STAT1/APOLD1/BCL2L1/BIRC5/GPC1/CALU/SRC/SOD2/CCL2/SPIRE1/GPX1/NR4A3/BCL2/PTGS2/NR4A2
Network map of SARS CoV 2 signaling pathway	129	-0,5441	0,0416	0,0342	IRF9/IRAK1/JUNB/ACTB/IFIH1/HSPA8/C1R/CAMK4/IFITM1/NFKB2/TGFBR2/TRAF3/CTSB/GSN/IFI27/FYN/CEBPB/STAT1/RRM2/CCNB1/IL1A/CDK1/BIRC5/IL18RAP/CTSD/CTSL/APOC1/CCL2/CCNB2/CCL22/IFI6/CCL5/PTGS2/OAS2/GTSE1/IFIT1/CXCL16/IL1B/CCL3/IFI44L/MX1/TRPM2/CCL4
Circadian rhythm genes	131	-0,4886	0,0416	0,0342	CSNK1D/PRKG2/CRTC1/GNAQ/TNFRSF11A/NAGLU/NR1D2/PML/BHLHE40/CUL1/ATF4/JUND/PHLPP1/MAGED1/PRMT5/NAMPT/UTS2/PER3/TYMS/MAPK10/KLF10/HNRNPD/EGR3/CLOCK/AHCY/NPY2R/PPP1CB/DRD2/DBP/UTS2R/RAI1/HEBP1/RELB/PER1/SREBF1/PPP1CA/NOCT/TPH1/RORA/CRY1/TOP2A/USP2/CREM/SIK1/BHLHE41/HS3ST2
Measles virus infection	102	-0,5369	0,0416	0,0342	PIK3R2/CDK2/MAPK10/CCND3/CCND2/BAD/IRF9/IRAK1/IFIH1/HSPA8/HSPA1L/IRF7/CCNE1/STAT2/RAB9A/NFKB2/HSPA2/TRAF3/CYCS/STAT1/IL1A/BCL2L1/FASLG/BCL2/EIF2AK2/OAS2/OAS1/IL1B/MX1/OAS3

Description	setSize	enrichmentScore	p.adjust	qvalues	core_enrichment
Cell cycle	110	-0,4649	0,0416	0,0342	TGFB1/CUL1/CCNB3/MCM2/MCM5/PTTG1/CDK2/CDKN1A/RAD21/CCND3/CCND2/ANAPC13/YWHAQ/CDKN2B/MCM4/CDC16/PLK1/CCNE1/CCNA1/BUB1/CDC6/E2F2/CDC20/CCNB1/CDK1/CCNA2/CDKN2C/WEE1/ESPL1/MCM6/CCNB2/E2F1
Electron transport chain OXPHOS system in mitochondria	88	-0,5632	0,0416	0,0342	NDUFA13/SDHA/ATP5MC2/NDUFA3/COX11/COX6B1/SDHC/ATP5PD/COX17/NDUFB9/NDUFB6/SLC25A14/NDUFS4/NDUFA5/NDUFA10/NDUFS6/NDUFB4/NDUFB8/ATP5PB/UQCR10/NDUFC1/NDUFV2/UQCRQ/NDUFB10/COX4I1/ATP5F1D/ATP5ME/NDUFS5/COX5B/NDUFA11/ATP5PO/SDHD/NDUFS2/COX7A2/NDUFA9/COX7B/COX15/SLC25A6/NDUFS7/ATP5F1A/NDUFS8/SLC25A5/COX6C/NDUFA6/ATP5MC3/UCP2/UQCRC1/COX5A/NDUFA8/ATP5F1E/SDHB/ATP5IF1/NDUFC2/NDUFS1/NDUFAB1/NDUFB5/UQCRFS1/NDUFA1/COX7A1/NDUFB1/ATP5F1C/NDUFS3/ATP5F1B
Spinal cord injury	62	-0,5811	0,0416	0,0342	RTN4/TGFB1/MAPK3/RAC1/CDK2/MIF/MAPK1/MBP/PRKCA/SLIT1/ZFP36/ICAM1/AIF1/CDC42/NR4A1/IL1A/CDK1/VIM/LGALS3/CCL2/PTGS2/SEMA6A/PLXNA2/IL1B/E2F1/RTN4R
Metabolic epileptic disorders	63	-0,5725	0,0416	0,0342	DLAT/GOT2/ALDOC/MPC1/HADH/GAMT/MDH1/ETHE1/PDHA1/AASS/MPC2/PFKM/LDHB/DLD/HK1/GOT1/SQOR/SLC25A5/PFKL/ACO1/PSPH/ENO3/PGAM1/TPI1/ACAT1/LDHA/PGK1/ALDOA/HK2/PKM/GAPDH/SFXN1/SLC25A1/ENO2/ENO1/SLC2A3/PC/FBP1/CBS/PSAT1
Selenium micronutrient network	49	-0,6054	0,0416	0,0342	TXNRD3/SELENOK/SELENOH/CAT/SELENOT/GSR/SELENOI/PRDX1/GPX4/PRDX2/PNPO/SELENOM/ICAM1/NFKB2/SCARB1/PRDX3/ABCA1/SOD2/CCL2/GPX1/PTGS2/IL1B/CBS
Oxidative phosphorylation	50	-0,6155	0,0416	0,0342	ATP5PD/NDUFB9/NDUFB6/NDUFS4/NDUFA5/NDUFA10/NDUFS6/NDUFB4/NDUFB8/ATP5PB/NDUFC1/NDUFV2/NDUFB10/ATP5F1D/ATP5ME/NDUFS5/NDUFA11/ATP5PO/NDUFS2/NDUFA9/NDUFS7/ATP6AP1/ATP5F1A/NDUFS8/ATP6AP2/NDUFA6/ATP5MC3/NDUFA8/ATP5F1E/NDUFC2/NDUFS1/NDUFAB1/NDUFB5/NDUFB1/NDUFS3/ATP5F1B

Description	setSize	enrichmentScore	p.adjust	qvalues	core_enrichment
Metabolic reprogramming in colon cancer	39	-0,6035	0,0416	0,0342	FH/PFKL/DLST/PGD/SUCLG2/PSPH/SDHB/PGAM1/ACO2/LDHA/FASN/PGK1/SLC16A3/PKM/GAPDH/ENO1/IDH2/TIGAR/PSAT1
Pathogenic Escherichia coli infection	43	-0,6611	0,0416	0,0342	LY96/TUBB/TUBB4B/PRKCA/YWHAQ/TUBA4A/ACTB/TUBA1B/TUBA1C/CDC42/ITGB1/FYN/CTTN/EZR/TUBB3/NCK2/TUBB6/TUBB4A/TUBA1A
Netrin UNC5B signaling pathway	33	-0,6173	0,0416	0,0342	PIK3CA/MAP2K1/PTPA/MAPK3/RAC1/MAPK1/PRKCA/PTPN11/ICAM1/CIP2A/PPP1CA/FYN/ITGB4/IL1A/SRC/CCL2
SARS CoV 2 innate immunity evasion and cell specific immune response	42	-0,7020	0,0416	0,0342	IL6R/TRIM25/IRF7/STAT2/TRAF5/IFITM1/TRAF3/STAT1/DHX58/CCL2/HAVCR2/CCL5/IFIT2/CCL3/MX1/CCL4
Overview of proinflammatory and profibrotic mediators	27	-0,8284	0,0416	0,0342	OSM/IL1A/CCL2/CCL22/CCL23/CCL5/SPP1/AREG/CXCL16/IL1B/CCL3/CCL4L2/CCL4/CCL18
Host pathogen interaction of human coronaviruses interferon induction	31	-0,6822	0,0416	0,0342	IRF9/IFIH1/STAT2/TRAF3/STAT1/EIF2AK2/OAS2/OAS1/OAS3
Glycolysis and gluconeogenesis	31	-0,6662	0,0416	0,0342	DLAT/GOT2/ALDOC/MPC1/MDH1/PDHA1/MPC2/PFKM/LDHB/DLD/HK1/GOT1/PFKL/ENO3/PGAM1/TPI1/LDHA/PGK1/ALDOA/HK2/PKM/GAPDH/ENO2/ENO1/SLC2A3/PC/FBP1
Vitamin B12 metabolism	26	-0,7290	0,0416	0,0342	MCEE/ICAM1/NFKB2/SCARB1/ABCA1/SOD2/CCL2/TCN1/CCL5/IL1B/CBS
Gastric cancer network 1	22	-0,7388	0,0416	0,0342	INO80D/MYBL2/RUVBL1/KIF20B/MCM4/UBE2C/AURKA/LIN9/E2F7/CCNA1/TPX2/CENPF/TOP2A/KIF15
Photodynamic therapy induced NF kB survival signaling	21	-0,6965	0,0416	0,0342	BIRC3/ICAM1/NFKB2/RELB/IL1A/BIRC5/PTGS2/IL1B
Type I interferon induction and signaling during SARS CoV 2 infection	23	-0,7576	0,0416	0,0342	IRF9/IFIH1/TLR6/IRF7/STAT2/TRAF3/STAT1/EIF2AK2/OAS2/OAS1/OAS3
Regulation of sister chromatid separation at the metaphase anaphase transition	14	-0,7628	0,0420	0,0345	PTTG1/BUB1B/RAD21/BUB1/CENPE/CDC20/MAD2L1/ESPL1
HDAC6 interactions in the central nervous system	93	-0,5050	0,0462	0,0379	MDH1/SMAD2/SIRT2/SOD1/CTNNB1/CSNK2B/SMAD7/SQSTM1/CNOT6/DYNC1I2/HSP90AA1/STUB1/ATXN3/HDAC11/MAPK3/RAC1/HSPB1/PRDX1/TUBB/OPTN/MIF/MAPK1/PRDX2/VHL/HSPA4/MAPT/TUBA4A/TPPP/GRK2/HSPA8/AURKA/SGK1/TUBA1C/MAP1B/GARS1/RAD23B/PPP1CA/CDC20/CTTN/VIM/TUBB3/BIRC5/ISG15/BCL2

Description	setSize	enrichmentScore	p.adjust	qvalues	core_enrichment
NF1 copy number variation syndrome	92	-0,4938	0,0462	0,0379	H3C12/RAD51/MAPK3/H3C15/MCL1/H4C8/PRMT5/TUBB/MAPK1/RFC3/H4C13/H4C6/COPRS/H4C4/H3C10/H3C3/H3C2/ARF6/EXOC5/CCNE1/PER1/H4C9/H4C11/H3C6/EVI2A/H4C1/CRY1/CCNA2/H3C8/H3C7/BCL2/RTN4R
Retinoblastoma gene in cancer	83	-0,5040	0,0462	0,0379	SAP30/CDT1/CDK2/TYMS/RRM1/RPA1/CDKN1A/PLK4/CCND3/HMGB1/RFC3/STMN1/MCM4/CCNE1/E2F2/H2AZ1/RPA3/RRM2/CCNB1/CDK1/CCNA2/TOP2A/WEE1/KIF4A/MCM6/CCNB2/E2F1
Nucleotide excision repair in xeroderma pigmentosum	73	-0,5114	0,0462	0,0379	POLH/XPA/RFC5/H4C15/GPS1/POLD3/ERCC6/POLE/POLD1/H4C5/H4C3/BRCA1/H4C2/GTF2H4/ERCC4/CUL4B/H4C14/POLD2/RBX1/RFC2/RAD18/ERCC2/H4C8/CETN2/RPA1/RFC3/H4C13/H4C6/H4C4/CHD1L/H4C9/H4C11/RAD23B/H4C1/RPA3/CUL4A
Toll like receptor signaling pathway	70	-0,5368	0,0462	0,0379	PIK3CA/MAP2K1/PIK3CD/FADD/MAP2K3/TICAM2/TAB2/MAPK3/MAP2K4/PIK3R3/RAC1/PIK3R2/LY96/MAPK10/MAPK1/IRAK1/TLR6/IRF7/TRAF3/STAT1/CCL5/SPP1/IL1B/CCL3/CCL4
Clear cell renal cell carcinoma pathways	65	-0,5200	0,0462	0,0379	PFKM/LDHB/LDHD/HK1/TGFB1/PFKL/AKT1S1/PSPH/ENO3/VHL/TPI1/LDHA/FASN/PGK1/ALDOA/HK2/PKM/GAPDH/ENO2/ENO1/ZEB1/PGM1/BHLHE41/PSAT1
Parkin ubiquitin proteasomal system pathway	59	-0,5503	0,0462	0,0379	PSMC3/PSMD5/STUB1/UBE2L6/PSMC4/PSMC6/CUL1/TUBB/HSPA9/PSMC5/TUBB4B/HSPA4/TUBA4A/PSMD14/HSPA8/PSMC2/TUBA1B/HSPA1L/CCNE1/TUBA1C/HSPA2/HSPA5/TUBB3/TUBB6/TUBB4A/TUBA1A
G1 to S cell cycle control	59	-0,5471	0,0462	0,0379	MCM2/MCM5/CDK2/RPA1/CREB3/CDKN1A/CCND3/CCND2/CDKN2B/MCM4/CCNE1/CCNA1/E2F2/RPA3/CCNB1/CDK1/CDKN2C/WEE1/MCM6/CCNG2/E2F1
Cytosolic DNA sensing pathway	52	-0,5481	0,0462	0,0379	TRIM25/CGAS/RNF125/IRF7/TREX1/ISG15/CCL5/IL1B/CCL4L2/CCL4

Description	setSize	enrichmentScore	p.adjust	qvalues	core_enrichment
Microtubule cytoskeleton regulation	40	-0,5931	0,0462	0,0379	DPYSL2/GNAQ/CLIP1/TRIO/MAPKAPK2/RAC1/PRKCA/MAPT/TPPP/STMN1/CAMK4/CDC42/MAP1B/KIF2C/TESK2/CDK1/SRC/AURKB
DNA replication	39	-0,5797	0,0462	0,0379	PCNA/CDC7/MCM3/RFC5/POLD3/POLE/POLD1/POLD2/UBC/RFC2/GMNN/CDT1/MCM2/MCM5/CDK2/RPA1/RFC3/MCM4/CDC6/MCM10/RPA3/MCM6
Lung fibrosis	28	-0,6597	0,0462	0,0379	CEBPB/CMA1/CCL2/SKIL/CCL5/SPP1/IL1B/CCL3/CCL4
2q13 copy number variation syndrome	42	-0,5785	0,0462	0,0379	IL1RAP/RGPD8/RAC1/SOCS3/ZC3H8/TMEM87B/MAPK1/GATA3/ARF6/ZC3H6/STAT1/IL1A/LGALS3/GAS6/CKAP2L/IL1B
miRNA role in immune response in sepsis	27	-0,6549	0,0462	0,0379	IRAK1/IRF7/ICAM1/NFKB2/RELB/TRAF3/IL1A/CCL3/CCL4
Immune response to tuberculosis	22	-0,6584	0,0470	0,0386	PSMB8/IRF9/STAT2/IFITM1/IFI35/STAT1/IFIT3/OAS1/IFIT1/MX1

Annex Table 13. Differential gene expression in LAD2 cells with MITF-silenced versus LAD2 cells with shRNA-NT in an IgE-dependent pathway. LAD2 cells were infected with lentivirus (shRNA-NT and MITF shRNA-2) for 5 days and stimulated with streptavidin for 24 hours.

Gene	Log2FoldChange	padj	Biotype	Description
ENSG00000267166	-2,956	0,000		
MT-RNR1	-2,715	0,013	Mt_rRNA	mitochondrially encoded 12S rRNA [Source:HGNC Symbol;Acc:HGNC:7470]
MT-RNR2	-2,647	0,006	Mt_rRNA	mitochondrially encoded 16S rRNA [Source:HGNC Symbol;Acc:HGNC:7471]
CCL18	-2,631	0,000	protein_coding	C-C motif chemokine ligand 18 [Source:HGNC Symbol;Acc:HGNC:10616]
ADAMTS18	-2,347	0,018	protein_coding	ADAM metallopeptidase with thrombospondin type 1 motif 18 [Source:HGNC Symbol;Acc:HGNC:17110]
DCDC2	-2,319	0,000	protein_coding	doublecortin domain containing 2 [Source:HGNC Symbol;Acc:HGNC:18141]
DEFB119	-2,317	0,000	protein_coding	defensin beta 119 [Source:HGNC Symbol;Acc:HGNC:18099]
ENSG00000181514	-2,287	0,000		
CHCHD6	-2,226	0,000	protein_coding	coiled-coil-helix-coiled-coil-helix domain containing 6 [Source:HGNC Symbol;Acc:HGNC:28184]
EEPD1	-2,210	0,005	protein_coding	endonuclease/exonuclease/phosphatase family domain containing 1 [Source:HGNC Symbol;Acc:HGNC:22223]

Gene	Log2FoldChange	padj	Biotype	Description
7SK	-2,204	0,000	misc_RNA	7SK RNA [Source:RFAM;Acc:RF00100]
AK5	-2,092	0,000	protein_coding	adenylate kinase 5 [Source:HGNC Symbol;Acc:HGNC:365]
RNA5S1	-2,090	0,003	rRNA	RNA, 5S ribosomal 1 [Source:HGNC Symbol;Acc:HGNC:34362]
TRPM2	-2,057	0,000	protein_coding	transient receptor potential cation channel subfamily M member 2 [Source:HGNC Symbol;Acc:HGNC:12339]
CCL4L2	-2,008	0,030	protein_coding	C-C motif chemokine ligand 4 like 2 [Source:HGNC Symbol;Acc:HGNC:24066]
ENSG00000283907	-2,000	0,025		
KCNQ5-DT	-1,976	0,000	lncRNA	KCNQ5 divergent transcript [Source:HGNC Symbol;Acc:HGNC:55469]
LINC00589	-1,923	0,001	lncRNA	long intergenic non-protein coding RNA 589 [Source:HGNC Symbol;Acc:HGNC:32299]
HMGB3P7	-1,907	0,000	processed_pseudogene	high mobility group box 3 pseudogene 7 [Source:HGNC Symbol;Acc:HGNC:39299]
OAS3	-1,899	0,000	protein_coding	2'-5'-oligoadenylate synthetase 3 [Source:HGNC Symbol;Acc:HGNC:8088]
MX1	-1,874	0,040	protein_coding	MX dynamin like GTPase 1 [Source:HGNC Symbol;Acc:HGNC:7532]
HNRNPUL2-BSCL2	-1,859	0,000	protein_coding	HNRNPUL2-BSCL2 readthrough (NMD candidate) [Source:HGNC Symbol;Acc:HGNC:49189]
CPM	-1,796	0,000	protein_coding	carboxypeptidase M [Source:HGNC Symbol;Acc:HGNC:2311]
ANGPT4	-1,796	0,000	protein_coding	angiopoietin 4 [Source:HGNC Symbol;Acc:HGNC:487]
NEURL1B	-1,778	0,011	protein_coding	neuralized E3 ubiquitin protein ligase 1B [Source:HGNC Symbol;Acc:HGNC:35422]
PSAT1	-1,775	0,003	protein_coding	phosphoserine aminotransferase 1 [Source:HGNC Symbol;Acc:HGNC:19129]
ZC3H11B	-1,768	0,009	protein_coding	zinc finger CCCH-type containing 11B [Source:HGNC Symbol;Acc:HGNC:25659]
TMEM178A	-1,756	0,008	protein_coding	transmembrane protein 178A [Source:HGNC Symbol;Acc:HGNC:28517]
RTN4R	-1,725	0,000	protein_coding	reticulon 4 receptor [Source:HGNC Symbol;Acc:HGNC:18601]
EPHA5	-1,716	0,008	protein_coding	EPH receptor A5 [Source:HGNC Symbol;Acc:HGNC:3389]
CTSH	-1,705	0,000	protein_coding	cathepsin H [Source:HGNC Symbol;Acc:HGNC:2535]
HNRNPH2	-1,694	0,000	protein_coding	heterogeneous nuclear ribonucleoprotein H2 [Source:HGNC Symbol;Acc:HGNC:5042]
ENSG00000276012	-1,688	0,001		
SORBS3	-1,678	0,000	protein_coding	sorbin and SH3 domain containing 3 [Source:HGNC Symbol;Acc:HGNC:30907]
LINC00276	-1,674	0,014	lncRNA	long intergenic non-protein coding RNA 276 [Source:HGNC Symbol;Acc:HGNC:38663]
TSPAN10	-1,672	0,000	protein_coding	tetraspanin 10 [Source:HGNC Symbol;Acc:HGNC:29942]
E2F1	-1,650	0,006	protein_coding	E2F transcription factor 1 [Source:HGNC Symbol;Acc:HGNC:3113]
CLSPN	-1,644	0,000	protein_coding	claspin [Source:HGNC Symbol;Acc:HGNC:19715]

Gene	Log2FoldChange	padj	Biotype	Description
CCL3	-1,640	0,003	protein_coding	C-C motif chemokine ligand 3 [Source:HGNC Symbol;Acc:HGNC:10627]
CPNE5	-1,612	0,007	protein_coding	copine 5 [Source:HGNC Symbol;Acc:HGNC:2318]
GUCA1C	-1,603	0,003	protein_coding	guanylate cyclase activator 1C [Source:HGNC Symbol;Acc:HGNC:4680]
SLAMF7	-1,601	0,000	protein_coding	SLAM family member 7 [Source:HGNC Symbol;Acc:HGNC:21394]
PRC1	-1,581	0,001	protein_coding	protein regulator of cytokinesis 1 [Source:HGNC Symbol;Acc:HGNC:9341]
DPEP2	-1,574	0,001	protein_coding	dipeptidase 2 [Source:HGNC Symbol;Acc:HGNC:23028]
DTL	-1,574	0,001	protein_coding	denticleless E3 ubiquitin protein ligase homolog [Source:HGNC Symbol;Acc:HGNC:30288]
ENSG00000286223	-1,555	0,002		
CTSA	-1,554	0,000	protein_coding	cathepsin A [Source:HGNC Symbol;Acc:HGNC:9251]
HS3ST2	-1,531	0,000	protein_coding	heparan sulfate-glucosamine 3-sulfotransferase 2 [Source:HGNC Symbol;Acc:HGNC:5195]
IL1B	-1,519	0,001	protein_coding	interleukin 1 beta [Source:HGNC Symbol;Acc:HGNC:5992]
GRIP1	-1,517	0,039	protein_coding	glutamate receptor interacting protein 1 [Source:HGNC Symbol;Acc:HGNC:18708]
MGAT4C	-1,499	0,015	protein_coding	MGAT4 family member C [Source:HGNC Symbol;Acc:HGNC:30871]
ITGBL1	-1,486	0,000	protein_coding	integrin subunit beta like 1 [Source:HGNC Symbol;Acc:HGNC:6164]
ZNF165	-1,485	0,002	protein_coding	zinc finger protein 165 [Source:HGNC Symbol;Acc:HGNC:12953]
TMEM268	-1,478	0,005	protein_coding	transmembrane protein 268 [Source:HGNC Symbol;Acc:HGNC:24513]
MEGF6	-1,473	0,000	protein_coding	multiple EGF like domains 6 [Source:HGNC Symbol;Acc:HGNC:3232]
STARD10	-1,473	0,000	protein_coding	StAR related lipid transfer domain containing 10 [Source:HGNC Symbol;Acc:HGNC:10666]
CXCL16	-1,452	0,000	protein_coding	C-X-C motif chemokine ligand 16 [Source:HGNC Symbol;Acc:HGNC:16642]
VAT1L	-1,451	0,000	protein_coding	vesicle amine transport 1 like [Source:HGNC Symbol;Acc:HGNC:29315]
ENSG00000234389	-1,440	0,000		
JPH4	-1,429	0,000	protein_coding	junctophilin 4 [Source:HGNC Symbol;Acc:HGNC:20156]
GGH	-1,423	0,000	protein_coding	gamma-glutamyl hydrolase [Source:HGNC Symbol;Acc:HGNC:4248]
HTN1	-1,415	0,010	protein_coding	histatin 1 [Source:HGNC Symbol;Acc:HGNC:5283]
STON2	-1,411	0,025	protein_coding	stonin 2 [Source:HGNC Symbol;Acc:HGNC:30652]
IFIT1	-1,394	0,000	protein_coding	interferon induced protein with tetratricopeptide repeats 1 [Source:HGNC Symbol;Acc:HGNC:5407]
DNAH7	-1,387	0,019	protein_coding	dynein axonemal heavy chain 7 [Source:HGNC Symbol;Acc:HGNC:18661]
OAS1	-1,386	0,000	protein_coding	2'-5'-oligoadenylate synthetase 1 [Source:HGNC Symbol;Acc:HGNC:8086]

Gene	Log2FoldChange	padj	Biotype	Description
ENSG00000287891	-1,382	0,001		
SEMA6A	-1,374	0,010	protein_coding	semaphorin 6A [Source:HGNC Symbol;Acc:HGNC:10738]
IFIT2	-1,369	0,000	protein_coding	interferon induced protein with tetratricopeptide repeats 2 [Source:HGNC Symbol;Acc:HGNC:5409]
ENSG00000236841	-1,362	0,002		
ENSG00000289316	-1,342	0,011		
NCS1	-1,340	0,000	protein_coding	neuronal calcium sensor 1 [Source:HGNC Symbol;Acc:HGNC:3953]
PEPD	-1,331	0,000	protein_coding	peptidase D [Source:HGNC Symbol;Acc:HGNC:8840]
GEM	-1,325	0,024	protein_coding	GTP binding protein overexpressed in skeletal muscle [Source:HGNC Symbol;Acc:HGNC:4234]
BPNT2	-1,320	0,003	protein_coding	3'(2'), 5'-bisphosphate nucleotidase 2 [Source:HGNC Symbol;Acc:HGNC:26019]
ENSG00000261888	-1,316	0,001		
SYNE2	-1,298	0,004	protein_coding	spectrin repeat containing nuclear envelope protein 2 [Source:HGNC Symbol;Acc:HGNC:17084]
GTSE1	-1,297	0,008	protein_coding	G2 and S-phase expressed 1 [Source:HGNC Symbol;Acc:HGNC:13698]
TM4SF19	-1,296	0,000	protein_coding	transmembrane 4 L six family member 19 [Source:HGNC Symbol;Acc:HGNC:25167]
HTN3	-1,293	0,001	protein_coding	histatin 3 [Source:HGNC Symbol;Acc:HGNC:5284]
BAIAP2L1	-1,293	0,030	protein_coding	BAR/IMD domain containing adaptor protein 2 like 1 [Source:HGNC Symbol;Acc:HGNC:21649]
PRKAR1A	-1,291	0,000	protein_coding	protein kinase cAMP-dependent type I regulatory subunit alpha [Source:HGNC Symbol;Acc:HGNC:9388]
PTGS2	-1,264	0,009	protein_coding	prostaglandin-endoperoxide synthase 2 [Source:HGNC Symbol;Acc:HGNC:9605]
DLGAP1-AS2	-1,262	0,002	lncRNA	DLGAP1 antisense RNA 2 [Source:HGNC Symbol;Acc:HGNC:28146]
IFI30	-1,261	0,002	protein_coding	IFI30 lysosomal thiol reductase [Source:HGNC Symbol;Acc:HGNC:5398]
LINC01119	-1,259	0,023	lncRNA	long intergenic non-protein coding RNA 1119 [Source:HGNC Symbol;Acc:HGNC:49262]
LINC01010	-1,250	0,000	lncRNA	long intergenic non-protein coding RNA 1010 [Source:HGNC Symbol;Acc:HGNC:48978]
RASGRP3	-1,237	0,001	protein_coding	RAS guanyl releasing protein 3 [Source:HGNC Symbol;Acc:HGNC:14545]
ENSG00000234139	-1,232	0,000		
ZMYND15	-1,232	0,000	protein_coding	zinc finger MYND-type containing 15 [Source:HGNC Symbol;Acc:HGNC:20997]
AMACR	-1,222	0,000	protein_coding	alpha-methylacyl-CoA racemase [Source:HGNC Symbol;Acc:HGNC:451]
TUBA1A	-1,221	0,012	protein_coding	tubulin alpha 1a [Source:HGNC Symbol;Acc:HGNC:20766]
PADI2	-1,217	0,000	protein_coding	peptidyl arginine deiminase 2 [Source:HGNC Symbol;Acc:HGNC:18341]
ST8SIA1	-1,216	0,000	protein_coding	ST8 alpha-N-acetyl-neuraminide alpha-2,8-sialyltransferase 1 [Source:HGNC Symbol;Acc:HGNC:10869]

Gene	Log2FoldChange	padj	Biotype	Description
ENSG00000229771	-1,210	0,005		
ATP5F1B	-1,207	0,001	protein_coding	ATP synthase F1 subunit beta [Source:HGNC Symbol;Acc:HGNC:830]
IFI6	-1,202	0,000	protein_coding	interferon alpha inducible protein 6 [Source:HGNC Symbol;Acc:HGNC:4054]
EIF2AK2	-1,199	0,000	protein_coding	eukaryotic translation initiation factor 2 alpha kinase 2 [Source:HGNC Symbol;Acc:HGNC:9437]
GBP2	-1,196	0,001	protein_coding	guanylate binding protein 2 [Source:HGNC Symbol;Acc:HGNC:4183]
APOBEC3B	-1,189	0,016	protein_coding	apolipoprotein B mRNA editing enzyme catalytic subunit 3B [Source:HGNC Symbol;Acc:HGNC:17352]
RTN4RL1	-1,187	0,005	protein_coding	reticulon 4 receptor like 1 [Source:HGNC Symbol;Acc:HGNC:21329]
OR10D1P	-1,185	0,006	unprocessed_pseudogene	olfactory receptor family 10 subfamily D member 1 pseudogene [Source:HGNC Symbol;Acc:HGNC:8166]
BCL2	-1,180	0,012	protein_coding	BCL2 apoptosis regulator [Source:HGNC Symbol;Acc:HGNC:990]
FMNL2	-1,179	0,000	protein_coding	formin like 2 [Source:HGNC Symbol;Acc:HGNC:18267]
HISLA	-1,176	0,001	lncRNA	HIF1A stabilizing long noncoding RNA [Source:HGNC Symbol;Acc:HGNC:49467]
TSHZ2	-1,176	0,006	protein_coding	teashirt zinc finger homeobox 2 [Source:HGNC Symbol;Acc:HGNC:13010]
ENSG00000273997	-1,172	0,020		
STXBP5-AS1	-1,165	0,003	lncRNA	STXBP5 antisense RNA 1 [Source:HGNC Symbol;Acc:HGNC:44183]
MAS1	-1,160	0,000	protein_coding	MAS1 proto-oncogene, G protein-coupled receptor [Source:HGNC Symbol;Acc:HGNC:6899]
NEK2	-1,146	0,020	protein_coding	NIMA related kinase 2 [Source:HGNC Symbol;Acc:HGNC:7745]
KREMEN1	-1,141	0,000	protein_coding	kringle containing transmembrane protein 1 [Source:HGNC Symbol;Acc:HGNC:17550]
ENSG00000288767	-1,135	0,039		
LY6S	-1,124	0,001	protein_coding	lymphocyte antigen 6 family member S [Source:HGNC Symbol;Acc:HGNC:54397]
SERPINI1	-1,124	0,000	protein_coding	serpin family I member 1 [Source:HGNC Symbol;Acc:HGNC:8943]
SESTD1	-1,120	0,030	protein_coding	SEC14 and spectrin domain containing 1 [Source:HGNC Symbol;Acc:HGNC:18379]
PLEKHN1	-1,112	0,002	protein_coding	pleckstrin homology domain containing N1 [Source:HGNC Symbol;Acc:HGNC:25284]
RAB3IL1	-1,111	0,002	protein_coding	RAB3A interacting protein like 1 [Source:HGNC Symbol;Acc:HGNC:9780]
ESR2	-1,104	0,000	protein_coding	estrogen receptor 2 [Source:HGNC Symbol;Acc:HGNC:3468]
CKAP2L	-1,102	0,009	protein_coding	cytoskeleton associated protein 2 like [Source:HGNC Symbol;Acc:HGNC:26877]
SOX13	-1,101	0,000	protein_coding	SRY-box transcription factor 13 [Source:HGNC Symbol;Acc:HGNC:11192]
ENSG00000272397	-1,098	0,016		
ISCA2	-1,094	0,000	protein_coding	iron-sulfur cluster assembly 2 [Source:HGNC Symbol;Acc:HGNC:19857]

Gene	Log2FoldChange	padj	Biotype	Description
ENSG00000290729	-1,087	0,015		
TDRD3	-1,082	0,000	protein_coding	tudor domain containing 3 [Source:HGNC Symbol;Acc:HGNC:20612]
AMZ2	-1,070	0,000	protein_coding	archaelysin family metallopeptidase 2 [Source:HGNC Symbol;Acc:HGNC:28041]
SNX3	-1,068	0,000	protein_coding	sorting nexin 3 [Source:HGNC Symbol;Acc:HGNC:11174]
MBNL2	-1,063	0,000	protein_coding	muscleblind like splicing regulator 2 [Source:HGNC Symbol;Acc:HGNC:16746]
PYGL	-1,060	0,000	protein_coding	glycogen phosphorylase L [Source:HGNC Symbol;Acc:HGNC:9725]
KCNQ5	-1,059	0,004	protein_coding	potassium voltage-gated channel subfamily Q member 5 [Source:HGNC Symbol;Acc:HGNC:6299]
AURKB	-1,058	0,017	protein_coding	aurora kinase B [Source:HGNC Symbol;Acc:HGNC:11390]
ABI3BP	-1,056	0,016	protein_coding	ABI family member 3 binding protein [Source:HGNC Symbol;Acc:HGNC:17265]
EPB41L4A	-1,051	0,000	protein_coding	erythrocyte membrane protein band 4.1 like 4A [Source:HGNC Symbol;Acc:HGNC:13278]
TOMM20	-1,046	0,000	protein_coding	translocase of outer mitochondrial membrane 20 [Source:HGNC Symbol;Acc:HGNC:20947]
ENSG00000274624	-1,043	0,000		
GPNMB	-1,043	0,000	protein_coding	glycoprotein nmb [Source:HGNC Symbol;Acc:HGNC:4462]
C1orf54	-1,039	0,015	protein_coding	chromosome 1 open reading frame 54 [Source:HGNC Symbol;Acc:HGNC:26258]
ACSL1	-1,035	0,000	protein_coding	acyl-CoA synthetase long chain family member 1 [Source:HGNC Symbol;Acc:HGNC:3569]
GAB2	-1,034	0,008	protein_coding	GRB2 associated binding protein 2 [Source:HGNC Symbol;Acc:HGNC:14458]
PIK3AP1	-1,024	0,000	protein_coding	phosphoinositide-3-kinase adaptor protein 1 [Source:HGNC Symbol;Acc:HGNC:30034]
SULT1C2	-1,022	0,001	protein_coding	sulfotransferase family 1C member 2 [Source:HGNC Symbol;Acc:HGNC:11456]
KIF15	-1,020	0,035	protein_coding	kinesin family member 15 [Source:HGNC Symbol;Acc:HGNC:17273]
CD68	-1,017	0,000	protein_coding	CD68 molecule [Source:HGNC Symbol;Acc:HGNC:1693]
PTP4A2	-1,015	0,000	protein_coding	protein tyrosine phosphatase 4A2 [Source:HGNC Symbol;Acc:HGNC:9635]
CCNG2	-1,010	0,000	protein_coding	cyclin G2 [Source:HGNC Symbol;Acc:HGNC:1593]
GAS6	-1,009	0,049	protein_coding	growth arrest specific 6 [Source:HGNC Symbol;Acc:HGNC:4168]
ARHGAP11A	-1,008	0,005	protein_coding	Rho GTPase activating protein 11A [Source:HGNC Symbol;Acc:HGNC:15783]
WARS1	-1,005	0,013	protein_coding	tryptophanyl-tRNA synthetase 1 [Source:HGNC Symbol;Acc:HGNC:12729]
THBS4-AS1	-1,003	0,000	lncRNA	THBS4 antisense RNA 1 [Source:HGNC Symbol;Acc:HGNC:40583]
GIHCG	1,006	0,001	lncRNA	GIHCG inhibitor of miR-200b/200a/429 expression [Source:HGNC Symbol;Acc:HGNC:52649]
RHBDL1	1,008	0,003	protein_coding	rhomboid like 1 [Source:HGNC Symbol;Acc:HGNC:10007]

Gene	Log2FoldChange	padj	Biotype	Description
ANKRD55	1,009	0,048	protein_coding	ankyrin repeat domain 55 [Source:HGNC Symbol;Acc:HGNC:25681]
ENSG00000264659	1,019	0,009		
LRATD1	1,024	0,027	protein_coding	LRAT domain containing 1 [Source:HGNC Symbol;Acc:HGNC:20743]
CCP110	1,025	0,049	protein_coding	centriolar coiled-coil protein 110 [Source:HGNC Symbol;Acc:HGNC:24342]
BAIAP2L2	1,029	0,048	protein_coding	BAR/IMD domain containing adaptor protein 2 like 2 [Source:HGNC Symbol;Acc:HGNC:26203]
LINC00954	1,033	0,015	lncRNA	long intergenic non-protein coding RNA 954 [Source:HGNC Symbol;Acc:HGNC:48668]
TSPAN6	1,043	0,007	protein_coding	tetraspanin 6 [Source:HGNC Symbol;Acc:HGNC:11858]
LINC02302	1,049	0,007	lncRNA	long intergenic non-protein coding RNA 2302 [Source:HGNC Symbol;Acc:HGNC:53221]
MUC20P1	1,056	0,008	unprocessed_pseudogene	mucin 20, cell surface associated pseudogene 1 [Source:HGNC Symbol;Acc:HGNC:51921]
ANKRD24	1,058	0,020	protein_coding	ankyrin repeat domain 24 [Source:HGNC Symbol;Acc:HGNC:29424]
TLN2	1,067	0,030	protein_coding	talin 2 [Source:HGNC Symbol;Acc:HGNC:15447]
ENSG00000247679	1,069	0,000		
TRIM73	1,072	0,000	protein_coding	tripartite motif containing 73 [Source:HGNC Symbol;Acc:HGNC:18162]
FAM183BP	1,084	0,031	processed_pseudogene	family with sequence similarity 183 member B, pseudogene [Source:HGNC Symbol;Acc:HGNC:34511]
RD3	1,088	0,001	protein_coding	RD3 regulator of GUCY2D [Source:HGNC Symbol;Acc:HGNC:19689]
RPL5P21	1,094	0,024	processed_pseudogene	ribosomal protein L5 pseudogene 21 [Source:HGNC Symbol;Acc:HGNC:37029]
ABCA15P	1,099	0,001	transcribed_unitary_pseudogene	ATP binding cassette subfamily A member 15, pseudogene [Source:HGNC Symbol;Acc:HGNC:34405]
LRRTM2	1,101	0,026	protein_coding	leucine rich repeat transmembrane neuronal 2 [Source:HGNC Symbol;Acc:HGNC:19409]
LINC00937	1,106	0,026	lncRNA	long intergenic non-protein coding RNA 937 [Source:HGNC Symbol;Acc:HGNC:48629]
NPHP3-ACAD11	1,108	0,036	protein_coding	NPHP3-ACAD11 readthrough (NMD candidate) [Source:HGNC Symbol;Acc:HGNC:48351]
LY6G5C	1,112	0,000	protein_coding	lymphocyte antigen 6 family member G5C [Source:HGNC Symbol;Acc:HGNC:13932]
ENSG00000278997	1,121	0,000		

Gene	Log2FoldChange	padj	Biotype	Description
PDE3A	1,125	0,000	protein_coding	phosphodiesterase 3A [Source:HGNC Symbol;Acc:HGNC:8778]
ADCY4	1,132	0,000	protein_coding	adenylate cyclase 4 [Source:HGNC Symbol;Acc:HGNC:235]
CFP	1,139	0,006	protein_coding	complement factor properdin [Source:HGNC Symbol;Acc:HGNC:8864]
NTRK3	1,147	0,002	protein_coding	neurotrophic receptor tyrosine kinase 3 [Source:HGNC Symbol;Acc:HGNC:8033]
RPL17P22	1,150	0,009	processed_pseudogene	ribosomal protein L17 pseudogene 22 [Source:HGNC Symbol;Acc:HGNC:35761]
ITGA4	1,170	0,000	protein_coding	integrin subunit alpha 4 [Source:HGNC Symbol;Acc:HGNC:6140]
LAMB2P1	1,170	0,001	unprocessed_pseudogene	laminin subunit beta 2 pseudogene 1 [Source:HGNC Symbol;Acc:HGNC:6488]
SOX4	1,172	0,000	protein_coding	SRY-box transcription factor 4 [Source:HGNC Symbol;Acc:HGNC:11200]
NKPD1	1,176	0,047	protein_coding	NTPase KAP family P-loop domain containing 1 [Source:HGNC Symbol;Acc:HGNC:24739]
ENSG00000236833	1,179	0,039		
AMH	1,186	0,001	protein_coding	anti-Mullerian hormone [Source:HGNC Symbol;Acc:HGNC:464]
RSPO4	1,199	0,000	protein_coding	R-spondin 4 [Source:HGNC Symbol;Acc:HGNC:16175]
KCNJ14	1,200	0,006	protein_coding	potassium inwardly rectifying channel subfamily J member 14 [Source:HGNC Symbol;Acc:HGNC:6260]
AFF2	1,200	0,000	protein_coding	ALF transcription elongation factor 2 [Source:HGNC Symbol;Acc:HGNC:3776]
KCND1	1,201	0,001	protein_coding	potassium voltage-gated channel subfamily D member 1 [Source:HGNC Symbol;Acc:HGNC:6237]
ASGR1	1,203	0,011	protein_coding	asialoglycoprotein receptor 1 [Source:HGNC Symbol;Acc:HGNC:742]
DNAH8	1,215	0,039	protein_coding	dynein axonemal heavy chain 8 [Source:HGNC Symbol;Acc:HGNC:2952]
CCDC154	1,216	0,001	protein_coding	coiled-coil domain containing 154 [Source:HGNC Symbol;Acc:HGNC:34454]
SAMD14	1,221	0,001	protein_coding	sterile alpha motif domain containing 14 [Source:HGNC Symbol;Acc:HGNC:27312]
MT2A	1,221	0,009	protein_coding	metallothionein 2A [Source:HGNC Symbol;Acc:HGNC:7406]
FAT3	1,225	0,004	protein_coding	FAT atypical cadherin 3 [Source:HGNC Symbol;Acc:HGNC:23112]
NEIL1	1,227	0,005	protein_coding	nei like DNA glycosylase 1 [Source:HGNC Symbol;Acc:HGNC:18448]
ITPRID2-DT	1,237	0,000	lncRNA	ITPRID2 divergent transcript [Source:HGNC Symbol;Acc:HGNC:55386]
SPRED3	1,241	0,002	protein_coding	sprouty related EVH1 domain containing 3 [Source:HGNC Symbol;Acc:HGNC:31041]
PID1	1,247	0,007	protein_coding	phosphotyrosine interaction domain containing 1 [Source:HGNC Symbol;Acc:HGNC:26084]
GRIN2C	1,266	0,000	protein_coding	glutamate ionotropic receptor NMDA type subunit 2C [Source:HGNC Symbol;Acc:HGNC:4587]
GABRB2	1,272	0,000	protein_coding	gamma-aminobutyric acid type A receptor subunit beta2 [Source:HGNC Symbol;Acc:HGNC:4082]
ENSG00000259080	1,279	0,031		

Gene	Log2FoldChange	padj	Biotype	Description
TAS1R3	1,288	0,018	protein_coding	taste 1 receptor member 3 [Source:HGNC Symbol;Acc:HGNC:15661]
XKR6	1,288	0,037	protein_coding	XK related 6 [Source:HGNC Symbol;Acc:HGNC:27806]
LINC01637	1,295	0,043	lncRNA	long intergenic non-protein coding RNA 1637 [Source:HGNC Symbol;Acc:HGNC:52424]
CFAP47	1,295	0,000	protein_coding	cilia and flagella associated protein 47 [Source:HGNC Symbol;Acc:HGNC:26708]
ENSG00000259278	1,302	0,015		
MT1E	1,304	0,000	protein_coding	metallothionein 1E [Source:HGNC Symbol;Acc:HGNC:7397]
BCAN-AS1	1,327	0,000	lncRNA	BCAN antisense RNA 1 [Source:HGNC Symbol;Acc:HGNC:55233]
C1GALT1P2	1,346	0,003	processed_pseudogene	C1GALT1 pseudogene 2 [Source:HGNC Symbol;Acc:HGNC:51615]
SLC23A3	1,353	0,014	protein_coding	solute carrier family 23 member 3 [Source:HGNC Symbol;Acc:HGNC:20601]
SLC22A20P	1,357	0,000	transcribed_unitary_pseudogene	solute carrier family 22 member 20, pseudogene [Source:HGNC Symbol;Acc:HGNC:29867]
PARD6G	1,358	0,001	protein_coding	par-6 family cell polarity regulator gamma [Source:HGNC Symbol;Acc:HGNC:16076]
LINC02940	1,374	0,011	lncRNA	long intergenic non-protein coding RNA 2940 [Source:HGNC Symbol;Acc:HGNC:55955]
ENSG00000260182	1,378	0,000		
ENSG00000248015	1,383	0,000		
ENSG00000286797	1,402	0,001		
ITGA2B	1,422	0,000	protein_coding	integrin subunit alpha 2b [Source:HGNC Symbol;Acc:HGNC:6138]
KAZN	1,440	0,000	protein_coding	kazrin, periplakin interacting protein [Source:HGNC Symbol;Acc:HGNC:29173]
ENSG00000256407	1,463	0,023		
WFIKKN1	1,486	0,000	protein_coding	WAP, follistatin/kazal, immunoglobulin, kunitz and netrin domain containing 1 [Source:HGNC Symbol;Acc:HGNC:30912]
ENSG00000260927	1,488	0,000		
CCR5	1,501	0,000	protein_coding	C-C motif chemokine receptor 5 [Source:HGNC Symbol;Acc:HGNC:1606]
FGFR2	1,526	0,000	protein_coding	fibroblast growth factor receptor 2 [Source:HGNC Symbol;Acc:HGNC:3689]
SLC27A3	1,529	0,000	protein_coding	solute carrier family 27 member 3 [Source:HGNC Symbol;Acc:HGNC:10997]
ALDH2	1,530	0,001	protein_coding	aldehyde dehydrogenase 2 family member [Source:HGNC Symbol;Acc:HGNC:404]
COL11A2	1,540	0,000	protein_coding	collagen type XI alpha 2 chain [Source:HGNC Symbol;Acc:HGNC:2187]
SLC18A2-AS1	1,557	0,000	lncRNA	SLC18A2 antisense RNA 1 [Source:HGNC Symbol;Acc:HGNC:55843]
ISG20	1,628	0,000	protein_coding	interferon stimulated exonuclease gene 20 [Source:HGNC Symbol;Acc:HGNC:6130]
TRIM74	1,635	0,001	protein_coding	tripartite motif containing 74 [Source:HGNC Symbol;Acc:HGNC:17453]

Gene	Log2FoldChange	padj	Biotype	Description
CEBPA	1,688	0,027	protein_coding	CCAAT enhancer binding protein alpha [Source:HGNC Symbol;Acc:HGNC:1833]
NFE2	1,770	0,000	protein_coding	nuclear factor, erythroid 2 [Source:HGNC Symbol;Acc:HGNC:7780]
KCNAB3	1,806	0,000	protein_coding	potassium voltage-gated channel subfamily A regulatory beta subunit 3 [Source:HGNC Symbol;Acc:HGNC:6230]
IQCN	1,919	0,000	protein_coding	IQ motif containing N [Source:HGNC Symbol;Acc:HGNC:29350]
C2orf66	1,962	0,000	protein_coding	chromosome 2 open reading frame 66 [Source:HGNC Symbol;Acc:HGNC:33809]
ASIC4	2,057	0,000	protein_coding	acid sensing ion channel subunit family member 4 [Source:HGNC Symbol;Acc:HGNC:21263]
PDE4D	2,093	0,000	protein_coding	phosphodiesterase 4D [Source:HGNC Symbol;Acc:HGNC:8783]
ENSG00000259283	2,256	0,005		
COL7A1	2,265	0,000	protein_coding	collagen type VII alpha 1 chain [Source:HGNC Symbol;Acc:HGNC:2214]
CA1	2,316	0,000	protein_coding	carbonic anhydrase 1 [Source:HGNC Symbol;Acc:HGNC:1368]
PTCHD1	2,371	0,000	protein_coding	patched domain containing 1 [Source:HGNC Symbol;Acc:HGNC:26392]
MGAM2	2,604	0,000	protein_coding	maltase-glucoamylase 2 (putative) [Source:HGNC Symbol;Acc:HGNC:28101]
CNTNAP5	3,708	0,001	protein_coding	contactin associated protein family member 5 [Source:HGNC Symbol;Acc:HGNC:18748]

REFERENCES

1. Marshall JS. Mast-cell responses to pathogens. Vol. 4, Nature Reviews Immunology. 2004. p. 787–99.
2. Espinosa-Riquer ZP, Segura-Villalobos D, Ramírez-Moreno IG, Rodríguez MJP, Lamas M, Gonzalez-Espinosa C. Signal transduction pathways activated by innate immunity in mast cells: Translating sensing of changes into specific responses. Vol. 9, Cells. Multidisciplinary Digital Publishing Institute (MDPI); 2020. p. 1–39.
3. Bischoff SC. Role of mast cells in allergic and non-allergic immune responses: Comparison of human and murine data. Vol. 7, Nature Reviews Immunology. 2007. p. 93–104.
4. Ansari YSE, Kanagaratham C, Oettgen HC. Mast Cells as Regulators of Adaptive Immune Responses in Food Allergy. Vol. 93, YALE JOURNAL OF BIOLOGY AND MEDICINE. 2020. p. 711–8.
5. Navinés-Ferrer A, Serrano-Candelas E, Lafuente A, Muñoz-Cano R, Martín M, Gastaminza G. MRGPRX2-mediated mast cell response to drugs used in perioperative procedures and anaesthesia. Sci Rep. 2018 Dec;8(1).
6. McNeil BD. MRGPRX2 and Adverse Drug Reactions. Vol. 12, Frontiers in Immunology. Frontiers Media S.A.; 2021.
7. Lecce M, Molfetta R, Milito ND, Santoni A, Paolini R. Fcεri signaling in the modulation of allergic response: Role of mast cell-derived exosomes. Vol. 21, International Journal of Molecular Sciences. MDPI AG; 2020. p. 1–13.
8. Anvari S, Miller J, Yeh CY, Davis CM. IgE-Mediated Food Allergy. Clin Rev Allergy Immunol. 2019 Oct;57(2):244–60.
9. Bahri R, Bulfone-Paus S. Mast Cell Activation Test (MAT). In: Gibbs BF, Falcone FH, editors. Basophils and Mast Cells: Methods and Protocols [Internet]. New York, NY: Springer US; 2020. p. 227–38. Available from: https://doi.org/10.1007/978-1-0716-0696-4_19
10. Tejedor Alonso MA, Moro Moro M, Múgica García MV. Epidemiology of anaphylaxis. Clin Exp Allergy. 2015 Jun;45(6):1027–39.
11. Bahri R, Custovic A, Korosec P, Tsoumani M, Barron M, Wu J, et al. Mast cell activation test in the diagnosis of allergic disease and anaphylaxis. J Allergy Clin Immunol. 2018 Aug;142(2):485-496.e16.
12. Santos AF, Toit GD, O'Rourke C, Becares N, Couto-Francisco N, Radulovic S, et al. Biomarkers of severity and threshold of allergic reactions during oral peanut challenges. J Allergy Clin Immunol. 2020 Aug;146(2):344–55.
13. Nicolaou N, Custovic A. Molecular diagnosis of peanut and legume allergy. Vol. 11, Current Opinion in Allergy and Clinical Immunology. 2011. p. 222–8.
14. Akiyama M, Alshehri W, Ishigaki S, Saito K, Kaneko Y. Human T follicular helper cells and their impact on IgE and IgG4 production across allergy, malignancy, and IgG4-related disease. Allergol Int. 2025 Jan;74(1):25–32.
15. Tong X, Guan C, Ji T, Cao C, Jiang J, Liu M, et al. Increased circulating T follicular helper 13 subset correlates with high IgE levels in pediatric allergic asthma. Vol. 52, European Journal of Immunology. John Wiley and Sons Inc; 2022. p. 2010–2.
16. Gowthaman U, Chen JS, Zhang B, Flynn WF, Lu Y, Song W, et al. Identification of a T follicular helper cell subset that drives anaphylactic IgE. Science. 2019 Aug;365(6456).
17. Guo Y, Proaño-Pérez E, Muñoz-Cano R, Martin M. Anaphylaxis: Focus on transcription factor activity. Vol. 22, International Journal of Molecular Sciences. MDPI AG; 2021.
18. Sharkia I, Erlich TH, Landolina N, Assayag M, Motzik A, Rachmin I, et al. Pyruvate dehydrogenase has a major role in mast cell function, and its activity is regulated by mitochondrial microphthalmia transcription factor. J Allergy Clin Immunol. 2017 Jul;140(1):204-214.e8.
19. Allergologia RCAGMDRS de VMFGCLCEVTMVKBJHAIBRCAR van RA di, Bollatesi OC, SpA L, CLB R van R. Lipid Transfer Protein: A Pan-Allergen in Plant-Derived Foods That Is Highly Resistant to Pepsin Digestion [Internet]. Vol. 124, Allergens Int Arch Allergy Immunol. 2001. p. 67–9. Available from: www.karger.com/journals/iaa
20. Egger M, Hauser M, Mari A, Ferreira F, Gadermaier G. The role of lipid transfer proteins in allergic diseases. Curr Allergy Asthma Rep. 2010 Sep;10(5):326–35.

21. Fernández-Rivas M, González-Mancebo E, Rodríguez-Pérez R, Benito C, Sánchez-Monge R, Salcedo G, et al. Clinically relevant peach allergy is related to peach lipid transfer protein, Pru p 3, in the Spanish population. 2003;
22. Scheurer S, Van Ree R, Vieths S. The Role of Lipid Transfer Proteins as Food and Pollen Allergens Outside the Mediterranean Area. Curr Allergy Asthma Rep. 2021 Feb;21(2):7.
23. Tam IYS, Lau HYA, Tam SY, Lee TH. Mast cell activation test using patient-derived mast cells exhibits distinct combinatorial phenotypic profiles among allergic patients. Vol. 75, Allergy: European Journal of Allergy and Clinical Immunology. Blackwell Publishing Ltd; 2020. p. 1796–9.
24. Goding CR, Arnheiter H. MITF—the first 25 years. Genes Dev. 2019 Aug 1;33(15–16):983–1007.
25. Martin M. Mast Cells: When the Best Defense Is an Attack? Vol. 23, International Journal of Molecular Sciences. MDPI; 2022.
26. Mendoza RP, Fudge DH, Brown JM. Cellular energetics of mast cell development and activation. Vol. 10, Cells. MDPI; 2021. p. 1–17.
27. Tauber M, Basso L, Martin J, Bostan L, Pinto MM, Thierry GR, et al. Landscape of mast cell populations across organs in mice and humans. J Exp Med. 2023 Oct;220(10).
28. John ALS, Rathore APS, Ginhoux F. New perspectives on the origins and heterogeneity of mast cells. Vol. 23, Nature Reviews Immunology. Nature Research; 2023. p. 55–68.
29. Akashi K, Traver D, Miyamoto T, Weissman IL. A clonogenic common myeloid progenitor that gives rise to all myeloid lineages. Nature. 2000 Mar;404(6774):193–7.
30. Arinobu Y, Iwasaki H, Gurish MF, Mizuno S ichi, Shigematsu H, Ozawa H, et al. Developmental checkpoints of the basophil/mast cell lineages in adult murine hematopoiesis. Proc Natl Acad Sci. 2005 Dec 13;102(50):18105–10.
31. Qi X, Hong J, Chaves L, Zhuang Y, Chen Y, Wang D, et al. Antagonistic Regulation by the Transcription Factors C/EBPα and MITF Specifies Basophil and Mast Cell Fates. Immunity. 2013 Jul;39(1):97–110.
32. Kirshenbaum AS, Goff JP, Semere T, Foster B, Scott LM, Metcalfe DD. Demonstration That Human Mast Cells Arise From a Progenitor Cell Population That Is CD34+, c-kit+, and Expresses Aminopeptidase N (CD13). Blood. 1999 Oct 1;94(7):2333–42.
33. Dahlin JS, Hallgren J. Mast cell progenitors: Origin, development and migration to tissues. Mol Immunol. 2015 Jan;63(1):9–17.
34. Komi DEA, Wöhrl S, Bielory L. Mast Cell Biology at Molecular Level: a Comprehensive Review. Vol. 58, Clinical Reviews in Allergy and Immunology. Springer; 2020. p. 342–65.
35. Dahlin JS, Maurer M, Metcalfe DD, Pejler G, Sagi-Eisenberg R, Nilsson G. The ingenious mast cell: Contemporary insights into mast cell behavior and function. Vol. 77, Allergy: European Journal of Allergy and Clinical Immunology. John Wiley and Sons Inc; 2022. p. 83–99.
36. Moon TC, Laurent CDS, Morris KE, Marcet C, Yoshimura T, Sekar Y, et al. Advances in mast cell biology: New understanding of heterogeneity and function. Vol. 3, Mucosal Immunology. Nature Publishing Group; 2010. p. 111–28.
37. Trivedi NH, Guentzel MN, Rodriguez AR, Yu JJ, Forsthuber TG, Arulanandam BP. Mast cells: multitalented facilitators of protection against bacterial pathogens. Expert Rev Clin Immunol. 2013 Feb;9(2):129–38.
38. Jiménez M, Cervantes-Garćıa D, E. Córdova-Dávalos L, Jesabel Pérez-Rodríguez M, Gonzalez-Espinosa C, Salinas E. Responses of Mast Cells to Pathogens: Beneficial and Detrimental Roles. Front Immunol. 2021;12.
39. Galli SJ, Nakae S, Tsai M. Mast cells in the development of adaptive immune responses. Nat Immunol. 2005 Feb;6(2):135–42.
40. Krystel-Whittemore M, Dileepan KN, Wood JG. Mast cell: A multi-functional master cell. Vol. 6, Frontiers in Immunology. Frontiers Media S.A.; 2016.
41. Agier J, Pastwińska J, Brzezińska-Błaszczyk E. An overview of mast cell pattern recognition receptors. Inflamm Res. 2018;67:737–46.
42. Mekori YA, Metcalfe DD. Mast cells in innate immunity. Immunol Rev. 2000 Feb;173:131–40.
43. Mukai K, Tsai M, Saito H, Galli SJ. Mast cells as sources of cytokines, chemokines, and growth factors. Vol. 282, Immunological Reviews. Blackwell Publishing Ltd; 2018. p. 121–50.
44. Portales-Cervantes L, Dawod B, Marshall JS. Mast Cells and Natural Killer Cells—A Potentially Critical Interaction. Viruses. 2019 Jun 4;11(6):514.

45. Kalkusova K, Smite S, Darras E, Taborska P, Stakheev D, Vannucci L, et al. Mast Cells and Dendritic Cells as Cellular Immune Checkpoints in Immunotherapy of Solid Tumors.
46. Dudeck J, Mohammed Ghouse S, H.K. Lehmann C, Hoppe A, Schubert N, A. Nedospasov S, et al. Mast-Cell-Derived TNF Amplifies CD8+ Dendritic Cell Functionality and CD8+ T Cell Priming. Cell Rep. 2015;13:399–411.
47. Mekori YA, Metcalfe DD. Mast cell–T cell interactions. J Allergy Clin Immunol. 1999 Sep;104(3):517–23.
48. Urb M, Sheppard DC. The Role of Mast Cells in the Defence against Pathogens. Heitman J, editor. PLoS Pathog. 2012 Apr 26;8(4):e1002619.
49. Komi DEA, Grauwet K. Role of Mast Cells in Regulation of T Cell Responses in Experimental and Clinical Settings. Clin Rev Allergy Immunol. 2018;54:432–45.
50. Palm AKE, Garcia-Faroldi G, Lundberg M, Pejler G, Kleinau S. Activated mast cells promote differentiation of B cells into effector cells. Sci Rep. 2016;6.
51. Sanmarco LM, Polonio CM, Wheeler MA, Quintana FJ. Functional immune cell–astrocyte interactions. J Exp Med. 2021;218(9).
52. Msallam R, Malissen B, Launay P, Blank U, Gautier G, Davoust J. Mast Cell Interaction with Foxp3+ Regulatory T Cells Occur in the Dermis after Initiation of IgE-Mediated Cutaneous Anaphylaxis. Cells. 2022 Sep 29;11(19):3055.
53. Piconese S, Gri G, Tripodo C, Musio S, Gorzanelli A, Frossi B, et al. Mast cells counteract regulatory T-cell suppression through interleukin-6 and OX40/OX40L axis toward Th17-cell differentiation. Blood. 2009 Sep 24;114(13):2639–48.
54. Bahri R, Bulfone-Paus S. Mast Cell Activation Test (MAT). Methods Mol Biol Clifton NJ. 2020;2163:227–38.
55. Castells M. Diagnosis and management of anaphylaxis in precision medicine. J Allergy Clin Immunol. 2017;140(2):321–33.
56. Gilfillan AM, Beaven MA. Regulation of Mast Cell Responses in Health and Disease. Crit Rev Immunol. 2011;31(6):475–530.
57. McNeil HP, Adachi R, Stevens RL. Mast Cell-restricted Tryptases: Structure and Function in Inflammation and Pathogen Defense. J Biol Chem. 2007 Jul;282(29):20785–9.
58. Schwartz L. Tryptase: a clinical indicator of mast cell-dependent events. Allergy proceedings. 1994;15(3):119–23.
59. Iwaki S, Tkaczyk C, Satterthwaite AB, Halcomb K, Beaven MA, Metcalfe DD, et al. Btk Plays a Crucial Role in the Amplification of FcεRI-mediated Mast Cell Activation by Kit. J Biol Chem. 2005 Dec;280(48):40261–70.
60. Jones BL, Kearns GL. Histamine: New Thoughts About a Familiar Mediator. Clin Pharmacol Ther. 2011 Feb;89(2):189–97.
61. Bongers G, de Esch I, Leurs R. Molecular pharmacology of the four histamine receptors. Adv Exp Med Biol. 2010;709:11–9.
62. Leurs R, Vischer HF, Wijtmans M, de Esch IJP. En route to new blockbuster anti-histamines: surveying the offspring of the expanding histamine receptor family. Trends Pharmacol Sci. 2011 Apr;32(4):250–7.
63. Hofstra CL, Desai PJ, Thurmond RL, Fung-Leung WP. Histamine H4 receptor mediates chemotaxis and calcium mobilization of mast cells. J Pharmacol Exp Ther. 2003 Jun;305(3):1212–21.
64. Boyce JA. Eicosanoid mediators of mast cells: receptors, regulation of synthesis, and pathobiologic implications. Chem Immunol Allergy. 2005;87:59–79.
65. Boyce JA. Eicosanoids in asthma, allergic inflammation, and host defense. Curr Mol Med. 2008 Aug;8(5):335–49.
66. Hellman L, Akula S, Fu Z, Wernersson S. Mast Cell and Basophil Granule Proteases - In Vivo Targets and Function. Front Immunol. 2022 Jul 5;13:918305.
67. Payne V, Kam PCA. Mast cell tryptase: a review of its physiology and clinical significance. Anaesthesia. 2004 Jul;59(7):695–703.
68. Vibhushan S, Bratti M, Montero-Hernández JE, El Ghoneimi A, Benhamou M, Charles N, et al. Mast Cell Chymase and Kidney Disease. Int J Mol Sci [Internet]. 2021;22(1). Available from: https://www.mdpi.com/1422-0067/22/1/302

69. Caughey GH. Mast cell tryptases and chymases in inflammation and host defense. Immunol Rev. 2007 Jun;217(1):141–54.
70. Metcalfe DD, Baram D, Mekori YA. Mast Cells [Internet]. Vol. 77, REVIEWS Jol. 1997. Available from: www.physiology.org/journal/physrev
71. Okayama Y, Kirshenbaum AS, Metcalfe DD. Expression of a functional high-affinity IgG receptor, Fc gamma RI, on human mast cells: Up-regulation by IFN-gamma. J Immunol Baltim Md 1950. 2000 Apr 15;164(8):4332–9.
72. Katsanos GS, Anogeianaki A, Orso C, Tetè S, Salini V, Antinolfi PL, et al. Mast cells and chemokines. J Biol Regul Homeost Agents. 2008 Sep;22(3):145–51.
73. Okayama Y. Mast cell-derived cytokine expression induced via Fc receptors and Toll-like receptors. Chem Immunol Allergy. 2005;87:101–10.
74. Okayama Y, Hagaman DD, Metcalfe DD. A comparison of mediators released or generated by IFN-gamma-treated human mast cells following aggregation of Fc gamma RI or Fc epsilon RI. J Immunol Baltim Md 1950. 2001 Apr 1;166(7):4705–12.
75. Moiseeva EP, Bradding P. Mast cells in lung inflammation. Adv Exp Med Biol. 2011;716:235–69.
76. Tsai M, Grimbaldeston M, Galli SJ. Mast cells and immunoregulation/immunomodulation. Adv Exp Med Biol. 2011;716:186–211.
77. Shelburne CP, Abraham SN. The mast cell in innate and adaptive immunity. Adv Exp Med Biol. 2011;716:162–85.
78. Berin MC. Targeting type 2 immunity and the future of food allergy treatment. J Exp Med. 2023;220(4):e20221104.
79. Ziegler SF, Liu YJ. Thymic stromal lymphopoietin in normal and pathogenic T cell development and function. Nat Immunol. 2006 Jul;7(7):709–14.
80. Morrey C, Brazin J, Seyedi N, Corti F, Silver RB, Levi R. Interaction between sensory C-fibers and cardiac mast cells in ischemia/reperfusion: activation of a local renin-angiotensin system culminating in severe arrhythmic dysfunction. J Pharmacol Exp Ther. 2010 Oct;335(1):76–84.
81. Moon TC, Befus AD, Kulka M. Mast Cell Mediators: Their Differential Release and the Secretory Pathways Involved. Front Immunol [Internet]. 2014 Nov 14 [cited 2025 Mar 12];5. Available from: http://journal.frontiersin.org/article/10.3389/fimmu.2014.00569/abstract
82. Blank U, Madera-Salcedo IK, Danelli L, Claver J, Tiwari N, SÃ¡nchez-Miranda E, et al. Vesicular Trafficking and Signaling for Cytokine and Chemokine Secretion in Mast Cells. Front Immunol [Internet]. 2014 Sep 22 [cited 2025 Mar 15];5. Available from: http://journal.frontiersin.org/article/10.3389/fimmu.2014.00453/abstract
83. De Matteis MA, Luini A. Exiting the Golgi complex. Nat Rev Mol Cell Biol. 2008 Apr;9(4):273–84.
84. Dvorak AM, Tepper RI, Weller PF, Morgan ES, Estrella P, Monahan-Earley RA, et al. Piecemeal degranulation of mast cells in the inflammatory eyelid lesions of interleukin-4 transgenic mice. Evidence of mast cell histamine release in vivo by diamine oxidase-gold enzyme-affinity ultrastructural cytochemistry. Blood. 1994 Jun 15;83(12):3600–12.
85. Tsai M, Valent P, Galli SJ. KIT as a master regulator of the mast cell lineage. J Allergy Clin Immunol. 2022 Jun;149(6):1845–54.
86. Dahlin JS, Ekoff M, Grootens J, Löf L, Amini RM, Hagberg H, et al. KIT signaling is dispensable for human mast cell progenitor development. Blood. 2017 Oct 19;130(16):1785–94.
87. Meininger C, Yano H, Rottapel R, Bernstein A, Zsebo K, Zetter B. The c-kit receptor ligand functions as a mast cell chemoattractant. Blood. 1992 Feb 15;79(4):958–63.
88. Rönnstrand L. Signal transduction via the stem cell factor receptor/c-Kit. Vol. 61, Cellular and Molecular Life Sciences. 2004. p. 2535–48.
89. Tkaczyk C. NTAL phosphorylation is a pivotal link between the signaling cascades leading to human mast cell degranulation following Kit activation and Fc RI aggregation. Blood. 2004 Jul 1;104(1):207–14.
90. Hundley TR, Gilfillan AM, Tkaczyk C, Andrade MV, Metcalfe DD, Beaven MA. Kit and FcεRI mediate unique and convergent signals for release of inflammatory mediators from human mast cells. Blood. 2004 Oct 15;104(8):2410–7.
91. Jensen BM, Akin C, Gilfillan AM. Pharmacological targeting of the KIT growth factor receptor: a therapeutic consideration for mast cell disorders. Br J Pharmacol. 2008 Aug;154(8):1572–82.

92. Kraft S, Kinet JP. New developments in FcεRI regulation, function and inhibition. Vol. 7, Nature Reviews Immunology. 2007. p. 365–78.
93. Sibilano R, Frossi B, Pucillo CE. Mast cell activation: A complex interplay of positive and negative signaling pathways. Vol. 44, European Journal of Immunology. Wiley-VCH Verlag; 2014. p. 2558–66.
94. Gilfillan AM, Austin SJ, Metcalfe DD. Mast cell biology: Introduction and overview. Vol. 716, Advances in Experimental Medicine and Biology. 2011. p. 2–12.
95. Kim MS, Rådinger M, Gilfillan AM. The multiple roles of phosphoinositide 3-kinase in mast cell biology. Trends Immunol. 2008 Oct;29(10):493–501.
96. Suzuki R, Leach S, Liu W, Ralston E, Scheffel J, Zhang W, et al. Molecular editing of cellular responses by the high-affinity receptor for IgE. Science. 2014;343(6174):1021–5.
97. Dema B, Suzuki R, Rivera J. Rethinking the role of immunoglobulin e and its high-affinity receptor: New insights into allergy and beyond. Vol. 164, International Archives of Allergy and Immunology. S. Karger AG; 2014. p. 271–9.
98. Saitoh S, Arudchandran R, Manetz TS, Zhang W, Sommers CL, Love PE, et al. LAT is essential for Fc(epsilon)RI-mediated mast cell activation. Immunity. 2000 May;12(5):525–35.
99. Kurosaki T, Baba Y. Ca2+ signaling and STIM1. Vol. 103, Progress in Biophysics and Molecular Biology. 2010. p. 51–8.
100. Kinet JP. THE HIGH-AFFINITY IGE RECEPTOR (FcεRI): From Physiology to Pathology. Annual Review of Immunology [Internet]. 1999;17:931–72. Available from: www.annualreviews.org.
101. Toru H, Nonoyama S, Suzuki K, Yata JI, Nakahata T. Induction of the high-affinity IgE receptor (FceRI) on human mast cells by IL-4 [Internet]. Vol. 8, International Immunology. 1996. p. 1367–73. Available from: https://academic.oup.com/intimm/article/8/9/1367/730830
102. Plattner K, Bachmann MF, Vogel M. On the complexity of IgE: The role of structural flexibility and glycosylation for binding its receptors. Front Allergy. 2023 Mar 28;4:1117611.
103. Turner H, Kinet JP. Signalling through the high-af®nity IgE receptor FceRI [Internet]. 1999. Available from: www.nature.com
104. Stathopulos PB, Ikura M. Partial unfolding and oligomerization of stromal interaction molecules as an initiation mechanism of store operated calcium entry. Biochem Cell Biol Biochim Biol Cell. 2010 Apr;88(2):175–83.
105. Ren R, Li Y. STIM1 in tumor cell death: angel or devil? Cell Death Discov. 2023 Nov 6;9(1):408.
106. Luik RM, Wang B, Prakriya M, Wu MM, Lewis RS. Oligomerization of STIM1 couples ER calcium depletion to CRAC channel activation. Nature. 2008 Jul 24;454(7203):538–42.
107. Zhou Y, Mancarella S, Wang Y, Yue C, Ritchie M, Gill DL, et al. The short N-terminal domains of STIM1 and STIM2 control the activation kinetics of Orai1 channels. J Biol Chem. 2009 Jul 17;284(29):19164–8.
108. Luik RM, Wu MM, Buchanan J, Lewis RS. The elementary unit of store-operated Ca2+ entry: local activation of CRAC channels by STIM1 at ER-plasma membrane junctions. J Cell Biol. 2006 Sep 11;174(6):815–25.
109. Ke Y, Gannaban R, Liu J, Zhou Y. STIM1 and lipid interactions at ER-PM contact sites. Am J Physiol Cell Physiol. 2025 Jan 1;328(1):C107–14.
110. Baba Y, Nishida K, Fujii Y, Hirano T, Hikida M, Kurosaki T. Essential function for the calcium sensor STIM1 in mast cell activation and anaphylactic responses. Nat Immunol. 2008 Jan;9(1):81–8.
111. Li Y, Guo B, Xie Q, Ye D, Zhang D, Zhu Y, et al. STIM1 Mediates Hypoxia-Driven Hepatocarcinogenesis via Interaction with HIF-1. Cell Rep. 2015 Jul 21;12(3):388–95.
112. Lioudyno MI, Kozak JA, Penna A, Safrina O, Zhang SL, Sen D, et al. Orai1 and STIM1 move to the immunological synapse and are up-regulated during T cell activation. Proc Natl Acad Sci U S A. 2008 Feb 12;105(6):2011–6.
113. Nunes-Hasler P, Maschalidi S, Lippens C, Castelbou C, Bouvet S, Guido D, et al. STIM1 promotes migration, phagosomal maturation and antigen cross-presentation in dendritic cells. Nat Commun. 2017 Nov 24;8(1):1852.
114. Yan CH, Bai WY, Zhang ZM, Shen JL, Wang YJ, Sun JW. The roles and mechanism of STIM1 in tumorigenesis and metastasis. Yi Chuan Hered. 2023 May 20;45(5):395–408.

115. Vaeth M, Maus M, Klein-Hessling S, Freinkman E, Yang J, Eckstein M, et al. Store-Operated Ca(2+) Entry Controls Clonal Expansion of T Cells through Metabolic Reprogramming. Immunity. 2017 Oct 17;47(4):664-679.e6.
116. Liu P, Yang Z, Wang Y, Sun A. Role of STIM1 in the Regulation of Cardiac Energy Substrate Preference. Int J Mol Sci. 2023 Aug 25;24(17):13188.
117. Kiatsurayanon C, Niyonsaba F, Chieosilapatham P, Okumura K, Ikeda S, Ogawa H. Angiogenic peptide (AG)-30/5C activates human keratinocytes to produce cytokines/chemokines and to migrate and proliferate via MrgX receptors. J Dermatol Sci. 2016 Sep;83(3):190–9.
118. Dong X, Han S, Zylka MJ, Simon MI, Anderson DJ. A diverse family of GPCRs expressed in specific subsets of nociceptive sensory neurons. Cell. 2001 Sep 7;106(5):619–32.
119. Azimi E, Reddy VB, Lerner EA. Brief communication: MRGPRX2, atopic dermatitis and red man syndrome. Itch Phila Pa. 2017 Mar;2(1):e5.
120. Porebski G, Kwiecien K, Pawica M, Kwitniewski M. Mas-Related G Protein-Coupled Receptor-X2 (MRGPRX2) in Drug Hypersensitivity Reactions. Front Immunol. 2018 Dec;9.
121. McNeil BD, Pundir P, Meeker S, Han L, Undem BJ, Kulka M, et al. Identification of a mast-cell-specific receptor crucial for pseudo-allergic drug reactions. Nature. 2015 Mar;519(7542):237–41.
122. Lieberman P, Garvey LH. Mast Cells and Anaphylaxis. Curr Allergy Asthma Rep. 2016 Mar;16(3):20.
123. Grimbaldeston MA. Mast cell-MrgprB2: sensing secretagogues or a means to overreact? Immunol Cell Biol. 2015 Mar;93(3):221–3.
124. Gaudenzio N, Sibilano R, Marichal T, Starkl P, Reber LL, Cenac N, et al. Different activation signals induce distinct mast cell degranulation strategies. J Clin Invest. 2016 Oct 3;126(10):3981–98.
125. Tatemoto K, Nozaki Y, Tsuda R, Konno S, Tomura K, Furuno M, et al. Immunoglobulin E-independent activation of mast cell is mediated by Mrg receptors. Biochem Biophys Res Commun. 2006 Nov 3;349(4):1322–8.
126. Navinés-Ferrer A, Serrano-Candelas E, Lafuente A, Muñoz-Cano R, Martín M, Gastaminza G. MRGPRX2-mediated mast cell response to drugs used in perioperative procedures and anaesthesia. Sci Rep. 2018;8(1):1–11.
127. Kühn H, Kolkhir P, Babina M, Düll M, Frischbutter S, Fok JS, et al. Mas-related G protein–coupled receptor X2 and its activators in dermatologic allergies. J Allergy Clin Immunol. 2021 Feb;147(2):456–69.
128. Macphee CH, Dong X, Peng Q, Paone DV, Skov PS, Baumann K, et al. Pharmacological blockade of the mast cell MRGPRX2 receptor supports investigation of its relevance in skin disorders. Front Immunol. 2024 Oct 18;15:1433982.
129. Babina M, Guhl S, Artuc M, Zuberbier T. Allergic FcεRI- and pseudo-allergic MRGPRX2-triggered mast cell activation routes are independent and inversely regulated by SCF. Allergy. 2018 Jan;73(1):256–60.
130. Babina M, Wang Z, Artuc M, Guhl S, Zuberbier T. MRGPRX2 is negatively targeted by SCF and IL-4 to diminish pseudo-allergic stimulation of skin mast cells in culture. Exp Dermatol. 2018 Nov;27(11):1298–303.
131. Wang Z, Guhl S, Franke K, Artuc M, Zuberbier T, Babina M. IL-33 and MRGPRX2-Triggered Activation of Human Skin Mast Cells-Elimination of Receptor Expression on Chronic Exposure, but Reinforced Degranulation on Acute Priming. Cells. 2019 Apr 11;8(4).
132. Babina M, Wang Z, Franke K, Guhl S, Artuc M, Zuberbier T. Yin-Yang of IL-33 in Human Skin Mast Cells: Reduced Degranulation, but Augmented Histamine Synthesis through p38 Activation. J Invest Dermatol. 2019 Jul;139(7):1516-1525.e3.
133. Fux M, Pecaric-Petkovic T, Odermatt A, Hausmann OV, Lorentz A, Bischoff SC, et al. IL-33 is a mediator rather than a trigger of the acute allergic response in humans. Allergy. 2014 Feb;69(2):216–22.
134. Lazki-Hagenbach P, Ali H, Sagi-Eisenberg R. Authentic and Ectopically Expressed MRGPRX2 Elicit Similar Mechanisms to Stimulate Degranulation of Mast Cells. Cells. 2021 Feb 12;10(2):376.
135. Lerner L, Babina M, Zuberbier T, Stevanovic K. Beyond Allergies—Updates on The Role of Mas-Related G-Protein-Coupled Receptor X2 in Chronic Urticaria and Atopic Dermatitis. Cells. 2024 Jan 25;13(3):220.

136. Gyoja F. A genome-wide survey of bHLH transcription factors in the Placozoan Trichoplax adhaerens reveals the ancient repertoire of this gene family in metazoan. Gene. 2014;542(1):29–37.
137. Simionato E, Ledent V, Richards G, Thomas-Chollier M, Kerner P, Coornaert D, et al. Origin and diversification of the basic helix-loop-helix gene family in metazoans: insights from comparative genomics. BMC Evol Biol. 2007 Mar 2;7:33.
138. Lowings P, Yavuzer U, Goding CR. Positive and negative elements regulate a melanocyte-specific promoter. Mol Cell Biol. 1992 Aug;12(8):3653–62.
139. Bentley NJ, Eisen T, Goding CR. Melanocyte-specific expression of the human tyrosinase promoter: activation by the microphthalmia gene product and role of the initiator. Mol Cell Biol. 1994 Dec;14(12):7996–8006.
140. Yavuzer U, Goding CR. Melanocyte-specific gene expression: role of repression and identification of a melanocyte-specific factor, MSF. Mol Cell Biol. 1994 May;14(5):3494–503.
141. Brown AD, Lynch K, Langelaan DN. The C-terminal transactivation domain of MITF interacts promiscuously with co-activator CBP/p300. Sci Rep. 2023 Sep 26;13(1):16094.
142. Levy C, Khaled M, Fisher DE. MITF: master regulator of melanocyte development and melanoma oncogene. Trends Mol Med. 2006 Sep;12(9):406–14.
143. Lu SY, Li M, Lin YL. Mitf induction by RANKL is critical for osteoclastogenesis. Mol Biol Cell. 2010 May 15;21(10):1763–71.
144. Kawakami A, Fisher DE. The master role of microphthalmia-associated transcription factor in melanocyte and melanoma biology. Lab Invest. 2017 Jun;97(6):649–56.
145. Hertwig P. Neue Mutationen und Koppelungsgruppen bei der Hausmaus. Z Für Indukt Abstamm-Vererbungslehre. 1942;80:220–46.
146. Hodgkinson CA, Moore KJ, Nakayama A, Steingrímsson E, Copeland NG, Jenkins NA, et al. Mutations at the mouse microphthalmia locus are associated with defects in a gene encoding a novel basic-helix-loop-helix-zipper protein. Cell. 1993 Jul 30;74(2):395–404.
147. Hartman ML, Czyz M. MITF in melanoma: mechanisms behind its expression and activity. Cell Mol Life Sci CMLS. 2015 Apr;72(7):1249–60.
148. Lee SH, Lee JH, Lee YM, Kim DK. Involvement of MITF-A, an alternative isoform of mi transcription factor, on the expression of tryptase gene in human mast cells. Exp Mol Med. 2010;42(5):366–75.
149. Lee YN, Noel P, Shahlaee A, Carter M, Kapur R, Wayne A, et al. Kit Signaling Regulates Mitf Expression in Mastocytosis. Blood. 2006 Nov 16;108(11):3601.
150. Proaño-Pérez E, Serrano-Candelas E, García-Valverde A, Rosell J, Gómez-Peregrina D, Navinés-Ferrer A, et al. The microphthalmia-associated transcription factor is involved in gastrointestinal stromal tumor growth. Cancer Gene Ther. 2023 Feb;30(2):245–55.
151. Agostini F, Agostinis R, Medina DL, Bisaglia M, Greggio E, Plotegher N. The Regulation of MiTF/TFE Transcription Factors Across Model Organisms: from Brain Physiology to Implication for Neurodegeneration. Mol Neurobiol. 2022 Aug;59(8):5000–23.
152. Ma P, Mali RS, Munugalavadla V, Krishnan S, Ramdas B, Sims E, et al. The PI3K pathway drives the maturation of mast cells via microphthalmia transcription factor. Blood. 2011 Sep 29;118(13):3459–69.
153. Pongas G, Cheson BD. PI3K signaling pathway in normal B cells and indolent B-cell malignancies. Semin Oncol. 2016 Dec;43(6):647–54.
154. Zhao H, Zhang J, Shao H, Liu J, Jin M, Chen J, et al. miRNA-340 inhibits osteoclast differentiation via repression of MITF. Biosci Rep. 2017 Aug 31;37(4):BSR20170302.
155. Haflidadóttir BS, Bergsteinsdóttir K, Praetorius C, Steingrímsson E. miR-148 regulates Mitf in melanoma cells. PloS One. 2010 Jul 14;5(7):e11574.
156. Hushcha Y, Blo I, Oton-Gonzalez L, Mauro GD, Martini F, Tognon M, et al. microRNAs in the Regulation of Melanogenesis. Int J Mol Sci. 2021 Jun 5;22(11).
157. Sato S, Roberts K, Gambino G, Cook A, Kouzarides T, Goding CR. CBP/p300 as a co-factor for the Microphthalmia transcription factor. Oncogene. 1997 Jun 26;14(25):3083–92.
158. Koludrovic D, Laurette P, Strub T, Keime C, Le Coz M, Coassolo S, et al. Chromatin-Remodelling Complex NURF Is Essential for Differentiation of Adult Melanocyte Stem Cells. PLoS Genet. 2015 Oct;11(10):e1005555.

159. Liu Z, Chen K, Dai J, Xu P, Sun W, Liu W, et al. A unique hyperdynamic dimer interface permits small molecule perturbation of the melanoma oncoprotein MITF for melanoma therapy. Cell Res. 2023 Jan;33(1):55–70.
160. Rajendran V, Kalita P, Shukla H, Kumar A, Tripathi T. Aminoacyl-tRNA synthetases: Structure, function, and drug discovery. Int J Biol Macromol. 2018 May;111:400–14.
161. Rubio Gomez MA, Ibba M. Aminoacyl-tRNA synthetases. RNA N Y N. 2020 Aug;26(8):910–36.
162. Freist W, Gauss DH. Lysyl-tRNA synthetase. Biol Chem Hoppe Seyler. 1995 Aug;376(8):451–72.
163. Motzik A, Nechushtan H, Foo SY, Razin E. Non-canonical roles of lysyl-tRNA synthetase in health and disease. Trends Mol Med. 2013 Dec 1;19(12):726–31.
164. Ofir-Birin Y, Fang P, Bennett SP, Zhang HM, Wang J, Rachmin I, et al. Structural Switch of Lysyl-tRNA Synthetase between Translation and Transcription. Mol Cell. 2013 Jan;49(1):30–42.
165. Motzik A, Amir E, Erlich T, Wang J, Kim BG, Han JM, et al. Post-translational modification of HINT1 mediates activation of MITF transcriptional activity in human melanoma cells. Oncogene. 2017 Aug 17;36(33):4732–8.
166. Shahlaee AH, Brandal S, Lee YN, Jie C, Takemoto CM. Distinct and Shared Transcriptomes Are Regulated by Microphthalmia-Associated Transcription Factor Isoforms in Mast Cells1. J Immunol. 2007 Jan 1;178(1):378–88.
167. Lee YN, Brandal S, Noel P, Wentzel E, Mendell JT, McDevitt MA, et al. KIT signaling regulates MITF expression through miRNAs in normal and malignant mast cell proliferation. Blood. 2011 Mar 31;117(13):3629–40.
168. Proaño-Pérez E, Ollé L, Guo Y, Aparicio C, Guerrero M, Muñoz-Cano R, et al. MITF Downregulation Induces Death in Human Mast Cell Leukemia Cells and Impairs IgE-Dependent Degranulation. Int J Mol Sci. 2023 Feb;24(4).
169. Guo Y, Ollé L, Proaño-Pérez E, Aparicio C, Guerrero M, Muñoz-Cano R, et al. MRGPRX2 signaling involves the Lysyl-tRNA synthetase and MITF pathway. Front Immunol. 2023;14.
170. Castells M, Madden M, Oskeritzian CA. Mast Cells and Mas-related G Protein-coupled Receptor X2: Itching for Novel Pathophysiological Insights to Clinical Relevance. Vol. 25, Current Allergy and Asthma Reports. Springer; 2025.
171. Haq R, Yokoyama S, Hawryluk EB, Jönsson GB, Frederick DT, McHenry K, et al. *BCL2A1* is a lineage-specific antiapoptotic melanoma oncogene that confers resistance to BRAF inhibition. Proc Natl Acad Sci. 2013 Mar 12;110(11):4321–6.
172. Li Y, Liu B, Harmacek L, Long Z, Liang J, Lukin K, et al. The transcription factors GATA2 and microphthalmia-associated transcription factor regulate Hdc gene expression in mast cells and are required for IgE/mast cell–mediated anaphylaxis. J Allergy Clin Immunol. 2018 Oct;142(4):1173–84.
173. Srivastava M, Kaplan MH. Transcription Factors in the Development and Pro-Allergic Function of Mast Cells. Front Allergy. 2021;2(June):1–13.
174. Ohanna M, Giuliano S, Bonet C, Imbert V, Hofman V, Zangari J, et al. Senescent cells develop a parp-1 and nuclear factor-κB-associated secretome (PNAS). Genes Dev. 2011;25(12):1245–61.
175. Ballotti R, Cheli Y, Bertolotto C. The complex relationship between MITF and the immune system: a Melanoma ImmunoTherapy (response) Factor? Mol Cancer. 2020 Dec;19(1):170.
176. Wiedemann GM, Aithal C, Kraechan A, Heise C, Cadilha BL, Zhang J, et al. Microphthalmia-Associated Transcription Factor (MITF) Regulates Immune Cell Migration into Melanoma. Transl Oncol. 2019 Feb;12(2):350–60.
177. Riesenberg S, Groetchen A, Siddaway R, Bald T, Reinhardt J, Smorra D, et al. MITF and c-Jun antagonism interconnects melanoma dedifferentiation with pro-inflammatory cytokine responsiveness and myeloid cell recruitment. Nat Commun. 2015 Nov 4;6(1):8755.
178. Chelombitko MA, Chernyak B V., Fedorov A V., Zinovkin RA, Razin E, Paruchuru LB. The Role Played by Mitochondria in FcεRI-Dependent Mast Cell Activation. Front Immunol. 2020;11(October).
179. Paruchuru LB, Govindaraj S, Razin E. The Critical Role Played by Mitochondrial MITF Serine 73 Phosphorylation in Immunologically Activated Mast Cells. Cells. 2022;11(3).
180. Hua J, Chen H, Chen Y, Zheng G, Li F, Qu J, et al. MITF acts as an anti-oxidant transcription factor to regulate mitochondrial biogenesis and redox signaling in retinal pigment epithelial cells. Exp Eye Res. 2018;170(February):138–47.

181. Lee A, Lim J, Lim JS. Emerging roles of MITF as a crucial regulator of immunity. Vol. 56, Experimental and Molecular Medicine. Springer Nature; 2024. p. 311–8.
182. Judge A, Dodd MS. Metabolism. Essays Biochem. 2020 Oct 8;64(4):607–47.
183. Mendoza RP, Anderson CC, Fudge DH, Roede JR, Brown JM. Metabolic Consequences of IgE- and Non-IgE–Mediated Mast Cell Degranulation. J Immunol. 2021;207(11):2637–48.
184. Schilling CH, Schuster S, Palsson BO, Heinrich R. Metabolic pathway analysis: basic concepts and scientific applications in the post-genomic era. Biotechnol Prog. 1999 Jun;15(3):296–303.
185. Pearce EL, Pearce EJ. Metabolic pathways in immune cell activation and quiescence. Immunity. 2013 Apr 18;38(4):633–43.
186. Kim J whan, Tchernyshyov I, Semenza GL, Dang CV. HIF-1-mediated expression of pyruvate dehydrogenase kinase: a metabolic switch required for cellular adaptation to hypoxia. Cell Metab. 2006 Mar;3(3):177–85.
187. Gatenby RA, Gillies RJ. Why do cancers have high aerobic glycolysis? Nat Rev Cancer. 2004 Nov 1;4(11):891–9.
188. Unno N, Menconi MJ, Salzman AL, Smith M, Hagen S, Ge Y, et al. Hyperpermeability and ATP depletion induced by chronic hypoxia or glycolytic inhibition in Caco-2BBe monolayers. Am J Physiol-Gastrointest Liver Physiol. 1996 Jun 1;270(6):G1010–21.
189. Everts B, Amiel E, van der Windt GJW, Freitas TC, Chott R, Yarasheski KE, et al. Commitment to glycolysis sustains survival of NO-producing inflammatory dendritic cells. Blood. 2012 Aug 16;120(7):1422–31.
190. Yu Q, Wang Y, Dong L, He Y, Liu R, Yang Q, et al. Regulations of Glycolytic Activities on Macrophages Functions in Tumor and Infectious Inflammation. Front Cell Infect Microbiol [Internet]. 2020;10. Available from: https://www.frontiersin.org/journals/cellular-and-infection-microbiology/articles/10.3389/fcimb.2020.00287
191. Linke M, Fritsch SD, Sukhbaatar N, Hengstschläger M, Weichhart T. mTORC1 and mTORC2 as regulators of cell metabolism in immunity. FEBS Lett. 2017 Oct;591(19):3089–103.
192. Goretzki A, Lin YJ, Schülke S. Immune metabolism in allergies, does it matter?—A review of immune metabolic basics and adaptations associated with the activation of innate immune cells in allergy. Vol. 76, Allergy: European Journal of Allergy and Clinical Immunology. John Wiley and Sons Inc; 2021. p. 3314–31.
193. Sharkia I, Hadad Erlich T, Landolina N, Assayag M, Motzik A, Rachmin I, et al. Pyruvate dehydrogenase has a major role in mast cell function, and its activity is regulated by mitochondrial microphthalmia transcription factor. J Allergy Clin Immunol. 2017;140(1):204-214.e8.
194. Buttgereit T, Pfeiffenberger M, Frischbutter S, Krauß PL, Chen Y, Maurer M, et al. Inhibition of Complex I of the Respiratory Chain, but Not Complex III, Attenuates Degranulation and Cytokine Secretion in Human Skin Mast Cells. Int J Mol Sci. 2022;23(19).
195. Kitahata Y, Nunomura S, Terui T, Ra C. Prolonged culture of mast cells with high-glucose medium enhances the Fc epsilon RI-mediated degranulation response and leukotriene C4 production. Int Arch Allergy Immunol. 2010;152 Suppl 1:22–31.
196. Nagai K, Fukushima T, Oike H, Kobori M. High glucose increases the expression of proinflammatory cytokines and secretion of TNFα and β-hexosaminidase in human mast cells. Eur J Pharmacol. 2012 Jul 15;687(1–3):39–45.
197. Goretzki A, Zimmermann J, Lin YJ, Schülke S. Immune Metabolism–An Opportunity to Better Understand Allergic Pathology and Improve Treatment of Allergic Diseases? Front Allergy. 2022;3.
198. Piotin A, Oulehri W, Charles AL, Tacquard C, Collange O, Mertes PM, et al. Oxidative Stress and Mitochondria Are Involved in Anaphylaxis and Mast Cell Degranulation: A Systematic Review. Vol. 13, Antioxidants. Multidisciplinary Digital Publishing Institute (MDPI); 2024.
199. Iyer SS, He Q, Janczy JR, Elliott EI, Zhong Z, Olivier AK, et al. Mitochondrial cardiolipin is required for Nlrp3 inflammasome activation. Immunity. 2013;39(2):311–23.
200. Zhang Q, Raoof M, Chen Y, Sumi Y, Sursal T, Junger W, et al. Circulating mitochondrial DAMPs cause inflammatory responses to injury. Nature. 2010;464(7285):104–7.
201. Akira S, Takeda K. Toll-like receptor signalling. Nat Rev Immunol. 2004;4(7):499–511.
202. Chelombitko MA, Chernyak B V., Fedorov A V., Zinovkin RA, Razin E, Paruchuru LB. The Role Played by Mitochondria in FcεRI-Dependent Mast Cell Activation. Front Immunol. 2020;11(October).

203. Iyer D, Mishra N, Agrawal A. Mitochondrial Function in Allergic Disease. Curr Allergy Asthma Rep. 2017;17(5).
204. Chelombitko MA, Chernyak BV, Fedorov AV, Zinovkin RA, Razin E, Paruchuru LB. The Role Played by Mitochondria in FcεRI-Dependent Mast Cell Activation. Vol. 11, Frontiers in Immunology. Frontiers Media S.A.; 2020.
205. Scarpelli M, Todeschini A, Volonghi I, Padovani A, Filosto M. Mitochondrial diseases: Advances and issues. Appl Clin Genet. 2017;10:21–6.
206. Jang H, Kim M, Hong JY, Cho HJ, Kim CH, Kim YH, et al. Mitochondrial and nuclear mitochondrial variants in allergic diseases. Allergy Asthma Immunol Res. 2020;12(5):877–84.
207. Perales-Chorda C, Obeso D, Twomey L, Rojas-Benedicto A, Puchades-Carrasco L, Roca M, et al. Characterization of anaphylaxis reveals different metabolic changes depending on severity and triggers. Clin Exp Allergy. 2021;51(10):1295–309.
208. Goretzki A, Lin YJ, Schülke S. Immune metabolism in allergies, does it matter?—A review of immune metabolic basics and adaptations associated with the activation of innate immune cells in allergy. Allergy Eur J Allergy Clin Immunol. 2021;76(11):3314–31.
209. Zhang B, Weng Z, Sismanopoulos N, Asadi S, Therianou A, Alysandratos KD, et al. Mitochondria distinguish granule-stored from de novo synthesized TNF secretion in human mast cells. Int Arch Allergy Immunol. 2012;159(1):23–32.
210. Kraus F, Roy K, Pucadyil TJ, Ryan MT. Function and regulation of the divisome for mitochondrial fission. Nature. 2021;590(7844):57–66.
211. Rossi A, Pizzo P, Filadi R. Calcium, mitochondria and cell metabolism: A functional triangle in bioenergetics. Vol. 1866, Biochimica et Biophysica Acta - Molecular Cell Research. Elsevier B.V.; 2019. p. 1068–78.
212. Kraus F, Roy K, Pucadyil TJ, Ryan MT. Function and regulation of the divisome for mitochondrial fission. Vol. 590, Nature. Nature Research; 2021. p. 57–66.
213. Coombs RRA, Gell PGH. Classification of allergic reactions responsible for drug hypersensitivity reactions. Clinical Aspects of Immunology. 1968;
214. Descotes J, Choquet-Kastylevsky G. Gell and Coombs's classification: is it still valid? Toxicology. 2001 Feb;158(1–2):43–9.
215. Theoharides TC, Alysandratos KD, Angelidou A, Delivanis DA, Sismanopoulos N, Zhang B, et al. Mast cells and inflammation. Vol. 1822, Biochimica et Biophysica Acta - Molecular Basis of Disease. 2012. p. 21–33.
216. Rajan TV. The Gell–Coombs classification of hypersensitivity reactions: a re-interpretation. Trends Immunol. 2003 Jul;24(7):376–9.
217. Rodriguez-Coira J, Villaseñor A, Izquierdo E, Huang M, Barker-Tejeda TC, Radzikowska U, et al. The Importance of Metabolism for Immune Homeostasis in Allergic Diseases. Front Immunol. 2021 Jul 28;12:692004.
218. Varricchi G, Harker J, Borriello F, Marone G, Durham SR, Shamji MH. T follicular helper (T_{fh}) cells in normal immune responses and in allergic disorders. Allergy. 2016 Aug;71(8):1086–94.
219. Johansson SGO, Bieber T, Dahl R, Friedmann PS, Lanier BQ, Lockey RF, et al. Revised nomenclature for allergy for global use: Report of the Nomenclature Review Committee of the World Allergy Organization, October 2003. J Allergy Clin Immunol. 2004 May;113(5):832–6.
220. Galli SJ, Tsai M, Piliponsky AM. The development of allergic inflammation. Nature. 2008;24(454):445–54.
221. Jutel M, Agache I, Zemelka-Wiacek M, Akdis M, Chivato T, Del Giacco S, et al. Nomenclature of allergic diseases and hypersensitivity reactions: Adapted to modern needs: An EAACI position paper. Allergy. 2023 Nov;78(11):2851–74.
222. Finkelman FD. Anaphylaxis: lessons from mouse models. J Allergy Clin Immunol. 2007 Sep;120(3):506–15; quiz 516–7.
223. Bruhns P. Properties of mouse and human IgG receptors and their contribution to disease models. Blood. 2012 Jun 14;119(24):5640–9.
224. Khodoun MV, Strait R, Armstrong L, Yanase N, Finkelman FD. Identification of markers that distinguish IgE- from IgG-mediated anaphylaxis. Proc Natl Acad Sci U S A. 2011 Jul 26;108(30):12413–8.

225. Mayorga C, Ariza A, Muñoz-Cano R, Sabato V, Doña I, Torres MJ. Biomarkers of immediate drug hypersensitivity. Allergy. 2024 Mar;79(3):601–12.
226. Muñoz-Cano R, Pascal M, Bartra J, Picado C, Valero A, Kim DK, et al. Distinct transcriptome profiles differentiate nonsteroidal anti-inflammatory drug–dependent from nonsteroidal anti-inflammatory drug–independent food-induced anaphylaxis. J Allergy Clin Immunol. 2016 Jan;137(1):137–46.
227. Justiz Vaillant AA, Vashisht R, Zito PM. Immediate Hypersensitivity Reactions. StatPearls [Internet]; 2025.
228. Valent P, Akin C, Metcalfe DD. Mastocytosis: 2016 updated WHO classification and novel emerging treatment concepts. Blood. 2017 Mar 16;129(11):1420–7.
229. Alaggio R, Amador C, Anagnostopoulos I, Attygalle AD, Araujo IB de O, Berti E, et al. The 5th edition of the World Health Organization Classification of Haematolymphoid Tumours: Lymphoid Neoplasms. Leukemia. 2022 Jul;36(7):1720–48.
230. Valent P, Horny HP, Escribano L, Longley BJ, Li CY, Schwartz LB, et al. Diagnostic criteria and classification of mastocytosis: a consensus proposal. Leuk Res. 2001 Jul;25(7):603–25.
231. Damman J, Diercks GFH, Van Doorn MB, Pasmans SG, Hermans MAW. Cutaneous Lesions of Mastocytosis: Mast Cell Count, Morphology, and Immunomolecular Phenotype. Am J Dermatopathol. 2023 Oct;45(10):697–703.
232. Fabbro D, Ruetz S, Bodis S, Pruschy M, Csermak K, Man A, et al. PKC412--a protein kinase inhibitor with a broad therapeutic potential. Anticancer Drug Des. 2000 Feb;15(1):17–28.
233. Gotlib J, Berubé C, Growney JD, Chen CC, George TI, Williams C, et al. Activity of the tyrosine kinase inhibitor PKC412 in a patient with mast cell leukemia with the D816V KIT mutation. Blood. 2005 Oct 15;106(8):2865–70.
234. Barete S, Lortholary O, Damaj G, Hirsch I, Chandesris MO, Elie C, et al. Long-term efficacy and safety of cladribine (2-CdA) in adult patients with mastocytosis. Blood. 2015 Aug 20;126(8):1009–16; quiz 1050.
235. Kluin-Nelemans HC, Oldhoff JM, Van Doormaal JJ, Van ’t Wout JW, Verhoef G, Gerrits WBJ, et al. Cladribine therapy for systemic mastocytosis. Blood. 2003 Dec 15;102(13):4270–6.
236. Walls AF, Jones DB, Williams JH, Church MK, Holgate ST. Immunohistochemical identification of mast cells in formaldehyde-fixed tissue using monoclonal antibodies specific for tryptase. J Pathol. 1990 Oct;162(2):119–26.
237. Ustun C, Reiter A, Scott BL, Nakamura R, Damaj G, Kreil S, et al. Hematopoietic stem-cell transplantation for advanced systemic mastocytosis. J Clin Oncol Off J Am Soc Clin Oncol. 2014 Oct 10;32(29):3264–74.
238. Desai M, Oppenheimer J. Elucidating asthma phenotypes and endotypes: progress towards personalized medicine. Ann Allergy Asthma Immunol Off Publ Am Coll Allergy Asthma Immunol. 2016 May;116(5):394–401.
239. Bossé Y, Lemire M, Poon AH, Daley D, He JQ, Sandford A, et al. Asthma and genes encoding components of the vitamin D pathway. Respir Res. 2009 Oct 24;10(1):98.
240. Braman SS. The global burden of asthma. Chest. 2006;130(1 Suppl):4S-12S.
241. Corren J. Asthma phenotypes and endotypes: an evolving paradigm for classification. Discov Med. 2013 Apr;15(83):243–9.
242. Allakhverdi Z, Comeau MR, Jessup HK, Yoon BRP, Brewer A, Chartier S, et al. Thymic stromal lymphopoietin is released by human epithelial cells in response to microbes, trauma, or inflammation and potently activates mast cells. J Exp Med. 2007 Feb 19;204(2):253–8.
243. Eiwegger T, Akdis CA. IL-33 links tissue cells, dendritic cells and Th2 cell development in a mouse model of asthma. Eur J Immunol. 2011 Jun;41(6):1535–8.
244. Zheng H, Zhang Y, Pan J, Liu N, Qin Y, Qiu L, et al. The Role of Type 2 Innate Lymphoid Cells in Allergic Diseases. Front Immunol. 2021 Jun 9;12:586078.
245. Matsuyama T, Machida K, Mizuno K, Matsuyama H, Dotake Y, Shinmura M, et al. The Functional Role of Group 2 Innate Lymphoid Cells in Asthma. Biomolecules. 2023 May 26;13(6).
246. Malik B, Bartlett NW, Upham JW, Nichol KS, Harrington J, Wark PAB. Severe asthma ILC2s demonstrate enhanced proliferation that is modified by biologics. Respirology. 2023 Aug 1;28(8):758–66.

247. Brightling CE, Bradding P, Symon FA, Holgate ST, Wardlaw AJ, Pavord ID. Mast-cell infiltration of airway smooth muscle in asthma. N Engl J Med. 2002 May 30;346(22):1699–705.
248. Navinés-Ferrer A, Serrano-Candelas E, Molina-Molina GJ, Martín M. IgE-Related Chronic Diseases and Anti-IgE-Based Treatments. J Immunol Res. 2016;2016:1–12.
249. Voehringer D. Protective and pathological roles of mast cells and basophils. Nat Rev Immunol. 2013 May;13(5):362–75.
250. Matsuzawa S, Sakashita K, Kinoshita T, Ito S, Yamashita T, Koike K. IL-9 enhances the growth of human mast cell progenitors under stimulation with stem cell factor. J Immunol Baltim Md 1950. 2003 Apr 1;170(7):3461–7.
251. Rojas-Ramos E, Avalos AF, Pérez-Fernandez L, Cuevas-Schacht F, Valencia-Maqueda E, Terán LM. Role of the chemokines RANTES, monocyte chemotactic proteins-3 and -4, and eotaxins-1 and -2 in childhood asthma. Eur Respir J. 2003 Aug;22(2):310–6.
252. Prakash YS. Airway smooth muscle in airway reactivity and remodeling: what have we learned? Am J Physiol Lung Cell Mol Physiol. 2013 Dec;305(12):L912-933.
253. Figueiredo IAD, Ferreira SRD, Fernandes JM, Silva BA da, Vasconcelos LHC, Cavalcante F de A. A review of the pathophysiology and the role of ion channels on bronchial asthma. Front Pharmacol. 2023 Sep 28;14:1236550.
254. Zheng L, Li B, Qian W, Zhao L, Cao Z, Shi S, et al. Fine epitope mapping of humanized anti-IgE monoclonal antibody omalizumab. Biochem Biophys Res Commun. 2008 Oct 31;375(4):619–22.
255. Presta LG, Lahr SJ, Shields RL, Porter JP, Gorman CM, Fendly BM, et al. Humanization of an antibody directed against IgE. J Immunol Baltim Md 1950. 1993 Sep 1;151(5):2623–32.
256. Serrano-Candelas E, Martinez-Aranguren R, Valero A, Bartra J, Gastaminza G, Goikoetxea MJ, et al. Comparable actions of omalizumab on mast cells and basophils. Clin Exp Allergy. 2016 Jan;46(1):92–102.
257. Seluk L, Davis AE, Rhoads S, Wechsler ME. Novel asthma treatments: Advancing beyond approved novel step-up therapies for asthma. Ann Allergy Asthma Immunol Off Publ Am Coll Allergy Asthma Immunol. 2025 Jan;134(1):9–18.
258. Grattan C. The urticarias: pathophysiology and management. Clin Med Lond Engl. 2012 Apr;12(2):164–7.
259. Kolkhir P, Giménez-Arnau AM, Kulthanan K, Peter J, Metz M, Maurer M. Urticaria. Nat Rev Dis Primer. 2022;8(1):61.
260. Peck G, Hashim MJ, Shaughnessy C, Muddasani S, Elsayed NA, Fleischer ABJ. Global Epidemiology of Urticaria: Increasing Burden among Children, Females and Low-income Regions. Acta Derm Venereol. 2021 Apr 22;101(4):adv00433.
261. Kaplan A, Lebwohl M, Giménez-Arnau AM, Hide M, Armstrong AW, Maurer M. Chronic spontaneous urticaria: Focus on pathophysiology to unlock treatment advances. Allergy. 2023 Feb;78(2):389–401.
262. Viegas L, Ferreira M, Kaplan A. The Maddening Itch: An Approach to Chronic Urticaria. J Investig Allergol Clin Immunol. 2014;24.
263. Kaplan A, Lebwohl M, Giménez-Arnau AM, Hide M, Armstrong AW, Maurer M. Chronic spontaneous urticaria: Focus on pathophysiology to unlock treatment advances. Allergy. 2023 Feb;78(2):389–401.
264. Saini SS, Bindslev-Jensen C, Maurer M, Grob JJ, Bülbül Baskan E, Bradley MS, et al. Efficacy and safety of omalizumab in patients with chronic idiopathic/spontaneous urticaria who remain symptomatic on H1 antihistamines: a randomized, placebo-controlled study. J Invest Dermatol. 2015 Jan;135(1):67–75.
265. Maurer M, Rosén K, Hsieh HJ, Saini S, Grattan C, Gimenéz-Arnau A, et al. Omalizumab for the treatment of chronic idiopathic or spontaneous urticaria. N Engl J Med. 2013 Mar 7;368(10):924–35.
266. Maurer M, Berger W, Giménez-Arnau A, Hayama K, Jain V, Reich A, et al. Remibrutinib, a novel BTK inhibitor, demonstrates promising efficacy and safety in chronic spontaneous urticaria. J Allergy Clin Immunol. 2022 Dec;150(6):1498-1506.e2.
267. Shtessel M, Limjunyawong N, Oliver ET, Chichester K, Gao L, Dong X, et al. MRGPRX2 Activation Causes Increased Skin Reactivity in Patients with Chronic Spontaneous Urticaria. J Invest Dermatol. 2021 Mar;141(3):678-681.e2.

268. Zuberbier T, Aberer W, Asero R, Abdul Latiff AH, Baker D, Ballmer-Weber B, et al. The EAACI/GA^{2}LEN/EDF/WAO guideline for the definition, classification, diagnosis and management of urticaria. Allergy. 2018 Jul;73(7):1393–414.
269. Kucuksezer UC, Ozdemir C, Cevhertas L, Ogulur I, Akdis M, Akdis CA. Mechanisms of allergen-specific immunotherapy and allergen tolerance. Allergol Int. 2020;69(4):549–60.
270. Gülen T, Akin C. Anaphylaxis and Mast Cell Disorders. Immunol Allergy Clin North Am. 2022 Feb;42(1):45–63.
271. Pawankar R. Allergic diseases and asthma: A global public health concern and a call to action. World Allergy Organ J. 2014;7(1):1–3.
272. Burbank AJ, Sood AK, Kesic MJ, Peden DB, Hernandez ML. Environmental determinants of allergy and asthma in early life. J Allergy Clin Immunol. 2017;140(1):1–12.
273. Simons FER, Ardusso LRF, Bil MB, El-Gamal YM, Ledford DK, Ring J, et al. World Allergy Organization anaphylaxis guidelines: Summary. J Allergy Clin Immunol. 2011;127(3).
274. Pumphrey RSH. Lessons for management of anaphylaxis from a study of fatal reactions. Clin Exp Allergy. 2000;30(8):1144–50.
275. Ruiz-Garcia M, Bartra J, Alvarez O, Lakhani A, Patel S, Tang A, et al. Cardiovascular changes during peanut-induced allergic reactions in human subjects. J Allergy Clin Immunol. 2021;147(2):633–42.
276. Turner PJ, Ruiz-Garcia M, Patel N, Abrantes G, Burrell S, Vazquez-Ortiz M, et al. Delayed symptoms and orthostatic intolerance following peanut challenge. Clin Exp Allergy. 2021;51(5):696–702.
277. Torres Jaen MJ. Alergológica 2015. Alergológica 2015. 2017. 230–247 p.
278. Cardona V. Galaxia 2016. 2016.
279. Cardona V, Ansotegui IJ, Ebisawa M, El-Gamal Y, Fernandez Rivas M, Fineman S, et al. World allergy organization anaphylaxis guidance 2020. World Allergy Organ J. 2020;13(10).
280. Perez-Codesido S, Rosado-Ingelmo A, Privitera-Torres M, Pérez Fernández E, Nieto-Nieto A, Gonzalez-Moreno A, et al. Incidence of Fatal Anaphylaxis: A Systematic Review of Observational Studies. J Investig Allergol Clin Immunol. 2022;32(4):245–60.
281. Turner PJ, Campbell DE, Motosue MS, Campbell RL. Global Trends in Anaphylaxis Epidemiology and Clinical Implications. J Allergy Clin Immunol Pract. 2020;8(4):1169–76.
282. Tejedor-Alonso MA, Moro-Moro M, Múgica-García M V. Epidemiology of anaphylaxis: Contributions from the last 10 years. J Investig Allergol Clin Immunol. 2015;25(3):163–75.
283. Muñoz-Cano R, San Bartolome C, Casas-Saucedo R, Araujo G, Gelis S, Ruano-Zaragoza M, et al. Immune-Mediated Mechanisms in Cofactor-Dependent Food Allergy and Anaphylaxis: Effect of Cofactors in Basophils and Mast Cells. Front Immunol. 2021;11(February):1–8.
284. Muñoz-Cano R, Pascal M, Araujo G, Goikoetxea MJ, Valero AL, Picado C, et al. Mechanisms, cofactors, and augmenting factors involved in anaphylaxis. Front Immunol. 2017;8(SEP):1–7.
285. Fundación Seaic. Guía de actuación en Anafilaxia: GALAXIA 2022. 2022.
286. Du Toit G, Santos A, Roberts G, Fox AT, Smith P, Lack G. The diagnosis of IgE-mediated food allergy in childhood. Pediatr Allergy Immunol Off Publ Eur Soc Pediatr Allergy Immunol. 2009 Jun;20(4):309–19.
287. Sicherer SH, Sampson HA. Food allergy: A review and update on epidemiology, pathogenesis, diagnosis, prevention, and management. J Allergy Clin Immunol. 2018 Jan;141(1):41–58.
288. Santos AF, Riggioni C, Agache I, Akdis CA, Akdis M, Alvarez-Perea A, et al. EAACI guidelines on the management of IgE-mediated food allergy. Allergy. 2025 Jan;80(1):14–36.
289. Piletta-Zanin A, Ricci C, Santos AF, Eigenmann PA. BAT and MAT for diagnosis of peanut allergy: A systematic review and meta-analysis. Pediatr Allergy Immunol. 2024 Jun;35(6):e14140.
290. Salcedo G, Sanchez-Monge R, Diaz-Perales A, Garcia-Casado G, Barber D. Plant non-specific lipid transfer proteins as food and pollen allergens. Clin Exp Allergy J Br Soc Allergy Clin Immunol. 2004 Sep;34(9):1336–41.
291. Asero R, Mistrello G, Roncarolo D, Amato S, Caldironi G, Barocci F, et al. Immunological cross-reactivity between lipid transfer proteins from botanically unrelated plant-derived foods: a clinical study. Allergy. 2002 Oct;57(10):900–6.
292. McKenna OE, Asam C, Araujo GR, Roulias A, Goulart LR, Ferreira F. How relevant is panallergen sensitization in the development of allergies? Pediatr Allergy Immunol. 2016 Sep;27(6):560–8.

293. Hauser M, Roulias A, Ferreira F, Egger M. Panallergens and their impact on the allergic patient. Vol. 6, Allergy, Asthma and Clinical Immunology. 2010.
294. Asero R, Mistrello G, Roncarolo D, de Vries SC, Gautier MF, Ciurana CL, et al. Lipid transfer protein: a pan-allergen in plant-derived foods that is highly resistant to pepsin digestion. Int Arch Allergy Immunol. 2001 Mar;124(1–3):67–9.
295. García AN, Ramos ÁM, Espinosa RP, Gómez LC, Jiménez FO. Implicación clínica de la reactividad cruzada entre alergenos. 2004;
296. Pastorello EA, Ortolani C, Farioli L, Pravettoni V, Ispano M, Borga A, et al. Allergenic cross-reactivity among peach, apricot, plum, and cherry in patients with oral allergy syndrome: an in vivo and in vitro study. J Allergy Clin Immunol. 1994 Oct;94(4):699–707.
297. Lleonart R, Cisteró A, Carreira J, Batista A, Moscoso del Prado J. Food allergy: identification of the major IgE-binding component of peach (Prunus persica). Ann Allergy. 1992 Aug;69(2):128–30.
298. Baldo BA. MRGPRX2, drug pseudoallergies, inflammatory diseases, mechanisms and distinguishing MRGPRX2- and IgE/FcεRI-mediated events. Br J Clin Pharmacol. 2023 Nov;89(11):3232–46.
299. Schlumberger HD. Pseudo-allergic reactions to drugs and chemicals. Ann Allergy. 1983 Aug;51(2 Pt 2):317–24.
300. Jurakić Toncić R, Marinović B, Lipozencić J. Nonallergic hypersensitivity to nonsteroidal antiinflammatory drugs, angiotensin-converting enzyme inhibitors, radiocontrast media, local anesthetics, volume substitutes and medications used in general anesthesia. Acta Dermatovenerol Croat ADC. 2009;17(1):54–69.
301. Gomes ER, Demoly P. Epidemiology of hypersensitivity drug reactions. Curr Opin Allergy Clin Immunol. 2005 Aug;5(4):309–16.
302. Sturm GJ, Varga E -M., Roberts G, Mosbech H, Bilò MB, Akdis CA, et al. EAACI guidelines on allergen immunotherapy: Hymenoptera venom allergy. Allergy. 2018 Apr;73(4):744–64.
303. Koenig JFE, Bruton K, Phelps A, Grydziuszko E, Jiménez-Saiz R, Jordana M. Memory generation and re-activation in food allergy. ImmunoTargets Ther. 2021;10:171–84.
304. Bacher P, Heinrich F, Stervbo U, Nienen M, Vahldieck M, Iwert C, et al. Regulatory T Cell Specificity Directs Tolerance versus Allergy against Aeroantigens in Humans. Cell. 2016 Nov 3;167(4):1067-1078.e16.
305. Seumois G, Ramírez-Suástegui C, Schmiedel BJ, Liang S, Peters B, Sette A, et al. Single-cell transcriptomic analysis of allergen-specific T cells in allergy and asthma. Sci Immunol. 2020 Jun 12;5(48).
306. Rudensky AY. Regulatory T cells and Foxp3. Immunol Rev. 2011 May;241(1):260–8.
307. Lozano-Ojalvo D, Tyler SR, Aranda CJ, Wang J, Sicherer S, Sampson HA, et al. Allergen recognition by specific effector Th2 cells enables IL-2-dependent activation of regulatory T-cell responses in humans. Allergy. 2023 Mar;78(3):697–713.
308. Burton OT, Noval Rivas M, Zhou JS, Logsdon SL, Darling AR, Koleoglou KJ, et al. Immunoglobulin E signal inhibition during allergen ingestion leads to reversal of established food allergy and induction of regulatory T cells. Immunity. 2014 Jul 17;41(1):141–51.
309. Noval Rivas M, Burton OT, Oettgen HC, Chatila T. IL-4 production by group 2 innate lymphoid cells promotes food allergy by blocking regulatory T-cell function. J Allergy Clin Immunol. 2016 Sep;138(3):801-811.e9.
310. Palomares F, Pérez-Sánchez N, Nieto N, Núñez R, Cañas JA, Martín-Astorga MDC, et al. Group 2 innate lymphoid cells are key in lipid transfer protein allergy pathogenesis. Front Immunol. 2024 Apr 25;15:1385101.
311. Palomares F, Gómez F, Bogas G, Maggi L, Cosmi L, Annunziato F, et al. Innate lymphoid cells type 2 in LTP-allergic patients and their modulation during sublingual immunotherapy. Allergy. 2021 Jul;76(7):2253–6.
312. Mita H, Yasueda H, Akiyama K. Affinity of IgE antibody to antigen influences allergen-induced histamine release. Clin Exp Allergy J Br Soc Allergy Clin Immunol. 2000;30(11):1583–9.
313. Suzuki R, Leach S, Liu W, Ralston E, Scheffel J, Zhang W, et al. Molecular editing of cellular responses by the high-affinity receptor for IgE. Science. 2014;343(6174):1021–5.
314. Liang Y, Niederstrasser H, Edwards M, Jackson CE, Cooper JA. Distinct Roles for CARMIL Isoforms in Cell Migration. Wang YL, editor. Mol Biol Cell. 2009 Dec;20(24):5290–305.

315. Wang J, Lin J, Bardina L, Goldis M, Nowak-Wegrzyn A, Shreffler WG, et al. Correlation of IgE/IgG4 milk epitopes and affinity of milk-specific IgE antibodies with different phenotypes of clinical milk allergy. J Allergy Clin Immunol. 2010;125(3).
316. He JS, Subramaniam S, Narang V, Srinivasan K, Saunders SP, Carbajo D, et al. IgG1 memory B cells keep the memory of IgE responses. Nat Commun. 2017 Dec;8(1).
317. Xiong H, Dolpady J, Wabl M, de Lafaille MAC, Lafaille JJ. Sequential class switching is required for the generation of high affinity IgE antibodies. J Exp Med. 2012 Feb;209(2):353–64.
318. Sahoo A, Wali S, Nurieva R. T helper 2 and T follicular helper cells: Regulation and function of interleukin-4. Cytokine Growth Factor Rev. 2016 Aug;30:29–37.
319. Haniuda K, Kitamura D. Multi-faceted regulation of IgE production and humoral memory formation. Allergol Int. 2021 Apr;70(2):163–8.
320. Olatunde AC, Hale JS, Lamb TJ. Cytokine-skewed Tfh cells: functional consequences for B cell help. Trends Immunol. 2021 Jun;42(6):536–50.
321. Ho IC, Tai TS, Pai SY. GATA3 and the T-cell lineage: essential functions before and after T-helper-2-cell differentiation. Nat Rev Immunol. 2009 Feb;9(2):125–35.
322. Gowthaman U, Chen JS, Eisenbarth SC. Regulation of IgE by T follicular helper cells. J Leukoc Biol. 2020;107(3):409–18.
323. Chen JS, Grassmann JDS, Gowthaman U, Olyha SJ, Simoneau T, Berin MC, et al. Flow cytometric identification of TFH13 cells in mouse and human. J Allergy Clin Immunol. 2021;147(2):470–83.
324. Gowthaman U, Chen JS, Zhang B, Flynn WF, Lu Y, Song W, et al. Identification of a T follicular helper cell subset that drives anaphylactic IgE. Science. 2019;365(6456).
325. Su HC. Insights into the pathogenesis of allergic disease from dedicator of cytokinesis 8 deficiency. Curr Opin Immunol. 2023 Feb;80:102277.
326. Yao Y, Wang ZC, Wang N, Zhou PC, Chen CL, Song J, et al. Allergen immunotherapy improves defective follicular regulatory T cells in patients with allergic rhinitis. J Allergy Clin Immunol. 2019 Jul;144(1):118–28.
327. Clement RL, Daccache J, Mohammed MT, Diallo A, Blazar BR, Kuchroo VK, et al. Follicular regulatory T cells control humoral and allergic immunity by restraining early B cell responses. Nat Immunol. 2019 Oct;20(10):1360–71.
328. Mateja A, Wang Q, Chovanec J, Kim J, Wilson KJ, Schwartz LB, et al. Defining baseline variability of serum tryptase levels improves accuracy in identifying anaphylaxis. J Allergy Clin Immunol. 2022 Mar;149(3):1010-1017.e10.
329. Lemon-Mulé H, Nowak-Wegrzyn A, Berin C, Adina K. Knight M. Pathophysiology of Food-Induced Anaphylaxis. Curr Allergy Asthma Rep. 2008;8:201–8.
330. Bahri R, Custovic A, Korosec P, Tsoumani M, Barron M, Wu J, et al. Mast cell activation test in the diagnosis of allergic disease and anaphylaxis. J Allergy Clin Immunol. 2018;142(2):485-496.e16.
331. Santos AF, Du Toit G, O'Rourke C, Becares N, Couto-Francisco N, Radulovic S, et al. Biomarkers of severity and threshold of allergic reactions during oral peanut challenges. J Allergy Clin Immunol. 2020;146(2):344–55.
332. Nicolaou N, Poorafshar M, Murray C, Simpson A, Winell H, Kerry G, et al. Allergy or tolerance in children sensitized to peanut: prevalence and differentiation using component-resolved diagnostics. J Allergy Clin Immunol. 2010;125(1).
333. Osborne NJ, Koplin JJ, Martin PE, Gurrin LC, Lowe AJ, Matheson MC, et al. Prevalence of challenge-proven IgE-mediated food allergy using population-based sampling and predetermined challenge criteria in infants. J Allergy Clin Immunol. 2011;127(3):668-676.e2.
334. Ebo DG, Faber M, Elst J, Van Gasse AL, Bridts CH, Mertens C, et al. In Vitro Diagnosis of Immediate Drug Hypersensitivity During Anesthesia: A Review of the Literature. J Allergy Clin Immunol Pract. 2018 Aug;6(4):1176–84.
335. Bousquet PJ, Gaeta F, Bousquet-Rouanet L, Lefrant JY, Demoly P, Romano A. Provocation tests in diagnosing drug hypersensitivity. Curr Pharm Des. 2008;14(27):2792–802.
336. Mertes PM, Malinovsky JM, Jouffroy L, Aberer W, Terreehorst I, Brockow K, et al. Reducing the risk of anaphylaxis during anesthesia: 2011 updated guidelines for clinical practice. J Investig Allergol Clin Immunol. 2011;21(6):442–53.
337. Ebo DG, Bahri R, Tontini C, Van Gasse AL, Mertens C, Hagendorens MM, et al. Mast cell versus basophil activation test in allergy: Current status. Clin Exp Allergy. 2024 Jun;54(6):378–87.

338. Santos AF, Shreffler WG. Road map for the clinical application of the basophil activation test in food allergy. Clin Exp Allergy J Br Soc Allergy Clin Immunol. 2017 Sep 1;47(9):1115–24.
339. Elst J, Sabato V, van der Poorten MLM, Van Gasse AL, Van Houdt M, Bridts CH, et al. Basophil and mast cell activation tests by flow cytometry in immediate drug hypersensitivity: Diagnosis and beyond. J Immunol Methods. 2021;495(April):113050.
340. Santos AF, Couto-Francisco N, Bécares N, Kwok M, Bahnson HT, Lack G. A novel human mast cell activation test for peanut allergy. J Allergy Clin Immunol. 2018;142(2):689-691.e9.
341. Chirumbolo S, Bjørklund G, Vella A. Mast cell activation test versus basophil activation test and related competing issues. J Allergy Clin Immunol. 2018;142(3):1018–9.
342. Shannalee R. Martinez, Maresha S. Gay and LZ. An optimized protocol for the generation and functional analysis of human mast cells from CD34+ enriched cell populations. Physiol Behav. 2016;176(1):139–48.
343. Reber LL, Hernandez JD, Galli SJ. The pathophysiology of anaphylaxis. J Allergy Clin Immunol. 2017;140(2):335–48.
344. Ebo DG, Bahri R, Eggel A, Sabato V, Tontini C, Elst J. Flow cytometry–based basophil and mast cell activation tests in allergology: State of the art. J Allergy Clin Immunol. 2025 Feb;155(2):286–97.
345. Butterfield JH, Weiler D, Dewald G, Gleich GJ. Establishment of an immature mast cell line from a patient with mast cell leukemia. Leuk Res. 1988;12(4):345–55.
346. Kirshenbaum AS, Akin C, Wu Y, Rottem M, Goff JP, Beaven MA, et al. Characterization of novel stem cell factor responsive human mast cell lines LAD 1 and 2 established from a patient with mast cell sarcoma/leukemia; Activation following aggregation of FcεRI or FcγRI. Leuk Res. 2003;27(8):677–82.
347. Laidlaw TM, Steinke JW, Tiñana AM, Feng C, Xing W, Lam BK, et al. Characterization of a novel human mast cell line that responds to stem cell factor and expresses functional FcεRI. J Allergy Clin Immunol. 2011;127(3):815-822.e5.
348. Saleh R, Wedeh G, Herrmann H, Bibi S, Cerny-Reiterer S, Sadovnik I, et al. A new human mast cell line expressing a functional IgE receptor converts to tumorigenic growth by KIT D816V transfection. Blood. 2014 Jul 3;124(1):111–20.
349. Elst J, Ebo DG, Faber MA, Van Gasse AL, Decuyper II, van der Poorten MLM, et al. Culturing cells with mast cell phenotype and function: Comparison of peripheral blood and bone marrow as a source. J Immunol Methods. 2021;495(April):113061.
350. Luo Y, Fernandez Vallone V, He J, Frischbutter S, Kolkhir P, Moñino-Romero S, et al. A novel approach for studying mast cell–driven disorders: Mast cells derived from induced pluripotent stem cells. J Allergy Clin Immunol. 2021;
351. Rådinger M, Jensen BM, Kuehn HS, Kirshenbaum A, Gilfillan AM. Generation, isolation, and maintenance of human mast cells and mast cell lines derived from peripheral blood or cord blood. Curr Protoc Immunol. 2010;(SUPPL. 90):1–12.
352. Schmetzer O, Valentin P, Smorodchenko A, Domenis R, Gri G, Siebenhaar F, et al. A novel method to generate and culture human mast cells: Peripheral CD34+ stem cell-derived mast cells (PSCMCs). J Immunol Methods. 2014;413:62–8.
353. Luo Y, Vallone VF, He J, Frischbutter S, Kolkhir P, Moñino-Romero S, et al. A novel approach for studying mast cell–driven disorders: Mast cells derived from induced pluripotent stem cells. J Allergy Clin Immunol. 2022 Mar;149(3):1060-1068.e4.
354. Zbären N, Brigger D, Bachmann D, Helbling A, Jörg L, Horn MP, et al. A novel functional mast cell assay for the detection of allergies. J Allergy Clin Immunol. 2022 Mar 1;149(3):1018-1030.e11.
355. Gupta RS, Warren CM, Smith BM, Blumenstock JA, Jiang J, Davis MM, et al. The Public Health Impact of Parent-Reported Childhood Food Allergies in the United States. Pediatrics. 2018 Dec;142(6).
356. Warrington R, Silviu-Dan F, Wong T. Drug allergy. Allergy Asthma Clin Immunol. 2018 Sep;14(S2):60.
357. Muraro A, Worm M, Alviani C, Cardona V, DunnGalvin A, Garvey LH, et al. EAACI guidelines: Anaphylaxis (2021 update). Allergy. 2022 Feb;77(2):357–77.
358. Kazmi W, Berin MC. Oral tolerance and oral immunotherapy for food allergy: Evidence for common mechanisms? Cell Immunol. 2023 Jan;383:104650.

359. Beitia JM, Vega Castro A, Cárdenas R, Peña-Arellano MI. Pru p 3 Sublingual Immunotherapy in Patients with Lipid Transfer Protein Syndrome: Is It Worth? Int Arch Allergy Immunol. 2021;182(5):447–54.
360. Suhrkamp I, Scheffold A, Heine G. T-cell subsets in allergy and tolerance induction. Eur J Immunol. 2023 Oct;53(10):2249983.
361. Wood RA, Togias A, Sicherer SH, Shreffler WG, Kim EH, Jones SM, et al. Omalizumab for the Treatment of Multiple Food Allergies. N Engl J Med. 2024;390(10):889–99.
362. Rachid R, Stephen-Victor E, Chatila TA. The microbial origins of food allergy. J Allergy Clin Immunol. 2021 Mar;147(3):808–13.
363. Shu SA, Yuen AWT, Woo E, Chu KH, Kwan HS, Yang GX, et al. Microbiota and Food Allergy. Clin Rev Allergy Immunol. 2019 Aug;57(1):83–97.
364. Bunyavanich S, Berin MC. Food allergy and the microbiome: Current understandings and future directions. J Allergy Clin Immunol. 2019 Dec;144(6):1468–77.
365. Zubeldia-Varela E, Barker-Tejeda T, Obeso D, Villaseñor A, Barber D, Pérez-Gordo M. Microbiome and Allergy: New Insights and Perspectives. J Investig Allergol Clin Immunol. 2022 Oct 10;32(5):327–44.
366. Poto R, Fusco W, Rinninella E, Cintoni M, Kaitsas F, Raoul P, et al. The Role of Gut Microbiota and Leaky Gut in the Pathogenesis of Food Allergy. Nutrients [Internet]. 2024;16(1). Available from: https://www.mdpi.com/2072-6643/16/1/92
367. Muraro A, Werfel T, Hoffmann-Sommergruber K, Roberts G, Beyer K, Bindslev-Jensen C, et al. EAACI Food Allergy and Anaphylaxis Guidelines: Diagnosis and management of food allergy. Allergy Eur J Allergy Clin Immunol. 2014;69(8):1008–25.
368. Yin Y, Bai Y, Olivera A, Desai A, Metcalfe DD. An optimized protocol for the generation and functional analysis of human mast cells from CD34+ enriched cell populations. J Immunol Methods. 2017 Sep;448:105–11.
369. Quan PL, Ollé L, Sabaté-Brescó M, Guo Y, Muñoz-Cano R, Wagner A, et al. SARS-CoV-2 vaccine excipients polyethylene glycol and trometamol do not induce mast cell degranulation, in an in vitro model for non-IgE-mediated hypersensitivity. Front Allergy. 2022;3.
370. Kirshenbaum AS, Akin C, Wu Y, Rottem M, Goff JP, Beaven MA, et al. Characterization of novel stem cell factor responsive human mast cell lines LAD 1 and 2 established from a patient with mast cell sarcoma/leukemia; Activation following aggregation of FcεRI or FcγRI. Leuk Res. 2003 Aug;27(8):677–82.
371. Ribó P, Guo Y, Aranda J, Ainsua-Enrich E, Navinés-Ferrer A, Guerrero M, et al. Mutation in KARS: A novel mechanism for severe anaphylaxis. J Allergy Clin Immunol. 2021 May;147(5):1855-1864.e9.
372. Faloon PW, Bennion M, Weiner WS, Smith RA, Wurst J, Weiwer M, et al. A Small Molecule Inhibitor of the MITF Molecular Pathway. In: Probe Reports from the NIH Molecular Libraries Program. Bethesda (MD): National Center for Biotechnology Information (US); 2010.
373. Álvarez-Errico D, Oliver-Vila I, Ainsua-Enrich E, Gilfillan AM, Picado C, Sayós J, et al. CD84 Negatively Regulates IgE High-Affinity Receptor Signaling in Human Mast Cells. J Immunol. 2011 Dec;187(11):5577–86.
374. Serrano-Candelas E, Ainsua-Enrich E, Navinés-Ferrer A, Rodrigues P, García-Valverde A, Bazzocco S, et al. Silencing of adaptor protein SH3BP2 reduces KIT/PDGFRA receptors expression and impairs gastrointestinal stromal tumors growth. Mol Oncol. 2018 Aug;12(8):1383–97.
375. Belleau JT, Gandhi RK, McPherson HM, Lew DB. Research upregulation of CD23 (FcεRII) expression in human airway smooth muscle cells (huASMC) in response to IL-4, GM-CSF, and IL-4/GM-CSF. Clin Mol Allergy. 2005 May;3.
376. Chen JS, Grassmann JDS, Gowthaman U, Olyha SJ, Simoneau T, Berin MC, et al. Flow cytometric identification of TFH13 cells in mouse and human. Vol. 147, Journal of Allergy and Clinical Immunology. Mosby Inc.; 2021. p. 470–83.
377. Jang JS, Simon VA, Feddersen RM, Rakhshan F, Schultz DA, Zschunke MA, et al. Quantitative miRNA Expression Analysis Using Fluidigm Microfluidics Dynamic Arrays. BMC Genomics. 2011;12:1–8.

378. Spurgeon SL, Jones RC, Ramakrishnan R. High throughput gene expression measurement with real time PCR in a microfluidic dynamic array. PLoS ONE. 2008;3(2).
379. Navinés-Ferrer A, Ainsua-Enrich E, Serrano-Candelas E, Proaño-Pérez E, Muñoz-Cano R, Gastaminza G, et al. MYO1F Regulates IgE and MRGPRX2-Dependent Mast Cell Exocytosis. J Immunol. 2021 May;206(10):2277–89.
380. Monteiro L de B, Davanzo GG, de Aguiar CF, Moraes-Vieira PMM. Using flow cytometry for mitochondrial assays. MethodsX. 2020;7.
381. Cantó-Santos J, Valls-Roca L, Tobías E, García-García FJ, Guitart-Mampel M, Esteve-Codina A, et al. Unravelling inclusion body myositis using a patient-derived fibroblast model. J Cachexia Sarcopenia Muscle. 2023 Apr;14(2):964–77.
382. Solsona-Vilarrasa E, Fucho R, Torres S, Nuñez S, Nuño-Lámbarri N, Enrich C, et al. Cholesterol enrichment in liver mitochondria impairs oxidative phosphorylation and disrupts the assembly of respiratory supercomplexes. Redox Biol. 2019 Jun;24:101214.
383. Fucho R, Solsona-Vilarrasa E, Torres S, Nuñez S, Insausti-Urkia N, Edo A, et al. Zonal expression of StARD1 and oxidative stress in alcoholic-related liver disease. J Lipid Res. 2023 Aug;64(8):100413.
384. Pastorello EA, Farioli L, Pravettoni V, Ortolani C, Ispano M, Monza M, et al. The major allergen of peach (Prunus persica) is a lipid transfer protein. J Allergy Clin Immunol. 1999;103(3 II):520–6.
385. Mori Y, Okazaki F, Inuo C, Yamaguchi Y, Masuda S, Sugiura S, et al. Evaluation of serum IgE in peach-allergic patients with systemic reaction by using recombinant Pru p 7 (gibberellin-regulated protein). Allergol Immunopathol (Madr). 2018;46(5):482–90.
386. Tejedor Alonso MA, Moro Moro M, Múgica García M V. Epidemiology of anaphylaxis. Clin Exp Allergy. 2015;45(6):1027–39.
387. Tejedor-Alonso MA, Moro-Moro M, Mosquera González M, Rodriguez-Alvarez M, Pérez Fernández E, Latasa Zamalloa P, et al. Increased incidence of admissions for anaphylaxis in Spain 1998-2011. Allergy Eur J Allergy Clin Immunol. 2015;70(7):880–3.
388. Pascal M, Vazquez-Ortiz M, Folque MM, Jimenez-Feijoo R, Lozano J, Dominguez O, et al. Asymptomatic LTP sensitisation is common in plant-food allergic children from the Northeast of Spain. Allergol Immunopathol (Madr). 2016;44(4):351–8.
389. Bousquet J, Anto JM, Bachert C, Bousquet PJ, Colombo P, Crameri R, et al. Factors responsible for differences between asymptomatic subjects and patients presenting an IgE sensitization to allergens. A GA2LEN project. Allergy Eur J Allergy Clin Immunol. 2006;61(6):671–80.
390. Hauser M, Roulias A, Ferreira F, Egger M. Panallergens and their impact on the allergic patient. Allergy Asthma Clin Immunol. 2010;6(1):1–14.
391. Muraro A, Werfel T, Hoffmann-Sommergruber K, Roberts G, Beyer K, Bindslev-Jensen C, et al. EAACI Food Allergy and Anaphylaxis Guidelines: Diagnosis and management of food allergy. Allergy Eur J Allergy Clin Immunol. 2014;69(8):1008–25.
392. Dema B, Suzuki R, Rivera J. Rethinking the role of immunoglobulin E and its high affinity receptor: New insights in allergy and beyond. Int Arch Allergy Immunol. 2014;164(4):271–9.
393. Bergoug M, Doudeau M, Godin F, Mosrin C, Vallée B, Bénédetti H. Neurofibromin Structure, Functions and Regulation. Cells. 2020 Oct 27;9(11).
394. Báez-Flores J, Rodríguez-Martín M, Lacal J. The therapeutic potential of neurofibromin signaling pathways and binding partners. Commun Biol. 2023 Apr 20;6(1):436.
395. Wang B, Han J, Elisseeff JH, Demaria M. The senescence-associated secretory phenotype and its physiological and pathological implications. Nat Rev Mol Cell Biol. 2024 Dec;25(12):958–78.
396. Yang FC, Chen S, Clegg T, Li X, Morgan T, Estwick SA, et al. Nf1+/- mast cells induce neurofibroma like phenotypes through secreted TGF-beta signaling. Hum Mol Genet. 2006 Aug 15;15(16):2421–37.
397. Patmore DM, Welch S, Fulkerson PC, Wu J, Choi K, Eaves D, et al. In vivo regulation of TGF-β by R-Ras2 revealed through loss of the RasGAP protein NF1. Cancer Res. 2012 Oct 15;72(20):5317–27.
398. Schreck R, Baeuerle PA. NF-κB as Inducible Transcriptional Activator of the Granulocyte-Macrophage Colony-Stimulating Factor Gene. Mol Cell Biol. 1990;10(3):1281–6.
399. Liu T, Zhang L, Joo D, Sun SC. NF-κB signaling in inflammation. Signal Transduct Target Ther. 2017;2(March).

400. Favaro F, Luciano-Mateo F, Moreno-Caceres J, Hernández-Madrigal M, Both D, Montironi C, et al. TRAIL receptors promote constitutive and inducible IL-8 secretion in non-small cell lung carcinoma. Cell Death Dis. 2022;13(12):1–12.
401. Wang X, Richard ML, Li P, Henry B, Schutt S. Expression of granulocyte-macrophage colony-stimulating factor is regulated by Fli-1 transcription factor, a potential drug target. J Immunol. 2021;206(1):59–66.
402. Friščić J, Böttcher M, Reinwald C, Bruns H, Wirth B, Popp SJ, et al. The complement system drives local inflammatory tissue priming by metabolic reprogramming of synovial fibroblasts. Immunity. 2021 May;54(5):1002-1021.e10.
403. Bossi F, Rizzi L, Bulla R, Debeus A, Tripodo C, Picotti P, et al. C7 is expressed on endothelial cells as a trap for the assembling terminal complement complex and may exert anti-inflammatory function. Blood. 2009 Apr 9;113(15):3640–8.
404. Cardona V, Ansotegui IJ, Ebisawa M, El-Gamal Y, Rivas MF, Fineman S, et al. World allergy organization anaphylaxis guidance 2020. World Allergy Organ J. 2020 Oct;13(10).
405. Simons FER, Ardusso LRF, Bil MB, El-Gamal YM, Ledford DK, Ring J, et al. World Allergy Organization anaphylaxis guidelines: Summary. J Allergy Clin Immunol. 2011;127(3).
406. Pampura A, Esakova N, Zimin S, Filippova E. Anaphylaxis biomarkers: present and future. Eur Ann Allergy Clin Immunol. 2024;56(06):243.
407. White MV. The role of histamine in allergic diseases. J Allergy Clin Immunol. 1990 Oct;86(4 Pt 2):599–605.
408. Li Y, Gao J, Zhao D, Guan X, Morris SC, Finkelman FD, et al. The Hdc GC box is critical for Hdc gene transcription and histamine-mediated anaphylaxis. J Allergy Clin Immunol. 2023 Jul 1;152(1):195-204.e3.
409. Lang A, Kubala S, Grieco MC, Mateja A, Pongracic J, Liu Y, et al. Severe food allergy reactions are associated with α-tryptase. J Allergy Clin Immunol. 2023 Oct 1;152(4):933–9.
410. Lyons JJ, Chovanec J, O'Connell MP, Liu Y, Šelb J, Zanotti R, et al. Heritable risk for severe anaphylaxis associated with increased α-tryptase–encoding germline copy number at TPSAB1. J Allergy Clin Immunol. 2021 Feb;147(2):622–32.
411. Zhou X, Whitworth HS, M. EK, Brown TA, Goswami R, Eren E, et al. Mast Cell Chymase: A Useful Serum Marker in Anaphylaxis. J Allergy Clin Immunol. 2011 Feb 1;127(2):AB143.
412. Scudamore CL, Thornton EM, McMillan L, Newlands GF, Miller HR. Release of the mucosal mast cell granule chymase, rat mast cell protease-II, during anaphylaxis is associated with the rapid development of paracellular permeability to macromolecules in rat jejunum. J Exp Med. 1995 Dec 1;182(6):1871–81.
413. Dispenza MC, Bochner BS, MacGlashan DW. Targeting the FcεRI Pathway as a Potential Strategy to Prevent Food-Induced Anaphylaxis. Vol. 11, Frontiers in Immunology. Frontiers Media S.A.; 2020.
414. Takahashi K, Ra C. The High Affinity IgE Receptor (FcεRI) as a Target for Anti-allergic Agents. Allergol Int. 2005 Jan 1;54(1):1–5.
415. Serra-Pages M, Olivera A, Torres R, Picado C, Mora F de, Rivera J. E-prostanoid 2 receptors dampen mast cell degranulation via cAMP/PKA-mediated suppression of IgE-dependent signaling. J Leukoc Biol. 2012 Dec;92(6):1155–65.
416. Torres-Atencio I, Ainsua-Enrich E, De Mora F, Picado C, Martín M. Prostaglandin E2 Prevents Hyperosmolar-Induced Human Mast Cell Activation through Prostanoid Receptors EP2 and EP4. PLoS ONE. 2014 Oct 20;9(10).
417. Kulesza A, Paczek L, Burdzinska A. The Role of COX-2 and PGE2 in the Regulation of Immunomodulation and Other Functions of Mesenchymal Stromal Cells. Biomedicines. 2023 Feb 3;11(2):445.
418. Globig P, Morakabati P, Höfer V, Willmes DM, Babina M, Worm M. Acetylsalicylic acid aggravates anaphylaxis in a PGE2-dependent manner. J Clin Invest. 2025 Mar 3;135(5).
419. Laouini D, ElKhal A, Yalcindag A, Kawamoto S, Oettgen H, Geha RS. COX-2 inhibition enhances the TH2 immune response to epicutaneous sensitization. J Allergy Clin Immunol. 2005 Aug;116(2):390–6.

420. Cardoso AP, Pinto ML, Castro F, Costa ÂM, Marques-Magalhães Â, Canha-Borges A, et al. The immunosuppressive and pro-tumor functions of CCL18 at the tumor microenvironment. Cytokine Growth Factor Rev. 2021;60(February):107–19.
421. Huoman J, Haider S, Simpson A, Murray CS, Custovic A, Jenmalm MC. Childhood CCL18, CXCL10 and CXCL11 levels differentially relate to and predict allergy development. Kalaycı Ö, editor. Pediatr Allergy Immunol. 2021 Nov;32(8):1824–32.
422. de Nadaï P. Involvement of CCL18 in inflammatory allergic diseases. J Allergy Clin Immunol. 2004 Feb 1;113(2):S262.
423. Conductier G, Blondeau N, Guyon A, Nahon JL, Rovère C. The role of monocyte chemoattractant protein MCP1/CCL2 in neuroinflammatory diseases. J Neuroimmunol. 2010;224(1–2):93–100.
424. Jiang S, Wang Q, Wang Y, Song X, Zhang Y. Blockade of CCL2/CCR2 signaling pathway prevents inflammatory monocyte recruitment and attenuates OVA-Induced allergic asthma in mice. Immunol Lett. 2019 Oct 1;214:30–6.
425. Dijkstra D, Leurs R, Chazot P, Shenton FC, Stark H, Werfel T, et al. Histamine downregulates monocyte CCL2 production through the histamine H4 receptor. J Allergy Clin Immunol. 2007 Aug 1;120(2):300–7.
426. Vantur R, Rihar M, Koren A, Rijavec M, Kopac P, Bidovec-Stojkovic U, et al. Chemokines during anaphylaxis: the importance of CCL2 and CCL2-dependent chemotactic activity for basophils. Clin Transl Allergy. 2020 Dec 15;10(1):63.
427. Kaneko N, Kurata M, Yamamoto T, Morikawa S, Masumoto J. The role of interleukin-1 in general pathology. Inflamm Regen. 2019;39(1):1–16.
428. Yeung K, Mraz V, Geisler C, Skov L, Bonefeld CM. The role of interleukin- 1B in the immune response to contact allergens. Contact Dermatitis. 2021 Oct;85(4):387–97.
429. Krause K, Metz M, Makris M, Zuberbier T, Maurer M. The role of interleukin-1 in allergy-related disorders. Curr Opin Allergy Clin Immunol. 2012 Oct;12(5):477–84.
430. Wang HR, Wei SZ, Song XY, Wang Y, Zhang WB, Ren C, et al. IL-1β and Allergy: Focusing on Its Role in Allergic Rhinitis. Caruso C, editor. Mediators Inflamm. 2023 Apr 12;2023:1–11.
431. Travis MA, Sheppard D. TGF-β Activation and Function in Immunity. Annu Rev Immunol. 2014;32(1):51–82.
432. Schmidt-Weber CB, Blaser K. The role of TGF-beta in allergic inflammation. Immunol Allergy Clin North Am. 2006 May;26(2):233–44, vi–vii.
433. Tirado-Rodriguez B, Ortega E, Segura-Medina P, Huerta-Yepez S. TGF- β: an important mediator of allergic disease and a molecule with dual activity in cancer development. J Immunol Res. 2014;2014:318481.
434. Li Y, Gao J, Kamran M, Harmacek L, Danhorn T, Leach SM, et al. GATA2 regulates mast cell identity and responsiveness to antigenic stimulation by promoting chromatin remodeling at super-enhancers. Nat Commun. 2021;12(1):1–17.
435. Marriott AS, Vasieva O, Fang Y, Copeland NA, McLennan AG, Jones NJ. NUDT2 Disruption Elevates Diadenosine Tetraphosphate (Ap4A) and Down-Regulates Immune Response and Cancer Promotion Genes. PloS One. 2016;11(5):e0154674.
436. Tanwar J, Sharma A, Saurav S, Shyamveer, Jatana N, Motiani RK. MITF is a novel transcriptional regulator of the calcium sensor STIM1: Significance in physiological melanogenesis. J Biol Chem. 2022;298(12):1–15.
437. Miller AJ, Du J, Rowan S, Hershey CL, Widlund HR, Fisher DE. Transcriptional Regulation of the Melanoma Prognostic Marker Melastatin (TRPM1) by MITF in Melanocytes and Melanoma. Cancer Res. 2004 Jan 15;64(2):509–16.
438. Mukai K, Tsai M, Saito H, Galli SJ. Mast cells as sources of cytokines, chemokines, and growth factors. Immunol Rev. 2018;282(1):121–50.
439. Rigoulet M, Bouchez CL, Molinié T, Cuvellier S, Mazat JP, Ransac S, et al. Mitochondria: Ultrastructure, dynamics, biogenesis, and main functions. Mitochondrial Physiology and Vegetal Molecules: Therapeutic Potential of Natural Compounds on Mitochondrial Health. Elsevier Inc.; 2021. 3–34 p.
440. Hua J, Chen H, Chen Y, Zheng G, Li F, Qu J, et al. MITF acts as an anti-oxidant transcription factor to regulate mitochondrial biogenesis and redox signaling in retinal pigment epithelial cells. Exp Eye Res. 2018 May;170:138–47.

441. Pascal M, Muñoz-Cano R, Milà J, Sanz ML, Diaz-Perales A, Sánchez-López J, et al. Nonsteroidal anti-inflammatory drugs enhance IgE-mediated activation of human basophils in patients with food anaphylaxis dependent on and independent of nonsteroidal anti-inflammatory drugs. Clin Exp Allergy. 2016;46(8):1111–9.
442. Deng S, Yin J. Clinical utility of basophil activation test in diagnosis and predicting severity of mugwort pollen-related peach allergy. World Allergy Organ J. 2019;12(6):100043.
443. Cañas JA, Pérez-Sánchez N, Lopera-Doblas L, Palomares F, Molina A, Bartra J, et al. Basophil Activation Test Utility as a Diagnostic Tool in LTP Allergy. Int J Mol Sci. 2022 Apr 29;23(9):4979.
444. Tam IYS, Lau HYA, Tam SY, Lee TH. Mast cell activation test using patient-derived mast cells exhibits distinct combinatorial phenotypic profiles among allergic patients. Allergy Eur J Allergy Clin Immunol. 2020;75(7):1796–9.
445. Elst J, van der Poorten MLM, Van Gasse AL, De Puysseleyr L, Hagendorens MM, Faber MA, et al. Mast cell activation tests by flow cytometry: A new diagnostic asset? Clin Exp Allergy. 2021;51(11):1482–500.
446. Adamko DJ, Khamis MM, Steacy LM, Regush S, Bryce R, Ellis AK, et al. A novel human mast cell activation test for peanut allergy. J Allergy Clin Immunol. 2018 Aug;142(2):689-691.e9.
447. Wachholz PA, Soni NK, Till SJ, Durham SR. Inhibition of allergen-IgE binding to B cells by IgG antibodies after grass pollen immunotherapy. J Allergy Clin Immunol. 2003;112(5):915–22.
448. Noh G, Ahn HS, Cho NY, Lee S, Oh JW. The clinical significance of food specific IgE/IgG4 in food specific atopic dermatitis. Pediatr Allergy Immunol Off Publ Eur Soc Pediatr Allergy Immunol. 2007 Feb;18(1):63–70.
449. Santos AF, James LK, Bahnson HT, Shamji MH, Couto-Francisco NC, Islam S, et al. IgG4 inhibits peanut-induced basophil and mast cell activation in peanut-tolerant children sensitized to peanut major allergens. J Allergy Clin Immunol. 2015;135(5):1249–56.
450. Carballo I, Alvela L, Pérez LF, Gude F, Vidal C, Alonso M, et al. Serum Concentrations of IgG4 in the Spanish Adult Population: Relationship with Age, Gender, and Atopy. PLOS ONE. 2016 Feb;11(2):e0149330.
451. Carballo I, González-Quintela A, Sopeña B, Vidal C. Immunoglobulin g4–related disease: What an allergist should know. J Investig Allergol Clin Immunol. 2021;31(3):212–27.
452. Qin L, Tang LF, Cheng L, Wang HY. The clinical significance of allergen-specific IgG4 in allergic diseases. Front Immunol. 2022;13(October):1–9.
453. Pascal M, Moreno C, Dávila I, Tabar AI, Bartra J, Labrador M, et al. Integration of in vitro allergy test results and ratio analysis for the diagnosis and treatment of allergic patients (INTEGRA). Clin Transl Allergy. 2021;11(7):1–14.
454. Gomez G, Ramirez CD, Rivera J, Patel M, Norozian F, Wright H V., et al. TGF-β1 Inhibits Mast Cell FcεRI Expression. J Immunol. 2005;174(10):5987–93.
455. Weissler KA, Frischmeyer-Guerrerio PA. Genetic evidence for the role of transforming growth factor-β in atopic phenotypes. Curr Opin Immunol. 2019;60(301):54–62.
456. Flinterman AE, Knol EF, Lencer DA, Bardina L, den Hartog Jager CF, Lin J, et al. Peanut epitopes for IgE and IgG4 in peanut-sensitized children in relation to severity of peanut allergy. J Allergy Clin Immunol. 2008;121(3):3–15.
457. Shreffler WG, Beyer K, Chu THT, Burks AW, Sampson HA. Microarray immunoassay: Association of clinical history, in vitro IgE function, and heterogeneity of allergenic peanut epitopes. J Allergy Clin Immunol. 2004;113(4):776–82.
458. Wang J, Lin J, Bardina L, Goldis M, Nowak-Węgrzyn A, Shreffler WG, et al. Correlation of IgE/IgG4 milk epitopes and affinity of milk-specific IgE antibodies with different phenotypes of clinical milk allergy. J Allergy Clin Immunol. 20010;125(3):695–702.
459. Coppé JP, Desprez PY, Krtolica A, Campisi J. The senescence-associated secretory phenotype: the dark side of tumor suppression. Annu Rev Pathol. 2010;5:99–118.
460. Schoetz U, Klein D, Hess J, Shnayien S, Spoerl S, Orth M, et al. Early senescence and production of senescence-associated cytokines are major determinants of radioresistance in head-and-neck squamous cell carcinoma. Cell Death Dis. 2021 Dec 15;12(12):1162.
461. Chiba T, Matsuzaka Y, Warita T, Sugoh T, Miyashita K, Tajima A, et al. NFKBIL1 Confers Resistance to Experimental Autoimmune Arthritis Through the Regulation of Dendritic Cell Functions. Scand J Immunol. 2011 May;73(5):478–85.

462. Bakos E, Thaiss CA, Kramer MP, Cohen S, Radomir L, Orr I, et al. CCR2 Regulates the Immune Response by Modulating the Interconversion and Function of Effector and Regulatory T Cells. J Immunol. 2017 Jun 15;198(12):4659–71.
463. Fang Y, Yu S, Ellis JS, Sharav T, Braley-Mullen H. Comparison of sensitivity of Th1, Th2, and Th17 cells to Fas-mediated apoptosis. J Leukoc Biol. 2010 Feb 23;87(6):1019–28.
464. Serrano Hernández A. Células colaboradoras (TH1, TH2, TH17) y reguladoras (Treg, TH3, NKT) en la artritis reumatoide. Reumatol Clínica. 2009 Apr;5:1–5.
465. Haque T, Leak L, Youngblood E, Laky K, Frischmeyer-Guerrerio P. Mast cell-intrinsic TGF-b signaling modulates mast cell effector function and allergic responses. J Immunol. 2024 May 1;212(1_Supplement):1058_4788-1058_4788.
466. Haque TT, Weissler KA, Schmiechen Z, Laky K, Schwartz DM, Li J, et al. TGFβ prevents IgE-mediated allergic disease by restraining T follicular helper 2 differentiation. Sci Immunol. 2024 Jan 19;9(91):eadg8691.
467. Lyons JJ, Chovanec J, O'Connell MP, Liu Y, Šelb J, Zanotti R, et al. Heritable risk for severe anaphylaxis associated with increased α-tryptase–encoding germline copy number at TPSAB1. J Allergy Clin Immunol. 2021;147(2):622–32.
468. Siegel AM, Stone KD, Cruse G, Lawrence MG, Olivera A, Jung MY, et al. Diminished allergic disease in patients with STAT3 mutations reveals a role for STAT3 signaling in mast cell degranulation. Bone. 2011;23(1):1–7.
469. Schutyser E, Richmond A, Van Damme J. Involvement of CC chemokine ligand 18 (CCL18) in normal and pathological processes. J Leukoc Biol. 2005 Mar 22;78(1):14–26.
470. Chang Y, Nadai PD, Azzaoui I, Morales O, Delhem N, Vorng H, et al. The chemokine CCL18 generates adaptive regulatory T cells from memory $CD4^+$ T cells of healthy but not allergic subjects. FASEB J. 2010 Dec;24(12):5063–72.
471. Amniai L, Ple C, Barrier M, De Nadai P, Marquillies P, Vorng H, et al. Natural Killer Cells from Allergic Donors Are Defective in Their Response to CCL18 Chemokine. Int J Mol Sci. 2021 Apr 9;22(8):3879.
472. Oštrić Pavlović I, Radović S, Krtinić D, Spirić J, Kusić N, Veličković A, et al. Tryptase: The Silent Witness of Past and Ongoing Systemic Events. Medicina (Mex). 2024 Aug 23;60(9):1380.
473. Yang BG, Kim AR, Lee D, An SB, Shim YA, Jang MH. Degranulation of Mast Cells as a Target for Drug Development. Cells. 2023 May 29;12(11):1506.
474. Gülen T. A Puzzling Mast Cell Trilogy: Anaphylaxis, MCAS, and Mastocytosis. Diagnostics. 2023 Oct 25;13(21):3307.
475. Khan M, Ricks A, Yao L. ELEVATED HISTAMINE LEVELS WITH NORMAL TRYPTASE IN ANAPHYLAXIS. Ann Allergy Asthma Immunol. 2022 Nov 1;129(5):S109.
476. Moñino-Romero S, Lexmond WS, Singer J, Bannert C, Amoah AS, Yazdanbakhsh M, et al. Soluble Fcε RI : A biomarker for IgE-mediated diseases. Allergy. 2019 Jul;74(7):1381–4.
477. Oettgen HC, Geha RS. IgE in asthma and atopy: cellular and molecular connections. J Clin Invest. 1999 Oct 1;104(7):829–35.
478. Yamaguchi M, Lantz CS, Oettgen HC, Katona IM, Fleming T, Miyajima I, et al. IgE Enhances Mouse Mast Cell FceRI Expression In Vitro and In Vivo: Evidence for a Novel Amplification Mechanism in IgE-dependent Reactions. J Exp Med. 1997;185(4):663–72.
479. Rajakulasingam K, Till S, Ying S, Humbert M, Barkans J, Sullivan M, et al. Increased Expression of High Affinity IgE (FcεRI) Receptor-a Chain mRNA and Protein-bearing Eosinophils in Human Allergen-induced Atopic Asthma. Am J Respir Crit Care Med. 1998;158:233–40.
480. Muñoz-Cano RM, Casas R, Araujo G, De La Cruz C, Martin M, Roca-Ferrer J, et al. Prostaglandin E2 decreases basophil activation in patients with food-induced anaphylaxis. Allergy. 2021 May;76(5):1556–9.
481. Rastogi S, Willmes DM, Nassiri M, Babina M, Worm M. PGE2 deficiency predisposes to anaphylaxis by causing mast cell hyperresponsiveness. J Allergy Clin Immunol. 2020 Dec;146(6):1387-1396.e13.
482. Torres R, Picado C, Mora F de. The PGE2-EP2-mast cell axis: An antiasthma mechanism. Vol. 63, Molecular Immunology. Elsevier Ltd; 2015. p. 61–8.

483. Molina-Holgado E, Ortiz S, Molina-Holgado F, Guaza C. Induction of COX-2 and PGE(2) biosynthesis by IL-1beta is mediated by PKC and mitogen-activated protein kinases in murine astrocytes. Br J Pharmacol. 2000 Sep;131(1):152–9.
484. Taniura S, Kamitani H, Watanabe T, Eling TE. Induction of cyclooxygenase-2 expression by interleukin-1beta in human glioma cell line, U87MG. Neurol Med Chir (Tokyo). 2008;48(11):500–5; discussion 505.
485. Uracz W, Uracz D, Olszanecki R, Gryglewski RJ. Interleukin 1beta induces functional prostaglandin E synthase in cultured human umbilical vein endothelial cells. J Physiol Pharmacol Off J Pol Physiol Soc. 2002 Dec;53(4 Pt 1):643–54.
486. Huang ZF, Massey JB, Via DP. Differential regulation of cyclooxygenase-2 (COX-2) mRNA stability by interleukin-1 beta (IL-1 beta) and tumor necrosis factor-alpha (TNF-alpha) in human in vitro differentiated macrophages. Biochem Pharmacol. 2000 Jan 15;59(2):187–94.
487. Estrada C, Mirabal-Ortega L, Méry L, Dingli F, Besse L, Messaoudi C, et al. MITF activity is regulated by a direct interaction with RAF proteins in melanoma cells. Commun Biol. 2022 Jan 28;5(1):101.
488. Srivastava M, Kaplan MH. Transcription Factors in the Development and Pro-Allergic Function of Mast Cells. Vol. 2, Frontiers in Allergy. Frontiers Media S.A.; 2021.
489. Takemoto CM, Yoon YJ, Fisher DE. The identification and functional characterization of a novel mast cell isoform of the microphthalmia-associated transcription factor. J Biol Chem. 2002 Aug 16;277(33):30244–52.
490. Tanwar J, Sharma A, Saurav S, Shyamveer, Jatana N, Motiani RK. MITF is a novel transcriptional regulator of the calcium sensor STIM1: Significance in physiological melanogenesis. J Biol Chem. 2022 Dec;298(12).
491. Wang J, Xu C, Zheng Q, Yang K, Lai N, Wang T, et al. Orai1, 2, 3 and STIM1 promote store-operated calcium entry in pulmonary arterial smooth muscle cells. Cell Death Discov. 2017 Nov 27;3(1):17074.
492. Butorac C, Krizova A, Derler I. Review: Structure and Activation Mechanisms of CRAC Channels. In: Islam MdS, editor. Calcium Signaling [Internet]. Cham: Springer International Publishing; 2020 [cited 2025 Feb 26]. p. 547–604. (Advances in Experimental Medicine and Biology; vol. 1131). Available from: http://link.springer.com/10.1007/978-3-030-12457-1_23
493. Peavy RD, Metcalfe DD. Understanding the mechanisms of anaphylaxis. 2009;
494. Nishikiori N, Watanabe M, Sato T, Furuhashi M, Okura M, Hida T, et al. Significant and Various Effects of ML329-Induced MITF Suppression in the Melanoma Cell Line. Cancers. 2024 Jan 7;16(2):263.
495. Lee YN, Nechushtan H, Figov N, Razin E. The Function of Lysyl-tRNA Synthetase and Ap4A as Signaling Regulators of MITF Activity in FcRI-Activated Mast Cells ally, MITF was found to be in complex with USF2 (Nechushtan et al., 1997). Using a construct containing the basic-helix-loop-helix-leucine zipper (bHLH-zip) motif of MITF as bait in yeast two-hybrid library screening, we have previously min of Ap 4 A exposure, the dissociation was complete. Vol. 20, Immunity. 2004. p. 145–51.
496. Kolkhir P, Ali H, Babina M, Ebo D, Sabato V, Elst J, et al. MRGPRX2 in drug allergy: What we know and what we do not know. J Allergy Clin Immunol. 2023 Feb;151(2):410–2.
497. Subramanian H, Gupta K, Ali H. Roles of Mas-related G protein–coupled receptor X2 on mast cell–mediated host defense, pseudoallergic drug reactions, and chronic inflammatory diseases. J Allergy Clin Immunol. 2016 Sep;138(3):700–10.
498. Yuan F, Zhang C, Sun M, Wu D, Cheng L, Pan B, et al. MRGPRX2 mediates immediate-type pseudo-allergic reactions induced by iodine-containing iohexol. Biomed Pharmacother. 2021 May;137:111323.
499. Nagamine M, Kaitani A, Izawa K, Ando T, Yoshikawa A, Nakamura M, et al. Neuronal substance P-driven MRGPRX2-dependent mast cell degranulation products differentially promote vascular permeability. Front Immunol. 2024;15:1477072.
500. Mi YN, Ping NN, Cao YX. Ligands and Signaling of Mas-Related G Protein-Coupled Receptor-X2 in Mast Cell Activation. Rev Physiol Biochem Pharmacol. 2021;179:139–88.

501. Roy S, Chompunud Na Ayudhya C, Thapaliya M, Deepak V, Ali H. Multifaceted MRGPRX2: New insight into the role of mast cells in health and disease. J Allergy Clin Immunol. 2021 Aug 1;148(2):293–308.
502. Li Z, Schneikert J, Bal G, Jin M, Franke K, Zuberbier T, et al. Intrinsic Regulatory Mechanisms Protect Human Skin Mast Cells from Excessive MRGPRX2 Activation: Paucity in LAD2 (Laboratory of Allergic Diseases 2) Cells Contributes to Hyperresponsiveness of the Mast Cell Line. J Invest Dermatol. 2024;2.
503. Wang Z, Li Z, Bal G, Franke K, Zuberbier T, Babina M. β-arrestin-1 and β-arrestin-2 Restrain MRGPRX2-Triggered Degranulation and ERK1/2 Activation in Human Skin Mast Cells. Front Allergy. 2022;3(July):1–10.
504. Piotin A, Oulehri W, Charles AL, Tacquard C, Collange O, Mertes PM, et al. Oxidative Stress and Mitochondria Are Involved in Anaphylaxis and Mast Cell Degranulation: A Systematic Review. Antioxidants. 2024;13(8).
505. Yamamoto H, Itoh N, Kawano S, Yatsukawa Y ichi, Momose T, Makio T, et al. Dual role of the receptor Tom20 in specificity and efficiency of protein import into mitochondria. Proc Natl Acad Sci. 2011 Jan 4;108(1):91–6.
506. Kadenbach B. Complex IV – The regulatory center of mitochondrial oxidative phosphorylation. Mitochondrion. 2021;58(September 2020):296–302.
507. Grevel A, Pfanner N, Becker T. Coupling of import and assembly pathways in mitochondrial protein biogenesis. Biol Chem. 2019 Dec 18;401(1):117–29.
508. Liang H, Ward WF. PGC-1α: a key regulator of energy metabolism. Adv Physiol Educ. 2006 Dec;30(4):145–51.
509. Vazquez F, Lim JH, Chim H, Bhalla K, Girnun G, Pierce K, et al. PGC1α Expression Defines a Subset of Human Melanoma Tumors with Increased Mitochondrial Capacity and Resistance to Oxidative Stress. Cancer Cell. 2013 Mar;23(3):287–301.
510. Haq R, Shoag J, Andreu-Perez P, Yokoyama S, Edelman H, Rowe GC, et al. Oncogenic BRAF regulates oxidative metabolism via PGC1α and MITF. Cancer Cell. 2013 Mar;23(3):302–15.
511. Navinés-Ferrer A, Ainsua-Enrich E, Serrano-Candelas E, Proaño-Pérez E, Muñoz-Cano R, Gastaminza G, et al. MYO1F Regulates IgE and MRGPRX2-Dependent Mast Cell Exocytosis. J Immunol. 2021;206(10):2277–89.
512. Chen HY, Chiang DML, Lin ZJ, Hsieh CC, Yin GC, Weng IC, et al. Nanoimaging granule dynamics and subcellular structures in activated mast cells using soft X-ray tomography. Sci Rep. 2016;6(April):1–11.
513. Zhang B, Alysandratos KD, Angelidou A, Asadi S, Sismanopoulos N, Delivanis DA, et al. Human mast cell degranulation and preformed TNF secretion require mitochondrial translocation to exocytosis sites: Relevance to atopic dermatitis. J Allergy Clin Immunol. 2011;127(6):1522–31.
514. Wang C, Zhao L, Su Q, Fan X, Wang Y, Gao S, et al. Phosphorylation of MITF by AKT affects its downstream targets and causes TP53-dependent cell senescence. Int J Biochem Cell Biol. 2016 Nov;80:132–42.
515. Giuliano S, Cheli Y, Ohanna M, Bonet C, Beuret L, Bille K, et al. Microphthalmia-associated transcription factor controls the DNA damage response and a lineage-specific senescence program in melanomas. Cancer Res. 2010 May 1;70(9):3813–22.
516. Zhang J, Mou Y, Gong H, Chen H, Xiao H. Microphthalmia-Associated Transcription Factor in Senescence and Age-Related Diseases. Gerontology. 2021;67(6):708–17.
517. Čunátová K, Reguera DP, Vrbacký M, Fernández-Vizarra E, Ding S, Fearnley IM, et al. Loss of COX4I1 Leads to Combined Respiratory Chain Deficiency and Impaired Mitochondrial Protein Synthesis. Cells. 2021 Feb 10;10(2).
518. Diaz F. Cytochrome c oxidase deficiency: Patients and animal models. Mitochondrial Dysfunct. 2010 Jan 1;1802(1):100–10.
519. Di Maio R, Barrett PJ, Hoffman EK, Barrett CW, Zharikov A, Borah A, et al. α-Synuclein binds to TOM20 and inhibits mitochondrial protein import in Parkinson's disease. Sci Transl Med. 2016 Jun 8;8(342):342ra78.
520. Chelombitko MA, Fedorov AV, Ilyinskaya OP, Zinovkin RA, Chernyak BV. Role of Reactive Oxygen Species in Mast Cell Degranulation. Biochem Biokhimiia. 2016 Dec;81(12):1564–77.

521. Goretzki A, Zimmermann J, Lin YJ, Schülke S. Immune Metabolism–An Opportunity to Better Understand Allergic Pathology and Improve Treatment of Allergic Diseases? Front Allergy. 2022;3(March):1–15.
522. Li X, Shen H, Zhang M, Teissier V, Huang EE, Gao Q, et al. Glycolytic reprogramming in macrophages and MSCs during inflammation. Front Immunol. 2023 Aug 22;14:1199751.
523. Lee A, Park H, Lim S, Lim J, Koh J, Jeon YK, et al. Novel role of microphthalmia-associated transcription factor in modulating the differentiation and immunosuppressive functions of myeloid-derived suppressor cells. J Immunother Cancer. 2023 Jan;11(1):e005699.
524. Gao H, Nepovimova E, Heger Z, Valko M, Wu Q, Kuca K, et al. Role of hypoxia in cellular senescence. Pharmacol Res. 2023 Aug 1;194:106841.
525. Wan M, Yu Q, Xu F, You LX, Liang X, Kang Ren K, et al. Novel hypoxia-induced HIF-1αactivation in asthma pathogenesis. Respir Res. 2024 Jul 25;25(1):287.